CAROLINA POWER & LIGHT COMPANY

RALEIGH, NORTH CAROLINA

PLANT UNIQUE ANALYSIS REPORT

MARK 1 CONTAINMENT PROGRAM

BRUNSWICK STEAM ELECTRIC PLANT

UNITS 1 & 2

OCTOBER 1, 1982

PREPARED BY: UNITED ENGINEERS AND CONTRUCTORS, INC.

PHILADELPHIA, PENNSYLVANIA

TABLE OF CONTENTS

TABLE OF CONTENTS

TABLE OF CONTENTS

TABLE OF CONTENTS

TABLE OF CONTENTS

TABLE OF CONTENTS

TABLE OF CONTENTS

TABLE OF CONTENTS

TABLE OF CONTENTS

LIST OF TABLES

LIST OF TABLES

LIST OF TABLES

LIST OF TABLES

LIST OF TABLES

LIST OF TABLES

LIST OF FIGURES

LIST OF FIGURES

LIST OF FIGURES

LIST OF FIGURES

LIST OF FIGURES

LIST OF FIGURES

LIST OF FIGURES

LIST OF FIGURES

INTRODUCTION

The Brunswick Steam Electric Plant (Units 1 and 2) is owned and operated by Carolina Power and Light Company. It is located near Wilmington, North Carolina. Both units contain General Electric boiling water reactor (BWR) nuclear steam supply systems housed in a containment structure designated as the Mark I containment system.

Subsequent to the establishment of the original design criteria for the boiling water reactor Mark I containment system design, additional load conditions were identified which relate to the pressure suppression concept. These additional loads result from the dynamic effects of drywell air and steam being rapidly forced into the suppression pool during a postulated LOCA and from suppression pool response to safety/relief valve (SRV) operation generally associated with plant transient operating conditions. The LOCA loads were identified in the course of performing large-scale testing of an advanced design pressure suppression containment (Mark III). The SRV loads were identified during in-plant testing of Mark I containments.

Consequently, in February and April 1975, the NRC transmitted letters to all utilities owning BWR facilities with the Mark I containment design, requesting that the owners quantify the hydrodynamic loads and assess the effect of these loads on the containment structure. Recognizing that the additional evaluation effort would be very similar for all Mark I BWR plants, the affected utilities formed an "ad hoc" Mark I Owners Group with General Electric designated as the lead technical organization.

A short term program (STP) was begun immediately and completed in 1977. This program verified that licensed Mark I BWR facilities could continue to operate safely, without endangering the health and safety of the public, while a methodical, comprehensive long term program (LTP) was being conducted.

The objectives of the long term program were to establish conservative design basis loads and to restore the originally intended design-safety margins for each Mark I containment system. This report

presents the results of the long term program, plant unique analysis for the Brunswick Steam Electric Plant (Units 1 and 2).

SUMMARY

A summary of the plant unique analysis results is as follows:

1) Torus - The Brunswick suppression chamber consists of a reinforced concrete, steel lined torus. This structure satisfies the LTP criteria without modification.

2) Vent System - The Brunswick vent system is a typical Mark I configuration and satisfies the LTP criteria with the addition of the following modifications: vent system deflector, vent header/downcomer intersection reinforcement, SRV penetration reinforcement and vent system support columns to the top of the torus.

3) Safety Relief Valve Discharge Lines - In order to satisfy LTP criteria for SRV discharges, standard Mark I T-quencher discharge devices will be added to all SRV discharge lines.

4) Miscellaneous Piping and Structures - All miscellaneous piping and structures within the torus meet the LTP criteria with the addition of new supports and/or the strengthening of existing supports where required.

Photographs and drawings of the modifications are included in Section 4.

1.0 SUPPRESSION CHAMBER ANALYSIS

1.1 INTRODUCTION

This report includes the analysis of the suppression chamber (torus) in Units 1 and 2 of Brunswick Steam Electric Plant. The structure is analyzed for the loads applied at normal operation and for Loss of Coolant Accident (LOCA) related loads as defined in Reference 1-1. The stresses which are developed in the suppression chamber for all the load combinations defined in Reference 1-2 are calculated to show the integrity of the structure.

A finite element direct stiffness technique for the analysis of axisymmetric solids of revolution under symmetric and arbitrary loadings (References 1-3 and 1-4) is used for the overall analysis of the suppression chamber. A utility program, based on Reference 1-13 and developed in United Engineers and Constructors Inc. (UE&C), is used for liner anchor analysis. The results from a large opening analysis, performed previously using a modified version of SAMIS computer program, is used to calculate stresses around the suppression chamber large openings. The changes and additions to the general program of Reference 1-3 are performed in UE&C. Several utility programs are developed and used as pre-or-post processor to the finite element computer programs. The computer programs used in the analysis are verified.

1.2 PHYSICAL DESCRIPTION OF SUPPRESSION CHAMBER

The primary containment structure of the Brunswick Nuclear Power Plant consists of the drywell and the pressure suppression chamber. See Figure 1.2-1. The suppression chamber is a reinforced concrete torus which encircles the bottom of the drywell. It is supported on the same mat foundation as drywell. It can be assumed to be physically independent of the drywell under all axisymmetric loads

such as dead load, hydrostatic load, pressure, temperature, pool swell, condensation oscillation and post chugging loads. A paper joint is provided between the bottom of the suppression chamber and the mat foundation to allow radial expansion of the chamber. The suppression chamber is keyed vertically to the drywell along the outside perimeters of the drywell pedestal.

The pressure suppression chamber consists of a continuous 16 sided steel liner of circular cross section which is enveloped by reinforced concrete. The liner has an internal diameter of 29'-0" and a major diameter of approximately 109'-0". Maximum water level in the torus is 2'-4" below the horizontal surface passing through the center of the circular liner. Figure 1.2-2 shows a typical vertical cross section of the suppression chamber.

The suppression chamber is reinforced with a single layer of continuous closed hoop reinforcing equally spaced around the perimeter of the liner. Meridional reinforcings in the form of closed rings, placed radially to the centerline of the containment, are also provided. Diagonal seismic reinforcings are provided and are located along the vertical faces and top of the suppression chamber. Figure 1.2-3 shows the typical reinforcing used in the concrete around the steel torus.

The suppression chamber contains eight symmetrically located vent openings corresponding to the vent openings in the drywell. The main hoop reinforcings which would normally occur in the openings is banded above and below the openings. The meridional bars which would normally occur at these locations are grouped on either side. The vents are locally reinforced by closed rings around the perimeter of each opening. See Section 1.10 for vent openings.

1.3 DESCRIPTION OF THE APPLIED LOADS

The loads applied to the suppression chamber under normal operating conditions and postulated Loss of Coolant Accident (LOCA)

are defined in detail in Structural Acceptance Criteria and Load Definition Report (References 1-1 and 1-2). LOCA loads are given for Design Basis Accident (DBA), Intermediate Break Accident (IBA) and Small Break Accident (SBA). The load due to safety/relief valve actuation (S/RV) caused by a normal operational transient and/or LOCA are also given in detail in Reference 1-1. The Operating Basis (OBE) and Safe Shutdown (SSE) seismic loads applied to the suppression chamber during an earthquake were derived from the definitions given in the Final Safety Analysis Report (FSAR). The characteristic, maximum magnitude, duration and other information related to the loads applied to the suppression chamber during normal operation, LOCA and earthquake are given briefly in the following subsections. The assumptions made to idealize the applied loads for the analysis are also given in the following subsections.

1.3.1 Dead Load

The dead load consists of the weight of the suppression chamber (liner and reinforced concrete) and the weight of the water in the torus. It is a symmetric load with respect to the suppression chamber axis of revolution.

1.3.2 Normal Operating Temperature

Temperature range, during normal operation of the suppression chamber, for the free air volume and for the suppression pool is 76-92°F. Temperature is symmetric with respect to the suppression chamber axis of revolution. It is assumed to vary linearly through the thickness of the structure to outside temperature of 70°F. A conservative temperature of 100°F is used in the analysis as normal operating temperature.

1.3.3 Normal Operating Internal Pressure

Suppression chamber pressure during normal operation is as high as 1.25 psig and as low as 0.15 psig. Since normal operating

loads do not control design, this internal pressure is neglected in the analysis.

1.3.4 S/RV Load

The S/RV load caused by actuating one or more safety/relief valves in normal operation and/or LOCA is an oscillatory, attenuated pressure which applies to the torus shell. Figure 1.3-1 shows a typical S/RV shell pressure loading transient. Ther are eleven safety relief valves in Brunswick torus of which a single valve or a combination of several valves may actuate during normal operation or LOCA.

The pressure distribution of a single S/RV along the longitudinal direction, as shown in Figure 1.3-2, and around meridional direction, as shown in Figure 1.3-3, is the same for all eleven valves; however, the maximum positive and negative pressure at torus bottom dead center and the frequency of the load is different for each valve and for various loading conditions. For example, the maximum positive pressure at torus bottom dead center due to a single S/RV at SBA is calculated to be as low as 14.4 psi (in excess to normal water and atmospheric pressure) for S/RV line number 27 and is as high as 16.5 psi for S/RV line number 34. For the other S/RV lines the pressure is between 14.4 and 16.5 psi. The maximum negative pressure at torus bottom dead center at SBA varies between 13.7 to 15.1 psi. The frequency of load for a single S/RV actuation at SBA varies between 6.7 to 7.7 Hz. for various S/RV lines.

The maximum positive and negative pressure of torus bottom dead center due to multiple S/RV actuation at normal and SBA conditions and due to single S/RV actuation at normal condition is generally lower than the values given above. The maximum positive pressure calculated for each single S/RV at SBA condition is used conservatively in lieu of positive and negative pressure at torus bottom dead center for single and multiple S/RV actuation in the present analysis. Table 1.3-1 shows Line number, maximum positive and negative pressure and frequency of each S/RV line at SBA, calculated using QBUBS program

given in Reference 1-6. The pressure distribution of a single S/RV actuation along longitudinal and meridional directions of torus shell are calculated using equations given in Reference 1-7.

The frequency of S/RV load, even with 40% increase as suggested in Reference 1-6, is around 11 Hz. It is far enough from frequencies of torus which start from 30 Hz., that no dynamic amplification is expected. Therefore S/RV load is treated as static load in the present analysis.

1.3.5 Quasi - Static Pressures

The LOCA-induced pressure transients of suppression chamber for DBA, IBA and SBA conditions are given in Reference 1-8. A modification to the maximum pressure in each case is given in Reference 1-9. Based on the information given in these references the pressure inside the torus reaches to its maximum value in 30 seconds in DBA, where the rise time is 560 seconds in IBA and 800 seconds in SBA. The minimum rise time of 30 seconds in DBA condition as compared to first natural period of torus which is about 0.03 second suggests that the internal pressure during LOCA may be treated as a static load. The maximum values of internal pressure for various loading conditions, used in the present analysis as static loads, are given in Table 1.3-2.

1.3.6 LOCA Temperatures

The LOCA-induced temperature transients of suppression chamber for DBA, IBA and SBA conditions are given in Reference 1-8. The maximum temperature in the torus during the pool swell phenomenon which occurs in the DBA condition is 90°F. The maximum torus temperature in other phases of DBA is 127°F. Temperature in torus may reach as high as 168°F in IBA and up to 140°F in SBA conditions. In the present study the torus is conservatively analyzed for three

inside temperatures of 100°F for pool swell, 140°F for SBA and other phases of DBA and 168°F for IBA condition. The inside temperature is assumed to change linearly to an outside temperature of 70°F.

1.3.7 Pool Swell Pressure

Pool swell and the loads associated with pool swell, applied to the torus shell, are given in detail in Section 4.3 of Reference 1-1. A typical average submerged torus pressure history and a typical torus airspace pressure history, given in this reference, show that the pressure inside the torus reaches about 32.5 psi in 1.4 seconds. This maximum pressure applies uniformly at the airspace and the submerged part of the torus 1.4 seconds after break initiation at DBA.

The pressure at the airspace and the submerged portion of torus is not the same at all instants of the pressure build up time (rise time). The effect is a maximum upward net pressure of approximately 7 psi at 0.5 second after the break. The resulting upward force is less than the combined weight of the suppression chamber and the pool water and does not produce any tension force at critical cross sections along meridional direction. The effect of this upward force is minimal compared with the tension produced by the uniform pressure of 32.5 psi at 1.4 seconds after break.

The time (1.4 seconds) required for the internal pressure to reach its maximum during pool swell as compared with torus breathing period (0.03 seconds) is large enough to give a dynamic load factor very close to unity. Therefore the pool swell load used in this analysis is assumed to be a uniform static pressure of 32.5 psi applied at the torus shell in addition to the quasi-static pressure of 11 psi given in Table 1.3-2.

1.3.8 Froth Impingement

The froth impingement load on the torus shell during the LOCA pool swell transient is relatively small and is neglected in torus analysis. Reference 1-1 gives description of froth formation

mechanisms and equations to calculate the corresponding load. The maximum calculated froth impingement load is 3.6 psi at the center of non-vent bay 12.5 ft. above torus center line; it then reduces to zero at the highest level of the torus shell. The load can be neglected compared to the high uniform pressure applied to the torus during pool swell phenomenon.

1.3.9 Condensation Oscillation Loads

Following the pool swell transient of a postulated LOCA, there is a period during which condensation oscillation occurs at the downcomer exit at DBA. Condensation oscillation phenomenon, associated with the pulsating movement of the steam-water interface caused by variations in condensation rate, produces an oscillatory pressure on the submerged portion of the torus shell. The pressure is maximum at torus shell bottom dead center and reduces linearly to zero at the pool water level.

The maximum pressure at torus shell bottom dead center, as given in Reference 1-1, is in terms of amplitude as a function of frequency range of 1 Hz. to 50 Hz. incremented by 1 Hz. The total pressure at torus shell bottom dead center at any time during condensation oscillation phenomenon may be written as:

$$P_{c.o.} = \Sigma_{n=1}^{50} A_n \text{ Cos } \omega_n t = \Sigma_{n=1}^{50} A_n \text{ Cos } 2\pi nt$$

where

$\Sigma_{n=1}^{50} |A_n| = 15.37$ psi is the maximum possible pressure at torus shell bottom dead center.

1.3.10 Chugging Loads

The chugging phenomenon, as described in Reference 1-1, occurs during a postulated Loss of Coolant Accident (LOCA) at SBA, IBA or DBA when the steam flow through the containment vent system falls below

the rate necessary to maintain steady condensation at the downcomer exits. Therefore steam bubbles form at the downcomer exits, oscillate or grow in size and collapse at a critical size. The resulting loads on the submerged portion of the torus shell consist of a pre-chugging load which is a low frequency oscillatory pressure associated with the oscillating bubbles as they grow, and a post-chugging load which is a high frequency oscillatory pressure associated with the collapsing bubbles.

1.3.10.1 Pre-Chugging Load

Pre-chugging produces a maximum pressure at torus bottom dead center equivalent to $\pm$ 2 psi. This pressure decreases linearly to zero along the wetted perimeter of torus in a vertical cross section. The circumferential distribution of pre-chugging load shall be either an asymmetric distribution as shown in Figure 1.3-4 or a symmetric uniform distribution of $\pm$ 2 psi at bottom dead center, whichever produces the maximum response. The frequencies of the pre-chugging load is in the range of 6.9 to 9.5 Hz. which is much lower than torus frequencies that starts from 30 Hz. Therefore, the oscillation of the pre-chugging load is neglected in the torus analysis.

1.3.10.2 Post-chugging Load

Post-chugging produces an oscillatory pressure on the wetted perimeter of the torus which has a maximum value at the bottom dead center and attenuates linearly to zero at the pool water level. The load is symmetric, having the same value and distribution at all vertical cross sections of the torus along the circumference. The post-chugging pressure at the torus bottom dead center, given in Reference 1-1, is written as:

$$P_{post\text{-}chug} = \sum_{n=1}^{50} B_n \cos 2\pi nt$$

where,

$\sum_{n=1}^{50} |B_n|$ = 3.7 psi is the maximum possible pressure at the torus bottom dead center.

1.3.11 Seismic Loads

A seismic analysis of combined stick models of drywell, torus and outer structure using response spectra method has previously been performed and are reported in References 1-11 and 1-12. The maximum horizontal acceleration at the top of the suppression chamber for SSE and OBE are conservatively calculated to be $\pm$ 0.32g and $\pm$ 0.23g respectively. The maximum vertical spectra acceleration for the OBE is found to be $\pm$ 0.1g and for the SSE $\pm$ 0.13g. In the present analysis these accelerations multiplied by torus mass are applied statically to the torus to calculate the forces and moments developed in the torus due to seismic loads. The horizontal seismic load is asymmetric and the vertical seismic load is symmetric with respect to the suppression chamber axis of revolution.

1.4 LOADING COMBINATIONS

Loading combinations are defined in Section 3 of the Load Definition Report (Reference 1-1) and are discussed in detail in Structural Acceptance Criteria (Reference 1-2). The twenty seven event combinations identified in Table 3.1 of Reference 1-1 and the additional load combination specified in Section 5.6.2 of the same reference actually represents sixty five load combinations which are considered in the present analysis. These sixty five load combina-

tions and the load factors used in combining the load components are given in Tables 1.4-1 and 1.4-2 respectively.

The static equivalents of dynamic loads are used in analysis of the torus as explained in Section 1.5. The total number of loading cases that is considered in combining the results of each individual load analysis is one hundred thirty cases in two sets of sixty five as follows:

Set 1, hereafter, is refered to as positive, is

Σ L.F * (static loads) + Σ L.F * |static equivalent of dynamic loads |

Set 2, hereafter, is referred to as negative, is

Σ L.F * (static loads) - L.F * |static equivalent of dynamic loads|

L.F is load factor which may be zero or nonzero as given in Table 1.4-2.

The forces and moments in the torus, calculated as given above, are conservative.

1.5 METHOD OF ANALYSIS

The loads applied to the suppression chamber, as discussed in Section 1.3, are categorized into two groups of static and dynamic loads. Dead load, normal and LOCA temperature, normal and LOCA internal pressure and pool swell are static loads. S/RV and pre-chugging are dynamic loads with dynamic load factors equal to unity (see Section 1.3). Condensation oscillation, post-chugging and seismic loads are dynamic loads with dynamic load factors greater than one.

The condensation oscillation and post-chugging are treated as static loads in the present analysis using fluid structure interaction factor of 1.13 and dynamic load factor of 1.5. The fluid structure

interaction factor is defined as the ratio of torus responses due to condensation oscillation loads considering the effect of the fluid in the torus to the torus responses due to the same loads neglecting the fluid. See Appendix A-1 for more detail. The fluid structure interaction and the dynamic load factors are obtained from a study performed to estimate the effect of interaction between the fluid and the suppression chamer on the overall response of the torus when subjected to condensation oscillation loads. It is assumed that the post-chugging load, which has distribution and variation similar to condensation oscillation loading, yields the same fluid structure interaction and dynamic load factors. Finite element technique using NASTRAN Program has been used to perform a frequency response dynamic analysis of the torus under oscillation loading and results are presented in Appendix A-1.

The earthquake loads are also applied to the torus as static loads using the amplified accelerations obtained from a response spectra dynamic analysis as discussed in Section 1.3.11.

Therefore, only static analysis of the suppression chamber is needed to calculate the stresses in the rebars and check the integrity of the structure under the applied forces. The finite element technique for the analysis of axisymmetric solids of revolution under symmetric and arbitrary static loading, as given in References 1-3 and 1-4, has been used to calculate the forces and moments developed in various cross sections of the torus. Hereafter, the finite element program for analysis of axisymmetric solid of revolution under symmetric loading is referred to as "WILSON I" Program and the finite element program for analysis of the same type of structure under symmetric and arbitrary loading is referred to as "WILSON II" Program.

WILSON I Program is used for analysis of torus under the following thermal loadings:

i. Inside temperature of 100°F, outside temperature of 70°F with temperature varies linearly through torus thickness.

ii. Inside temperature of 140°F, same as above.

iii. Inside temperature of 168°F, same as above.

The WILSON II Program is used for analysis of torus under the following symmetric and asymmetric loadings:

i. Dead load of the suppression chamber without the pool water, hereafter referred to as dead load (symmetric loading).

ii. Internal pressure of 1 psi, hereafter is referred to as unit uniform pressure (symmetric loading).

iii. Hydrostatic pressure distribution on the wetted perimeter of torus with maximum pressure of 1 psi at torus bottom dead center, hereafter referred to as unit hydrostatic pressure (symmetric loading).

iv. Horizontal earthquake load with a horizontal acceleration equal to one g, hereafter is referred to as unit horizontal earthquake (asymmetric loading).

v. Safety/relief valve load for a single S/RV as defined in Section 1.3.4 with a maximum pressure at the torus bottom dead center equal to 1 psi, hereafter referred to as unit S/RV (asymmetric loading).

The results of the above WILSON I and II analyses are the stresses in the centroid of the elements in the finite element model. These stresses are used to calculate forces and moments in various sections of the torus using a utility program (Force and Moment) to simplify hand calculations.

The forces and moments developed in various sections of torus due to the loads defined in Section 1.3 are then calculated as follows:

a) Dead Load Forces and Moments

Dead load forces and moments, defined in Section 1.3.1, is calculated as:

(Dead load forces and moments) + (static water pressure at bottom dead center) * (forces and moments due to unit hydrostatic pressure)

b) LOCA Pressure Forces and Moments

LOCA pressure forces and moments are calculated by multiplying the internal pressure in the torus as given in Section 1.3.5 for various cases of SBA, IBA or DBA, by forces and moments calculated due to unit uniform pressure.

c) Pool Swell Forces and Moments

Pool Swell forces and moments are calculated by multiplying the pool swell internal pressure (32.5 psi) by forces and moments calculated due to unit uniform pressure.

d) S/RV Load Forces and Moments

Forces and moments due to a single S/RV actuation is equal to forces and moments calculated for a single unit S/RV multiplied by the maximum S/RV pressure at torus bottom dead center due to S/RV actuation. For multiple S/RV actuation the total forces and moments for all locations at any vertical cross section along the torus circumference are calculated as follows:

When more than one valve actuate at the same time the effect of any valve is exactly the same as the other valves except for the fact that the same effect occurs at a different location along the torus circumference. Therefore, by proper summation of forces and moments calculated for a single S/RV for various vertical cross sections along circumference, the total forces and moments for multiple S/RV actuation are calculated for any combination of eleven safety/relief valves. The absolute valves of eleven S/RV effects are added to obtain the maximum conservative effect of multiple S/RV actuation. A utility program (S/RV Combination) is developed and used to simplify hand calculation.

e) Condensation Oscillation Forces and Moments

The forces and moments due to condensation oscillation load are calculated using the following:

$F_{cond.\ osci.} = \pm (P_{c.o.}) * (DLF) * (FSI) * (forces\ and\ moments\ due\ to\ unit\ hydrostatic\ pressure)$

where,

DLF and FSI are dynamic load factor and fluid structure interaction factor respectively; $P_{c.o.}$ is the maximum possible pressure at torus shell bottom dead center as given in Section 1.3.9.

f) Pre-chugging Forces and Moments

The forces and moments due to pre-chugging load is calculated as follows:

$F_{pre-chug} = \pm (P_{pre-chug}) * (FSI) * (F)$

where,

$P_{pre-chug}$ is the maximum possible pressure at torus bottom dead center for pre-chugging as given in Section 1.3.10.1; and F is defined as:

F = Maximum of (unit hydrostatic forces and moments and unit S/RV forces and moments)

The unit S/RV forces and moments are assumed to be approximately the same as unit pre-chugging forces and moments developed by asymmetric pre-chugging load.

g) Post-chugging Forces and Moments

The forces and moments due to post-chugging load are calculated using the following:

$F_{post-chug} = \pm (P_{post-chug}) * (FSI) * (DLF) * (forces\ and\ moments\ due\ to\ unit\ hydrostatic\ pressure)$

where

$P_{post-chug}$ is the maximum possible pressure at torus bottom dead center for post chugging load as given in Section 1.3.10.2.

h) Earthquake Load Forces and Moments

The earthquake load forces and moments are calculated using the following equation:

$$F_{EQ} = \pm \sqrt{F_{EQV}^2 + F_{EQH}^2}$$

where

F_{EQV} and F_{EQH} are forces and moments due to vertical and horizontal earthquake respectively calculated as follows:

$F_{EQV} = \alpha$ * (dead load forces and moments)

$F_{EQH} = \alpha$ * (unit horizontal earthquake forces and moments)

Values of α, for OBE and SSE cases of horizontal and vertical earthquake, are given in Section 1.3.11.

1.6 FINITE ELEMENT IDEALIZATION

The suppression chamber is approximated as an axisymmetric solid of revolution. A vertical cross section of the chamber, as shown in Figures 1.2-2, 1.6-1 and 1.6-2, is discretized into 602 triangular, quadrilateral and truncated cone shell elements. Each element in the vertical cross section of the structure actually represents an axisymmetric ring with triangular, quadrilateral or line cross section.

The global coordinate system R-Z-T, in which the coordinates of nodes are specified, and the local coordinates system N-S-T, in which the material properties of the elements are defined, are shown in Figure 1.2-2. S is in the meridional direction (local hoop) and T is in the global hoop direction. Material coordinate systems of the shell elements are assumed to be coincident with the meridional axis of the shell elements.

The concrete portion of the suppression chamber is idealized as triangular and quadrilateral elements. There are a total of 410 quadrilateral and triangular elements with 439 nodes. Figure 1.6-1

shows the computer plot of the concrete portion of the model. The visual check of the model insures that the geometric data used in analysis is correct.

The liner, which is a series of sixteen interconnected cylinders along the circumference of suppression chamber, is idealized as a pure circular torus of isotropic steel with a constant thickness of 3/8". Truncated conical shell elements are used to model the liner.

The hoop and meridional reinforcing bars are idealized as independent layers of truncated cone shell elements of toroidal shape. The hoop reinforcing bars are modelled as fourty eight shell elements having a thickness of 0.2 in. with stiffness property only in the hoop direction. The meridional reinforcing bars are modelled as fourty eight shell elements having a thickness of 0.37 in. with stiffness property only in the meridional direction.

The seismic bars on top of the torus are also modeled as two independent layers of shell elements, having a thickness of 0.04 in. with stiffness properties only in their respective global hoop and radial directions. The seismic bars on the sides of the torus, which consist of two reinforcing bars perpendicular to each other and running at 45° with respect to global Z axis, are modeled as one layer of twenty four shell elements with a thickness of 0.084 inch having stiffness in both hoop and meridional directions.

Total number of shell elements used in modeling the reinforcing bars and liner is 192. Figure 1.6-2 shows the finite element model of the liner and the reinforcing bars.

It should be noted that the actual reinforcement in the torus is not uniform. The meridional reinforcing rings are closer to each other in the inside radius of torus than the outside, resulting in a non-uniform distribution of reinforcing bars in the meridional direction. Also, there are more hoop reinforcing bars above and below vent openings than in the other areas of the torus vertical cross section. To simplify the modeling, an average reinforcement area is used in

calculating the equivalent thickness of the shell elements in the hoop and meridional directions. It can be shown that a reasonable change in reinforcing bars does not change the forces and moments in various section of torus drastically. The controlling load applied to the torus is internal pressure that induces forces and moments which are not significantly affected by reinforcing in the torus. However, the final stresses in the reinforcing bars are calculated using forces and moments obtained from the finite element analysis and the actual area of reinforcing bars at each section of the torus.

1.7 MATERIAL PROPERTIES

The stress strain relationships used in the analysis are based on the following material properties:

a) Concrete: (uncracked)

Isotropic

$E = 3{,}000{,}000.$ psi

$\nu = 0.15$

b) Concrete: (cracked)

Orthotropic

$E_N = 3{,}000{,}000.$ psi

$E_S = E_T = 0.0$ psi

$\nu = 0.0$

$G = 1{,}304{,}348.0$ psi

c) Liner

Isotropic

$E = 30{,}000{,}000.$ psi

$\nu = 0.3$

d) Hoop Reinforcing

Orthotropic

$E_N = E_S = 0.0$ $E_T = 30{,}000{,}000.$ psi

$\nu = 0.0$

$G = 0.0$

e) Meridional Reinforcing

Orthotropic

$E_N = E_T = 0.0$

$E_S = 30{,}000{,}000.$ psi

$\nu = 0.0$

$G = 0.0$

f) Seismic Rebars

$E_N = 0.0$ $E_S = E_T = 30{,}000{,}000.$ psi

$\nu = 0.0$

$G = 0.0$

E is modulus of elasticity, ν poisson's ratio, G shear modulus and N-S-T is the local material coordinate system shown in Figure 1.2-2.

Coefficients of thermal expansion used in the analysis are as follows:

α for concrete = 0.0000055 /F°

α for liner = 0.0000065 /F°

1.8 FINITE ELEMENT ANALYSIS OF SUPPRESSION CHAMBER

The finite element analysis is performed for temperature loads, dead load, unit uniform pressure, unit hydrostatic pressure, unit S/RV load and unit horizontal earthquake using the method of Section 1.5. The assumptions made, the computer runs and the results of these analyses are given below.

Two separate computer runs are made for each load component given above. In the first runs the concrete elements are assumed to be uncracked. The results are used in loading combinations 1, 2, 3, 64 and 65, where internal pressure is not included in the loadings. In the second runs the concrete elements are assumed to be fully cracked in the circumferential (T) and in the meridional (S) directions. The latter assumption is especially valid for all the other sixty loading combinations where internal pressure produces high tensile stresses in the concrete. The assumption of cracked torus, although a good approximation for the analysis, is not exact. The applied pressure does not develop crack close to the boundaries

(bottom of torus and especially bottom corner adjacent to the drywell) due to frictional resistance and the key between the torus and the drywell. The liner is assumed to contribute to the stiffness of the structure in all the finite element computer runs.

The stresses calculated in these analyses are given in the global R-Z-T coordinate system. Stresses are transformed to local N-S-T coordinate system and are integrated using a utility program to calculate normal forces, shear forces and moments at locations 1 to 8 along meridional direction shown in Figure 1.8-1. For asymmetric loads of S/RV and earthquake, stresses and subsequently forces and moments are calculated for locations 1 to 8 along meridional direction for nine vertical cross sections of the suppression chamber along circumferential direction of the torus shown in Figure 1.8-2.

The forces and moments calculated at each section are as follows: (Note that the notations used here for forces and moments are different from the notations normally used in shell analysis.)

F_S: Normal force in meridional direction per unit length in T-direction; positive force produces tension in section.

M_T: Moment related to F_S, calculated with respect to the center of area of the cross section. Positive moment produces tension in the liner.

F_T: Normal force in circumferential direction (global hoop) per unit length in S-direction; positive force produces tension in section.

M_S: Moment related to F_T, calculated with respect to the center of area of the cross section. Positive moment produces tension in the liner.

F_{NS}: Shear force in the direction of N on the plane whose normal is S (S-plane) per unit length in T-direction. (Radial shear S)

F_{NT}: Shear force in the direction of N on the plane whose normal is T (T-plane) per unit length in S-direction. (Radial shear T)

F_{ST}: Shear force in the direction of S on the plane whose normal is T (T-plane) per unit length of T or S direction. (Tangential shear)

Figure 1.8-3 shows a cross section of the torus and directions of the forces and moments.

Boundary conditions and other assumptions made in finite element analysis of each of the six load components of the load combinations, mentioned in Section 1.5 and above, are given in the following sections.

1.8.1 Temperature Analysis

WILSON I Program is used for analysis of suppression chamber under three different inside temperatures of 100°F, 140°F and 168°F. The outside temperature is kept at 70°F and the temperature is assumed to decrease linearly through the thickness of the suppression chamber. The base of the structure is allowed to move freely in the radial direction (global R axis) and is restrained in the Z direction.

Temperature analysis is performed for cracked and uncracked concrete. The properties of the cracked concrete are given in Section 1.7. Since temperature rise inside the torus produces high compressive stress in the liner side and high tensile stress in the concrete elements close to the outside face of the torus, concrete can not be assumed to be uncracked in the absence of internal pressure. Therefore, the torus is assumed to crack partially for the loading cases where temperature is included but internal pressure does not exist (cases 2, 3, 64 and 65). In lieu of a cracking analysis to find the correct cracking pattern for thermal loadings, the modulus of elasticity of the concrete is assumed to be approximately 1/3 of the values given in Section 1.7 for uncracked concrete.

Forces and moments are calculated for fully cracked and partially cracked torus due to thermal loadings. The forces and moments are calculated once including the liner force and in another case excluding the liner force in integration. Table 1.8-1 shows the forces and moments for the eight locations of a vertical cross section of the torus for inside temperature of 100°F, 140°F and 168°F assuming concrete is partially cracked. Table 1.8-2 shows the same forces and

moments for fully cracked concrete. The forces and moments are shown with and without the liner effect.

1.8.2 Dead Load, Unit Internal Pressure and Unit Hydrostatic Pressure Analyses

WILSON II Program is used for dead load, unit internal pressure and unit hydrostatic pressure analyses. The base of the structure is allowed to move freely in R direction and is restrained in Z direction. Concrete is assumed to be fully cracked in local S and T directions. Concrete is assumed to be uncracked in another set of analyses. Material properties for these two cases are given in Section 1.7. Table 1.8-3 shows forces and moments calculated for dead load for two cases of cracked and uncracked concrete. Table 1.8-4 shows forces and moments for unit hydrostatic analysis and Table 1.8-5 shows forces and moments for unit internal pressure analysis.

1.8.3 Unit S/RV Analysis

S/RV load is an asymmetric non self-balanced load which is applied to the torus shell. To prevent the rigid body motion of the structure, due to this asymmetric load, the inner corner of the structure at the base (node 439) is restrained in the R direction. WILSON II and a utility program is used to calculate forces and moments for various locations along meridional direction for nine vertical cross sections of the torus along circumferential direction. The maximum of all the forces and moments along circumferential direction (T) is used in loading combinations. Table 1.8-6 shows the forces and moments for unit S/RV analysis.

1.8.4 Unit Horizontal Earthquake Analysis

WILSON II Program is used for analysis of suppression chamber under unit horizontal earthquake load. Due to the nature of the load, which is asymmetric and non self-balanced, the torus tends to move in the direction of the applied loads unless it is restrained in R or T

direction. The suppression chamber is keyed to the drywell pedestal and thus does not move freely due to horizontal earthquake. The actual boundary condition is complicated and can not be modelled in two dimensional finite element analysis. In lieu of a three dimensional complex finite element analysis, the analysis is performed for two different boundary conditions as follows:

i. The inner bottom corner of the model (node 439) is restrained in the R direction, and the base is restrained in the Z direction. The results from this analysis are justified for shear forces F_{TZ} in global coordinates (F_{ST} in local) at vertical section 5 along circumferential direction (Figure 1.8-2), where this component of shear has the maximum value along the torus circumference. Vertical section 5 is free to move in the direction of applied load under this boundary condition. The shear force F_{ZR} in global coordinate (F_{NS} in local) obtained from this analysis is not accurate. This component of shear is maximum at vertical section 1. This section, in reality, tends to move in the direction of applied load, but is restrained from moving in this analysis.

ii. The inner bottom corner of the model (node 439) is restrained from moving in the circumferential (T) direction. The nodes on the base restrained in the Z direction. The results from this analysis is justified for shear force F_{NS} and for forces and moments F_S, M_T, and M_S which are maximum at vertical section 1. This section is free to move radially but does not tend to move in the T direction due to the symmetry of the applied load with respect to axis $\theta = 0.0$ (Figure 1.8-2).

The forces and moments due to unit horizontal earthquake are taken from the two preceeding analyses and are used in the loading combinations. The shear forces F_{NT} and F_{ST} at vertical section 5 are taken from the first analysis and the forces and moments F_S, F_T, F_{NS}, M_T and M_S are taken from the second analysis. The approach, if not

exactly representing the actual boundary condition, is conservative and eliminates a need for a three dimensional complex finite element analysis. Table 1.8-7 shows the forces and moments for unit horizontal earthquake for the two preceeding boundary conditions assuming concrete is fully cracked in T and S directions.

1.9 LOAD COMBINATION ANALYSIS

Forces and moments for each component of loads applied to the torus are calculated using the procedure given in Section 1.5. Then they are combined according to the load factors given in Table 1.4-2. Two sets of "positive" and "negative" forces and moments as defined in Section 1.4 are calculated for each of the eight locations along the meridional direction for all the sixty five loading cases given in Table 1.4-1. Table 1.9-1 shows a typical force and moment calculated for meridional location 1 for all the loading cases assuming concrete is cracked in meridional and circumferential directions. Internal pressure is not included in load cases 1, 2, 3, 64 and 65, thus concrete can not be assumed to be cracked. As a result forces and moments for these cases given in Table 1.9-1 are not valid. Table 1.9-2 shows a typical forces and moments for these cases assuming concrete is uncracked. A utility program called Load Combination Program is developed and used to simplify hand calculation and obtain the forces and moments for various load cases.

1.9.1 Shear Stress Calculation

The average radial shear stresses on plane S and T and the average tangential shear stress in the concrete are calculated for various meridional sections for all the loading cases using shear resultants F_{NS}, F_{NT} and F_{ST} respectively. The allowable radial and tangential shear stresses in concrete are also calculated for all the sections and loading cases using equations given in ASME Section III, Division 2, Subsections CC-3421.4 and CC-3421.5. Actual reinforcement

areas at each cross section are used in calculating allowable shear stresses of concrete. Factors of safety for all shearing stresses are then calculated. Table 1.9-3 shows typical allowable shear stresses, average shear stresses and factors of safety calculated for location 1 of the meridional sections assuming concrete is cracked in meridional and circumferential directions.

The factors of safety for shearing stresses are generally greater than one with the exception of the tangential shear stresses in meridional locations 5 and 6 for cracked concrete. These results suggest that the concrete alone is capable of resisting all the shearing forces at all the sections except for locations 5 and 6. However, seismic reinforcing bars are provided at location 5 which carry the tangential shearing forces developed due to earthquake. No reinforcing bar is provided at meridional location 6 to resist the tangential shearing forces. However, the high shearing force in this section which is due to seismic loads is developed in the section because of the very approximate conservative approach discussed in Sections 1.8 and 1.8.4 with concrete fully cracked. With partially cracked concrete, to account for the effect of boundaries, tangential shearing forces decrease drastically, resulting in smaller shear stresses in the concrete. Furthermore, if one assumes that the horizontal seismic loads are taken by a ring action of the suppression chamber, as may be the case (Figure 1.9-1), earthquake does not develop shearing forces in concrete but increases the stress in the hoop reinforcing bars by approximately 10 ksi. Note that the maximum possible hoop stress in the reinforcing bars, given in section 1.9.2, is not affected by this new approach; because seismic load is not a component of the loading case which induces the maximum hoop stress in the reinforcing bars.

1.9.2 Normal Stress Calculation

Stresses in the meridional bars (S-Stress) and global hoop bars (T-Stress) are calculated for all the loading cases and at all

the meridional locations shown in Figure 1.8-1. These stresses are calculated for the following conditions.

i. Thermal loadings are neglected in loading combinations; only mechanical loads included.

ii. Thermal loading included in loading combinations; but effect of liner is neglected in force and moment calculation of thermal loading.

iii. Thermal loading included in loading combinations; effect of liner is also included in force and moment calculation of thermal loading.

The stresses in the rebars for case (i) are calculated for two conditions; using liner as a strength element and neglecting the liner as a strength element.

The stresses are calculated for case (ii) assuming that all forces are to be taken by reinforcing bars only. The stresses are calculated for case (iii) assuming forces and moments are to be taken by the liner and reinforcing bars together.

Actual area of the reinforcing bars at each section are used in normal stress calculation. Coupling between the shearing forces and normal forces are neglected. Concrete is considered to be fully cracked and not capable of resisting any axial forces. A typical result of stress calculations are given in Table 1.9-4. In this table concrete is assumed to be cracked for all loading cases.

Normal stresses are calculated in the rebars and also in the seismic bars considering the coupling between the shearing and normal forces for a few loading cases and sections where tangential shearing forces are considerable (Reference 1-14). Compressive stresses are also calculated in the concrete where the applied moments at the section are big enough to develop such stresses even though the section is under normal axial tensile forces. This condition arises when thermal loading is included in loading combinations.

Maximum mechanical stress in the meridional bars is 26.14 ksi, occurring at location 7 for loading case 27 with the liner having no

stiffness. Maximum mechanical stress in the hoop bars is 30.13 ksi, occurring at location 1 for loading case 40 neglecting liner. The mechanical stresses in meridional and hoop bars decrease to 9.04 ksi and 11.59 ksi respectively if liner is included in carrying section loads. In this case the stress in the liner in meridional direction is 19.45 ksi and in hoop direction is 9.27 ksi; the maximum meridional bar stress, including liner, is 10.51 ksi and maximum hoop bar stress in 15.62 ksi. The maximum meridional stress in the liner is 19.45 ksi and maximum hoop stress in the liner is 10.85 ksi. Note that these maxima do not necessarily occur at the same locations and the same loading conditions as the case where liner is neglected. The maximum stresses in the reinforcing bars and in the liner are below the yield stresses of bars (F_y = 50 ksi) and of liner (F_y = 28 ksi) respectively.

Maximum stress in the meridional bars when thermal loading is included but liner is neglected (liner is included in finite element analysis and force and moment calculation but is neglected in stress calculation) is 32.59 ksi which occurs at location 7 for loading case 27. Maximum stress in the hoop bars for the same condition is 44.48 ksi which occurs at location 1 for loading case 27. If the liner is also used as load carrying member, the maximum stress in meridional bars decreases to 19.34 ksi and the maximum stress in hoop bars decreases to 38.55 ksi. Note that these new maxima do not necessarily occur at the same locations as given above. When thermal loading is included, if one assumes that concrete does not take any compressive force, the maximum compressive stress in the liner is 10.66 ksi. The maximum compressive stress in the concrete (assuming liner is neglected) is less than 1.0 ksi under both thermal and mechanical loadings. Table 1.9-5 shows a summary of the maximum stresses in the torus for various conditions given above.

1.10 LARGE OPENING ANALYSIS

The suppression chamber has eight symmetrically located vent openings with 7'-1" diameter, each corresponding to the vent openings in the drywell. The main hoop reinforcing bars which would normally occur in the openings are banded above and below the openings. The meridional bars which would normally occur at these locations are grouped on either side. The vents are locally reinforced by closed rings around the perimeters of each opening. Reinforcing for areas left void by banding the main hoop and meridional reinforcing is provided by fill steel. Radial stirrups are provided around each vent opening to accomodate the radial shears due to the presence of the openings. Figure 1.10-1 shows the reinforcings around the suppression chamber vent openings.

The smallest thickness of the suppression chamber concrete wall in the vicinity of the vent opening is approximately 37 inches. It is a common practice to consider openings whose diameters are less than 2.5 times the wall thickness as small openings (Reference 1-15, Volume I). The ratio of vent opening diameter to 2.5 times the wall thickness is approximately 0.92. This ratio is less than one and the openings could be regarded as small; however, to be conservative, the vent openings are considered to be large enough to merit a more detailed analysis to calculate the stresses in the liner and the reinforcing bars.

A finite element method was previously used for three dimensional analysis of drywell and suppression chamber including the vent openings (Reference 1-15, Volume I). Due to the geometric symmetry of the structure, a representative 45° sector was chosen for the analysis. A composite mesh of interconnected laminated triangular plate elements was used to discretize the 45° section of the suppression chamber. Each triangular element was a composite of independent layers of concrete and reinforcing bars. The closed hoop rings provided around each large opening were idealized as general line elements. Symmetric boundary conditions were applied along the

22.5° and -22.5° vertical edge of the sector. The loading combinations used in that analysis included internal pressure, thermal, dead and seismic loadings. No hydrodynamic loads were used.

The results of the above analysis are given in Volume II of Reference 1-15 in a series of stress plots around the vent openings. Another two dimensional analysis, neglecting vent openings, had also been performed; the result of which are reported in Reference 1-16. Table 1.10-1 shows the stresses available for two load cases obtained from the analyses of References 1-15 and 1-16. The percentage increases in stresses for reinforcing bars and the liner including the vent openings are also shown in Table 1.10-1. From this table it can conservatively be concluded that the meridional bar stress close to the opening increases by 20%, the hoop bar stress by 75%, the meridional liner stress by 40% and the hoop liner stress by 55% due to vent openings.

As mentioned above the hydrodynamic loads had not been included in the preceding analysis. However, the effect of the hydrodynamic loads on the stresses in the vicinity of the vent opening is minimal compared to the effect of other loads, particularly the internal pressure, in the various load combinations. Table 1.10-2 shows the hydrodynamic stresses for sixty five load cases for locations 4 and 5 as obtained from the present analysis neglecting the opening. Note that the thermal, dead load, seismic and internal pressure are omitted from the load combinations. As seen the stresses (maximum 3.23 ksi) induced from hydrodynamic loadings in the locations close to the opening (locations 4 and 5) are negligible compared to the maximum stresses in the liner and reinforcings. Therefore, it can be concluded that the percentage increases in the liner and rebar stresses due to the vent openings obtained from the previously performed analysis, neglecting the hydrodynamic loads is not going to be affected by the hydrodynamic loads.

Therefore, to calculate the stresses in the liner and rebars in the vicinity of the openings, the stresses calculated in the present analysis neglecting the vent openings, can be multiplied by the percentage increase given in Table 1.10-3.

Table 1.10-4 shows the maximum possible liner and reinforcing stresses calculated in the present analysis, neglecting vent openings, for locations 4 and 5. It also shows the same stresses increased by the factors given in Table 1.10-3 to obtain a measure for rebar and liner stresses including the effect of the vent openings. As seen all the resulting stresses are below the allowable stresses of 0.9 F_y for liner and reinforcings. The stresses far from the openings are not affected due to the vent openings in the suppression chamber.

1.11 LINER ANCHOR ANALYSIS

The liner in the suppression chamber is a continuous sixteen sided steel plate of circular cross section with a uniform thickness of 3/8". It is attached to the concrete by 1/2" diameter, 8½" long Nelson studs spaced at 15" in the meridional and hoop directions. The distance between rows or columns of studs in these directions is 7.5" and the spacing of the studs on the 45° line from meridional or hoop direction is approximately 10.6". Figure 1.11-1 shows the stud arrangements on the liner plates.

The liner plate can experience compressive stresses due to temperature rise and/or dynamic and static loads applied to the suppression chamber. The main source of compressive stresses in the liner is temperature rise. Non-uniformity of the compressive stresses throughout the circumference of the liner shell and possible initial deflection of liner between two studs can produce unbalanced forces on studs, buckling of the liner plate between the studs and displacement of the studs in the vicinity of the buckled panel. The liner stud analysis performed for the suppression chamber to calculate the stud deformation and the strain in the liner are given in the following.

The maximum compressive stress in the liner for fully cracked concrete, as obtained from the analysis described in Section 1.8 for sixty five different load combinations, in 10.66 ksi. The maximum compressive stress in the liner for uncracked concrete (see Section 1.8-1 for assumption made in thermal analysis) is 19.5 ksi. Although the torus is not uncracked it is conservatively assumed that the maximum possible compressive stress in the liner is equal to 19.5 ksi. This maximum compressive stress in the liner is referred to as "initial stress in the liner" before buckling of any panel in liner anchor analysis.

To perform the liner anchor analysis, four mathematical models are constructed to a one inch strip of the liner. The studs are modelled as springs with a predefined load displacement curve as given in Reference 1-17 and shown in Figure 1.11-2. The ultimate displacements of the studs is approximately 0.167 inches. The curve is obtained from a shear test performed on studs embedded in concrete. Figure 1.11-3 shows a typical mathematical model of the liner stud system. The panel located at the center of the model buckles due to an initial assumed maximum deflection Δ_o equal to 1/8". The initial and final buckled shape of the panel together with the geometry of the straight and buckled panels for various models used in the analysis are shown in Figure 1.11-3. The length of the buckled panel in two of the models are increased by 100% to account for a missing anchor condition as required by Article CC-3123 of ASME Section III, Division 2.

The stiffness of the buckled panel in the model is small compared to the stiffness of the straight panels. The buckled panel resists load in bending as compared to the straight panels which resist load by axial deformation. Figure 1.11-4 shows the load displacement curve, defining the stiffness of the buckled panel obtained using the procedure given in Reference 1-13.

The detailed procedure for calculation of the stud deformation using the liner-stud model is given in Reference 1-13. The method is an

iterative technique to solve a system of nonlinear equations obtained from equilibrium of each node in the model. A program called LADT (Liner Anchorage Displacement due to Temperature) is developed and used to simplify the hand calculations. The total inital compressive stress in the liner is assumed to be the result from a thermal load and to be constant in all panels of the model prior to buckling. After buckling occurs, the stress in the panels decreases due to deformation of the studs toward the buckled panel. The deflections of the studs far from the buckled panel are assumed to be zero and are input as boundary condition to the mathematical model.

The output from the LADT Program is the maximum displacement of studs and the final compressive stresses in the panels. Having the displacements at both ends of the buckled panel, together with the assumed final buckled shape, the maximum outward displacement of the buckled panel and the average strain at the straight and buckled panel are calculated and shown in Tables 1.11-1 and 1.11-2. The allowable stud displacement and the allowable strains in the liner as given in Articles CC-3730 and CC-3720 of ASME III, Division 2 are also given in the same tables. The maximum stud displacements obtained from the analysis and the calculated average strain in the buckled panel are smaller that the allowables.

1.12 CONCENTRATED LOAD ON THE TORUS

At approximately 0.6 second after pool swell initiation an upward pressure on the downcomers and vent headers in the torus tends to move the headers upward. To prevent the upward displacement, the vent headers are connected to the suppression chamber inner surface at the top of the vent headers by columns. The load applied to the torus through these columns at each of the eight locations of the vent headers is approximately 342 kips considering the dynamic load factor due to the nature of the load. To prevent excessive shear and normal stresses in the torus, each of these loads are distributed along the

torus circumference (Global hoop direction) using four columns at each vent header as shown in Figure 1.12-1. A 12" by 12" plate is used to transfer the load from each column to the torus. At each vent header two of the four columns carry 102 kips per column and the other two columns carry 69 kips per column.

In addition to the concentrated load applied to the torus during pool swell, dead load, hydrostatic load, earthquake loads, S/RV, Quasi-static pressure and pool swell pressure are also applied to the torus at the same time. The Quasi-static pressure at 0.6 second after DBA break is 4 psi and the torus air pressure due to pool swell is about 12 psi. The loading combination during pool swell (cases 40, 44, 48, 49, 56 and 57) are given in Table 1.4-1.

To calculate the stresses in the torus at t = 0.6 second after DBA break, forces and moments at various sections of the torus are calculated for load cases mentioned above and are added to the forces and moments induced in the torus due to the concentrated loads. The forces and moments due to the loads other than concentrated loads are calculated using the procedure described in Section 1.5. The forces and moments due to concentrated loads are calculated as given below.

The load due to each vent header is applied at four points, two along the meridional and two along the circumference of the torus. The spacing between the points is approximately 5.5 ft. in meridional and 7'-8" in circumferenctial directions. The headers are equally spaced and are located at eight different locations of torus circumference. The applied loads to the torus are mainly taken by the rigidity of the torus in the radial direction. Therefore it can be concluded that an axisymmetric analysis of the torus due to a concentrated axisymmetric load of 37 kip/ft (maximum load of each pair of column divided by minimum spacing of columns) applied at node 1 of the finite element model in Figure 1.6-1 gives stresses and displacements which are close enough to the results of an asymmetric analysis of the torus.

Two axisymmetric analyses of the torus for cracked and uncracked concrete were performed for a load of 1000 lb/in applied at node 1. Forces and moments were calculated and scaled up to obtain the response for 37 kip/ft. Then the results of these analyses were added to the forces and moments for six pool swell cases. Then the stresses (normal and shear) were obtained and compared to the allowables. All the stresses including those close to the vent opening and close to the applied load are smaller than the allowables.

1.13 SUMMARY OF SUPPRESSION CHAMBER ANALYSIS

The objective of the suppression chamber analysis was to calculate the maximum possible stresses in concrete, reinforcing bars and the liner. To achieve the objective, a series of analyses as outlined in Sections 1.9.1, 1.9.2, 1.10, 1.11 and 1.12 were performed to consider all ranges of loading possibilites.

The calculated shear stresses are normally less than the allowable specified shear stresses of the concrete. The high tangential shear force in location 5 along meridional is resisted by seismic bars in the section.

The mechanical stresses in the hoop and meridional reinforcing bars are much smaller than the allowable stress of 0.9 F_y = 45 ksi. The maximum stress in the meridional bars including the thermal loading is also much smaller than 45 ksi. The maximum hoop stress in the bars including the thermal loading is close to the allowable if liner is not included in the stress calculation. If the liner is included in the stress calculation the comparable maximum hoop bar stress reduces to 30 ksi.

With the liner having no load carrying capacity, the total mechanical and thermal stresses in reinforcing bars, which are at some cases close to allowable stresses (about 35 ksi), are not realistic. In these cases the high thermal loadings are accompanied by high internal pressure during IBA. If liner is included in calculating

stresses, the reinforcing bar stresses decrease to far below the allowable; the resulting stresses in the liner are either in low compression (-8 ksi) or in low tension (7 ksi). The stresses in liner for some other loading cases, where moments are high in the sections, are higher than these values but do not correspond to the maximum stresses in the reinforcing bars. The liner is capable of resisting low stresses given above. Note that according to ASME Section III, Division 2 the stresses in the reinforcing bars may exceed the yield when the effects of thermal gradients through the concrete section are included.

It was found that the controlling loading cases which induces the highest stresses in the reinforcing bars are those with high internal pressure. Therefore the effect of other loads such as S/RV, chugging, condensation oscillation and so on is not much on the design stresses.

To study the effect of dynamic loadings on the final stresses, the dynamic load factor and the fluid structure interaction factor was increased by 100%, the S/RV loads were also increased by 100%. As the result, the stresses in the reinforcing bars generally were increased between 0.0 to 40%. Obviously, the stress for the loading cases that do not include hydrodynamic loads did not change. Also the maximum mechanical hoop reinforcing bar stress did not change. The maximum hoop reinforcing bar stress, with thermal loading included in the stress calculations changed 9.2% to 48.58 ksi; the corresponding meridional stress changed 38% to 45.06 ksi. The maximum tensile stresses in the liner, when used as a strength element, changed up to 38% to a maximum of 26.44 ksi. The maximum compressive strength in the liner increased 38% to a maximum of -14.66 ksi. The change in stresses of the liner and reinforcing bars for most of the loading cases were between 0.0 to 10%.

The stresses in the vicinity of the large openings were also calculated. The stresses due to concentrated loads applied to the top of the torus were calculated and added to the stresses due to the

other loads. The resulting stresses were checked against the allowables. The liner anchor analysis were also performed. The maximum anchore displacement and the liner strains were obtained and compared with the allowables. The stresses, strain and deformations in the suppression chamber were all below the allowables.

APPENDIX A.1

SUPPRESSION CHAMBER ANALYSIS-FLUID STRUCTURE INTERACTION

A.1.1 INTRODUCTION

The primary containment structure of the Brunswick Steam Electric Plant consists of the drywell and the pressure suppression chamber. See Figure 1.2-1. The suppression chamber is a reinforced concrete torus encircling the lower part of the drywell containment structure. The concrete envelopes a continuous sixteen sided steel liner of circular cross section. The major centerline diameter of the torus is 109'-0". The cross section diameter of the circular liner is 29'-0". Maximum water level in the torus is 2'-4" below the horizontal diameter of the torus. A paper joint is provided between the bottom of the torus and the mat foundation to allow the radial growth of the torus. Figure A.1-1 shows the typical cross section of the torus.

Recent studies (References 1-18, 1-19, 1-20 and 1-21) have demonstrated that the interaction between the fluid and the structure can have a significant influence on the response of the overall system when subject to certain dynamic loadings. This observation is true when mass of the fluid comprises the major part of the total system mass. In the concrete torus, concrete mass is approximately four times that of fluid mass. The concrete torus has a continuous support at the bottom mat whereas the steel torus in other Mark I plants is supported with pairs of columns or saddles.

The present study has been performed to investigate the effect of fluid structure interaction (FSI) on the dynamic response of the Brunswick concrete torus. A normal mode and a frequency response analysis of the torus for Condensation Oscillation (CO) loadings was performed.

Also in this study the dynamic load factor (DLF), the ratio of stresses calculated for condensation oscillation loads applied to the torus shell without FSI to stresses calculated for the same loads applied to the torus shell statically, are obtained. Two types of support conditions have been considered in the analysis to bound the solution:

Type I Support Condition: Both radial, U_r, and vertical, U_z, translations restrained.

Type II Support Condition: Only vertical translation, U_z, restrained.

The concrete in the torus has been assumed to be uncracked. The analysis has been done with the computer program NASTRAN. Results of this analysis is presented in this report.

Frequency response analysis gives displacements and stresses which are complex having real and imaginary parts or amplitudes and phase angles. Phase angles do not remain constant but vary from node to node. The sum of all the absolute amplitudes (1 to 50 Hz.) of stress/displacement has conservatively been used as an index to measure the effect of FSI.

A.1.2 CONCLUSIONS

Based on the present study, the following can be concluded about the effect of FSI on the Brunswick concrete torus on the normal modes and dynamic response under CO loading.

A.1.2.1 Normal Modes

With FSI, frequencies of normal modes decrease. The reduction in frequencies of normal modes in the range of 1 to 50 Hz. for type I support, where no radial growth at base is permitted, is only 0.2%. The reduction for type II support, where radial growth is permitted at base, is 3.5% with FSI. Modes shapes are not affected with inclusion of FSI. See Figures A.1-12 to A.1-18.

A.1.2.2 Hydrodynamic Pressure

The Load Definition Report (LDR) for Mark I program gives the baseline rigid wall pressure amplitude on torus bottom dead center (Table A.1-2). These amplitudes of pressures get modified due to FSI depending on the stiffness of the structure and fluid/structure mass ratio.

The sum of all the amplitudes of rigid wall pressure (1 to 50 Hz.) is 15.25 psi without FSI. With FSI, the value increases to a maximum of 15.347 psi and 15.443 psi for Type I and Type II support, respectively. Due to FSI, the change in the rigid wall pressure is 1.3%.

A.1.2.3 Displacement

In general, displacements increase due to FSI.

Radial Displacements: From Tables A.1-5 and A.1-6, it can be seen that the maximum change in the radial displacement is 4.2% and 11.4% for Type I and Type II support respectively.

Tangential Displacements: From Tables A.1-5 and A.1-6, it can be seen that the maximum change in the tangential displacement is 4.9% and 9% for Type I and Type II support respectively.

It can be concluded that in the concrete torus, displacements will change in the order of 10% due to FSI. It is then recommended that the concrete torus be analyzed for CO loading without FSI and fluid mass and the displacements so obtained be increased 10% to account for the FSI.

A.1.2.4 State of Stress

In general, stress levels increase due to FSI. Tables A.1-7 to A.1-9 show that the maximum change in the stress level

due to FSI is on the order of 13%. It can be conservatively concluded that the concrete torus can be analyzed for CO loading without FSI and fluid mass with the stress levels so obtained increased by 13% to account for the FSI.

A.1.2.5 Dynamic Load Factor

The stresses for CO loading without FSI and fluid mass, and the stresses for CO loading (neglecting its variation with time) are calculated. Table A.1-10 shows the ratio between these stresses (dynamic load factors) for the Type II support condition for various nodes of the torus model. This table shows that the dynamic load factors change from node to node and for various stresses. A careful inspection of the stresses and dynamic load factors reveals that the dynamic load factor (DLF) does not exceed 1.45 for stress components which have a considerable value. The dynamic load factors which have a value greater than 1.45 correspond to stresses with small values and are not reliable or typical. A dynamic load factor equal to 1.5 is recommended to be used conservatively for all components of stresses throughout the torus.

A.1.3 METHOD OF SOLUTION

Consider an elastic structure submerged in a finite acoustic fluid, where pressure P satisfies the wave equation

$$\nabla 2p = \ddot{P}/C^2 \qquad (1)$$

where C is the speed of sound in the fluid. If both structure and fluid are modeled with finite elements, the resulting matrix equations take the general forms (18, 19, 20)

$$\begin{bmatrix} M & 0 \\ -\rho\hat{A}^T & Q \end{bmatrix} \begin{Bmatrix} \ddot{u} \\ \ddot{P} \end{Bmatrix} + \begin{bmatrix} K & \hat{A} \\ 0 & \bar{H} \end{bmatrix} \begin{Bmatrix} u \\ P \end{Bmatrix} = \begin{Bmatrix} f \\ 0 \end{Bmatrix} \qquad (2)$$

where M and K are the usual structural mass and stiffness matrices, Q, and $\bar{H}$ are the inertia and stiffness matrices for the

fluid, $\hat{A}$ is the area matrix converting pressure to force at the fluid-structure interface nodes and ρ is the fluid's mass density. 'f' is the external force on the structure, u is the vector of the structure's nodal displacements and P is pressure at all nodes of the fluid as well as at the fluid-structure interface.

In the analysis, the rigid wall pressure on the torus shell is considered as an external force on the structure; in this case P in Equation (2) represents change in rigid wall pressure at the fluid structure interface and change in fluid pressure within the fluid due to fluid-structure interaction.

In Equation (2), $\bar{H}$ can be assembled from standard 3-D elasticity finite elements (References 1-19 and 1-20) if the Z component of displacement at each point is retained and Hooke's law is specified as:

$$\begin{Bmatrix} \sigma_{xx} \\ \sigma_{yy} \\ \sigma_{zz} \\ \sigma_{xy} \\ \sigma_{yz} \\ \sigma_{xz} \end{Bmatrix} = \begin{bmatrix} 1 & -1 & -1 & & & \\ -1 & 1 & -1 & & & \\ -1 & -1 & 1 & & & \\ & & & 1 & & \\ & & & & 1 & \\ & & & & & 1 \end{bmatrix} \begin{Bmatrix} \varepsilon_{xx} \\ \varepsilon_{yy} \\ \varepsilon_{zz} \\ \gamma_{xy} \\ \gamma_{yz} \\ \gamma_{xz} \end{Bmatrix} \tag{3}$$

In terms of the usual engineering constants, Equation (3) is equivalent (numerically) to choosing shear modulus G and Young's modulus, E as

$$G = 1.0 \qquad E = 10^{20}G$$

In Equation (2) Q can be assembled from standard elasticity finite elements (References 1-19 and 1-20) if the mass density assigned to the material is numerically equal to $1/C^2$.

For an incompressible fluid $C \to \infty$ and the wave Equation (1) reduces to Laplace's equation

$$\nabla^2 p = 0 \tag{4}$$

Also $Q = 0$ so that P can be eliminated from Equation (2) to yield

$$(M + \rho \hat{A} \bar{H}^{-1} \hat{A}^T) \ddot{u} + Ku = f \tag{5}$$

Thus defining the added mass matrix

$$\bar{M}_a = \rho \hat{A} \bar{H}^{-1} \hat{A}^T \tag{6}$$

Note that matrix $\hat{A}$ is a rectangular matrix with zero elements related to nodes within the fluid (area is specified only for interface of fluid and structure); $\hat{A}$ could be partitioned as:

$$\hat{A} = \begin{bmatrix} A & 0 \\ 0 & 0 \end{bmatrix} \tag{7}$$

where A is a diagonal matrix;

then

$$\bar{M}_a = \rho A H^{-1} A^T \tag{8}$$

where H is a reduced stiffness matrix for the fluid related to the nodes of the fluid located on the interface of fluid and structure.* Using Equation (2), the hydrodynamic pressure P at the fluid nodes is given by:

$$P = \rho \bar{H}^{-1} \hat{A}^T \ddot{u} \tag{9}$$

then the hydrodynamic pressure at the fluid structure interfaces (P_1) is given by:

$$P_1 = \rho H^{-1} A^T \ddot{u}_1 \tag{10}$$

where $\ddot{u}_1$ is now the acceleration of the nodes at the interface of the fluid and structure which is a sub vector of the structural acceleration vector. From Equation (5) and (10) the following observations can be made about fluid-structure interaction for a system containing incompressible fluid:

---

* $H = H_{11} - H_{12} H_{22}^{-1} H_{12}^T$, where H_{11}, H_{12}, etc. are submatrices of $\bar{H}$ matrix related to nodes on interface and nodes in fluid.

i. Fluid-structure interaction does not affect the stiffness matrix of the structure.

ii. Fluid-structure interaction does not affect the equation of motion of the structure. The classical equation of motion of structure remains valid.

iii. Fluid-structure interaction does not introduce any additional degrees of freedom.

iv. Effect of fluid-structure interaction is to alter the mass matrix of the structure in the form of an "added mass" matrix related to the degrees of freedom at the fluid-structure interface.

v. Hydrodynamic pressure at the fluid-structure interaction is related to the acceleration at the fluid-structure interface.

A.1.3.1 Finite Element Discretization of Structure and Fluid

Figure A.1-1 shows the typical cross section of the Brunswick concrete torus. The torus has been assumed to be axisymmetric. Both fluid and concrete structure has been discretized with NASTRAN'S axisymmetric, triangular cross-section, ring element (TRIAX6) with mid-size grid points.

A.1.3.1.1 Finite Element for Fluid

Figures A.1-2 to A.1-4 shows the finite element mesh for the fluid. There are 128 TRIAX6 elements and 289 fluid nodes. At the fluid nodes translation in the Z-direction (degree of freedom 3) has been retained. The following material properties have been used in MAT1 Cards for the fluid elements.

$$G = \frac{1}{\rho} = 1.07 \times 10^4 \qquad \text{psi}/(\text{lb-sec}^2)/\text{in}^4$$

$$E = 10^{20}G = 1.07 \times 10^{24} \qquad "$$

A.1.3.1.2 Finite Element for Concrete

Figure A.1-5 shows the finite element mesh for the concrete structure. There are 136 "TRIAX6" elements and 340 nodes. At structural nodes, there are two degrees of freedom (U_r, U_z). The following material properties have been used in MAT1 cards for concrete elements.

$G = 1.35 \times 10^6$ psi

$E = 3.1 \times 10^6$ psi

$\nu = 0.15$

$\rho = 2.246 \times 10^{-4}$ (lb - sec^2)/in^4

A.1.3.2 DMAP ALTER in NASTRAN for "Added Mass" Matrix

Because of the value of material properties assumed in the analysis for the fluid elements, the added mass matrix $\bar{M}_a$ of the fluid is given as:

$$\bar{M}_a = \hat{A}\, \bar{H}^{-1}\, \hat{A}^T \qquad (11)$$

The added mas matrix $\bar{M}_a$ of the fluid has been calculated using DMAP ALTER in NASTRAN. The DMAP ALTERs for normal mode calculation and frequency response analysis are given in Appendices B.1 and C.1.

A.1.4 NORMAL MODE ANALYSIS

Normal modes of vibration have been calculated for the torus with and without FSI. Since the loading spectrum under LOCA (CO and CHUGGING) has frequencies 1 to 50 Hz., normal modes have been extracted only for the frequencies which are below 100 Hz. A generalized dynamic reduction (Reference 1-21) has been used instead of Guyon reduction procedures. Natural frequencies have been calculated for two types of boundary conditions.

Type I: Both radial (U_r) and vertical translations (U_z) are restrained at base. (radial movement restrained)

Type II: Only vertical translations (U_z) are restrained at base. (radial movement allowed)

Normal modes have been calculated for the torus with and without FSI for both types of boundary conditions.

The result of these analyses are given in Table A.1-1. The first six frequencies remain practically unaffected with FSI.

Figures A.1-6 to A.1-10 give the mode shapes for Type II B.C. for the torus with and without FSI. FSI has no significant influence on the mode shapes.

For Type I support, there are two normal modes having frequencies in the range of 1 to 50 Hz. When FSI is included in analysis, reduction in these two natural frequencies is below 0.2% (Table A.1-1).

For Type II support, there are three frequencies in the range of 1 to 50 Hz. When FSI is included in the analysis reduction in these three natural frequencies are 2.1%, 3.5% and 0.56% respectively (Table A.1-1).

A.1.5 FREQUENCY RESPONSE ANALYSIS FOR C.O. LOAD

The torus has been analyzed for a spectrum of loading to study the effect of FSI on:

i. Hydrodynamic pressure at fluid-structure interface
ii. Displacement of structure
iii. State of stress

The frequency response analysis (NASTRAN Rigid Format 26) has been performed for CO loading under DBA as defined in Table 4.4.1-2 of Reference 1-1. Table A.1-2 shows the amplitudes of the CO loading for frequencies ranging from 1 to 50 Hz. as used in this analysis. Figure A.1-19 shows the rigid wall pressure distribution of the CO loading.

A.1.5.1 Effect of FSI on Hydrodynamic Pressure

Because of the assumed material property for the fluid elements, the hydrodynamic pressure at the fluid structure interface is given as:

$$P_l = H^{-1} A^T \ddot{u}_l \tag{12}$$

For the n^{th} frequency of loading displacement u_l is written as:

$$u_l = \zeta_n \cos(\omega_n t + \alpha_n) \tag{13}$$

then

$$\ddot{u}_l = -\omega_n^2 \zeta_n \cos(\omega_n t + \alpha_n) \tag{14}$$
$$= -\omega_n^2 u_l$$

hence,

$$P_l(\omega_n) = \omega_n^2 H^{-1} A^T u_l \tag{15}$$

where

P_l is a subvector of

$$P = \omega_n^2 \bar{H}^{-1} \hat{A}^T u \tag{16}$$

Equation (16) has been included in NASTRAN by DMAP ALTER to calculate hydrodynamic pressure due to FSI at each fluid structure node. This hydrodynamic pressure represents the change in the rigid wall pressure due to FSI.

Table A.1-3 shows the change in the rigid wall pressure due to FSI at bottom dead center (Node 30016) for Type I support condition. The dashed line curve in Figure A.1-11 also shows the same rigid wall pressure change. The rigid wall pressure amplitude is maximum at 6 Hz. and is equal to 2.68 psi, the change in this maximum pressure due to FSI is .001 psi (.04%). The maximum change in the rigid wall pressure is .0082 psi at 50 Hz. For Type I support, the maximum change in the rigid wall pressure due to FSI is less than 2.5%. Table A.1-4 and the solid line curve in Figure A.1-11 give the change in the rigid wall pressure due to FSI for Type II support. The change in the maximum pressure amplitude which occurs at 6 Hz. is .0019 psi (.07%). The maximum change in the hydrodynamic pressure is 0.0162 psi at 50 Hz. For

Type II support, the maximum change in the rigid wall pressure due to FSI is less than 5%.

The sum of the amplitudes (1 to 50 Hz.) of the rigid wall pressure is 15.25 psi without FSI which changes to 15.347 and 15.443 psi for Type I and Type II support respectively.

A.1.5.2 Effect of FSI on Displacement

The frequency response analysis (NASTRAN Rigid Format 26) has been used to investigate the effect of FSI on the displacement at some selected grid points at the concrete torus. Radial displacements at nodes 36, 81, 126, 166, 211, 251, 291 which lie on the inside surface of the concrete torus have been considered.

Due to the n^{th} component of the frequency spectrum, the radial displacement $u_r^i(\omega_n,t)$ is given by the following:

$$u_r^i(\omega_n,t) = A_n^i \cos(\omega_n t+\phi_{in}) \qquad (17)$$

where ω_n = Frequency of the n^{th} component

A_n^i = Amplitude of radial displacement at i^{th} node and n^{th} component of frequency spectrum

ϕ_{in} = Phase angle at i^{th} node and n^{th} component of frequency spectrum

For the CO load, the frequency spectrum consists of 50 components ranging from 1 to 50 Hz.

Figures A.1-12 to A.1-18 show values of A_n^i for n = 1 to 50 Hz. and i = 36, 81, 126, 166, 211, 251, 291. In fact, these figures show the amplitudes of the radial displacement with and without FSI for Type II support. Total displacement for the CO loading is given as

$$U^i_r(t) = \sum_{n=1}^{50} u^i_r(\omega_n,t)$$

$$= \sum_{n=1}^{50} A^i_n \cos(\omega_n t+\phi_{in}) \qquad (18)$$

To simplify the analysis, we define a quantity

$$U^i = \sum_{n=1}^{50} |A^i_n| \qquad (19)$$

This quantity U^i has been used as an index to measure the effect of FSI. In fact, U^i is the sum of absolute radial or tangential displacement amplitude at node i in local cylindrical coordinate system.

Table A.1-5 shows that the maximum change in radial and tangential displacement for Type I support, is 4.2% and 4.9% respectively. Table A.1-6 shows that the maximum change in the radial and tangential displacement for Type II support, is 11.4% and 9% respectively.

A.1.5.3 Effect of FSI on Stress at Concrete Torus

Frequency Response Analysis has been used to study the effect of FSI on the state of stress at concrete torus. Displacement vectors obtained from Direct Frequency Analysis have real and imaginary parts. Stresses corresponding to these displacement vectors are also complex quantities. NASTRAN Rigid Format 26 can not handle complex stress computation for TRIAX6 element. Postprocessing of the complex displacement, obtained from Direct Frequency Response, was performed to calculate complex stress for TRIAX6 elements. Real and imaginary parts of displacement vectors were saved separately for each of the 50 frequencies. There were 100 sets of displacement vectors (50 real + 50 imaginary). These 100 sets of displacement vectors were input into the DSR2 (Stress Data Recovery - Phase 2) module in a subsequent normal mode analysis (Rigid Format 25). A FORTRAN program was written to separate the imaginary and real part of each stress tensor. The program also combines the real and imaginary parts to calculate amplitudes at each frequency. State of stress has been calculated for CO load.

At i^{th} node the radial stress, σ_{rr}^{ni}, for the n^{th} component of the frequency spectrum can be written as:

$$\sigma_{rr}^{ni}(\omega_n,t) = \sigma_{rR}^{ni} \cos\omega_n t + \sigma_{rI}^{ni} \sin\omega_n t$$
$$= \sigma_{rA}^{ni} \cos(\omega_n t + \beta in) \quad (20)$$

where

$\sigma_{rR}^{ni}\sigma_{rI}^{ni}$ are the real and imaginary part of the radial stress at node i for the n^{th} frequency spectrum

σ_{rA}^{ni} = Amplitude of the radial stress at n^{th} component of frequency spectrum

$$= \sqrt{\sigma_{rR}^{ni2} + \sigma_{rI}^{ni2}} \quad (21)$$

βin = The phase angle of radial stress at i^{th} node for the n^{th} component of frequency spectrum

$$= \tan^{-1} \sigma_{rI}^{ni}/\sigma_{rR}^{ni} \quad (22)$$

Hence, the total radial stress $\sigma_{rr}^{Ti}(t)$ at the i^{th} node is given as:

$$\sigma_{rr}^{Ti}(t) = \sum_{n=1}^{50} \sigma_{rr}^{ni}(\omega_n,t)$$

$$= \sum_{n=1}^{50} \sigma_{rA}^{ni} \cos(\omega_n t + \beta in) \quad (23)$$

Similar expression can be obtained for azimuth, axial and shear stress. The following steps have been performed to obtain an index to measure the effect of FSI in the concrete stresses.

Step I: Calculate real and imaginary part of stress for each frequency.

Step II: Calculate amplitude for each frequency.

Step III: Calculate, $\Sigma\sigma_A$, sum of absolute value of all the amplitudes (50 of them).

Step I to Step III have been performed for radial, azimuth, axial and shear stresses.

Values of $\Sigma\sigma A$ have been tabulated in Tables A.1-7 and A.1-8 for Type I and Type II support respectively. Table A.1-9 gives the percentage change in the state of stress due to FSI for the two types of support. Table A.1-7 shows that, in general, for Type I support (Radial and Vertical translations restrained) the stress level is lower. Table A.1-9 shows that percentage change due to FSI is highest at node 31 for radial stress (13.2%) azimuth (11.2%), axial (12.1%) and at node 291 for shear stress (7.1%) for Type II support. However, change in all other nodes are below 10%.

Hence, it can be conservatively concluded that due to FSI, the stress level in the concrete torus increases by 13%.

APPENDIX B.1

DMAP ALTER FOR NORMAL MODE CALCULATIONS

The DMAP ALTER for normal mode calculations (Solution Rigid Format 25) is given below. MBAR is the added mass matrix of the fluid.

```
ID NORMAL MODES OF THE COMBINED SYSTEM BASE RESTRAINED
SOL 25,0
DIAG 8,13,14
TIME 5.
ALTER 92
MTRXIN      ,,MATPOOL,EQEXIN,SIL,/STIF,,/V,N,LUSET/S,N,NOSTIF $
COND        FINIS,NOSTIF $
ADD         KGG,STIF/KXX $
EQUIV       KXX,KGG/ALWAYS $
ALTER 108,108
UPARTN      USET,KNN/KFF,KSF,KFS,KSS/N/F/C,N,S $
VEC         USET/CP/C,N,S/SG/SB $
PARTN       KSS,CP,/K11,,,///6 $
PARTN       KSF,,CP/K12,,,/1 $
DECOMP      K11/KL, $
FBS         KL,,K12/X $
MPYAD       K12,X,/MBAR/1////6 $
DIAGONAL    MBAR/MXXD/SQUARE $
MATGPR      GPL,USET,SIL,MXXD//F/F $
ALTER 125
ADD         MFF,MBAR/MTT $
EQUIV       MTT,MFF/ALWAYS $
ECHOOFF
ALTER 154
MTRXIN      ,,MATPOOL,EQEXIN,SIL,/FORCE1,,/V,N,LUSET/ $
DIAGONAL    FORCE1/P1/COLUMN $
MPYAD       PHIG,P1,/PF/1 $
MATPRN      PF// $
CEND
```

APPENDIX C.1

DMAP ALTER FOR FREQUENCY RESPONSE ANALYSIS

The DMAP ALTER for Frequency Response Analysis (Solution Rigid Format 26) is given below. MBAR is the added mass matrix for the fluid.

```
ID FREQUENCY RESPONSE OF THE COMBINED SYSTEM
SOL 26,1
DIAG 8,13
TIME 500.
ALTER 135
MTRXIN      ,,MATPOOL,EQEXIN,SIL,/STIF,,/V,N,LUSET/S,N,NOSTIF $
COND        FINIS,NOSTIF $
ADD         KGG,STIF/KXX $
EQUIV       KXX,KGG/ALWAYS $
ALTER 149,149
UPARTN      USET,KNN/KFF,KSF,KFS,KSS/N/F/C,N,S $
VEC         USET/CP/C,N,S/SG/SB $
PARTN       KSS,CP,/K11,,,///6 $
PARTN       KSF,,CP/K12,,,/1 $
DECOMP      K11/KL, $
FBS         KL,,K12/X $
MPYAD       K12,X,/MBAR/1////6 $
ATER 175
ADD         MFF,MBAR/MTT $
EQUIV       MTT,MFF/ALWAYS $
```

REFERENCES - SECTION 1

1-1 "Mark I Containment Program, Load Definition Report", General Electric NEDO - 21888, Class I, November 1981, Revision 2.

1-2 "Mark I Containment Program, Structural Acceptance Criteria, Plant Unique Analysis, Application Guide", General Electric NEDO - 245831, 78ND125, Class I, October 1979.

1-3 Ghosh, S. and Wilson, E. L., "Dynamic Stress Analysis of Axisymmetric Structures Under Arbitrary Loading", Revised June, 1980 by Rahmat O. Rabizadeh, Structural Analysis Group, United Engineers & Constructors, Inc.

1-4 Wilson, E. L., "A Digital Computer Program for the Finite Element Analysis of Axisymmetric Solids with Orthotropic, Nonlinear Material Properties", November, 1965.

1-5 Wilson, E. L. and Nickell, R. E., "Application of the Finite Element Method to Heat Conduction Analysis", Nuclear Engineering and Design. Volume 4, pp. (276-286), 1966.

1-6 "Mark I Containment Program, T-Quencher S/RV Discharge, Torus Shell Loads", by Sanchez, R. A. NEDO - 24555-P, Application Guide 4, Class III, Revision 2.

1-7 "Mark I SSE Question Response", Revision 1, General Electric Company Proprietary, Question 161.6, February 8, 1980.

1-8 "Mark I Containment Program, Plant Unique Load Definition, Brunswick Steam Electric Plant Units 1 & 2", General Electric Company, NEDO - 24582 Class I, March 1979.

1-9 "Mark I Containment Program Plant Unique Load Definition Reports", Memorandum MI-G-66, April 11, 1979 General Electric.

1-10 Biggs, John M., Introduction to Structural Dynamics, McGraw-Hill Book Company, 1964.

1-11 "Seismic Analysis of the Primary and Secondary Containments", CP&L Brunswick Steam Electric Plants Units 1 & 2, Design Report No. 4, November, 1970.

1-12 "Earthquake Analysis of Reactor Building and Primary Containment", CP&L Brunswick Steam Electric Plants, November 1969, by Manson, Holley and Biggs Consulting Engineers.

1-13 Winstead, T. L., Burdette, E. G., "Liner Anchorage Analysis for Nuclear Containments", ASCE, Journal of the Structural Division, October, 1975.

1-14 Duchan, N. B., "Analysis of Reinforced Concrete Membrane Subject to Tension and Shear", ACI Journal, September, 1972, pp. 578-583.

1-15 "Containment Large Opening Design Text, Figures and Stress Plots", CP&L, Brunswick Steam Electric Plant, Units 1 & 2, Design Report No. 11, Volumes I & II, December, 1971.

1-16 "Containment Design Report", CP&L, Brunswick Steam Electric Plant, Units 1 & 2, Design Report No. 7. December, 1970.

1-17 Design Data NELSON concrete Anchor, Studs for Securing Steel to Concrete. (NELSON Catalog).

1-18 Zienkiewicz, O. C., and Newton, R. E., "Coupled Vibrations of a Structure Submerged in a Compressible Fluid", Proc. Int. Symp. on Finite Element Techniques, Stuttgart, 1969.

1-19 Everstine, G. C., Schroeder, E. A., and Marcus, M. S., "The Dynamic Analysis of Submerged Structures", NASTRAN: Users' Experiences, NASA. TM. X-3278, September 1975, pp. 419-429.

1-20 Everstine, G. C., "A Nastran Implementation of the Doubly Asympotic Approximation for Underwater Shock Response", NASTRAN: Users' Experiences, N77-20485-20511, pp. 207-228.

1-21 MSC/NASTRAN Application Manual, Vol. 1, Section 2.4-1 to 2.4-34. April, 1978.

Table 1.3-1
Torus B ttom Dead Center Pressure and Frequency of
a Single S/RV Line at SBA

Sq. No.	S/RV Line No.	Positive Pressure psi *	Negative Pressure psi	Frequency HZ
1	11	15.52	-14.51	10.0
2	12	15.59	-14.77	9.67
3	18	15.3	-14.4	9.9
4	19	15.0	-14.2	10.1
5	20	14.8	-14.0	10.2
6	26	14.5	-13.7	10.4
7	27	14.4	-13.7	10.4
8	33	15.7	-14.7	9.9
9	34	16.5	-15.1	9.6
10	58	15.2	-14.3	10.0
11	59	15.8	-14.7	9.7

* The pressures in this column are also conservatively used in lieu of negative pressures, given in next column, for S/RV load at normal and LOCA conditions.

Table 1.3-2
Maximum Internal Pressure in the Suppression Chamber

Condition	Pressure in Psig
DBA	28.6
DBA, Pool Swell**	11.0
IBA	32.8
SBA	24.4

** During pool swell an additional pressure is developed in torus which is added to Quasi - Static pressure (see pool swell pressure).

TABLE 1.4-1

LOAD COMBINATIONS **

LOAD CASE	1	DEAD LOAD	+HYDR LOAD	+S/RV				
LOAD CASE	2	DEAD LOAD	+HYDR LOAD	+S/RV	+EQ.	OBE		
LOAD CASE	3	DEAD LOAD	+HYDR LOAD	+S/RV	+EQ.	SSE		
LOAD CASE	4	DEAD LOAD	+HYDR LOAD	+SBA				
LOAD CASE	5	DEAD LOAD	+HYDR LOAD	+SBA				PRE CHUG
LOAD CASE	6	DEAD LOAD	+HYDR LOAD	+SBA				POST CHUG
LOAD CASE	7	DEAD LOAD	+HYDR LOAD	+SBA	+S/RV			
LOAD CASE	8	DEAD LOAD	+HYDR LOAD	+SBA	+S/RV			PRE CHUG
LOAD CASE	9	DEAD LOAD	+HYDR LOAD	+SBA	+S/RV			POST CHUG
LOAD CASE	10	DEAD LOAD	+HYDR LOAD	+SBA	+EQ.	OBE		
LOAD CASE	11	DEAD LOAD	+HYDR LOAD	+SBA	+EQ.	SSE		
LOAD CASE	12	DEAD LOAD	+HYDR LOAD	+SBA	+EQ.	OBE		PRE CHUG
LOAD CASE	13	DEAD LOAD	+HYDR LOAD	+SBA	+EQ.	SSE		PRE CHUG
LOAD CASE	14	DEAD LOAD	+HYDR LOAD	+SBA	+EQ.	OBE		POST CHUG
LOAD CASE	15	DEAD LOAD	+HYDR LOAD	+SBA	+EQ.	SSE		POST CHUG
LOAD CASE	16	DEAD LOAD	+HYDR LOAD	+SBA	+S/RV	+EQ.	OBE	
LOAD CASE	17	DEAD LOAD	+HYDR LOAD	+SBA	+S/RV	+EQ.	SSE	
LOAD CASE	18	DEAD LOAD	+HYDR LOAD	+SBA	+S/RV	+EQ.	OBE	PRE CHUG
LOAD CASE	19	DEAD LOAD	+HYDR LOAD	+SBA	+S/RV	+EQ.	SSE	PRE CHUG
LOAD CASE	20	DEAD LOAD	+HYDR LOAD	+SBA	+S/RV	+EQ.	OBE	POST CHUG
LOAD CASE	21	DEAD LOAD	+HYDR LOAD	+SBA	+S/RV	+EQ.	SSE	POST CHUG
LOAD CASE	22	DEAD LOAD	+HYDR LOAD	+IBA				
LOAD CASE	23	DEAD LOAD	+HYDR LOAD	+IBA				PRE CHUG
LOAD CASE	24	DEAD LOAD	+HYDR LOAD	+IBA				POST CHUG
LOAD CASE	25	DEAD LOAD	+HYDR LOAD	+IBA	+S/RV			
LOAD CASE	26	DEAD LOAD	+HYDR LOAD	+IBA	+S/RV			PRE CHUG
LOAD CASE	27	DEAD LOAD	+HYDR LOAD	+IBA	+S/RV			POST CHUG
LOAD CASE	28	DEAD LOAD	+HYDR LOAD	+IBA	+EQ.	OBE		
LOAD CASE	29	DEAD LOAD	+HYDR LOAD	+IBA	+EQ.	SSE		
LOAD CASE	30	DEAD LOAD	+HYDR LOAD	+IBA	+EQ.	OBE		PRE CHUG
LOAD CASE	31	DEAD LOAD	+HYDR LOAD	+IBA	+EQ.	SSE		PRE CHUG
LOAD CASE	32	DEAD LOAD	+HYDR LOAD	+IBA	+EQ.	OBE		POST CHUG

..... Continued

TABLE 1.4-1 Continued

LOAD COMBINATIONS **

LOAD CASE	33	DEAD LOAD +HYDR LOAD	+IBA	+EQ.	SSE			POST CHUG
LOAD CASE	34	DEAD LOAD +HYDR LOAD	+IBA	+S/RV	+EQ.	OBE		
LOAD CASE	35	DEAD LOAD +HYDR LOAD	+IBA	+S/RV	+EQ.	SSE		
LOAD CASE	36	DEAD LOAD +HYDR LOAD	+IBA	+S/RV	+EQ.	OBE	PRE CHUG	
LOAD CASE	37	DEAD LOAD +HYDR LOAD	+IBA	+S/RV	+EQ.	SSE	PRE CHUG	
LOAD CASE	38	DEAD LOAD +HYDR LOAD	+IBA	+S/RV	+EQ.	OBE	POST CHUG	
LOAD CASE	39	DEAD LOAD +HYDR LOAD	+IBA	+S/RV	+EQ.	SSE	POST CHUG	
LOAD CASE	40	DEAD LOAD +HYDR LOAD	+DBA				POOL SWELL	
LOAD CASE	41	DEAD LOAD +HYDR LOAD	+DBA				COND. OSC.	
LOAD CASE	42	DEAD LOAD +HYDR LOAD	+DBA				PRE CHUG	
LOAD CASE	43	DEAD LOAD +HYDR LOAD	+DBA				POST CHUG	
LOAD CASE	44	DEAD LOAD +HYDR LOAD	+DBA	+S/RV			POOL SWELL	
LOAD CASE	45	DEAD LOAD +HYDR LOAD	+DBA	+S/RV			COND. OSC.	
LOAD CASE	46	DEAD LOAD +HYDR LOAD	+DBA	+S/RV			PRE CHUG	
LOAD CASE	47	DEAD LOAD +HYDR LOAD	+DBA	+S/RV			POST CHUG	
LOAD CASE	48	DEAD LOAD +HYDR LOAD	+DBA	+EQ.	OBE		POOL SWELL	
LOAD CASE	49	DEAD LOAD +HYDR LOAD	+DBA	+EQ.	SSE		POOL SWELL	
LOAD CASE	50	DEAD LOAD +HYDR LOAD	+DBA	+EQ.	OBE		COND. OSC.	
LOAD CASE	51	DEAD LOAD +HYDR LOAD	+DBA	+EQ.	SSE		COND. OSC.	
LOAD CASE	52	DEAD LOAD +HYDR LOAD	+DBA	+EQ.	OBE		PRE CHUG	
LOAD CASE	53	DEAD LOAD +HYDR LOAD	+DBA	+EQ.	SSE		PRE CHUG	
LOAD CASE	54	DEAD LOAD +HYDR LOAD	+DBA	+EQ.	OBE		POST CHUG	
LOAD CASE	55	DEAD LOAD +HYDR LOAD	+DBA	+EQ.	SSE		POST CHUG	
LOAD CASE	56	DEAD LOAD +HYDR LOAD	+DBA	+S/RV	+EQ.	OBE	POOL SWELL	
LOAD CASE	57	DEAD LOAD +HYDR LOAD	+DBA	+S/RV	+EQ.	SSE	POOL SWELL	
LOAD CASE	58	DEAD LOAD +HYDR LOAD	+DBA	+S/RV	+EQ.	OBE	COND. OSC.	
LOAD CASE	59	DEAD LOAD +HYDR LOAD	+DBA	+S/RV	+EQ.	SSE	COND. OSC.	
LOAD CASE	60	DEAD LOAD +HYDR LOAD	+DBA	+S/RV	+EQ.	OBE	PRE CHUG	
LOAD CASE	61	DEAD LOAD +HYDR LOAD	+DBA	+S/RV	+EQ.	SSE	PRE CHUG	
LOAD CASE	62	DEAD LOAD +HYDR LOAD	+DBA	+S/RV	+EQ.	OBE	POST CHUG	
LOAD CASE	63	DEAD LOAD +HYDR LOAD	+DBA	+S/RV	+EQ.	SSE	POST CHUG	
LOAD CASE	64	DEAD LOAD +HYDR LOAD						
LOAD CASE	65	DEAD LOAD +HYDR LOAD	+S/RV					

** NOTE TOTAL NUMBER OF LOADING CASES CONSIDERING SIGN OF DYNAMIC LOADS IS 130 IN TWO SETS OF 65
SET 1 POSITIVE SUM(D.L.,H.L.,TEMP.,LOCA P,POOL SWELL)+SUM(ABS(EQ.),ABS(S/RV),ABS(CHUG.),ABS(COND. OSC.))
SET 2 NEGATIVE SUM(D.L.,H.L.,TEMP.,LOCA P,POOL SWELL)-SUM(ABS(EQ.),ABS(S/RV),ABS(CHUG.),ABS(COND. OSC.))

TABLE 1.4-2

LOAD CASE	LOAD FACTORS D.L	H.L	T1	T2	T3	LOCA P	PL SWL	H. EQ.	V. EQ.	S/RV	PRE CH	POS CH	CON OS	***
1	1.40	1.40	0.	0.	0.	0.	0.	0.	0.	1.50	0.	0.	0.	
2	1.00	1.00	1.00	0.	0.	0.	0.	1.25	1.25	1.25	0.	0.	0.	
3	1.00	1.00	1.00	0.	0.	0.	0.	1.00	1.00	1.00	0.	0.	0.	
4	1.00	1.00	0.	1.00	0.	1.25	0.	0.	0.	0.	0.	0.	0.	
5	1.00	1.00	0.	1.00	0.	1.25	0.	0.	0.	0.	1.25	0.	0.	
6	1.00	1.00	0.	1.00	0.	1.25	0.	0.	0.	0.	0.	1.25	0.	
7	1.00	1.00	0.	1.00	0.	1.25	0.	0.	0.	1.25	0.	0.	0.	
8	1.00	1.00	0.	1.00	0.	1.25	0.	0.	0.	1.25	1.25	0.	0.	
9	1.00	1.00	0.	1.00	0.	1.25	0.	0.	0.	1.25	0.	1.25	0.	
10	1.00	1.00	0.	1.00	0.	1.10	0.	1.10	1.10	0.	0.	0.	0.	
11	1.00	1.00	0.	1.00	0.	1.00	0.	1.00	1.00	0.	0.	0.	0.	
12	1.00	1.00	0.	1.00	0.	1.10	0.	1.10	1.10	0.	1.10	0.	0.	
13	1.00	1.00	0.	1.00	0.	1.00	0.	1.00	1.00	0.	1.00	0.	0.	
14	1.00	1.00	0.	1.00	0.	1.10	0.	1.10	1.10	0.	0.	1.10	0.	
15	1.00	1.00	0.	1.00	0.	1.00	0.	1.00	1.00	0.	0.	1.00	0.	
16	1.00	1.00	0.	1.00	0.	1.10	0.	1.10	1.00	1.10	0.	0.	0.	
17	1.00	1.00	0.	1.00	0.	1.00	0.	1.00	1.00	1.00	0.	0.	0.	
18	1.00	1.00	0.	1.00	0.	1.10	0.	1.10	1.10	1.10	1.10	0.	0.	
19	1.00	1.00	0.	1.00	0.	1.00	0.	1.00	1.00	1.00	1.00	0.	0.	
20	1.00	1.00	0.	1.00	0.	1.10	0.	1.10	1.10	1.10	0.	1.10	0.	
21	1.00	1.00	0.	1.00	0.	1.00	0.	1.00	1.00	1.00	0.	1.00	0.	
22	1.00	1.00	0.	0.	1.00	1.25	0.	0.	0.	0.	0.	0.	0.	
23	1.00	1.00	0.	0.	1.00	1.25	0.	0.	0.	0.	1.25	0.	0.	
24	1.00	1.00	0.	0.	1.00	1.25	0.	0.	0.	0.	0.	1.25	0.	
25	1.00	1.00	0.	0.	1.00	1.25	0.	0.	0.	1.25	0.	0.	0.	
26	1.00	1.00	0.	0.	1.00	1.25	0.	0.	0.	1.25	1.25	0.	0.	
27	1.00	1.00	0.	0.	1.00	1.25	0.	0.	0.	1.25	0.	1.25	0.	
28	1.00	1.00	0.	0.	1.00	1.10	0.	1.10	1.10	0.	0.	0.	0.	
29	1.00	1.00	0.	0.	1.00	1.00	0.	1.00	1.00	0.	0.	0.	0.	
30	1.00	1.00	0.	0.	1.00	1.10	0.	1.10	1.10	0.	1.10	0.	0.	
31	1.00	1.00	0.	0.	1.00	1.00	0.	1.00	1.00	0.	1.00	0.	0.	
32	1.00	1.00	0.	0.	1.00	1.10	0.	1.10	1.10	0.	0.	1.10	0.	

..... Continued

TABLE 1.4-2 Continued

LOAD CASE	LOAD FACTORS D.L	H.L	T1	T2	T3	LOCA P	PL SWL	H. EQ.	V. EQ.	S/RV	PRE CH	POS CH	CON OS	***
33	1.00	1.00	0.	0.	1.00	1.00	0.	1.00	1.00	0.	0.	1.00	0.	
34	1.00	1.00	0.	0.	1.00	1.10	0.	1.10	1.10	1.10	0.	0.	0.	
35	1.00	1.00	0.	0.	1.00	1.00	0.	1.00	1.00	1.00	0.	0.	0.	
36	1.00	1.00	0.	0.	1.00	1.10	0.	1.10	1.10	1.10	1.10	0.	0.	
37	1.00	1.00	0.	0.	1.00	1.00	0.	1.00	1.00	1.00	1.00	0.	0.	
38	1.00	1.00	0.	0.	1.00	1.10	0.	1.10	1.10	1.10	0.	1.10	0.	
39	1.00	1.00	0.	0.	1.00	1.00	0.	1.00	1.00	1.00	0.	1.00	0.	
40	1.00	1.00	1.00	0.	0.	1.25	1.25	0.	0.	0.	0.	0.	0.	
41	1.00	1.00	0.	1.00	0.	1.25	0.	0.	0.	0.	0.	0.	1.25	
42	1.00	1.00	0.	1.00	0.	1.25	0.	0.	0.	0.	1.25	0.	0	
43	1.00	1.00	0.	1.00	0.	1.25	0.	0.	0.	0.	0.	1.25	0.	
44	1.00	1.00	1.00	0.	0.	1.00	1.00	0.	0.	1.00	0.	0.	0.	
45	1.00	1.00	0.	1.00	0.	1.00	0.	0.	0.	1.00	0.	0.	1.00	
46	1.00	1.00	0.	1.00	0.	1.00	0.	0.	0.	1.00	1.00	0.	0.	
47	1.00	1.00	0.	1.00	0.	1.00	0.	0.	0.	1.00	0.	1.00	0.	
48	1.00	1.00	1.00	0.	0.	1.10	1.10	1.10	1.10	0.	0.	0.	0.	
49	1.00	1.00	1.00	0.	0.	1.00	1.00	1.00	1.00	0.	0.	0.	0.	
50	1.00	1.00	0.	1.00	0.	1.10	0.	1.10	1.10	0.	0.	0.	1.10	
51	1.00	1.00	0.	1.00	0.	1.00	0.	1.00	1.00	0.	0.	0.	1.00	
52	1.00	1.00	0.	1.00	0.	1.00	0.	1.10	1.10	0.	1.10	0.	0.	
53	1.00	1.00	0.	1.00	0.	1.00	0.	1.00	1.00	0.	1.00	0.	0.	
54	1.00	1.00	0.	1.00	0.	1.10	0.	1.10	1.10	0.	0.	1.10	0.	
55	1.00	1.00	0.	1.00	0.	1.00	0.	1.00	1.00	0.	0.	1.00	0.	
56	1.00	1.00	1.00	0.	0.	1.00	1.00	1.00	1.00	1.00	0.	0.	0.	
57	1.00	1.00	1.00	0.	0.	1.00	1.00	1.00	1.00	1.00	0.	0.	0.	
58	1.00	1.00	0.	1.00	0.	1.00	0.	1.00	1.00	1.00	0.	0.	1.00	
59	1.00	1.00	0.	1.00	0.	1.00	0.	1.00	1.00	1.00	0.	0.	1.00	
60	1.00	1.00	0.	1.00	0.	1.00	0.	1.00	1.00	1.00	1.00	0.	0.	
61	1.00	1.00	0.	1.00	0.	1.00	0.	1.00	1.00	1.00	1.00	0.	0.	
62	1.00	1.00	0.	1.00	0.	1.00	0.	1.00	1.00	1.00	0.	1.00	0.	
63	1.00	1.00	0.	1.00	0.	1.00	0.	1.00	1.00	1.00	0.	1.00	0.	
64	1.40	1.40	1.00	0.	0.	0.	0.	0.	0.	0.	0.	0.	0.	
65	1.00	1.00	1.00	0.	0.	0.	0.	0.	0.	1.30	0.	0.	0.	

***

D.L Dead Load

H.L Hydrostatic Load

T_1 Temperature Load (T = 100°F)

T_2 Temperature Load (T = 140°F)

T_3 Temperature Load (T = 168°F)

LOCA P = LOCA Quasi-Static Pressure

PL SWL Pool Swell Pressure

H. EQ. Horizontal Earthquake Load

V. EQ. Vertical Earthquake Load

S/RV Safety Relief Value Load

PRE CH Pre-chugging Load

POS CH Post chugging Load

CON OS Condensation Oscillation Load

TABLE 1.8-1 TEMPERATURE FORCES AND MOMENTS FOR PARTIALLY CRACKED CONCRETE - LINER EXCLUDED

Units(lb/in, in-lb/in)

FORCES AND MOMENTS FOR INSIDE TEMPERATURE 100.OF

SECTION NO.	SECTION ANGLE	FS	MT	FT	MS	FNS	FNT	FST
1	3.750	2094.700	-40491.700	1523.600	-28384.900	-113.900	0.	0.
2	48.750	817.600	-36505.500	2338.200	-152088.199	63.700	0.	0.
3	93.750	1899.800	-36293.600	696.700	-24072.400	106.800	0.	0.
4	138.750	734.100	-47791.900	1437.200	-120045.200	-79.300	0.	0.
5	183.750	1873.500	-46824.300	-288.100	-37133.200	313.400	0.	0.
6	228.750	886.600	-110823.300	2195.200	-184470.900	14.200	0.	0.
7	273.750	1193.800	-24850.800	525.500	-22335.100	143.600	0.	0.
8	318.750	915.900	-62872.200	2508.100	-148475.801	-256.900	0.	0.

FORCES AND MOMENTS FOR INSIDE TEMPERATURE 140.OF

SECTION NO.	SECTION ANGLE	FS	MT	FT	MS	FNS	FNT	FST
1	3.750	4885.400	-94437.600	3558.400	-66109.700	-268.200	0.	0.
2	48.750	1907.400	-85983.600	5464.700	-357282.500	142.000	0.	0.
3	93.750	4546.900	-84878.000	1619.400	-56284.300	258.900	0.	0.
4	138.750	1674.600	-109889.700	3385.500	-281113.199	-204.300	0.	0.
5	183.750	4361.300	-109429.700	-674.400	-86555.600	743.200	0.	0.
6	228.750	2089.800	-257865.301	5109.900	-429490.898	-4.600	0.	0.
7	273.750	2810.100	-57981.000	1229.900	-52448.800	350.900	0.	0.
8	318.750	2196.400	-147123.500	5902.100	-240348.801	-589.300	0.	0.

FORCES AND MOMENTS FOR INSIDE TEMPERATURE 168.OF

SECTION NO.	SECTION ANGLE	FS	MT	FT	MS	FNS	FNT	FST
1	3.750	6841.400	-132261.600	4968.100	-92571.400	-384.600	0.	0.
2	48.750	2688.300	-120722.200	7662.800	-500716.699	216.900	0.	0.
3	93.750	6366.800	-118723.600	2256.200	-7884.400	354.000	0.	0.
4	138.750	2370.800	-155120.000	4725.300	-393342.301	-251.200	0.	0.
5	183.750	6097.300	-153329.801	-940.600	-121246.000	1042.800	0.	0.
6	228.750	2875.100	-360155.500	7159.000	-601681.297	-22.900	0.	0.
7	273.750	3909.100	-81181.600	1723.600	-73325.900	489.000	0.	0.
8	318.750	3072.000	-205601.699	8243.600	-486413.602	-838.600	0.	0.

.... Continued

TABLE 1.8-1 TEMPERATURE FORCES AND MOMENTS FOR PARTIALLY CRACKED CONCRETE - LINER INCLUDED

Units (lb/in, in-lb/in)

FORCES AND MOMENTS FOR INSIDE TEMPERATURE 100.0F

SECTION NO.	SECTION ANGLE	FS	MT	FT	MS	FNS	FNT	FST
1	3.750	125.500	-73786.400	-113.300	-56061.200	-113.900	0.	0.
2	48.750	-76.300	-81959.900	832.200	-228666.801	63.700	0.	0.
3	93.750	-25.700	-68849.900	-1101.400	-54475.100	106.800	0.	0.
4	138.750	-434.600	-97680.100	-120.200	-186526.400	-79.300	0.	0.
5	183.750	-137.900	-90911.600	-2287.200	-80952.000	313.400	0.	0.
6	228.750	-654.000	-191220.199	515.900	-272100.898	14.200	0.	0.
7	278.750	-389.300	-53204.900	-1159.400	-52511.200	143.600	0.	0.
8	318.750	-251.500	-122243.400	984.100	-225980.301	-256.900	0.	0.

FORCES AND MOMENTS FOR INSIDE TEMPERATURE 140.0F

SECTION NO.	SECTION ANGLE	FS	MT	FT	MS	FNS	FNT	FST
1	3.750	290.200	-172133.500	-261.000	-130687.700	-268.200	0.	0.
2	48.750	-178.800	-192062.199	1950.600	-535932.203	142.000	0.	0.
3	93.750	53.700	-160849.000	-2576.500	-127228.200	258.900	0.	0.
4	138.750	-1036.400	-226306.900	-248.300	-436230.699	-204.300	0.	0.
5	183.750	-332.300	-212308.699	-5339.000	-188799.500	743.200	0.	0.
6	228.750	-1505.200	-445464.898	1191.500	-633973.398	-4.600	0.	0.
7	278.750	-883.500	-124133.800	-2701.600	-122862.000	350.900	0.	0.
8	318.750	-527.300	-285638.199	2345.600	-421218.199	-589.300	0.	0.

FORCES AND MOMENTS FOR INSIDE TEMPERATURE 168.0F

SECTION NO.	SECTION ANGLE	FS	MT	FT	MS	FNS	FNT	FST
1	3.750	408.000	-241037.100	-379.000	-182980.600	-384.600	0.	0.
2	48.750	-232.200	-269224.898	2743.200	-750874.703	216.900	0.	0.
3	93.750	76.700	-225076.699	-3618.200	-178193.301	354.000	0.	0.
4	138.750	-1447.200	-318104.102	-362.000	-610506.797	-251.200	0.	0.
5	183.750	-473.700	-297358.699	-7470.900	-264387.500	1042.800	0.	0.
6	228.750	-2159.500	-622878.703	1672.800	-887975.797	-22.900	0.	0.
7	278.750	-1231.800	-173792.801	-3780.700	-171907.000	489.000	0.	0.
8	318.750	-741.000	-399518.602	3264.700	-739619.297	-838.600	0.	0.

TABLE 1.8-2 TEMPERATURE FORCES AND MOMENTS FOR CRACKED CONCRETE - LINER EXCLUDED

Units (lb/in, in-lb/in)

FORCES AND MOMENTS FOR INSIDE TEMPERATURE 100.0F

SECTION NO.	SECTION ANGLE	FS	MT	FT	MS	FNS	FNT	FST
1	3.750	1131.000	-13956.500	994.400	-12474.900	-44.500	0.	0.
2	48.750	635.600	5932.400	371.600	-3823.400	55.100	0.	0.
3	93.750	974.300	-11060.100	864.100	-10248.100	25.600	0.	0.
4	138.750	601.100	-3022.800	508.100	-9489.900	128.200	0.	0.
5	183.750	1020.000	-11064.900	788.400	-10068.500	37.800	0.	0.
6	228.750	334.900	8286.400	182.400	4513.100	-229.100	0.	0.
7	273.750	842.900	-8033.300	633.800	-6040.700	-41.400	0.	0.
8	318.750	680.200	-1896.700	524.100	-10356.900	-85.100	0.	0.

FORCES AND MOMENTS FOR INSIDE TEMPERATURE 140.0F

SECTION NO.	SECTION ANGLE	FS	MT	FT	MS	FNS	FNT	FST
1	3.750	2638.500	-32559.400	2320.000	-29104.800	-99.400	0.	0.
2	48.750	1413.200	17388.600	867.500	-8914.700	-50.600	0.	0.
3	93.750	2274.000	-25811.400	2018.600	-23916.400	52.900	0.	0.
4	138.750	1402.700	-7047.400	1185.700	-22134.000	274.400	0.	0.
5	183.750	2380.400	-25817.800	1839.500	-23493.200	103.800	0.	0.
6	228.750	781.800	19344.400	426.000	10540.500	-520.800	0.	0.
7	273.750	1966.200	-18739.700	1478.800	-14094.400	-107.400	0.	0.
8	318.750	1587.000	-4428.600	1222.500	-24174.000	-194.800	0.	0.

FORCES AND MOMENTS FOR INSIDE TEMPERATURE 168.0F

SECTION NO.	SECTION ANGLE	FS	MT	FT	MS	FNS	FNT	FST
1	3.750	3694.100	-45585.900	3248.300	-40750.000	-129.000	0.	0.
2	48.750	1978.300	24340.700	1213.800	-12490.200	-37.100	0.	0.
3	93.750	3183.500	-36134.900	2822.600	-33477.900	71.000	0.	0.
4	138.750	1963.600	-9868.000	1659.300	-30996.600	393.900	0.	0.
5	183.750	3334.600	-36164.100	2575.900	-32902.500	139.900	0.	0.
6	228.750	1099.000	27197.000	597.000	14771.600	-726.500	0.	0.
7	273.750	2752.800	-26238.900	2070.600	-19734.900	-148.800	0.	0.
8	318.750	2221.900	-6204.400	1712.000	-33842.800	-276.600	0.	0.

... Continued

TABLE 1.8-2 TEMPERATURE FORCES AND MOMENTS
FOR CRACKED CONCRETE - LINER INCLUDED

Units (lb/in, in-lb/in)

FORCES AND MOMENTS FOR INSIDE TEMPERATURE 100.0F

SECTION NO.	SECTION ANGLE	FS	MT	FT	MS	FNS	FNT	FST
1	3.750	3.800	-33014.900	145.800	-26823.500	-44.500	0.	0.
2	48.750	69.100	-22873.700	-337.500	-39881.700	55.100	0.	0.
3	93.750	27.900	-27061.700	59.300	-23854.800	25.600	0.	0.
4	138.750	-35.300	-30189.700	-206.700	-40001.100	128.200	0.	0.
5	183.750	-16.300	-33780.500	-96.600	-29466.800	37.600	0.	0.
6	228.750	-270.200	-23290.600	-506.500	-31435.200	-229.100	0.	0.
7	273.750	-75.300	-24477.700	-149.200	-20064.200	-41.400	0.	0.
8	318.750	-36.500	-38346.000	-188.400	-46591.800	-85.100	0.	0.

FORCES AND MOMENTS FOR INSIDE TEMPERATURE 140.0F

SECTION NO.	SECTION ANGLE	FS	MT	FT	MS	FNS	FNT	FST
1	3.750	8.800	-77022.800	339.600	-62589.000	-99.400	0.	0.
2	48.750	91.000	-49843.800	-787.000	-93044.400	-50.600	0.	0.
3	93.750	66.100	-63142.100	139.000	-55663.300	52.900	0.	0.
4	138.750	-82.000	-70425.400	-482.300	-93337.600	274.400	0.	0.
5	183.750	-37.600	-78820.800	-225.300	-68750.500	103.800	0.	0.
6	228.750	-629.700	-54314.400	-1181.300	-79351.800	-520.800	0.	0.
7	273.750	-176.400	-57114.500	-348.600	-46822.700	-107.400	0.	0.
8	318.750	-85.200	-89471.000	-439.500	-108696.700	-194.800	0.	0.

FORCES AND MOMENTS FOR INSIDE TEMPERATURE 168.0F

SECTION NO.	SECTION ANGLE	FS	MT	FT	MS	FNS	FNT	FST
1	3.750	12.300	-107838.500	475.900	-87625.300	-129.000	0.	0.
2	48.750	127.300	-69781.000	-1102.600	-130275.600	-37.100	0.	0.
3	93.750	92.500	-88399.200	-193.700	-77931.200	78.000	0.	0.
4	138.750	-114.800	-98590.400	-676.200	-130694.400	393.900	0.	0.
5	183.750	-52.700	-110409.600	-314.600	-96259.400	139.900	0.	0.
6	228.750	-882.700	-76218.200	-1653.800	-102681.500	-726.500	0.	0.
7	273.750	-247.200	-79964.300	-486.900	-65539.700	-148.800	0.	0.
8	318.750	-119.100	-125256.400	-614.500	-152159.301	-276.600	0.	0.

TABLE 1.8-3 DEAD LOAD FORCES AND MOMENTS FOR CRACKED CONCRETE

FORCES AND MOMENTS,(LB/IN,IN LB/IN)

D.L CONC. CRK. SECTION NUMBER 1

ANGLE	FS	MT	FT	MS	FNS	FNT	FST
0.	-1514.2818	-22031.3516	149.8132	-4555.6917	-28.1153	0.	0.

FORCES AND MOMENTS,(LB/IN,IN-LB/IN)

D.L CONC. CRK. SECTION NUMBER 2

ANGLE	FS	MT	FT	MS	FNS	FNT	FST
0.	-543.7111	-17643.0764	173.0475	7261.7942	-389.2667	0.	0.

FORCES AND MOMENTS,(LB/IN,IN-LB/IN)

D.L CONC. CRK. SECTION NUMBER 3

ANGLE	FS	MT	FT	MS	FNS	FNT	FST
0.	-268.2796	10356.7773	230.7150	2023.8264	67.0508	0.	0.

D.L CONC. CRK. SECTION NUMBER 4

ANGLE	FS	MT	FT	MS	FNS	FNT	FST
0.	-1052.1921	-32033.2085	-230.8619	-13325.6577	492.8980	0.	0.

FORCES AND MOMENTS,(LB/IN,IN-LB/IN)

D.L CONC. CRK. SECTION NUMBER 5

ANGLE	FS	MT	FT	MS	FNS	FNT	FST
0.	-1923.8658	-32961.1206	-818.2662	-12732.0387	-273.2509	0.	0.

FORCES AND MOMENTS,(LB/IN,IN-LB/IN)

D.L CONC. CRK. SECTION NUMBER 6

ANGLE	FS	MT	FT	MS	FNS	FNT	FST
0.	-756.1282	-26212.3860	124.0891	4485.6633	-898.6187	0.	0.

... Continued

TABLE 1.8-3 Continued

FORCES AND MOMENTS,(LB/IN,IN-LB/IN)

D.L CONC. CRK. SECTION NUMBER 7

ANGLE	FS	MT	FT	MS	FNS	FNT	FST
0.	85.0246	988.1900	165.8738	1579.4380	2.5704	0.	0.

FORCES AND MOMENTS,(LB/IN,IN-LB/IN)

D.L CONC. CRK. SECTION NUMBER 8

ANGLE	FS	MT	FT	MS	FNS	FNT	FST
0.	-2003.4904	-23223.2734	31.9980	153.7503	1586.3318	0.	0.

TABLE 1.8-4 UNIT HYDROSTATIC FORCES AND MOMENTS FOR CRACKED CONCRETE

FORCES AND MOMENTS,(LB/IN,IN-LB/IN)

HYDR. CONC. CRK. SECTION NUMBER 1

ANGLE	FS	MT	FT	MS	FNS	FNT	FST
0.	2.0359	-18.7177	17.4099	80.7817	-4.4158	0.	0.

FORCES AND MOMENTS,(LB/IN,IN-LB/IN)

HYDR. CONC. CRK. SECTION NUMBER 2

ANGLE	FS	MT	FT	MS	FNS	FNT	FST
0.	2.1406	212.4204	7.9699	338.0582	-0.6746	0.	0.

FORCES AND MOMENTS,(LB/IN,IN-LB/IN)

HYDR. CONC. CRK. SECTION NUMBER 3

ANGLE	FS	MT	FT	MS	FNS	FNT	FST
0.	0.9076	116.2919	6.9167	50.2561	2.1429	0.	0.

HYDR. CONC. CRK. SECTION NUMBER 4

ANGLE	FS	MT	FT	MS	FNS	FNT	FST
0.	-1.6577	-107.7558	3.8797	40.2728	2.7357	0.	0.

FORCES AND MOMENTS,(LB/IN,IN-LB/IN)

HYDR. CONC. CRK. SECTION NUMBER 5

ANGLE	FS	MT	FT	MS	FNS	FNT	FST
0.	-2.2531	-149.0354	3.0865	-0.1969	-0.9120	0.	0.

FORCES AND MOMENTS,(LB/IN,IN-LB/IN)

HYDR. CONC. CRK. SECTION NUMBER 6

ANGLE	FS	MT	FT	MS	FNS	FNT	FST
0.	28.3706	1216.2444	17.1145	774.3642	-31.3939	0.	0.

... Continued

TABLE 1.8-4 Continued

FORCES AND MOMENTS,(LB/IN,IN-LB/IN)

HYDR. CONC. CRK. SECTION NUMBER 7

ANGLE	FS	MT	FT	MS	FNS	FNT	FST
0.	69.0150	509.7685	31.4635	386.2129	1.6912	0.	0.

FORCES AND MOMENTS,(LB/IN,IN-LB/IN)

HYDR. CONC. CRK. SECTION NUMBER 8

ANGLE	FS	MT	FT	MS	FNS	FNT	FST
0.	0.9595	206.6263	24.9024	790.1612	23.5549	0.	0.

TABLE 1.8-5 UNIT PRESSURE FORCES AND MOMENTS FOR CRACKED CONCRETE

FORCES AND MOMENTS, (LB/IN, IN-LB/IN)

UNIT PRESSURE SECTION NUMBER 1

ANGLE	FS	MT	FT	MS	FNS	FNT	FST
0.	153.1689	685.5799	99.4032	778.5754	-3.1350	0.	0.

FORCES AND MOMENTS, (LB/IN, IN-LB/IN)

UNIT PRESSURE SECTION NUMBER 2

ANGLE	FS	MT	FT	MS	FNS	FNT	FST
0.	153.3745	5937.1799	94.5466	3798.0466	0.4682	0.	0.

FORCES AND MOMENTS, (LB/IN, IN-LB/IN)

UNIT PRESSURE SECTION NUMBER 3

ANGLE	FS	MT	FT	MS	FNS	FNT	FST
0.	172.8462	813.1804	87.6809	816.3145	1.7397	0.	0.

UNIT PRESSURE SECTION NUMBER 4

ANGLE	FS	MT	FT	MS	FNS	FNT	FST
0.	201.0454	5903.0883	73.4852	2275.8600	1.2735	0.	0.

FORCES AND MOMENTS, (LB/IN, IN-LB/IN)

UNIT PRESSURE SECTION NUMBER 5

ANGLE	FS	MT	FT	MS	FNS	FNT	FST
0.	211.1465	1672.9324	55.7592	883.1847	3.9152	0.	0.

FORCES AND MOMENTS, (LB/IN, IN-LB/IN)

UNIT PRESSURE SECTION NUMBER 6

ANGLE	FS	MT	FT	MS	FNS	FNT	FST
0.	184.5615	7528.3807	64.1777	3008.8639	-6.2226	0.	0.

... Continued

TABLE 1.8-5 Continued

FORCES AND MOMENTS,(LB/IN,IN-LB/IN)

UNIT PRESSURE SECTION NUMBER 7

ANGLE	FS	MT	FT	MS	FNS	FNT	FST
0.	161.3472	1208.3343	93.2975	986.1703	1.0784	0.	0.

FORCES AND MOMENTS,(LB/IN,IN-LB/IN)

UNIT PRESSURE SECTION NUMBER 8

ANGLE	FS	MT	FT	MS	FNS	FNT	FST
0.	148.5886	5168.5341	97.0492	3501.8200	-5.9892	0.	0.

TABLE 1.8-6 SINGLE UNIT S/RV FORCES AND MOMENTS FOR CRACKED CONCRETE

FORCES AND MOMENTS, (LB/IN, IN-LB/IN)

S/RV CONC. CRK. SECTION NUMBER 1

ANGLE	FS	MT	FT	MS	FNS	FNT	FST
0.	2.4090	2.3714	8.9095	30.0692	-3.4713	0.	0.
22.5000	-0.1987	-26.5910	2.6858	14.3481	-0.7114	-0.1915	-1.3085
45.0000	0.4347	-22.1306	1.9738	8.3106	-0.5550	-0.0257	0.4022
67.5000	0.2337	-18.5670	2.2847	8.4341	-0.7281	-0.0040	0.6025
90.0000	0.1021	-15.1504	2.3705	9.7234	-0.6952	-0.0233	0.3207
112.5000	0.1869	-10.9672	2.4481	10.3656	-0.6555	-0.0257	0.1420
135.0000	0.3054	-7.6330	2.5076	10.3183	-0.6598	-0.0191	0.0904
157.5000	0.2127	-6.3673	2.3830	10.1464	-0.5697	-0.0150	0.0493
180.0000	0.0835	-6.4207	2.2374	10.0353	-0.4739	0.0000	0.0000

FORCES AND MOMENTS, (LB/IN, IN-LB/IN)

S/RV CONC. CRK. SECTION NUMBER 2

ANGLE	FS	MT	FT	MS	FNS	FNT	FST
0	2.6591	144.9840	2.2895	105.9638	-0.2357	0.	0.
22.5000	0.0597	32.9738	1.5880	67.8408	-0.2884	2.0448	0.3234
45.0000	0.1360	21.7343	0.6350	33.5195	-0.2964	0.7342	0.3462
67.5000	0.3456	28.7085	0.9490	44.1331	-0.2827	0.2009	0.3547
90.0000	0.3259	29.5784	1.2954	55.0176	-0.2134	0.2167	0.1981
112.5000	0.2836	28.1544	1.3839	56.7173	-0.1534	0.2378	0.1453
135.0000	0.2869	27.5680	1.3629	54.9849	-0.1208	0.1880	0.0988
157.5000	0.2193	24.2160	1.3556	54.0917	-0.1027	0.1215	0.0393
180.0000	0.1415	20.9004	1.3625	54.0155	-0.0959	-0.0000	-0.0000

FORCES AND MOMENTS, (LB/IN, IN-LB/IN)

S/RV CONC. CRK. SECTION NUMBER 3

ANGLE	FS	MT	FT	MS	FNS	FNT	FST
0.	1.2203	45.7064	-0.1031	8.1563	0.8866	0.	0.
22.5000	0.3993	39.5774	1.2452	10.6403	0.3631	0.1953	1.5370
45.0000	0.0216	30.7197	1.0408	8.6063	0.1624	0.0760	0.9997
67.5000	0.3681	28.4481	1.1875	10.0875	0.2092	0.0534	0.6209
90.0000	0.2819	24.1933	1.3512	10.1347	0.2589	0.0602	0.4507
112.5000	0.1255	19.7376	1.2734	8.9444	0.2611	0.0481	0.3651
135.0000	0.0670	16.7900	1.1697	8.0380	0.2501	0.0334	0.2807
157.5000	0.0344	15.0343	1.1542	7.7410	0.2335	0.0207	0.1697
180.0000	0.0108	14.3768	1.1804	7.7528	0.2216	-0.0000	-0.0000

... Continued

TABLE 1.8-6 Continued

FORCES AND MOMENTS,(LB/IN,IN-LB/IN)

S/RV CONC. CRK. SECTION NUMBER 4

ANGLE	FS	MT	FT	MS	FNS	FNT	FST
0.	-0.7715	-14.3927	-2.4681	-74.0065	0.7835	0.	0.
22.5000	-0.5238	-11.2306	-1.0919	-37.7739	0.2966	-0.9210	1.2101
45.0000	0.2964	11.0030	0.5852	-2.4130	0.2562	-0.7950	1.4046
67.5000	0.1541	4.5920	1.0635	9.4728	0.4205	-0.5779	0.9285
90.0000	-0.0975	-6.3826	0.8236	6.9548	0.3915	-0.5528	0.8707
112.5000	-0.1572	-10.5066	0.5822	4.6918	0.3406	-0.4764	0.7179
135.0000	-0.1479	-11.2633	0.5043	4.8001	0.3271	-0.3383	0.4993
157.5000	-0.1385	-11.5145	0.5392	6.7415	0.3097	-0.1790	0.2625
180.0000	-0.1412	-11.8373	0.5745	8.0950	0.2930	0.0000	-0.0000

FORCES AND MOMENTS,(LB/IN,IN-LB/IN)

S/RV CONC. CRK. SECTION NUMBER 5

ANGLE	FS	MT	FT	MS	FNS	FNT	FST
0.	-1.7916	-97.5041	-8.6969	-98.5769	2.3158	0.	0.
22.5000	-1.4025	-75.0066	-6.1132	-47.3051	0.7532	-0.2332	-0.9845
45.0000	0.1164	-46.0324	-1.5175	-18.5307	0.6955	-0.0338	-0.1004
57.5000	-0.1410	-40.3855	-0.6564	-12.2663	0.3995	-0.0109	1.2278
90.0000	-0.0856	-33.4820	-0.6955	-8.8145	0.1786	-0.0299	1.2223
112.5000	0.0579	-26.8825	-0.4601	-5.6576	0.1031	-0.0390	0.8123
135.0000	0.1094	-22.5628	-0.1353	-3.5718	0.0802	-0.0286	0.4701
157.5000	0.0892	-19.5175	0.1558	-0.4029	-0.0102	-0.0218	0.2212
180.0000	0.0648	-18.1337	0.2804	1.8065	-0.0895	0.0000	-0.0000

FORCES AND MOMENTS,(LB/IN,IN-LB/IN)

S/RV CONC. CRK. SECTION NUMBER 6

ANGLE	FS	MT	FT	MS	FNS	FNT	FST
0.	10.7526	410.5197	-8.1846	-343.8544	-18.5766	0.	0.
22.5000	10.6173	417.1676	-1.0322	-24.4359	-29.8557	0.6392	-6.7557
45.0000	5.9679	245.8432	2.1759	100.5337	-17.3398	-0.3180	-0.9894
67.5000	5.3855	225.3908	1.7966	83.9646	-8.3198	-0.1361	0.8323
90.0000	5.1490	216.4222	1.7102	81.6408	-5.2843	0.0659	0.6414
112.5000	4.4635	189.5914	1.8876	88.1276	-3.6415	0.0633	0.5323
135.0000	3.8023	163.8358	2.0717	94.2458	-2.2440	0.0615	0.1917
157.5000	3.4137	148.6688	2.2322	100.9841	-1.5236	0.0908	-0.1724
180.0000	3.2942	143.9755	2.3329	105.8197	-1.4576	-0.0000	-0.0000

... Continued

TABLE 1.8-6 Continued

FORCES AND MOMENTS, (LB/IN, IN-LB/IN)

S/RV CONC. CRK. SECTION NUMBER 7

ANGLE	FS	MT	FT	MS	FNS	FNT	FST
0.	56.9856	369.8042	4.2572	129.8142	1.5517	0.	0.
22.5000	26.5068	189.8317	9.8322	129.6385	0.6821	0.2652	-4.7546
45.0000	15.8339	112.7542	5.4826	73.6870	0.3467	0.1365	-0.0740
67.5000	11.9285	84.7902	4.0019	54.2895	0.1561	0.1027	0.9835
90.0000	8.9347	65.5255	3.8815	48.4426	0.0728	0.0674	0.5485
112.5000	7.2471	54.1247	3.5650	42.8589	0.0611	0.0355	0.1078
135.0000	6.3204	47.3018	3.1337	37.4455	0.0685	0.0244	0.0528
157.5000	5.1452	39.8949	3.1454	35.6607	0.0494	0.0191	0.0847
180.0000	4.3554	35.3179	3.3359	36.1014	0.0337	0.0000	0.0000

FORCES AND MOMENTS, (LB/IN, IN-LB/IN)

S/RV CONC. CRK. SECTION NUMBER 8

ANGLE	FS	MT	FT	MS	FNS	FNT	FST
0.	-2.5819	77.9239	10.0138	213.2235	19.7226	0.	0.
22.5000	2.5260	163.0289	4.3391	200.5473	6.6699	-0.3604	-2.3791
45.0000	0.8131	116.3779	3.4249	126.1679	6.2749	-0.2478	0.2427
67.5000	0.0947	91.2473	3.3402	111.4361	6.1105	-0.0604	0.9799
90.0000	0.3004	81.8337	3.1394	111.6619	4.6981	0.0176	0.5940
112.5000	0.2945	67.7528	3.1441	107.4352	3.8338	0.0165	0.0866
135.0000	0.1243	54.3991	3.2218	101.1191	3.5146	0.0112	0.0823
157.5000	0.1396	46.2725	3.0456	97.8225	2.8706	0.0245	0.2019
180.0000	0.2344	43.5828	2.8552	97.3878	2.3231	0.0000	0.0000

TABLE 1.8-7 UNIT HORIZONTAL EARTHQUAKE FORCES AND MOMENTS FOR CRACKED CONCRETE

FORCES AND MOMENTS, (LB/IN, IN-LB/IN)

$U_\theta = 0.0$

HEQ. CRK. REV. 3 SECTION NUMBER 1

ANGLE	FS	MT	FT	MS	FNS	FNT	FST
0.	-277.1154	-6161.6882	1072.6819	3248.1588	282.7402	0.	0.
22.5000	-256.0213	-5692.6576	991.0288	3000.9073	261.2179	-38.9951	-271.7621
45.0000	-195.9502	-4356.9714	758.5006	2296.7950	199.9278	-72.0535	-502.1509
67.5000	-106.0475	-2357.9758	410.4976	1243.0164	108.2000	-94.1425	-656.0918
90.0000	0.0000	0.0003	-0.0000	-0.0001	-0.0000	-101.8991	-710.1487
112.5000	106.0475	2357.9764	-410.4977	-1243.0168	-108.2000	-94.1425	-656.0918
135.0000	195.9502	4356.9719	-758.5007	-2296.7952	-199.9275	-72.0535	-502.1509
157.5000	256.0213	5692.6578	-991.0289	-3000.9075	-261.2179	-38.9951	-271.7621
180.0000	277.1154	6161.6882	-1072.6819	-3248.1588	-282.7402	0.0000	0.0001

FORCES AND MOMENTS, (LB/IN, IN-LB/IN)

HEQ. CRK. REV. 3 SECTION NUMBER 2

ANGLE	FS	MT	FT	MS	FNS	FNT	FST
0.	718.6658	7354.5905	1407.6108	50330.5654	-672.5719	0.	0.
22.5000	663.9606	6794.7557	1300.4628	46499.3799	-621.3754	-329.7966	306.2270
45.0000	508.1734	5200.4808	995.3311	35589.0840	-475.5802	-609.3846	565.8337
67.5000	275.0215	2814.4798	538.6693	19260.6721	-257.3821	-796.1994	739.2973
90.0000	-0.0000	-0.0003	-0.0001	-0.0022	0.0000	-861.8000	800.2096
112.5000	-275.0215	-2814.4805	-538.6694	-19260.6768	257.3822	-796.1993	739.2973
135.0000	-508.1735	-5200.4814	-995.3312	-35589.0869	475.5802	-609.3846	565.8336
157.5000	-663.9606	-6794.7560	-1300.4628	-46499.3813	621.3754	-329.7965	306.2269
180.0000	-718.6658	-7354.5905	-1407.6108	-50330.5654	672.5719	0.0001	-0.0001

FORCES AND MOMENTS, (LB/IN, IN-LB/IN)

HEQ. CRK. REV. 3 SECTION NUMBER 3

ANGLE	FS	MT	FT	MS	FNS	FNT	FST
0.	503.3124	14338.8594	1479.3943	12292.3345	-237.4906	0.	0.
22.5000	465.0000	13247.3785	1366.7821	11356.6361	-219.4127	28.2940	667.2590
45.0000	355.8956	10139.1044	1046.0897	8691.9929	-167.9312	52.2806	1232.9339
67.5000	192.6093	5487.2435	566.1396	4704.0724	-90.8837	68.3078	1610.9058
90.0000	-0.0000	-0.0006	-0.0001	-0.0005	0.0000	73.9359	1743.6319
112.5000	-192.6094	-5487.2449	-566.1398	-4704.0735	90.8837	68.3078	1610.9057
135.0000	-355.8956	-10139.1053	-1046.0898	-8691.9937	167.9312	52.2806	1232.9338
157.5000	-465.0000	-13247.3790	-1366.7821	-11356.6366	219.4127	28.2940	667.2589
180.0000	-503.3124	-14338.8594	-1479.3943	-12292.3345	237.4906	-0.0000	-0.0002

... Continued

TABLE 1.8-7 Continued

FORCES AND MOMENTS,(LB/IN,IN-LB/IN)

$U_\theta = 0.0$

HEQ. CRK. REV. 3 SECTION NUMBER 4

ANGLE	FS	MT	FT	MS	FNS	FNT	FST
0.	-124.4391	21432.7629	1745.3733	41318.2769	-405.6130	0.	0.
22.5000	-114.9668	19801.2905	1612.5146	38173.1104	-374.7375	-441.9549	1489.8668
45.0000	-87.9917	15155.2517	1234.1652	29216.4336	-286.8117	-816.6262	2752.9149
67.5000	-47.6208	8201.9626	667.9254	15811.8190	-155.2214	-1066.9736	3596.8566
90.0000	0.0000	-0.0009	-0.0001	-0.0018	0.0000	-1154.8838	3893.2095
112.5000	47.6208	-8201.9647	-667.9255	-15811.8228	155.2214	-1066.9735	3596.8564
135.0000	87.9918	-15155.2529	-1234.1653	-29216.4358	286.8117	-816.6261	2752.9146
157.5000	114.9668	-19801.2915	-1612.5147	-38173.1113	374.7376	-441.9548	1489.8665
180.0000	124.4391	-21432.7629	-1745.3733	-41318.2769	405.6130	0.0001	-0.0003

FORCES AND MOMENTS,(LB/IN,IN-LB/IN)

HEQ. CRK. REV. 3 SECTION NUMBER 5

ANGLE	FS	MT	FT	MS	FNS	FNT	FST
0.	-1757.6439	-30545.9631	459.5048	-1998.9399	412.4096	0.	0.
22.5000	-1623.8512	-28220.7896	424.5271	-1846.7796	381.0168	21.6724	2387.7277
45.0000	-1242.8419	-21599.2573	324.9190	-1413.4639	291.6176	40.0453	4411.9456
67.5000	-672.6211	-11689.4330	175.8449	-764.9611	157.8223	52.3217	5764.4846
90.0000	0.0001	0.0013	-0.0000	0.0001	-0.0000	56.6326	6239.4332
112.5000	672.6213	11689.4359	-175.8449	764.9613	-157.8223	52.3217	5764.4844
135.0000	1242.8420	21599.2593	-324.9190	1413.4641	-291.6176	40.0453	4411.9451
157.5000	1623.8513	28220.7910	-424.5271	1846.7797	-381.0168	21.6723	2387.7272
180.0000	1757.6439	30545.9631	-459.5048	1998.9399	-412.4096	-0.0000	-0.0005

FORCES AND MOMENTS,(LB/IN,IN-LB/IN)

HEQ. CRK. REV. 3 SECTION NUMBER 6

ANGLE	FS	MT	FT	MS	FNS	FNT	FST
0.	-2628.2217	-101561.8682	395.0423	13164.1235	-1580.7644	0.	0.
22.5000	-2428.1602	-93830.9297	364.9715	12162.0642	-1460.4359	6203.8356	-3751.7040
45.0000	-1858.4333	-71815.0850	279.3371	9308.4408	-1117.7692	11463.1934	-6932.2451
67.5000	-1005.7768	-38866.0415	151.1761	5037.6917	-604.9323	14977.3838	-9057.4146
90.0000	0.0001	0.0044	-0.0000	-0.0006	0.0001	16211.4033	-9803.6747
112.5000	1005.7771	38866.0508	-151.1762	-5037.6929	604.9324	14977.3832	-9057.4142
135.0000	1858.4335	71815.0908	-279.3371	-9308.4417	1117.7693	11463.1924	-6932.2444
157.5000	2428.1603	93830.9336	-364.9715	-12162.0647	1460.4359	6203.8344	-3751.7032
180.0000	2628.2217	101561.8682	-395.0423	-13164.1235	1580.7644	-0.0014	0.0009

... Continued

TABLE 1.8-7 Continued

FORCES AND MOMENTS,(LB/IN,IN-LB/IN)

$U_\theta = 0.0$

HEQ. CRK. REV. 3 SECTION NUMBER 7

ANGLE	FS	MT	FT	MS	FNS	FNT	FST
0.	1146.7560	8773.8633	621.1985	7279.9621	-62.2871	0.	0.
22.5000	1059.4644	8105.9928	573.9126	6725.8079	-57.5458	-52.9248	-1446.0793
45.0000	810.8789	6204.0582	439.2537	5147.7104	-44.0437	-97.7922	-2672.0061
67.5000	438.8445	3357.6120	237.7224	2785.9206	-23.8363	-127.7717	-3491.1441
90.0000	-0.0001	-0.0004	-0.0000	-0.0003	0.0000	-138.2990	-3778.7871
112.5000	-438.8446	-3357.6128	-237.7224	-2785.9213	23.8363	-127.7716	-3491.1440
135.0000	-810.8790	-6204.0588	-439.2537	-5147.7109	44.0437	-97.7922	-2672.0059
157.5000	-1059.4644	-8105.9930	-573.9126	-6725.8081	57.5458	-52.9247	-1446.0790
180.0000	-1146.7560	-8773.8633	-621.1985	-7279.9621	62.2871	0.0000	0.0003

FORCES AND MOMENTS,(LB/IN,IN-LB/IN)

HEQ. CRK. REV. 3 SECTION NUMBER 8

ANGLE	FS	MT	FT	MS	FNS	FNT	FST
0.	300.4830	43232.1670	718.8830	27244.7393	1289.3660	0.	0.
22.5000	277.6101	39941.3140	664.1613	25170.8567	1191.2189	-162.8762	-845.9820
45.0000	212.4736	30569.7581	508.3271	19264.9397	911.7194	-300.9560	-1563.1709
67.5000	114.9899	16544.2327	275.1046	10426.1095	493.4190	-393.2179	-2042.3811
90.0000	-0.0000	-0.0019	-0.0000	-0.0012	-0.0001	-425.6160	-2210.6574
112.5000	-114.9899	-16544.2368	-275.1047	-10426.1122	-493.4191	-393.2179	-2042.3810
135.0000	-212.4736	-30569.7600	-508.3271	-19264.9412	-911.7195	-300.9559	-1563.1707
157.5000	-277.6101	-39941.3159	-664.1614	-25170.8577	-1191.2189	-162.8762	-845.9818
180.0000	-300.4830	-43232.1670	-718.8830	-27244.7393	-1289.3660	0.0000	0.0002

... Continued

TABLE 1.8-7 UNIT HORIZONTAL EARTHQUAKE FORCES AND MOMENTS FOR CRACKED CONCRETE

FORCES AND MOMENTS, (LB/IN, IN-LB/IN)

$U_R = 0.0$

HEQ. CONC. CRK. SECTION NUMBER 1

ANGLE	FS	MT	FT	MS	FNS	FNT	FST
0.	5.3439	-26081.4451	-3461.0668	-18482.0327	779.4719	0.	0.
22.5000	4.9371	-24096.1133	-3197.6088	-17075.1721	720.1381	-5.5171	710.7914
45.0000	3.7787	-18442.3665	-2447.3438	-13068.7705	551.1698	-10.1942	1313.3712
67.5000	2.2450	-9980.9363	-1324.4928	-7072.7675	298.2910	-13.3194	1716.0021
90.0000	-0.0000	0.0011	0.0002	0.0008	-0.0000	-14.4168	1857.3873
112.5000	-2.0450	9980.9386	1324.4932	7072.7691	-298.2910	-13.3194	1716.0021
135.0000	-3.7787	18442.3679	2447.3440	13068.7716	-551.1699	-10.1942	1313.3711
157.5000	-4.9372	24096.1140	3197.6089	17075.1726	-720.1381	-5.5171	710.7912
180.0000	-5.3439	26081.4451	3461.0668	18482.0327	-779.4719	0.0000	-0.0002

FORCES AND MOMENTS, (LB/IN, IN-LB/IN)

HEQ. CONC. CRK. SECTION NUMBER 2

ANGLE	FS	MT	FT	MS	FNS	FNT	FST
0.	741.0028	-16129.6531	-2089.4269	-76837.2627	-815.0858	0.	0.
22.5000	684.5973	-14901.8560	-1930.3787	-70988.3750	-753.0411	-591.3628	1183.4547
45.0000	523.9681	-11405.3870	-1477.4479	-54332.1489	-576.3527	-1092.6960	2186.7391
67.5000	283.5695	-6172.5504	-799.5890	-29404.3452	-311.9198	-1427.6761	2857.1122
90.0000	-0.0000	0.0007	0.0001	0.0034	0.0000	-1545.3055	3092.5160
112.5000	-283.5695	6172.5519	799.5892	29404.3525	311.9199	-1427.6760	2857.1121
135.0000	-523.9681	11405.3878	1477.4480	54332.1538	576.3527	-1092.6959	2186.7388
157.5000	-684.5973	14901.8571	1930.3788	70988.3779	753.0411	-591.3627	1183.4544
180.0000	-741.0028	16129.6531	2089.4269	76837.2627	815.0858	0.0001	-0.0003

FORCES AND MOMENTS, (LB/IN, IN-LB/IN)

HEQ. CONC. CRK. SECTION NUMBER 3

ANGLE	FS	MT	FT	MS	FNS	FNT	FST
0.	711.2783	11633.3586	-1791.2436	-5856.6533	-551.9483	0.	0.
22.5000	657.1355	10747.8220	-1654.8932	-5410.8420	-509.9337	57.1863	1829.5548
45.0000	502.9497	8226.0267	-1266.6005	-4141.2794	-390.2864	105.6665	3380.5766
67.5000	272.1944	4451.8932	-685.4792	-2241.2440	-211.2214	138.0599	4416.9360
90.0000	-0.0000	-0.0005	0.0001	0.0003	0.0000	149.4349	4780.8571
112.5000	-272.1945	-4451.8944	685.4793	2241.2446	211.2215	138.0599	4416.9359
135.0000	-502.9497	-8226.0275	1266.6006	4141.2796	390.2864	105.6664	3380.5762
157.5000	-657.1355	-10747.8224	1654.8933	5410.8423	509.9337	57.1863	1829.5545
180.0000	-711.2783	-11633.3586	1791.2436	5856.6533	551.9483	-0.0000	-0.0004

... Continued

TABLE 1.8-7 Continued

FORCES AND MOMENTS, (LB/IN, IN-LB/IN)

$U_R = 0.0$

HEQ. CONC. CRK. SECTION NUMBER 4

ANGLE	FS	MT	FT	MS	FNS	FNT	FST
0.	-102.3423	42756.6250	-1670.2393	-41205.0796	-817.4975	0.	0.
22.5000	-94.5519	39501.9712	-1543.0999	-38068.5293	-755.2692	-678.7903	2983.3715
45.0000	-72.3669	30233.4988	-1181.0375	-29136.3906	-578.0580	-1254.2408	5512.5518
67.5000	-39.1647	16362.2509	-639.1729	-15768.5000	-312.8427	-1638.7446	7202.4959
90.0000	0.0000	-0.0019	0.0001	0.0018	0.0000	-1773.7644	7795.9253
112.5000	39.1647	-16362.2548	639.1730	15768.5040	312.8428	-1638.7445	7202.4956
135.0000	72.3669	-30233.5015	1181.0376	29136.3931	578.0581	-1254.2407	5512.5513
157.5000	94.5519	-39501.9727	1543.0999	38068.5313	755.2692	-678.7901	2983.3709
180.0000	102.3423	-42756.6250	1670.2393	41205.0795	817.4975	0.0002	-0.0007

FORCES AND MOMENTS, (LB/IN, IN-LB/IN)

HEQ. CONC. CRK. SECTION NUMBER 5

ANGLE	FS	MT	FT	MS	FNS	FNT	FST
0.	-3077.1163	-63707.4121	-6556.6980	-63351.7158	1713.0645	0.	0.
22.5000	-2842.8848	-58857.9736	-6057.5991	-58529.3535	1582.6652	127.5716	3592.4513
45.0000	-2175.8498	-45047.9424	-4636.2855	-44796.4277	1211.3195	235.7216	6637.9846
67.5000	-1177.5614	-24379.7693	-2509.1395	-24243.6501	655.5613	307.9851	8672.9446
90.0000	0.0001	0.0028	0.0003	0.0028	-0.0001	333.3607	9387.5275
112.5000	1177.5616	24379.7754	2509.1401	24243.6563	-655.5615	307.9851	8672.9442
135.0000	2175.8499	45047.9458	4636.2859	44796.4312	-1211.3196	235.7216	6637.9839
157.5000	2842.8849	58857.9756	6057.5993	58529.3560	-1582.6653	127.5716	3592.4506
180.0000	3077.1163	63707.4121	6556.6980	63351.7158	-1713.0645	-0.0000	-0.0008

FORCES AND MOMENTS, (LB/IN, IN-LB/IN)

HEQ. CONC. CRK. SECTION NUMBER 6

ANGLE	FS	MT	FT	MS	FNS	FNT	FST
0.	-3105.0021	-160341.8164	-7927.1468	-345870.4883	-21797.2759	0.	0.
22.5000	-2868.6478	-148136.5195	-7323.7286	-319542.6680	-20138.0569	-936.8832	2523.0874
45.0000	-2195.5680	-113378.7803	-5605.3292	-244567.3652	-15413.0013	-1731.1344	4662.0577
67.5000	-1188.2328	-61360.1514	-3033.5875	-132358.8984	-8341.4558	-2261.8361	6091.2718
90.0000	0.0001	0.0070	0.0003	0.0151	0.0010	-2448.1937	6593.1451
112.5000	1188.2330	61360.1670	3033.5883	132358.9297	8341.4578	-2261.8360	6091.2716
135.0000	2195.5681	113378.7939	5605.3397	244567.3867	15413.0027	-1731.1342	4662.0572
157.5000	2868.6479	148136.5273	7323.7289	319542.6797	20138.0579	-936.8830	2523.0869
180.0000	3105.0021	160341.8164	7927.1468	345870.4883	21797.2759	0.0002	-0.0006

... Continued

TABLE 1.8-7 Continued

FORCES AND MOMENTS,(LB/IN,IN-LB/IN)

$U_R = 0.0$

HEQ. CONC. CRK. SECTION NUMBER 7

ANGLE	FS	MT	FT	MS	FNS	FNT	FST
0.	5409.1672	22707.9023	-4750.6995	-31927.4980	47.4547	0.	0.
22.5000	4997.4188	20979.3665	-4389.0740	-29497.1621	43.8424	34.1427	889.9140
45.0000	3824.8587	16056.9111	-3359.2518	-22576.1504	33.5555	63.0874	1644.3467
67.5000	2069.9985	8689.9375	-1818.0139	-12218.1235	18.1601	82.4277	2148.4425
90.0000	-0.0002	-0.0010	0.0002	0.0014	-0.0000	89.2191	2325.4573
112.5000	-2069.9990	-8689.9396	1818.0143	12218.1268	-18.1601	82.4277	2148.4424
135.0000	-3824.8590	-16056.9126	3359.2521	22576.1521	-33.5555	63.0874	1644.3465
157.5000	-4997.4191	-20979.3667	4389.0742	29497.1628	-43.8424	34.1427	889.9138
180.0000	-5409.1672	-22707.9023	4750.6995	31927.4980	-47.4547	-0.0000	-0.0002

FORCES AND MOMENTS,(LB/IN,IN-LB/IN)

HEQ. CONC. CRK. SECTION NUMBER 8

ANGLE	FS	MT	FT	MS	FNS	FNT	FST
0.	1815.9551	118487.6719	-4757.4427	-126194.7666	1767.1093	0.	0.
22.5000	1677.7238	109468.3330	-4395.3039	-116588.7617	1632.5961	-315.2886	585.4835
45.0000	1284.0742	83783.4346	-3364.0199	-89233.1758	1249.5349	-582.5774	1081.8324
67.5000	694.9359	45343.2651	-1820.5944	-48292.6431	676.2434	-761.1741	1413.4822
90.0000	-0.0001	-0.0052	0.0002	0.0055	-0.0001	-823.8889	1529.9421
112.5000	-694.9361	-45343.2764	1820.5948	48292.6548	-676.2436	-761.1740	1413.4821
135.0000	-1284.0743	-83783.4414	3364.0202	89233.1816	-1249.5350	-582.5774	1081.8323
157.5000	-1677.7239	-109468.3379	4395.3041	116588.7656	-1632.5962	-315.2886	585.4834
180.0000	-1815.9551	-118487.6719	4757.4427	126194.7666	-1767.1093	0.0001	-0.0001

... Continued

TABLE 1.9-1 TYPICAL FORCES AND MOMENTS FOR ALL LOADING COMBINATIONS
CRACKED CONCRETE

TOTAL FORCES AND MOMENTS ,POSITIVE.

BRUNSWICK TORUS LOAD COMBINATIONS CRK — TEMPERATURE EXCLUDED
SECTION NUMBER 1 ANGLE OF SECTION 3.750 MOMENTS UNIT IN-K/FT FORCES UNIT K/FT

LOAD CASE	FS	MT	FT	MS	FNS	FNT	FST
1	-23.837	-323.515	13.256	-31.406	1.915	0.146	1.261
2	-14.394	-186.035	14.264	-4.817	2.143	0.172	7.459
3	-14.503	-191.657	13.159	-9.874	1.788	0.153	7.973
4	38.022	-14.680	39.320	235.583	-2.967	0.	0.
5	38.103	-13.779	39.910	238.322	-2.817	0.006	0.044
6	38.213	-12.920	40.958	243.182	-2.552	0.	0.
7	39.202	25.594	46.938	267.016	-0.640	0.122	1.051
8	39.283	26.495	47.529	269.754	-0.490	0.128	1.095
9	39.393	27.355	48.576	274.615	-0.224	0.122	1.051
10	33.463	-10.213	38.217	212.938	-1.970	0.044	5.639
11	29.401	-23.139	36.169	192.947	-1.651	0.055	7.132
12	33.535	-9.419	38.736	215.348	-1.838	0.049	5.678
13	29.466	-22.418	36.642	195.138	-1.531	0.061	7.168
14	33.632	-8.663	39.658	219.626	-1.604	0.044	5.639
15	29.554	-21.730	37.480	199.026	-1.318	0.055	7.132
16	34.335	23.037	44.920	240.324	0.078	0.151	6.564
17	30.345	9.080	42.264	218.093	0.211	0.153	7.973
18	34.574	26.022	45.440	243.009	0.210	0.157	6.603
19	30.410	9.802	42.736	220.284	0.331	0.158	8.008
20	34.670	26.778	46.362	247.287	0.443	0.151	6.564
21	30.498	10.489	43.574	224.173	0.543	0.153	7.973
22	57.321	71.703	51.845	333.684	-3.717	0.	0.
23	57.403	72.604	52.435	336.422	-3.567	0.006	0.044
24	57.513	73.464	53.483	341.283	-3.302	0.	0.
25	58.501	111.977	59.463	365.116	-1.390	0.122	1.051
26	58.583	112.878	60.053	367.855	-1.240	0.128	1.095
27	58.693	113.738	61.101	372.716	-0.975	0.122	1.051
28	50.447	65.805	49.239	299.267	-2.673	0.044	5.639
29	44.840	45.968	46.189	271.427	-2.322	0.055	7.132
30	50.519	66.598	49.758	301.677	-2.541	0.049	5.678
31	44.906	46.689	46.661	273.618	-2.202	0.061	7.168
32	50.615	67.354	50.680	305.954	-2.307	0.044	5.639

... Continued

TABLE 1.9-1 Continued

TOTAL FORCES AND MOMENTS ,POSITIVE.

BRUNSWICK TORUS LOAD COMBINATIONS CRK — TEMPERATURE EXCLUDED

SECTION NUMBER 1 ANGLE OF SECTION 3.750 MOMENTS UNIT IN-K/FT FORCES UNIT K/FT

LOAD CASE	FS	MT	FT	MS	FNS	FNT	FST
33	44.993	47.376	47.499	277.507	-1.990	0.055	7.132
34	51.485	101.246	55.943	326.928	-0.625	0.151	6.564
35	45.784	78.187	52.284	296.573	-0.460	0.153	7.973
36	51.557	102.039	56.462	329.337	-0.493	0.157	6.603
37	45.850	78.908	52.756	298.764	-0.341	0.158	8.008
38	51.654	102.795	57.384	333.615	-0.259	0.151	6.564
39	45.937	79.596	53.594	302.653	-0.128	0.153	7.973
40	81.905	181.738	67.799	458.645	-3.206	0.	0.
41	48.467	35.826	52.386	316.201	-1.439	0.	0.
42	47.753	29.413	46.173	287.372	-3.015	0.006	0.044
43	47.863	30.272	47.220	292.233	-2.749	0.	0.
44	62.393	97.535	56.591	362.995	-2.110	0.038	0.259
45	35.643	-19.195	44.260	249.040	-0.828	0.038	0.259
46	35.072	-24.325	39.290	225.976	-2.088	0.043	0.295
47	35.160	-23.638	40.128	229.865	-1.876	0.038	0.259
48	72.080	162.636	63.278	409.233	-2.102	0.044	5.639
49	64.507	133.996	58.953	371.396	-1.711	0.055	7.132
50	42.655	34.233	49.715	283.882	-0.625	0.044	5.639
51	37.757	17.266	46.622	257.442	-0.428	0.055	7.132
52	36.770	5.060	40.836	231.792	-1.904	0.049	5.678
53	37.186	12.136	41.651	234.378	-1.689	0.061	7.168
54	42.124	29.346	45.169	262.790	-1.778	0.044	5.639
55	37.274	12.823	42.490	238.267	-1.476	0.055	7.132
56	64.365	128.970	59.557	373.495	-1.329	0.078	5.385
57	64.984	139.261	60.717	377.350	-1.023	0.093	7.391
58	37.615	12.240	47.227	259.540	-0.047	0.078	5.385
59	38.234	22.531	48.386	263.395	0.259	0.093	7.391
60	37.043	7.110	42.256	236.476	-1.307	0.083	5.421
61	37.663	17.401	43.416	240.332	-1.002	0.098	7.427
62	37.131	7.797	43.094	240.365	-1.095	0.078	5.385
63	37.751	18.088	44.254	244.220	-0.789	0.093	7.391
64	-25.253	-371.844	4.114	-69.126	-1.411	0.	0.
65	-16.811	-223.718	10.862	-16.686	1.260	0.127	1.093

TABLE 1.9-2 TYPICAL FORCES AND MOMENTS
UNCRACKED CONCRETE

TOTAL FORCES AND MOMENTS ,POSITIVE.

BRUNSWICK TORUS LOAD COMBINATIONS,UNCRK. TEMP. EXCLUDED UNCRACKED
SECTION NUMBER 1 ANGLE OF SECTION 3.750 MOMENTS UNIT IN-K/FT FORCES UNIT K/FT

LOAD CASE	FS	MT	FT	MS	FNS	FNT	FST
1	-23.732	-185.309	18.614	-24.521	2.239	0.054	0.815
2	-13.696	-66.096	19.557	-0.562	2.914	0.394	2.983
3	-13.881	-62.894	18.831	-0.452	2.934	0.424	3.108
4	-26.068	-207.030	10.705	-34.298	-0.699	0.	0.
5	-16.595	-129.054	14.501	-16.025	0.472	0.047	0.706

TOTAL FORCES AND MOMENTS ,NEGATIVE.

BRUNSWICK TORUS LOAD COMBINATIONS,UNCRK. TEMP. EXCLUDED UNCRACKED
SECTION NUMBER 1 ANGLE OF SECTION 3.750 MOMENTS UNIT IN-K/FT FORCES UNIT K/FT

LOAD CASE	FS	MT	FT	MS	FNS	FNT	FST
1	-28.404	-228.750	2.795	-44.075	-0.904	-0.054	-0.815
2	-23.544	-229.660	-4.265	-48.435	-4.693	-0.394	-2.983
3	-23.358	-232.863	-3.539	-48.545	-4.713	-0.424	-3.108
4	-26.068	-207.030	10.705	-34.298	-0.699	0.	0.
5	-20.645	-166.702	0.791	-32.972	-2.252	-0.047	-0.706

TABLE 1.9-3 TYPICAL SHEARING STRESSES AND FACTORS OF SAFETY

FACTOR OF SAFETY FOR SHEARING FORCES, POSITIVE. **

BRUNSWICK TORUS, SHEAR STRESS CHECK
SECTION NUMBER 1 ANGLE OF SECTION 3.750 SHEAR FORCES IN KIPS/FT NO TEMP. ONLY SHEAR DUE TO TEMP ADDED SHEAR STRESSES IN PSI

	RADIAL SHEAR S				RADIAL SHEAR T				TANGENTIAL SHEAR			
LOAD CASE	FNS	VUNS	VCNS	F.S.NS	FNT	VUNT	VCNT	F.S.NT	FST	VUT	VCT	F.S.T
1	1.92	4.72	188.39	39.92	0.15	0.36	102.39	284.12	1.26	3.11	80.72	25.99
2	2.14	5.28	198.39	37.57	0.17	0.42	101.84	240.84	7.46	18.38	80.72	4.39
3	1.79	4.40	198.44	45.05	0.15	0.38	102.44	271.97	7.97	19.65	80.72	4.11
4	-2.97	7.31	89.02	12.18	0.	0.	88.32	9999.00	0.	0.	80.72	9999.00
5	-2.82	6.94	88.97	12.82	0.01	0.02	88.00	5500.18	0.04	0.11	80.72	738.53
6	-2.55	6.29	88.92	14.14	0.	0.	87.43	9999.00	0.	0.	80.72	9999.00
7	-0.64	1.58	88.38	56.07	0.12	0.30	84.21	280.40	1.05	2.59	80.72	31.18
8	-0.49	1.21	88.34	73.16	0.13	0.32	83.89	265.21	1.09	2.70	80.72	29.92
9	-0.22	0.55	88.28	159.69	0.12	0.30	83.32	277.45	1.05	2.59	80.72	31.18
10	-1.97	4.85	91.48	18.85	0.04	0.11	88.91	824.43	5.64	13.89	80.72	5.81
11	-1.65	4.07	93.67	23.03	0.06	0.14	90.02	659.92	7.13	17.57	80.72	4.59
12	-1.84	4.53	91.44	20.19	0.05	0.12	88.63	726.93	5.68	13.99	80.72	5.77
13	-1.53	3.77	93.64	24.82	0.06	0.15	89.76	601.60	7.17	17.66	80.72	4.57
14	-1.60	3.95	91.39	23.12	0.04	0.11	88.14	817.21	5.64	13.89	80.72	5.81
15	-1.32	3.25	93.59	28.81	0.06	0.14	89.31	654.73	7.13	17.57	80.72	4.59
16	0.08	0.19	91.01	475.16	0.15	0.37	85.29	229.21	6.56	16.17	80.72	4.99
17	0.21	0.52	93.16	179.28	0.15	0.38	86.73	230.26	7.97	19.65	80.72	4.11
18	0.21	0.52	90.88	175.97	0.16	0.39	85.01	220.13	6.60	16.27	80.72	4.96
19	0.33	0.81	93.13	114.30	0.16	0.39	86.47	222.04	8.01	19.73	80.72	4.09
20	0.44	1.09	90.83	83.13	0.15	0.37	84.52	227.12	6.56	16.17	80.72	4.99
21	0.54	1.34	93.08	69.54	0.15	0.38	86.02	228.38	7.97	19.65	80.72	4.11
22	-3.72	9.16	78.60	8.58	0.	0.	81.56	9999.00	0.	0.	80.72	9999.00
23	-3.57	8.79	78.56	8.94	0.01	0.02	81.24	5077.58	0.04	0.11	80.72	738.53
24	-3.30	8.14	78.50	9.65	0.	0.	80.67	9999.00	0.	0.	80.72	9999.00
25	-1.39	3.42	77.96	22.76	0.12	0.30	77.44	257.88	1.05	2.59	80.72	31.18
26	-1.24	3.06	77.92	25.50	0.13	0.32	77.13	243.83	1.09	2.70	80.72	29.92
27	-0.97	2.40	77.86	32.42	0.12	0.30	76.56	254.94	1.05	2.59	80.72	31.18
28	-2.67	6.59	82.31	12.50	0.04	0.11	82.96	769.26	5.64	13.89	80.72	5.81
29	-2.32	5.72	85.34	14.92	0.06	0.14	84.61	620.26	7.13	17.57	80.72	4.59
30	-2.54	6.26	82.27	13.14	0.05	0.12	82.68	678.13	5.68	13.99	80.72	5.77
31	-2.20	5.43	85.30	15.72	0.06	0.15	84.35	565.35	7.17	17.66	80.72	4.57
32	-2.31	5.69	82.22	14.46	0.04	0.11	82.19	762.04	5.64	13.89	80.72	5.81

** FNS=SHEAR FORCE IN RADIAL S VUNS=STRESS IN RADIAL S VCNS=ALLOWABLE STRESS IN RADIAL S F.S.NS=FACTOR OF SAFETY
FNT=SHEAR FORCE IN RADIAL T VUNT=STRESS IN RADIAL T VCNT=ALLOWABLE STRESS IN RADIAL T F.S.NT=FACTOR OF SAFETY
FST=SHEAR FORCE IN TANGENT. VUT =STRESS IN TANGENT. VCT =ALLOWABLE STRESS IN TANGENT. F.S.T =FACTOR OF SAFETY

... Continued

TABLE 1.9-3 TYPICAL SHEARING STRESSES AND FACTORS OF SAFETY

FACTOR OF SAFETY FOR SHEARING FORCES, POSITIVE. **

SECTION NUMBER 1 ANGLE OF SECTION 3.750 SHEAR FORCES IN KIPS/FT SHEAR STRESSES IN PSI

	RADIAL SHEAR S				RADIAL SHEAR T				TANGENTIAL SHEAR			
LOAD CASE	FNS	VUNS	VCNS	F.S.NS	FNT	VUNT	VCNT	F.S.NT	FST	VUT	VCT	F.S.T
33	-1.99	4.90	85.26	17.39	0.06	0.14	83.90	615.08	7.13	17.57	80.72	4.59
34	-0.62	1.54	81.75	53.09	0.15	0.37	79.34	213.22	6.56	16.17	80.72	4.99
35	-0.46	1.13	84.83	74.79	0.15	0.38	81.32	215.90	7.97	19.65	80.72	4.1.
36	-0.49	1.22	81.71	67.24	0.16	0.39	79.06	204.72	6.60	16.27	80.72	4.96
37	-0.34	0.84	84.79	101.05	0.16	0.39	81.06	208.15	8.01	19.73	80.72	4.09
38	-0.26	0.64	81.66	127.77	0.15	0.37	78.57	211.13	6.56	16.17	80.72	4.99
39	-0.13	0.32	84.75	268.73	0.15	0.38	80.61	214.02	7.97	19.65	80.72	4.11
40	-3.21	7.90	65.33	8.27	0.	0.	72.94	9999.00	0.	0.	80.72	9999.00
41	-1.44	3.55	83.38	23.52	0.	0.	81.26	9999.00	0.	0.	80.72	9999.00
42	-3.01	7.43	83.77	11.28	0.01	0.02	84.62	5288.88	0.04	0.11	80.72	738.53
43	-2.75	6.77	83.71	12.36	0	0.	84.05	9999.00	0.	0.	80.72	9999.00
44	-2.11	5.20	75.86	14.59	0.04	0.09	78.99	845.33	0.26	0.64	80.72	126.45
45	-0.83	2.04	90.30	44.28	0.04	0.09	85.65	916.57	0.26	0.64	80.72	126.45
46	-2.09	5.15	90.61	17.61	0.04	0.11	88.33	831.40	0.29	0.73	80.72	111.21
47	-1.88	4.62	90.56	19.59	0.04	0.09	87.88	940.44	0.26	0.64	80.72	126.45
48	-2.10	5.18	70.63	13.64	0.04	0.11	75.38	698.98	5.64	13.89	80.72	5.81
49	-1.71	4.21	74.72	17.73	0.06	0.14	77.72	569.75	7.13	17.57	80.72	4.59
50	-0.63	1.54	86.52	56.15	0.04	0.11	82.71	766.87	5.64	13.89	80.72	5.81
51	-0.43	1.06	89.16	84.48	0.06	0.14	84.38	618.55	7.13	17.57	80.72	4.59
52	-1.90	4.69	89.69	19.11	0.05	0.12	87.50	717.63	5.68	13.99	80.72	5.77
53	-1.69	4.16	89.47	21.50	0.06	0.15	87.06	583.47	7.17	17.66	80.72	4.57
54	-1.78	4.38	86.80	19.81	0.04	0.11	85.16	789.63	5.64	13.89	80.72	5.81
55	-1.48	3.64	89.42	24.58	0.06	0.14	86.61	634.90	7.13	17.57	80.72	4.59
56	-1.33	3.27	74.80	22.85	0.08	0.19	77.39	404.16	5.39	13.27	80.72	6.08
57	-1.02	2.52	74.46	29.53	0.09	0.23	76.77	333.98	7.39	18.21	80.72	4.43
58	-0.05	0.11	89.24	778.31	0.08	0.19	84.05	438.92	5.39	13.27	80.72	6.08
59	0.26	0.64	88.90	139.32	0.09	0.23	83.42	362.94	7.39	18.21	80.72	4.43
60	-1.31	3.22	89.55	27.80	0.08	0.20	86.73	424.56	5.42	13.36	80.72	6.04
61	-1.00	2.47	89.21	36.14	0.10	0.24	86.11	354.85	7.43	18.30	80.72	4.41
62	-1.09	2.70	89.50	33.18	0.08	0.19	86.28	450.57	5.39	13.27	80.72	6.08
63	-0.79	1.94	89.17	45.85	0.09	0.23	85.65	372.64	7.39	18.21	80.72	4.43
64	-1.41	3.48	129.61	37.27	0.	0.	107.32	9999.00	0.	0.	80.72	9999.00
65	1.26	3.10	199.49	64.28	0.13	0.31	103.68	331.97	1.09	2.69	80.72	29.98

** FNS=SHEAR FORCE IN RADIAL S VUNS=STRESS IN RADIAL S VCNS=ALLOWABLE STRESS IN RADIAL S F.S.NS=FACTOR OF SAFETY
FNT=SHEAR FORCE IN RADIAL T VUNT=STRESS IN RADIAL T VCNT=ALLOWABLE STRESS IN RADIAL T F.S.NT=FACTOR OF SAFETY
FST=SHEAR FORCE IN TANGENT. VUT =STRESS IN TANGENT. VCT =ALLOWABLE STRESS IN TANGENT. F.S.T =FACTOR OF SAFETY

TABLE 1.9-4 TYPICAL STRESSES IN THE REINFORCING BARS AND THE LINER

STRESS IN LINER AND REBARS, POSITIVE

BRUNSWICK TORUS ANALYSIS
SECTION NUMBER 1 ANGLE OF SECTION 3.750 STRESS UNIT KSI

LOAD CASE	TEMPERATURE IS NOT INCLUDED						TEMPERATURE IS INCLUDED					
	WITH LINER				NO LINER		WITH LINER				NO LINER	
	BAR		LINER		BAR		BAR		LINER		BAR	
	S-STRESS	T-STRESS	S-STRESS	T-STRESS	S-STRESS	T-STRESS	S-STRESS	T-STRESS	S-STRESS	T-STRESS	S-STRESS	T-STRESS
1	-0.69	4.31	-4.68	0.79	-5.96	5.89	-0.69	4.31	-4.68	0.79	-5.96	5.89
2	-0.50	4.15	-2.75	1.10	-3.60	6.34	2.97	10.07	-5.82	-1.47	-0.21	11.64
3	-0.47	3.92	-2.81	0.97	-3.63	5.85	3.00	9.84	-5.88	-1.61	-0.23	11.15
4	5.74	7.23	3.34	5.12	9.51	17.48	13.83	21.05	-3.82	-0.88	17.42	29.85
5	5.75	7.36	3.36	5.19	9.53	17.74	13.83	21.17	-3.81	-0.81	17.44	30.11
6	5.76	7.57	3.38	5.32	9.55	18.20	13.84	21.39	-3.79	-0.69	17.47	30.58
7	5.57	8.87	3.76	5.99	9.80	20.86	13.65	22.69	-3.40	-0.01	17.72	33.23
8	5.57	9.00	3.78	6.06	9.82	21.12	13.66	22.81	-3.39	0.06	17.74	33.50
9	5.58	9.21	3.80	6.19	9.85	21.59	13.66	23.03	-3.37	0.19	17.76	33.96
10	5.03	7.30	2.96	4.8[illegible]	8.37	16.99	13.12	21.12	-4.20	-1.16	16.28	29.36
11	4.54	7.05	2.49	4.51	7.35	16.08	12.63	20.87	-4.67	-1.49	15.27	28.45
12	5.03	7.41	2.98	4.90	8.38	17.22	13.12	21.22	-4.19	-1.10	16.30	29.59
13	4.55	7.15	2.51	4.57	7.37	16.29	12.63	20.97	-4.66	-1.43	15.28	28.66
14	5.04	7.60	2.99	5.01	8.41	17.63	13.13	21.41	-4.17	-0.99	16.32	30.00
15	4.55	7.32	2.52	4.67	7.39	16.66	12.64	21.14	-4.64	-1.34	15.30	29.03
16	4.87	8.75	3.30	5.61	8.58	19.96	12.96	22.56	-3.86	-0.39	16.50	32.34
17	4.40	8.37	2.83	5.21	7.59	18.78	12.49	22.18	-4.33	-0.79	15.50	31.16
18	4.88	8.85	3.35	5.67	8.64	20.20	12.96	22.67	-3.82	-0.33	16.56	32.57
19	4.40	8.46	2.84	5.26	7.60	18.99	12.49	22.28	-4.32	-0.74	15.52	31.37
20	4.89	9.04	3.36	5.78	8.67	20.61	12.97	22.86	-3.80	-0.22	16.58	32.98
21	4.41	8.64	2.86	5.36	7.62	19.37	12.50	22.45	-4.31	-0.64	15.54	31.74
22	7.84	9.15	5.77	6.95	14.33	23.04	19.16	28.49	-4.26	-1.46	25.41	40.37
23	7.84	9.27	5.79	7.02	14.35	23.30	19.16	28.61	-4.25	-1.39	25.43	40.63
24	7.85	9.49	5.80	7.14	14.38	23.77	19.17	28.83	-4.23	-1.26	25.46	41.09
25	7.66	10.79	6.19	7.82	14.63	26.43	18.98	30.13	-3.84	-0.58	25.71	43.75
26	7.66	10.91	6.21	7.89	14.65	26.69	18.99	30.25	-3.83	-0.51	25.73	44.01
27	7.67	11.13	6.22	8.01	14.67	27.16	19.00	30.47	-3.81	-0.39	25.76	44.48
28	6.87	8.99	5.10	6.45	12.61	21.88	18.20	28.33	-4.93	-1.95	23.69	39.21
29	6.22	8.59	4.44	5.97	11.21	20.53	17.54	27.93	-5.60	-2.43	22.29	37.85
30	6.88	9.09	5.11	6.51	12.63	22.11	18.20	28.44	-4.92	-1.89	23.71	39.44
31	6.22	8.68	4.45	6.03	11.23	20.74	17.54	28.03	-5.58	-2.37	22.31	38.06
32	6.89	9.28	5.13	6.62	12.65	22.52	18.21	28.63	-4.90	-1.78	23.74	39.85

... Continued

TABLE 1.9-4 Continued

STRESS IN LINER AND REBARS, POSITIVE

BRUNSWICK TORUS ANALYSIS
SECTION NUMBER 1 ANGLE OF SECTION 3.750 STRESS UNIT KSI

LOAD CASE	TEMPERATURE IS NOT INCLUDED						TEMPERATURE IS INCLUDED					
	WITH LINER				NO LINER		WITH LINER				NO LINER	
	BAR		LINER		BAR		BAR		LINER		BAR	
	S-STRESS	T-STRESS	S-STRESS	T-STRESS	S-STRESS	T-STRESS	S-STRESS	T-STRESS	S-STRESS	T-STRESS	S-STRESS	T-STRESS
33	6.23	8.86	4.46	6.13	11.25	21.11	17.55	28.20	-5.57	-2.28	22.33	38.44
34	6.72	10.43	5.47	7.22	12.87	24.86	18.04	29.77	-4.56	-1.19	23.95	42.19
35	6.08	9.90	4.77	6.67	11.45	23.24	17.40	29.24	-5.26	-1.73	22.53	40.56
36	6.72	10.54	5.48	7.28	12.89	25.09	18.04✓	29.88	-4.55	-1.12	23.97✓	42.42✓
37	6.08	10.00	4.78	6.73	11.46	23.45	17.40	29.34	-5.25	-1.68	22.54	40.77
38	6.73	10.73	5.50	7.39	12.91	25.50	18.05	30.07✓	-4.53	-1.01	24.00	42.83
39	6.09	10.17	4.80	6.82	11.48	23.82	17.41	29.51	-5.23	-1.58	22.57	41.14
40	10.51✓	11.59✓	8.86✓	9.27✓	20.48✓	30.13✓	13.97	17.51	5.79	6.70	23.87	35.44
41	6.84	9.60	4.69	6.84	12.12	23.28	14.93	23.41	-2.48	0.84	20.03	35.66
42	6.79	8.31	4.57	6.10	11.94	20.52	14.88	22.13	-2.59	0.10	19.85	32.89
43	6.80	8.53	4.59	6.23	11.97	20.99	14.89	22.34	-2.58	0.23	19.88	33.36
44	8.36	10.01	6.43	7.57	15.60	25.15	11.83	15.93	3.36	5.00	18.99	30.46
45	5.43	8.41	3.09	5.63	8.91	19.67	13.52	22.23	-4.07	-0.37	16.83	32.04
46	5.39	7.39	3.00	5.04	8.77	17.46	13.48	21.20	-4.16	-0.96	16.68	29.84
47	5.40	7.56	3.01	5.14	8.79	17.83	13.48	21.37	-4.15	-0.86	16.71	30.21
48	9.22	11.13	7.82	8.50	18.02	28.12	12.69	17.05	4.75	5.92✓	21.41	33.43
49	8.36	10.54	6.91	7.83	16.13	26.20	11.82	16.46	3.84	5.26	19.52	31.50
50	6.00	9.38	4.15	6.36	10.66	22.10	14.09	23.20	-3.02	0.36	18.58	34.47
51	5.42	8.95	3.57	5.89	9.44	20.72	13.51	22.76	-3.60	-0.11	17.35	33.09
52	5.39	7.73	3.38	5.21	9.19	18.15	13.47	21.54	-3.78	-0.79	17.11	30.52
53	5.38	7.92	3.48	5.30	9.30	18.51	13.47	21.73	-3.69	-0.70	17.21	30.89
54	5.96	8.44	4.06	5.82	10.53	20.08	14.05	22.26	-3.10	-0.18	18.45	32.45
55	5.39	8.09	3.49	5.40	9.32	18.88	13.48	21.91	-3.67	-0.61	17.23	31.26
56	8.38	10.67	6.86	7.90	16.09	26.47	11.84	16.60	3.79	5.33	19.48	31.77
57	8.38	10.94	6.99	8.02	16.25	26.99	11.85	16.86	3.92	5.45	19.64	32.29
58	5.45	9.08	3.52	5.95	9.40	20.99	13.53	22.90	-3.65	-0.05	17.32	33.36
59	5.45	9.35	3.65	6.08	9.56	21.50	13.54	23.16	-3.51	0.08	17.47	33.88
60	5.41	8.05	3.42	5.36	9.26	18.78	13.49	21.87	-3.74	-0.64	17.18	31.15
61	5.41	8.32	3.56	5.49	9.42	19.30	13.50	22.13	-3.60	-0.51	17.33	31.67
62	5.41	8.23	3.44	5.46	9.28	19.15	13.50	22.04	-3.73	-0.54	17.20	31.53
63	5.42	8.49	3.57	5.59	9.44	19.67	13.50	22.31	-3.59	-0.41	17.35	32.04
64	-0.48	2.34	-5.18	-0.25	-6.31	1.83	2.98	8.26	-8.25✓	-2.83✓	-2.92	7.13
65	-0.53	3.38	-3.27	0.73	-4.20	4.83	2.94	9.30	-6.34	-1.85	-0.81	10.13

TABLE 1.9-5

SUMMARY OF THE MAXIMUM NORMAL STRESSES IN THE REINFORCING BARS AND THE LINER

Unit Ksi

Temp.	Case	Location	Bar Stresses		Liner Stresses	
			Meridional	Hoop	Meridional	Hoop
No Temperature	40	1	10.51	11.59	8.86	9.27
	40	1	20.48	30.13 *	0.0	0.0
	40	6	6.26	4.03	16.04	7.87
	40	6	17.28	19.77	0.0	0.0
	27	7	9.04	5.34	19.45 *	10.85 *
	27	7	26.14 *	27.03	0.0	0.0
	40	8	4.74	15.62	11.74	6.71
	40	8	17.17	29.04	0.0	0.0
With Temperature	27	1	19.0	30.47	-3.81	-0.39
	27	1	25.76	44.48 *	0.0	0.0
	25	1	19.34 *	26.85	-4.68	-2.33
	25	1	25.12	36.98	0.0	0.0
	35	4	11.17	15.37	-2.92	-10.66 *
	2	5	1.65	2.92	-9.74 *	-5.65
	27	7	14.84	15.97	12.19	4.23
	27	7	32.59 *	38.07	0.0	0.0
	27	8	11.99	38.55 *	-0.17	-7.06
	27	8	18.42	36.84	0.0	0.0

* Maximum Stresses

TABLE 1.10-1
LINER AND REINFORCING BARS STRESSES IN THE VICINITY
OF THE VENT OPENINGS FOR TWO DIFFERENT MODELS
(WITH AND WITHOUT OPENINGS)**

Load Case	Element	Stress Type	Stress in Ksi (No Opening) Location	Stress	Average Stress	Stress in Ksi (With Opening)	% Change
Internal Pressure of 62 psi	Reinforcing	Meridional	4	11.88	11.90	12.0	1.0
			5	11.92			
		Hoop	4	5.72	5.26	8.0	52.0
			5	4.80			
	Liner	Meridional	4	13.53	13.59	18.5	36.0
			5	13.64			
		Hoop	4	9.10	8.4	12.5	48.8
			5	7.70			
0.9D + 1.5P + 1.0T P = 62.0 T = 240°	Reinforcing	Meridional	4	21.7	23.0	27.0	17.4
			5	24.2			
		Hoop	4	12.2	12.2	18.0	47.5
			5	15.9	15.9	28.0	76.0
	Liner	Meridional	4	17.5	14.75	15.0	1.7
			5	12.0			
		Hoop	4	9.0	7.1	11.0	54.9
			5	5.2			

** Stresses obtained from References 15 and 16 (dated 1970 and 1971) where hydrodynamic loads were not included in the analyses.

TABLE 1.10-2
STRESS IN LINER AND REINFORCING BARS DUE TO HYDRODYNAMIC LOADS

Unit Ksi

BRUNSWICK TP.US , HYDRODYNAMIC LOADS
SECTION NU ER 4 ANGLE OF SECTION 138.750

TEMPERATURE IS NOT INCLUDED

LOAD CASE	WITH LINER				NO LINER	
	BAR		LINER		BAR	
	S-STRESS	T-STRESS	S-STRESS	T-STRESS	S-STRESS	T-STRESS
1	0.02	0.69	0.17	0.05	0.14	0.75
2	0.02	0.58	0.14	0.04	0.11	0.63
3	0.02	0.46	0.11	0.04	0.09	0.50
4	0.	0.	0.	0.	0.	0.
5	-0.01	0.03	0.02	0.00	0.01	0.03
6	-0.02	0.12	0.06	-0.02	0.02	0.10
7	0.02	0.58	0.14	0.04	0.11	0.63
8	0.01	0.61	0.16	0.05	0.12	0.66
9	0.00	0.70	0.20	0.02	0.14	0.72
10	0.	0.	0.	0.	0.	0.
11	0.	0.	0.	0.	0.	0.
12	-0.01	0.03	0.02	0.00	0.01	0.03
13	-0.01	0.03	0.02	0.00	0.01	0.03
14	-0.02	0.11	0.05	-0.02	0.02	0.08
15	-0.01	0.10	0.05	-0.02	0.02	0.08
16	0.02	0.51	0.12	0.04	0.10	0.55
17	0.02	0.46	0.11	0.04	0.09	0.50
18	0.01	0.54	0.14	0.04	0.11	0.58
19	0.01	0.49	0.13	0.04	0.10	0.53
20	0.00	0.62	0.18	0.02	0.12	0.64
21	0.00	0.56	0.16	0.02	0.11	0.58
22	0.	0.	0.	0.	0.	0.
23	-0.01	0.03	0.02	0.00	0.01	0.03
24	-0.02	0.12	0.06	-0.02	0.02	0.10
25	0.02	0.58	0.14	0.04	0.11	0.63
26	0.01	0.61	0.16	0.05	0.12	0.66
27	0.00	0.70	0.20	0.02	0.14	0.72
28	0.	0.	0.	0.	0.	0.
29	0.	0.	0.	0.	0.	0.
30	-0.01	0.03	0.02	0.00	0.01	0.03
31	-0.01	0.03	0.02	0.00	0.01	0.03
32	-0.02	0.11	0.05	-0.02	0.02	0.08

Continued ....

TABLE 1.10-2
STRESS IN LINER AND REINFORCING BARS
DUE TO HYDRODYNAMIC LOADS

Unit Ksi

BRUNSWICK TORUS . HYDRODYNAMIC LOADS
SECTION NUMBER 4 ANGLE OF SECTION 138.750

TEMPERATURE IS NOT INCLUDED

LOAD CASE	WITH LINER				NO LINER	
	BAR		LINER		BAR	
	S-STRESS	T-STRESS	S-STRESS	T-STRESS	S-STRESS	T-STRESS
33	-0.01	0.10	0.05	-0.02	0.02	0.08
34	0.02	0.51	0.12	0.04	0.10	0.55
35	0.02	0.46	0.11	0.04	0.09	0.50
36	0.01	0.54	0.14	0.04	0.11	0.58
37	0.01	0.49	0.13	0.04	0.10	0.53
38	0.00	0.62	0.18	0.02	0.12	0.64
39	0.00	0.56	0.16	0.02	0.11	0.58
40	0.	0.	0.	0.	0.	0.
41	-0.08	0.51	0.26	-0.10	0.09	0.40
42	-0.01	0.03	0.02	0.00	0.01	0.03
43	-0.02	0.12	0.06	-0.02	0.02	0.10
44	0.02	0.07	0.00	0.05	0.02	0.13
45	-0.04	0.48	0.21	-0.02	0.10	0.45
46	0.01	0.09	0.02	0.05	0.03	0.16
47	0.01	0.17	0.05	0.03	0.04	0.21
48	0.	0.	0.	0.	0.	0.
49	0.	0.	0.	0.	0.	0.
50	-0.07	0.45	0.23	-0.09	0.08	0.35
51	-0.06	0.41	0.21	-0.08	0.07	0.32
52	-0.01	0.03	0.02	0.00	0.01	0.03
53	-0.01	0.03	0.02	0.00	0.01	0.03
54	-0.02	0.11	0.05	-0.02	0.02	0.08
55	-0.01	0.10	0.05	-0.02	0.02	0.08
56	0.02	0.07	0.00	0.05	0.02	0.13
57	0.02	0.07	0.00	0.05	0.02	0.13
58	-0.04	0.48	0.21	-0.02	0.10	0.45
59	-0.04	0.48	0.21	-0.02	0.10	0.45
60	0.01	0.09	0.02	0.05	0.03	0.16
61	0.01	0.09	0.02	0.05	0.03	0.16
62	0.01	0.17	0.05	0.03	0.04	0.21
63	0.01	0.17	0.05	0.03	0.04	0.21
64	0.	0.	0.	0.	0.	0.
65	0.02	0.60	0.15	0.05	0.12	0.65

Continued ...

TABLE 1.10-2
STRESS IN LINER AND REINFORCING BARS
DUE TO HYDRODYNAMIC LOADS

Unit Ksi

BRUNSWICK TORUS , HYDRODYNAMIC LOADS
SECTION NUMBER 5 ANGLE OF SECTION 183.750

TEMPERATURE IS NOT INCLUDED

LOAD CASE	WITH LINER				NO LINER	
	BAR		LINER		BAR	
	S-STRESS	T-STRESS	S-STRESS	T-STRESS	S-STRESS	T-STRESS
1	-0.48	1.48	1.14	0.88	0.20	3.23
2	-0.40	1.23	0.95	0.73	0.17	2.69
3	-0.32	0.99	0.76	0.58	0.13	2.15
4	0.	0.	0.	0.	0.	0.
5	-0.02	0.05	0.04	0.04	0.01	0.13
6	-0.04	0.11	0.12	0.01	0.03	0.13
7	-0.40	1.23	0.95	0.73	0.17	2.69
8	-0.42	1.29	0.99	0.77	0.18	2.82
9	-0.44	1.34	1.07	0.74	0.20	2.82
10	0.	0.	0.	0.	0.	0.
11	0.	0.	0.	0.	0.	0.
12	-0.01	0.05	0.04	0.03	0.01	0.11
13	-0.01	0.04	0.03	0.03	0.01	0.10
14	-0.04	0.09	0.10	0.01	0.02	0.11
15	-0.03	0.08	0.09	0.01	0.02	0.10
16	-0.35	1.09	0.84	0.64	0.15	2.37
17	-0.32	0.99	0.76	0.58	0.13	2.15
18	-0.37	1.13	0.88	0.68	0.16	2.48
19	-0.33	1.03	0.80	0.62	0.14	2.26
20	-0.39	1.18	0.94	0.65	0.17	2.48
21	-0.35	1.07	0.86	0.59	0.16	2.26
22	0.	0.	0.	0.	0.	0.
23	-0.02	0.05	0.04	0.04	0.01	0.13
24	-0.04	0.11	0.12	0.01	0.03	0.13
25	-0.40	1.23	0.95	0.73	0.17	2.69
26	-0.42	1.29	0.99	0.77	0.18	2.82
27	-0.44	1.34	1.07	0.74	0.20	2.82
28	0.	0.	0.	0.	0.	0.
29	0.	0.	0.	0.	0.	0.
30	-0.01	0.05	0.04	0.03	0.01	0.11
31	-0.01	0.04	0.03	0.03	0.01	0.10
32	-0.04	0.09	0.10	0.01	0.02	0.11

Continued ...

TABLE 1.10-2
STRESS IN LINER AND REINFORCING BARS
DUE TO HYDRODYNAMIC LOADS

Unit Ksi

BRUNSWICK TORUS , HYDRODYNAMIC LOADS
SECTION NUMBER 5 ANGLE OF SECTION 183.750

TEMPERATURE IS NOT INCLUDED

LOAD CASE	WITH LINER BAR		LINER		NO LINER BAR	
	S-STRESS	T-STRESS	S-STRESS	T-STRESS	S-STRESS	T-STRESS
33	-0.03	0.08	0.09	0.01	0.02	0.10
34	-0.35	1.09	0.84	0.64	0.15	2.37
35	-0.32	0.99	0.76	0.58	0.13	2.15
36	-0.37	1.13	0.88	0.68	0.16	2.48
37	-0.33	1.03	0.80	0.62	0.14	2.26
38	-0.39	1.18	0.94	0.65	0.17	2.48
39	-0.35	1.07	0.86	0.59	0.16	2.26
40	0.	0.	0.	0.	0.	0.
41	-0.18	0.44	0.49	0.05	0.11	0.53
42	-0.02	0.05	0.04	0.04	0.01	0.13
43	-0.04	0.11	0.12	0.01	0.03	0.13
44	-0.05	0.31	0.17	0.23	0.05	0.77
45	-0.20	0.66	0.56	0.27	0.14	1.19
46	-0.07	0.35	0.20	0.26	0.06	0.87
47	-0.09	0.39	0.26	0.24	0.07	0.87
48	0.	0.	0.	0.	0.	0.
49	0.	0.	0.	0.	0.	0.
50	-0.16	0.38	0.43	0.04	0.10	0.46
51	-0.14	0.35	0.39	0.04	0.09	0.42
52	-0.01	0.05	0.04	0.03	0.01	0.11
53	-0.01	0.04	0.03	0.03	0.01	0.10
54	-0.04	0.09	0.10	0.01	0.02	0.11
55	-0.03	0.08	0.09	0.01	0.02	0.10
56	-0.05	0.31	0.17	0.23	0.05	0.77
57	-0.05	0.31	0.17	0.23	0.05	0.77
58	-0.20	0.66	0.56	0.27	0.14	1.19
59	-0.20	0.66	0.56	0.27	0.14	1.19
60	-0.07	0.35	0.20	0.26	0.06	0.87
61	-0.07	0.35	0.20	0.26	0.06	0.87
62	-0.09	0.39	0.26	0.24	0.07	0.87
63	-0.09	0.39	0.26	0.24	0.07	0.87
64	0.	0.	0.	0.	0.	0.
65	-0.42	1.28	0.99	0.76	0.17	2.80

TABLE 1.10-3

RECOMMENDED % CHANGE IN THE LINER AND REINFORCING BARS STRESSES DUE TO THE OPENINGS FOR USE IN THE PRESENT ANALYSIS

Reinforcing Bars	Meridional	20%
	Hoop	75%
Liner	Meridional	40%
	Hoop	55%

TABLE 1.10-4

TENSILE STRESSES IN THE LOCATIONS CLOSE TO THE OPENINGS OBTAINED FROM THE PRESENT ANALYSIS

Element	Type of Stress	Location	Ksi Max Stress (No opening)	Recommended Increase	Ksi Max Stress (with open)	Allowable Stress 0.9 F_y Ksi
Reinforcing Bars	Meridional	4	16.40	20%	19.68	45
		5	16.84	20%	20.21	45
	Hoop	4	19.14	75%	33.50	45
		5	24.48	75%	42.84	45
Liner	Meridional	4	13.18	40%	18.45	25.2
		5	11.17	40%	15.64	25.2
	Hoop	4	4.66	55%	7.22	25.2
		5	4.57	55%	7.08	25.2

TABLE 1.11-1

MAXIMUM STUDS DISPLACEMENT AS COMPARED TO THE ALLOWABLES

Case or Model Number	Deflection In Inches		
	Left	Right	Allowable*
1	0.022	0.019	
2	0.019	0.017	
3	0.027	0.025	0.084
4	0.025	0.022	

* Allowable Deflection = 1/2 of Ultimate Deflection

TABLE 1.11-2

STRAIN IN THE BUCKLED PANEL AS COMPARED TO THE ALLOWABLES

Case or Model Number	Strain (Bending & Membrane)	
	Compressive	Tensile
1	0.0061	0.0056
2	0.0095	0.0089
3	0.0025	0.0022
4	0.0039	0.0035
Allowable Strain	0.014	0.01

TABLE A.1-1

EFFECT OF FSI ON NATURAL FREQUENCIES OF BRUNSWICK CONCRETE TORUS

	Base Fully Restrained (I)			Radial Movement Allowed at Base (II)		
	Case IA	Case IB	% Change	Case IIA	Case IIB	% Change
1	28.30	28.35	-0.18	26.41	26.97	-2.08
2	33.41	33.45	-0.12	31.84	32.98	-3.46
3	51.66	52.0	-0.65	33.45	33.64	-0.56
4	66.21	66.33	-0.18	52.50	52.62	-0.23
5	78.38	78.44	-0.08	66.11	66.15	-0.06
6	88.13	91.44	-3.62	77.35	79.63	-2.86

Cases IA and IIA with FSI

Cases IB and IIB without FSI

All frequencies are in cycles/sec.

TABLE A.1-2

CONDENSATION OSCILLATION BASELINE RIGID WALL

TYPICAL PRESSURE AMPLITUDE ON TORUS BOTTOM DEAD CENTER *

FREQUENCY Hz.	AMPLITUDE	FREQUENCY Hz.	AMPLITUDE
1	.29	26	.25
2	.25	27	.57
3	.32	28	.13
4	.47	29	.19
5	1.18	30	.14
6	2.68	31	.08
7	.41	32	.03
8	.38	33	.03
9	.38	34	.03
10	.38	35	.05
11	.78	36	.08
12	.44	37	.10
13	.12	38	.07
14	.08	39	.06
15	.07	40	.09
16	.10	41	.33
17	.04	42	.33
18	.04	43	.33
19	.04	44	.33
20	.27	45	.33
21	.20	46	.33
22	.30	47	.33
23	.34	48	.33
24	.33	49	.33
25	.16	50	.33

* Refer to Figure A.1-19 for variation of pressure in the torus cross section

TABLE A.1-3

EFFECT OF FSI ON HYDRODYNAMIC PRESSURE (NODE 30016) *

TYPE I SUPPORT: (VERTICAL & RADIAL DISPLACEMENT RESTRAINED AT BASE)

FREQUENCY Hz	RIGID WALL PRESSURE	CHANGE IN PRESSURE DUE TO FSI	TOTAL HYDRODYNAMIC PRESSURE	% CHANGE
1	.29	.0000	.29	.00
2	.25	.0000	.25	.00
3	.32	.0000	.32	.00
4	.47	.0001	.4701	.02
5	1.18	.0003	1.1803	.03
6	2.68	.0010	2.6810	.04
7	.41	.0002	.4102	.05
8	.38	.0002	.3802	.05
9	.38	.0003	.3803	.08
10	.38	.0004	.3804	.11
11	.78	.0009	.7809	.12
12	.44	.0006	.4406	.14
13	.12	.0002	.1202	.17
14	.08	.0002	.0802	.25
15	.07	.0002	.0702	.29
16	.10	.0002	.1002	.20
17	.04	.0001	.0401	.25
18	.04	.0001	.0401	.25
19	.04	.0001	.0401	.25
20	.27	.0011	.2711	.41

* Bottom dead center of torus

TABLE A.1-3

EFFECT OF FSI ON HYDRODYNAMIC PRESSURE (NODE 30016)

TYPE I SUPPORT: (VERTICAL & RADIAL DISPLACEMENT RESTRAINED AT BASE)

FREQUENCY Hz	RIGID WALL PRESSURE	CHANGE IN PRESSURE DUE TO FSI	TOTAL HYDRODYNAMIC PRESSURE	% CHANGE
21	.20	.0009	.2009	.45
22	.30	.0015	.3015	.50
23	.34	.0019	.3419	.56
24	.33	.0020	.3320	.61
25	.16	.0011	.1611	0.69
26.4	.25	.0020	.2520	.80
27	.57	.0049	.5749	.86
28	.13	.0012	.1312	.92
29	.19	.0014	.1914	.74
30	.14	.0011	.1411	.79
31.84	.08	.0008	.0808	1.00
32	.03	.0003	.0303	1.00
33.45	.03	.0003	.0303	1.00
34	.03	.0003	.0303	1.00
35	.05	.0005	.0505	1.00
36	.08	.0009	.0809	1.13
37	.10	.0012	.1012	1.20
38	.07	.0013	.0713	1.86
39	.06	.0008	.0608	1.33
40	.09	.0013	.0913	1.44

TABLE A.1-3

EFFECT OF FSI ON HYDRODYNAMIC PRESSURE (NODE 30016)

TYPE I SUPPORT: (VERTICAL & RADIAL DISPLACEMENT RESTRAINED AT BASE)

FREQUENCY Hz	RIGID WALL PRESSURE	CHANGE IN PRESSURE DUE TO FSI	TOTAL HYDRODYNAMIC PRESSURE	% CHANGE
41	.33	.0050	.3350	1.52
42	.33	.0054	.3354	1.64
43	.33	.0057	.3357	1.73
44	.33	.0060	.3360	1.82
45	.33	.0063	.3363	1.91
46	.33	.0067	.3367	2.03
47	.33	.0070	.3370	2.12
48	.33	.0074	.3374	2.24
49	.33	.0078	.3378	2.36
50	.33	.0082	.3382	2.48

TABLE A.1-4

EFFECT OF FSI ON HYDRODYNAMIC PRESSURE (NODE = 30016) *
TYPE II SUPPORT: (RADIAL DISPLACEMENT NOT RESTRAINED AT BASE)

FREQUENCY HZ	RIGID WALL PRESSURE	CHANGE IN PRESSURE DUE TO FSI	TOTAL HYDRODYNAMIC PRESSURE	% CHANGE
1	0.29	0.0000	0.2900	0.00
2	0.25	0.0000	0.2500	0.00
3	0.32	0.0001	0.3201	0.03
4	0.47	0.0001	0.4701	0.02
5	1.18	0.0006	1.1806	0.05
6	2.68	0.0019	2.6819	0.07
7	0.41	0.0004	0.4104	0.10
8	0.38	0.0005	0.3805	0.13
9	0.38	0.0006	0.3806	0.16
10	0.38	0.0008	0.3808	0.21
11	0.78	0.0019	0.7819	0.24
12	0.44	0.0013	0.4413	0.30
13	0.12	0.0004	0.1204	0.33
14	0.08	0.0003	0.0803	0.38
15	0.07	0.0003	0.0703	0.43
16	0.10	0.0006	0.1006	0.60
17	0.04	0.0003	0.0403	0.75
18	0.04	0.0003	0.0403	0.75
19	0.04	0.0003	0.0403	0.75
20	0.27	0.0026	0.2726	0.96
21	0.20	0.0023	0.2023	1.15
22	0.30	0.0039	0.3039	1.30
23	0.34	0.0053	0.3453	1.56
24	0.33	0.0063	0.3363	1.91
25	0.16	0.0039	0.1639	2.44
26.4	0.25	0.0073	0.2573	2.92

* Bottom dead center of torus

TABLE A.1-4

EFFECT OF FSI ON HYDRODYNAMIC PRESSURE (NODE = 30016)

TYPE II SUPPORT: (RADIAL DISPLACEMENT NOT RESTRAINED AT BASE)

FREQUENCY ΔZ	RIGID WALL PRESSURE	CHANGE IN PRESSURE DUE TO FSI	TOTAL HYDRODYNAMIC PRESSURE	% CHANGE
27	0.57	0.0120	0.5820	2.11
28	0.13	0.0015	0.1315	1.15
29	0.19	0.0022	0.1922	1.16
30	0.14	0.0022	0.1422	1.57
31.84	0.08	0.0017	0.0817	2.13
32	0.03	0.0006	0.0306	2.00
33.45	0.03	0.0003	0.0303	1.00
34	0.03	0.0003	0.0303	1.00
35	0.05	0.0006	0.0506	1.20
36	0.08	0.0011	0.0811	1.38
37	0.10	0.0017	0.1017	1.70
38	0.07	0.0019	0.0719	2.71
39	0.06	0.0013	0.0613	2.17
40	0.09	0.0021	0.0921	2.33
41	0.33	0.0084	0.3384	2.55
42	0.33	0.0092	0.3392	2.79
43	0.33	0.0099	0.3399	3.00
44	0.33	0.0107	0.3407	3.24
45	0.33	0.0115	0.3415	3.48
46	0.33	0.0124	0.3424	3.76
47	0.33	0.0133	0.3433	4.03
48	0.33	0.0142	0.3442	4.30
49	0.33	0.0152	0.3452	4.61
50	0.33	0.0162	0.3462	4.91

TABLE A.1-5

EFFECT OF FSI ON DISPLACEMENTS

(DBA C.O. LOAD GIVEN IN TABLE A.1-2)

Boundary Condition: Radial Growth Restrained at Base (Type I Support)

Tabulated displacements are sum of absolute displacement amplitudes for different frequencies (1 to 50 Hz.)

Node	Radial Displacement x10^3* inch			Tangential Displacement x 10^3* inch		
	CASE IA	CASE IB	% CHANGE	CASE IA	CASE IB	% CHANGE
36	0.39	0.39	0.0	0.19	0.19	0.0
81	0.15	0.15	0.0	0.0	0.0	0.0
126	0.45	0.44	2.3	0.32	0.31	3.2
166	1.14	1.10	3.6	0.34	0.34	0.0
211	0.34	0.33	3.0	1.16	1.12	3.6
251	1.65	1.60	3.1	0.43	0.41	4.9
291	0.50	0.48	4.2	0.75	0.72	4.2

Case IA with FSI

Case IB without FSI

*Local cylindrical co-ordinate system with origin at the center of the torus.

TABLE A.1-6

EFFECT OF FSI ON DISPLACEMENTS

(DBA C.O. LOAD GIVEN IN TABLE A.1-2)
Boundary Condition: Radial Growth at Base Permitted (Type II Support)

Tabulated displacements are sum of absolute displacement amplitudes for different frequencies (1 to 50 Hz.)

	Radial Displacement $x10^3$ * inch			Tangential Displacement $x10^3$* inch		
NODE	CASE IIA	CASE IIB	% CHANGE	CASE IIA	CASE IIB	% CHANGE
36	1.27	1.14	11.4	1.33	1.22	9.0
81	0.20	0.20	0.0	2.38	2.27	4.8
126	2.18	2.09	4.3	1.94	1.88	3.2
166	3.25	3.10	4.8	0.31	0.31	0.0
211	0.62	0.59	5.1	2.52	2.38	5.9
251	2.87	2.72	5.5	1.24	1.18	5.1
291	1.25	1.18	5.9	0.78	0.76	2.6

CASE IIA WITH FSI

CASE IIB WITHOUT FSI

*Local cylindrical co-ordinate system with origin at the center of the torus.

TABLE A.1-7

EFFECT OF FSI ON STATE OF STRESS AT CONCRETE TORUS
(DBA C.O. LOAD GIVEN IN TABLE A.1-2)
CASE IA: WITH FSI, CASE IB: WITHOUT FSI

Boundary Condition: Radial Growth at Base Restrained (Type I)
Tabulated stresses (Psi) are sum of absolute stress amplitudes for different frequencies (1 to 50 Hz)

NODE	RADIAL		AZIMUTH		AXIAL		SHEAR	
	CASE IA	CASE IB	CASE IA	CASE IB	CASE IA	CASE IB	CASE IA	CASE IB
31	3.2	3.2	3.6	3.5	2.9	2.8	6.0	6.0
81	4.6	4.5	1.6	1.6	15.2	15.1	0.1	0.1
85	2.0	2.0	2.1	2.1	12.0	12.0	0.2	0.2
125	2.4	2.3	3.8	3.7	23.0	22.5	4.3	4.3
165	0.56	0.53	4.8	4.6	7.6	7.4	0.6	0.6
211	1.6	1.5	2.8	2.7	2.1	2.0	1.6	1.5
241	6.9	6.6	2.9	2.8	0.2	0.2	0.9	0.9
245	7.3	7.0	1.8	1.7	0.4	0.4	0.36	0.34
251	8.8	8.5	3.0	2.8	0.3	0.3	0.46	0.44
291	1.7	1.6	2.8	2.6	2.2	2.1	1.8	1.7

TABLE A.1-8

EFFECT OF FSI ON STATE OF STRESS AT CONCRETE TORUS

(DBA C.O. LOAD GIVEN IN TABLE A.1-2)

WITH FSI, CASE IIB: WITHOUT FSI

Boundary Condition: Radial Growth at Base Permitted (TYPE II)

Tabulated Stresses (Psi) are sum of absolute stress amplitude for different frequencies (1 to 50 Hz.)

	RADIAL		AZIMUTH		AXIAL		SHEAR	
NODE	CASE IIA	CASE IIB	CASE IIA	CASE IIB	CASE IIA	CASE IIB	CASE IIA	CASE IIB
31	4.3	3.8	11.9	10.7	6.5	5.8	8.9	8.7
81	37.0	36.4	12.9	12.5	15.2	15.0	.3	.3
85	29.0	28.5	12.6	12.2	11.1	11.0	.5	.5
125	.4	.4	8.2	8.1	14.8	14.8	0.46	.44
165	.8	.8	12.3	11.8	9.8	9.4	0.95	0.92
211	2.3	2.3	7.6	7.2	2.9	2.8	2.2	2.2
241	16.2	15.3	7.6	7.2	.5	.5	2.5	2.4
245	15.7	14.9	4.2	4.0	0.96	.93	0.76	0.75
251	16.3	15.3	7.6	7.3	.6	.6	0.86	0.83
291	4.5	4.2	4.0	3.7	5.3	4.9	4.5	4.2

TABLE A.1-9

EFFECT OF FSI ON STATE OF STRESS FOR C.O. LOADINGS

TYPE I = Radial Growth Restrained at Base
TYPE II = Radial Growth Not Restrained at Base

% CHANGE IN STRESS DUE TO FSI								
	RADIAL		AZIMUTH		AXIAL		SHEAR	
NODE	TYPE I	TYPE II	TYPE I	TYPE II	TYPE I	TYPE II	TYPE I	TYPE II
31	0.0	13.2	2.9	11.2	3.6	12.1	0.0	2.3
81	2.2	1.6	0.0	3.2	0.7	1.3	0.0	0.0
85	0.0	1.8	0.0	3.3	0.0	0.9	0.0	0.0
125	4.3	0.0	2.7	1.2	2.2	0.0	0.0	4.5
165	5.7	0.0	4.3	4.2	2.7	4.3	0.0	3.3
211	6.7	0.0	3.7	5.6	5.0	3.6	6.7	0.0
241	4.5	5.9	3.6	5.6	0.0	0.0	0.0	4.2
245	4.3	5.4	5.9	5.0	0.0	3.2	5.9	1.3
251	3.5	6.5	7.1	4.1	0.0	0.0	4.5	3.6
291	6.3	7.1	7.7	8.1	4.8	8.2	5.9	7.1

TABLE A.1-10

DYNAMIC LOAD FACTOR FOR STRESS,

CONDENSATION OSCILLATION LOAD

RADIAL GROWTH ALLOWED AT BASE

NODE	RADIAL STRESS	AZIMUTH	AXIAL	SHEAR
1	1.52	4.21	2.71	2.16
3	3.69	5.10	7.74	44.98
5	4.89	7.28	3.21	3.73
11	1.13	7.27	3.26	4.43
13	1.60	16.59	3.91	1.52
15	1.72	65.38	18.34	2.67
21	1.31	41.21	12.02	1.24
23	2.07	22.77	1.38	1.12
25	1.62	14.27	2.13	1.38
31	2.39	10.78	6.54	1.09
33	1.64	7.61	1.12	1.10
35	1.48	10.18	1.24	1.50
41	1.63	5.05	3.31	1.06
43	1.20	4.98	1.05	1.08
45	1.00	9.22	1.17	1.24
51	1.15	3.16	1.06	1.05
53	1.12	3.47	1.06	1.04
55	1.16	4.50	1.05	1.30
61	1.09	2.22	1.00	1.05
63	1.09	2.42	1.03	1.05
65	1.10	2.88	1.05	1.15
71	1.07	1.58	1.00	1.04
73	1.08	1.73	1.00	1.05
75	1.08	1.89	1.00	1.21
81	1.07	1.33	1.00	1.04
83	1.07	1.39	1.00	1.07
85	1.08	1.41	1.00	1.09

TABLE A.1-10

DYNAMIC LOAD FACTOR FOR STRESS,

CONDENSATION OSCILLATION LOAD

RADIAL GROWTH ALLOWED AT BASE

NODE	RADIAL STRESS	AZIMUTH	AXIAL	SHEAR
91	1.07	1.27	1.00	1.04
93	1.08	1.30	1.00	1.05
95	1.08	1.30	1.00	1.23
101	1.10	1.26	1.00	1.05
103	1.09	1.30	1.00	1.08
105	1.09	1.30	1.04	1.13
111	1.25	1.29	1.03	1.08
113	1.11	1.30	1.05	1.07
115	1.15	1.31	1.03	1.62
121	4.93	1.31	1.46	1.17
123	1.19	1.29	1.06	1.06
125	1.13	1.36	1.46	1.10
131	1.31	1.37	1.88	1.46
133	1.51	1.26	1.16	1.07
135	1.30	1.28	1.66	1.28
141	1.11	1.47	1.47	4.53
143	1.48	1.24	1.51	1.06
145	1.24	1.15	13.19	1.19
151	1.07	1.57	1.17	1.36
153	1.28	1.27	9.78	1.87
155	1.2	1.14	1.63	1.61
161	1.28	1.54	1.26	1.12
163	1.50	1.42	5.21	1.88
165	2.1	1.36	1.20	1.70
171	2.85	1.54	7.68	2.79
173	2.10	1.81	5.64	1.62

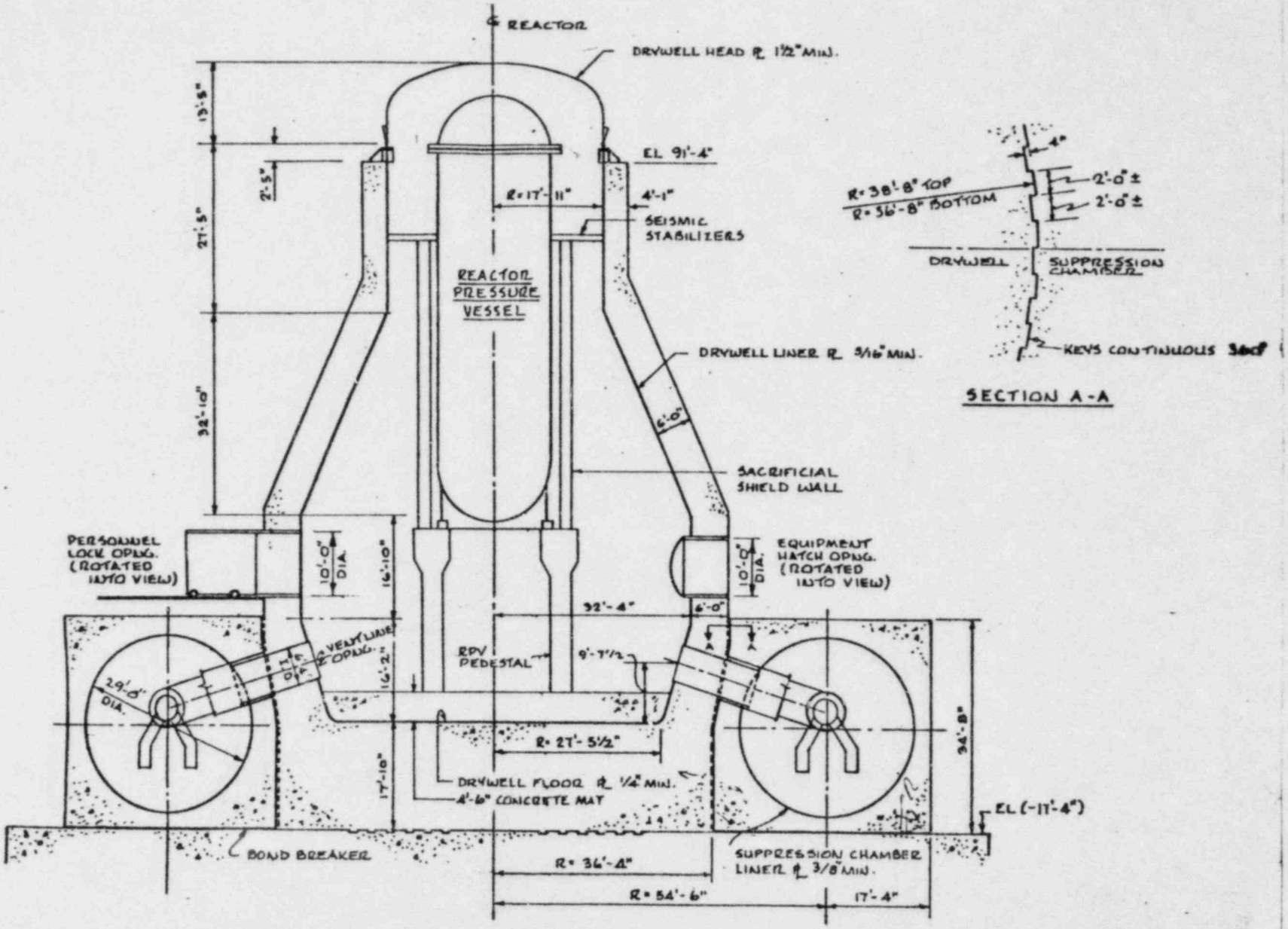

Figure 1.2-1 Section Through Primary Containment Structure

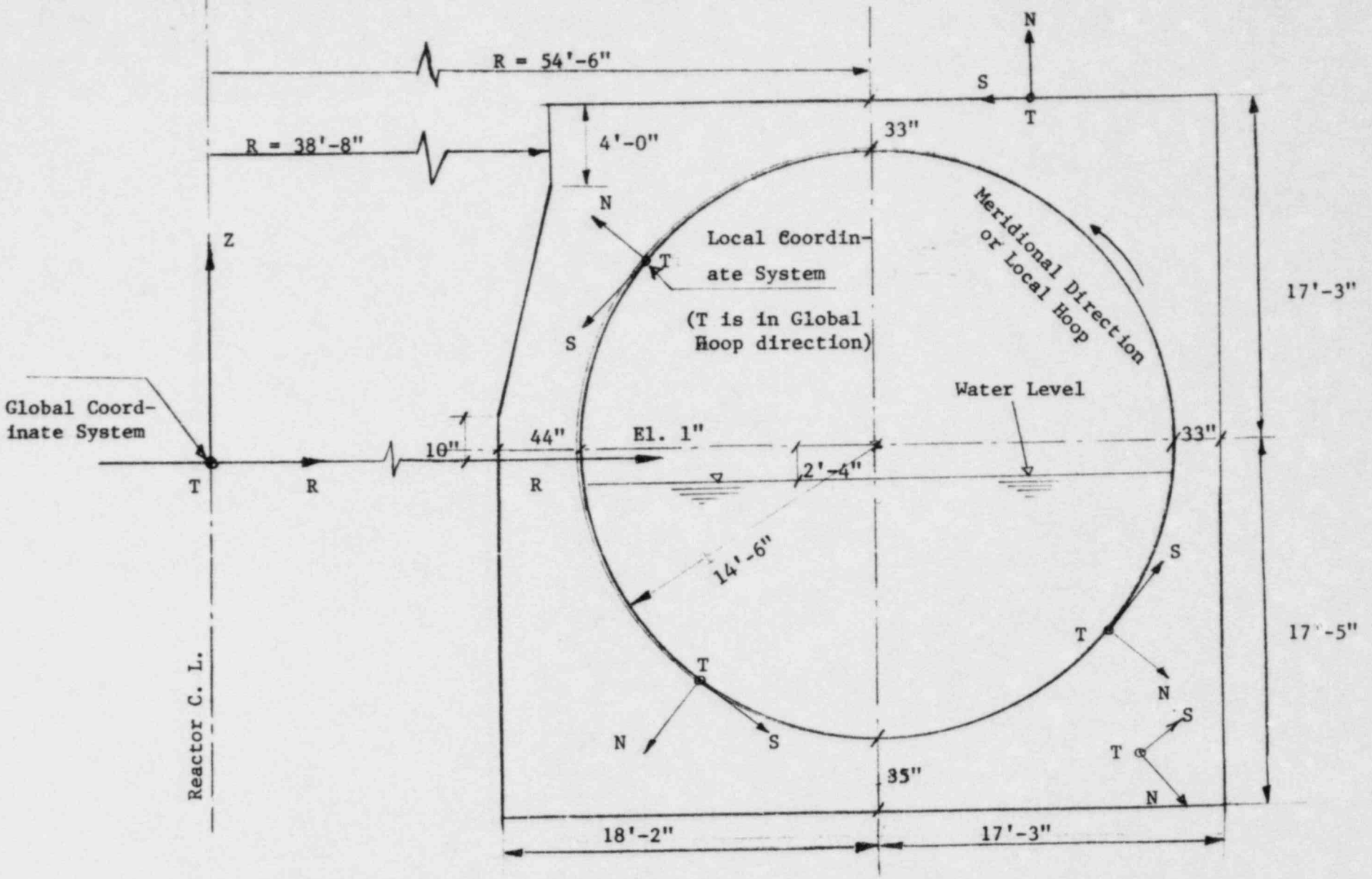

Figure 1.2-2 Typical Cross Section of Suppression Chamber With Local and Global Coordinate Systems

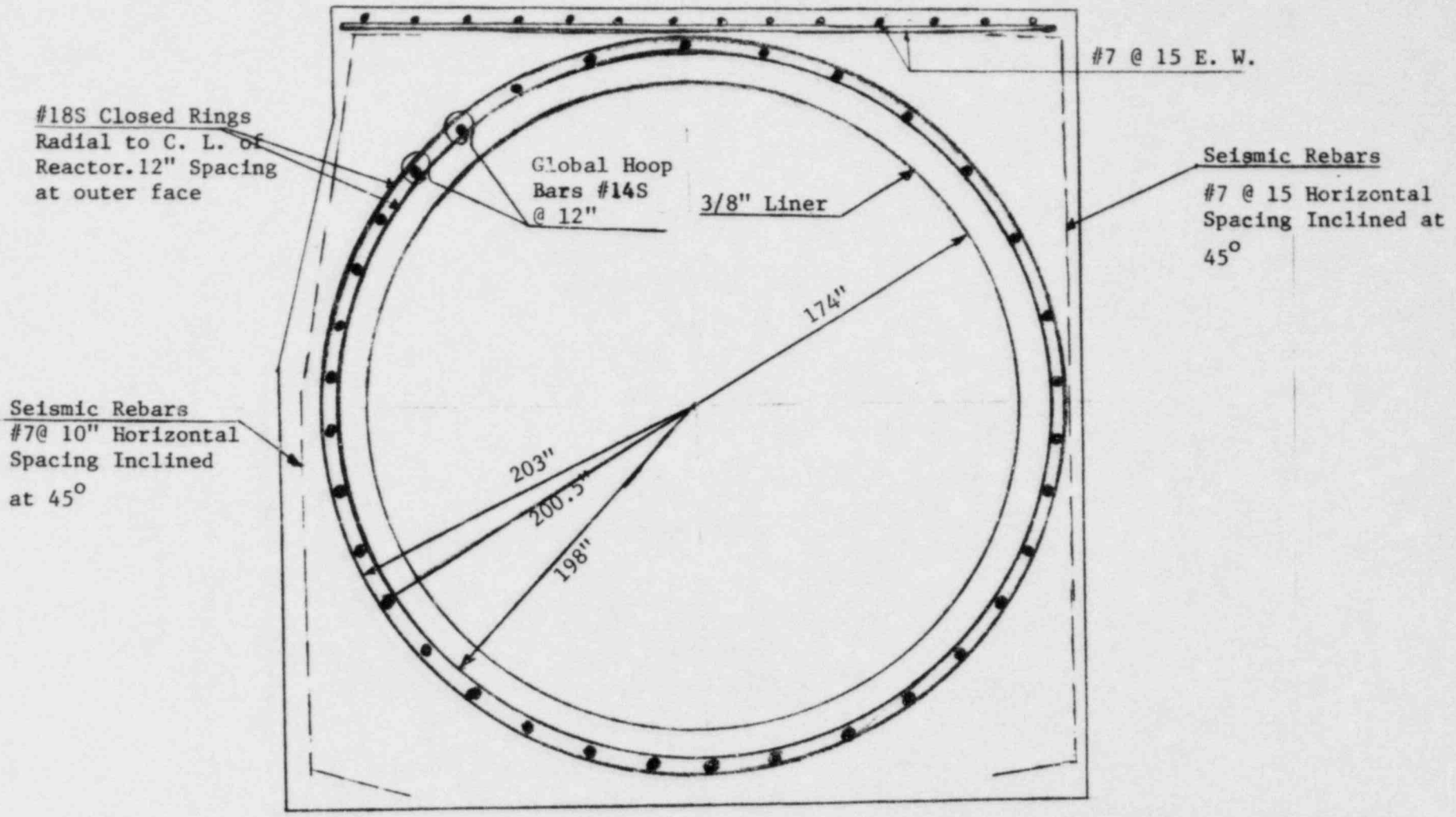

Figure 1.2-3 Suppression Chamber Reinforcements

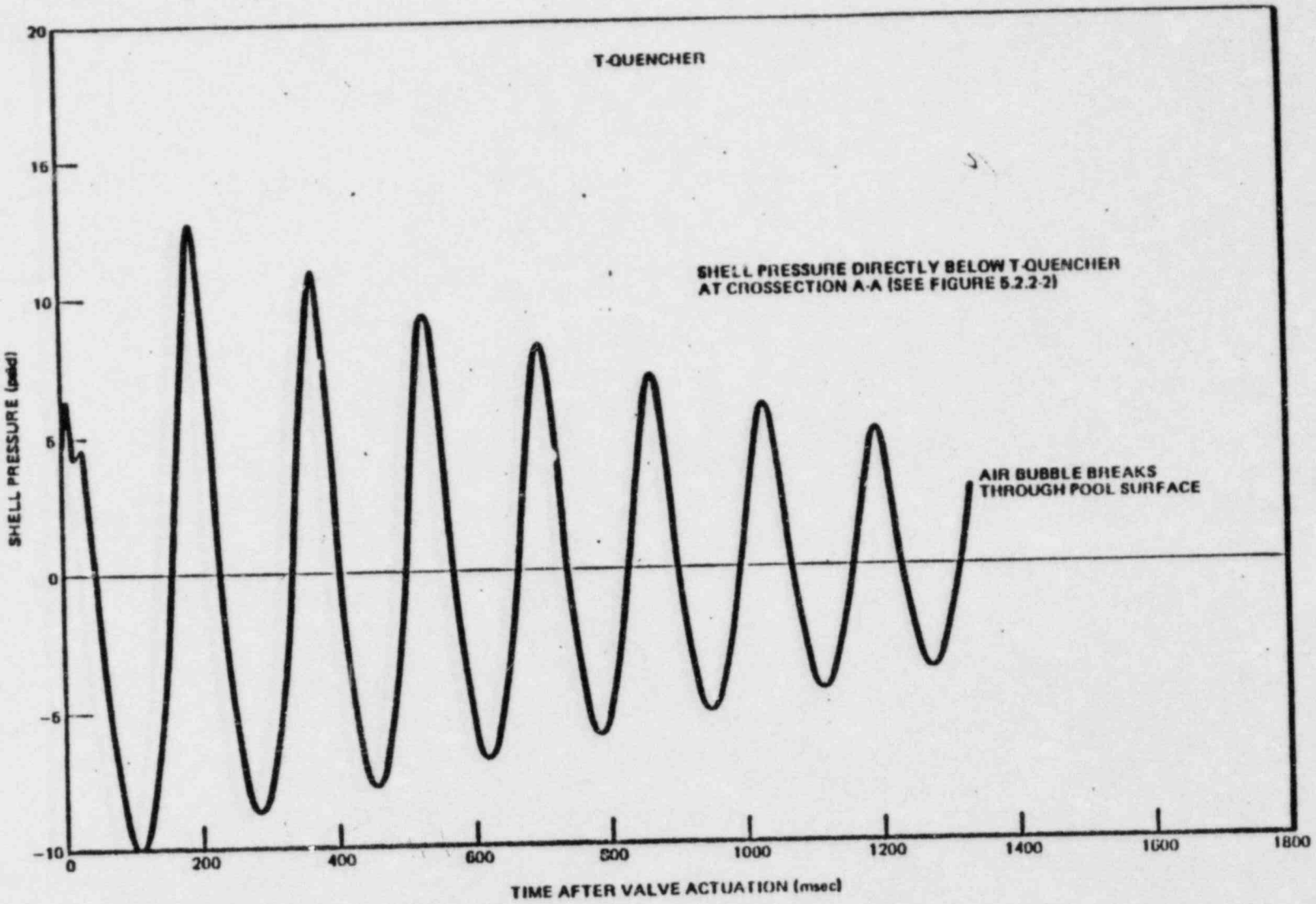

Figure 1.3-1 Sample Prediction of Torus Shell Pressure Loading Transient Due to a S/RV Actuation

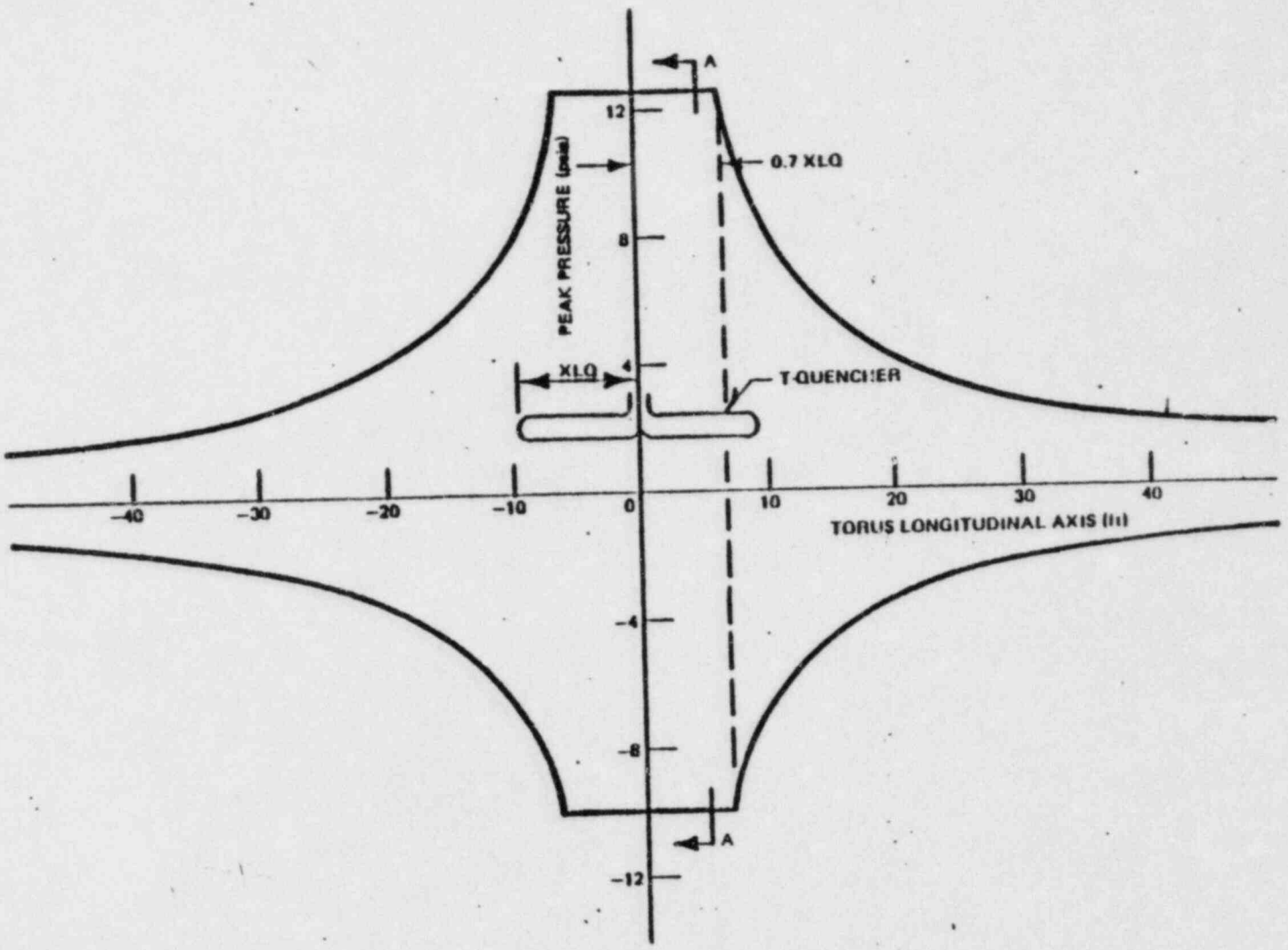

Figure 1.3-2 Sample prediction of Torus Shell Longitudinal Pressure Distribution Due to a S/RV Actuation

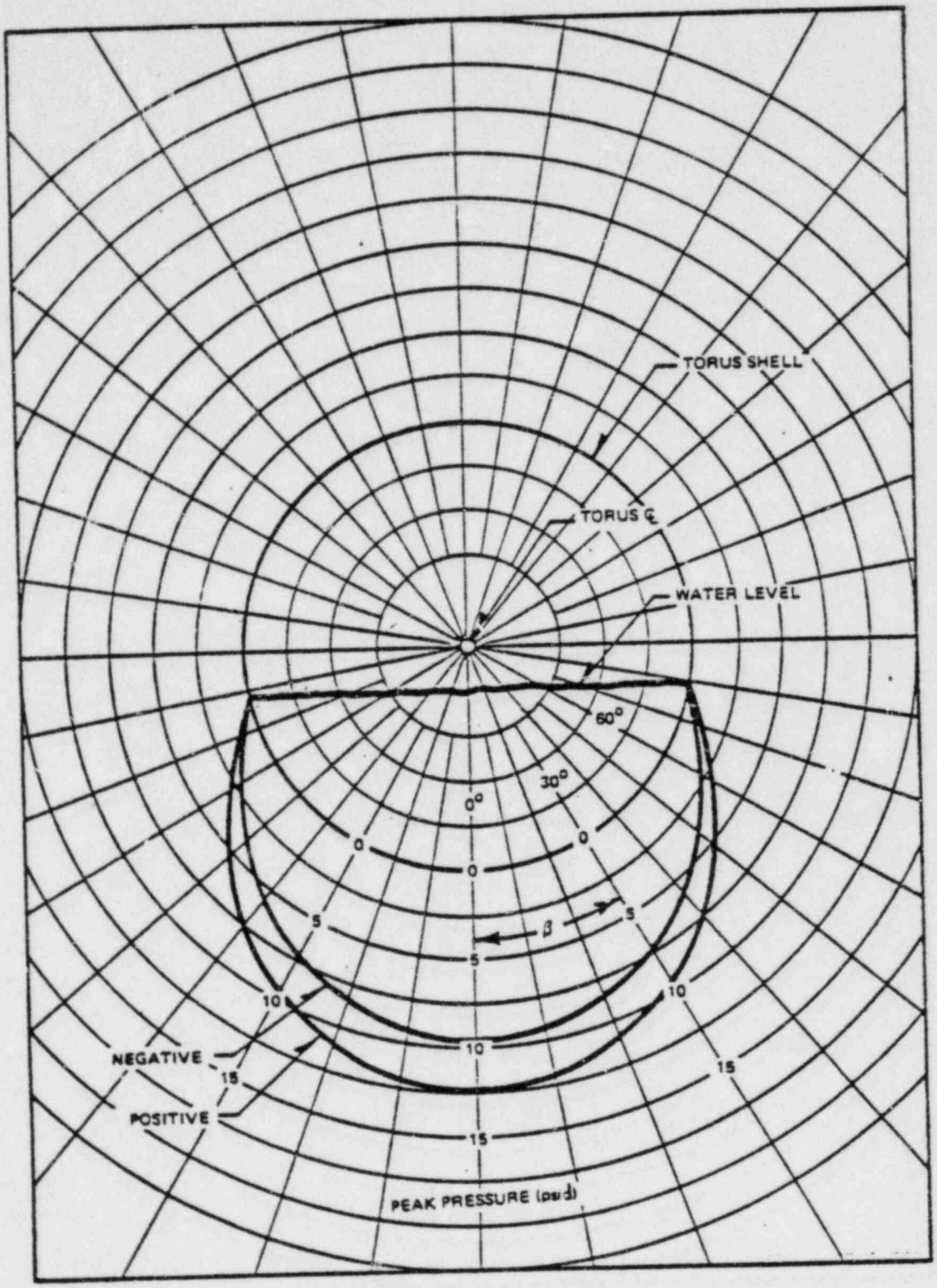

Figure 1.3-3 Sample Prediction of Torus Shell Radial Pressure Distribution at Section A-A in Figure 1.3-2 Due to a S/RV Actuation

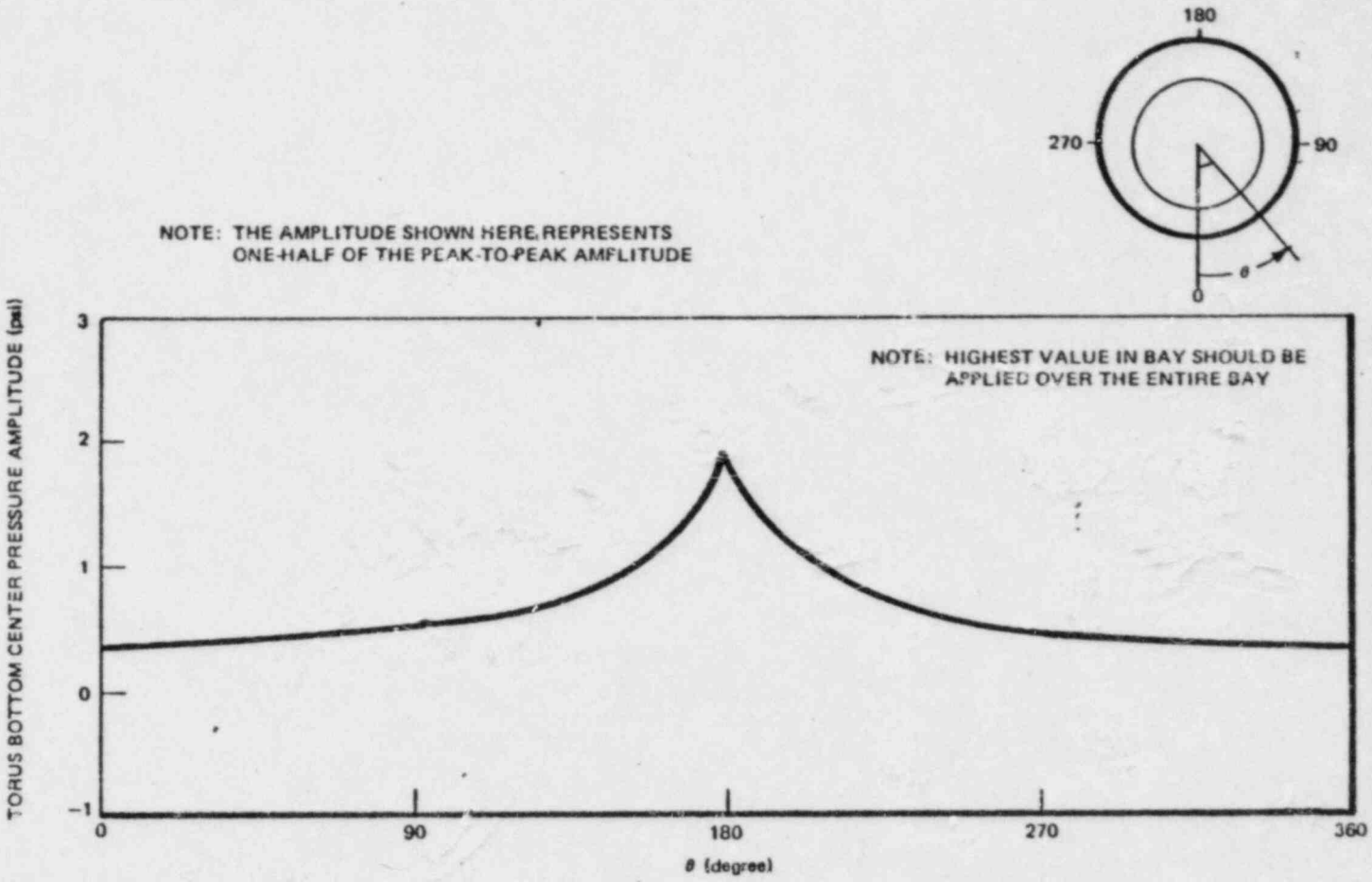

Figure 1.3-4 Mark I Chugging - Torus Asymmetric Circumferential Distribution for Pressure Amplitude

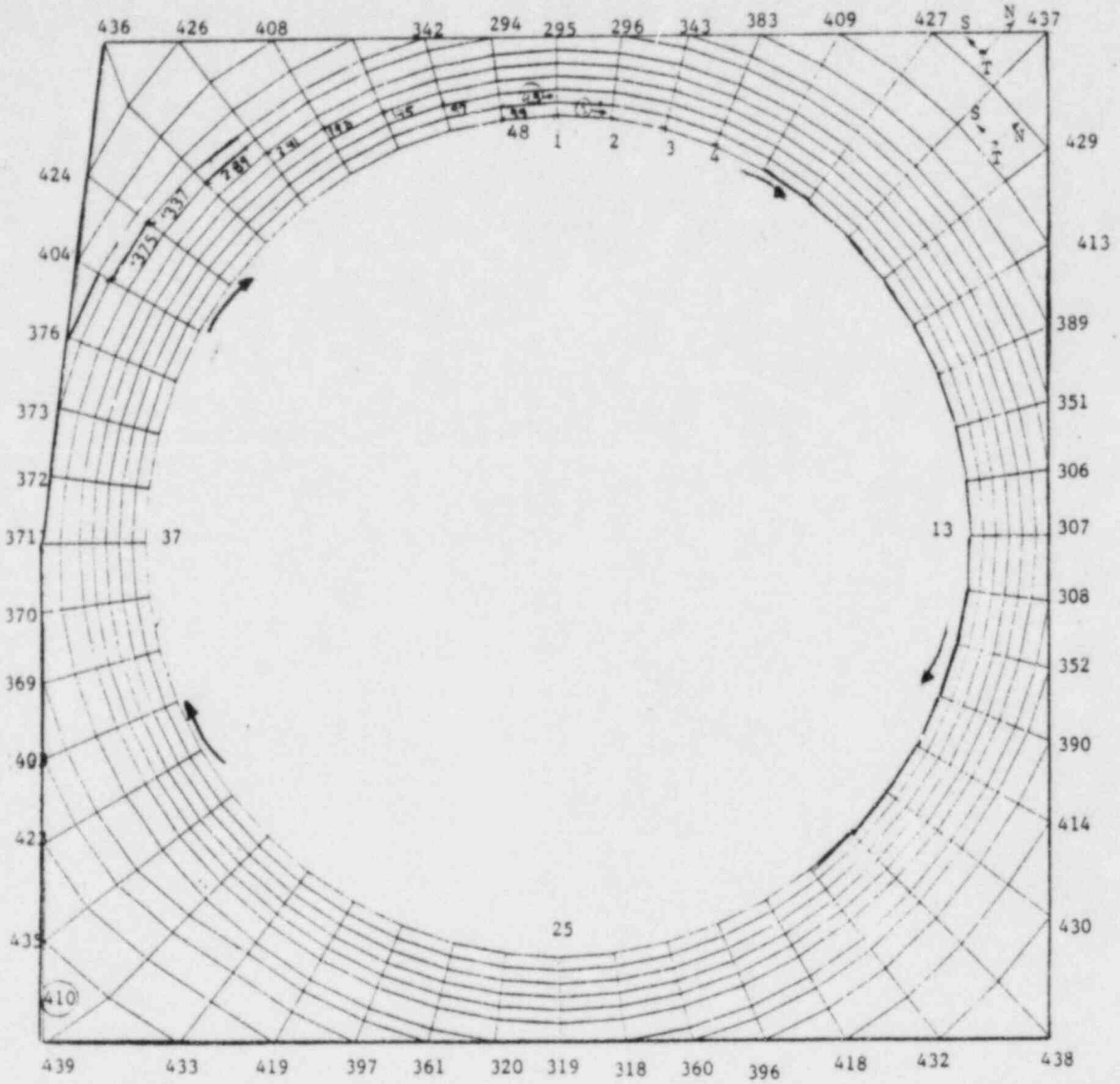

Figure 1.6-1 Finite Element Discretization of the Concrete Portion of the Suppression Chamber (Quadilateral & Triangular Elements)

Numbers in circles: Elements Number

Other numbers: Nodes Number

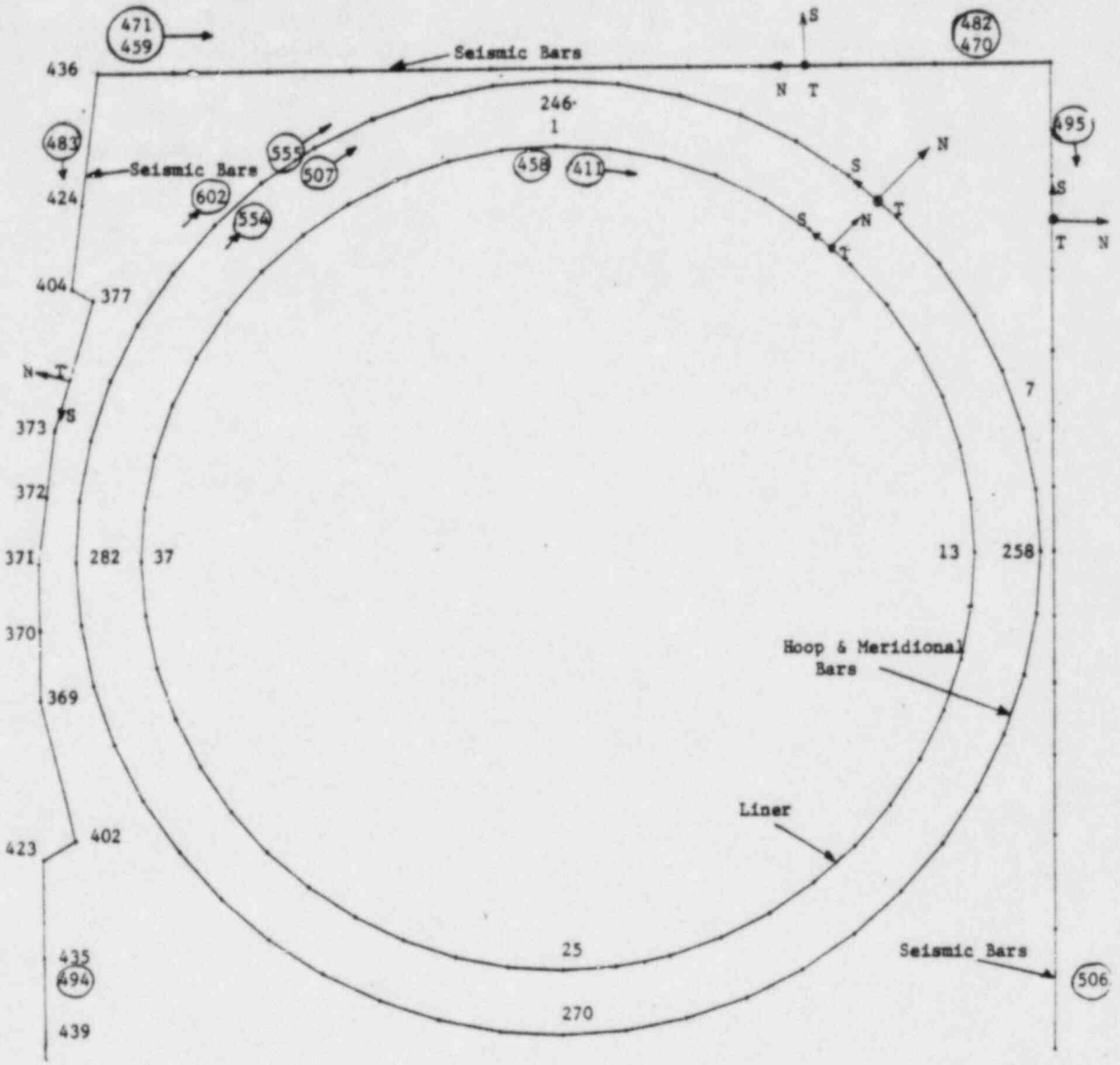

Figure 1.6-2 Finite Element Discretization of the Liner and Reinforcing Bars (Shell Elements)

Numbers in Circle: Elements Number Other numbers are Nodes Number

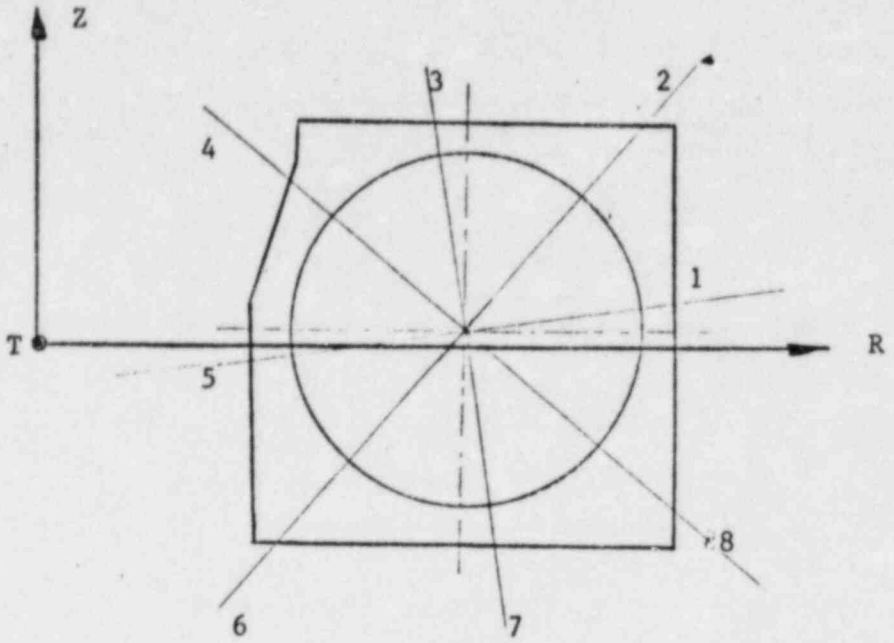

Figure 1.8-1 Locations Along Meridional Direction Where Forces and Moments are Calculated.

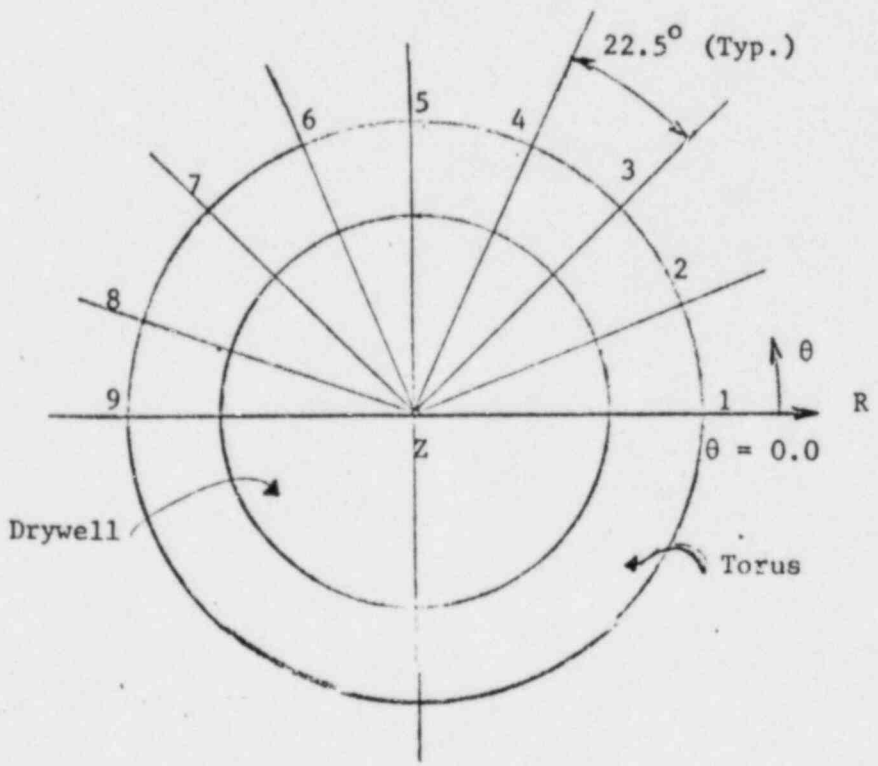

Figure 1.8-2 Sections Along Circumferential Direction of the Torus Where Forces and Moments are Calculated for All of the Locations Along Meridional.

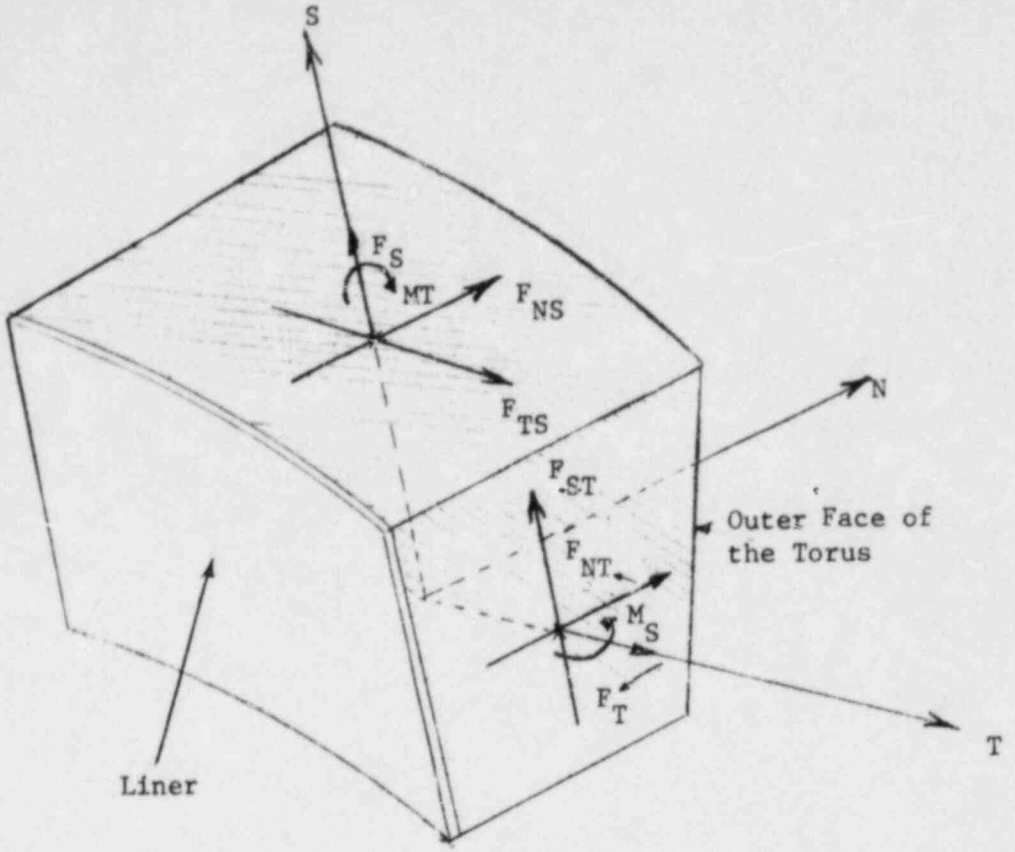

Figure 1.8-3 Forces and Moments Directions at Meridional and Circumferential Cross Section of the Torus

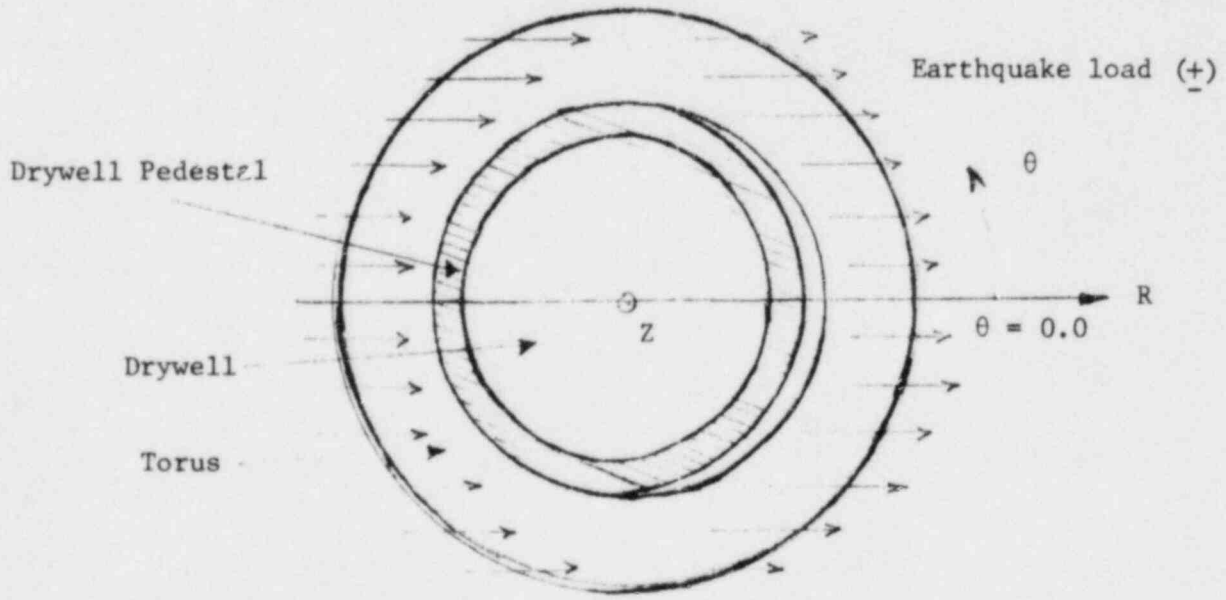

Figure 1.9-1 Earthquake Load and Possible Movement of Torus (Ring Action)

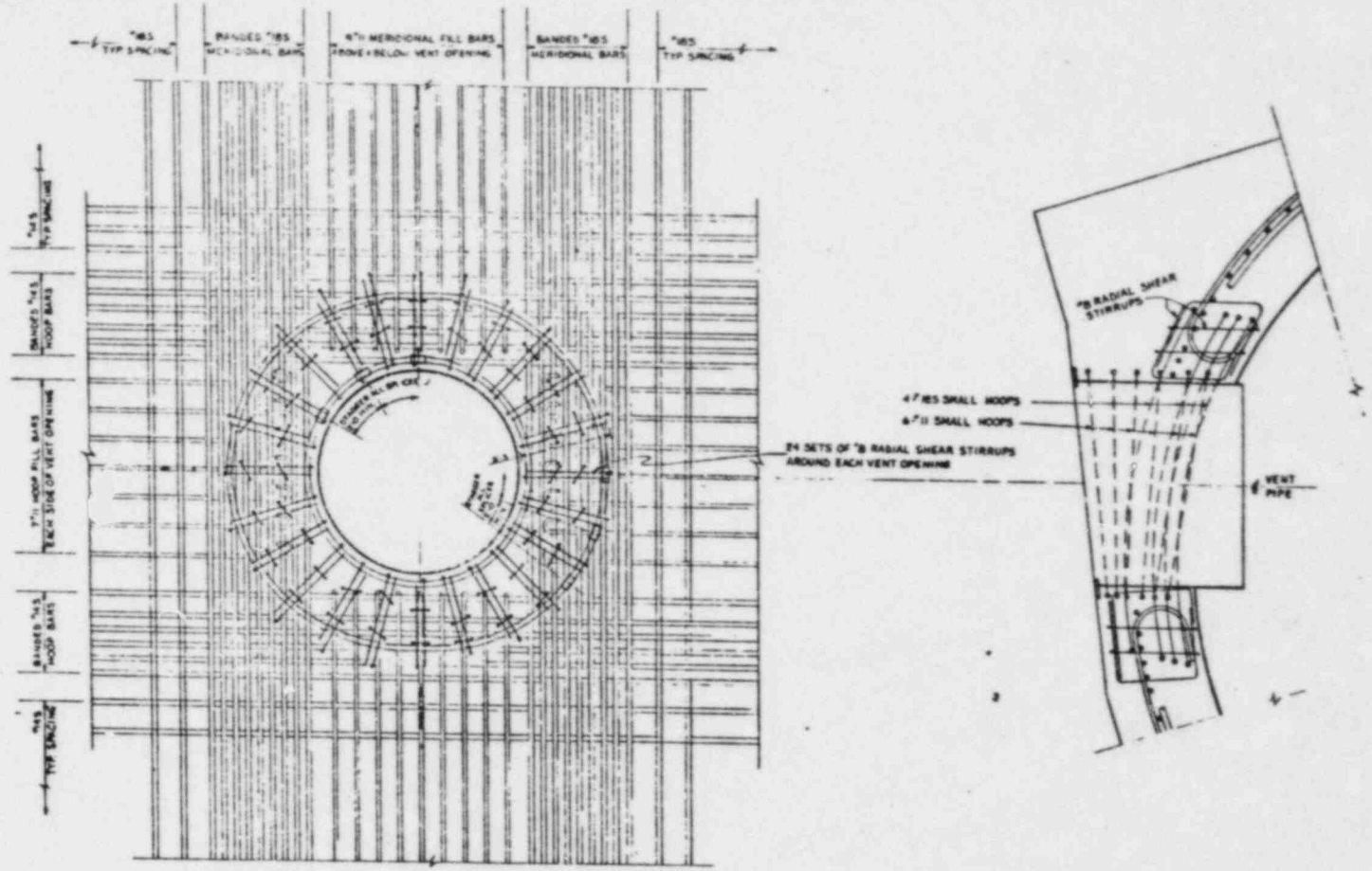

Figure 1.10-1 Typical Reinforcing Details Around Vent Openings in the Suppression Chamber

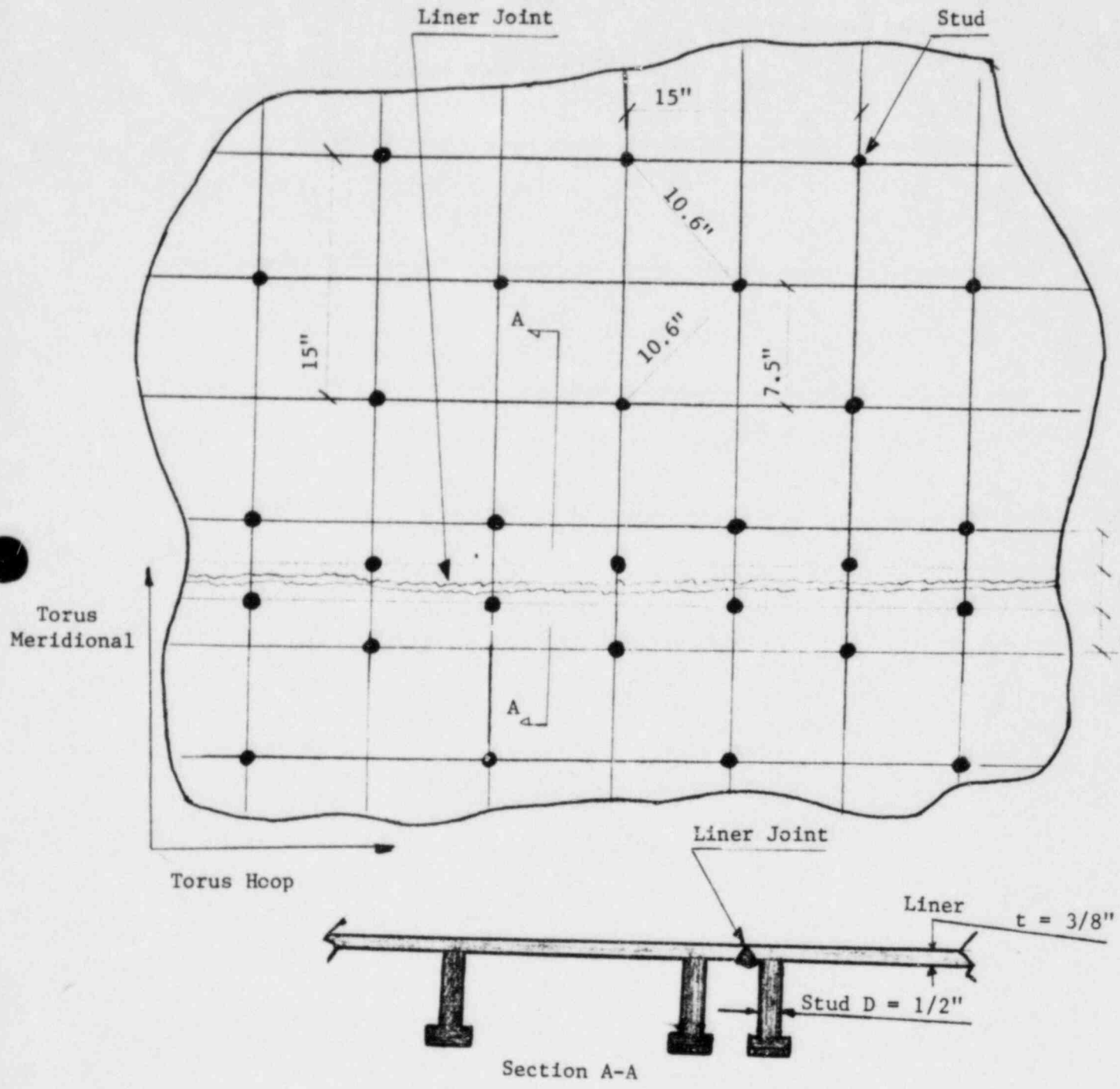

Figure 1.11-1 Stud Arrangement on Brunswick Torus Liner

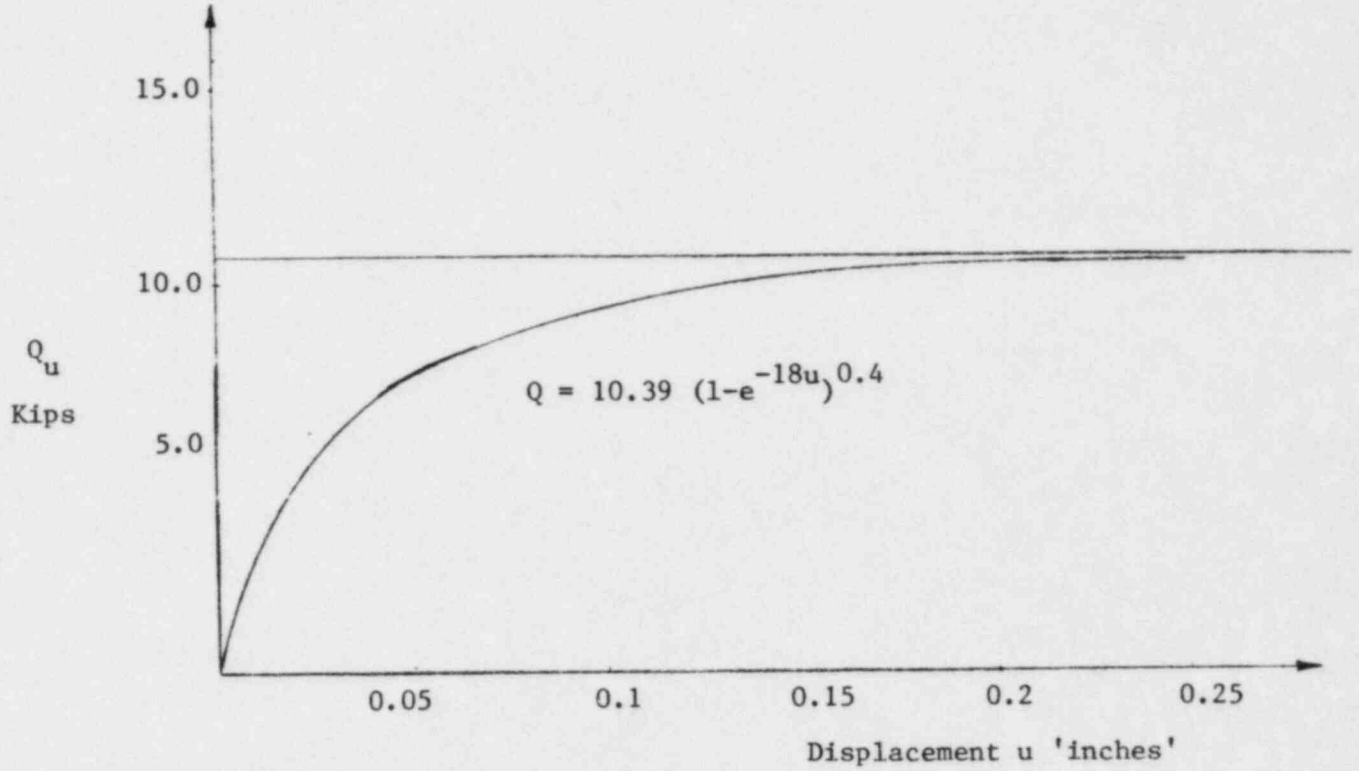

Figure 1.11-2 Load Displacement Curve for 1/2" Nelson Studs

Ref: Nelson Stud Catalog

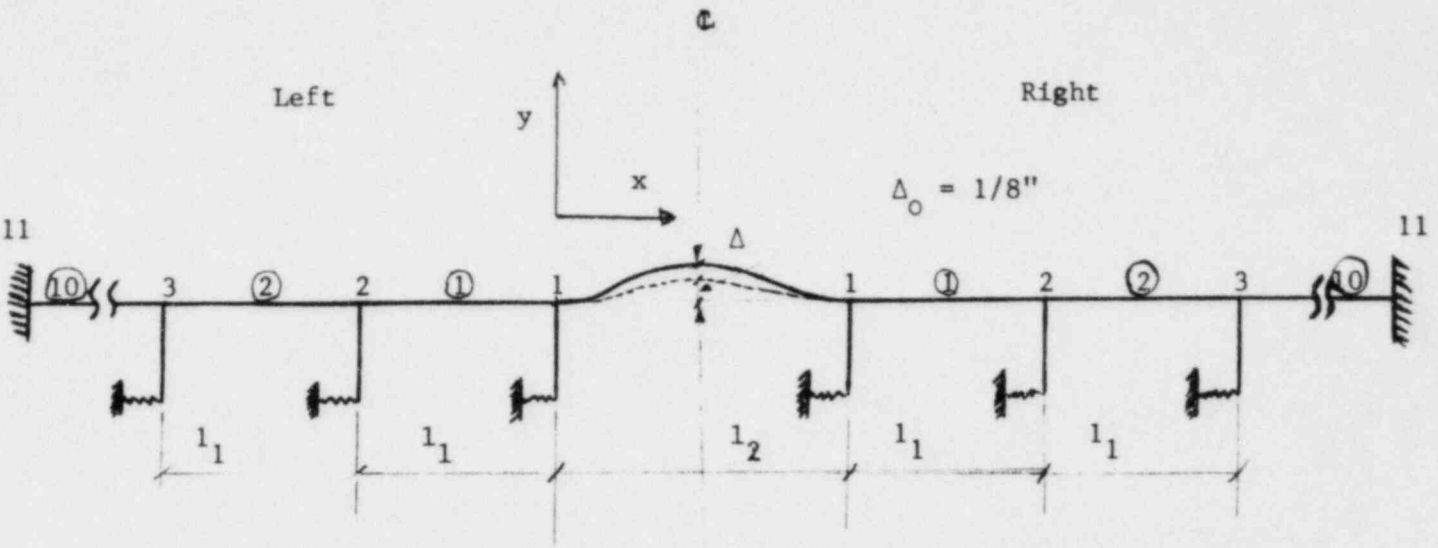

$y_o = \Delta_o \sin^2 \frac{\pi x}{l_2}$ assumed initial shape of the liner plate.

$y = \Delta \sin^2 \frac{\pi x}{l_2}$ buckled shape of the liner plate

t_L = Thickness of left panels = 0.405 in.

t_R = Thickness of right panels = 0.375 in.

t = Thickness of buckled panel = 0.375 in.

Geometry of Models

Case	Model	l_1 in.	l_2 in.
1	1	15.0	15.0
2	2	10.6	10.6
3	3	15.0	30.0
4	4	10.6	21.2

Figure 1.11-3 Mathematical Models for Liner-Stud Analysis

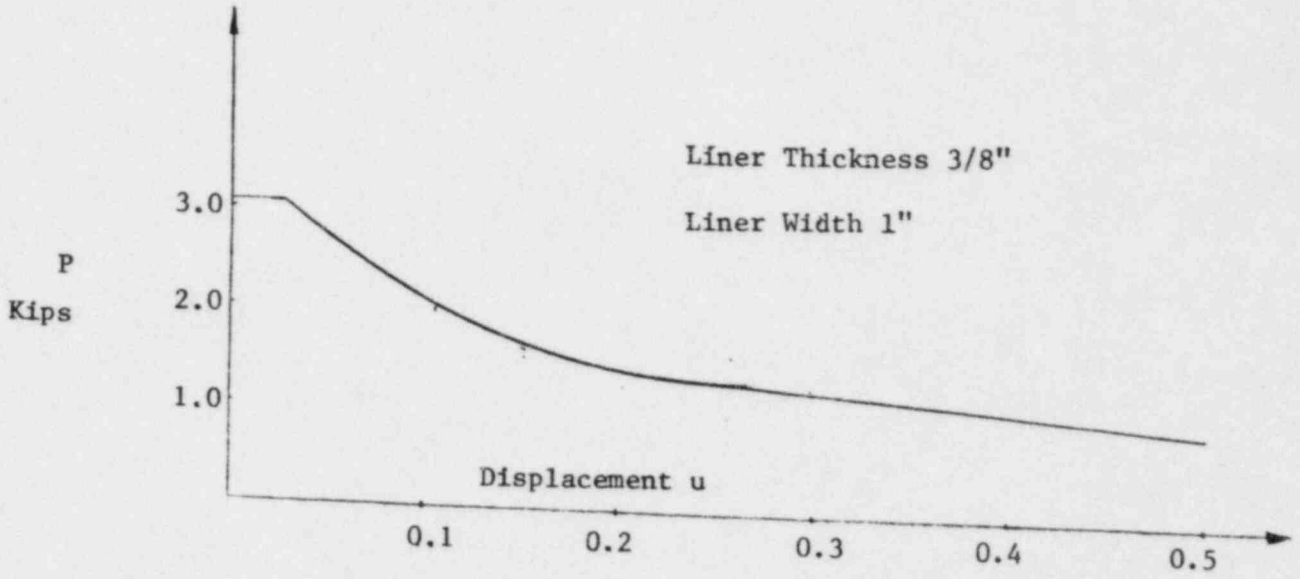

Figure 1.11-4 Load Displacement Curve for a 15" Long Liner Plate

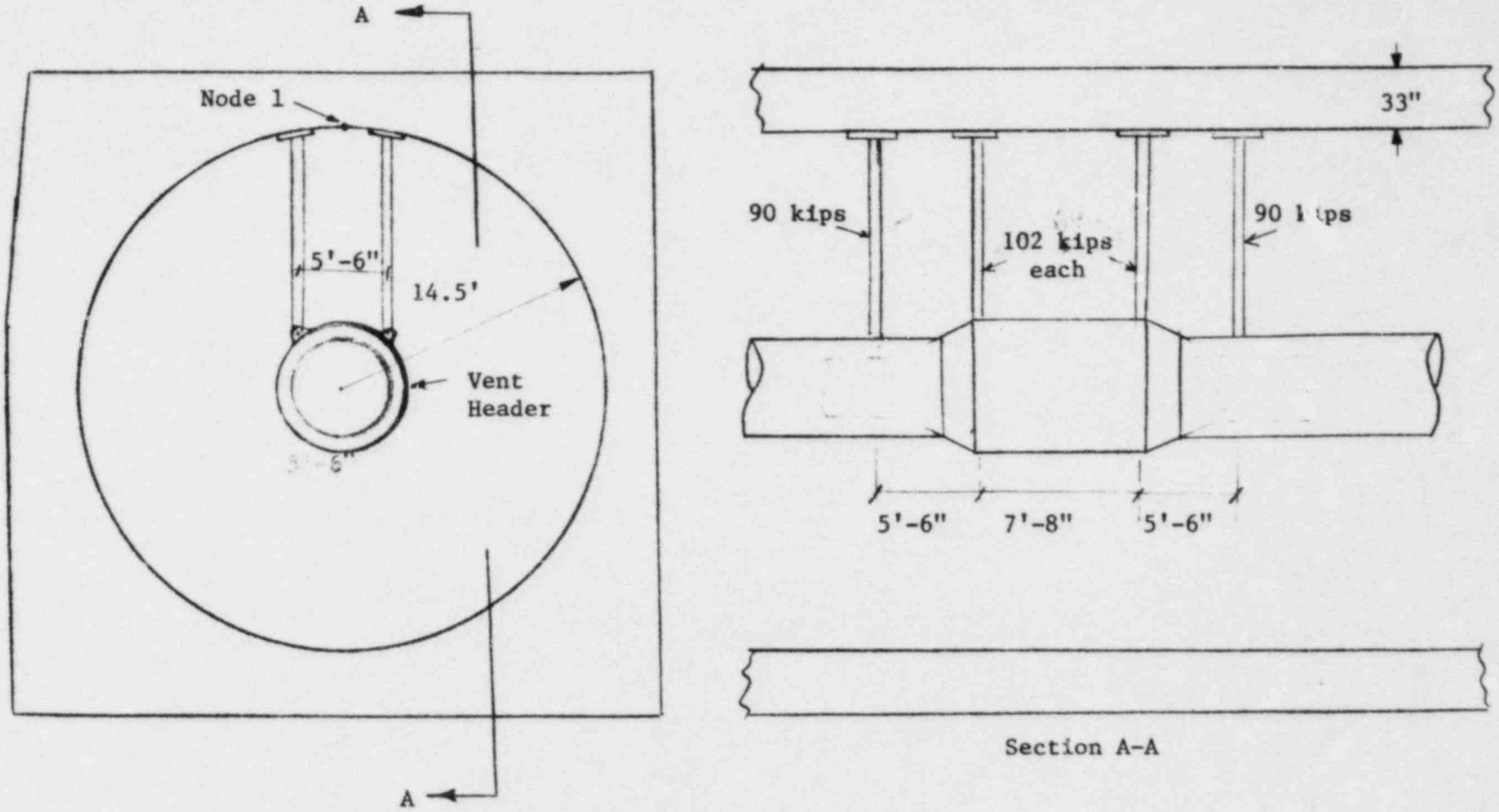

Figure 1.12-1 Vertical Uploads and Columns to Distribute the Loads to the Torus

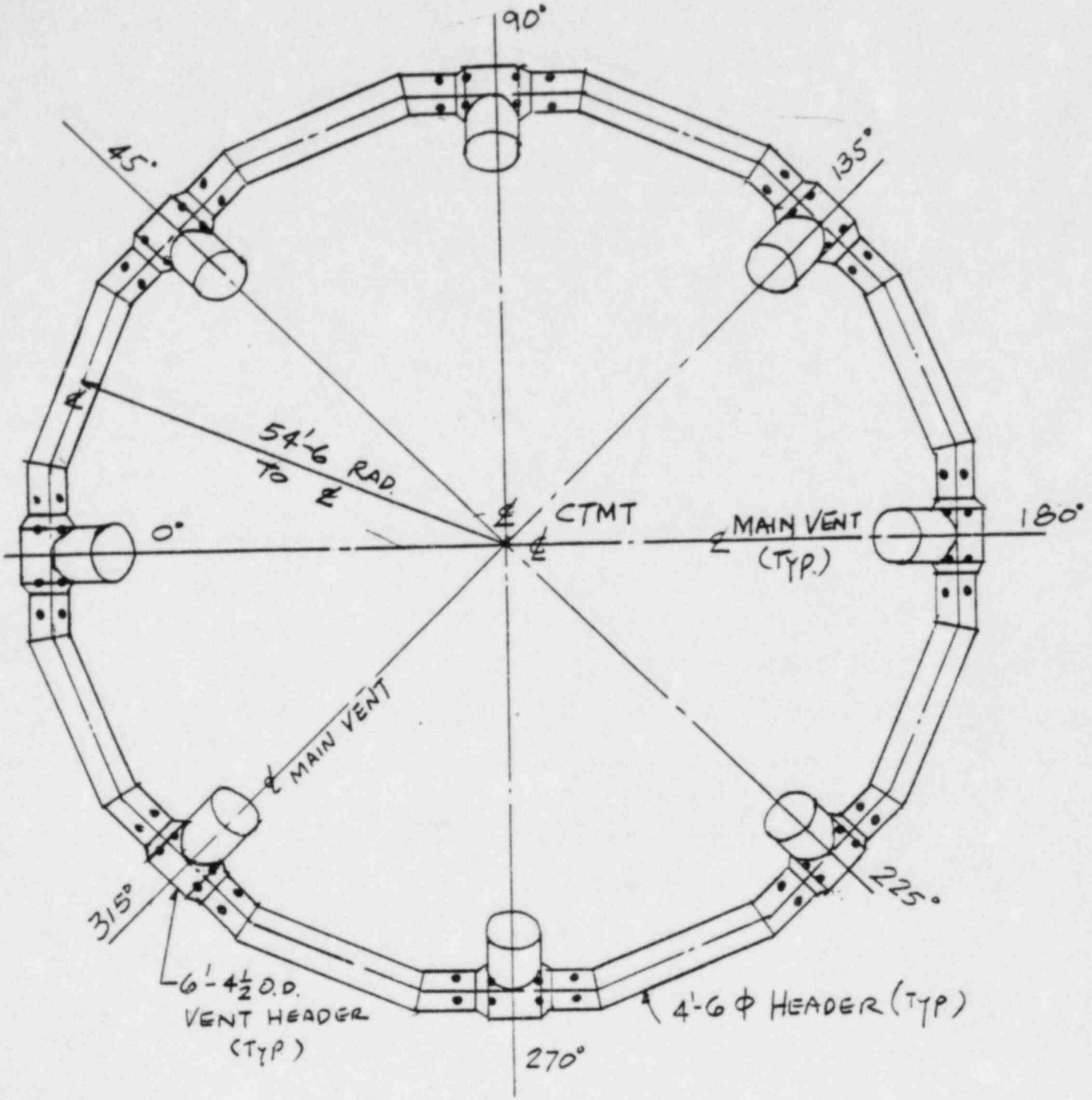

Figure 1.12-2 Plan of Header, Vent Header and Columns

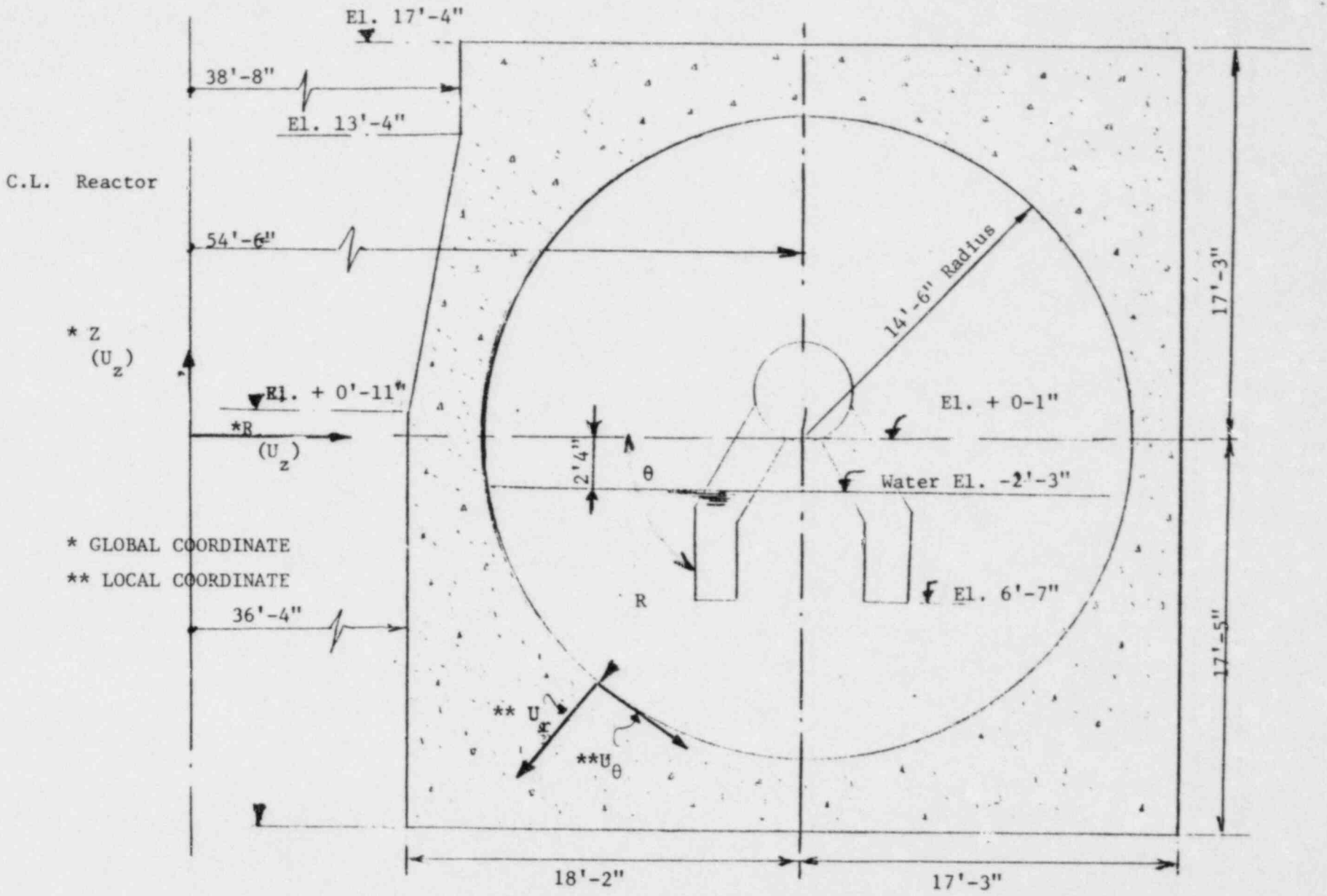

Figure A.1-1 Axisymmetric Cross Section of Concrete Torus

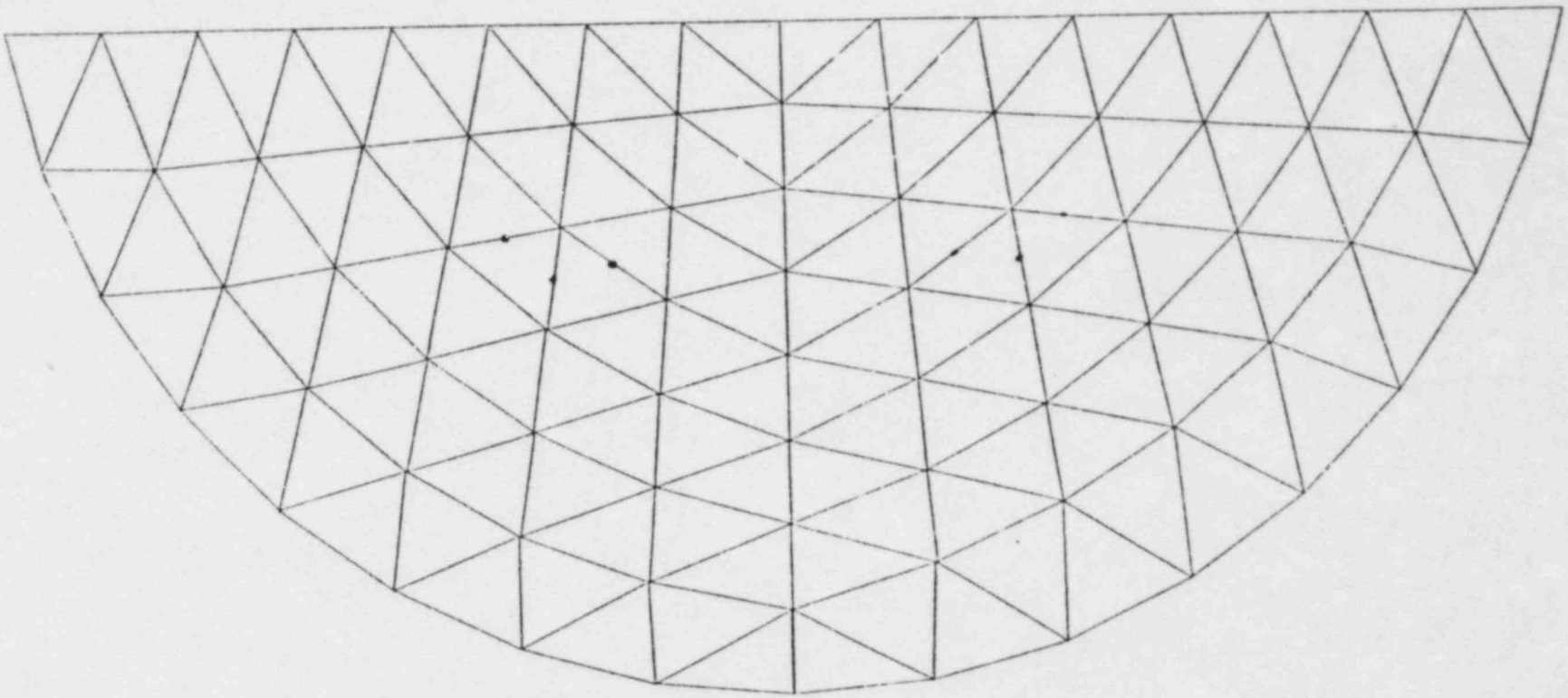

Figure A.1-2: Finite Element Mesh for Fluid

128 Axisymmetric Triangles Ring Elements "TRIAX 6"
289 Nodes

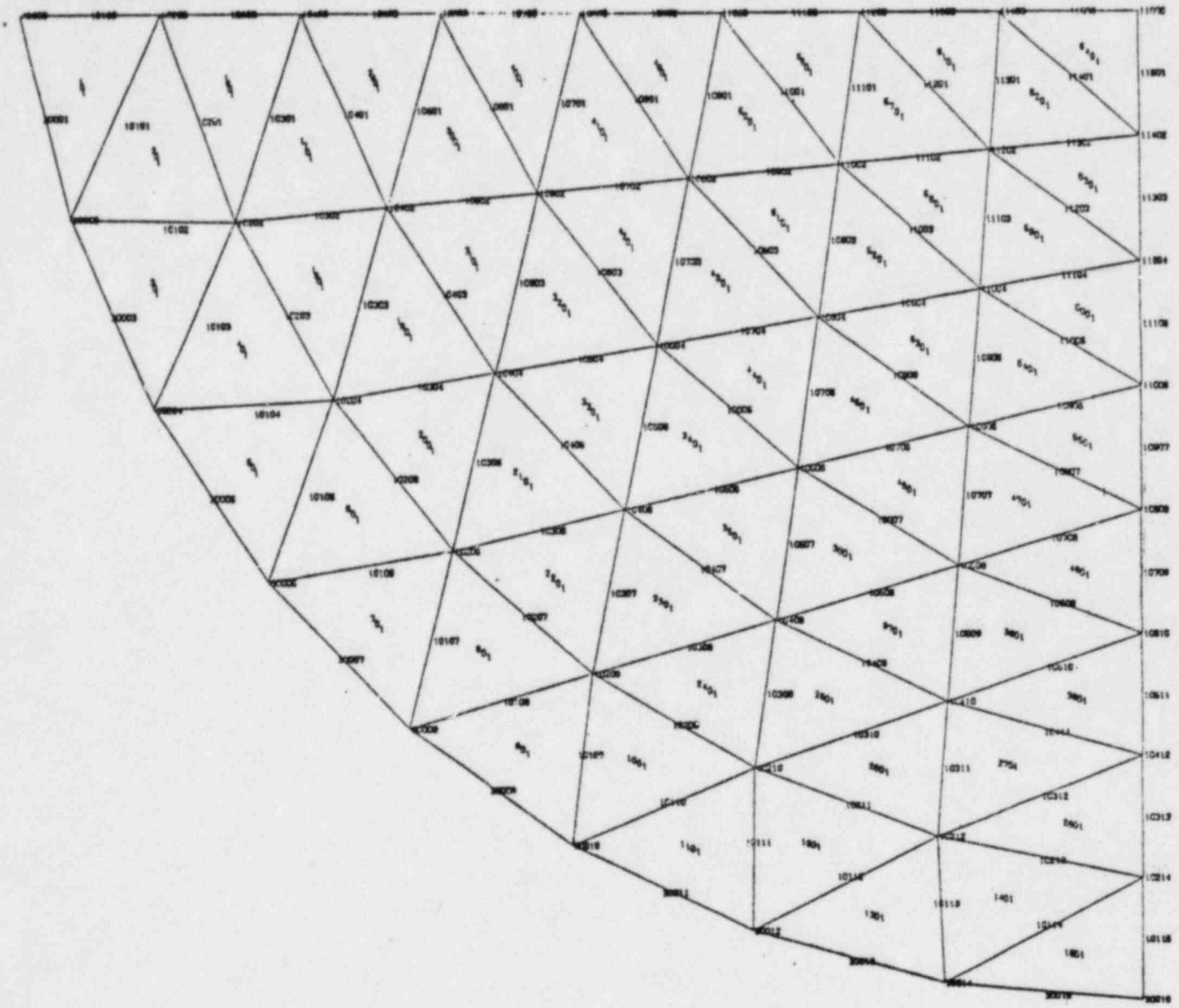

Figure A.1-3: Right Half of Fluid Mesh
Nastran "TRIAX 6" Element

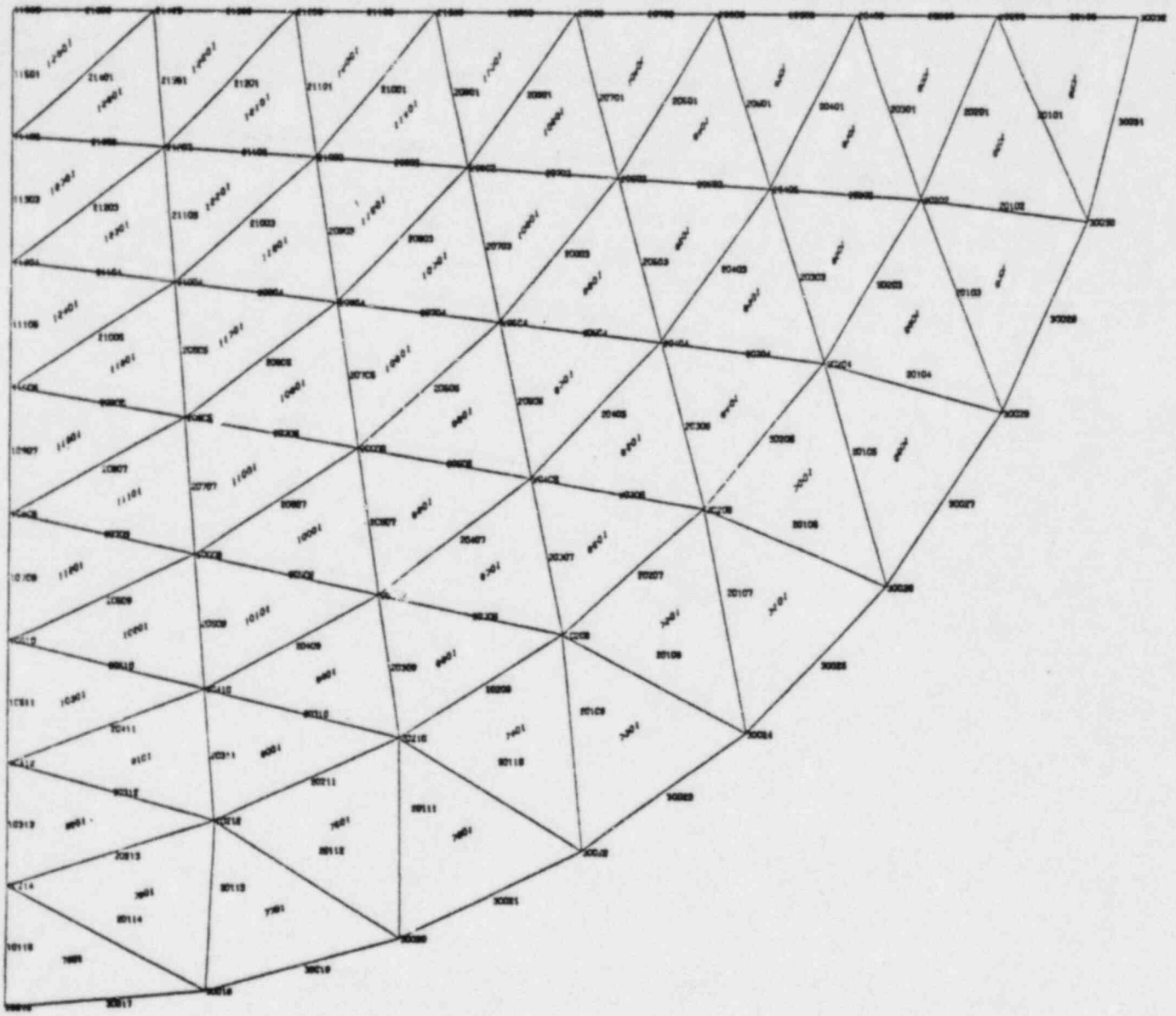

Figure A.1-4 Left Half of Fluid Mesh
Nastran "TRIAX 6" Elements

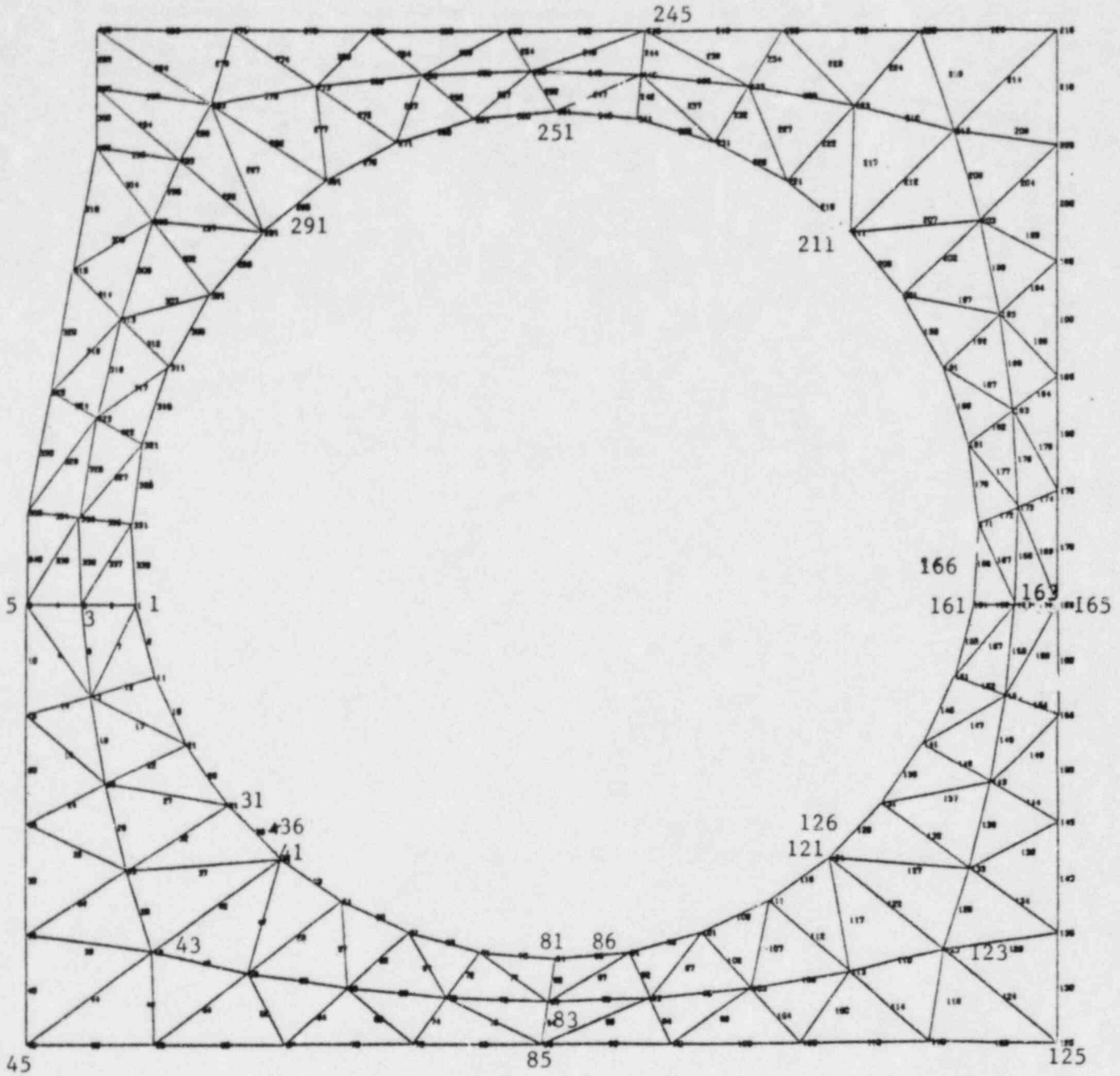

Figure A.1-5 Finite Element Mesh of Concrete Torus
136 "TRIAX 6" Elements
340 Nodes

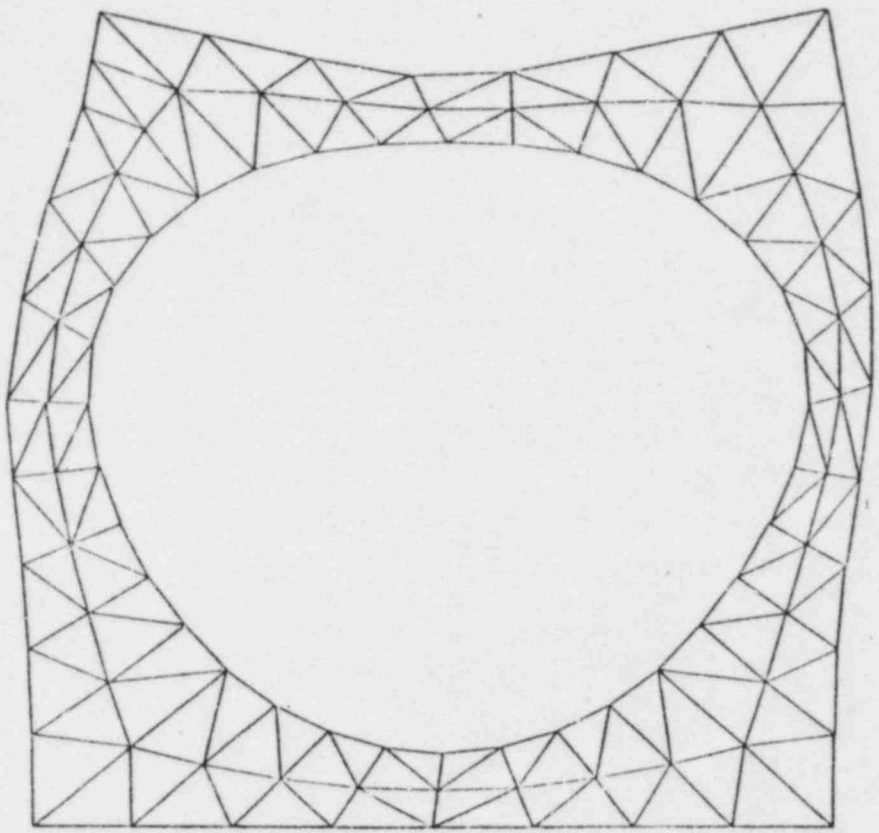

NORMAL MODES ANALYSIS OF THE STRUCTURE ONLY

MODAL DEFOR. SUBCASE 1 MODE 1 FREQ. 26.96561

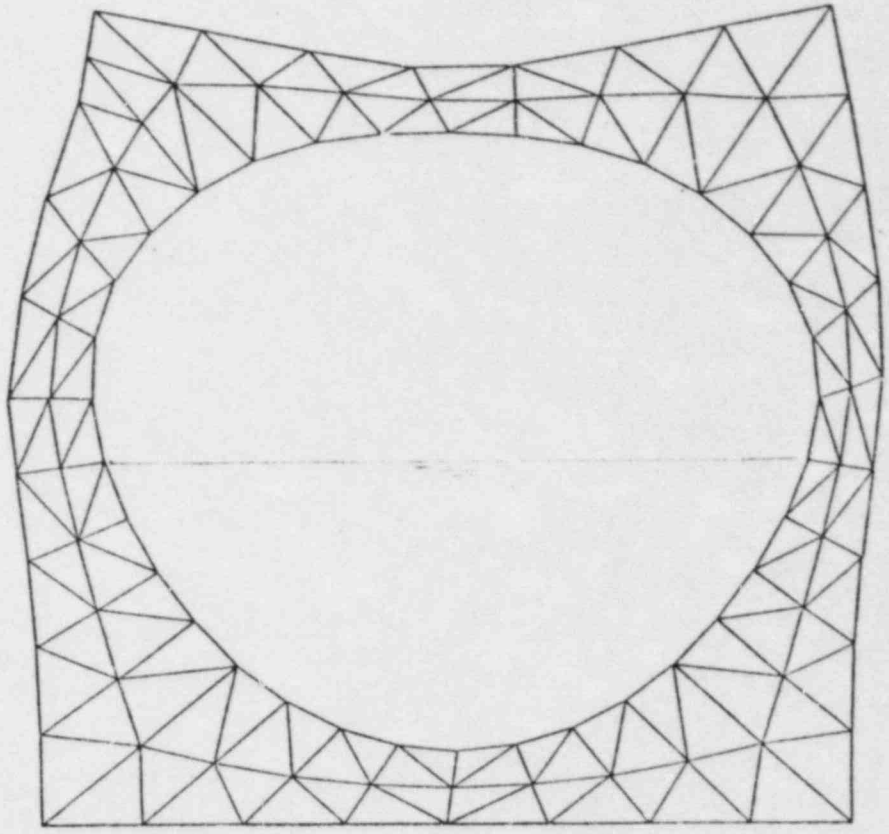

NORMAL MODES ANALYSIS OF THE COMBINED SYSTEM

MODAL DEFOR. SUBCASE 1 MODE 1 FREQ. 26.40548

Figure A.1-6 Effect of FSI on Mode 1 (Radial Movement Allowed)

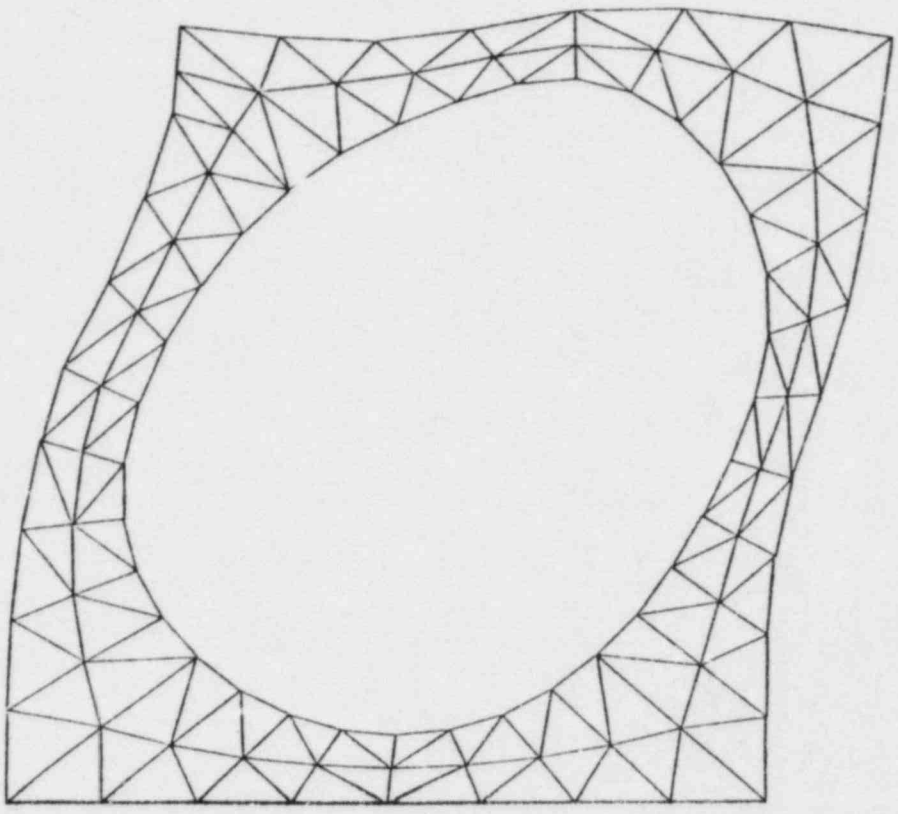

NORMAL MODES ANALYSIS OF THE STRUCTURE ONLY

MODAL DEFOR. SUBCASE 2 MODE 2 FREQ. 32.97632

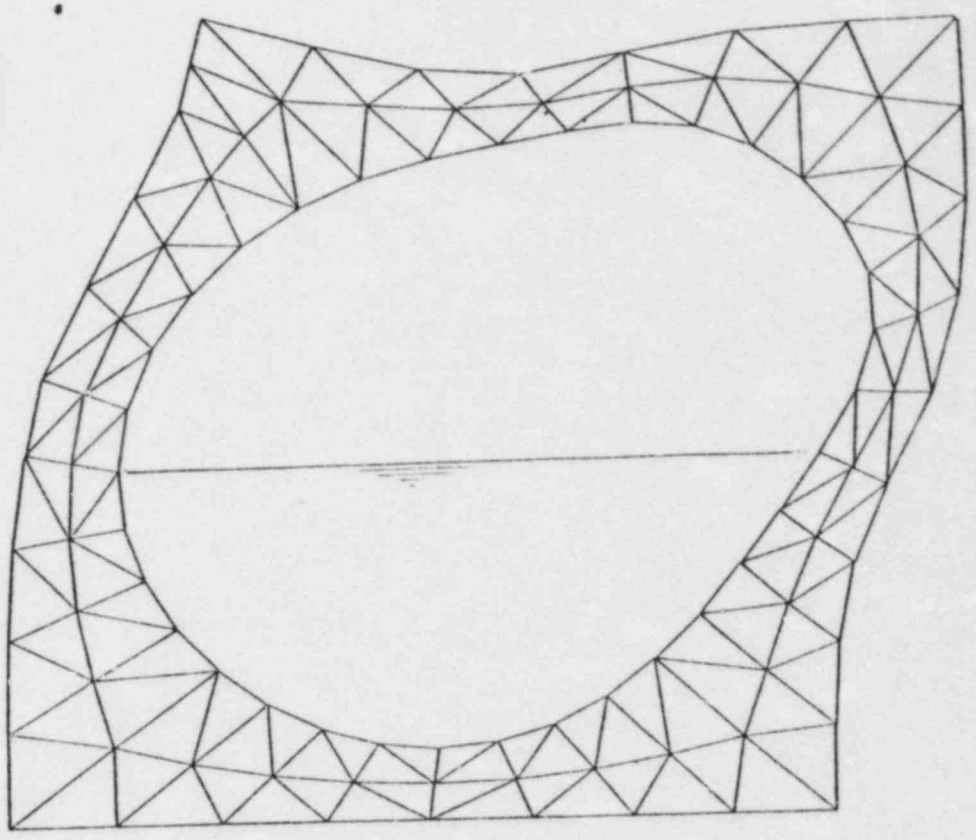

NORMAL MODES ANALYSIS OF THE COMBINED SYSTEM

MODAL DEFOR. SUBCASE 2 MODE 2 FREQ. 31.84038

Figure A.1-7 Effect of FSI on Mode 2 (Radial Movement Allowed)

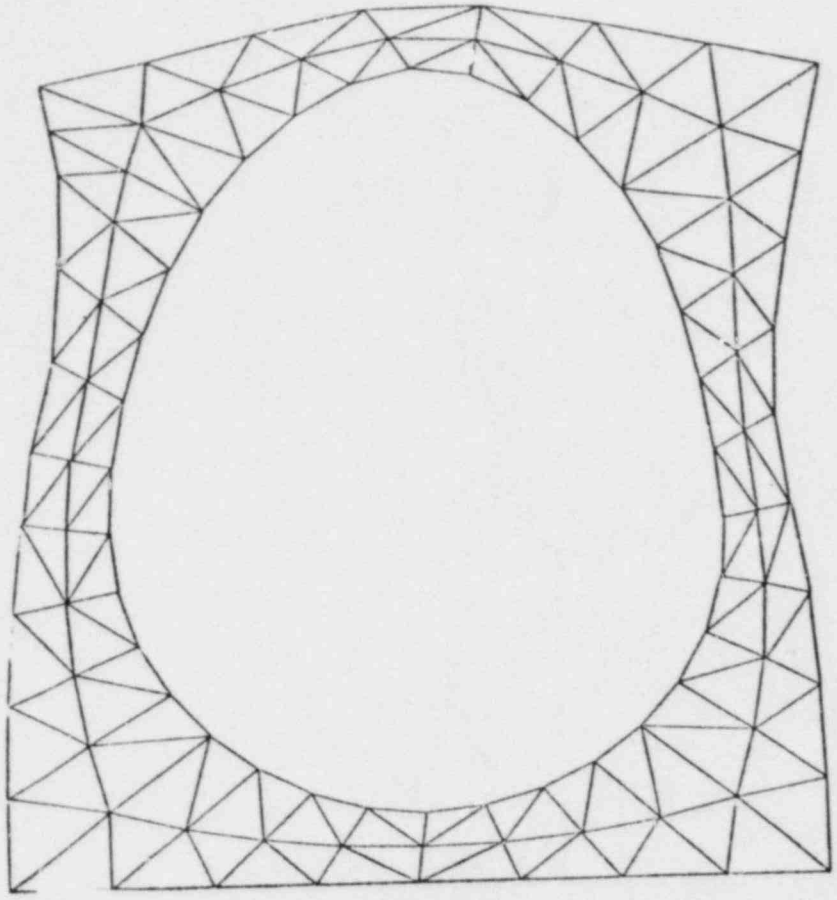

NORMAL MODES ANALYSIS OF THE STRUCTURE ONLY

MODAL DEFOR. SUBCASE 3 MODE 3 FREQ. 33.64432

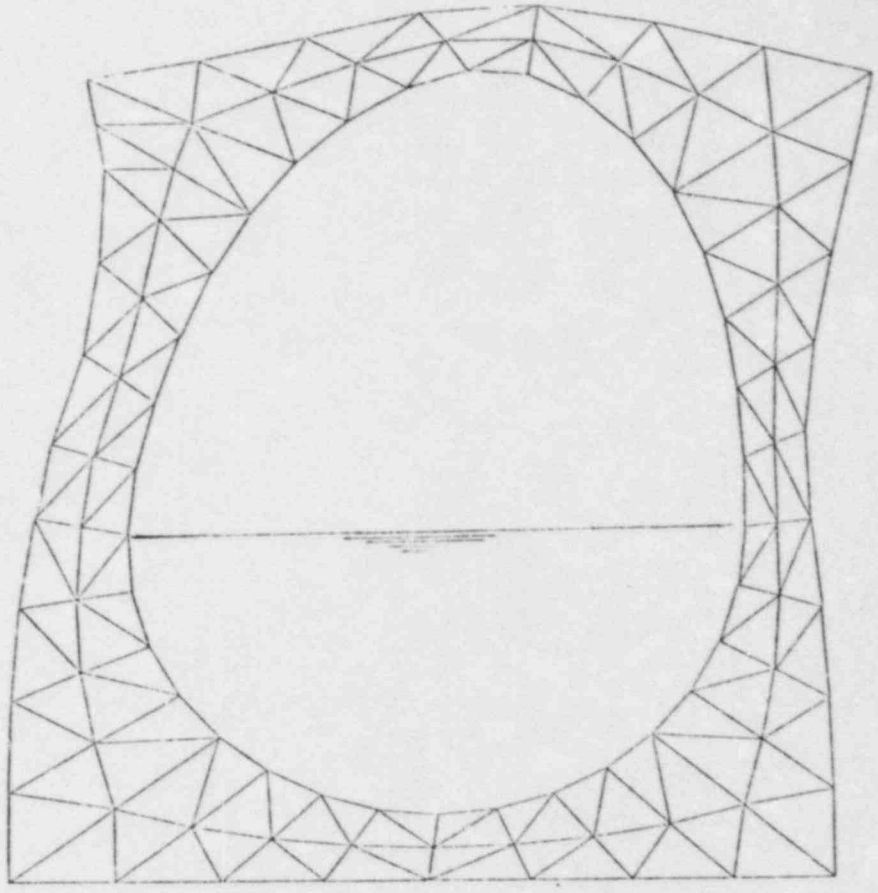

NORMAL MODES ANALYSIS OF THE COMBINED SYSTEM

MODAL DEFOR. SUBCASE 3 MODE 3 FREQ. 33.45044

Figure A.1-8 Effect of FSI on Mode 3 (Radial Movement Allowed)

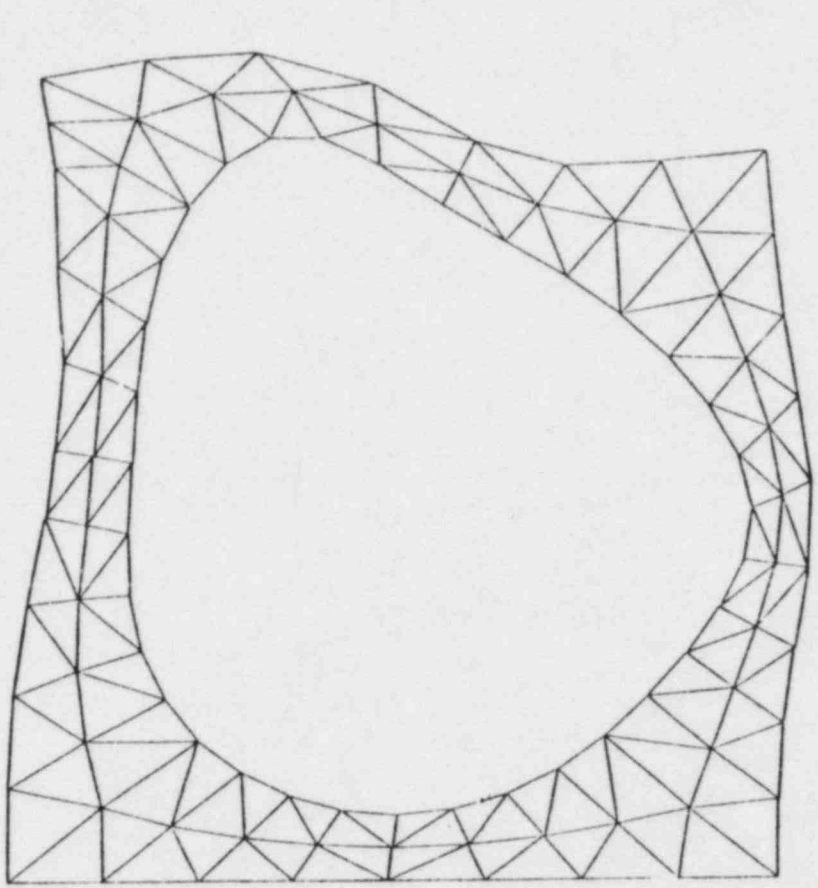

NORMAL MODES ANALYSIS OF THE STRUCTURE ONLY

MODAL DEFOR. SUBCASE 4 MODE 4 FREQ. 52.62469

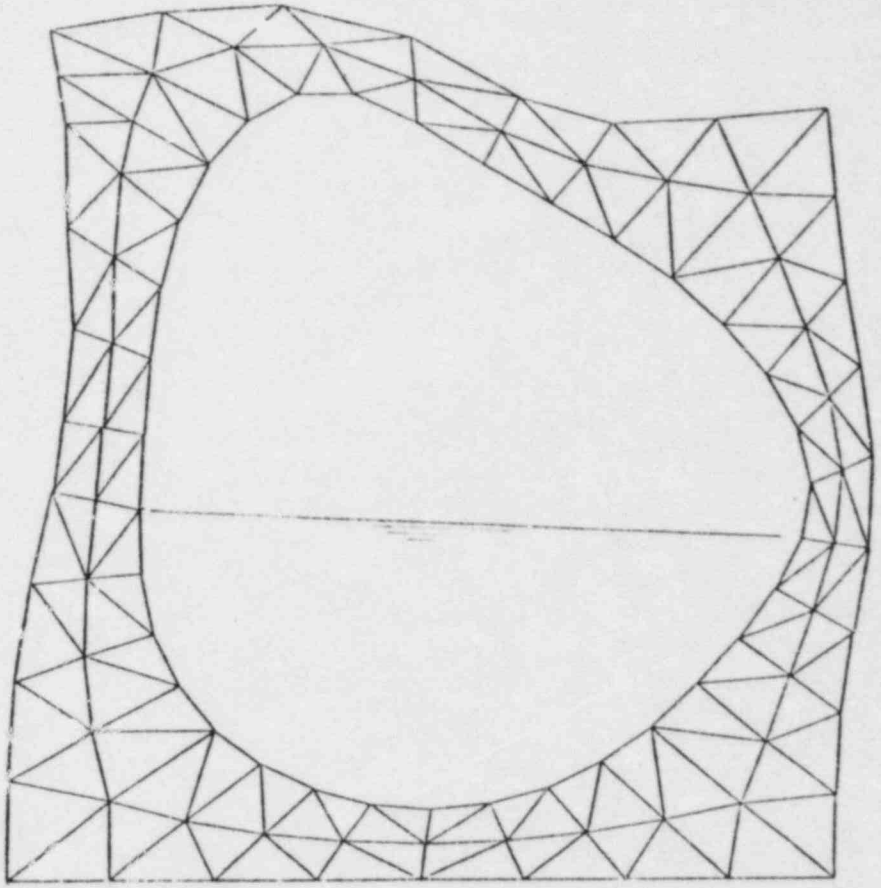

NORMAL MODES ANALYSIS OF THE COMBINED SYSTEM

MODAL DEFOR. SUBCASE 4 MODE 4 FREQ. 52.50384

Figure A.1-9 Effect of FSI on Mode 4 (Radial Movement Allowed)

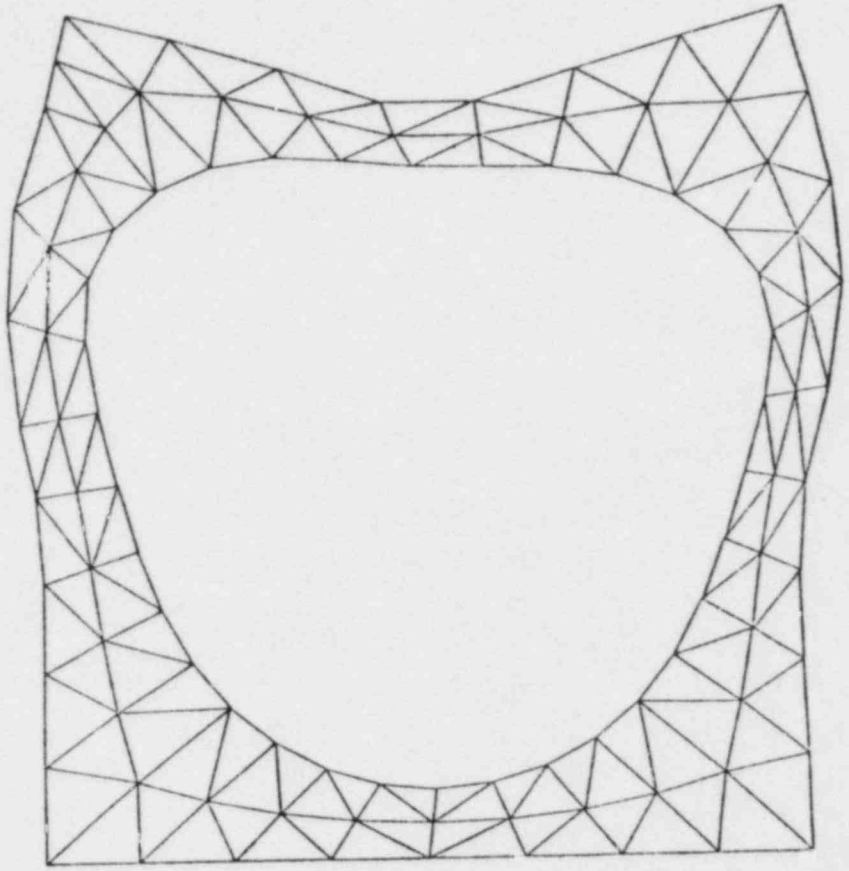

NORMAL MODES ANALYSIS OF THE STRUCTURE ONLY

MODAL DEFOR. SUBCASE 5 MODE 5 FREQ. 66.14927

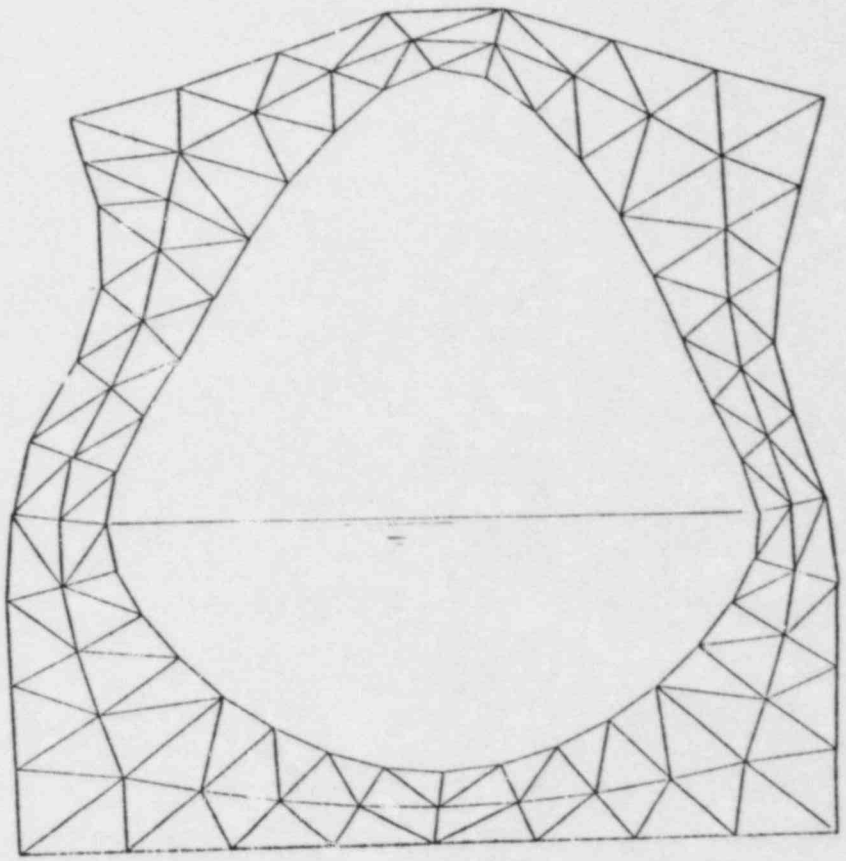

NORMAL MODES ANALYSIS OF THE COMBINED SYSTEM

MODAL DEFOR. SUBCASE 5 MODE 5 FREQ. 66.11057

Figure A.1-10 Effect of FSI on Mode 5 (Radial Movement Allowed)

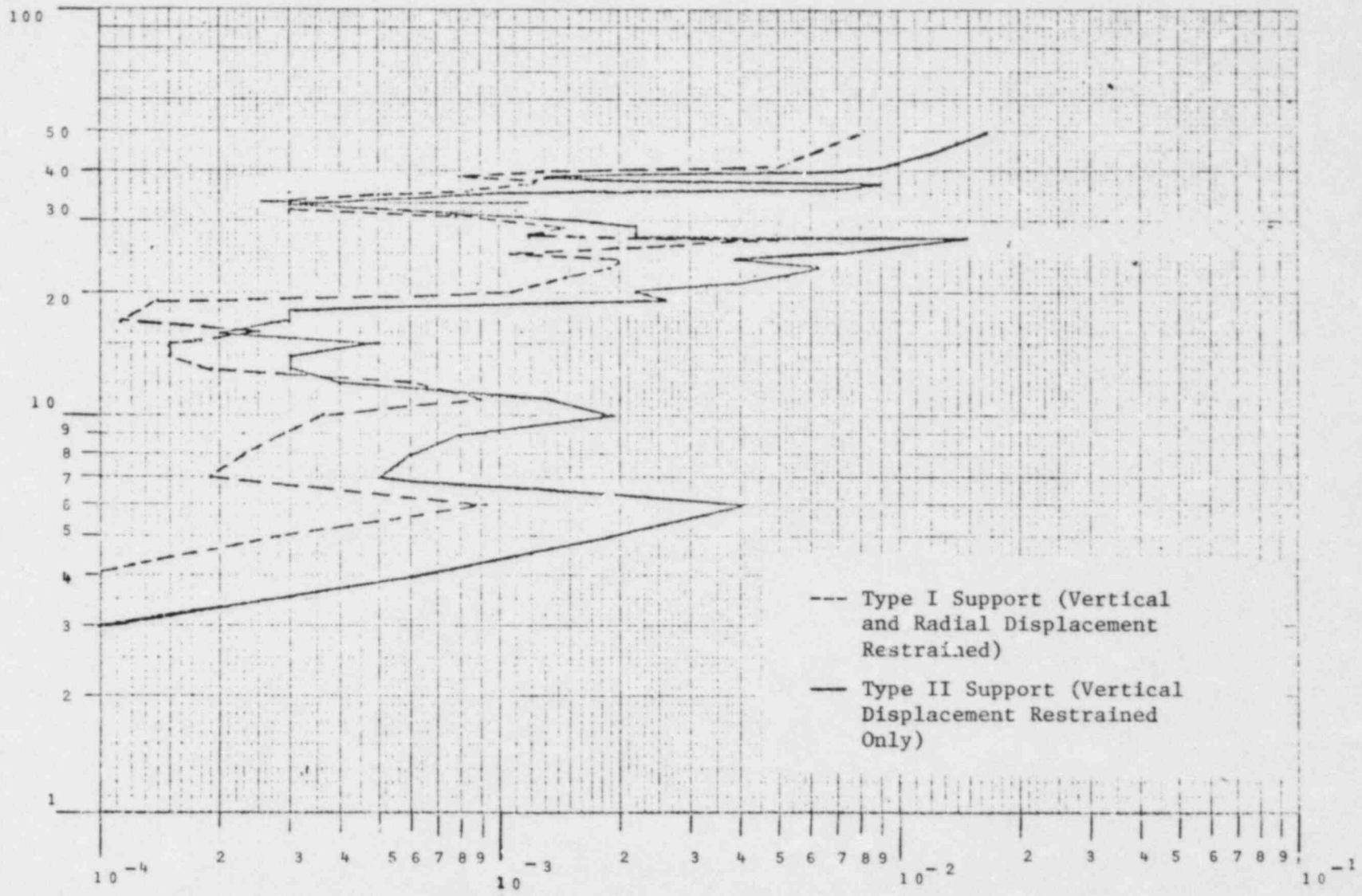

Figure A.1-11 Effect of FSI on Rigid Wall Pressure Amplitudes

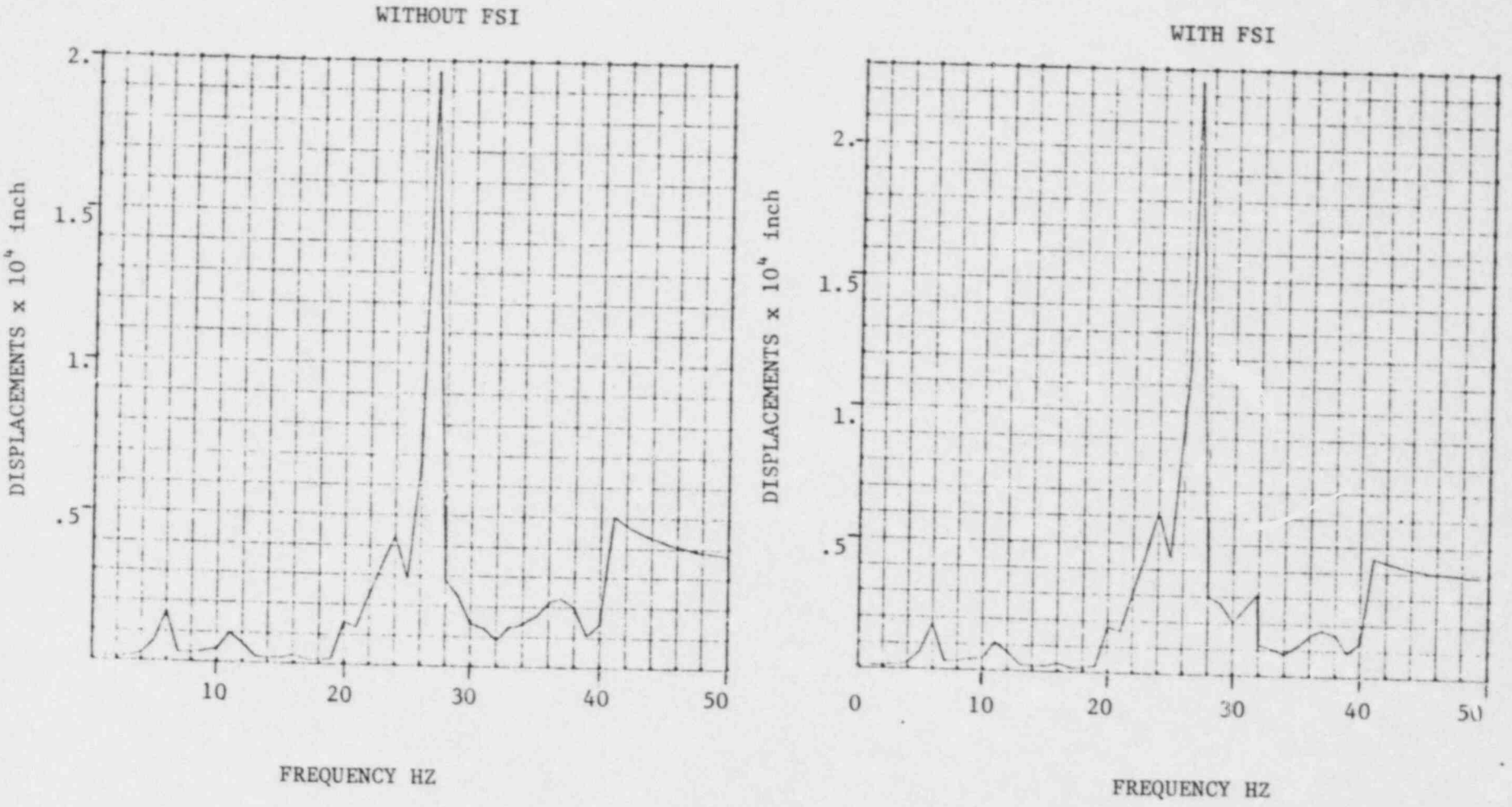

Figure A.1-12 Effect of FSI on Radial Displacement (Node 36) (Type II Support)

(CO Load NEDO 21888, Table 4.1.1-2 Ref. 1)

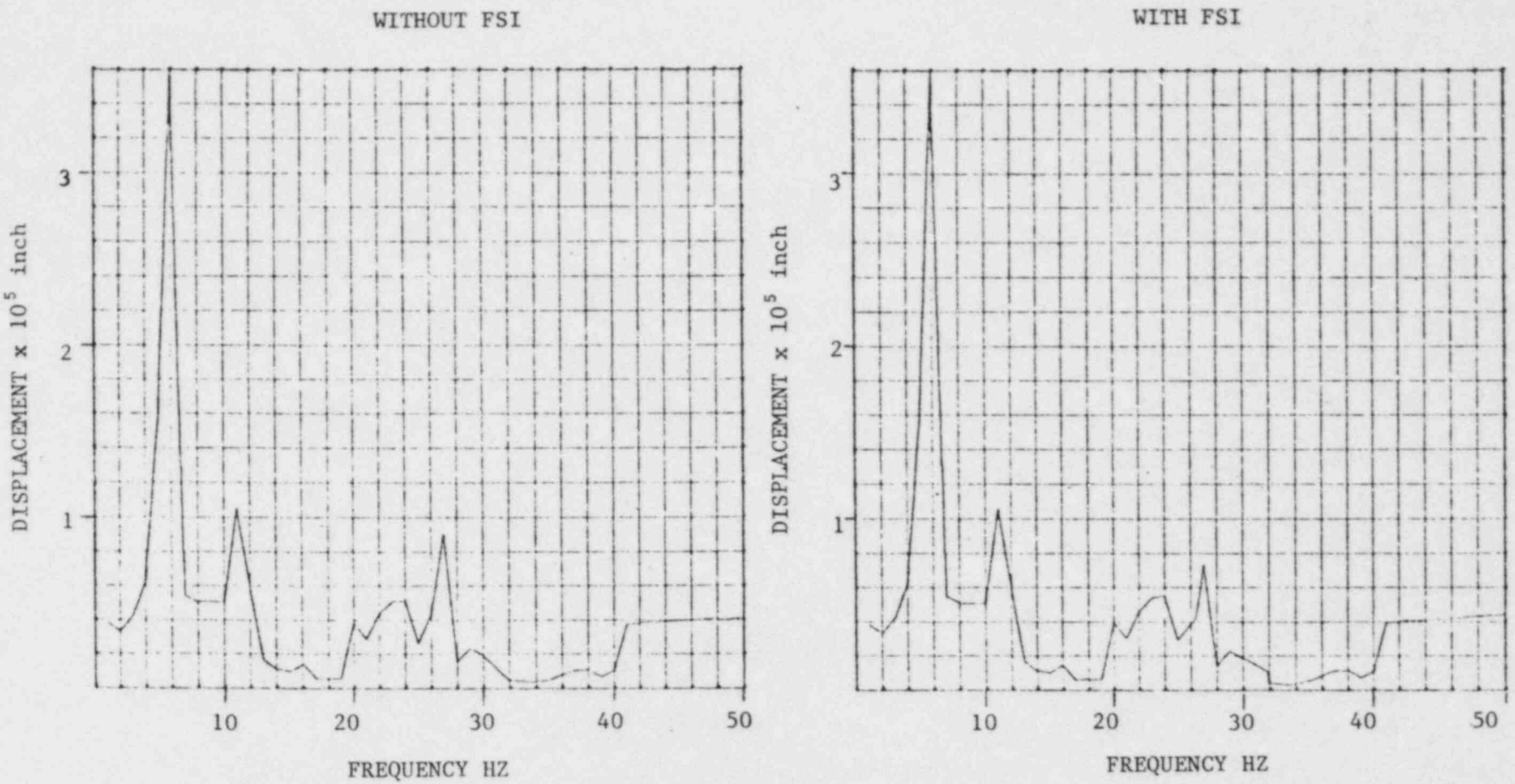

Figure A.1-13 Effect of FSI on Radial Displacement (Node 81) (Type II Support)

(CO Load NEDO 21888, Table 4.1.1-2, Ref. 1)

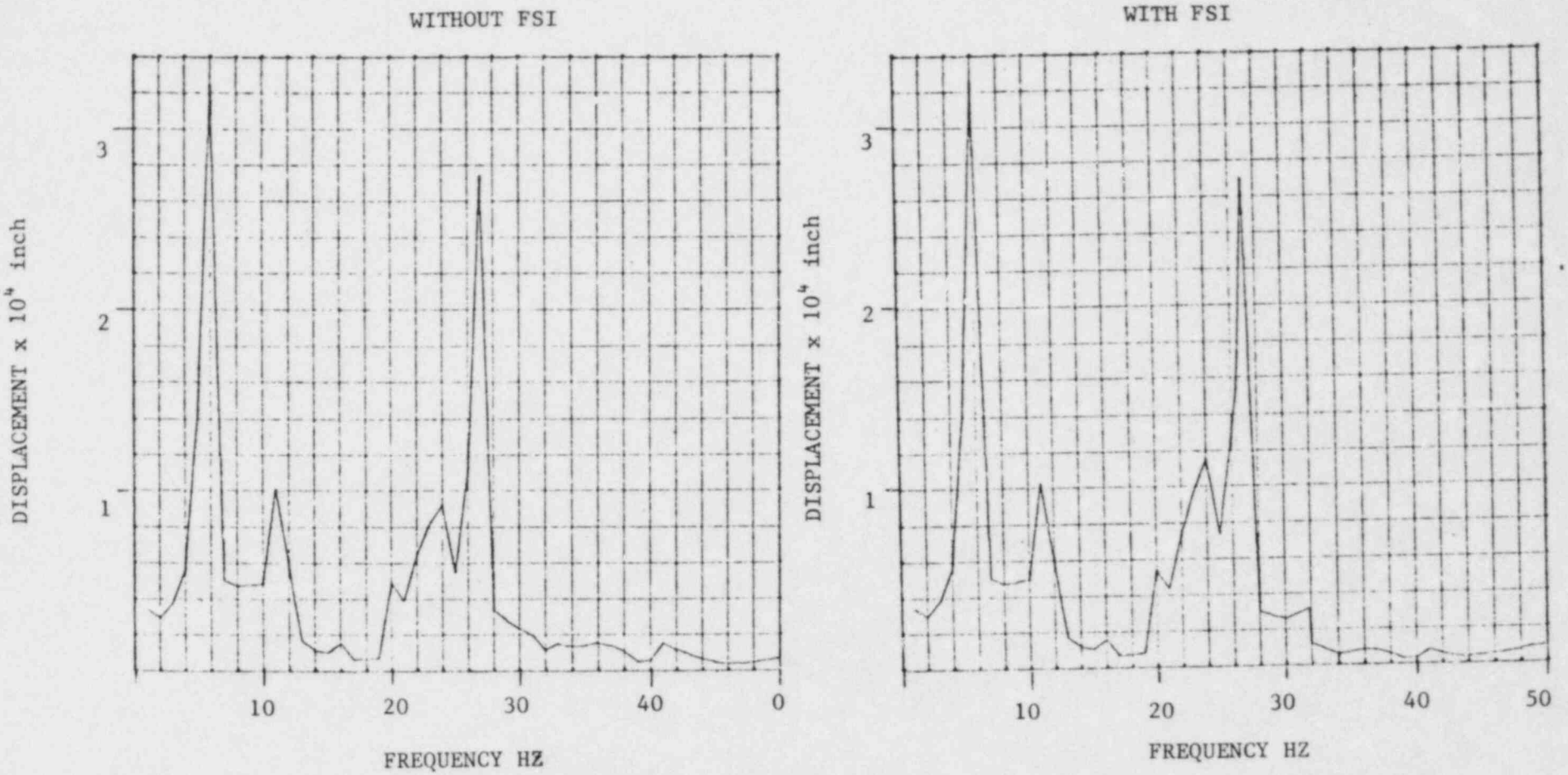

Figure A.1-14 Effect of FSI on Radial Displacement (Node 126) (Type II Support)

(CO Load NEDO 21888, Table 4.1.1-2, Ref. 1)

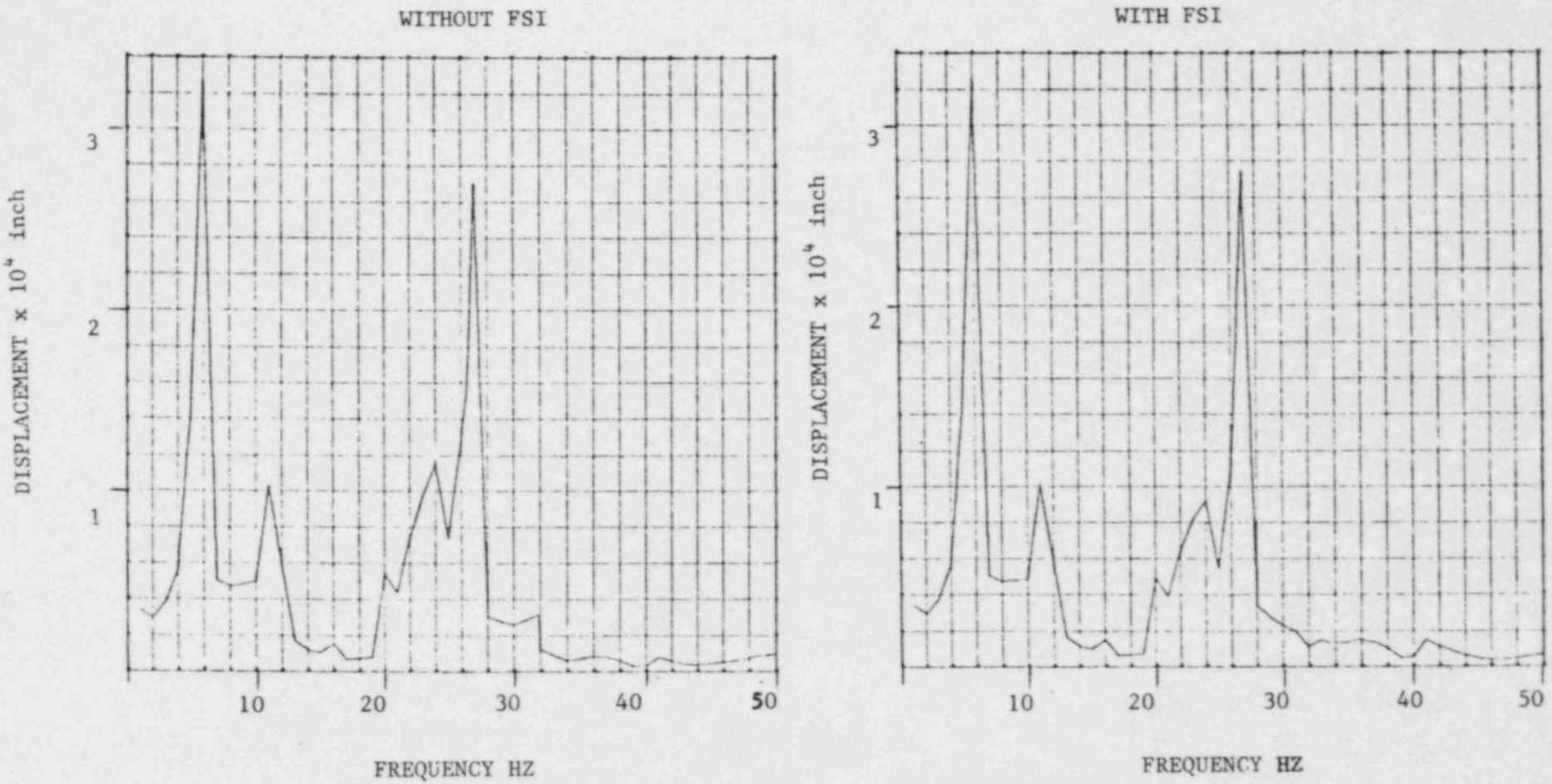

Figure A.1-15 Effect of FSI on Radial Displacement (Node 166) (Type II Support)

(CO Load NEDO 21888, Table 4.1.1-2, Ref. 1)

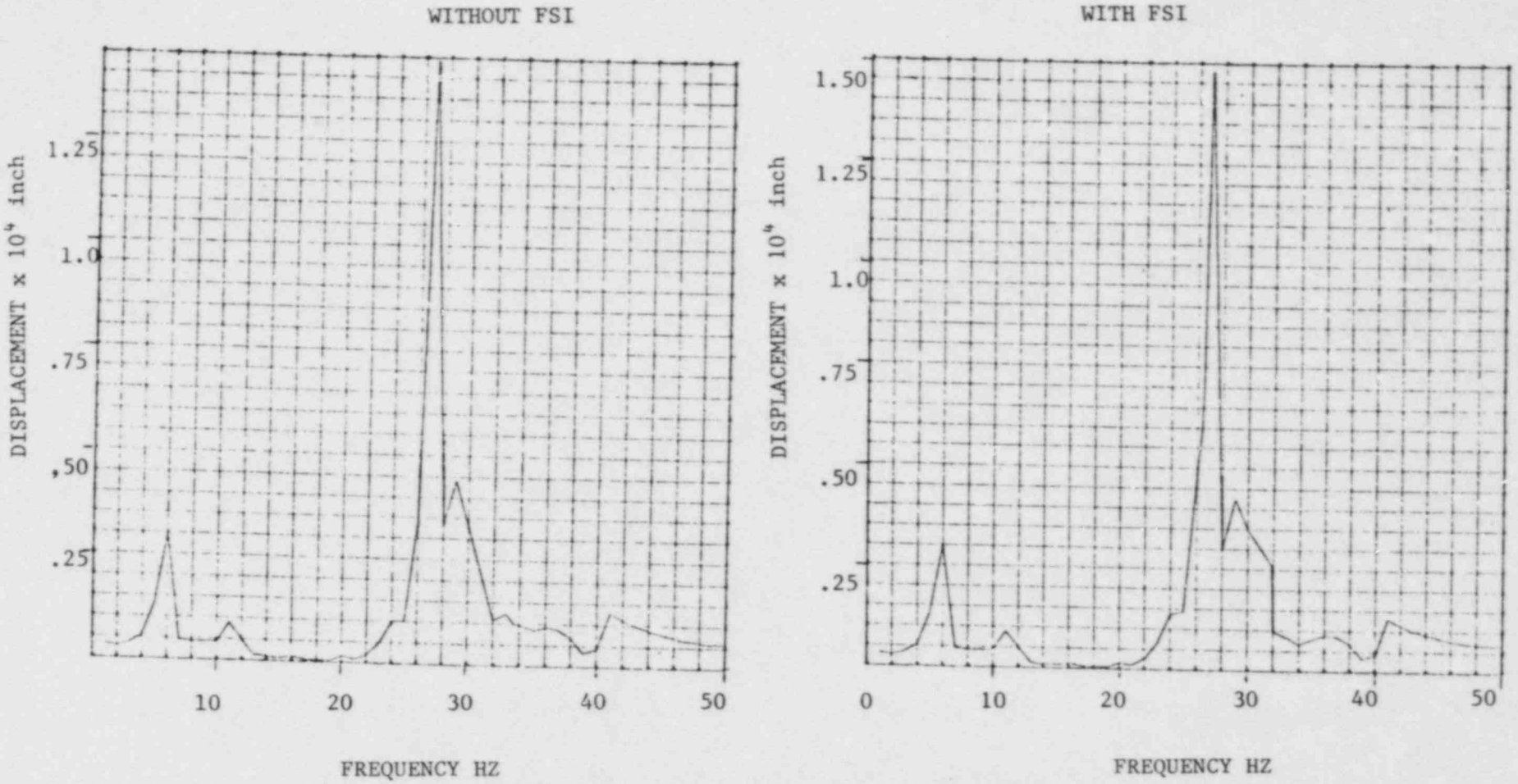

Figure A.1-16 Effect of FSI on Radial Displacement (Node 211) (Type II Support)

(CO Load NEDO 21888, Table 4.1.1-2, Ref. 1)

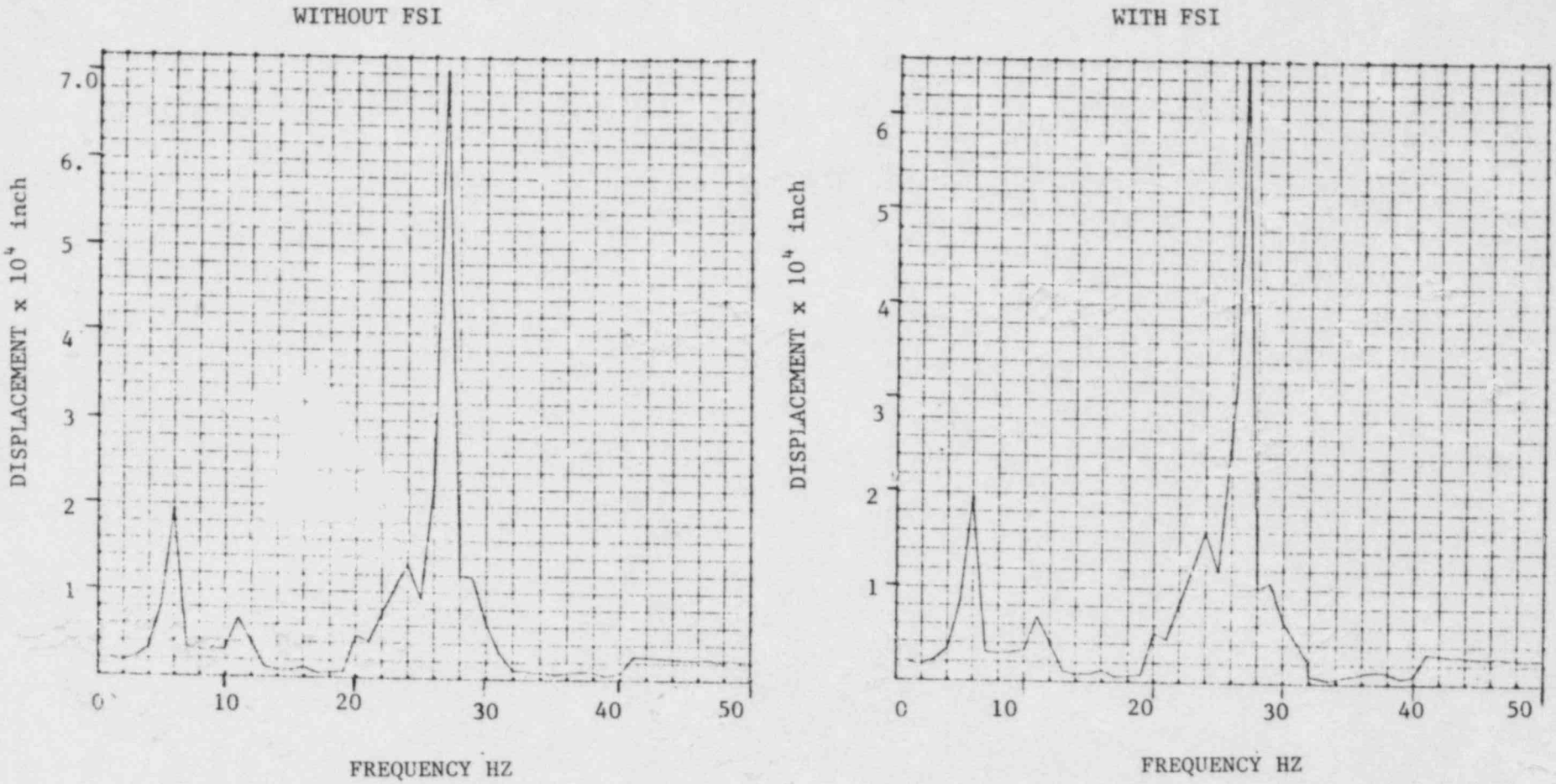

Figure A.1-17 Effect of FSI on Radial Displacement (Node 251) (Type II Support)

(CO Load NEDO 21888, Table 4.1.1-2, Ref. 1)

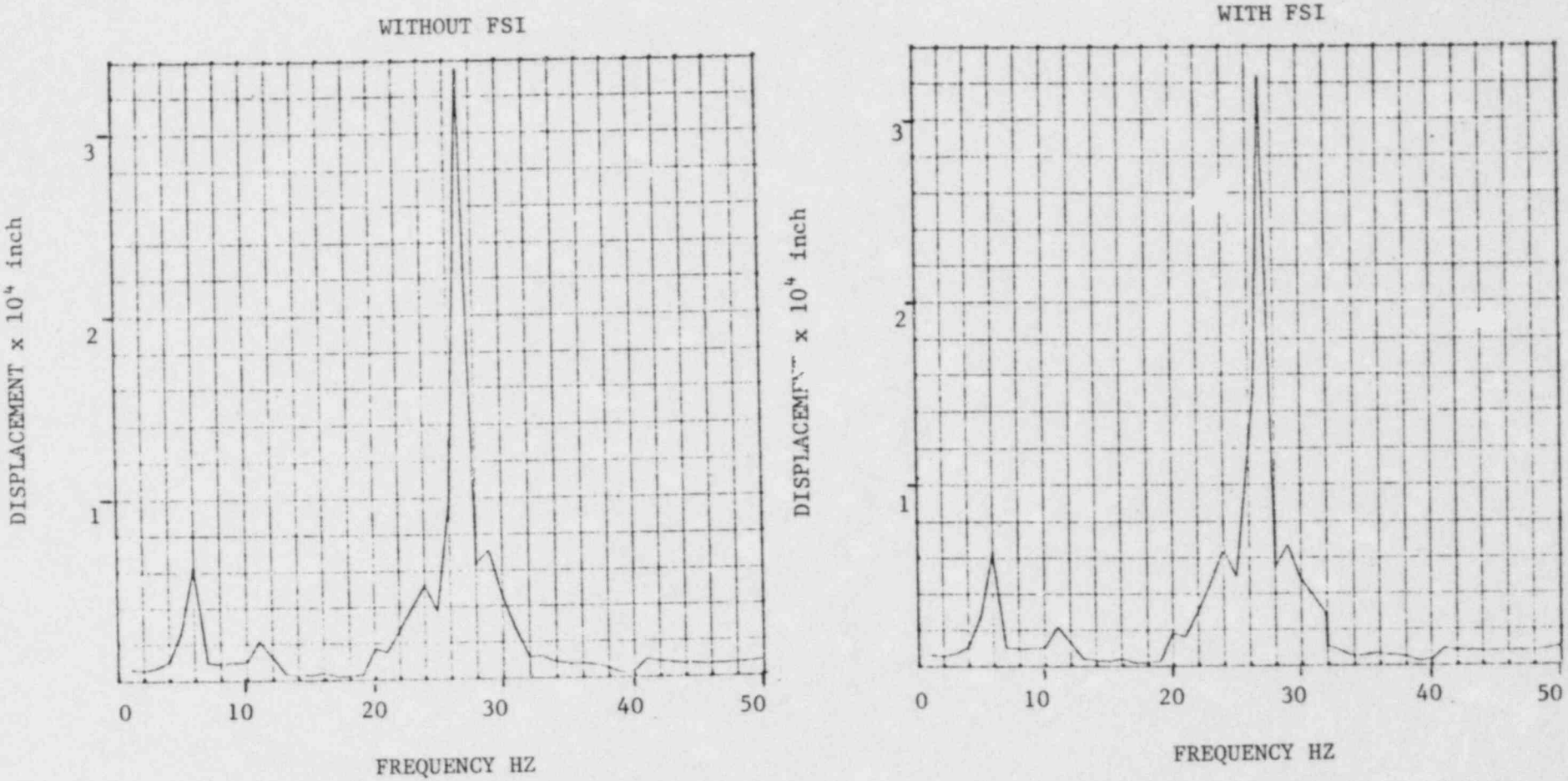

Figure A.1-18 Effect of FSI on Radial Displacement (Node 291) (Type II Support)

(CO Load NEDO 21888, Table 4.1.1-2, Ref. 1)

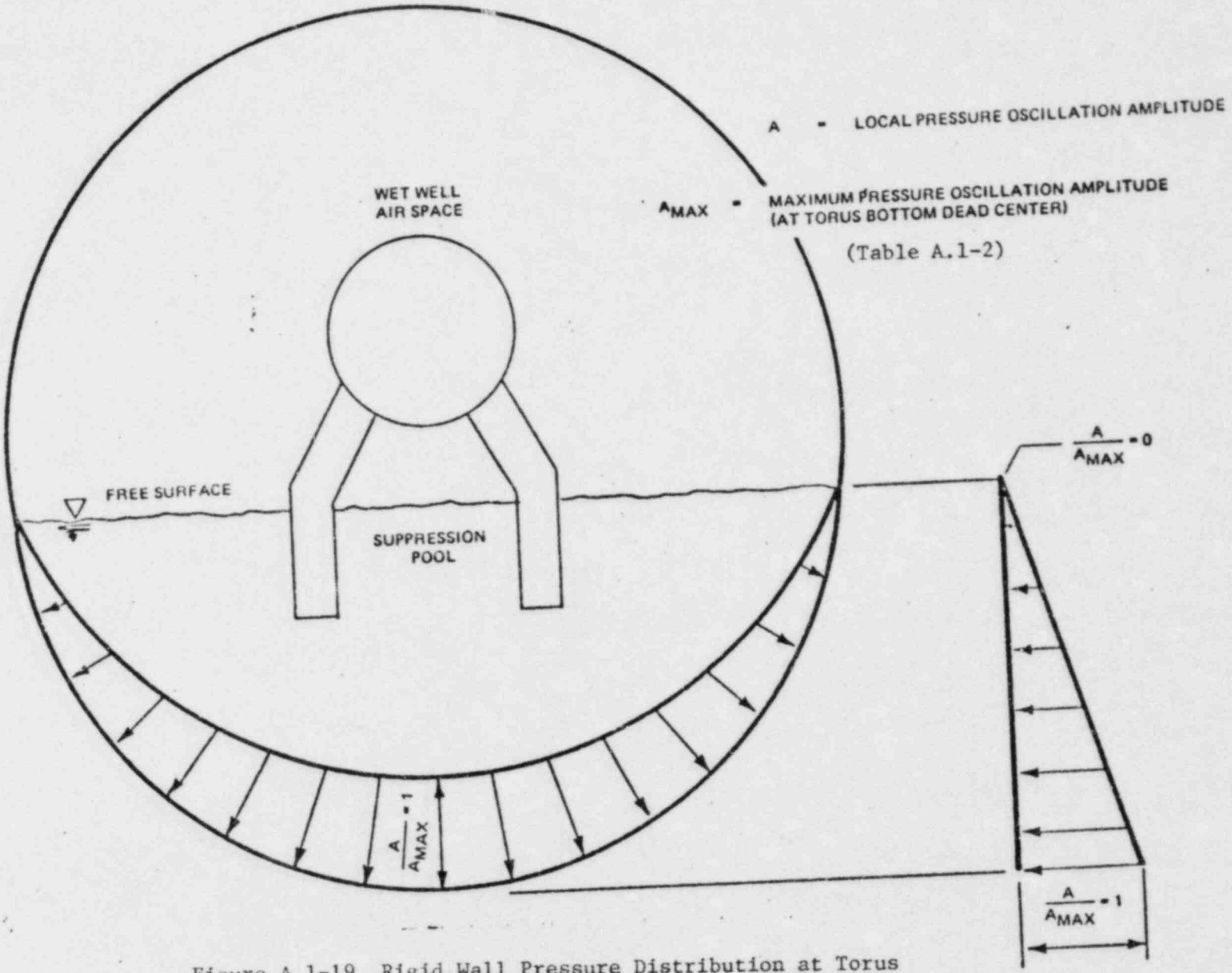

Figure A.1-19 Rigid Wall Pressure Distribution at Torus Cross Section

2.0 LOAD DEFINITIONS AND STRUCTURAL EVALUATION OF MISCELLANEOUS INTERNAL STRUCTURES

2.1 INTRODUCTION

The Mark I Long Term Program requires that all structures within the suppression chamber be evaluated for hydrodynamic loads resulting from the postulated Loss-of-Coolant Accident (LOCA) and Safety Relief Valve (SRV) actuation events.

The objective of this section is to describe the calculation of these hydrodynamic loads and to present the analyses and evaluation of the miscellaneous structures inside the suppression chamber based on the calculated loads. A list of acronyms used in this section is given in Table 2.1-1.

2.1.1 Miscellaneous Structures Inside the Suppression Chamber

The following structures were evaluated based on the loads developed under the Mark I Long Term Program:

A. SRV Discharge Lines and Supports

B. Submerged Structures
   1. HPCI turbine exhaust line
   2. Vent header support columns
   3. Platform support columns
   4. Pump suction strainer piping (RCIC, RHR, HPCI, Core Spray)
   5. Core spray test line
   6. RCIC barometric condenser line
   7. HPCI turbine drain pot line
   8. RCIC turbine exhaust line
   9. Liquid level indicators

C. Structures Above the Suppression Pool
   1. RHR containment cooling line
   2. Monorail

3. RHR test lines
4. Access hatch
5. Drywell/wetwell vacuum breaker flange
6. RCIC vacuum breaker line
7. HPCI vacuum breaker line
8. Electric penetration box
9. Vent purge inlet and outlet
10. Spare penetrations

2.2 LOAD DEVELOPMENT

Based on the Load Definition Report (LDR) (Reference 2-1) miscellaneous structures within the suppression chamber must be analyzed for the following hydrodynamic loads in combination with seismic loads and dead weight.

A. LOCA Related Loads
   1. Containment system temperature and pressure load
   2. Pool swell impact and drag loads, froth impingement loads and pool fallback loads
   3. LOCA water jet loads
   4. LOCA air bubble induced drag loads
   5. LOCA steam induced condensation oscillation drag loads
   6. LOCA steam induced chugging drag loads

B. SRV Discharge Loads
   1. SRV discharge line clearing transient loads
   2. Torus shell loads (applied to shell only)
   3. SRV reflood transient
   4. T-Quencher water jet loads
   5. T-Quencher air bubble induced drag loads
   6. Thrust loads on T-Quencher arms
   7. Maximum SRVDL and T-Quencher wall temperature

The calculations of these loads are documented in the calculation books listed in Appendix A.2 (A through C).

2.2.1 LOCA Related Loads

For a postulated pipe break inside the drywell, three LOCA cases selected on the basis of postulated break size, are referred to as Design Basis Accident (DBA), Intermediate Break Accident (IBA) and Small Break Accident (SBA). The application of loads from each case is illustrated in Figures 3.0-2 through 3.0-5 of Reference 2-1.

2.2.1.1 Containment System Temperature

Containment temperature and pressure loads for Brunswick are provided by GE and are documented in the Plant Unique Load Definition (Reference 2-2)

2.2.1.2 Pool Swell Impact and Drag Loads

During the pool swell transient, the rising pool will impact structures that are located above the initial pool surface and below the maximum pool swell height. Two sets of procedures are given in Application Guide 10 (Reference 2-3). The first set is consistent with the original LDR methodology. Alternately, a second set of procedures is evolved from the NRC's acceptance criteria (Reference 2-4). The alternate procedure has been used to calculate the pool swell impact and drag loads. There are two sets of pool swell profiles (pool swell displacement distribution and pool swell velocity distribution curves) for Brunswick. The first set is a result of Brunswick quarter scale test with wingless deflector. The second set is the load definition for Brunswick developed by the General Electric Company based on the Monticello test. When calculating pool swell loads, the first set of curves were used for structures located in the region without the deflector while the second set of curves were used for structures located in the region with the winged deflector.

The pool swell impact and drag loads are time history forces. Time history dynamic analysis using STARDYNE program (Reference 2-5)

was performed for all piping systems in the suppression chamber. When analyzing the penetration sleeves and other structural components such as the access hatch and the electric penetration box, these loads were treated statically and the dynamic effects were considered by calculating dynamic load factors. An in-house program "DLFPSWL" (Reference 2-6) was developed to facilitate the calculation.

2.2.1.3 Froth Impingement Loads

Two sets of procedures are given in Application Guide 10 (Reference 2-3) for calculating froth impingement loads. The first set provides procedures to define the generic froth load. To allow for plant-specific variations in the froth source velocity, departure angle, and froth density, the second set of procedures allow the QSTF plant-specific movies to be used to define these parameters. The first set of procedures was employed in the entire calculation. Later it was discovered that the calculated loads on RHR test lines, RHR containment cooling line and monorail were too conservative to permit feasible modifications. Calculations were then conducted using the test film in order to get more realistic loads. The modifications on RHR test lines, RHR containment cooling line and the monorail were pursued using the maximum average velocity calculated from the films and the froth density defined by the NRC.

The froth impingement loads are defined as rectangular pulses. The dynamic effects were considered using Bigg's methods (Reference 2-7).

2.2.1.4 Pool Fallback Loads

Pool fallback loads occur on structures inside the torus which are between the maximum bulk pool swell height and the downcomer exit level. Application Guide 10 (Reference 2-3) outlines the procedures for calculating the loads. The loads are defined in the form of time histories by combining the acceleration drag (proportional to acceleration) with the standard drag (proportional to velocity

squared). In structural evaluation, this load was treated statically and the dynamic effects were considered by calculating the dynamic load factors. To facilitate the calculation, an in-house program "DLFPFBK" (Reference 2-8) was developed.

2.2.1.5 LOCA Jet Loads

All structures below the downcomer exit level receive the water jet loads and the bulk pool motion loads. The Application Guide 10 (Reference 2-3) outlines a step-by-step procedure to calculate these loads. The calculation procedure is complex and repetitive. A computer program written by Bechtel (Reference 2-9) was used to replace tedious hand calculations.

The code (Reference 2-9) computes component velocities in a rectangular coordinate system and then computes component forces from these velocities in the same coordinate system. Let $F_{x'}$ and $F_{y'}$ be the component forces, $V_{x'}$ and $V_{y'}$ be the component velocities, the standard drag loads are computed as:

$$F_{x'} = K\, V_{x'}^2 \text{ and } F_{y'} = K\, V_{y'}^2 \qquad (1)$$

where

$$K = C_D A_p\, \rho\, /2g_c$$

In the above expression, C_D is the standard drag coefficient, A_p is the projected area, ρ is the water density and g_c is the gravitational acceleration. The computer code then computes the resultant load as:

$$F_{resultant} = \sqrt{F_{x'}^2 + F_{y'}^2} = K \sqrt{V_{x'}^4 + V_{y'}^4} \qquad (2)$$

Another method which is different from Equation (2) is to combine velocities in different directions and to yield resultant

velocities. Resultant forces are then computed from these resultant velocities. These can be represented in the expression below:

$$V_{resultant} = \sqrt{V_{x'}^2 + V_{y'}^2} \quad (3)$$

$$F_{resultant} = K(V_{x'}^2 + V_{y'}^2) \quad (4)$$

Comparing Equations (2) with (4), it is seen the second method gives resultant forces as much as $\sqrt{2}$ larger. This factor was applied to the loads computed from the LOCAJET code as shown in Equation (2) to obtain more conservative results.

The resultant loads are time history forces. All submerged structures which experience these loads were analyzed by the STARDYNE program (Reference 2-5).

2.2.1.6 LOCA Bubble Induced Drag Loads

All submerged structures below the pool surface will be exposed to transient hydrodynamic loads due to LOCA air bubbles. Application Guide 1 (Reference 2-10) provides procedures to evaluate using the GE computer code LOCAFOR. The resultant loads are time history forces. For structural evaluation, this load was simplified as a rectangular pulse with an amplitude equal to the peak load from the entire time history. Dynamic load factors were calculated by Bigg's method (Reference 2-7) and were incorporated in the static analysis using the STARDYNE program (Reference 2-5).

2.2.1.7 Condensation Oscillation Loads

Condensation oscillation in the suppression pool produces three dimensional flow fields that result in drag forces on structures submerged in the suppression pool. The GE computer code CONDFOR (Reference 2-11) was used to calculate the loads. The loads were computed on the basis of both the average and maximum source strengths. The average source strength was applied at all downcomers

to calculate the average loads on the submerged structures. The maximum source strength, which is defined as twice the average source strength, was applied at the downcomer nearest to the structure to calculate the maximum drag loads on the structure.

According to the NRC criteria (Reference 2-4) the total drag, which is the sum of standard and acceleration drags, shall be computed by using a conservative coefficient of $C_d = 3.6$ for $U_m\ T/D > 2.74$, where U_m is the maximum velocity, T is the period of bubble oscillation and D is the cylinder diameter. For $U_m\ T/D \leq 2.74$, the drag forces shall be computed on the basis of acceleration drag alone. In developing the loads for Brunswick, both standard and acceleration drags were considered disregarding the value of $U_m\ T/D$.

The NRC criteria states that the loads may be applied quasi-statically to structures, only if the highest significant Fourier components occur at frequencies less than half the lowest structural frequency. When the structures are rigid enough to allow application of the load on a quasi-static basis, dynamic load factors were calculated using the in-house program code DLFCO (Reference 2-12).

Because fluid-structure interaction (FSI) may alter the flow field, the condensation oscillation loads have to also include the effects of the FSI-induced acceleration flow field if the local fluid acceleration is less than twice the torus boundary acceleration. For simplicity, the FSI-induced acceleration was included in the structural evaluation using the in-house program DLFFSI (Reference 2-13) regardless of the magnitude of the local fluid acceleration with respect to torus boundary acceleration. Loads calculated by DLFFSI were then combined absolutely with condensation oscillation induced drag loads.

2.2.1.8 Chugging Loads

Chugging drag loads were calculated by the GE computer code CONDFOR (Reference 2-11). Prechug analysis was performed in a manner identical to the condensation oscillation method because of the almost harmonic character of the prechug pressure traces. Due to the less

synchronized nature of the postchug signal, the loads were computed based on maximum source applied at the two downcomers nearest to the structure with phasing which would result in maximum forces. The effects of fluid-structure interaction and U_m T/D were dealt with in the same manner as for condensation oscillation loads.

For prechug, loads can be applied quasi-statically to structures if the highest significant Fourier components occur at frequencies less than half the lowest structural frequency. The dynamic effects were considered by calculating the dynamic load factors using Bigg's method (Reference 2-7). For postchug, the loads were applied dynamically when the lowest structural natural frequency times the duration of the spike in the source strength is less than 3. Dynamic analysis was performed by the STARDYNE program (Reference 2-5). When the product of the fundamental structural frequency with the duration of the spike in the source strength is greater than 3, the postchug loads were analyzed quasi-statically using the dynamic load factors calculated by the in-house program DLFPCH (Reference 2-14).

2.2.2 SRV Discharge Loads

Following an actuation of a Safety Relief Valve (SRV), pressure and thrust loads are exerted on the SRV piping and discharge device (T-Quencher). In addition, the expulsion of water and then air into the suppression pool through the T-Quencher results in pressure loads on the submerged portion of the torus shell and drag loads on submerged structures. In general, there are three load cases on submerged structures due to SRV actuations. These loads cases are:

Case 1. Any one Valve

Case 2. ADS Valves

Case 3. Multiple Valves

Various load cases which are applicable to Brunswick are listed in Table 2.2.2-1. Among these load cases, C3.2 and C3.3 are not evaluated. These loads will be eliminated by lowering the MSIV

isolation water level trip and modifying the SRV logic. Computer analyses were performed for load cases A1.1, A1.2 (SBA) and C3.1. It was found that A1.2 (SBA) bounds A1.2 (IBA), thus ony A1.2 (SBA) was analyzed. It was also found that A1.3 is bounded by A1.1 and A2.2 is bounded by A3.2 (SBA). Furthermore, load cases A3.1 and A3.2 are deduced from A1.1 and A1.2, respectively.

2.2.2.1 SRV Discharge Line Clearing Transient Loads

Using the GE computer code RVFOR04 (Reference 2-15), the SRV discharge line clearing transient loads were obtained. The program provides the following transients:

a) SRVDL pressure
b) SRVDL thrust
c) T-Quencher pressure
d) Water clearing velocity and acceleration
e) Discharge pressure
f) Water clearing time

The peak dynamic value of the SRVDL pressure was used to evaluate the design adequacy of the SRVDL and the steady state value (exit pressure) to verify that the SRV back-pressure requirements are met. The SRVDL thrust force was used in evaluation of the design adequacy of the SRVDL and discharge devices, their restraints, and the connection of the SRV to the main steam line. For ease of the manipulations of the thrust forces in the evaluation of SRVDL, two post-processor programs, SAG092 and SAG093 (References 2-16 and 2-17), were developed to reformat and plot the data. It should also be noted that the RVFOR04 code cannot correctly calculate the water thrust in the elbow upstream of the discharge device for the case when the elbow is directly connected to the discharge device such as the one at Brunswick. Corrections to the RVFOR04 results were made in terms of Reference 2-18.

Internal T-Quencher pressure was used in the evaluation of the design adequacy of the T-Quencher. Water clearing velocity and

acceleration were used to calculate the thrust loads exerted on the T-Quencher arms plus the drag loads on submerged structures in the suppression pool due to T-Quencher water jets. The discharge pressure and water clearing time were used as input for the evaluation of SRV air bubble pressures and torus shell pressures.

2.2.2.2 Torus Shell Loads

The pressure loading on the wetted portion of the torus shell that results from the air discharge through a T-Quencher device when a safety relief valve actuates was calculated using the GE computer code QBUBS02 (Reference 2-19). Loads and frequencies on all eleven SRV discharge lines at Brunswick were calculated. The loads were used in the evaluation of the torus shell. For load case C3.1 the pressure amplitude was taken from that predicted on load case A1.1 while the bubble frequency is still based on the load case C3.1. The predicted frequency of the torus shell pressure has to be adjusted by $\pm$ 25 percent for first actuations and $\pm$ 40 percent for subsequent actuations to account for data scatter per the requirements of the load definition.

2.2.2.3 SRV Reflood Transient

The GE computer code RVRIZ02 (Reference 2-20) was employed to determine the transient water rise in the SRVDL following SRV closure. The reflood transient was input to the RVFOR04 code for the analysis of the SRVDL clearing transient for subsequent actuations. The design reflood transient was evaluated for eleven SRV discharge lines under load case C3.1. The reflood water column length is the maximum value which occurs at or after the minimum predicted interval between SRV closure and a subsequent actuation. Since the minimum interval between actuations has not been determined, the water column length was conservatively evaluated at its maximum value (i.e., the first peak).

The calculated reflood height is not only used for the subsequent analysis, it is also used to check if the water leg reaches or exceeds the elevation of the va uum breaker at any time during the design reflood transient. [illegible] n-inch check valves at Brunswick, the water leg was found below the elevation of the vacuum breaker under normal operating condition (Case C3.1).

2.2.2.4 T-Quencher Water Jet Loads

Drag loads on submerged structures due to T-Quencher water jet discharges were calculated per Reference 2-21. Since the water jets from the arm of one quencher will not interact with the water jet from any adjacent quencher, only single valve actuations need to be considered. Calculations were made for load cases A1.1, A1.2 (SBA) and C3.1. Load case A1.3 was replaced by the more conservative loads from case A1.1. The load is defined as a rectangular pulse. The dynamic effects were considered by Bigg's method (Reference 2-7) in the structural evaluation.

2.2.2.5 T-Quencher Bubble Induced Drag Loads

T-Quencher bubble induced drag loads on submerged structures as well as on the T-Quencher, the submerged SRV piping and the T-Quencher support pipe were calculated using the GE computer code TQFORBF (Reference 2-22). Loads for cases A1.1, A1.2 (SBA), A3.1 and A3.2 (SBA) were calculated. Load cases A1.3 and A2.2 are bounded by load cases A1.1 and A3.2, respectively. Based on the load definition, the pressures for subsequent actuations are bounded by pressures of first actuations. Thus, for load case C3.1, the pressure amplitudes were taken from load case A3.1. The load definition also requires a range of $\pm$ 40% be applied to the predicted frequencies for subsequent actuations and $\pm$ 25% for first actuations.

Loads obtained from the GE code TQFORBF are sinusoidal time history loads with nearly constant periods but with variant amplitudes. For simplicity, the peak amplitude in the entire time history was used. The assumed simple harmonic forcing function was used in the structural analysis by the STARDYNE program (Reference 2-5).

2.2.2.6 Thrust Loads on T-Quencher Arms

Uneven water clearing between the two arms of a T-Quencher results in a thrust load along the axis of the T-Quencher arms. Uneven water clearing between the two sides of an arm results in a thrust load perpendicular to the T-Quencher arms. Both of these loads were calculated per Application Guide 10 (Reference 2-3). It is apparent from the application guide that the maximum thrust loads occur at the maximum mass flowrate. Thus loads were calculated for the SRV discharge line which has the maximum mass flowrate. Load cases A1.1, A1.2 (SBA) and C3.1 were calculated and used in the evaluation of the T-Quencher and support systems. These loads are defined as static concentrated loads. They were applied on the T-Quencher arms in all possible combinations to result in the maximum twisting moment on the entire discharge device and the maximum bending moment at the center of the discharge device.

2.2.2.7 Maximum SRVDL and T-Quencher Wall Temperature

The maximum SRV discharge pipe temperature (upstream of the discharge device) at a given location along the line is assumed to be the saturation temperature corresponding to the steady state pressure predicted by the SRV clearing model at the location. The SRVDL wall temperature is thus determined by finding the saturation temperature corresponding to the steady state pressure predicted from code RVFOR04 using the steam tables. The T-Quencher temperature is defined generically as 370°F per Reference 2-7. A local pool temperature limit of 200°F has also been established by the NRC (Reference 2-4). This temperature was used in the evaluation of submerged structures.

2.3 STRUCTURAL EVALUATION

Structural analyses were carried out for SRV line supports in the wetwall, miscellaneous submerged structures and structures above the pool (excluding vent system). Structural evaluations were then conducted according to load combinations and service limits defined in

the Plant Unique Analysis Application Guide (Reference 2-23). The computer analysis models and results are documented in the calculation books listed in Appendix A.2 (D through F).

2.3.1 Method of Analysis

Hand calculation or finite element program STARDYNE (Reference 2-5) was used for the structural analysis. Depending on the nature of loading, either a static or dynamic analysis was performed. In general, dead weight, thermal and seismic loads were treated as static loads. LOCA and SRV induced loads were analyzed by either a dynamic or a static analysis complying with the requirement of the LDR (Reference 2-1) and the NRC criteria (Reference 2-4). When performing the static analysis, dynamic load factors were calculated and the loads were adjusted accordingly. When performing the dynamic analysis, the structural natural frequencies and their corresponding mode shapes were first calculated. All the calculated modes were then used in the dynamic analysis. The damping coefficients were determined from the NRC's Regulatory Guide 1.61 (Reference 2-24). When calculating the natural frequencies for the submerged structures, it is necessary to include the hydrodynamic mass in addition to the mass of the structure itself. For a circular cylinder, the added hydrodynamic mass was taken as the water mass equivalent to the cross section of the structure (References 2-11 and 2-25). For a plate, the added mass varies with the aspect ratio and was calculated per Reference 2-11. In performing the dynamic analysis for structures subject to pool swell impact loads, the hydrodynamic mass of impact (Reference 2-4) was added to account for the effect of fluid-structure-interaction during impact. Application Guide 10 (Reference 23) provides the calculation procedures.

2.3.1.1 SRV Discharge Line and Supports in Wetwell

There are eleven SRV discharge lines in Unit 1 as well as in Unit 2 at Brunswick. Each line has different geometry and supports

above the vent header. However, below the vent header the T-Quencher discharge device and its supports are identical for all lines. The analysis was thus broken into two parts. Above the vent header, each line was analyzed separately. Below the vent header, the same analysis applied to all lines. This section covers the analysis of the SRV line below the vent header. The sketches of T-Quencher and supports are shown in Figure 2.3.1-1. The T-Quencher is a 12" schedule 80 pipe made of SA312 TP316L stainless steel. It is supported on the 14" diameter schedule 120 pipe by six U-bolts and saddles. The 14" pipe is supported laterally by three pairs of 8" diameter pipe and is supported at each end by a vertical (8" diameter) pipe and two diagonal (3" diameter) pipes. In the center the 14" pipe is supported vertically by a 12" diameter pipe which is bolted to a W12x120 section. The materials of these components are shown in Table 2.3.2-1.

For structural analysis, the T-Quencher and supports were modelled as shown in Figure 2.3.1-2. Node 1 is where the SRV line penetrates the header and Node 40 is the intersection of the header and the 24 inch pipe support which connects the SRV line by two 6 x 1 inch plates. Stiffnesses at Node 1 and 40 were calculated using a finite element model. The stiffnesses are listed in Table 2.3.1-1. The U-bolts provide restraint in the x2 and x3 directions. The stiffnesses of the U-bolts are also given in Table 2.3.1-1. The support pipe is restrained in the x1 and x2 directions at Node 22 and restrained in the x2 direction at Node 37. At Node 30, the center support provides restraints in the vertical and rotational directions. At Nodes 24, 29 and 35, the 8" diameter pipes restrain the support pipes from movement in the lateral (x3) and rotational directions.

The T-Quencher and supports have to sustain LOCA and SRV induced loads in addition to dead weight and seismic loads. LOCA induced loads on eleven T-Quenchers are identical. Loads calculated from Section 2.2.1 can be used directly. SRV induced loads vary with the initial conditions and geometry of each line. For structural evaluation, the most conservative SRV loads from eleven lines were

selected and used in the analysis in combination with other loads. Table 2.3.1-2 shows the method of analysis for each load.

2.3.1.2 Submerged Structures

Submerged structures in the torus can be classified as:

a) Component supports - e.g., platform support columns, header support columns.

b) Attached piping and supports - e.g., HPCI turbine exhaust line, RCIC turbine exhaust line.

c) Strainers and their flanges - e.g., HPCI, RCIC, strainers.

Header columns are 6" diameter schedule 80 pipes made of SA333 Grade 1 carbon steel. As seen in Figure 2.3.1-3, the header columns are connected to the header and to the bottom anchor plate by 2 3/4" diameter pins. In the analysis, pin-pin end conditions were assumed. The columns were analyzed for the submerged structure loads. It was assumed that the uplift loads on the header resulting from pool swell are resisted by the columns above the header (see Figure 2.3.1-3).

Platform support columns are made up of two back-to-back angles. They are pin connected at the bottom while the top is supported by a wide flange in the radial direction and by a diagonal rod and the grating in the circumferential direction of the torus. Stiffnesses contributed by these members were considered (Table 2.3.1-3) in the analysis.

Header columns and platform support columns are linear type supports and are designed according to ASME Code Subsection NF. Complete structural evaluations are reported in Sections 2.3.2.2 and 2.3.2.3.

Attached piping systems are partially submerged in the suppression chamber. A typical example is shown in Figure 2.3.1-4 where Node 9 represents the high water elevation. The pipe is connected to a penetration sleeve which runs from Node 3 to Node 1. The pipe continues outside the torus. For analysis purpose, the piping model is cut off at Node 1 where fully rigidity is provided by

the sleeve which is embedded in the concrete. The submerged portion of attached piping is normally supported at a plate and a clamp above the last elbow. Sometimes supports are added near the end of the line. Portions below the high water elevation must be analyzed for submerged structure loads resulting from SRV and LOCA, while those above the water including sleeve must consider pool swell loads. Some attached piping must also be evaluated for the loads from the discharge of fluid/steam inside the line itself.

Strainers are connectd to a flange which penetrates the torus wall as shown in Figure 2.3.1-5. The analysis of the strainer will be done by the strainer supplier while the flange and penetration sleeve were analyzed in the same way as other submerged structures.

These structures were analyzed by the STARDYNE finite element program (Reference 2-5). Loads and methods of analysis are listed in Table 2.3.1-4. Condensation oscillation and chugging induced loads were analyzed either statically or dynamically following the NRC criteria as described in Sections 2.2.1.7 and 2.2.1.8.

2.3.1.3 Structures Above the Pool

Structures above the pool can be classified as:

a) Attached piping and penetration sleeves - e.g., torus spray header, RHR test lines.

b) Structures for maintenance - e.g., monorail.

c) Structures housing instruments - e.g., penetration box.

As described in the preceeding section, most attached piping is partially submerged and penetrates the torus wall above the water level. The torus spray header and DW/WW vacuum breaker flange are attached piping completely above the pool. The computer models for these structures have no differences from the submerged the structures except the treatment of hydrodynamic mass as explained in Section 2.3.1.

The monorail is made of 12 I @ 31.8 LB and is supported every 7 ft. 10-1/3 in. along the circumference of the containment. The main loads on the monorail are the froth impingement forces which are

repeated every sector from the center of the non-vent bay to the center of the vent bay. For simplicity, the monorail was analyzed as a continuous beam taken from the sector that defines a full range of froth impingement loads.

Structures housing instruments such as the penetration box are composed of plates welded along the joint edges. Each plate which receives loads during the pool swell event was analyzed as a simply supported plate.

Loads and methods for analyzing structures above the pool are listed in Table 2.3.1-5. For pool swell impact and drag loads, dynamic analysis was performed for the attached piping. Other structures including penetration sleeves, structures for maintenance and instruments, however, were analyzed statically. The dynamic effects were considered using the code DLFPSWL (Reference 2-6). Dynamic load factors for froth impingement forces were calculated by Bigg's method (Reference 2-7) and those for pool fallback loads were calculated by the code DLFPFBK (Reference 2-8).

2.3.2 Results of Analysis

Structures listed in Section 2.1 were analyzed according to methods described in Section 2.3.1. The results were then evaluated based on the load combinations given in Reference 2-23. Presented herein are the results of T-Quencher supports, component supports covered by the ASME Code Subsection NF and required piping modifications. The load combination number and service level referred in this section conform with Reference 2-23.

2.3.2.1 T-Quencher Supports

The SRV piping is Class 3 essential piping. Therefore, service level B is required to be maintained for support components. Table 2.3.2-1 contains the results for evaluation of the T-Quencher supports and connections. The computed stresses are within allowables.

2.3.2.2 Vent Header Support Columns

The vent header support columns are classified as internal supports. The stresses must satisfy service level A, B or C limits depending on load combinations. Table 2.3.2-2 shows the columns and connections are acceptable.

2.3.2.3 Platform Support Columns

Platform support columns are classified as internal structures. Structural evaluations reveal that the existing columns are vulnerable to submerged structure loads as shown in Table 2.3.2-3. The evaluation did not include the uplift load acting on the platform during the pool swell events. It has been decided to remove all platforms and walkways from the plant except for platforms at three bays (45°, 225° and 315° Azimuth) for plant maintenance and for instrument piping support. All platform grating will be removed during plant operation.

All the existing beams and columns, except the crossing rod assemblies, will be replaced by 6" diameter pipes. New 6" diameter pipe columns will be added above the platforms to resist pool swell loads.

2.3.2.4 RHR Containment Cooling Line

The analysis model for RHR containment cooling line (also known as torus spray header) is shown in Figure 2.3.2-1. The line is continuous along the circumference of containment beyond Node 23. The analysis model is cut off at Node 23 because there are no pool swell loads acting on the line beyond Node 23. Analysis of the existing line showed that it was not acceptable. Additional supports will be provided at Nodes 10, 14, 18 and 22. Also a new froth impingement load definition based on the test film has been developed and was utilized in the analysis. The line is found acceptable with four additional supports. Design of the additional supports is presented in Section 4.

2.3.2.5 Monorail

The monorail is classified as an internal structure. The service level E limit is allowed yet it must be shown that element failure does not result in significant damage to safety-related items. Based on the generic froth impingement forces, the monorail is not acceptable. Modifiation has been made based on the froth impingement loads developed from the test film and is presented in Section 4.

2.3.2.6 RHR Test Line

The RHR test line as shown in Figure 2.3.2-2 was analyzed. Full anchorage is assumed at Node 1 and guide are provided at Node 2. Nodes 9, 13, 18, 22 and 30 are frame-type supports. The line is submerged below Node 27. Analysis based on these existing supports showed that the piping and supports were highly overstressed due to froth impingement forces alone. After adding additional supports at Nodes 11, 16, 40 and 21, the line is found adequate for the froth impingement forces calculated per the test film in combination with other loads.

2.3.2.7 Access Hatch

The access hatch is a 48-in. pipe which penetrates the torus shell and is sealed with a 2 3/4-in. plate. The structure was analyzed for pool swell impact and drag loads as well as froth impingement force using hand calculations. The resultant stresses were found less than 10 percent of allowables.

2.3.2.8 Drywell/Wetwell Vacuum Breaker Flange

The vacuum breaker is bolted to the flange pipe which has a diameter of either 18-in. or 21-in. The flange is welded to the vent header. The evaluation of the vacuum breaker will be done by others. Only the flange and the junction at the flange and vent header were analyzed. The governing load case is the froth impingement force combined with safe shutdown earthquake and dead load. The maximum stress in the flange is 5.6 ksi as compared with the allowable of 42 ksi.

The junction at the flange and vent header is classified as class MC vessel. Local stresses were evaluated using a computer program (Reference 2-26) based on Bijlaard's method. The evaluation results for 18-in. flange as shown in Table 2.3.2-4 showed the calculated stresses are within the allowable limits. Since the loads on the 21-in. flange are about the same as those on the 18-in. flange, the local stress at the junction of 21-in. flange and vent header can be concluded the same way as the 18-in. flange.

2.3.2.9 Electric Penetration Box

The electric penetration box is a 24x24x24-in. stainless steel box. The bottom of the box is subjected to the pool swell impact and drag load while the door receives froth impingement forces. Hand calculations showed maximum stresses of 353 ksi at the bottom plate and 357 ksi at the door. These stresses are unacceptable as compared with allowable of 31.95 ksi. These loads are too large to accomodate feasible structural modifications. It has been decided to relocate the electric penetration box to eliminate loads resulting from pool swell.

Appendix A.2 List of Calculation Books

Listed below are calculation books related with the load development and analysis of the miscellaneous structures in the suppression chamber:

A. SRV Discharge Induced Loads

1. Calculation of the Safety Relief Valve Discharge Line Clearing Transient, Calculation Set No. 9527-E-SC-DL-1-F.
2. Calculation of the Safety Relief Valve Discharge Line Reflood Transient, Calculation Set No. 9527-E-SC-DL-2-F.
3. Calculation of the T-Quencher S/RV Discharge Torus Shell Loads, Calculation Set No. 9527-E-SC-DL-3-F.

B. Submerged Structural Loads

1. Calculation of LOCA Bubble Induced Loads on Submerged Structures, Calculation Set No. 9527-E-SC-SL-1-F.
2. Calculation of LOCA Water Jet Induced Loads on Submerged Structures, Calculation Set No. 9527-E-SC-SL-2-F.
3. Calculation of Condensation Oscillation and Chugging Induced Loads on Submerged Structures, Calculation Set No. 9527-E-SC-SL-3-F.
4. Calculation of the T-Quencher S/RV Bubble Induced Loads on Submerged Structures, Calculation Set No. 9527-E-SC-SL-4-F.
5. Calculation of the T-Quencher Water Jet Induced Loads on Submerged Structures, Calculation Set No. 9527-E-SC-SL-5-F.

C. Pool Swell Induced Loads

1. Calculation of Impact and Drag Loads, Froth Impingement Loads and Pool Fallback Loads, Calculation Set No. 9527-E-SC-AP-1F.

D. Analysis of T-Quencher Supports

1. Analysis of SRV Discharge Line and T-Quencher Supports, Calculation Set No. 9527-E-SC-SR-3-F.

E. Analysis of Submerged Structures

1. Analysis of HPCIS Turbine Exhaust Line, Calculation Set No. 9527-E-SC-SS-1-F.
2. Analysis of Header Column, Calculation Set No. 9527-E-SC-SS-2-F.
3. Analysis of Platform Column, Calculation Set No. 9527-E-SC-SS-3-F.
4. Analysis of RCICS, RHR, HPCIS, Core Spray Pump Suctions and Strainers, Calculation Set No. 9527-E-SC-SS-4-F.
5. Analysis of Core Spray Test Line, Calculation Set No. 9527-E-SC-SS-5-F.
6. Analysis of RCICS Barometric Condenser and HPCI Turbine Drain Pot Lines, Calculation Set No. 9527-E-SC-SS-6-F.
7. Analysis of RCIC Turbine Exhaust Line, Calculation Set No. 9527-E-SC-SS-7-F.
8. Analysis of Liquid Level Indicators, Calculation Set No. 9527-E-SC-SS-8-F.

F. Analysis of Structures Above the Pool

1. Analysis of RHR Containment Cooling Line, Calculation Set No. 9527-E-SC-AP-2-F.
2. Analysis of Monorail, Calculation Set No. 9527-E-SC-AP-3-F.
3. Analysis of RHR Test Line, Calculation Set No. 9527-E-SC-AP-4-F.
4. Analysis of Access Hatch, Calculation Set No. 9527-E-SC-AP-5-F.
5. Analysis of DW/WW Vacuum Breaker Flange, Calculation Set No. 9527-E-SC-AP-6-F.
6. Analysis of RCIC Vacuum Breaker and HPCIS Vacuum Breaker Lines, Calculation Set No. 9527-E-SC-AP-7-F.
7. Analysis of Electric Penetration Box, Calculation Set No. 9527-E-SC-AP-8-F.
8. Analysis of Vent Purge Inlet, Vent Purge Outlet and Spare Penetrations, Calculation Set No. 9527-E-SC-AP-9-F.

REFERENCES - SECTION 2

2-1 Mark I Containment Program, Load Definition Report, General Electric Company, Report No. NEDO-21888, November, 1981.

2-2 Mark I Containment Program, Plant Unique Load Definition, Brunswick Steam Electric Plant: Units 1 and 2, General Electric Company, Report No. NEDO-24582, March, 1979.

2-3 Mark I Containment Program, Application Guide 10, General Electric Company, Report No. NEDE-24555-P, September, 1980.

2-4 Safety Evaluation Report, Mark I Containment Long-Term Program, Resolution of Generic Technical Activity A-7, Office of Nuclear Reactor Rgulation, U.S. Nuclear Regulatory Commission, Report No. NUREG-0661, July, 1980.

2-5 STARDYNE for Scope 3.4 operating system, Control Data Corporation, 1978.

2-6 DLFPSWL, a program to calculate dynamic load factors for pool swell impact and drag on (i) cylindrical targets and (ii) flat targets, UE&C proprietary program, May, 1981.

2-7 J. M. Biggs, Introduction to Structural Dynamics, McGraw-Hill Book Co.

2-8 DLFPFBK, a program to calculate dynamic load factors for pool fallback loads, UE&C proprietary program, May, 1981.

2-9 LOCAJET, a program to calculate drag loads on submerged structures in Mark I Containment due to LOCA water jet, Bechtel Power Corporation, July, 1980.

2-10 Mark I Containent Program, Application Guide 1, LOCA Bubble Induced Loads on Submerged Structures, General Electric Company, Report No. NEDE-24555-P, September, 1980.

2-11 Mark I Containment Program, Application Guide 2, Condensation Oscillation and Chugging Induced Loads on Submerged Structures, General Electric Company, Report No. NEDE-24555-P, September, 1980.

2-12 DLFCO, a program to calculate dynamic load factors for condensation oscillation, UE&C proprietary program, May, 1981.

2-13 DLFFSI, a program to calculate dynamic load factors for fluid-structure induced acceleration, UE&C proprietary program, May, 1981.

2-14 DLFPCH, a program to calculate dynamic load factors for postchug, UE&C proprietary program, May, 1981.

2-15 Mark I Containment Program, Application Guide 3, Safety Relief Valve Discharge Line Clearing Transient, General Electric Company, Report No. NEDE-24555-P.

2-16 REFORM, a program to select the segment forces at varying time steps and the associated water thrust values, UE&C proprietary program No. SAG092, August, 1979.

2-17 SPPLOT, a program to plot the data selected by the REFORM program (SAG092), UE&C proprietary program No. SAG093, August, 1979.

2-18 Mark I SSE Question Response, Question No. 203.4, General Electric Company, February, 1980.

2-19 Mark I Containment Program, Application Guide 4, T-Quencher S/RV Discharge Torus Shell Loads, General Electric Company, Report No. NEDE-24555-P.

2-20 Mark I Containment Program, Application Guide 9, Safety Relief Valve Discharge Line Reflood Transient, General Electric Company, Report No. NEDE-24555-P.

2-21 Mark I Containment Program Application Guide 6, T-Quencher Water Jet Induced Loads on Submerged Structures, General Electric Company, Report No. NEDE-24555-P, September, 1980.

2-22 Mark I Containment Program Application Guide 5, T-Quencher SRV Bubble Induced Loads on Submerged Structures, General Electric Company, Report No. NEDE-24555-P, October, 1980.

2-23 Mark I Containment Program Structural Acceptance Criteria, Plant Unique Analysis Application Guide, Task 3.1.3, General Electric Company, Report No. NEDO-24583-1, October, 1979.

2-24 U.S. Atomic Energy Commission, Regulatory Guide 1.61, Damping Values for Seismic Design of Nuclear Power Plants.

2-25 Blevins, R. D., Flow-Induced Vibration, Van Nostrand Reinhold Company.

2-26 CYLNOZ, UE&C Program No. ME-418, Rev. 3.0, February, 1980.

TABLE 2.1-1

List of Acronyms

ADS	Automatic Depressurization System
DBA	Design Basis Accident
DLF	Dynamic Load Factor
FSI	Fluid Structure Interaction
GE	General Electric
HPCI	High Pressure Coolant Injection
IBA	Intermediate Break Accident
LDR	Load Definition Report
LOCA	Loss of Coolant Accident
MSIV	Main Steam Isolation Valve
NOC	Normal Operating Conditions
NRC	Nuclear Regulatory Commission
PULD	Plant Unique Load Definition
QSTF	Quarter Scale Test Facility
RCIC	Reactor Core Isolation Cooling
RHR	Residual Heat Removal
SBA	Small Break Accident
SRSS	Square Root Sum of the Squares
SRV	Safety Relief Valve
SRVDL	Safety Relief Valve Discharge Line

TABLE 2.2.2-1

SRV LOAD CASES

Design Initial Condition	Load Case	Any One Valve	ADS Valves	Multiple Valves
1 NOC, First Act.		A1.1		A3.1
2 SBA/IBA, First Act.		A1.2	A2.2	A3.2
3 DBA, First Act.		A1.3		
1 NOC, Subsequent Act.				C3.1
2 SBA/IBA, Sub. Act. air in S/RVDL				C3.2
3 SBA/IBA, Sub. Act. steam in S/RVDL				C3.3

TABLE 2.3.1-1

Spring Constants for Restraints in T-Quencher Model

Support Location	Node	Spring Constant (k/ft or ft-k/rad)					
		x1	x2	x3	x4	x5	x6
SRV - Header Penetration	1	Rigid	15,600	Rigid	4,866.7	Rigid	9,250
24" Ø Support - Header Intersection	40	Rigid	46,200	Rigid	143,333.3	Rigid	57,500
1½" Ø U-bolt	21-23	0	118,800	2,640	0	0	0
	18-26						
	16-28						
	10-31						
	12-33						
	15-36						

TABLE 2.3.1-2

Methods for Analyzing T-Quencher and Supports

Load Case	Method of Analysis
Dead Weight	Static
Thermal	Static
Seismic	Static (DLF)
SRV Water Clearing Thrust Loads	Dynamic
T-Quencher Water Jet Loads	Static (DLF = 2)
T-Quencher Air Bubble Induced Drag Loads	Dynamic
Thrust Loads on T-Quencher Arms	Static
Pool Fallback Loads	Static (DLF)
LOCA Water jet Loads	Dynamic
LOCA Air Bubble Induced Drag Loads	Static (DLF = 2)
Condensation Oscillation	Static (DLF)
Prechug	Dynamic
Postchug	Dynamic

TABLE 2.3.1-3

Spring Constants for Restraints in Platform Columns

Column Assembly	Sring Constant (k/in) x1 (Radial)	x3 (Circumferential)	Remarks
C	1951	128	CBI Dwg. No. 215-217
D	1568	141	

TABLE 2.3.1-4

Method for Analyzing Submerged Structures

Load Case	Method of Analysis
Dead Weight	Static
Thermal	Static
Seismic	Static (DLF)
Fluid/Steam Dischage Thrust Loads	Dynamic
T-Quencher Water Jet Loads	Static (DLF = 2)
T-Quencher Air Bubble Induced Drage Loads	Dynamic
Pool Fallback Loads	Static (DLF)
LOCA Water Jet Loads	Dynamic
LOCAL Air Bubble Induced Drag	Static (DLF = 2)
Condensation Oscillation	Static (DLF)
Prechug	Static (DLF)
Postchug	Static/Dynamic

TABLE 2.3.1-5

Methods for Analyzing Structures Above the Pool

Load Case	Method of Analysis
Dead Weight	Static
Thermal	Static
Seismic	Static (DLF)
Pool Swell Impact and Drag Loads	Static (DLF)/Dynamic
Froth Impingement Loads	Static (DLF)
Pool Fallback Loads	Static (DLF)

TABLE 2.3.2-1
(Sheet 1 of 3)

Evaluation of T-Quencher Supports

Structure & Component	Service Level (Load Case)	Load Comb. No.	Stress Type	Stress (KSI) 1 Computed	2 Allowable	Unless Note 1 / 2 Ratio	Remarks
14" ϕ SCH. 120 SA106 GR. B Support Pipe	B (DBA)	27	Flexure	7.5	21.0	0.36	
			Shear	3.2	12.7	0.25	
Splice Bolts 8'-1" ϕ SA193 B7	B (DBA)	27	Tension	30.8	44.3	0.70	
			Shear	3.2	18.7	0.17	
Splice Plate 13/16" SA516 GR 70	B (DBA)	27	Flexure	12.6	26.0	0.48	
8" ϕ SCH. 100 Horiz. Brace SA106 GR B	B (DBA)	27	Axial	3.42	19.1	0.18	
			Flexure	2.73	21.0	0.13	
						0.31	
Studs 14-3/2" ϕ	Normal Extreme Environ.	3	Shear	29.1^k	41.4^k	0.70	
1½" ϕ Pin SA193 B7	B (DBA)	27	Bearing	51.2^k	70.0^k	0.73	
Welds to Liner	B (DBA)	27	Shear	39.9^k	59.8^k	0.67	
1½" ϕ U-Bolts SA193 B7	B (NOC)	3	Tension	10.1	86.1	0.12	
			Shear	23.0	27.1	0.85	
						0.97	
24" ϕ SCH. 80 SA106 GR. B Support Pipe	B (DBA)	27	Axial	2.3	21.0	0.11	Assuming 2-SRV/Line
			Flexure	15.9	23.1	0.69	
						0.80	
Strap Plates SA516 GR. 70	B (SBA/IBA)	15	Tension	4.71	20.76	0.23	
			Flexure	13.0	20.76	0.63	
						0.86	

TABLE 2.3.2-1
(Sheet 2 of 3)

Evaluation of T-Quencher Supports

Structure & Component	Service Level (Load Case)	Load Comb. No.	Stress Type	Stress (KSI) 1 Computed	2 Allowable	Unless Note 1 / 2 Ratio	Remarks
Welds at Node 3	B (DBA)	27	Shear	2.6k/in.	4.64k/in.	0.56	
Welds at Node 41	B (DBA)	27	Tension Shear	3.3k/in.	7.42k/in.	0.44	
Welds 1"x9" Plates to 1" Cap Plate	B (DBA)	27	Tension Shear	1.94k/in.	4.64k/in.	0.42	
Welds Cap Plate to 24" ϕ Support Pipe	B (DBA)	27	Tension Shear	3.22k/in.	4.64k/in.	0.69	
Center Support 12" ϕ SCH. 100 SA106 GR B	B (DBA)	27	Comp.	6.90	19.10	0.36	
4 -1½" ϕ Bolt SA193 B7	B (DBA)	27	Tension	13.60	58.30	0.23	
1-1/4" Cap Plate SA516 GR 70	B (DBA)	27	Flexure	17.30	26.00	0.67	
Header Columns Anchor	B (NOC)	3	Tension	75.10k	100.60k	0.75	
End Support Vert. Anchor 6-1/2" ϕ Stud	Normal Extreme Environ.	3	Tension	19.9k	21.20k	0.94	SRSS

TABLE 2.3.2-1
(Sheet 3 of 3)

Evaluation of T-Quencher Supports

Structure & Component	Service Level (Load Case)	Load Comb. No.	Stress Type	Stress (KSI) 1 Computed	2 Allowable	Unless Note 1 / 2 Ratio	Remarks
Horiz. Capa. 3/4" Plate SA516 GR 70	B (SBA/IBA)	15	Bearing	19.31	31.14	0.62	
3" ϕ SCH. 80 45° Brace SA106 GR B	B (SBA/IBA)	15	Comp.	5.99	19.10	0.31	
1-1/4" ϕ Pin SA193 B7	B (SBA/IBA)	15	Shear	7.37	24.10	0.31	
TS 5x5x0.5 SA36	B (DBA)	27	Tension	3.53	19.70	0.18	
			Flexure	13.57	21.60	0.63	
						0.81	
2-1"x5"x1'-4 Plates SA36	B (DBA)	27	Flexure	17.67	21.60	0.82	
Welds	B (DBA)	27	Shear	13.33	21.0	0.63	
8" ϕ SCH. 100	(Load Negligible)						

TABLE 2.3.2-2

Evaluation of Vent Header Support Columns
6" Diameter Schedule 80

Structure and Component	Service Level	Load Comb. No. (Max)	Stress Type	Stress (KSI) 1 Calculated	2 Allowable	Combined 1/2 Ratio	Remarks
Support Column (SA333)	B	18 (DBA)	Axial & Bending	1.78 15.15	12.92 19.34	0.14 0.78 0.92	
Support Column (SA333)	C	25 (DBA)	Axial & Bending	4.51 13.21	16.05 20.31	0.28 0.65	
Connection Plates (SA516) & Pin (SA36)	B	18 (DBA)	Bearing Shear Axial & Bending	9.20 3.20 3.20 11.70 14.90	31.14 9.84 25.95	0.30 0.33 0.57	Plate Pin Plate
Welds	Stress Negligible						

TABLE 2.3.2-3

Evaluation of Existing and Modified Platform Support Columns

Structure	Service Level	Load Comb. No. (Max)	Stress Type	Stress (KSI) 1 Calculated	2 Allowable	1 / 2 Ratio	Remarks
'C'							
2 6x4x3/8 (A36)	C	11 (SBA/IBA)	Bending	32.18	17.57	1.83	N.G.
'D'							
2 6x4x3/8 (A36)	C	11 (SBA/IBA)	Bending	184.39	16.65	11.07	N.G.
	D	14 (SBA/IBA)	Bending	184.39	16.65	11.07	N.G.
Modified							
		22					
'D'	B	24	Bending	20.44	22.50	0.91	OK
6" ø, t=1"		25					
SA106 B		(DBA)	Axial	0.88	14.86	0.06	
						0.97	

Note: Pool Swell Load on Grating to be Resisted by Additional Columns Above Grating

TABLE 2.3.2-4

Evaluation of Local Stress at Junction of Breaker Flange and Vent Header

Member	Service Level	Load Combination No.	Stress (KSI) Computed	Stress (KSI) Allowable
Junction of	A	16	9.61	31.95
18" flange and	B	18	9.71	31.95
vent header	C	19	9.78	50.55

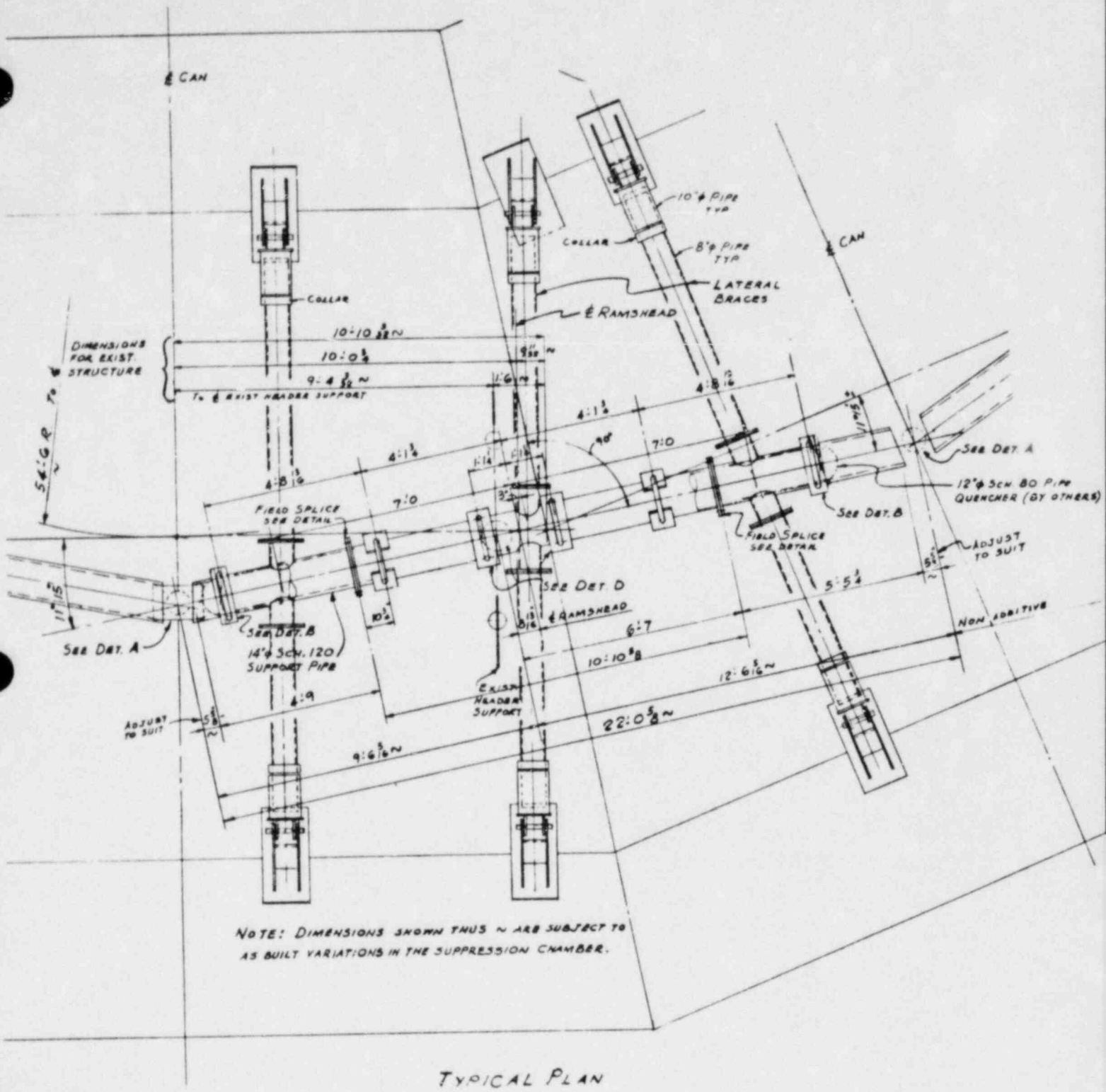

NOTE: DIMENSIONS SHOWN THUS N ARE SUBJECT TO AS BUILT VARIATIONS IN THE SUPPRESSION CHAMBER.

TYPICAL PLAN

Figure 2.3.1-1 Sketches for T-Quencher and Supports (Page 1 of 7)

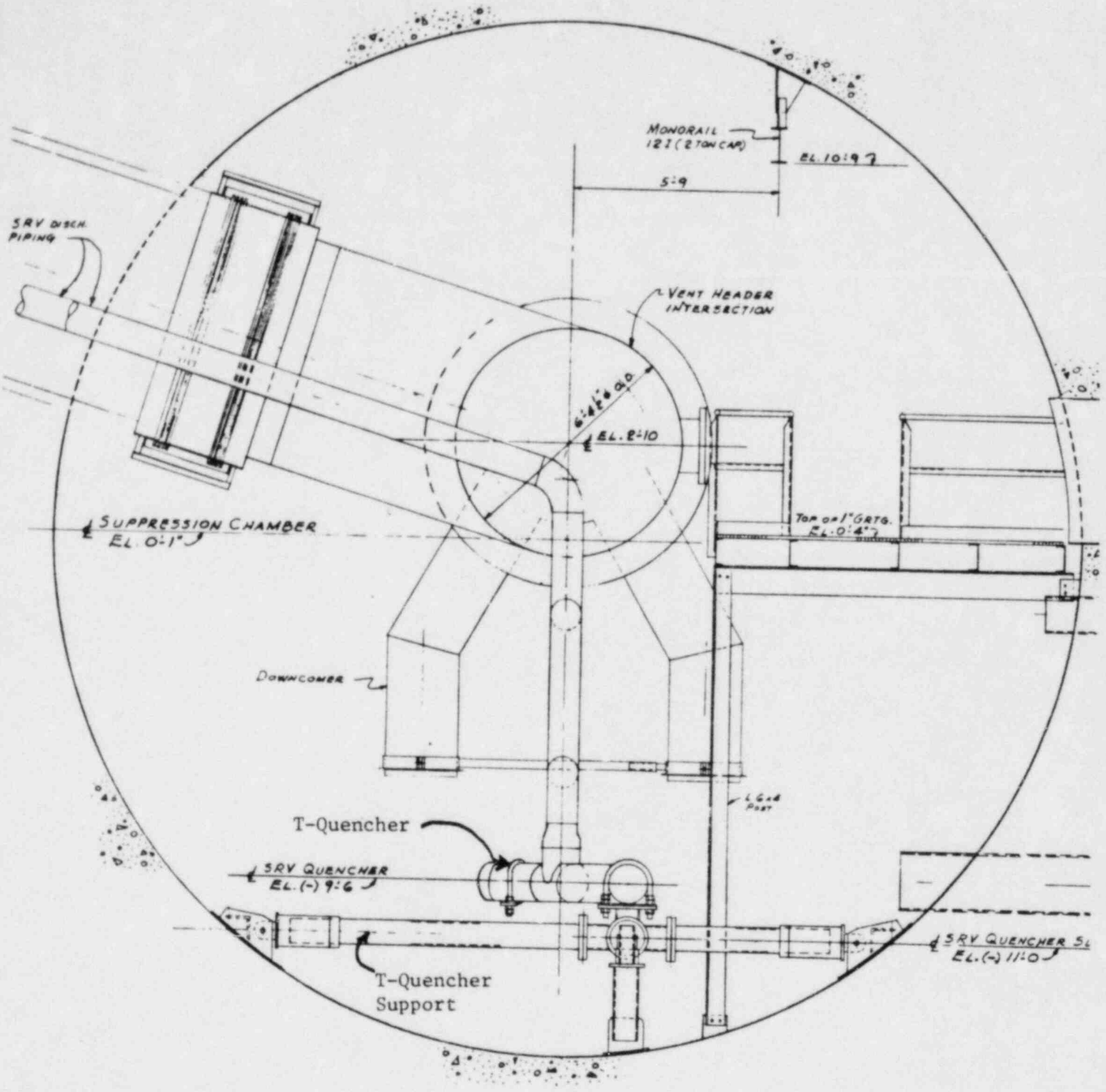

Elevation

Figure 2.3.1-1 Sketches for T-Quencher and Supports (Page 2 of 7)

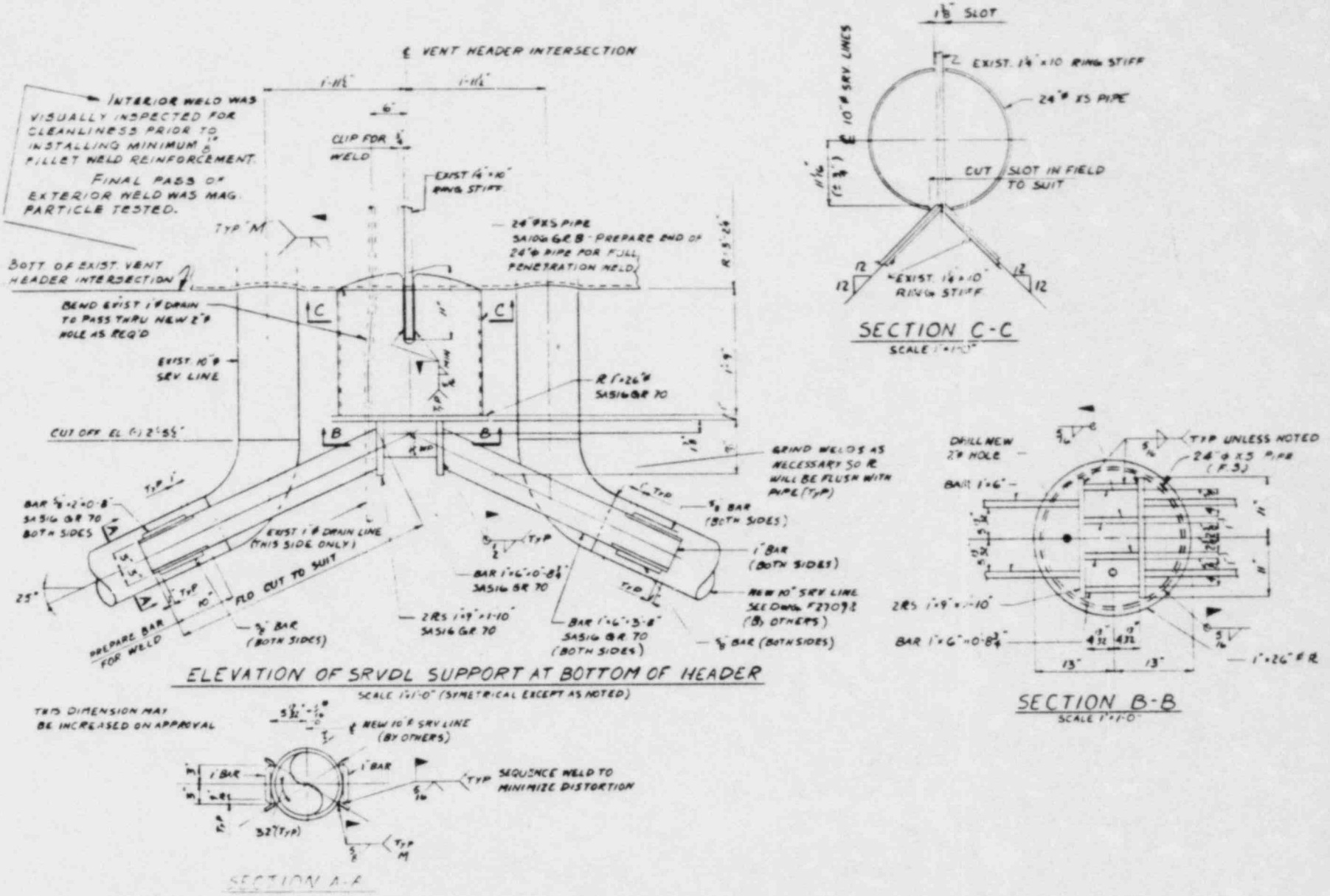

Figure 2.3.1-1 Sketches for T-Quencher and Supports (Page 3 of 7)

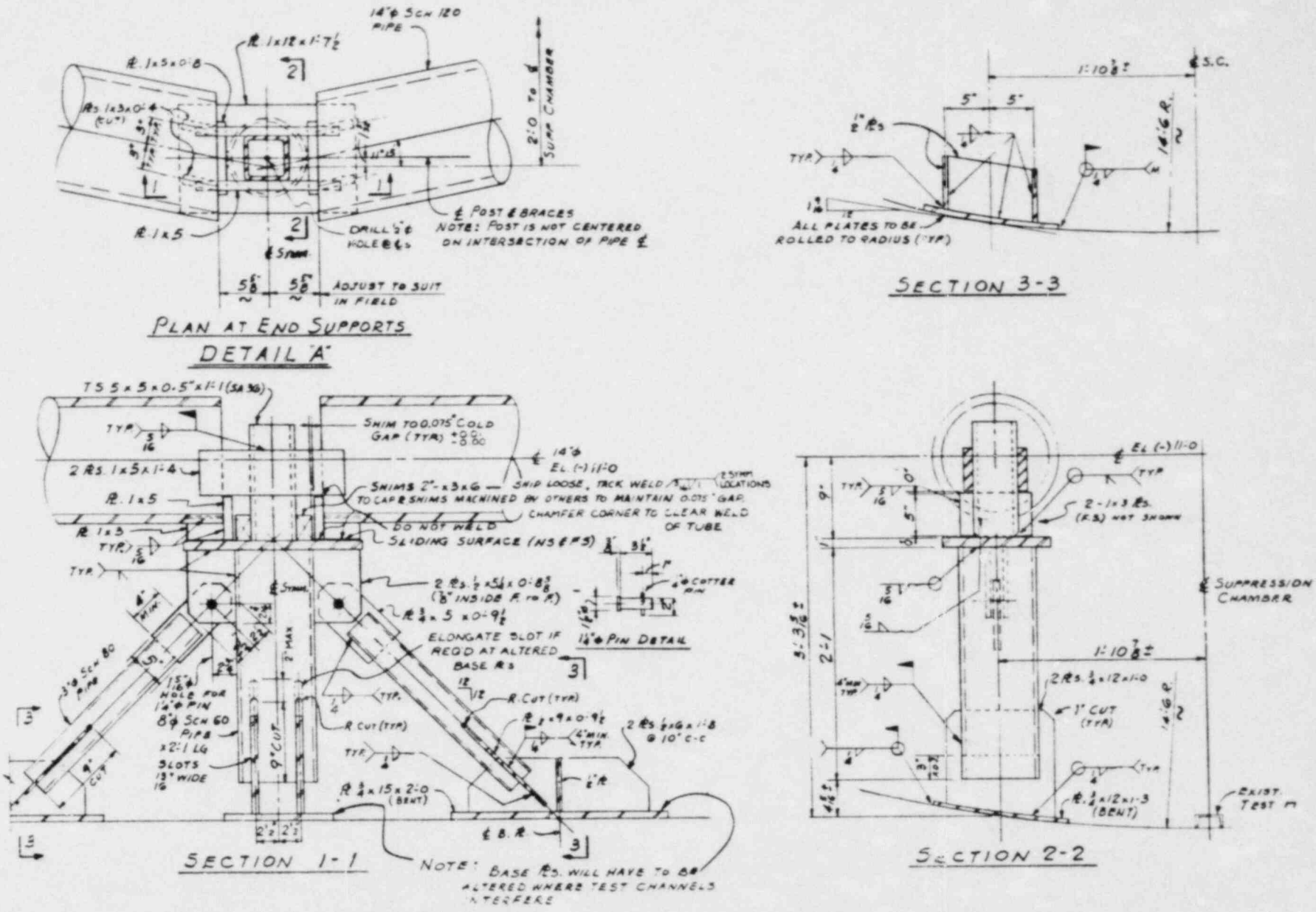

Figure 2.3.1-1 Sketches for T-Quencher and Supports (Page 4 of 7)

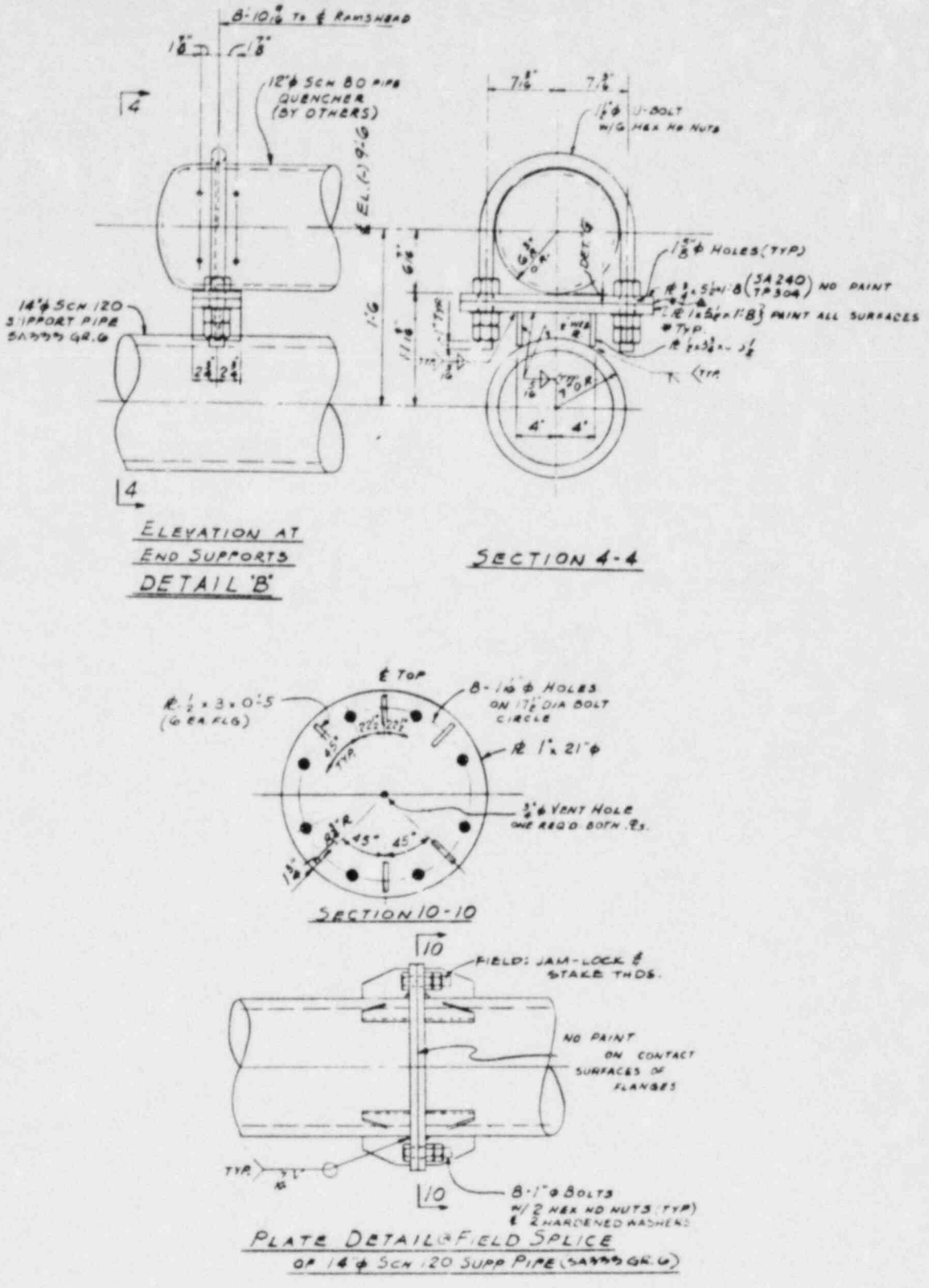

Figure 2.3.1-1 Sketches for T-Quencher and Supports (Page 5 of 7)

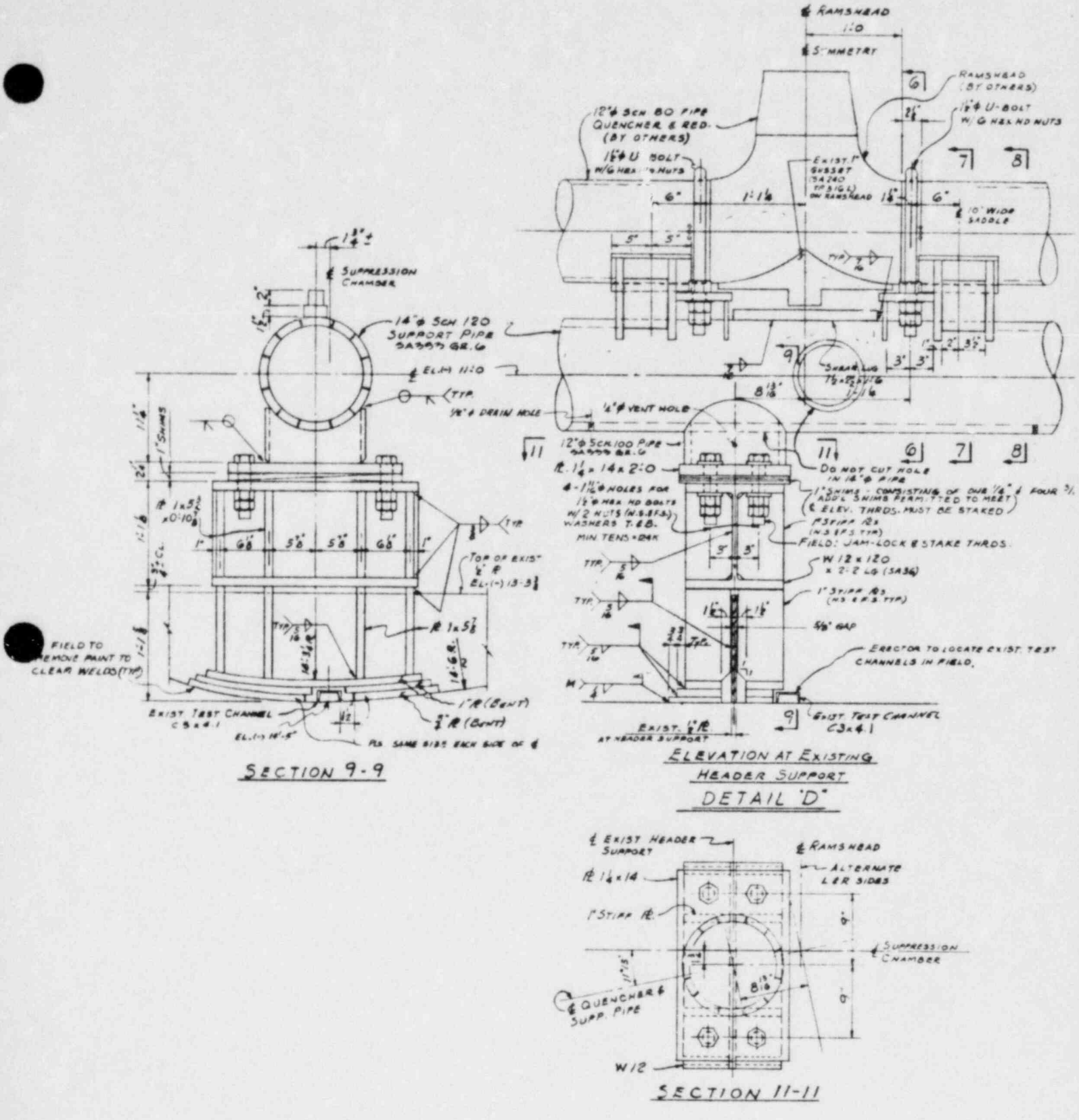

Figure 2.3.1-1 Sketches for T-Quencher and Supports (Page 6 of 7)

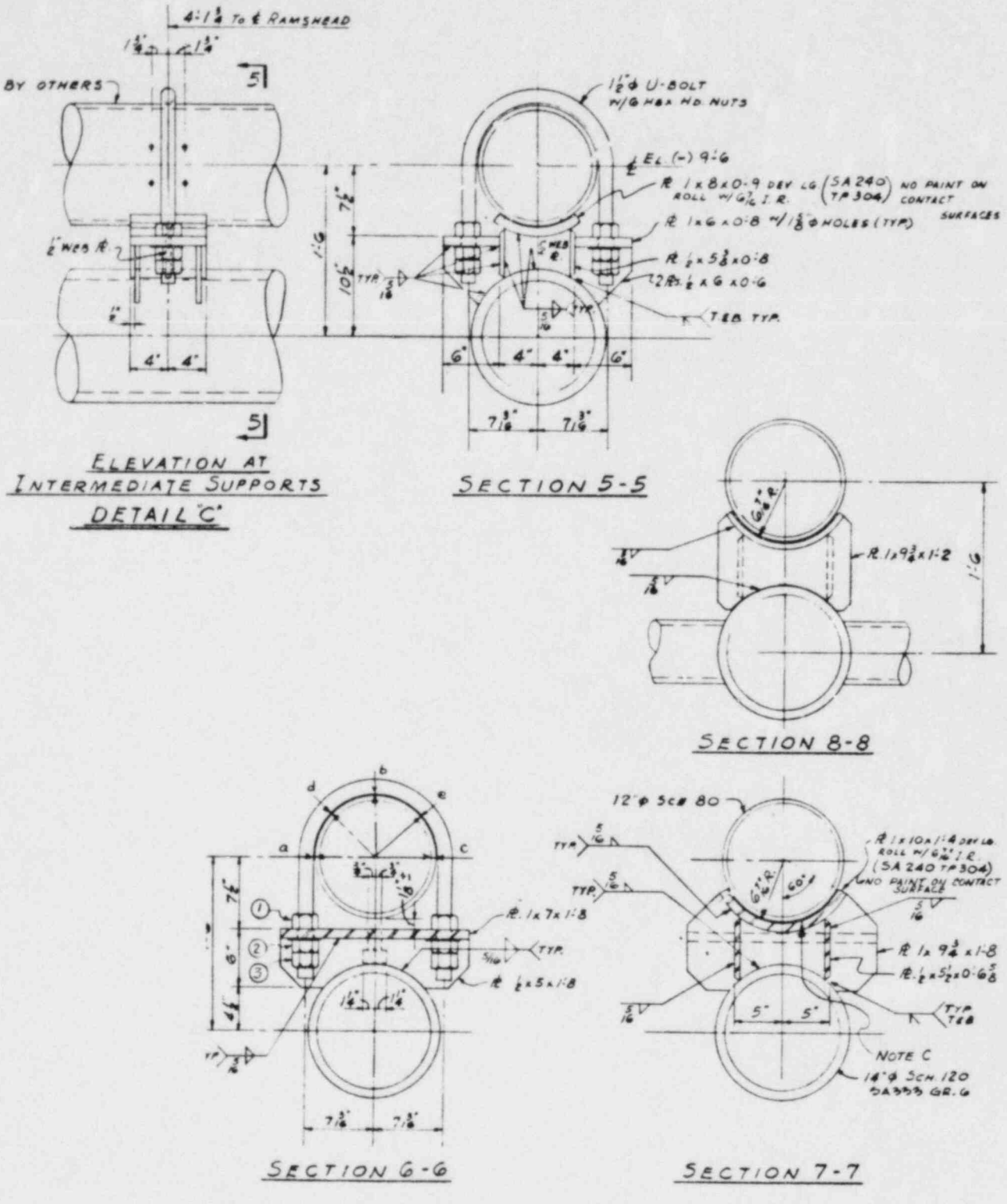

Figure 2.3.1-1 Sketches for T-Quencher and Supports (Page 7 of 7)

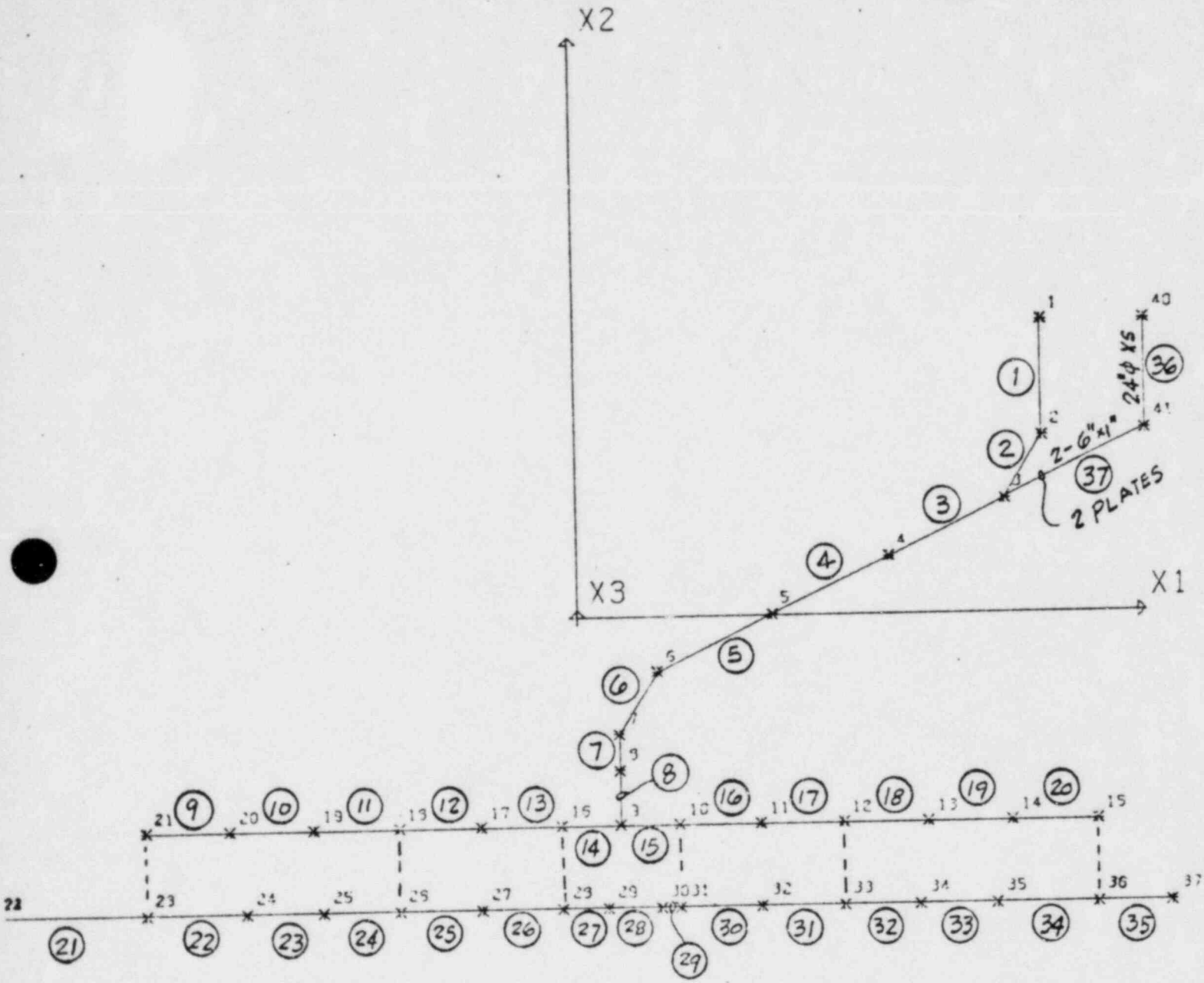

Figure 2.3.1-2 STARDYNE Finite Element Model For T-Quencher and Supports

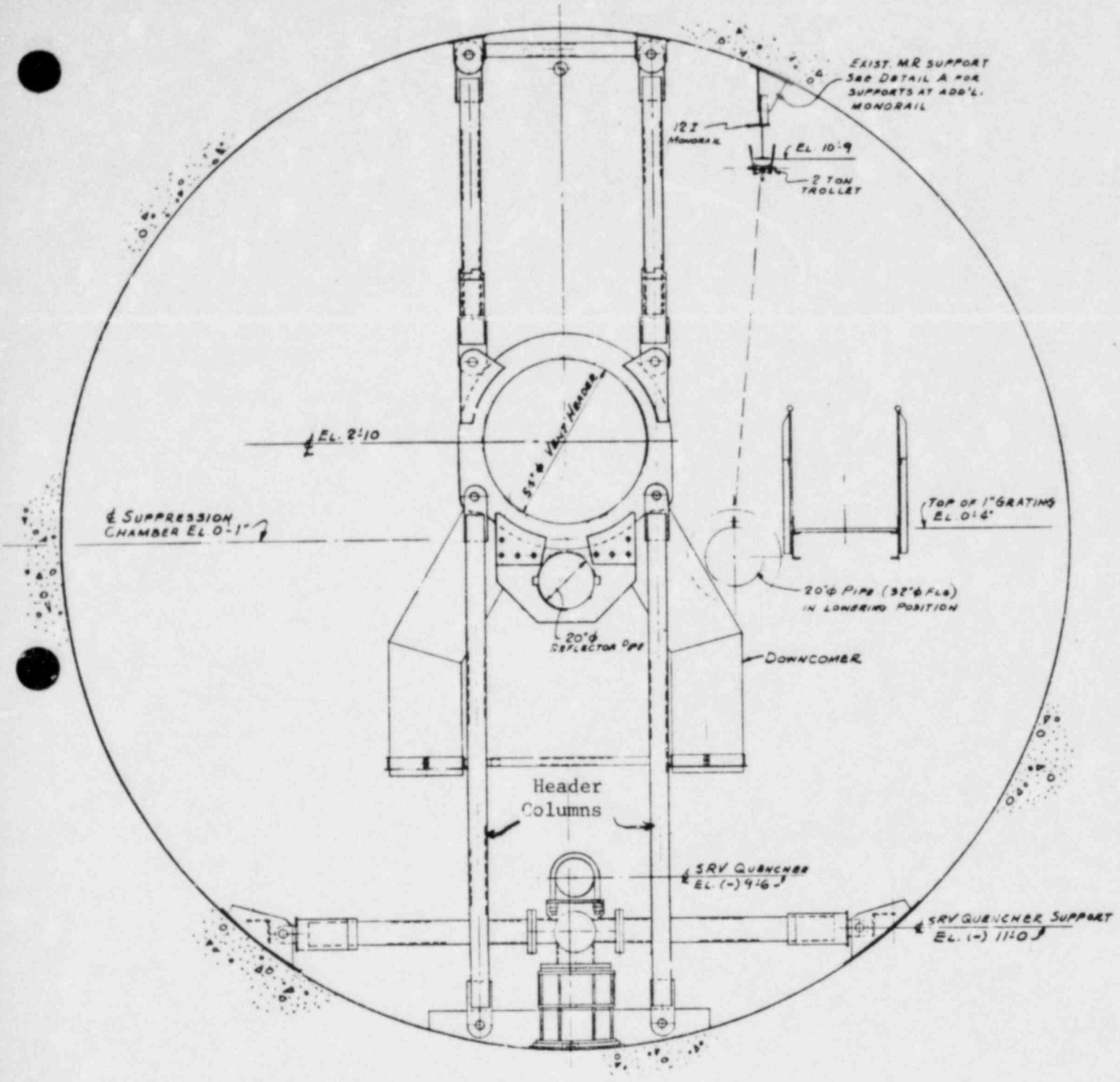

Figure 2.3.1-3 Sketch for Header Columns

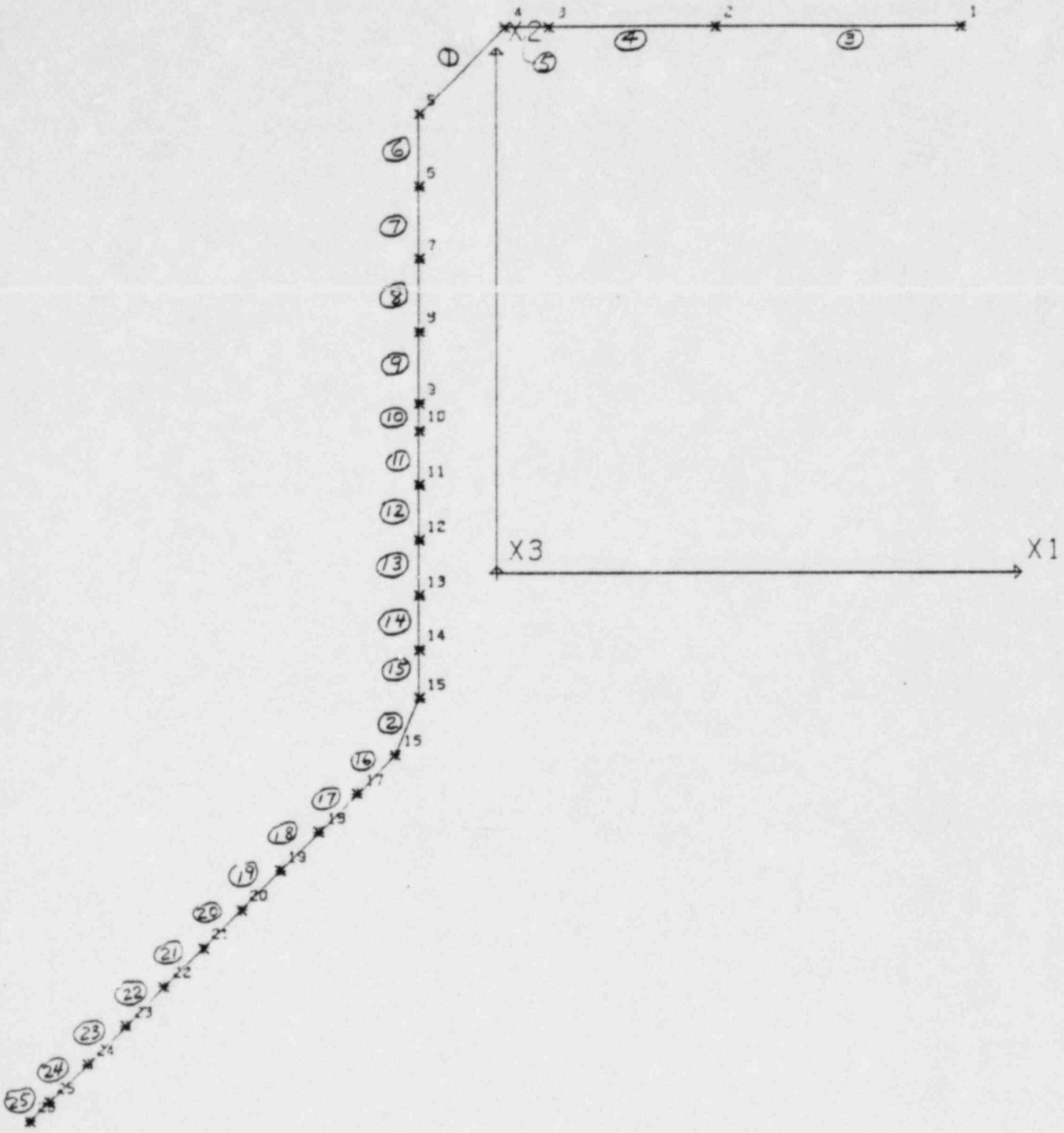

Figure 2.3.1-4 STARDYNE Finite Element Model For RCIC Turbine Exhaust Line

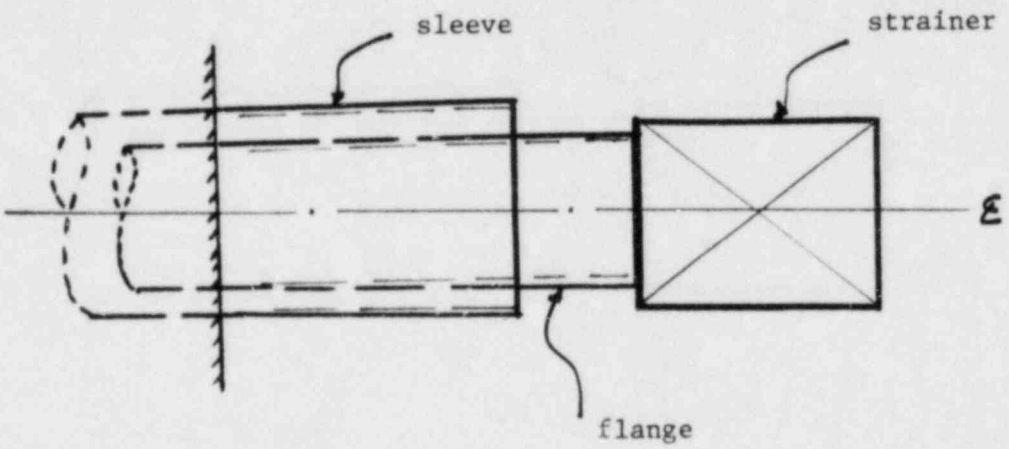

Figure 2.3.1-5 Strainer and Flange

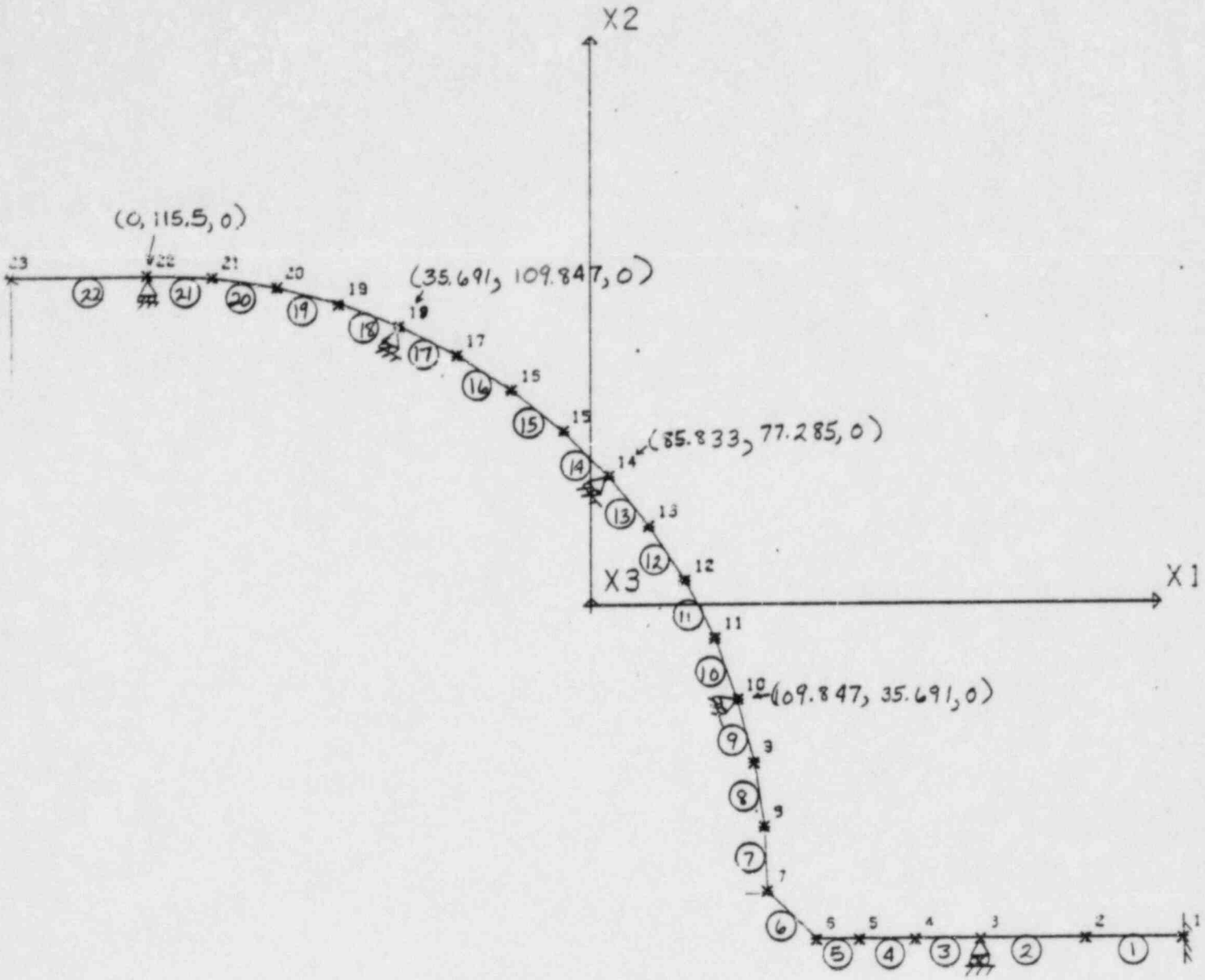

Figure 2.3.2-1 STARDYNE Finite Element Model For Torus Spray Header

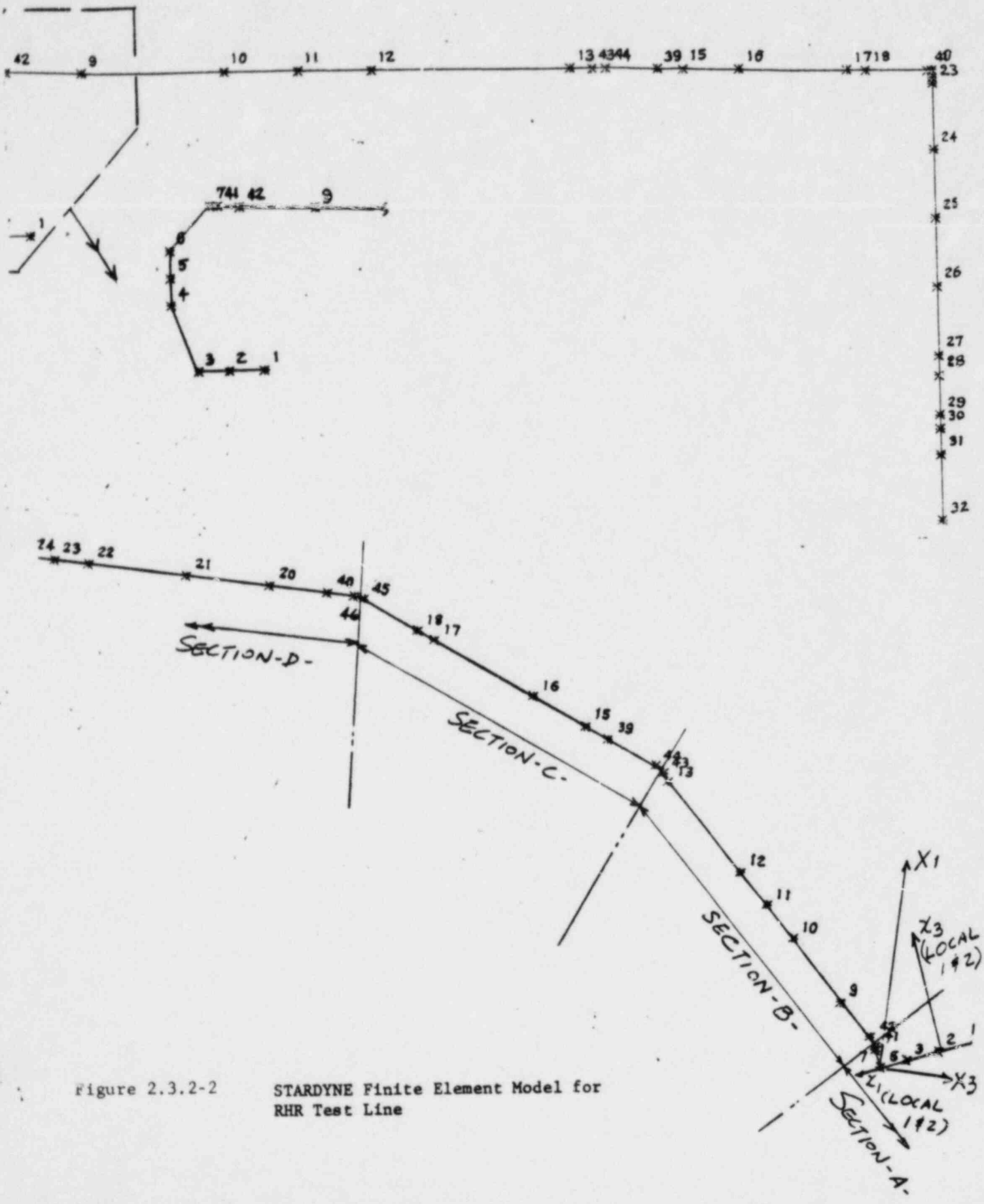

Figure 2.3.2-2 STARDYNE Finite Element Model for RHR Test Line

3.0 VENT SYSTEM ANALYSIS

3.1 INTRODUCTION

The vent system structures, as required by the Mark I Long Term Program (Reference 3-1), have to be evaluated for hydrodynamic loads resulting from postulated loss of coolant accident (LOCA) and safety relief valve (SRV) discharge loads together with dead loads and seismic loads.

This section describes the procedures for calculation and application of the loads and presents the methods of analysis and evaluation of the structures for various load combinations.

3.2 PHYSICAL DESCRIPTION OF VENT SYSTEM STRUCTURES

The primary containment system consists of two basic components: the drywell and the toroidal suppression chamber (see Figure 3.2-1). The drywell houses the reactor pressure vessel. The suppression chamber for the Brunswick Steam Electric Plant is a reinforced concrete torus which encircles the drywell. The torus is partially filled with water. Inside the torus is another torus-like steel header, 4'-6" in diameter, called the vent header (see Figures 3.2-2 and 3.2-3). The vent header is located above the water level and is supported by columns. There are thirty two sets of columns which support the vent header and are anchored to the torus concrete. Attached to the vent header are forty eight pairs of downcomers. The lower ends of the downcomers are submerged in water as shown in Figure 3.2-2. The drywell and vent header are connected by eight symmetrically located vent pipes. The vent pipes are connected to the torus by means of bellows which allow radial, lateral and axial growth of the vent (see Figure 3.2-4). The vent system has sixteen identical $22\frac{1}{2}^{o}$ segments. The vent header consists of sixteen cylindrical segments, eight vent bays and eight non-vent bays. In the event of a

loss of coolant accident, steam is discharged to the suppression pool through the eight vents, the vent header and ninety six downcomers. A deflecter pipe has been provided to mitigate the effect of pool swell loads on the vent header pipe.

Safety relief valves (eleven per unit) are designed to prevent primary system overpressurization and are activated during both normal operating and accident conditions. SRV's are attached to the main steam lines in the drywell. Safety relief valve discharge lines (SRVDL) are routed from the main steam lines in the drywell to the suppression pool in the torus. These discharge lines penetrate the vent system at the vent/vent header intersections. The locations of the eleven penetrations in each unit are shown in Figure 3.2-5.

The deflector was installed directly beneath the ring header to divert pool swell flow away from the ring header and reduce the impact pressure on the ring header. The typical deflector is a 20-inch pipe with two angles welded at sides. It is supported at the ring header and runs continuously from one vent bay to the adjacent vent bay, and ends with cantilevers at two ends before it meets the SRV discharge lines (Figure 3.2-6). At the vent bay the angles were not directly attached to the pipe as the typical deflector, instead, a clamp bar (Detail C) was used. This was due to the fact that the field installation required angles not to be welded to the pipe beforehand. Also for ease of installation in each assembly the deflector was composed of three pipes with one straight pipe in the middle and two bent pipes at ends. Slip-on flanges were used to connect these three pipes.

The deflector sits on a 1 inch support plate (Plate "A") which is accompanied by four 3/4-inch cheek plates (Plate "B") and four 3/4-inch stiffener plates (Plate "C"). The support plate was welded to the ring plate which is an extension of ring header collar. Cheek plates were bolted and welded to the support plate. In addition, there are two trunnion lugs (Figure 3.2-6, Section 1-1) and two pairs

of thermal lugs (Figure 3.2-6, Detail A). Trunnion lugs were devised for transmitting horizontal and vertical loads as well as bending moments from the deflector to the support system. Thermal lugs were provided to transfer axial loads due to seismic and thermal loads.

3.3 DESCRIPTION OF APPLIED LOADS

The loads applied to the structures of the vent system can be classified into two categories:

a) Normal, seismic and SRV loads

b) LOCA loads

3.3.1 Normal, Seismic and SRV Loads

These are loads applied to the structure under normal operating and seismic conditions and include the following:

i) Dead load

ii) Normal operating temperature loads

iii) Normal operating internal pressure loads

iv) Seismic loads

v) SRV discharge loads

3.3.1.1 Dead Loads

These are the structural gravitational loads. These loads are always present and will be applied to structure under both normal and accident conditions.

3.3.1.2 Normal Operating Temperature Loads

Under normal operating conditions the temperature range in the suppression chamber for the free air volume and the suppression pool is 76-92°F.

3.3.1.3 Normal Operating Internal Pressure Loads

During normal operating conditions the suppression chamber pressure varies between 0.15 psig and 1.25 psig. The suppression chamber pressure and drywell pressure are essentially equal due to drywell/wetwell vacuum breakers.

3.3.1.4 Seismic Loads

Seismic response for the entire primary containment system complete with the suppression chamber and the vent system was generated using the design response spectra curves documented in the Final Safety Analysis Report (Reference 3-2). Design Response Spectra are attached in this report (Figure 3.3.1.4-1 and Table 3.3.1.4-1) for reference.

3.3.1.5 SRV Loads

SRV loads are described in Reference 3-4. The SRV air bubble drag loads were generated using General Electric's TEEQFOR03 program. The computation for SRV loads is contained in Reference 3-5 (Calculation Set 9527-E-SC-SL-4-F) which indicates the loads for various location of the bubbles and their phasing. The most critical load case was applied to the submerged portion of the downcomers.

3.3.2 LOCA Loads

Postulated loss of coolant accident can occur due to steam pipe break in the drywell. Depending upon the size of the pipe break, the LOCA conditions can be classified as Design Basis Accident (DBA), Intermediate Break Accident (IBA), and Small Break Accident (SBA). Various SRV actuations and seismic conditions must be considered to occur simultaneously with a LOCA. Structural Acceptance Criteria Plant Unique Analysis Application Guide (Reference 3-6) Table 3-1, Page 3-3/3-4 gives all possible load combinations associated with each accident condition (see Table 3.4.1-1)

Pool swell takes place during the first few seconds following the onset of a Design Basis Accident. It is the result of the initial vent system air being rapidly forced into the torus suppression pool and causing the pool to swell into the torus air space. In the process of the pool rising, it impacts the structures in the torus air space up to a certain height and flows past these structure thus resulting in hydrodynamic loads.

Condensation oscillation occurs following the initial air clearing when the flow into the torus is an air/steam mixture. The discharge of steam into the pool and its subsequent condensation causes pool pressure oscillations which are transmitted to submerged structures and to the torus shell.

As the steam vents from the drywell into the wetwell, the reactor vessel depressurizes and the steam flow rate to the vent system decreases. The reduced steam flow rate leads to a reduction in the drywell/wetwell pressure differential. Steam condensation during this period of reduced steam flow is characterized by movement of the water/steam interface up and down within the downcomer. This phenomenon is referred to as chugging.

A schematic of loading condition combinations for various accident conditions is given in Figures 3.0-1 to 3.0-5 of Reference 3-1. Various structures affected by the loads are given in Table 3.0-3, Page 3-5 of the above reference and reproduced as Table 3.3.2-1 and Table 3.3.2-2.

A brief description of the LOCA loads affecting the vent system structures is given below:

3.3.2.1 Containment Pressure and Temperature

The internal pressure and temperature during LOCA in the vent system structures are defined in Section 4.1 of Reference 3-1. The internal pressure loads cause hoop stresses in the header and downcomers. The hoop stresses in the vent and vent header are insignificant. The temperature loads on the vent system do not

cause any stresses because the bellows and support columns have been designed to allow thermal growth.

3.3.2.2 Vent System Thrust Loads

Vent system thrust loads are caused due to the rapid pressurization of the system. Most rapid pressurization occurs in the initial 30 second period following the onset of DBA. After a 30 second period the thrust loads remain practically constant. The critical location for the header loads are vent/vent header intersection, vent header miters and downcomer miters. These loads are described in Reference 3-1, Section 4.2.

3.3.2.3 Pool Swell Load

In the event of a postulated design basis LOCA due to a break in a large pressurized line, the drywell and vent system are pressurized and the water initially in the downcomers is accelerated downward into the suppression pool. After the downcomers are cleared of water, air is discharged into the wetwell below the pool surface, which forces the water above the air bubbles to rise.

As the pool surface rises, it impacts structures in its path. The phenomenon consists of two events, the impact of the pool on structure, and the drag on the structure as the pool flows past it following impact. The portion of the vent system of this plant which is subjected to this impact transient loading includes the lower portion of the main vent, vent header, vent header deflector, and downcomers.

The pool swell deflector loads were defined by General Electric and presented in the Plant Unique Load Definition (PULD) (Reference 3-7). According to NRC criteria (Reference 3-15), the deflector loads should be adjusted to include the initial impact pressure spike. The criteria also requires that the plant-unique loads be adjusted to account for the effects of (a) impact time delays and (b) pool swell velocity and acceleration differences which

results from uneven spacing of downcomer pairs. Pursuant to NRC criteria, the initial impact pressure was caluclated as

$$F = \frac{7\rho V^2 d}{2} \qquad (1)$$

and the duration of the spike was calculated as

$$t = \frac{0.136d}{V} \qquad (2)$$

where

F = Vertical upward force on deflector per unit length

d = Diameter of deflector

V = Impact velocity

ρ = Water density

t = Time from beginning of impact

To account for longitudinal variations in impact and velocities, pool surface displacements and velocities were adjusted using the normalized displacement and normalized velocity factors found in Figures 4.3.4-2 and 4.3.4-3 of Reference 3-8.

For the purpose of load definition, PULD presents the deflector load histories calculated for three Z/L locations, 0, 0.5 and 1.0. A value of Z/L equal to zero corresponds to the center of a vent bay; a value of one corresponds to the center of a non-vent bay. The station Z/L = 0.5 was designated as having the multiplier, K = 1.0. The value of K was defined in Reference 3-16 for the convenience of calculating loads at other Z/L as shown below:

For $0 \leq Z/L \leq 0.5$

$$F(Z/L) = \frac{[F(0.5)-F(0)]\ [k(Z/L)-0.830]}{0.170} + F(0) \qquad (3)$$

For $0.5 \leq Z/L \leq 1.0$

$$F(Z/L) = \frac{[F(1.0)-F(0.5)]\ [k(Z/L)-1.0]}{0.350} + F(0.5) \qquad (4)$$

where F = loads correspond to Z/L

A typical curve for pool swell impact and drag loads is shown in Figure 3.3.2.3-1

Froth fallback load resulting from the froth located between the header and deflector was found to be very small as compared with the impact and drag loads. The pool swell impact and drag loads were applied at directions of $\pm$ 10° from the upward vertical.

3.3.2.4 Condensation Oscillation Loads

Condensation oscillation loads and chugging loads refer to the oscillatory pressure loads imparted to the structures as a result of the unsteady, transient behavior of the condensation of the steam (released during a LOCA) occuring near the end of the downcomers. It is convenient to divide the phenomena into two types:

1) "Condensation Oscillations", which occur at relatively high vent-flow rates; and
2) "Chugging", which occurs at lower vent-flow rates. These loads are described in the next section.

Condensation oscillation is characterized by continuous harmonic pressure oscillations, with the adjacent downcomer pairs oscillating in phase. Oscillating loads on the vent system are caused by the harmonic pressure oscillations superimposed on the prevailing local static pressures in the vent system. For a detailed description of these loads refer to Section 4.4 of Reference 3-1.

The amplitude, frequency and duration of the CO loads depends upon the break size of the accident and as such CO loads are given for the following accident conditions:

1) DBA CO condition

2) IBA CO condition

CO loads do not occur for the SBA condition. Duration of the CO loads is as given in Table 3.3.2.4-1.

Condensation oscillation loads are specified for all three components of the vent system: main vents, vent header and downcomers. The Load Definition Report (LDR) defines the following loads for the DBA and IBA CO condition.

1. Main vent and vent header internal pressurizaiton load
2. Downcomer internal pressurization load
3. Downcomer dynamic load

For the downcomer dynamic load two component of loadings exist:

1) An internal pressure load of equal magnitude in each downcomer in a pair; and
2) A differential pressure load between downcomers in a pair

The CO loads on the vent system structures are tabulated in Table 3.3.2.4-2.

The CO loadings for various conditions are shown graphically in Figures 3.3.2.4-1 to 3.3.2.4-5.

Application of CO Load:

A. Main vent and vent header internal pressurization load
   1. Internal pressurization load $\pm$ 2.5 psig at 4-8 Hz frequency
   2. Main vent and vent header natural frequency in hoop modes is greater than 60 Hz
   3. Responds statically to load in the 4-8 Hz range
   4. Stress levels are low for this load

B. Downcomers - Internal Pressurization Load
   1. CO loads on downcomer are
      a) Internal pressurization load
      b) Dynamic load: DBA = $\pm$ 5.5 psig
         IBA = $\pm$ 2.1 psig

2. Internal pressurization load for both DBA and IBA conditions are within frequency range 4-8 Hz
3. Downcomer natural frequency in hoop mode is > 60 Hz
4. Responds statically to loads in 4-8 Hz range
5. Stress levels are low for this load

C. Downcomer - Dynamic Loads

1. Unequal pressure in downcomer pair causes swing motion.
2. Simultaneous swing motion of downcomer pairs produce dynamic loading on downcomer/vent header system
3. Downcomer pairs swing in-and-out-of-phase.
4. Eight dynamic load cases to be analyzed as shown in Figure 3.3.2.4-6.
5. Sum response from internal and differential pressure as shown in Figure 3.3.2.4.-1
6. For all dynamic loading use 3 harmonics; the lowest downcomer frequency being the first dominant CO frequency, F_1 and the other two harmonics at $2F_1$ and $3F_1$ frequencies.
7. Use one times the water weight at the submerged portion of the downcomer as added hydrodynamic weight.
8. 2% damping was used for CO evaluation, which is considered convservative.

3.3.2.5 Chugging Loads

As discussed earlier in Section 3.3.2.1 chugging occurs as the flow rate of the steam is reduced. During this phase vapor bubbles are formed at the downcomer end which collapse suddenly and intermittently to produce lateral loads on downcomers. These loads are defined for DBA, IBA and SBA conditions. The duration of this load is as given in Table 3.3.2.4-5.

Chugging loads are defined in LDR Section 4.5. Chugging load definition is based on the data obtained from the instrumented downcomers of the Mark I FSTF.

FSTF downcomer lateral loads are defined as Resultant Static Equivalent Loads (RSEL) which, when applied statically to the end of the downcomer, will reproduce at any given time the measured response at the downcomer/vent header junction.

The maximum design loads for the individual plants are obtained by scaling the maximum measured RSEL from the FSTF. The scaling factors are derived on the basis of a comparison of dynamic characteristics of the plant unique downcomers with that of FSTF.

Procedure for determining chugging lateral loads on downcomers is based on the following assumption:

a) Downcomers can be considered rigid when compared to the flexible downcomer/vent header intersection. Therefore the downcomer responds dynamically in any given direction as a single-degree-of-freedom system.

b) Chugging loads are approximated as triangular loads for the purpose of dynamic scaling. A typical chugging pulse is shown in Figure 3.3.2.4-7.

c) For fatigue evaluation, the FSTF RSEL reversal histograms must be scaled by the ratios of the chugging duration in the plant to the duration used in the FSTF.

d) Maximum chugging load on an individual downcomer can occur in any arbitrary direction with equal probability.

e) All downcomers experience chugging in phase.

3.3.2.5.1 Evaluation of Maximum Chugging Design Load

Maximum design load P_{max} is given by

$$P_{max} = P_1 \frac{DLF}{DLF_1}$$

Equation 4.5.3.1
Reference 3-8

where

P_{max} = Maximum design load for plant unique downcomer

P_1 = Maximum RSEL design load obtained from FSTF

DLF = Plant unique dynamic load factor

DLF_1 = Dynamic load factor of FSTF downcomer

The dynamic load factors are given by

$$DLF = \frac{2}{\omega t_d}\left[2 \cos\left(\omega \frac{t_d}{2}\right) - \cos(\omega t_d) - 1\right]$$

Equation 4.5.3.2
Reference 3-8

where

ω = lowest natural frequency of downcomer

t_d = duration of the triangular chug pulse load = .003 secs.

Since ωt_d is small, above equation is simplified to

$$DLF = \pi \ f \ t_d$$

Equation 4.5.3.2
Reference 3-8

Since the chugging load is random in direction, plant unique maximum design chugging lateral load as a function of direction is given by

$$P_{EW} = P_1 \ \text{Sin} \ \theta \frac{DLF_{EW}}{DLF_{EW,\ 1}}$$

$$P_{NS} = P_1 \cos\theta \frac{DLF_{NS}}{DLF_{NS,\,1}}$$

where

θ = angle from N-S direction where P_{max} is applied

DLF_{ij} = plant unique dynamic load factor of downcomer/vent header based on natural frequency in i-j direction

$DLF_{ij,1} = DLF_{ij}$ from FSTF

From equation 4.5.3-3 Reference 3-8

$$DLF_{ij} = \pi\, f_{ij}\, t_d$$

where f_{ij} = lowest natural frequency of downcomer/vent header in the i-j direction

The E-W natural frequency of FSTF downcomer is given in Reference 3-8 (Mark I Containment Program, Application Guide 10) as 2.9 Hz.

The N-S natural frequency is found by the square root of the ratio of the rotational stiffnesses

$$f_{NS} = f_{EW}\sqrt{\frac{K_{NS}}{K_{EW}}}$$

For FSTF $\frac{K_{NS}}{K_{EW}} = 5.76$

i) Reference 3-8, Mark I Containment Program Development of Downcomer Lateral Load from FSTF.

$f_{NS} = 6.96$ Hz

ii) GE letter MI-G-27, dated 5-11-82.

The procedure for obtaining the plant unique maximum design load for chugging can be enumerated as follows:

Step 1 Determine the lowest natural frequency of the plant unique downcomer using 2 times the water mass as added water mass in the submerged segment of downcomer in both E-W and N-S directions

Step 2 Determine plant unique dynamic load factors

$$DLF_{EW} = \pi \ f_{EW} \ t_d$$

$$DLF_{NS} = \pi \ f_{NS} \ t_d$$

where t_d = .003 sec. (Reference 8)

Step 3 Determine FSTF DLF_1

$$DLF_{EW,1} = \pi \ f_{EW,1} \ t_d$$

$$DLF_{NS,1} = \pi \ f_{NS,1} \ t_d$$

where:

$$f_{EW,1} = 2.9 \text{ Hz}$$

$$f_{NS,1} = 6.96 \text{ Hz}$$

$$t_d = .003 \text{ sec.}$$

Step 4 Determine maximum design lateral load

$$P_{EW} = P_1 \text{ Sin } \theta \frac{DLF_{EW}}{DLF_{EW,1}}$$

and

$$P_{NS} = P_1 \text{ Cos } \theta \frac{DLF_{NS}}{DLF_{NS,1}}$$

where P_1 = 3046 lbs., max. RSEL observed in FSTF tests

P_{EW} and P_{NS} are then applied as static loads at downcomer tips to obtain maximum response at the vent header/downcomer intersection.

3.3.5.2 Procedure for Fatigue Evaluation Due to Chugging

For fatigue evaluation, the number of RSEL reversals during the entire chugging phase in the FSTF were counted and presented in the form of RSEL reversal histograms. Since the chugging load may be oriented in any lateral direction, these histograms were obtained for eight angular sections around the downcomer as shown in

Figure 3.5.3-1. The histograms are based on 95% probability of non-exceedence. FSTF chugging RSEL reversal date is given Table 4.5.3-1 of A.G.10 (Reference 3-8) and the histograms for each of eight sections are shown in Figures 4.5.3-2 through 4.5.3.-9 of A.G.10. Procedure for fatigue evaluation for a typical point near the downcomer/vent header junction is described in Section 4.5.3.2. of A.G.10.

3.4 DESIGN LOAD COMBINATIONS AND CODE ALLOWABLES

3.4.1 Load Combinations for Vent System

Load combinations for vent system structures are shown in Table 3.4-1. Following load combinations have been determined to be more critical than the others.

1. Load Combination #11: CO (IBA) + SRV
   Chugging (IBA) + SRV
2. Load Combination #23: CO (DBA) + SRV
   Chugging (DBA) + SRV

SRV discharge loads for single and multiple valve actuations were generated and it was determined that multiple valve actuation for SBA/IBA condition (A3.2S) was found to be the most severe. SRV (A3.2S) was used conservatively for all load cases in the above load combinations.

3.4.2 Code Allowables

This section describes the structural acceptance criteria which have been used in the evaluation of the vent system structures. The structural acceptance criteria are based on the Plant Unique Analysis Application Guide (Reference 3-6) and Application Guide 10. (Reference 3-8) and ASME Section III Code including Addenda through Summer 1977.

The vent, vent header and the downcormers are classified as class MC components and criteria of Subsection NE-3000 of the code are

to be applied for qualification of these components. Accordingly stress intensity limits for various load combinations and service level assignments (as per Table 3.4-1) have to be satisfied. Table 3.4-2 shows the allowable stress intensity limits.

The following design stress intensity valves were used.

S_{mc} = 19.3 KSI at = 200°F $S_{mc} = S_m$ as listed in Table I-10.0, Appendix I.

Reference: ASME Section III, Division 1, Subsection NE paragraph NE-3134, Summer 1977 Addenda.

S_{ml} = 23.1 KSI at = 200°F Reference: ASME Section III, Division 1, Subsection NE, paragraph NE-3134, Summer 1977 Addenda. $S_{ml} = S_m$ as listed in Table I-1.0, Appendix I.

3.5 METHOD OF ANALYSIS

3.5.1 Seismic Analysis

The postulated earthquake creates horizontal and vertical inertia loads on the vent system. These loads are non-symmetric loads. A 180° lumped mass beam model of the vent system structures with symmetric boundary conditions was formed and coupled with the Brunswick Containment Stick Model to form a three-dimensional beam model. The vent/vent header intersection was represented in the beam model by an 18 x 18 spring stiffness matrix. The spring stiffness matrix was generated from a finite element model of the vent/vent header intersection. The intersection finite element model was used to formulate a stiffness matrix. Using static condensation, the stiffness matrix was reduced to boundary degrees of freedoms conforming to three boundary nodes. This 18 x 18 super-element stiffness matrix, shown in Table 3.6.2.1-1 was used in the 180° beam model.

The downcomer/vent header intersection was represented by a 12 x 12 diagonal stiffness matrix. The downcomer/vent header spring stiffness was developed by applying unit loads at the intersection

using a shell model of the downcomer/vent header intersection. This shell model is described in Section 3.6.1. The 12 x 12 stiffness matrix is shown in Table 3.6-1.

The Householder-QR method was used to extract eigenvalues of the 180° beam model. Design response spectra curves for Brunswick (Fig. 3.3.1.4-1) were used as seismic input. Peak responses were evaluated at salient points using Stardyne Dynre-4 program. A description of the 180° beam model is included in Section 3.6.2.1.

3.5.2 Analysis for Pool Swell Loads

The vent header is made up of sixteen straight sections or bays with eight vent pipes connecting into alternate bays. Thus a typical repeatable segment including one half of a "non-vent" bay and one half of a "vent" bay can be identified. The configuration of a typical 22 1/2° segment of the vent system is shown in Figure 3.5.2-1. The segment includes a portion of the ring header, one half of a vent pipe and six downcomers. Sixteen such segments make up the complete vent system. A typical 22 1/2° degree segment is chosen for analysis. The 22 1/2° beam model has been used for all dynamic analysis for LOCA loads and is described in Section 3.6.4. The response results have then been applied to an appropriate finite element shell model as equivalent static loads to obtain stresses for code evaluation.

For pool swell transient, a 22 1/2° beam model with one times the water weight as added water weight for the submerged segment of the downcomers was used. Eigenvalues were obtained using the HQR method and the time history response was obtained using Stardyne Dynre-1 program. This analysis is described in Section 3.8.1.

3.5.2.1 Methods of Analysis for Pool Swell Loads for Vent System Structures

The magnitudes and time-dependent characteristics of the loading at each component (vent, vent header and downcomer) are developed based on Section 4.3.3 of LDR for load definition and

assumptions, Section 4.3.3 of Application Guide 10 for procedure of calculations, pages 37-48 of the PULD for plant unique characteristics and General Electric EDT #171.1 dated May 8, 1980. Due to the relative location in the impact path of the three components of concern, their loadings are generated individually.

The 22 1/2° degree beam model has been used for the analysis of the vent system structure subjected to these impact loadings due to the symmetrical nature of the loading and the structural geometry.

The dynamic response of the structure due to impact on the downcomer portion between the intersection of vent header and first miter bend of the downcomer is accounted for by applying a dynamic load factor of 2 as suggested in the LDR. Dynamic analysis is performed to find the dynamic responses due to impact on main vent and vent header. A one-time water mass for the submerged portion of downcomer in addition to the structural mass has been used for this analysis with a 2% structural damping.

The generated force vector at each nodal point from the dynamic analysis due to main vent and vent header impact is then combined statically with the effect of impact on downcomer sloped portion (dynamic load factor of 2 is included) to obtain the total structural responses of the vent system due to pool swell impact on those three components.

3.5.2.2 Methods of Analysis for Pool Swell Loads for Vent/Vent Header Intersection

Pool swell time history loads were applied to the 22 1/2° beam model and the time history response was obtained at the support columns. From this response dynamic load factors were computed for various locations in the model. The dynamic load factor obtained at support column locations was applied to the pool swell pressure load acting upon the vent/vent header intersection. The resulting equivalent static pressure loads were then applied to the vent/vent header intersection shell model (Half Shell Model #3). Stresses at

the critical element locations were used for code evaluation. Column reactions were obtained for design of support columns and attachments.

3.5.3 Analysis for Chugging Loads

Chugging produces lateral loads on downcomers. The maximum design resultant static equivalent loads have been calculated based on the dynamic characteristics of the plant unique downcomers. 22 1/2° beam model with 2 x water weight as added water weight in the submerged portion of downcomers was used. HQR method of analysis was used to extract eigenvalues. The lowest natural frequencies in-plane and out-of-plane of a typical downcomer pair were noted. FSTF definition of scaling factor is based on the assumption that downcomers are rigid as compared to the downcomer/vent header intersection flexibility. This was verified by applying unit loads at downcomer tips of the downcomer/vent header intersection shell model. The same unit loads were also applied at downcomer tips in the 22 1/2° beam model and the correspondence of the beam model and shell model was established by comparing tip displacements. A computer plot of the displaced shape is shown in Figure 3.6-11. This establishes the validity of the rigid downcomer assumption. Plant unique dynamic load factors in E-W and N-S directions were computed using the formula DLF $= \pi f t_d$ where t_d (= .003) is the triangular pulse duration as shown in Figure 3.3.8 of Reference 1. Plant unique RSEL's were computed for E-W and N-S directions and for each of the eight sectorial orientations (Figure 3.5.3-1) using the procedure outlined in Section 3.3.5.1. Unit loads were applied at tips of downcomers using the downcomer/vent header shell model. Static analysis was done using Stardyne Static program. Plant unique RSEL's were then factored into the unit loads and Stardyne Post program was used to compute element stresses and stress intensities. The method of analysis described above is presented schematically in Figure 3.5.3-2. The maximum stress intensities for membrane and bending for chugging were thus obtained.

3.5.4 Analysis for Condensation Oscillation Loads

CO loads are oscillatory internal pressure loads. The vent system structures, wherever axisymmetric (frequency 60 Hz) are not excited by axisymmetric internal pressure harmonics (frequency 4-8 Hz). These pressures at such locations have been applied statically and hoop stresses have been evaluated. At locations where there is a change of direction in the flow path, the internal pressure causes thrust loads due to imbalance. Such locations are vent/vent header intersection, vent header miter and downcomer miter. Evaluation of these imbalances forces, due to CO internal pressure at vent/vent header intersection and at vent header miter, are inherent in the vent system thrust load analysis and have been discussed in Section 3.3.2.2.

The CO internal pressure loads on downcomer miters were integrated over the geometrically unsymmetrical segment of the miter. For each downcomer pair two situations were considered: firstly, the unbalanced miter force resultant harmonics for internal pressure loading of both downcomers; secondly, the differential pressure harmonics were applied to one downcomer. The response from the two situations was then superimposed. Both IBA and DBA conditions of accident were evaluated. A schematic of the method is shown in Figure 3.5.4-1.

3.5.5 Analysis for Safety Relief Valve Loads

SRV actuations cause velocity and acceleration drag loads on submerged structures. From the velocity and acceleration fields, the drag forces are calculated using TEEQFOR03 computer program (Reference 3-9). T-quencher discharge loads are not only plant unique but also SRV line unique. Individual lines have different geometry and different set pressures. SRV time history loads were generated for single and multiple valve actuations. It was determined that A3.2(SBA) SRV time history loads were governing loads for peak response. These loads are lateral loads having in-plane and

out-of-plane components on the submerged segments of the downcomers. 22 1/2° beam model with 2 x water weight on submerged portion of downcomers as added weight was used for analysis. Structural frequencies were obtained using Stardyne Householder-QR method. The frequency content of the SRV load transients was determined using a response spectra technique. The SRV time history was then adjusted to conform to the structural frequencies so as to obtain maximum responses. A typical plot of the adjusted SRV A3.2 (SBA) time history is shown in Figure 3.8.1-1. These time histories were then applied at two nodal locations in each downcomer to correspond with the two locations for which the SRV time history was generated using TEEQFORØ3 program. 4% damping was used and peak downcomer tip displacement responses was generated using Starydyne Dynre-1 program. These peak tip displacements were then applied to vent header/downcomer intersection shell model which was then post processed to obtain peak stress intensities in all elements. The above method is presented schematically in Figure 3.5.5-1.

3.5.6 Analysis for Thrust Loads

Due to the symmetry of the thrust loading and structural geometry of vent system, the 22 1/2 degree beam model has been utilized to investigate the structural response of the vent system subjected to thrust loads. The new column supports located at both sides of the intersection of main vent and vent header have been deleted for the analysis due to their proximity to the main vent, which tends to attract downward force from the thrust on main vent and the fact that their downward restraint capacity is negligible due to their design.

With the transient nature of the thrust loading, dynamic analysis has been performed to find the responses of the vent system structure. A one-time water mass at the submerged portion of downcomer has been incorporated in the modal extraction of the

structure and a 2% modal damping has been used to calculate the dynamic responses.

3.5.7 Fatigue Evaluation

The vent system structures are subjected to a number of cyclic loading conditions. ASME Code and Mark I LTP acceptance criteria require fatigue evaluation for cyclic loads.

3.5.7.1 Evaluation Procedure

a) Determine total number of loading events for loads which cause cyclic stresses.

b) Identify critical location for fatigue damage.

c) Calculate stress range for each cyclic load and critical location.

d) Determine equivalent maximum stress cycles.

e) Select suitable stress concentration factors.

f) Perform a fatigue evaluation in accordance with the ASME Code.

The assumptions and procedures for carrying out steps (a) thru (e) are described below. Actual fatigue evaluations at the selected locations are summarized in Section 3.8.

3.5.7.2 Loadings Considered for Fatigue

Vent system structures are subjected to the following cyclic loadings:

1. Seismic loads.
2. SRV air bubble drag loads on downcomers.
3. LOCA loads: including condensation oscillation and chugging loads.

Seismic loads, applied to shell model as equivalent static loads, do not produce high stresses. These stresses yield a very low usage factor. Fatigue evaluation for these loads is not discussed further.

3.5.7.2.1 SRV Air Bubble Drag Loads

SRV air bubble loads have been applied as lateral loads on submerged portion of downcomers. Based on the actual SRV actuations counted, it is estimated that a total of 400 actuations would occur over the 40 year estimate plant life. Each SRV event (actuation) produces cyclic response transients with amplitude (stress range) varying among successive cycles. Amplitude decays to zero after each event (see downcomer tip displacement response curve Figure 3.8.1-3). For the purpose of a conservative fatigue evaluation, an estimated 2000 equivalent maximum stress cycles have been used.

3.5.7.2.2 Condensation Oscillation Loads

Condensation oscillation loads have three harmonics which have been applied at frequencies f, 2f and 3f (see Section 3.3.2.4). These loads are internal pressure oscillations and do not excite the shell modes of the structure. The differential pressure harmonics applied at downcomer miters contribute significantly because one of the harmonics is applied at the lowest downcomer frequancy. Number of cycles for the CO load harmonics is obtained by multiplying the duration of the event by the frequency of the harmonics. Conservatively, the total stress intensity has been used for each harmonic. Maximum stress range and number of cycles for each harmonic is thus obtained.

3.5.7.2.3 Chugging Loads

Chugging loads are applied as maximum RSEL (resultant static equivalent loads). Plant unique RSEL's are scaled from the FSTF resultant static equivalent load. The step by step procedures for computing number of stress reversals for chugging loads for fatigue evaluation is as given below.

- Compute plant unique RSEL's

$$P_{max} = F_1 \times \frac{DLF}{(DLF)_1}$$

where

F_1 = RSEL from FSTF data

F_1 = 3936

$DLF = \pi\ t_d\ f$

$DLF_1 = \pi\ t_d\ f_1$

- Compute RSEL components in N-S and E-W directions for each of the eight sectors using equations.
  Apply RSEL components at downcomer tips of vent header/downcomer shell model for each sector.
- Compute maximum stress intensity for each element for all the eight sectors.
- For each element scale stress intensities for each sector to the maximum stress intensity obtained in the previous step. Scale Factor = $\frac{\text{S.I. OF ELEMENT FOR SECTOR}}{(\text{S.I.})_{\text{max. OF ELEMENT}}}$
- Use FSTF stress reversal histograms Figures 4.5.3.2 through 4.5.3-9 of LDR (Reference 3-1) for each sector for computing number of stress reversals. Rescale the RSEL (%) scale by multiplying each histogram by the scale factor obtained in previous step.

- Sum all eight histograms to obtain total number of stress reversals for every 10% of the maximum stress intensity range.
- Multiply total number of stress reversals by the ratio

$$\frac{\text{IBA/DBA CHUGGING DURATION}}{\text{FSTF CHUGGING DURATION}}$$

This ratio is 1.76 for IBA and .0586 for DBA.

In this manner we obtain the stress range and number reversals for each element for chugging loads.

3.5.7.3 Critical Fatigue Locations

The downcomer/vent header intersection is the area where maximum stresses occur due to CO, chugging and SRV loads. This intersection is identified as the most critical location in the vent system for fatigue evaluation.

3.5.7.4 Stress Concentration Factors

In the areas of stress concentration, a refined finite element mesh was used to obtain accurate stresses. For fatigue evaluation of welds in the area of high stress concentrations a fatigue concentration factor of 2.0 for welds was used.

3.5.7.5 Code Procedure for Determination of Fatigue Usage Factor

Using the stress ranges, stress concentration factors and number of stress reversals (cycles) determined in the previous sections, a code fatigue evaluation was carried out. The step by step procedure is outline below.

- Determine peak stress intensity range for selected elements by multiplying maximum stress intensity by stress concentration factor.

- Peak S.I. range = $|Si-Sj|_{max}$ x SCF

- Determine alternating stress intensity range by using the formula

$$S_a = 1/2 \times \text{Peak S.I. range} \times \frac{E_c}{E}$$

where

S_a = alternating stress intensity range

E = Elastic modulus for SA 516 Grade 70 for temperature 200°c = 27.7×10^6 Ksi

E_c = Elastic modulus used for code fatigue curves as given in ASME Code = 30×10^6 ksi

(Ref. Fig I-9.1 Appx. I of ASME Code Section III Appendices)

- For the alternating stress intensity range, read allowable stress cycles for fatigue design curves using Figure I-9.1 Appendix I of ASME Code Section III Appendices

- Repeat calculations for each cyclic load

- Compute cummulative usage factor using the formula

- Cummulative usage factor $= \Sigma \frac{n_i}{N_i}$

where summation is for all cyclic loads.

n_i = Equivalent maximum stress cycles for the i_{th} cyclic load

N_i = Number of maximum allowable stress cycles for the alternating stress intensity range, S_a, obtained from the code fatigue design curve.

Cummulative usage for fatigue should be < 1.0

3.5.7.6 Use of Program "Fatigue"

For fatigue evaluation of chugging loads, a Fortran coding of the procedure using the FSTF histograms and the code fatigue design curves was done. This in-house program "Fatigue" (Reference 3-14) was verified. The program was used in conjunction with output of stress intensities using Stardyne "Post" program.

For other cyclic loads, such as CO and SRV, the maximum stress intensities were obtained from Post program. The usage factor was calculated by direct use of code fatigue curves.

3.5.8 Evaluation of SRV Discharge Line Penetration of Vent/Vent Header Intersection

Actuations of an SRV are assumed to occur at any time during the life of the plant. One or more of the eleven SRVDL can be actuated during normal plant operations or possibly during a LOCA. The variations in loading which are associated with the random occurence of these actuations requires that the nature and origin of the loads acting on the SRVDL be considered in the analysis of the penetration.

Specifically, differences in magnitude, direction, and timing between a normal operational and LOCA related SRVDL discharge are important considerations. An important distinction occurs between the upstream and downstream sections of the discharge line. The downstream portion of the line lies within the wetwell airspace and the supression pool. This location of the line causes it to be subjected to higher loads during a LOCA than the upstream portion of the line which lies in the drywell airspace. In the drywell airspace, the upstream portion of the line is protected from the direct effects of quenching and other suppression pool phenomena. For this reason, statically applied equivalents of the peak loads from time history analyses were differentiated as being upstream loads or downstream loads (Reference 3-4). Also, some of the loads related to an SRV

discharge do not occur simultaneously on the upstream and downstream legs of a line. This effect was included through the separation of these load components into separate static cases.

3.6 MATHEMATICAL MODELS

Mathematical models used for vent system evaluation are described in this section. As necessitated by the type of loads and methods of analysis used, two types of models were used:

1) Shell models
2) Beam models

Finite element shell models were used to obtain stresses in the local regions of intersections in the vent system. These models were also used to obtain local stiffness coefficients for incorporation in the beam models. Regions where local effects were desired to be evaluated are:

a) Downcomer/vent header intersection (Shell Model #1)
b) Vent/vent header intersection (Half Shell Model #3)

Shell models used for computing local stiffness coefficients are:

a) Vent/vent header intersection superelement (Shell Model #3)
b) Downcomer/vent header intersection (Shell Model #1)

Shell models were used for static analysis. Salient features of these shell models are described in Section 3.6.1. Beam models were used for dynamic analysis. There were two types of beam models used:

a) 180° Beam model for asymmetric loads
b) 22½° Beam model for symmetric loads.

Justification for using 180° beam model or 22½° beam model has already been discussed under methods of analysis. To recapitulate, the 180° beam model has been used for seismic analysis of the vent

system. 22½° Beam model was used for pool swell, thrust, CO, SRV and chugging loads. Salient features of the beam models are discussed in Section 3.6.2.

3.6.1 Shell Models

Finite element discretization of the intersection regions was done using STARDYNE QUAD-PLATE and TRI-PLATE elements. QUAD-PLATE is a quadrilateral thin-plate 4-node planar element. The element has five degrees of freedom per node - three translations and two rotations. The in-plane displacement function is an iso-parametric formulation with incompatible modes. The curvature and slope terms have a quasi-linear strain formulation. TRI-PLATE is a linear curvature comaptible triangular plate element which simulates thin plate behavior. A variation of this element is "Martin element" which can be used when transverse sheer effects and/or transverse shear stresses are desired. The displacement of a TRI-PLATE element is defined by three translations and two rotations at each corner of the element. "Martin" triangular plate element can be used for both thin and thick plate behavior. "Martin" element with constant strain formulation (linear variation of displacement) was used in the present analysis. A complete description of these elements is contained in References 3-10 and 3-11.

The basic form of finite element mesh was dictated by the geometry of the intersection, the location of the stiffeners and other geometric discontinuities. The mesh was graduated in accordance with anticipated stress gradients. The mesh refinement was arrived at by using various test problems and the solution verified by classical methods. In most areas of the shell models the QUAD-PLATE element was used. Triangular plate elements were used in transition areas. The shell models extend over the region of the discontinuity plus sufficient distance into the uniform region of the shell to allow local stress effects to die out. The model symmetry and geometry input were checked by using Stardyne's "Static", "PLOT 3D" and CONSTAR

(plot) programs. A brief description of the individual shell models and the finite element mesh of each model is given below:

3.6.1.1 Downcomer/Vent Header Intersection (Shell Model #1)

This is a finite element shell model consisting of a typical tied downcomer pair attached to a segment of the vent header. The header segment extends to 87.5" in length on either side of the downcomer pair. The geometry and finite element model of shell model No. 1 are shown in Figures 3.6.1.1-1 through 3.6.1.1-10. The CONSTAR/PLOT 3D plots of the mesh are shown in Figures 3.6.1.1-11 through 3.6.1.1-13. The tie between the downcomers is represented by STARDYNE BEAMG elements. The nodes at the end of each downcomer are connected to a central node (Node 1277 and Node 1346) by means of rigid links. This allows these central nodes to be used as points of load application. Fixed boundary conditions are imposed at the two extremities of the vent header segment.

This shell model is used for two purposes; firstly to compute downcomer/vent header intersection stiffness matrix and secondly to apply equivalent static loads for CO, SRV and chugging loads to compute element stresses and stress intensities. Procedure for computing downcomer/vent header intersection stiffness matrix is given in Calculation Set 9527-E-SC-VS-1-F (Reference 3-13). This stiffness matrix is used in beam models as matrix addition elements at header and downcomer junction nodes and is shown in Table 3.6.1.1-1. The method for application of CO loads, SRV loads and chugging loads to this model has been discussed under method of analysis Sections 3.5.7.2.1 through 3.5.7.2.3.

3.6.1.2 Vent/Vent Header Intersection (Shell Model #3)

A typical vent/vent header intersection is shown in Figure 3.6.1.2-1. Of the eight vent/vent header intersections in the ring header, six intersections have penetrations for SRV discharge lines.

Locations of the eleven SRV discharge pipes are indicated in Figure 3.2.3. The vent header is 54.25" in diameter everywhere except at the areas of the vent/vent header intersections where the diameter is enlarged to 76.25" through a conical transition. It was required to determine the local stiffness properties of this intersection in order to form analytical beam models for dynamic analysis of vent system structures.

A representative vent/vent header intersection model was chosen which consists of a 12" long segment of the vent pipe, two 10" long segments of the header pipe, one on either side of the conical transitions, the enlarged portion of the header and the three 1 1/4" thick collar stiffeners. A finite element model of this intersection is shown in Figures 3.6.1.2-2 through 3.6.1.2-3.

The nodes at the extremities of each cylindrical segment are connected to a central node through rigid links. These three nodes (Nodes 2820, 2821 and 2822) correspond to the three nodes in the 180° beam model at the junction of the vent and vent header beam elements. Stardyne QUAD-PLATE and triangular plate elements were used. A graduated refined mesh was used in the areas of discontinuity.

Stardyne static analysis was used to compute the reduced stiffness matrix. Analytical procedure used to obtain the reduced stiffness matrix is given in Calculation Set 9527-E-SC-VS-1-F (Reference 3-13). The stiffness matrix was reduced to the boundary degrees of freedom corresponding to the three boundary nodes (Nodes 2820, 2821 and 2822) using static condensation. This reduced matrix k_s is shown in Table 3.6.1.2-1. The entire intersection was thus used as a superelement.

Two variations of the above matrix were used in the beam models. One for the 180° beam model and the other for the 22½° beam model. The 180° beam model was used for seismic analysis wherein seismic response was also required at SRV discharge line penetrations. To accomplish this a 4-node beam model interconnecting the three boundary nodes of the superelement was made. The superelement k_s and

the 4-node beam model reduced stiffness matrix k_B were then superimposed together to yield the same reduced stiffness matrix as obtained originally for the superelement. The effective difference matrix (k_S-k_B) was used in conjuction with the 4-node replacement model in the 180° beam model.

The other variation of the superelement was made with the 22½° beam model where the symmetric half of the vent/vent header intersection was to be used. The reduced stiffness matrix of the superelement was modified retaining only the appropriate stiffness coefficients using symmetric boundary conditions at Node 2822 on the vent. This stiffness matrix is shown in Table 3.6.2.2-1.

3.6.1.3 Vent/Vent Header (Half Shell Model #3)

This shell model was used for evaluation of the intersection for pool swell loads. Pool swell loads were applied as equivalent static pressure loads on the Half Shell Model #3. It was called Half Shell Model #3 because only symmetric half of the intersection shell model was used; the load and the structure both being symmetric about the center line of the vent. The model contains the vent/vent header intersection and the vent segment extending up to the drywell. A sufficient length of the header (45.7765") past the conical section has been included so that local effects die out. The header segment beyond this length is modelled as beam elements which are connected to the shell by means of rigid links. The supporting columns near the header miter have been represented in the model as ground springs at Node 2220 and the columns at the transition cone have been represented as beam elements connected to the enlarged diameter of the header by means of a 1" x 6" ring welded to the header. The finite element discretization of the model is shown in Figures 3.6.1.3-1 through 3.6.1.3-6. The bellows are attached to the vent by means of springs representing the axial and lateral stiffness of the bellows. The vent drywell junction nodes have been fully restrained. Symmetric boundary conditions have been applied to all nodes at the vent center line.

Node 2222 represents the far end of the model on the header. Symmetric boundary conditions have been applied at this node.

3.6.1.4 SRVDL Penetration of Vent/Vent Header Intersection

This shell model was used to evaluate the penetration of the vent/vent header intersection by the SRV discharge line (SRVDL) (Figures 3.6.1.4-1 and 3.6.1.4-2) under loads acting on the SRVDL system. The geometry of the penetration and the application of appropriate boundary conditions permitted the isolation of one SRVDL in a finite element idealization of one half of the vent/vent header intersection. The use of only one half of the intersection allowed for significant mesh refinement in the region of the penetration.

The model (Figures 3.6.1.4-3 and 3.6.1.4-4) consists of one half of the vent/vent header intersection model with short segments of the vent and vent header included (similar to Shell Model No. 3). Upstream SRV loads were applied to the end of a portion of the upstream SRVDL, while downstream SRV loads were applied to the point at which the SRV support is connected to the downstream portion of the SRVDL (Figure 3.6.1.4-5). Also included in the model are idealizations of the SRVDL penetration reinforcement (Figure 3.6.1.4-6) and the intersection ring stiffener.

The majority of the idealization consists of STARDYNE QUAD-PLATE and TRI-PLATE elements to model the primary components. Rigid link elements (Figure 3.6.1.4-5) were used to distribute applied loads and support reactions along the outermost edges of the cylindical members of the model. Beam elements were used to model portions of the SRVDL support and matrix elements were used to provide concentrated values of stiffness where necessary.

3.6.1.5 Deflector Support Shell Model

The deflector support shell model as shown in Figure 3.6.1.5-1 includes the deflector support plate, header ring plate, header columns, the header and cheek plates. The header columns were

represented by springs with a stiffness of 2100 k/in. The model includes the header extending three feet on both sides to ensure that critical local stresses in the header were examined. At the boundary of the header it was assumed that there were no movements in the axial and horizontal directions. The cheek plates were connected to ring plate and the support plate by rigid beams. The model consists of 726 nodes, 60 rigid beams, 232 triangular plate elements and 516 quadrilateral plate elements.

3.6.2 Beam Models

Lumped mass beam models have been used for dynamic analysis of the vent system structures. Asymmetric loads were applied using a 180° beam model. Taking advantage of the repeatibility of the geometry, a typical 22½° segment was considered representative of the vent system for all symmetric loading. STARDYNE BEAMG & PIPEG elements were used for the vent header, vent, downcomers and the deflector. The support columns for the vent header were represented as axial members. These columns were translationally restrained at support points located at the torus but allow horizontal translation of the header. These support columns are designed to take only compression loads. The downcomers are connected to the header by means of rigid links of lengths equal to the radius of the header. The downcomer/header intersection stiffness is represented by matrix addition elements "MADDEL's". Each matrix addition element has downcomer/vent header stiffness coefficient input as a symmetric stiffness matrix. A 12 x 12 stiffness coefficient matrix is included for each "Maddel". Each downcomer/vent header intersection has one Maddel. The 12 x 12 spring stiffness matrix is shown in Table 3.6.1.1-1. The mass nodes have been chosen judiciously to represent their physical location. An adequate number of mass nodes has been provided so that all nodes of interest are preserved. The miter at the header and the downcomers was represented by beam elements with beam properties representing the miter flexibilities. Salient

features of the 180° Beam model and the 22½° beam model are discussed below.

3.6.2.1 180° Beam Model

The 180° beam model of the vent system structures is connected to the Brunswick containment lumped mass stick model by means of rigid links. Together these structures form a three dimensional beam model. The containment model and 180° beam model are described below.

1. Containment Model

Brunswick containment model consists of the following components:

- o Pressurized Reactor Vessel
- o Concrete Pedestal
- o Shield Wall
- o Drywell
- o Reactor Building
- o Foundation Mat
- o Seismic Springs
- o Soil Springs

A lumped mass finite element idealization is shown in Figures 3.6.2.1-1 and 3.6.2.1-3. Nodes 1 to 45 and beam elements 801 to 902 have been allocated to the containment model. Soil spring stiffnesses are represented by STARDYNE matrix addition elements (MADDELS 223 and 224). The soil springs have been attached to the containment at the bottom of the foundation mat (Node 999) at El. (-)28 ft. The reactor vessel to shield wall and shield wall to drywell lateral springs are represented by MADDELS 225 and 226.

2. 180° Beam Model Description

This beam model consists of four vents, 180° of header/downcomer system, the deflector and the supporting columns as shown in Figure 3.6.2.2-1.

A lumped mass finite element idealization of the 180° beam model is shown in Figures 3.6.2.1-4 through 3.6.2.1-7. Nodes 100 to 900 and nodes 35 and 1000 and beam elements 1 to 800 and 910 to 951 have been allocated to this model.

The 180° beam model is connected to node 999 of the containment model by means of rigid links. These rigid links interconnect all ground support locations which are identified as vent to drywell connections (Nodes 299, 499, 699 and 899) and column nodes at anchorage points with the torus shell (Nodes 128 to 131, 171 to 174, 328 to 331, 371 to 374, 528 to 531, 571 to 574, 728 to 731 and 771 to 774) as shown in Figures 3.6.2.1-8 to 3.6.2.1-11.

As has been mentioned earlier in Section 3.5.1, the 180° beam model was used for seismic analysis of the vent system. The infinitely rigid system formed by the rigid links, makes it convenient to input the Design Response Spectra Curves. Notable features of the model are given below:

- Bellows are represented by equivalent beam elements 948 to 951.

- Superelement stiffness matrix obtained from Shell Model No. 3 was modified to include a 4-node beam model and the resulting stiffness matrix (see Table 3.6.2.1-1) was used in the 180° beam model as MADDEL No. 1 to 4.

MADDEL No.	NODES FORMING THE ELEMENT
1	150, 151 & 152
2	350, 351 & 352
3	550, 551 & 552
4	750, 751 & 752

- The downcomer/vent header intersection stiffness matrix was represented in the model by MADDELS 5 to 15, 25 to 36, 45 to 56 and 65 to 76.

- Damping values used are as follows:

Structural Steel	5%
Concrete	7%
Soil	7%
Vent System Structures	4%

Composite Damping determined by STARDYNE, was used for seismic evaluation of the above three-dimensional 180° beam model.

- Symmetric boundary conditions were applied at nodes 100, 200, 900 & 1000 of the header and the deflector. Node 999 was restrained for vertical and all out-of-plane rotations and translations.

3.6.2.2 22½° Beam Model

This beam model contains a 22½° segment of the vent system. It has three downcomer pairs, the deflector and the header segments, two sets of support columns and a symmetric half of a vent as shown in Figure 3.5-1. A finite element discretization of this model is shown in Figures 3.6.2.2-1 through 3.6.2.2-11. This model was used for dynamic analysis of CO loads, SRV loads, pool swell and thrust loads. The frequency characteristics of the structural model were used for the determination of Resultant Static Equivalent loads for chugging. Static analysis was done to verify correspondence of the beam model with the shell model. The model contains 146 nodes, 122 beam elements and 10 rigid links.

The rigid links were used to connect the downcomers to the header center line and to connect support columns to the header center

line. Downcomer/header intersection stiffnesses have been incorporated in the model as matrix addition elements Maddels 2 to 7. A symmetric half of the vent/vent header intersection stiffness matrix was used in the model as shown in Table 3.6.2.2-1. This matrix was derived from the reduced stiffness matrix of Shell Model No. 3 (superelement) described in Section 3.6.1.2 and shown in Table 3.6.1.2-1 using the asymmetric and symmetric contribution of coefficients in the stiffness matrix. Additional pertinent features of the model are given below.

- Adequate distribution of mass nodes has been used in the model to preserve all beam modes. Nodes have been assigned at all locations where dynamic loads have to be applied.

- Appropriate hydrodynamic weights have been added to submerged portion of downcomers as required by the type of loading (see methods of analysis Sections 3.5.3 through 3.5.5).

Type of Loading	Hydrodynamic Weight Added
Pool Swell	1 x Water Weight
CO	1 x Water Weight
Chugging	2 x Water Weight
SRV	2 x Water Weight

- For pool swell and CO loads 2% damping was used which was considered conservative. For SRV, a damping of 4% was used.

- Bellows have been represented in the model as equivalent beam elements. (Elements 23, 24 and 25)

- Symmetric and asymmetric boundary conditions were used for modal extractions. It was considered reasonable to use only symmetric boundary conditions for evaluation of dynamic response. Symmetric boundary conditions were applied at nodes 100, 117-120, 124, 152, 153 and 300. Vent node 121 was fully restrained. Column support nodes anchored to the torus shell were translationally restrained.

3.6.2.3 Deflector Beam Model

A deflector beam model was created (Figure 3.6.2.3-1) representing a half length of the deflector. Node 300 is the center line of the non-vent bay. When analyzing symmetric loads such as pool swell loads or dead weight, symmetric boundary conditions were assigned at Node 300. While evaluating non-symmetric loads such as seismic loads in the axial direction, anti-symmetric boundary conditions were assumed. Node 313 represents the cantilever end of the deflector. Free boundary conditions were assigned at this node. The defector is supported by the header at Node 310. Spring constants at the support were obtained from the unit load analysis of deflector support shell model. These constants are given in Table 3.6.2.3-1.

The beam model consists of 13 segments. The segments between Nodes 307 and 309 represent the miter bends. To account for the flexibility of the miter, stiffness at these segments were divided by the calculated flexibility factor. Node `04 represents a splice in which the loads are required for the evaluation of flange joints. The rest of the nodes were chosen to provide equal spaces.

3.7 VENT/VENT HEADER INTERSECTION - RESULTS OF ANALYSIS AND QUALIFICATION

The models used were:

- 22½ Degree Beam Model for Dynamic Analysis
- Half Shell Model No. 3 for Static Analysis

Applicable Loads:

- o Pool Swell Time History Loads
- o Equivalent Static Pressure Loads

3.7.1 Analysis and Results

The analysis followed the methodology described in Section 3.5.2 and is summarized below.

- o Pool Swell Time History Analysis using 22½° Beam Model. (Reference 3-13)
- o Obtain Column Reactions from Above Analysis. (see Table 3.7.1-1)
- o Compute Equivalent Static Pool Swell Loads which when Applied to Half Shell Model No. 3 will Yield Same Reaction in Columns. (see Table 3.7.1-2)
- o Perform Static Analysis
- o Obtain Column Reactions, Column Displacements and Maximum Principal Stresses in Support Ring (See Figures 3.7.1-1 to 3.7.1-6)

Obtain Stress Intensities by Post Processing

- o Summary of Stresses, See Table 3.7.1-3 for Qualifying Elements (See Figures 3.7.1-7 to 3.7.1-34)

3.7.2 Qualification of Main Vent/Vent Header Intersection For Pool Swell Loads

Qualification criteria are defined in Tables 3.4.1-1 and 3.4.1-2 and summarized below.

- o Qualification Criteria: Service Stress Intensity Limit A (Ref. Table 3.7.2-1)
- o At Discontinuities

$P_L < 1.5\ S_{mc}$ (= 28.95 ksi)

$P_L + P_b + Q < 3.0\ S_{ml}$ (= 69.3 ksi)

- At Continuities

$P_m < 1.0\ S_{mc}$ (= 19.3 ksi)

$P_L + P_b < 1.5\ S_{mc}$ (= 28.95 ksi)

3.7.3 Qualification of Bellows

The bellows have been qualified based on their rated capacities in terms of axial and lateral growth. Comnparison with the actual growth at the vent node obtained from the 22½° beam model for pool swell and thrust loads is shown in Table 3.7.3-1.

3.7.4 Qualification of Columns

The methodology for qualification of columns is summarized below:

- Obtain column reactions from analysis of thrust loads (see Table 3.7.4-1)
- Column reaction obtained from analysis of pool swell loads (see Table 3.7.4-1)
- Compare with column capacity (see Table 3.7.4-1)

3.7.5 Qualification of Support Ring

The support ring has been qualified

- Compare stresses from pool swell analysis to allowables (Table 3.7.5-1)

3.7.6 SRVDL Penetration of Vent/Vent Header Intersection -Results of Analysis and Qualification

The SRVDL penetration of the vent/vent header intersection, with its associated stiffening members, was subjected to a series of static analyses. The results of the analyses were used to evaluate the penetration and penetration stiffening in compliance with the ASME code. From the analyses, loading cases which were a result of LOCA induced loads on the SRVDL were found to cause the highest stresses in the components and connection details of the penentration region. The

evaluation of the stress and force values in each component of the penetration detail was required to insure its proper functioning.

The maximum stress intensity calculated for any element in the model for any load case was 23.6 ksi. This stress occured in the SRV support cylinder and is a local secondary bending stress for which the allowable is 69.3 ksi. The maximum secondary bending stress intensity calculated for the header for all load cases was 15.8 ksi. This value occured at the penetration line on the header itself. Its allowable stress is also 69.3 ksi. Based on these two comparisons, the stresses at the penetration are well below the allowable value. This low value of stress is a result of the header stiffening and SRV clamp details. These details were chosen so as to together channel the loads on the downstream SRVDL away from the penetration without inducing high stresses anywhere else at the penetration. The size of the particular clamp and stiffening plate details used, effectively transfer the load with no stress concentrations.

All welds along the header/stiffening plate/ring interface and clamp supports are sufficient to transfer the required forces. The bolts used in the clamp support angle/stiffening plate connection are sufficient to permit the force transfer as a friction type connection. Bolts used in the SRV clamp provide the necessary shear and tensile resistance to insure the effectiveness of the clamp in transferring the load from the SRVDL to the stiffening plates. The SRV clamp and angle supports were also found to be sufficient to transfer the applied loads without any overstress. Because of the relatively low stress levels, fatigue usage factors are well below 1.0 and therefore, fatigue does not present a problem in the SRVDL penetration region.

3.8 VENT HEADER/DOWNCOMER INTERSECTION-RESULTS OF ANALYSIS AND QUALIFICATION

The models used were:

- o 22½ Degree Beam Model for Dynamic Analysis
- o Shell Model No. 1 for Static Analysis

The applicable loads used for this analysis are:

- o SRV time history for A3.2S (SBA) actuation (SRV actuation concurrent with a small break LOCA)
- o Condensation Oscillation Harmonic Loads
- o Chugging RSEL's (Resultant Static Equivalent Loads)

3.8.1 SRV Time History Analysis and Results

The analysis followed the methodology described in section 3.5.5 and is summarized below.

- o 22½ Degree Beam Model-HQR Analysis
  - o 2x Water Mass as added Mass on Submerged Portion of Downcomers (See Fig. 3.6.2.2-2)
  - o Obtain Natural Frequencies for both x2 and x3 degrees of freedom using Symmetric Boundary Conditions (See Table 3.8.1-1)
  - o Obtain Natural Frequencies for both x2 and x3 degrees of freedom using Asymmetric Boundary Conditions (See Table 3.8.1-2)
- o SRV Time History
  - o Select the most critical time history (A3.2S (SBA)) for evaluation of response (TEEQFOR03, Reference 3-9)
  - o Determine frequency content of SRV time history using Response Spectra Method (Program SAG058) (See Table 3.8.1-3)
  - o Adjust frequency of SRV time history (within a ±40% Range) to resonate with structural frequencies. Figure 3.8.1-1 shows a typical input time history.

- o 22½ Degree Beam Model - Time History Analysis
  - o Apply SRV time histories for x2 and x3 degrees of freedom to submerged portion of downcomers. (See Figure 3.8.1-2)
  - o Obtain downcomer tip displacement response time history note peak responses in x2 and x3 degrees of freedom (See Figure 3.8.1-3 and Table 3.8.1-4)
- o Shell Model No. 1 - Static Analysis
  - o Apply Unit Loads at tips of both downcomers (Nodes 1277 and 1346)
  - o Obtain response from static analysis for unit loads. Note downcomer tip displacements and elemental stresses (See Table 3.8.1-5)
  - o Factor tip displacements due to SRV load obtained from 22½° Beam Model Response into Unit Load Tip Displacements. Run "Post" to obtain stresses and stress intensities. (See Table 3.8.1-6)

3.8.2 CO Loads Analysis and Results

The analysis followed the methodology described in Section 3.5.4 and is summarized below:

- o 22½ Degree Beam Model - HQR Analysis
  - o 1x water mass as added mass on submerged portion of downcomers
  - o Obtain natural frequencies using symmetric boundary conditions. (See Table 3.8.2-1)
- o Condensation Oscillation Harmonic Loads
  - o Integrate unbalanced force at downcomer miter due to ΔP and internal pressure (See Figure 3.8.2-1)
  - o Select lowest downcomer frequency in X2 direction and compute amplitude and frequencies of three harmonics of ΔP and internal pressure for IBA and DBA. (See Table 3.8.2-2 to Table 3.8.2-3)

- o 22½ Degree Beam Model - Harmonic Response Analysis
  - o Apply three sinuosidal harmonics for CO internal pressure (IBA) on each downcomer miter node and three sinusoidal harmonics for ΔP (IBA) on one downcomer of each downcomer pair. (See Figures 3.8.2-2 and 3.8.2-3)
  - o Obtain downcomer tip displacement response. (Table 3.8.2-4)
  - o Repeat Dynre-2 analysis for DBA condition and obtain downcomer tip displacement response. (Table 3.8.2-5)
- o Shell Model No. 1 - Static Analysis
  - o Use tip displacements and stresses due to unit loads (See Table 3.8.1-5)
  - o Factor tip displacements due to CO loads from 22½° beam model response into unit load tip displacements. Run "Post" to obtain stress intensities. (Table 3.8.2-6)

3.8.3 Chugging Loads Analysis and Results

The analysis followed the step by step procedure described in Section 3.3.2.5.1 and is summarized below:

- o 22½ Beam Model - HQR Analysis
  - o 2X Water Mass as added mass on submerged portion of downcomers
  - o Obtain natural frequencies using symmetric boundary conditions (See Table 3.6.2.2-2)
- o Compute maximum resultant static equivalent loads due to chugging to be applied statically to tips of downcomers (Step 4 of Section 3.3.2.5.1)

  Pmax (E-W) = 11.987 kips

  Pmax (N-S) = 4.58 kips

- o Shell Model No. 1 - Static Analysis
- o Obtain Element Stresses due to Unit Loads applied at downcomer tips (See Table 3.8.1-13)
  - o Factor Pmax (E-W) and Pmax (N-S) into unit downcomer stress to obtain maximum element stresses due to chugging loads in X_2 and X_3 directions. (Table 3.8.3-1)
  - o Run "Post" to compute maximum stress intensities for each element.

3.8.4 Combining Responses Due to SRV, CO and Chugging Loads and Qualification

Various load combinations have been described earlier in Section 3.4. These load combination are based on event timings. The SRV and chugging loads are random in nature and the peak responses have phase lags. Based on Reference 3-6, Section 6.3b, SRSS method of combining peak responses has been used. The load combination which yield the most critical stresses/stress intensities are given below:

3.8.4.1 CO + SRV

The responses due to CO (IBA) and CO (DBA) were combined with responses due to SRV using the absolute sum method. Resulting stresses in the maximum stressed elements are shown in Table 3.8.4.1-1.

3.8.4.2 Chugging + SRV

It was determined that IBA Chugging and SRV A3.2S gave the worst load combination. The stresses due to chugging IBA and SRV loads were combined by SRSS method and the elements with the maximum stress intensities were identified. The load factors for possible combinations are shown in Tables 3.8.4.2-1 through 3.8.4.2-3. Maximum stress intensities on selected elements due to eight SRSS load combination are shown in Tables 3.8.4.2-4 through 3.8.4.2-11. Contour

plots of maximum shear stress is shown in Figures 3.8.4-1 through 3.8.4.2-4 to identify stress intensity distribution over the entire range of elements in the vicinity of the vent header/downcomer intersection.

3.8.4.3 Qualification of Downcomer/Vent header Intersection For SRV, CO And Chugging Loads

From Table 3.4-1, the following structural acceptance criteria is applicable.

LOAD COMBINATION	QUALIFYING SERVICE LEVEL	CODE ALLOWABLES (KSI) P_m	P_L	P_L+P_b	P_L+P_b+Q
CO(IBA) + SRV	A	1.0 S_{mc}	1.5x1.3 S_{mc}	1.5x1.3 S_{mc}	3.0 S_{ml}
CHUGGING(IBA) + SRV	A	(19.3)	(37.63)	(37.63)	(69.3)
CO(DBA)	A	1.0 S_{mc}	1.5x1.3 S_{mc}	1.5x1.3 S_{mc}	3.0 S_{ml}
CHUGGING(DBA)	A	(19.3)	(37.63)	(37.63)	(69.3)
CO(DBA)+SRV	C	1.2 S_{mc}	1.5 S_y	1.5 S_y	N/A
CHUGGING(DBA)+SRV	C	(23.16)	(51.90)	(51.90)	

The above criteria was applied to CO (DBA) + SRV and Chugging (IBA) + SRV Load Cases. The results are presented in Table 3.8.4.3-1.

3.8.5 Fatigue Evaluation

Procedure for fatigue evaluation for SRV, CO and chugging loads has been described in Section 3.5.7 under methods of analysis. Step by step evaluation for each of the loads for the most critical locations at the downcomer/vent header intersection is given below.

3.8.5.1 Fatigue Evaluation for SRV Loads

Step 1. Compute maximum stress intensities. (See Table 3.8.1-14)

Step 2. Compute maximum alternating stress S_a.

$$S_a = 1/2 \times \text{Peak S.I. range} \times \frac{Ec}{E}$$

where SCF = Stress Concentration Factor for weld at intersection.

SCF = 2.0

$E_c = 30.0 \times 10^6$

$E = 27.7 \times 10^6$

(Si-Sj) max = max stress intensity

QUAD #	$\lvert(S_i-S_j)\rvert$ MAX	S_a
2503	18.92	20.43 KSI
36	38.89	42.12 KSI

Step 3. Determine number of stress cycles for SRV, for 40 year plant life

n = 2000 @ maximum Sa

Step 4. Compute maximum allowable stress cycles N from S-N curve (ASME Code Section III Division 1 Appendices)

$N = 7 \times 10^4$

Step 5. Compute usage factor.

Usage Factor = n/N

QUAD	n	N	$\frac{n}{N}$
2503	2000	7×10^4	.0286
36	2000	7×10^3	.286

Fatigue usage factors for SRV loads are shown in Table 3.8.5-1.

3.8.5.2 Fatigue Evaluation For CO Loads

Step 1. Compute maximum stress intensities. (See Table 3.8.2-6)

Step 2. Compute maximum alternating stress Sa (See Step 2 of SRV for procedure)

For CO DBA,

Sa = 37.32 KSI (For QUAD 2503)

Compute Sa for all critical elements for both DBA and IBA.

Step 3. Compute number of stress cycles.

Duration of event for CO DBA = 30 sec.

For Δ P

HARMONIC	FREQ.	NO. OF CYCLES
1st	6.642	199
2nd	13.284	399
3rd	19.926	598

Step 4. Use Sa = 37.32 KSI for all harmonics. (This is a conservative approximation)

Step 5. Compute maximum allowable stress cycles for each harmonic from S-N curves.

Step 6. Compute usage factor n/N for all three harmonics and add.

HARMONIC	Sa	N	N	n/N
1st	37.32 ksi	199	11000	.0181
2nd	37.32 ksi	399	11000	.0363
3rd	37.32 ksi	598	11000	.0544

Σ n/N = 0.108

The usage factor for the most critical elements for the CO DBA are shown in Table 3.8.5-2. For CO IBA the stress intensity

is low and does not give any significant usage factor.

3.8.5.3 Fatigue Evaluation for Chugging Loads

Step 1. Compute chugging RSEL's for fatigue for E-W and N-S direction using the procedure described in section 3.3.2.5-1 and in section 3.5.7.2.-3

P_{max} (E-W) = 15.490 KIPS
P_{max} (N-S) = 5.918 KIPS

Step 2. Compute weighting factor for P_{max} (N-S) using the formula

weighting factor = $P_{max}(N-S)/P_{max}(E-W)$

Step 3. Apply $P_{max} = P_{max}$ (E-W) in each of the eight sectors and compute components in N-S and E-W direction. (See Figure 3.8.5.3-1)

Step 4. Scale N-S components to E-W components using the weighting factor.

Step 5. Compute stresses by factoring each sector loads into unit load stresses obtained from static analysis of Shell Model No. 1.

Step 6. Run Post to compute stress intensities for each selected element for each sector loads.

Step 7. Use output from Post run to compute usage factor using program FATIGUE (Reference 3-14).

The usage factor for critical elements due to chugging loads is shown in Table 3.8.5-3.

3.8.5.4 Qualification of Downcomer/Vent header Intersection For Fatigue

Commulative usage for both IBA and DBA cases is evaluated and results are tabulated in Table 3.8.5.4-1.

It can be seen that the cumulative usage factor is less than 1.0.

3.9 DEFLECTOR AND SUPPORTS - RESULTS OF ANALYSIS AND QUALIFICATION

3.9.1 Structural Analysis

Structural analyses were performed in accordance with the Plant Unique Analysis Application Guide (PUAAG) (Reference 3-6). Finite element models for the vent system were analyzed using the STARDYNE program (Reference 3-17). The computer analysis models and results are documented in the calculation books listed in Reference 3-19.

The beam model was used to calculate bending moments, shear loads and axial forces in each element and at the support. Beam element loads were directly used for the evaluation of the deflector while loads at the support were input in the shell model for subsequent analyses. The shell model was used to calculate membrane stresses, bending stresses and stress intensities for the evaluation of the support.

3.3.9.1 Beam Model Dynamic Analysis

Dynamic analysis was performed to determine the loads in the deflector and supports due to pool swell impact and drag loads. In applying the load to the deflector, NRC Criteria (Reference 3-15) requires the inertia due to the added mass of water below the deflector be accounted for. The added mass per unit length of deflector was estimated by:

$$M_H = \frac{Igc}{V}$$

where

M_H = hydrodynamic mass per unit length (lbm/ft),
I = total impulse per unit length associated with the transient (lb ft-sec/ft),
V = impact velocity (ft/sec),
g_c = gravitational constant (ft-lbm/lbf-sec^2)

Two percent of critical damping was used. The first 37 modes were included in the analyses.
The load at each elements and reactions at the support were output as functions of time. The maximum magnitudes were used to combine with other loads for the structural evaluation.

3.9.1.2 Beam Model Static Analysis

Static analyses were performed for dead weight, LOCA thermal and seismic loads. LOCA temperatures intermediate break accident and large break accident were considered. Seismic loads were taken from vent system 180° beam model analysis. Earthquakes in three directions were considered. The largest components in each direction were then combined by the square root sum of the squares method and were used in the evaluation.

3.9.1.3 Shell Model Static Analysis

To facilitate the evaluation of deflector supports due to combined loads, the following static analyses were performed for unit load cases:

1. Horizontal force of 100 kips in the deflector
2. Vertical force of 100 kips in the deflector
3. Axial force of 100 kips in the deflector
4. Moment of 100 in-kips about vertical axis in the deflector
5. Torque of 100 in-kips about axial axis in the deflector
6. Axial force of 100 kips at bottom of the header ring plate

Unit load cases 1 thru 5 were used to obtain all combined loads resulting from beam model analysis. Case 3 and Case 6 were combined to simulate relative movements of deflector and header due to a LOCA thermal and earthquake in the axial direction or pool swell impact and drag loads.

3.9.2 Structural Evaluation

Structural evaluations were conducted according to load combinations and service limits defined in the PUAAG (Reference 3-6). The load combination number and service level referred in this section conform with Reference 3-6. For each structural component, the allowable stresses used for the evaluation were based on the ASME code (Reference 3-18).

3.9.2.1 Deflector and Supports

According to PUAAG (Reference 3-6), deflector and associated hardware were considered to be internal structures. The design rules of Subsection NF, ASME Code (Reference 3-18) were to be met. Using results from beam model analysis, the evaluation of deflector is shown in Table 3.9.2.1-1. At deflector miters and the deflector flange connections, stresses due to stress intensity factors were taken into account. Table 3.9.2.1-1 shows the deflector and its connections are acceptable.

The deflector support was evaluated using the results of shell model analysis. For the support plate, cheek plates and ring plate, the governing code is Subsection NF. Membrane stress (σ_1) and bending stress (σ_2) in the principal axes were to be checked. As shown in Table 3.9.2.1-2, the support hardware and connections are within acceptable limits. The deflector loads also induced stresses in the header where the deflector is attached. The allowables for the header were governed by Subsection NE, ASME Code (Reference 3-18). Membrane stress intensity (P_m), local membrane stress intensity (P_L), bending stress intensity (P_b) and secondary stress (Q) due to structure discontinuity were to be evaluated. As shown in Table 3.9.2.1-3, the stress intensities induced by deflector loads were far below the allowables. Adding the maximum stress intensity of 6.34 ksi resulting from the overall ring header analysis, the combined header stress intensities at the deflector support are acceptable.

3.10 SUMMARY AND CONCLUSIONS

It was intended to qualify the vent system structures for LOCA and SRV hydrodynamic loads and all other applicable loads. The loads, as defined in LDR (Reference 3-1) were applied in accordance with the procedures described in the Application Guide 10 (Reference 3-8) and Plant Unique Analysis Application Guide (Reference 3-6). The stress analysis was done using appropriate mathematical models. Stresses due to various loading conditions were combined based on the event times of occurrence and the critical locations in the vent system structures were identified. The Structural Acceptance Criteria based on ASME Code and Mark I LTP were applied for qualification of each critical component. The cummulative fatigue damage was assessed based on forty year plant life. It was identified that the following modifications to the existing vent system structures are necessary in order to ensure the intended margins of safety:

1) All downcomers be reduced in length by 12" and tie location accordingly adjusted

2) All downcomer/vent header intersections be stiffened by providing ½" plate stiffeners as shown in Figure 3.6.11-2

3) Four additional columns be provided at each vent/vent header intersection. These columns are to be attached to the header by means of a 1" x 6" ring welded to the header. Figures 3.5-1 and 3.6.1.3-3 show the position of the ring and the orientation of the columns.

The above modifications have been included in all the mathematical models used for this analysis. The modified vent system satisfies the required structural acceptance criteria.

REFERENCES - SECTION 3

3-1 "Mark I Containment Program, Load Definition Report," General Electric NEDO - 21888, Class I, November 1981, Revision 2.

3-2 "Final Safety Analysis Report, Brunswick Steam Electric Plant, Units 1 & 2" Carolina Power & Light Company.

3-3 STARDYNE for NOS Operating System, Control Data Corporation, 1978.

3-4 Plant Unique Analysis Report, Load Definitions and Structual Evaluation of Miscellaneous Internal Structures for Brunswick Units 1 & 2.

3-5 Calculation Set No. 9527-E-SC-SL-4-F.

3-6 "Mark I Containment Program, Structural Acceptance Criteria, Plant Unique Analysis, Application Guide." General Electric NEDO-24583-1, 79ND125, Class I, October 1979.

3-7 "Mark I Containment Program, Plant Unique Load Definition, Brunswick Steam Electric Plant, Units 1 & 2" NEDO-24582 Class I, March 1979, General Electric.

3-8 "Mark I Containment Program, Application Guide 10," General Electric NEDE-24555-P, September 1980.

3-9 "Mark I Containment Program, Application Guide 5, T-Quencher SRV Bubble Induced Loads on Submerged Structures," General Electric NEDE-24555-P, January 1981.

3-10 STARDYNE User Information Manual, Control Data Corporation.

3-11 MRI/STARDYNE Theoretical Manual, Control Data Corporation.

3-12 WRC Bulletin 256.

3-13 Calculation Set No. 9527-E-SC-VS-1-F.

3-14 FATIGUE, UE&C Program, Rev. 0.0, March 1982.

3-15 Safety Evaluation Report, Mark I Containment Long-Term Program, Resolution of Generic Technical Activity A-7, Office of Nuclear Reactor Regulation, U.S. Nuclear Regulator Commission, Report No. NUREG-0661, July, 1980.

3-16 Mark I Containment Program, Vent Header Deflector Load Definition, Task Number 7.3.3, General Electric Co., Report No. NEDO-24612, April, 1979.

REFERENCES - SECTION 3

3-17 STARDYNE for Scope 3.4 Operating System, Control Data Corporation, 1978.

3-18 ASME Boiler and Pressure Vessel Code Section III, Nuclear Power Plant Components, including Addenda through Summer 1977.

3-19 Calculation Set No. 9527-E-SC-DV-1-F.

TABLE 3.3.1.4-1

INPUT RESPONSE SPECTRA CURVES

DESIGN RESPONSE SPECTRA NORMALIZED AS FOLLOWS WAS USED

DBE	0.16g	(Horizontal)
DBE	2/3 Horizontal = 0.107g	(Vertical)

COMPOSITE VISCOUS MODAL DAMPING WAS USED WITH THE FOLLOWING MATERIAL DAMPING VALUES

MATERIAL	% DAMPING FOR DBE
Steel	5
Concrete	4
Vent System	2

TABLE 3.3.2-1

STRUCTURAL LOADING DUE TO LOCA
LOADS ON VENT SYSTEM STRUCTURES

LOCA LOADS	VENT SYSTEM STRUCTURES		
	MAIN VENTS	VENT HEADER	DOWN-COMERS
1. Containment Pressure and Temperature	X	X	X
2. Vent System Thrust Loads	X	X	X
3. Pool Swell	X	X	X
3A. Impact and Drag	X	X	X
3B. Froth Impingement	X	X	X
4. Condensation Oscillation	X	X	X
5. Chugging	X	X	X

TABLE 3.3.2-2

STRUCUTRAL LOADING DUE TO
NON-LOCA SRV LOADS

NON-LOCA LOADS	VENT SYSTEM STRUCTURES		
	MAIN VENT	VENT HEADER	DOWN-COMERS
1. T-Quencher Loads			
1A. Jet Loads on Submerged Structures			X
1B. Air Bubble Drag			X

TABLE 3.3.2.4-1

CO - ONSET & DURATION

Break Size	Onset Time After Break	Duration After Onset
DBA	5 Sec.	30 Sec.
IBA	5 Sec.	900 Sec. (CO + Chugging)
SBA	Not Applicable	Not Applicable

TABLE 3.3.2.4-2

MAIN VENT & VENT HEADER INTERNAL PRESSURE

Characteristics	DBA	IBA
Amplitude	± 2.5 psi	± 2.5 psi
Frequency Range	@ frequency of Max. Response in 4-8 Hz range	@ frequency of Max. Response in 6-10 Hz range
Forcing Function	Sinusoidal	Sinusoidal
Spatial Distribution	Uniform	Uniform

Downcomer Internal Pressure (DBA)

	Internal Pressure	Frequency Range
Dominant Frequency	± 3.6 psi	4-8 Hz
Second Harmonic	± 1.3 psi	8-16 Hz
Third Harmonic	± 0.6 psi	12-24 Hz

Downcomer Differential Pressure Δ P(DBA)

	Differential Pressure	Frequency Range
Dominant Frequency	± 2.8 psi	4-8 Hz
Second Harmonic	± 2.6 psi	8-16 Hz
Third Harmonic	± 1.3 psi	12-24 Hz

Downercomer Internal Pressure (IBA)

	Internal Pressure	Frequency Range
Dominant Frequency	± 1.1 psi	6-10 Hz
Second Harmonic	± 0.8 psi	12-20 Hz
Third Harmonic	± 0.2 psi	18-30 Hz

Downcomer Differential Pressure Δ P (IBA)

	Differential Pressure	Frequency Range
Dominant Frequency	± 0.2 psi	6-10 Hz
Second Harmonic	± 0.2 psi	12-20 Hz
Third Harmonic	± 0.2 psi	18-30 Hz

TABLE 3.3.2.4-3

DOWNCOMER CO

DUE TO DBA

LOAD DEFINITION

o DYNAMIC LOAD

MODE	AMPLITUDE	FREQUENCY
Dominant CO Freq.	Internal P ±3.6 psi plus delta P ±2.85 psi	A single fundamental freq. in the range of 4-8 Hz simultaneously with its second and third harmonics
Second Harmonic	Internal P ±1.3 psi plus delta P ±2.6 psi	2 x fundamental freq. simultaneously with fundamental and third harmonic
Third Harmonic	Internal P ±0.6 psi plus delta P ±1.2 psi	3 X Fundamental freq. simultaneously with fundamental and second harmonic

o APPLICATION

Eight load cases to be analyzed
Sum response from internal and differential pressure
Use the worst of eight cases.

TABLE 3.3.2.4-4

DOWNCOMER CO

DUE TO IBA

LOAD DEFINITION

o DYNAMIC LOAD

MODE	AMPLITUDE	FREQUENCY
Dominant CO Freq.	Internal P ±1.1 psi plus delta P ±0.2 psi	A single fundamental freq. in the range of 6-10 Hz simultaneously with its second and third harmonics
Second Harmonic	Internal P ±0.8 psi plus delta P ±0.2 psi	2 x fundamental freq. simultaneously with fundamental and third harmonic
Third Harmonic	Internal P ±0.2 psi plus delta P ±0.2 psi	3 X fundamental freq. simultaneously with fundamental and second harmonic

o APPLICATION

Eight load cases to be analyzed
Sum response from internal and differential pressure
Use the worst of eight cases.

TABLE 3.3.2.4-5

CHUGGING ONSET & DURATION

Break Size	Onset Time After Break	Duration After Onset
DBA	35 seconds	30 seconds
IBA	5 seconds	900 seconds (CO + Chugging)
SBA	300 seconds	900 seconds

TABLE 3.4.1-1

CLASS MC COMPONENTS AND INTERNAL STRUCTURES (Page 1 of 3)

(Reference NEDO - 24583-1 Table 5-1)

EVENT COMBINATIONS		SRV	SRV + EQ		SBA IBA		SBA + EQ IBA + EQ				SBA + SRV IBA + SRV		SBA + SRV + EQ IBA + SRV + EQ				DBA		DBA + EQ				DBA + SRV		DBA + EQ + SRV			
						CO, CH			CO, CH			CO, CH			CO, CH				FS		CO, CH			CO, CH		FS		CO, CH	
TYPE OF EARTHQUAKE			O	S			O	S	O	S			O	S	O	S			O	S	O	S			O	S	O	S
COMBINATION NUMBER		1	2	3	4	5	6	7	8	9	10	11	12	13	14	15	16	17	18	19	20	21	22	23	24	25	26	27
LOADS																												
Normal (2)	N	X	X	X	X	X	X	X	X	X	X	X	X	X	X	X	X	X	X	X	X	X	X	X	X	X	X	X
Earthquake	EQ		X	X			X	X	X	X			X	X	X	X			X	X	X	X			X	X	X	X
SRV Discharge	SRV	X	X	X							X	X	X	X	X	X							X	X	X	X	X	X
LOCA Thermal	T_A				X	X	X	X	X	X	X	X	X	X	X	X							X	X	X	X	X	X
LOCA Reactions	R_A				X	X	X	X	X	X	X	X	X	X	X	X	X	X	X	X	X	X	X	X	X	X	X	X
LOCA Quasi-Static Pressure	P_A				X	X	X	X	X	X	X	X	X	X	X	X	X	X	X	X	X	X	X	X	X	X	X	X
LOCA Pool Swell	P_{FS}																X	X	X	X			X	X	X	X	X	X
LOCA Condensation Oscillation	P_{CO}					X			X	X		X			X	X		X			X	X		X			X	X
LOCA Chugging	P_{CH}					X			X	X		X			X	X		X			X	X		X			X	X
STRUCTURAL ELEMENT	ROW																											
External Class MC																												
Torus, External Vent Pipe, Bellows, Drywall (at Vent), Attachment Welds, Torus Supports, Seismic Restraints	1	A	B	C	A	A	B	C	B	C	A	A	B	C	B	C	A (3, 6)	A	B (3, 6)	C	B	C	C	C	C	C	C	C
Internal Vent Pipe																												
General and Attachment Welds	2	A	B	C	A	A	B	C	B	C	A	A	B	C	B	C	A (3, 5)	A	B (3, 5)	C	B	C	C	C	C	C	C	C
At Penetrations (e.g., Header)	3	A	B	C	A	A	B	C	B	C	A	A	B	C	B	C	A (3)	A	B (3)	C	B	C	C	C	C	C	C	C
Vent Header																												
General and Attachment Welds	4	A	B	C	A	A	B	C	B	C	A	A	B	C	B	C	A (3, 5)	A	B (3, 5)	C	B	C	C	C	C	C	C	C
At Penetrations (e.g., Downcomers)	5	A	B	C	A	A (4)	B	C	B (4)	C	A	A (4)	B	C	B (4)	C	A (3, 4, 5)	A (4)	B (3, 4, 5)	C	B (4)	C	C	C	C	C	C	C
Downcomers																												
General and Attachment Welds	6	A	B	C	A	A	B	C	B	C	A	A	B	C	B	C	A (3, 5)	A	B (3, 5)	C	B	C	C	C	C	C	C	C
Internal Supports	7	A	B	C	A	A	B	C	B	C	A	A	B	C	B	C	A	A	B	C	B	C	C	C	C	C	C	C
Internal Structures																												
General	8	A	B	C	A	A	C	D	C	D	C	C	D	E	D	E	E	E	E	E	E	E	E	E	E	E	E	E
Vent Deflector	9	A	B	C	A	A	C	D	C	D	C	C	D	D	D	D	D	D	D	D	D	D	D	D	D	D	D	D

TABLE 3.4.1-1

CLASS MC COMPONENTS AND INTERNAL STRUCTURES (Page 2 of 3)

(1) Where drywell to wetwell pressure differential is normally utilized as a load mitigator, an additional evaluation shall be performed without SRV loadings but assuming loss of the pressure differential. In the additional evaluation, Level D Service Limits shall apply for all structural elements except Row 8 Internal Structures, which need not be evaluated. If drywell to wetwell pressure differential is not employed as a load mitigator, the listed Service Limits shall be applicable.

(2) Normal loads (N) consist of the combination of dead loads (D), live loads (L), thermal effects during operation (T_o), and pipe reactions during operation (R_o).

(3) Evaluation of primary-plus-secondary stress intensity range (NE-3221.4) and of fatigue (NE-3221.5) are not required.

(4) When considering the limits on local membrane stress intensity (NE-3221.2), and primary-membrane-plus-primary bending stress intensity (NE-3221.3), the S_{mc} value may be replaced by 1.3 S_{mc}.

(NOTE: The modification to the limits does not affect the normal limits on primary-plus-secondary stress intensity range (NE-3221.4 or NE-3228.3) nor the normal limits on fatigue evaluation (NE-3221.5(e) or Appendix II-1500). The modification is that the limits on local membrane stress intensity (NE-3221.2) and on primary-membrane-plus-primary bending stress intensity (NE-3221.3) have been modified by using 1.3 S_{mc} in place of the normal S_{mc}.

This modification is a conservative approximation to results from limit analysis testing as reported in Reference 3 and is consistent with the requirements of NE-3228.2.)

TABLE 3.4.1-1

CLASS MC COMPONENTS AND INTERNAL STRUCTURES (Page 3 of 3)

(5) Service Level Limits specified apply to the overall structural response of the vent system. An additional evaluation shall be performed to demonstrate that shell stresses due to the local pool swell impingement pressures do not exceed Service Level C Limits.

(NOTE: The ratio of the dynamic collapse load to the static collapse load was established as permitted by Code Case N-197, and is reported in Reference 4.)

(6) For the torus shell, the S_{mc} value may be replaced by 1.0 S_{mc} times the dynamic load factor derived from the torus structural model. As an alternative, the 1.0 multiplier may be replaced by the plant unique ratio of the torus dynamic failure pressure to the static failure pressure.

(NOTE: The ratio of the dynamic collapse load to the static collapse was established as permitted by Code Case N-197 and is reported in Reference 5.)

TABLE 3.4.2-1

SUMMARY OF STRESS INTENSITY LIMITS

(Reference Table NE-3221-1)

	Loading Condition					
Symbol	Design Stress Intensity Limit	Level A Service Stress Intensity Limit	Level B Service Stress Intensity Limit and Level C Service Stress Limit Where the Structure Is Not Integral and Continuous	Level C Service Stress Intensity Limit Where the Structure Is Integral and Continuous and Level D Service Stress Limit Where the Structure Is Not Integral and Continuous and at Partial Penetration Welds (2)	Level D Service Stress Intensity Limit Where the Structure Is Integral and Continuous (Elastic Analysis) (4)	Level D Service Stress Intensity Limit Where the Structure is Integral and Continuous (Inelastic Analysis) (4)
P_m	1.0 S_{mc}	1.0 S_{mc}	1.0 S_{mc}	1.2 S_{mc} or * 1.0 S_r	S_r	S_r
P_L	1.5 S_{mc}	1.5 S_{mc}	1.5 S_{mc}	1.8 S_{mc} or * 1.5 S_r	1.5 S_r	S_r
$P_L + P_b$	1.5 S_{mc}	1.5 S_{mc}	1.5 S_{mc}	1.8 S_{mc} or * 1.5 S_r	1.5 S_r	S_r
$P_L + P_b + Q$	N/A (1)	3.0 S_{m1}	3.0 S_{m1} (3)	N/A (1)	N/A (1)	N/A (1)
$P_L + P_b + Q + F$	N/A (1)	S_a	S_a (3)	N/A (1)	N/A (1)	N/A (1)

NOTES:

(1) N/A - No evaluation required.

(2) Limits identified by (*) indicates a choice of the larger of two limits.

(3) Evaluation not required for Level C Service.

(4) S_r is 85% of the general primary membrane allowable permitted in Appendix F. In the application of the rules of Appendix F, S_{m1}, if applicable, shall be as specified in Tables I-1.0.

TABLE 3.6.1.1-1 DOWNCOMER/VENT HEADER INTERSECTION STIFFNESS MATRIX

NODE A	NODE B	1	2	3	4	5	6
1		567000					
2			3000000				
3				10000000			
4					1000000000		
5						92759425	
6							2365790000
1		-567000					
2			-3000000				
3				-10000000			
4					-1000000000		
5						-92759425	
6							-2365790000
	1						567000
	2						3000000
	3						10000000
	4						1000000000
	5						92759425
	6						2365790000

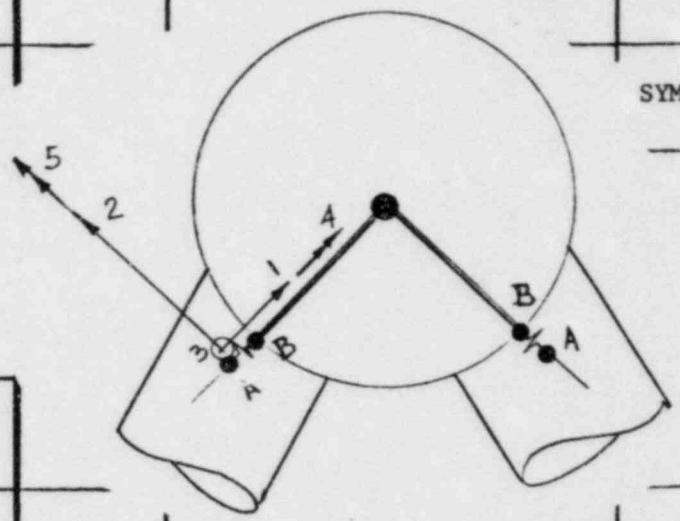

SYMMETRIC

DOCUMENT/ PAGE PULLED

ANO. 8211170424

NO. OF PAGES 3

REASON

☐ PAGE ILLEGIBLE

☐ HARD COPY FILED AT: PDR CF

OTHER _____

☐ BETTER COPY REQUESTED ON ___/___/___

☒ PAGE TOO LARGE TO FILM

☒ HARD COPY FILED AT: PDR (CF)

OTHER _____

☒ FILMED ON APERTURE CARD NO 8211170424-01

thru

8211170424-03

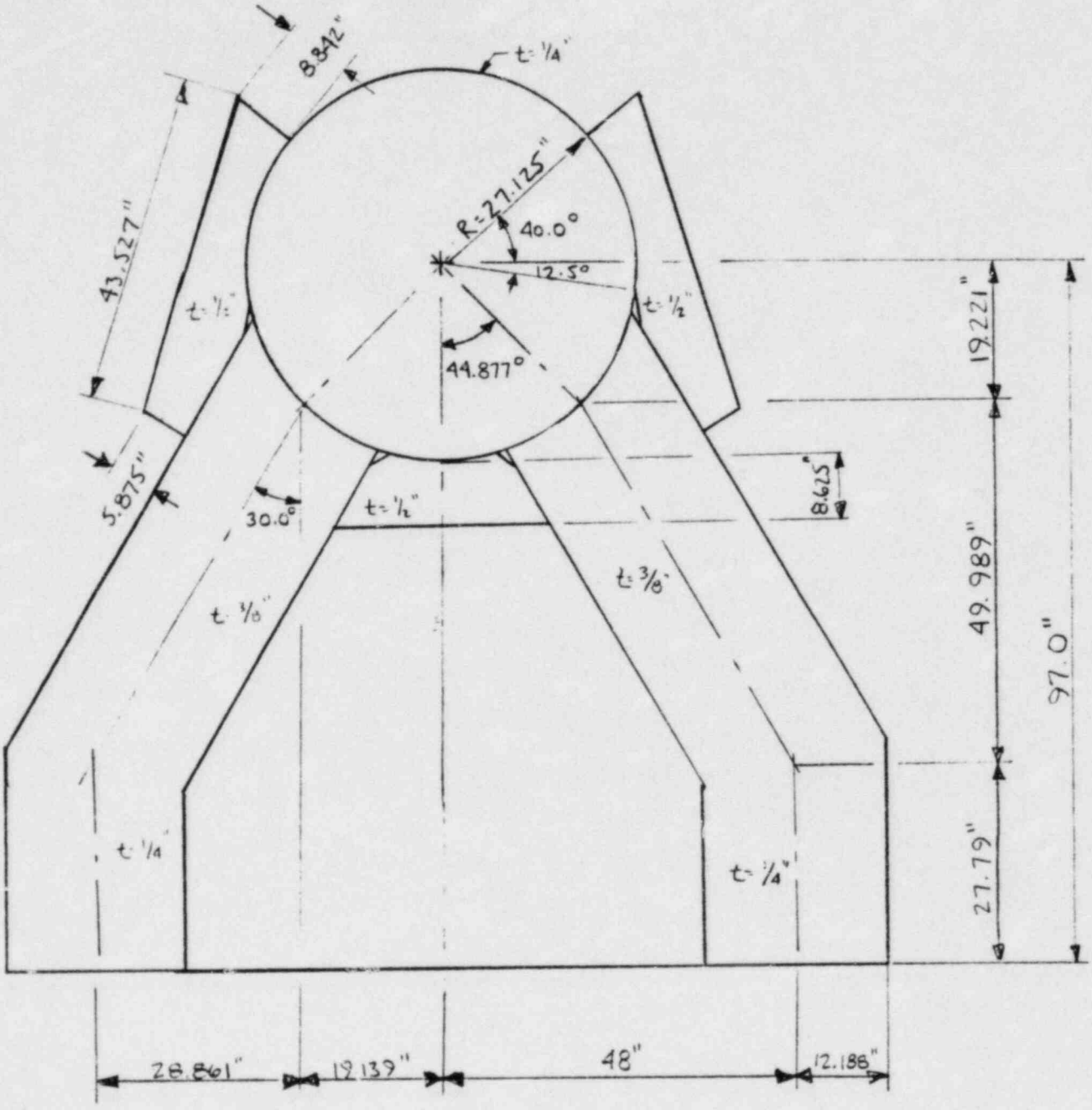

Figure 3.6.1.1-2 Downcomer/Vent Header Section A-A

DOCUMENT/ PAGE PULLED

ANO. 8211170424

NO. OF PAGES 1

REASON

☐ PAGE ILLEGIBLE

☐ HARD COPY FILED AT. PDR CF

OTHER _____

☐ BETTER COPY REQUESTED ON __/__/__

☒ PAGE TOO LARGE TO FILM

☒ HARD COPY FILED AT. PDR (CF)

OTHER _____

☒ FILMED ON APERTURE CARD NO 8211170424-04

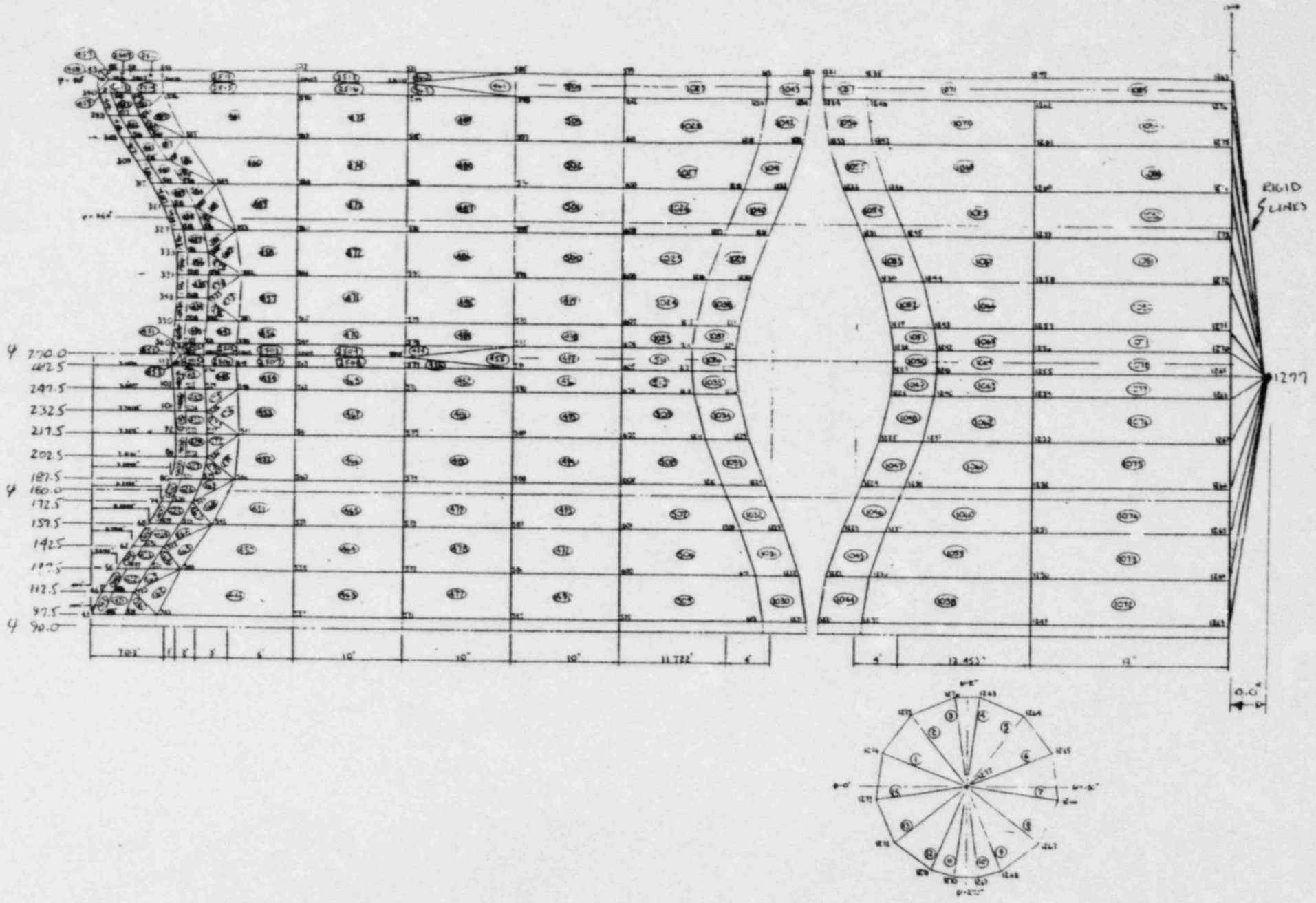

Figure 3.6.1.1-4 Downcomer 1

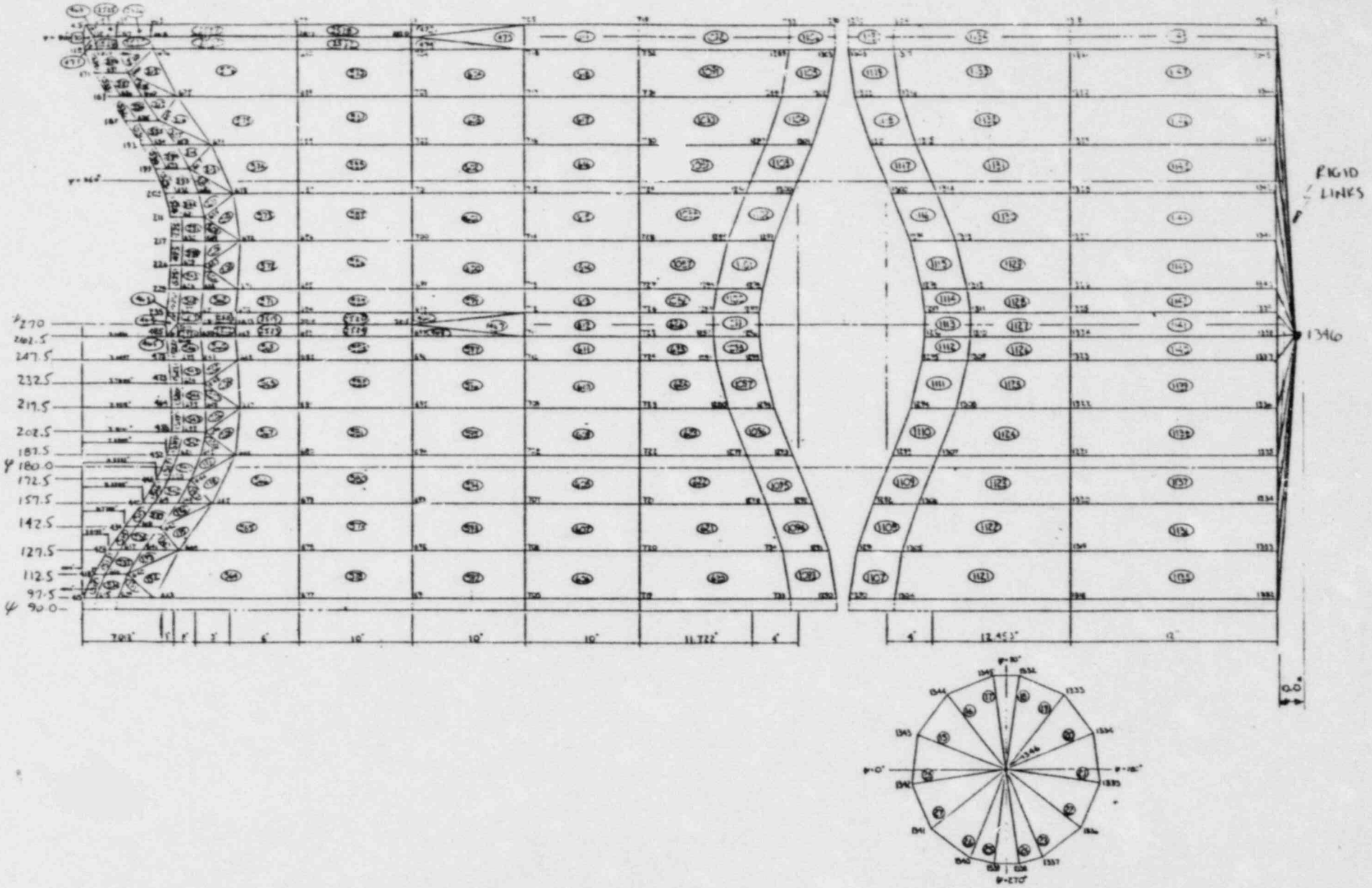

Figure 3.6.1.1-5 Downcomer 2

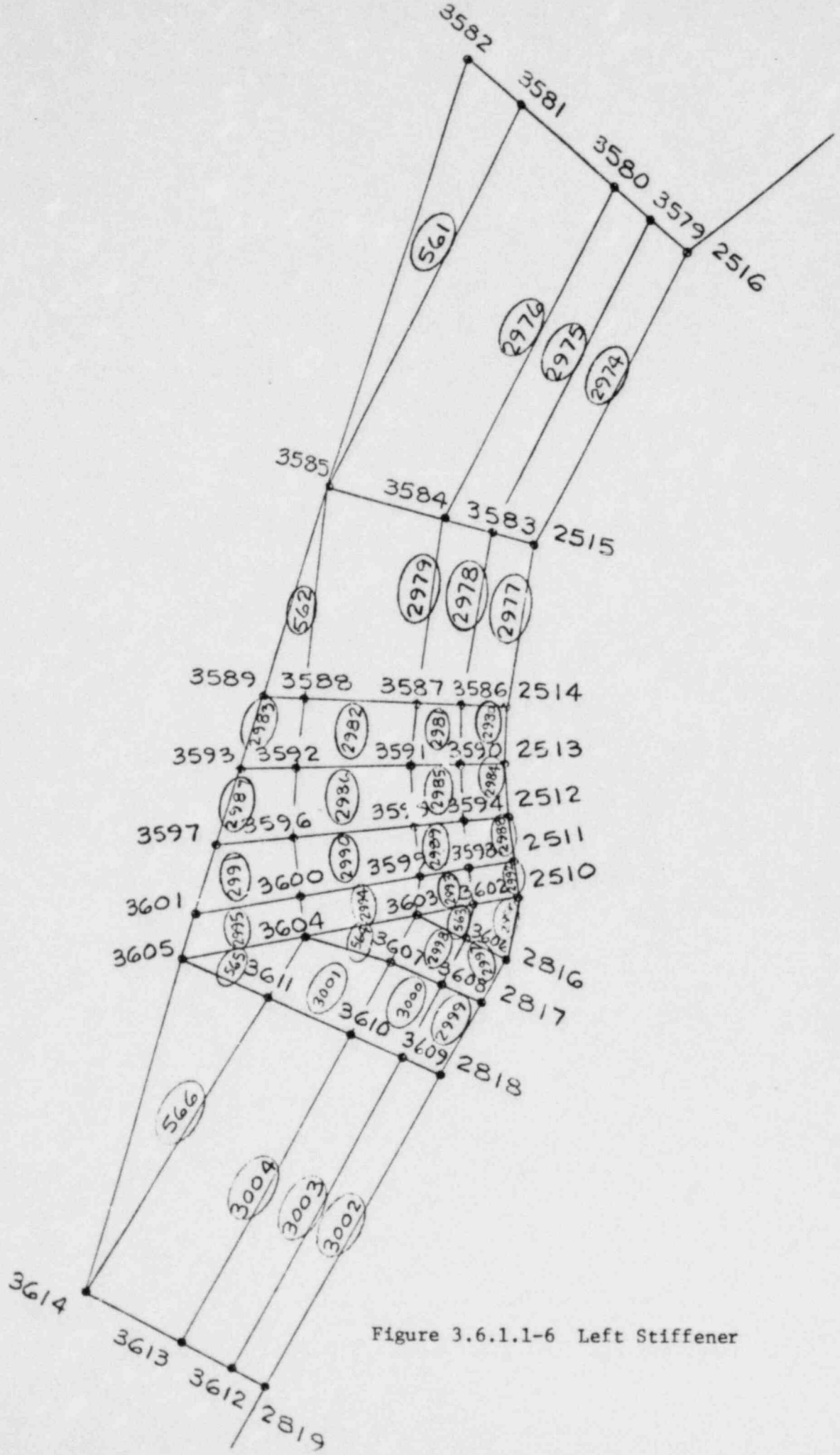

Figure 3.6.1.1-6 Left Stiffener

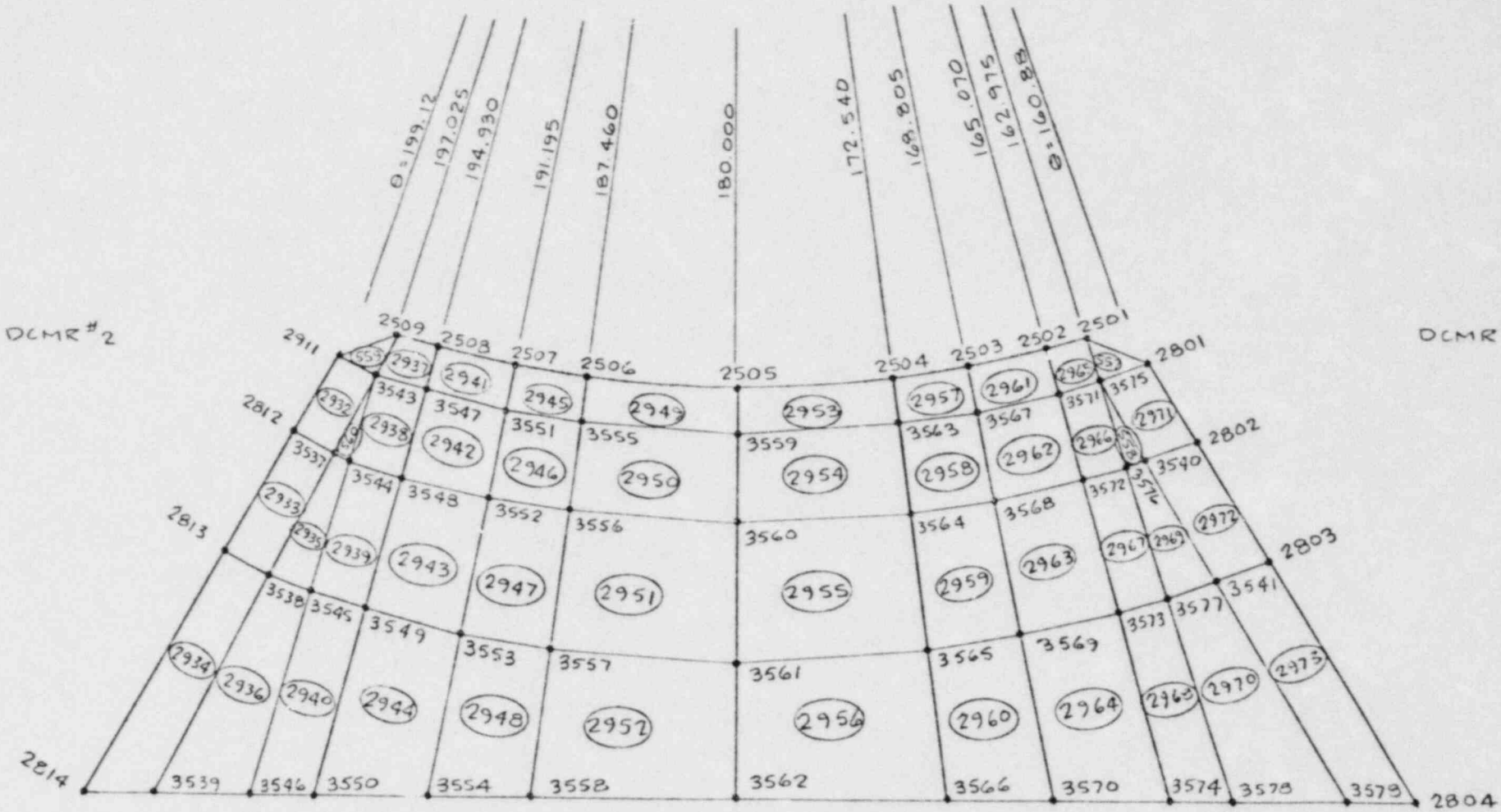

Figure 3.6.1.1-7 Center Stiffener

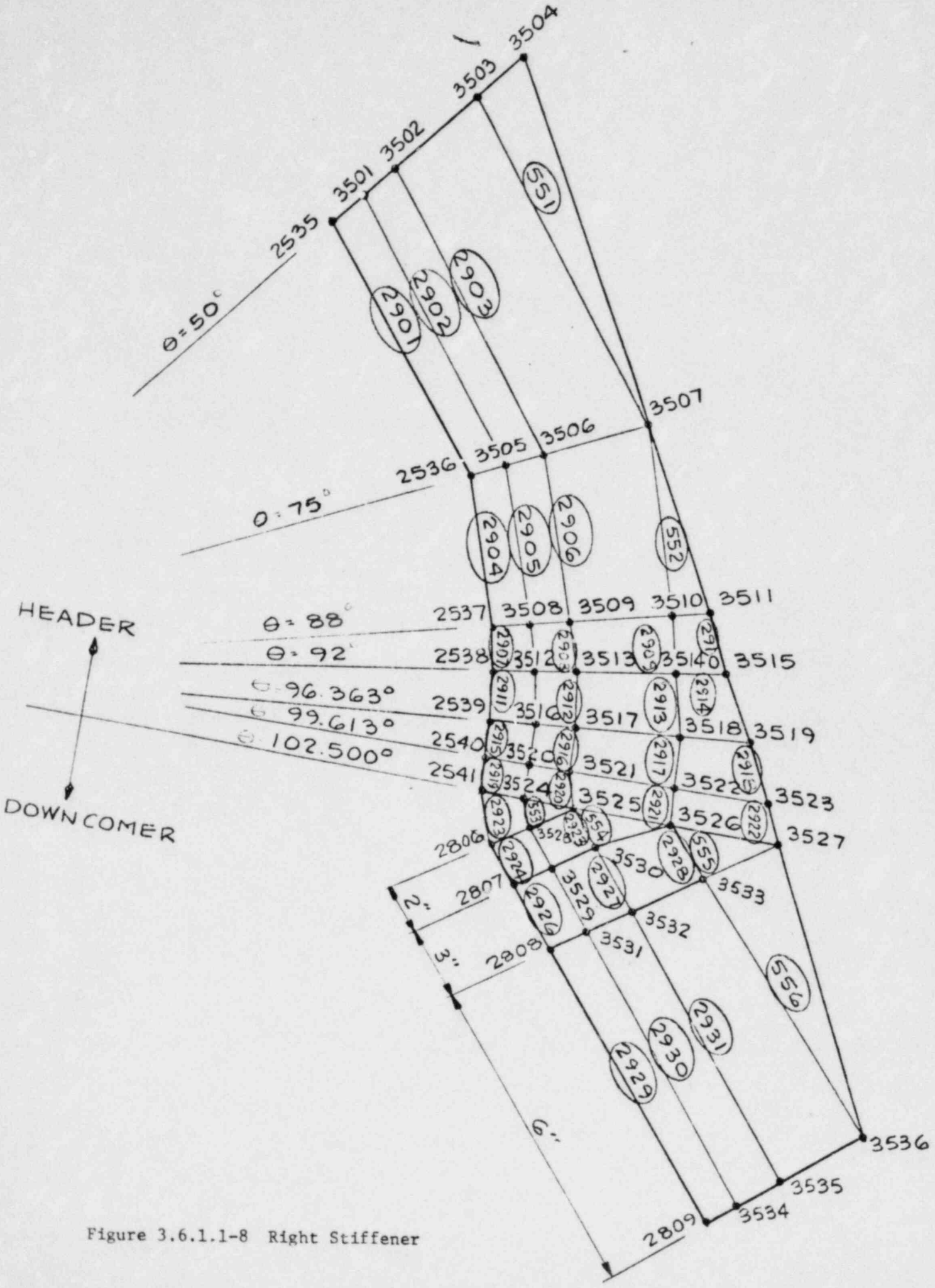

Figure 3.6.1.1-8 Right Stiffener

DOCUMENT/ PAGE PULLED

ANO. 8211170424

NO. OF PAGES 2

REASON

☐ PAGE ILLEGIBLE

☐ HARD COPY FILED AT. PDR CF

OTHER _____

☐ BETTER COPY REQUESTED ON ___/___/___

☒ PAGE TOO LARGE TO FILM

☒ HARD COPY FILED AT. PDR (CF)

OTHER _____

☒ FILMED ON APERTURE CARD NO 8211170424 05

then

8211170424-06

TABLE 3.6.2.3-1

SPRING CONSTANTS FOR DEFLECTOR SUPPORT

	Spring Constants (K/in or in-K/rad)					
Node	K_1	K_2	K_3	P_1	P_2	P_3
310	2,500	17.42	1,692	8,620	Rigid	0

TABLE 3.7.1-1

COLUMN REACTIONS (KIPS)

COLUMN LOCATION (Header Node No.)	BEAM ELEM. NO.	REACTION DUE TO POOL SWELL LOAD	REACTION DUE TO THRUST LOAD
114	29	18.66	14.47
	30	12.44	9.64
	32	25.99	15.95
	35	17.32	19.63
150	89	36.32	0.0
	91	45.55	0.0
	90	24.21	0.0
	92	30.36	0.0

TABLE 3.7.1-2

EQUIVALENT POOL SWELL LOADS APPLIED AS PRESSURE LOAD. TOTAL LOAD = 164500 LBS

ELEMENT TYPE	ELEMENT NUMBER FROM	TO	PRESSURE (PSI)
TRIAB	990	1008	40.83204
TRIAB	1021	1024	40.83204
TRIAB	903	916	40.83204
TRIAB	935	937	40.83204
TRIAB	950		40.83204
TRIAB	508	510	40.83204
QUAD	951	989	40.83204
QUAD	1009	1020	40.83204
QUAD	917	934	40.83204
QUAD	938	949	40.83204
QUAD	864	902	40.83204
QUAD	446	507	40.83204
QUAD	511	516	40.83204
QUAD	415	425	40.83204

TABLE 3.7.1-3

VENT/VENT HEADER INTERSECTION
(HALF SHELL MODEL #3)
SUMMARY OF STRESS INTENSITIES (KSI)
DUE TO POOL SWELL LOADS

AREA	ELEMENT	$P_L + P_b + Q$	P_m OR P_L	$P_L + P_b$
Intersection	QUAD 801	41.14	16.20	N/A
	QUAD 802	25.29	16.14	N/A
Main Vent	QUAD 828	N/A	11.14	22.82
	QUAD 989	N/A	9.37	17.63
At Collar Intersection	QUAD 403	21.60	12.00	N/A
	QUAD 710	19.85	12.57	N/A
At Stiffener Ring	QUAD 405	22.46	17.89	N/A
	QUAD 783	20.29	16.53	N/A
Vent Header	QUAD 406	N/A	17.23	19.52
	QUAD 417	N/A	15.55	18.12
Conical Section	QUAD 190	N/A	3.97	6.09
	QUAD 203	N/A	4.42	4.62
Cone-Vent Header Intersection	QUAD 161	17.38	11.82	N/A
	QUAD 169	17.40	11.85	N/A

TABLE 3.7.2-1

QUALIFICATION OF VENT/VENT HEADER INTERSECTION FOR POOL SWELL LOAD
QUALIFICATION CRITERIA: SERVICE LEVEL A

AREA	ELEMENT NUMBER	STRESS INTENSITY VALUES (KSI) $P_L + P_b + Q$ ALLOWABLE	$P_L + P_b + Q$ ACTUAL	P_m or P_L ALLOWABLE	P_m or P_L ACTUAL	$P_L + P_b$ ALLOWABLE	$P_L + P_b$ ACTUAL	REMARKS
	QUAD 800		28.18		10.97			
Vent Header	QUAD 801		41.14		16.20			
Intersection	QUAD 802	69.3	25.29	28.95	16.14	N/A	N/A	
(Area of Discontinuity)	QUAD 961		31.14		11.01			
	QUAD 962		34.72		12.75			
	QUAD 827				8.05		9.36	Critical Element
Main Vent	*QUAD 828	N/A	N/A	19.3	11.14	28.95	22.82	Bending Stress
	TRIAB 841				7.88		14.88	
	QUAD 989				9.37		17.63	
	QUAD 403		21.60		12.00			
Vent Header At	QUAD 414	69.3	20.05	28.95	12.56	N/A	N/A	
Intersection Collar	QUAD 710		19.85		12.57			
(Area of Discontinuity)	QUAD 711		19.10		12.09			
	QUAD 864		15.18		14.31			
	QUAD 393		21.41		14.54			
Vent Header At	QUAD 405	69.3	22.46	28.95	17.89	N/A	N/A	
Stiffener Ring	QUAD 782		18.31		15.74			
(Area of Discontinuity)	QUAD 783		20.29		16.53			
	QUAD 395				11.19		13.88	Critical Element
Vent Header	QUAD 406	N/A	N/A	19.3	17.23	28.95	19.52	Membrane Stress
	QUAD 407				15.27		16.66	
	QUAD 417				15.55		18.12	
	QUAD 190				3.97		6.09	
Conical Section	QUAD 198	N/A	N/A	19.3	3.63	28.95	5.42	
	QUAD 203				4.42		4.62	
	QUAD 161		17.38		11.82			
Cone-Vent Header	QUAD 162	69.3	7.38	28.95	6.68	N/A	N/A	
Intersection	QUAD 169		17.40		11.85			
(Area of Discontinuity)	QUAD 170		6.71		6.13			

TABLE 3.7.3-1

QUALIFICATION OF BELLOWS FOR POOL SWELL AND THRUST LOADS

NODE 119	AXIAL DISPLACEMENT (IN)		LATERAL DISPLACEMENT (IN)	
	ACTUAL	ALLOWABLE*	ACTUAL	ALLOWABLE*
Pool Swell	0.00418	0.375	0.0259	0.500
Thrust	0.00266	0.375	0.00166	0.500

*From Chicago Bridge & Iron Company Drawing # F.P. 9527-1085.

TABLE 3.7.4-1

QUALIFICATION OF COLUMNS FOR POOL SWELL & THRUST LOADS

COLUMN NO.	POOL SWELL (KSI)	THRUST (KSI)	SUMMATION		COLUMN CAPACITY (KIPS) (REF 14)	REMARKS
29	18.66	14.47	33.13		138.16	Acceptable
				55.21		
30	12.44	9.64	22.08			
32	25.99	15.95	41.94			
				69.89	138.16	Acceptable
35	17.32	10.63	27.95			
TOTAL	74.41	50.69	125.10			
89	36.32	0.0	36.32			
				81.87	138.16	Acceptable
91	45.55	0.0	45.55			
90	24.21	0.0	24.21			
				54.56	138.16	Acceptalbe
92	30.36	0.0	30.36			
TOTAL	136.44	0.0	136.44			

TABLE 3.7.5-1

QUALIFICATION OF SUPPORT RING FOR POOL SWELL LOAD

Qualification of the support ring is summarized below:

- From Table 3.4-1 support ring is to qualify for Level A Stress Intensities
- Allowables for Level A from Table 3.4-2.

$$P_L < 1.5\, S_{mc} = 28.95 \text{ksi}$$

$$P_L + P_b + Q < 3\, S_{ml} = 69.3 \text{ ksi}$$

ELEMENT	P_L		$P_L + P_b + Q$		REMARKS
	ACTUAL	ALLOWABLE	ACTUAL	ALLOWABLE	
TRIAB 2100	16.05	28.95	17.02	69.3	Acceptable
TRIAB 2105	16.08	28.95	16.61	69.3	Acceptable

TABLE 3.8.1-1

22½ Degree Beam Model
with 2x Water Mass

NATURAL FREQUENCY TABLE
(Symmetric Boundary Conditions)

MODE NO.	NATURAL FREQUENCY (HZ.)	ASSOCIATED NODE-D.O.F.	REMARKS
1	10.465	25-3	First Mode In X3 Direction
2	10.659	257-3	
3	10.788	217-3	
4	10.866	258-3	
5	10.945	254-3	
6	11.019	259-3	
7	11.274	255-2	First Mode In X2 Direction
8	14.330	122-3	
9	15.021	259-2	
10	15.612	257-2	
11	16.234	259-2	

TABLE 3.8.1-2

22½ Beam Model With 2x Water Mass

NATURAL FREQUENCY TABLE
(Asymmetric Boundary Conditions)

MODE NO.	NATURAL FREQUENCY (HZ.)	ASSOCIATED NODE-D.O.F.	REMARKS
1	9.628	308-3	Deflector Mode
2	10.433	254-3	
3	10.741	234-3	
4	10.806	257-3	
5	10.886	258-3	
6	10.929	256-3	
7	11.118	259-3	
8	14.110	257-2	
9	14.333	122-3	
10	15.695	225-2	
11	15.819	259-2	
12	24.830	123-3	
13	26.839	313-2	
14	31.136	234-1	
15	31.187	251-1	

TABLE 3.8.1-3

FREQUENCY CONTENT OF SRV TIME HISTORY

SAG058 RESPONSE SPECTRA OF SRV TIME HISTORY

SRV-T/H	SEGMENT #1*		SEGMENT #2*	
	X2	X3	X2	X3
A1.2S	9.3334 HZ.	9.3289 HZ.	9.32 HZ.	9.32 HZ.
A3.2S	9.4606 HZ.	10.341 HZ.	9.18 HZ.	10.42 HZ.

STRUCTURAL FREQUENCY

X3: $f_{(3)}$ = 10.465 HZ.

X2: $f_{(2)}$ = 11.274 HZ.

* See Figure 3.8.1-2 for identification of water segments 1 and 2.

TABLE 3.8.1-4

DOWNCOMER MAXIMUM PEAK TIP
DISPLACEMENT RESPONSES DUE TO SRV TIME HISTORY

INPUT SRV T/H	DOWNCOMER TIP NODE	DISPLACEMENT RESPONSE (IN) X2	X3	REMARKS
SRV A3.2S - X2 Adjusted To f = 11.274 HZ	216	-0.1989	-0.0714299	at t = .225229 SEC
SRV A3.2S - X3 Adjusted To f = 10.465 HZ	233	0.00761975	0.[illegible]294	at t = .413047 SEC

TABLE 3.8.1-5

TIP DISPLACEMENT AND MAXIMUM STRESSES
FOR SHELL MODEL NO. 1 WITH UNIT LOADS
APPLIED TO DOWNCOMERS TIPS (NODES 1277, 1346)

UNIT LOAD	DOWNCOMER TIP DISPLACEMENT			STRESS	MAX ELEMENT NUMBER
	1	2	3	MAX	
FX_1 = 1,000 lbs.	.001307	--	--	.147 KSI	QUAD #36
				.040 KSI	QUAD #2508
FX_2 = 1,000 lbs.	--	.02864	--	1.848 KSI	TRIAB #305,302
				4.230 KSI	QUAD #2503,2519
				.6974 KSI	QUAD #36
FX_3 = 1,000 lbs.	--	--	.07456	9.42 KSI	TRIAB #57,58
				9.597 KSI	QUAD #36,312
				.337 KSI	QUAD #2503

TABLE 3.8.1-6

MAXIMUM STRESS
INTENSITIES DUE TO SRV LOADS

ELEMENT NO	RESONANCE FREQUENCY-D.O.F.	MAXIMUM STRESS INTENSITY (KSI)
QUAD 2503	11.274 - X_2	18.92
QUAD 36	11.274 - X_2	11.95
QUAD 2503	10.465 - X_3	15.42
QUAD 36	10.465 - X_3	38.89

TABLE 3.8.2-1

22½° BEAM MODEL WITH 1X WATER MASS
NATURAL FREQUENCY TABLE
(Symmetric Boundary Conditions)

MODE NO.	NATURAL FREQUENCY (HZ.)	ASSOCIATED NODE-D.O.F.
1	13.284	255-2
2	13.493	26-3
3	13.898	217-3
4	13.972	29-3
5	14.112	256-3
6	14.190	255-3
7	14.331	122-3
8	14.437	259-3
9	15.965	300-2
10	17.878	300-1
11	19.828	257-2
12	20.228	259-2

TABLE 3.8.2-2

DOWNCOMER TIP
DISPLACEMENTS DUE TO CO IBA

DOWNCOMER TIP NODE	DISPLACEMENT D.O.F.	TIP DISPLACEMENT DUE TO INTERNAL PRESSURE HARMONICS			TIP DISPLACEMENTS DUE TO Δ P HARMONICS			MAXIMUM TIP DISPLACEMENT
		1ST HARMONIC	2ND HARMONIC	3RD HARMONIC	1ST HARMONIC	2ND HARMONIC	3RD HARMONIC	
208	X_1	.00071	.00102	.00025	.00027	.00439	.00097	.0076
	X_2	.00014	.00485	.00026	.00155	.02273	.00315	.0327
	X_3	.00019	.00327	.00003	.00007	.00676	.00011	.0104
216	X_1	.00109	.00241	.00021	.00068	.00874	.00106	.0142
	X_2	.00059	.00485	.00021	.00159	.02275	.00316	.0331
	X_3	.00018	.00208	.00004	0.0	.00207	.00006	.0044

TABLE 3.8.2-3

DOWNCOMER TIP
DISPLACEMENTS DUE TO CO DBA

DOWNCOMER TIP NODE	DISPLACEMENT D.O.F.	TIP DISPLACEMENT DUE TO INTERNAL PRESSURE HARMONICS			TIP DISPLACEMENTS DUE TO Δ P HARMONICS			MAXIMUM TIP DISPLACEMENT
		1ST HARMONIC	2ND HARMONIC	3RD HARMONIC	1ST HARMONIC	2ND HARMONIC	3RD HARMONIC	
208	X_1	.00231	.00166	.00075	.003874	.057045	.005804	.0714466
	X_2	.00046	.00789	.00077	.022051	.29552	.0188945	.3455795
	X_3	.00061	.00531	.00009	.0009377	.087922	.0006529	.1031327

TABLE 3.8.2-4

CO IBA LOAD HARMONICS
(Pressure Amplitudes and Frequencies

HARMONIC NO	INTERNAL PRESSURE (PSI)	Δ P (PSI)	FREQUENCY RANGE (HZ)	EXCITING FREQUENCY (HZ)
1st	1.10	0.20	6-10	6.642
2nd	0.80	0.20	12-20	13.284
3rd	0.20	0.20	18-30	19.926

TABLE 3.8.2-5

CO DBA LOAD HARMONICS
(Pressure Amplitudes and Frequencies)

HARMONIC NO.	INTERNAL PRESSURE (PSI)	Δ P (PSI)	FREQUENCY RANGE (HZ)	EXCITING FREQUENCY (HZ)
1st	2.85	3.6	4.8	6.642
2nd	2.6	1.3	8.16	13.284
3rd	1.2	0.6	12.24	19.926

TABLE 3.8.2-6

MAXIUMUM STRESS INTENSITIES

DUE TO CO HARMONIC LOADS

ACCIDENT CONDITION	ELEMENT NO	MAX STRESS INTENSITY (KSI)
IBA	QUAD 2503	3.28
	QUAD 36	1.19
DBA	QUAD 2503	34.46
	QUAD 36	13.36

TABLE 3.8.3-1

STRUCTURAL EVALUATION DUE TO CHUGGING

RSEL: PMAX (N-S) = 4580.0 lbs.
PMAX (E-W) = 11987.0 lbs.

MAX = MAX DUE TO UNIT LOAD X RSEL

UNIT LOAD	ELEMENT NO.	UMAX (UNIT LOAD)	MAX X RSEL
FX_2 = 1000 lbs.	TRIA #302	1.848 KSI	= 22.152 KSI
	305	1.848 KSI	
	QUAD #2503	4.23 KSI	= 50.705 KSI
	2519	4.23 KSI	
FX_3 = 1000 lbs.	TRIA #57	9.42 KSI	= 43.14 KSI
	58	9.42 KSI	
	QUAD #36	9.597 KSI	= 43.954 KSI
	312	9.597 KSI	

TABLE 3.8.4.1-1

MAXIMUM STRESS INTENSITIES
DUE TO CO AND SRV LOAD COMBINATION

	ELEMENT NO.	MAX S.I. CO (KSI)	MAX S.I. SRV (KSI)	TOTAL (KSI)
CO IBA	QUAD 36	1.19	11.95	13.14
	QUAD 2503	3.28	18.92	22.20
CO DBA	QUAD 36	13.36	38.89	52.25
	QUAD 2503	34.46	18.92	53.38

TABLE 3.8.4.2-1

CHUGGING AND SRV INDIVIDUAL LOADS

LOAD CASE	DESCRIPTION
1	CHUGGING-X_2 (E-W)
2	CHUGGING-(-)X_2 (W-E)
3	CHUGGING-X_3 (N-S)
4	CHUGGING-(-)X_3 (S-N)
5	SRV-X_2
6	SRV-X_3

TABLE 3.8.4.2-2

SRSS COMBINATION OF INDIVIDUAL CHUGGING AND SRV LOADS FOR STRESS INTENSITIES

LOAD COMBINATION	SRSS COMBINATION
1	$((1)^2 + (5)^2)^{1/2}$
2	$((2)^2 + (5)^2)^{1/2}$
3	$((3)^2 + (5)^2)^{1/2}$
4	$((4)^2 + (5)^2)^{1/2}$
5	$((1)^2 + (6)^2)^{1/2}$
6	$((2)^2 + (6)^2)^{1/2}$
7	$((3)^2 + (6)^2)^{1/2}$
8	$((4)^2 + (6)^2)^{1/2}$

TABLE 3.8.4.2-3

COMBINING STRESS INTENSITIES
DUE TO SRV AND CHUGGING BY SRSS METHOD

LOAD COMB. NO.	APPLIED FORCE	FACTOR FOR UNIT LOAD CASE NO. 2	FACTOR FOR UNIT LOAD CASE NO. 3
1	CHUGGING-X_2 (E-W)	11.987	
2	CHUGGING-X_2 (W-E)	-11.987	
3	CHUGGING-X_3 (N-S)		4.580
4	CHUGGING-X_3 (S-N)		-4.580
5	SRV-X_2	-6.948 x .6322 = -4.393	-0.958
6	SRV-X_3	-0.266 x .6322 = -0.168	4.063

TABLE 3.8.4.2-4

SRSS LOAD COMBINATION NO. 1 OF SRV AND CHUGGING LOADS

TOP MAXIMUM 10 ELEMENTS IN +3 FACE

ELEM	CASE 1	CASE 5	SRSS OF +3	SRSS OF -3
Q2519	38730.000	14410.000	41323.855	54124.583
Q2503	38730.000	14410.000	41323.855	54124.583
Q2523	38730.000	13980.000	41175.883	53894.031
Q2507	38730.000	13980.000	41175.883	53894.031
Q2520	38470.000	14150.000	40989.796	45258.264
Q2504	38470.000	14150.000	40989.796	45258.264
Q2524	38470.000	14050.000	40955.383	45210.075
Q2508	38470.000	14050.000	40955.383	45210.075
T 305	30950.000	11550.000	33034.906	22228.580
T 302	30950.000	11550.000	33034.906	22238.647

TOP MAXIMUM 10 ELEMENTS IN -3 FACE

ELEM	CASE 1	CASE 5	SRSS OF +3	SRSS OF -3
Q2519	50710.000	18920.000	41323.855	54124.583
Q2503	50710.000	18920.000	41323.855	54124.583
Q2523	50710.000	18250.000	41175.883	53894.031
Q2507	50710.000	18250.000	41175.883	53894.031
Q2520	42470.000	15640.000	40989.796	45258.264
Q2504	42470.000	15640.000	40989.796	45258.264
Q2524	42470.000	15500.000	40955.383	45210.075
Q2508	42470.000	15500.000	40955.383	45210.075
T 302	20830.000	7789.000	33034.906	22238.647
T 305	20820.000	7787.000	33034.906	22228.580
T 305	30950.000	11550.000	33034.906	22228.580
T 302	30950.000	11550.000	33034.906	22238.647

TABLE 3.8.4.2-5

SRSS LOAD COMBINATION NO. 2 OF SRSS AND CHUGGING LOADS

--TOP MAXIMUM 10 ELEMENTS IN +3 FACE--

ELEM	CASE 2	CASE 5	SRSS OF +3	SRSS OF -3
Q2519	38730.000	14410.000	41323.855	54124.583
Q2503	38730.000	14410.000	41323.855	54124.583
Q2523	38730.000	13980.000	41175.883	53894.031
Q2507	38730.000	13980.000	41175.883	53894.031
Q2520	38470.000	14150.000	40989.796	45258.264
Q2504	38470.000	14150.000	40989.796	45258.264
Q2524	38470.000	14050.000	40955.383	45210.075
Q2508	38470.000	14050.000	40955.383	45210.075

--TOP MAXIMUM 10 ELEMENTS IN -3 FACE--

ELEM	CASE 2	CASE 5	SRSS OF +3	SRSS OF -3
Q2519	50710.000	18920.000	41323.855	54124.583
Q2503	50710.000	18920.000	41323.855	54124.583
Q2523	50710.000	18250.000	41175.883	53894.031
Q2507	50710.000	18250.000	41175.883	53894.031
Q2520	42470.000	15640.000	40989.796	45258.264
Q2504	42470.000	15640.000	40989.796	45258.264
Q2524	42470.000	15500.000	40955.383	45210.075
Q2508	42470.000	15500.000	40955.383	45210.075
T 302	20830.000	7789.000	33034.906	22238.647
T 305	20820.000	7787.000	33034.906	22228.580

TABLE 3.8.4.2-6

SRSS LOAD COMBINATION NO. 3 OF SRV AND CHUGGING LOADS

—TOP MAXIMUM 10 ELEMENTS IN +3 FACE——

	ELEM	CASE 3	CASE 5	SRSS OF +3	SRSS OF -3
T	56	38930.000	12180.000	40790.897	44219.672
T	15	38930.000	12180.000	40790.897	44207.375
Q	312	37780.000	11550.000	39506.087	45535.987
Q	36	37770.000	11550.000	39496.524	45545.636
T	16	38920.000	4758.000	39209.756	43074.214
T	55	38920.000	4756.000	39209.513	43093.698
Q	128	37770.000	6127.000	38263.730	44408.129
Q	220	37760.000	6127.000	38253.859	44418.021
T	19	36460.000	11030.000	38091.895	44420.448
T	57	36440.000	11030.000	38072.753	44473.796

—TOP MAXIMUM 10 ELEMENTS IN -3 FACE——

	ELEM	CASE 3	CASE 5	SRSS OF +3	SRSS OF -3
Q	36	43950.000	11950.000	39496.524	45545.636
Q	312	43940.000	11950.000	39506.087	45535.987
T	57	43160.000	10730.000	38072.753	44473.796
T	19	43110.000	10710.000	38091.895	44420.448
Q	220	43940.000	6499.000	38253.859	44418.021
Q	128	43930.000	6499.000	38263.730	44408.129
T	56	42630.000	11750.000	40790.897	44219.672
T	15	42620.000	11740.000	40790.897	44207.375
T	58	43150.000	7459.000	36999.656	43789.944
T	17	43100.000	7458.000	37009.331	43740.505

TABLE 3.8.4.2-7

SRSS LOAD COMBINATION NO. 4 OF SRV AND CHUGGING LOADS

-------TOP MAXIMUM 10 ELEMENTS IN +3 FACE-------

	ELEM	CASE 4	CASE 5	SRSS OF +3	SRSS OF -3
T	56	38930.000	12180.000	40790.897	44219.672
T	15	38930.000	12180.000	40790.897	44207.375
Q	312	37780.000	11550.000	39506.087	45535.987
Q	36	37770.000	11550.000	39496.524	45545.636
T	16	38920.000	4758.000	39209.756	43074.214
T	55	38920.000	4756.000	39209.513	43093.698
Q	128	37770.000	6127.000	38263.730	44408.129
Q	220	37760.000	6127.000	38253.859	44418.021
T	18	36460.000	11030.000	38091.895	44420.448
T	57	36440.000	11030.000	38072.753	44473.796

-------TOP MAXIMUM 10 ELEMENTS IN -3 FACE-------

	ELEM	CASE 4	CASE 5	SRSS OF +3	SRSS OF -3
Q	36	43950.000	11950.000	39496.524	45545.636
Q	312	43940.000	11950.000	39506.087	45535.987
T	57	43160.000	10730.000	38072.753	44473.796
T	18	43110.000	10710.000	38091.895	44420.448
Q	220	43940.000	6499.000	38253.859	44418.021
Q	128	43930.000	6499.000	38263.730	44408.129
T	56	42630.000	11750.000	40790.897	44219.672
T	15	42620.000	11740.000	40790.897	44207.375
T	58	43150.000	7459.000	36999.656	43789.944
T	17	43100.000	7458.000	37009.331	43740.505

TABLE 3.8.4.2-8

SRSS LOAD COMBINATION NO. 5 OF SRV AND CHUGGING LOADS

———TOP MAXIMUM 10 ELEMENTS IN +3 FACE———

ELEM	CASE 1	CASE 6	SRSS OF +3	SRSS OF -3
Q2523	38730.000	1538.000	38762.542	50758.965
Q2507	38730.000	1588.000	38762.542	50758.965
Q2519	38730.000	773.300	38737.729	50733.439
Q2503	38730.000	773.700	38737.727	50733.439
Q2524	38470.000	984.300	38482.590	42488.776
Q2508	38470.000	984.300	38482.590	42488.776
Q2520	38470.000	722.100	38476.776	42485.730
Q2504	38470.000	722.000	38476.775	42485.730
T 27	24790.000	28220.000	37555.516	34538.848
T 73	24770.000	28210.000	37541.404	34555.927

———TOP MAXIMUM 10 ELEMENTS IN -3 FACE———

ELEM	CASE 1	CASE 6	SRSS OF +3	SRSS OF -3
Q2523	50710.000	2229.000	38762.542	50758.965
Q2507	50710.000	2229.000	38762.542	50758.965
Q2519	50710.000	1542.000	38737.729	50733.439
Q2503	50710.000	1542.000	38737.727	50733.439
Q2524	42470.000	1263.000	38482.590	42488.776
Q2508	42470.000	1263.000	38482.590	42488.776
Q2520	42470.000	1156.000	38476.776	42485.730
Q2504	42470.000	1156.000	38476.775	42485.730
Q 220	8331.000	39090.000	35063.412	39967.908
Q 128	8329.000	39080.000	35084.858	39957.711

TABLE 3.8.4.2-9

SRSS LOAD COMBINATION NO. 6 OF SRV AND CHUGGING LOADS

—TOP MAXIMUM 10 ELEMENTS IN +3 FACE——

ELEM	CASE 2	CASE 6	SRSS OF +3	SRSS OF -3
Q2523	38730.000	1588.000	38762.542	50758.965
Q2507	38730.000	1588.000	38762.542	50758.965
Q2519	38730.000	773.800	38737.729	50733.439
Q2503	38730.000	773.700	38737.727	50733.439
Q2524	38470.000	984.300	38482.590	42488.776
Q2508	38470.000	984.300	38482.590	42488.776
Q2520	38470.000	722.100	38476.776	42485.730
Q2504	38470.000	722.000	38476.775	42485.730
T 27	24780.000	28220.000	37555.516	34538.848
T 73	24770.000	28210.000	37541.404	34555.927

—TOP MAXIMUM 10 ELEMENTS IN -3 FACE——

ELEM	CASE 2	CASE 6	SRSS OF +3	SRSS OF -3
Q2523	50710.000	2229.000	38762.542	50758.965
Q2507	50710.000	2229.000	38762.542	50758.965
Q2519	50710.000	1542.000	38737.729	50733.439
Q2503	50710.000	1542.000	38737.727	50733.439
Q2524	42470.000	1263.000	38482.590	42488.776
Q2509	42470.000	1263.000	38482.590	42488.776
Q2520	42470.000	1156.000	38476.776	42485.730
Q2504	42470.000	1156.000	38476.775	42485.730
Q 220	8331.000	39090.000	35063.412	39967.908
Q 128	8329.000	39090.000	35084.858	39957.711

TABLE 3.8.4.2-10

SRSS LOAD COMBINATION NO. 7 OF SRV AND CHUGGING LOADS

—TOP MAXIMUM 10 ELEMENTS IN +3 FACE——

	ELEM	CASE 3	CASE 6	SRSS OF +3	SRSS OF -3
T	16	38920.000	34680.000	52129.347	57019.032
T	55	38920.000	34670.000	52122.695	57040.621
T	15	38930.000	34390.000	51944.364	56901.269
T	56	38930.000	34380.000	51937.744	56922.011
Q	128	37770.000	33650.000	50585.526	58797.035
Q	220	37760.000	33630.000	50564.756	58811.153
Q	312	37790.000	33380.000	50413.816	58671.782
Q	36	37770.000	33360.000	50393.080	58685.898
T	17	36450.000	32380.000	48755.173	57651.835
T	58	36440.000	32370.000	48741.056	57722.423

—TOP MAXIMUM 10 ELEMENTS IN -3 FACE——

	ELEM	CASE 3	CASE 6	SRSS OF +3	SRSS OF -3
Q	220	43940.000	39090.000	50564.756	58811.153
Q	128	43930.000	39080.000	50585.526	58797.035
Q	36	43950.000	38890.000	50393.080	58685.898
Q	312	43940.000	38880.000	50413.816	58671.782
T	58	43150.000	38340.000	48741.056	57722.423
T	57	43160.000	38230.000	48681.331	57656.903
T	17	43100.000	38290.000	48755.173	57651.835
T	18	43110.000	38180.000	48709.564	57586.322
T	55	42620.000	37910.000	52122.695	57040.621
T	16	42600.000	37900.000	52129.347	57019.032

TABLE 3.8.4.2-11

SRSS LOAD COMBINATION NO. 8 OF SRV AND CHUGGING LOADS

——TOP MAXIMUM 10 ELEMENTS IN +3 FACE——

	ELEM	CASE 4	CASE 6	SRSS OF +3	SRSS OF -3
T	16	38920.000	34680.000	52129.347	57019.032
T	55	38920.000	34670.000	52122.695	57040.621
T	15	38930.000	34390.000	51944.364	56901.269
T	56	38930.000	34380.000	51937.744	56922.011
Q	128	37770.000	33650.000	50585.526	58797.035
Q	220	37760.000	33630.000	50564.756	58811.153
Q	312	37780.000	33380.000	50413.816	58671.782
Q	36	37770.000	33360.000	50393.080	58685.898
T	17	36450.000	32380.000	48755.173	57651.835
T	58	36440.000	32370.000	48741.056	57722.423

---TOP MAXIMUM 10 ELEMENTS IN -3 FACE——

	ELEM	CASE 4	CASE 6	SRSS OF +3	SRSS OF -3
Q	220	43940.000	39090.000	50564.756	58811.153
Q	128	43930.000	39080.000	50585.526	58797.035
Q	36	43950.000	38890.000	50393.080	58685.898
Q	312	43940.000	38880.000	50413.816	58671.782
T	58	43150.000	38340.000	48741.056	57722.423
T	57	43160.000	38230.000	48681.331	57656.903
T	17	43100.000	38290.000	48755.173	57651.835
T	18	43110.000	38180.000	48709.564	57586.322
T	55	42620.000	37910.000	52122.695	57040.621
T	16	42600.000	37900.000	52129.347	57019.032

TABLE 3.8.4.3-1

QUALIFICATION OF DOWNCOMER/
VENT HEADER INTERSECTION

STRESS INTENSITY VALUES (KSI)

LOAD COMBINATION	ELEMENT NO.	ALLOW	ACTUAL	ALLOW	ACTUAL	ALLOW	ACTUAL	ALLOW	ACTUAL	REMARKS
	TRIAB 55	69.3	57.04	37.63	24.74	N/A	N/A	N/A	N/A	Discontinuity
CHUGGING +	QUAD 220	69.3	58.81	37.63	21.17	N/A	N/A	N/A	N/A	Discontinuity
(IBA)	QUAD 205	N/A	N/A	N/A	N/A	37.63	19.81	19.3	16.53	
SRV	QUAD 269	N/A	N/A	N/A	N/A	37.63	25.08	19.3	14.57	
	QUAD 2503	N/A	N/A	51.90	16.17	N/A	N/A	N/A	N/A	Discontinuity
CO (DBA) +	QUAD 262	N/A	N/A	51.90	29.51	N/A	N/A	N/A	N/A	Discontinuity
SRV	QUAD 275	N/A	N/A	N/A	N/A	34.74	15.25	23.16	9.65	

o $P_L = 1.5\ S_{mc}$ for areas of continuity

TABLE 3.8.5-1

EVALUATION OF FATIGUE USAGE FACTOR FOR SRV LOADS

ELEMENT	MAXIMUM STRESS INTENSITY	MAXIMUM ALTERNATING STRESS	EQUIVALENT MAXIMUM STRESS CYCLES	NUMBER OF ALLOWABLE CYCLES	FATIGUE USAGE FACTOR
QUAD 2503	18.92 ksi	20.43 ksi	2000	7×10^4	0.0286
QUAD 36	38.89 ksi	42.12 ksi	2000	7×10^3	0.286

TABLE 3.8.5-2

EVALUATION OF FATIGUE USAGE FACTOR FOR CO LOADS

ELEMENT NUMBER	HARMONIC	MAXIMUM STRESS INTENSITY (KSI)	MAXIMUM ALTERNATING STRESS (KSI)	NUMBER OF CYCLES	NUMBER OF ALLOWABLE CYCLES	FATIGUE USAGE FACTOR	TOTAL
QUAD 2503	1st	34.46	37.32	199	11,000	0.0181	
	2nd	34.46	37.32	399	11,000	0.0362	0.108
	3rd	34.46	37.32	598	11,000	0.0544	
QUAD 36	1st	13.36	14.47	199	300,000	0.0007	
	2nd	13.36	14.47	399	300,000	0.0013	0.004
	3rd	13.36	14.47	598	300,000	0.0020	

TABLE 3.8.5-3

EVALUATION OF FATIGUE USAGE FACTOR FOR IBA CHUGGING

ELEMENT NO.	FATIGUE USAGE FACTOR
QUAD 2503	0.09
QUAD 36	0.15
QUAD 312	0.15
QUAD 128	0.14
QUAD 220	0.14
TRIAB 15	0.14
TRIAB 17	0.14
TRIAB 18	0.14
TRIAB 56	0.14
TRIAB 57	0.14
TRIAB 58	0.14

Reference: Calculation Set 9527-E-SC-VS-1-F

TABLE 3.8.5.4-1

CUMULATIVE FATIGUE USAGE FACTOR

EVENT	ELEMENT NO.	SRV	CO	CHUGGING	TOTAL
IBA	QUAD 2503	0.0286	0.0	0.09	0.12
	QUAD 36	0.286	0.0	0.15	0.44
DBA	QUAD 2503	0.0286	0.108	0.0	0.14
	QUAD 36	0.286	0.004	0.0	0.29

TABLE 3.9.2.1-1
(Page 1 of 2)

EVALUATION OF RING HEADER DEFLECTOR

Structure & Component	Service Level	Load Comb. No.	Stress Type	Stress (ksi Unless Noted) (1) Computed	(2) Allowable	(1)/(2) Ratio	Remarks
Deflector 20" Sch. 120 SA106 Gr.B	D	18	Flexure Axial Shear	13.41 0.13 0.753	42.0 21.8 28.0	0.425 0.027	Linear Combination
Wing L8x8x½ SA36	D	18	Flexure Axial	17.75 0.113	40.6 22.42	0.442	Liner Combination
Deflector Miter 20" Sch. 120 SA106 Gr.B	D	18	Flexure Axial Shear	7.649 0.085 0.113	42.0 0.085 28.0	0.185 0.027	Linear Combination
Weld at Deflection to Wing	-	18	Shear	6.075^{k}	7.155^{k}	0.849	
Clamp Bar 4 x 5/8 SA36	D	18	Flexure	30.866	51.04	0.605	
Weld at Clamp Bar to Wing	-	18	Shear	10.792^{k}	12.70^{k}	0.85	
1" Bolts SA193 Gr.87	-	18	Tension Shear	14.072 16.297	62.5 25.83	0.449	Square Combination
Flange 20"	D	18	Flexure	3577^{in-k}	5831^{kin-k}	0.613	
1 5/8" Stud Bolts SA193 Gr.B7	-	18	Tension Shear	8.31 1.463	62.5 25.83	0.02	Square Combination

TABLE 3.9.2.1-1
(Page 2 of 2)

EVALUATION OF RING HEADER DEFLECTOR

Structure & Component	Service Level	Load Comb. No.	Stress Type	Stress (ksi Unless Noted) (1) Computed	(2) Allowable	(1)/(2) Ratio	Remarks
Deflector at Flange	D	18	Flexure	14	36	0.039	
Weld at Deflector to Flange	-	18	Shear	5.87k/in	12.726k/in	0.461	

TABLE 3.9.2.1-2
(Page 1 of 2)

EVALUATION OF DEFLECTOR SUPPORTS

Structure & Component	Service Level	Load Comb. No.	Stress Type	Stress (ksi Unless Noted) (1) Computed	(2) Allowable	(1)/(2) Ratio	Remarks
Cheek plate "B" 3/4 in. SA516 Gr. 70	A	4	$\sigma 1$	3.088	17.5	0.176	
			$\sigma 1+\sigma 2$	4.264	26.25	0.162	
	C	6	$\sigma 1$	6.945	21.0	0.331	
			$\sigma 1+\sigma 2$	9.671	31.5	0.307	
	D	16	$\sigma 1$	8.155	26.25	0.311	
			$\sigma 1+\sigma 2$	8.919	39.375	0.227	
	D	18	$\sigma 1$	10.30	26.25	0.392	
			$\sigma 1+\sigma 2$	12.68	39.375	0.322	
Support Hate "A" 1 in. SA516 Gr. 70	A	4	$\sigma 1$	1.06	17.5	0.061	
			$\sigma 1+\sigma 2$	3.967	26.25	0.151	
	C	6	$\sigma 1$	2.137	21.0	0.102	
			$\sigma 1+\sigma 2$	8.878	31.5	0.282	
	D	16	$\sigma 1$	4.705	26.25	0.179	
			$\sigma 1+\sigma 2$	5.419	39.375	0.138	
	D	18	$\sigma 1$	4.930	26.25	0.188	
			$\sigma 1+\sigma 2$	9.237	39.375	0.235	
1¼" Bolts SA193 Gr.B7	-	18	Tension	0.254	62.5	0.227	Square Combination
			Shear	12.318	25.83		

TABLE 3.9.2.1-2
(Page 2 of 2)

EVALUATION OF DEFLECTOR SUPPORTS

Structure & Component	Service Level	Load Comb. No.	Stress Type	Stress (ksi Unless Noted) (1) Computed	(2) Allowable	(1)/(2) Ratio	Remarks
Weld at cheek plate to support plate	-	18	Shear	2.4k/in	4.6k/in	0.522	
Weld at cheek plate to ring plate							
1/2 in.	-	18	Shear	7.095k/in	7.42k/in	0.956	
9/16 in.	-	18	Shear	3.578k/in	8.35k/in	0.429	
Trunnion Lug 3 x 2½ x 11 SA516 Gr. 70	D	18	Flexure	17.497	25.95	0.674	
			Shear	7.291	13.84	0.527	
Weld at Trunnion Lug to Deflector	-	18	Shear	2.90k/in	4.77k/in	0.608	
Thermal Lug Bar 1 x 2 SA516 Gr. 70	D	18	Bearing	14.865	41.52	0.358	
Weld at Thermal Lug to Deflector							
3/8 in.	-	18	Shear	4.955k/in	5.57k/in	0.889	
3/16 in.	-	18	Shear	1.573k/in	2.78k/in	0.566	
3/4 Plate "C" SA516 Gr. 70	D	18	Shear	11.98	27.68	0.433	
			Bearing	10.484	41.52	0.253	

TABLE 3.9.2.1-3
(Page 1 of 2)

STRESSES IN THE DEFLECTOR SUPPORT AND THE HEADER AT THE DEFLECTOR ATTACHMENT

Structure & Component	Service Level	Load Comb. No.	Stress Type	Stress (ksi) Computed	Allowable
Common to Header and Ring Plate	A	4	P_L	2.12	28.95
			P_L+P_b+Q	18.84	69.3
	B	6	P_L	5.88	28.95
			P_L+P_b+Q	48.14	69.3
	A	16	P_L	7.234	28.95
	B	18	P_L	6.72	28.95
Header	A	4	P_m	2.25	19.3
			P_L+P_b	4.63	28.95
	B	6	P_m	5.28	19.3
			P_L+P_b	11.0	28.95
	A	16	P_m	4.86	19.3
			P_L+P_b	5.67	28.95
	B	18	P_m	6.56	19.3
			P_L+P_b	11.67	28.95
Ring Plate	A	4	P_m	0.47	19.3
			P_L+P_b	5.58	28.95
	B	6	P_m	0.82	19.3
			P_L+P_b	12.62	28.95

TABLE 3.9.2.1-3
(Page 2 of 2)

STRESSES IN THE DEFLECTOR SUPPORT AND THE HEADER AT THE DEFLECTOR ATTACHMENT

Structure & Component	Service Level	Load Comb. No.	Stress Type	Stress (ksi) Computed	Allowable
Ring Plate	A	16	P_m	7.54	19.3
			P_L+P_b	10.20	28.95
	B	18	P_m	7.89	19.3
			P_L+P_b	17.46	28.95

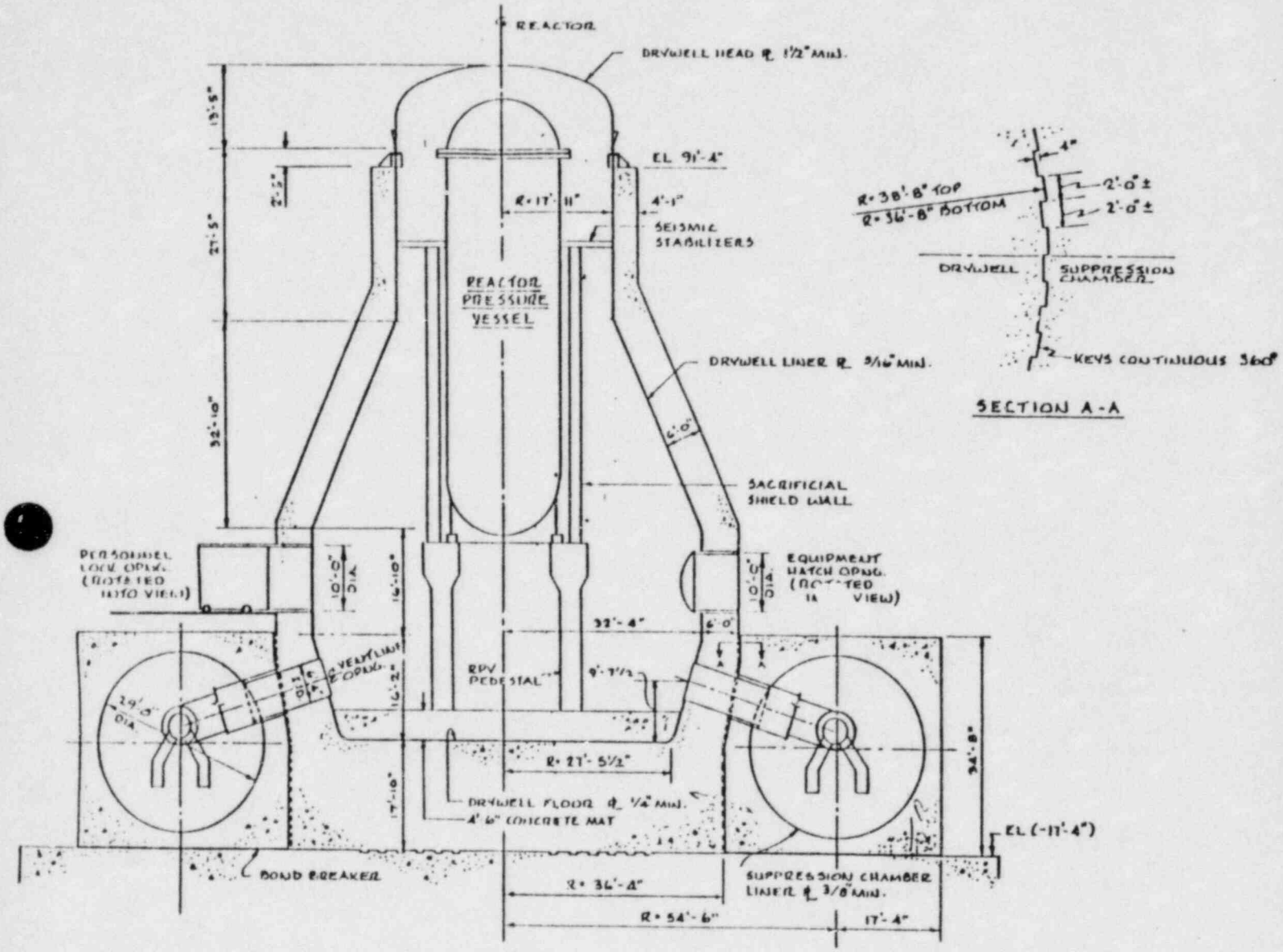

Figure 3.2-1 Drywell & Suppression Chamber

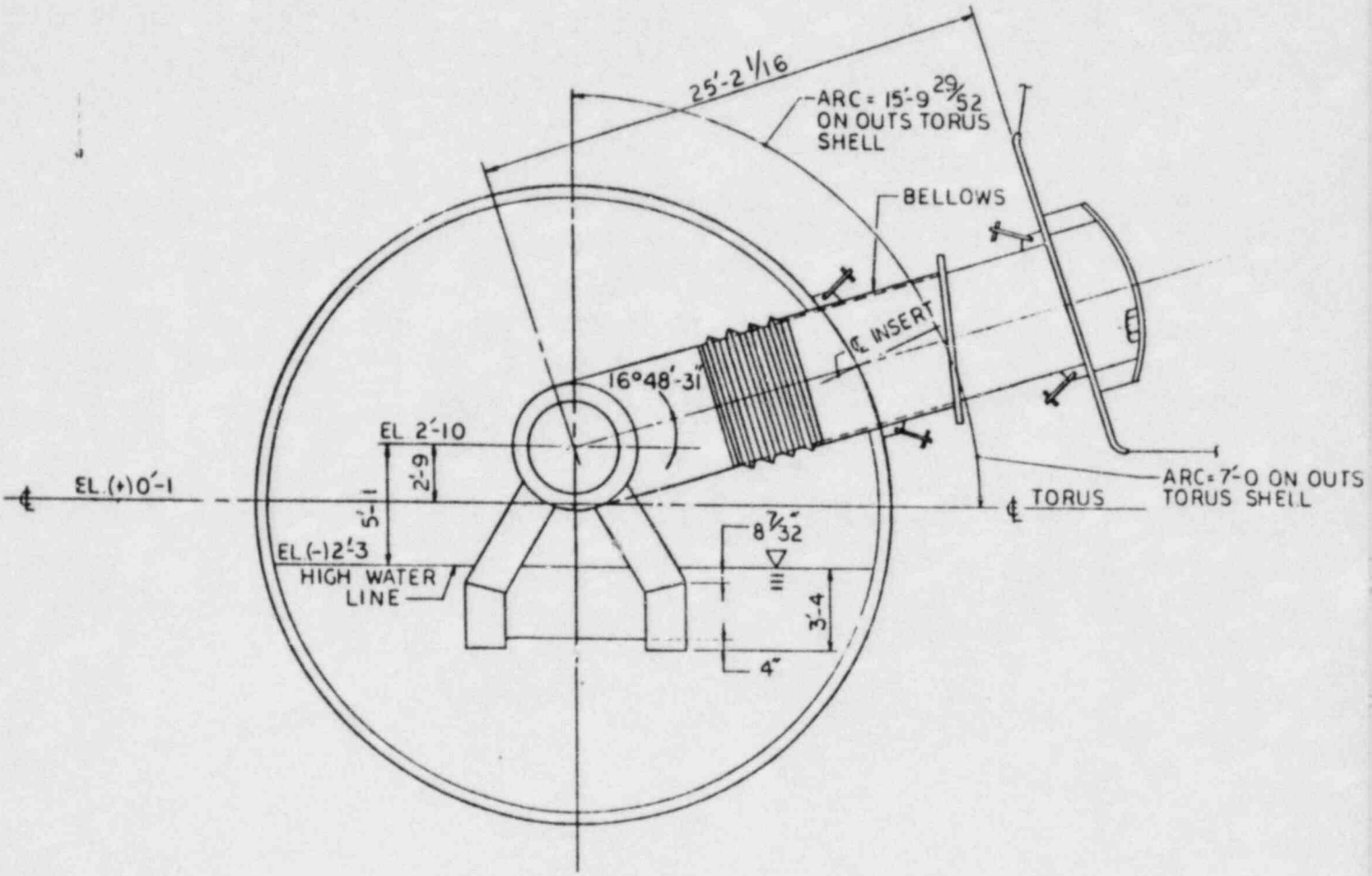

Figure 3.2-2 Section "A-A" Vent & Bellows

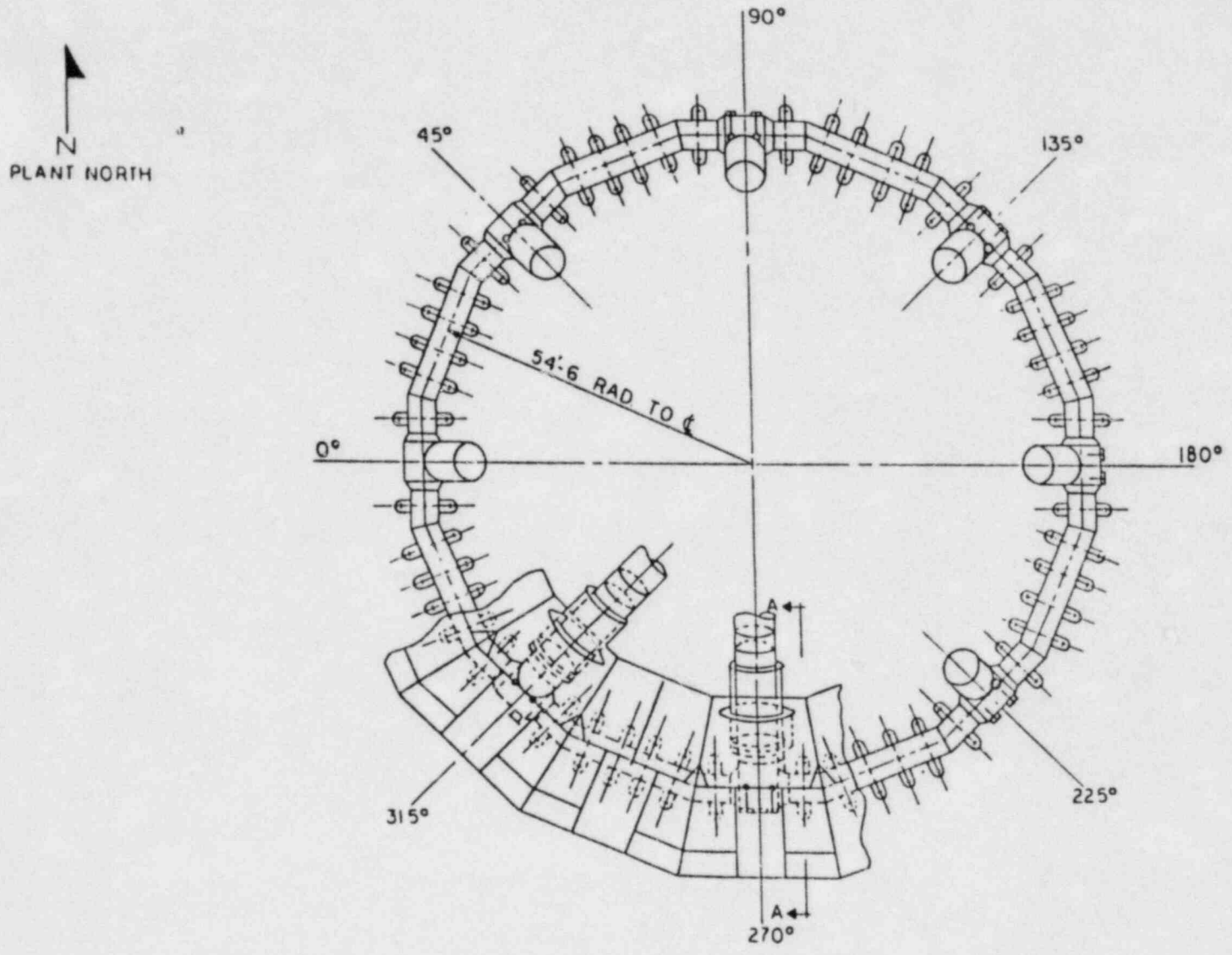

Figure 3.2-3 Plan View Vent Header Assembly

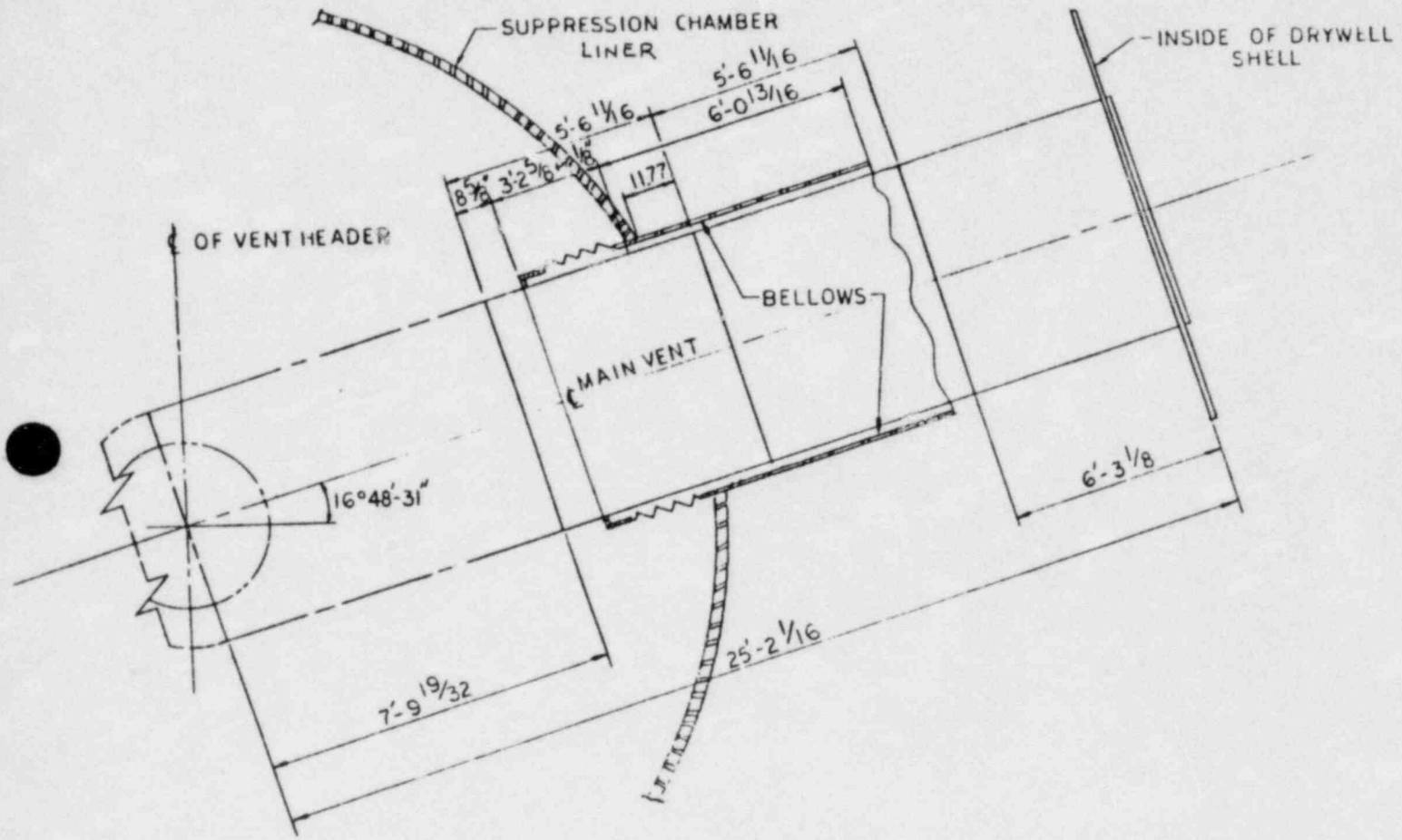

Figure 3.2-4 Detail of Bellows @ Vent & Torus Attachment

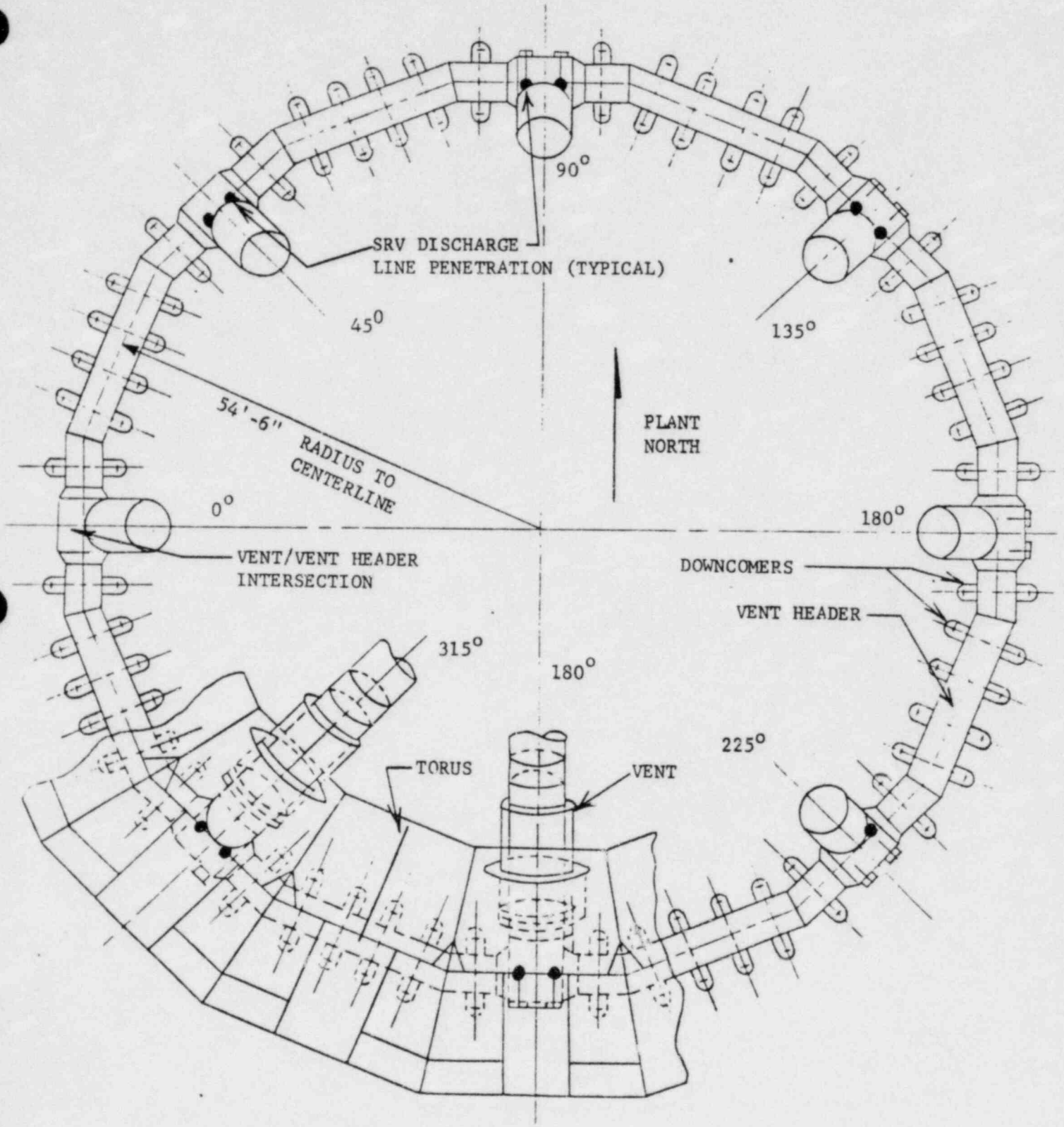

Figure 3.2-5 Location of SRV Discharge Line Penetrations of Vent/Vent Header Intersections

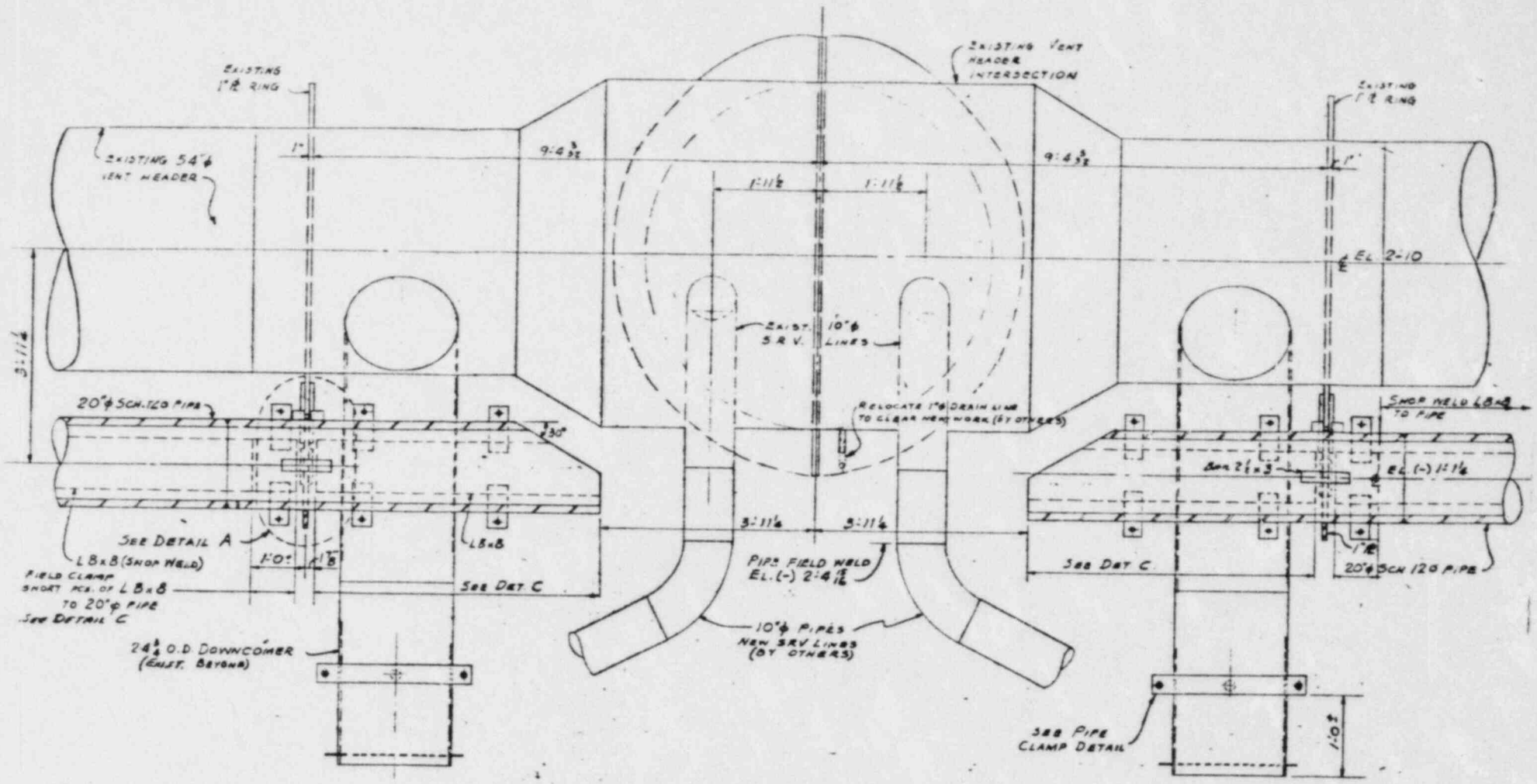

Figure 3.2-6 Sketches for Ring Header Deflector
(Page 1 of 4)

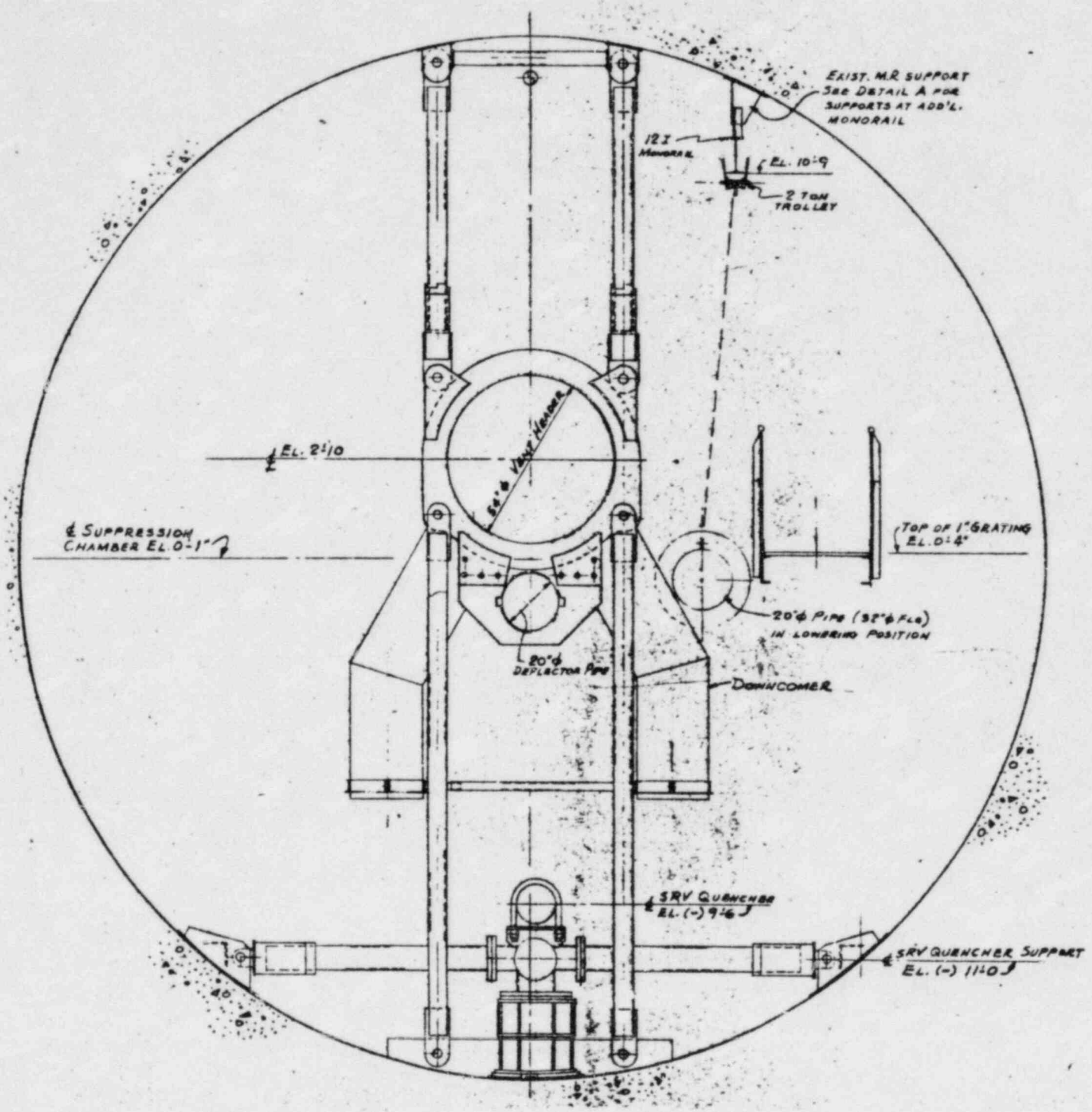

Figure 3.2-6 Sketches for Ring Header Deflector
(Page 2 of 4)

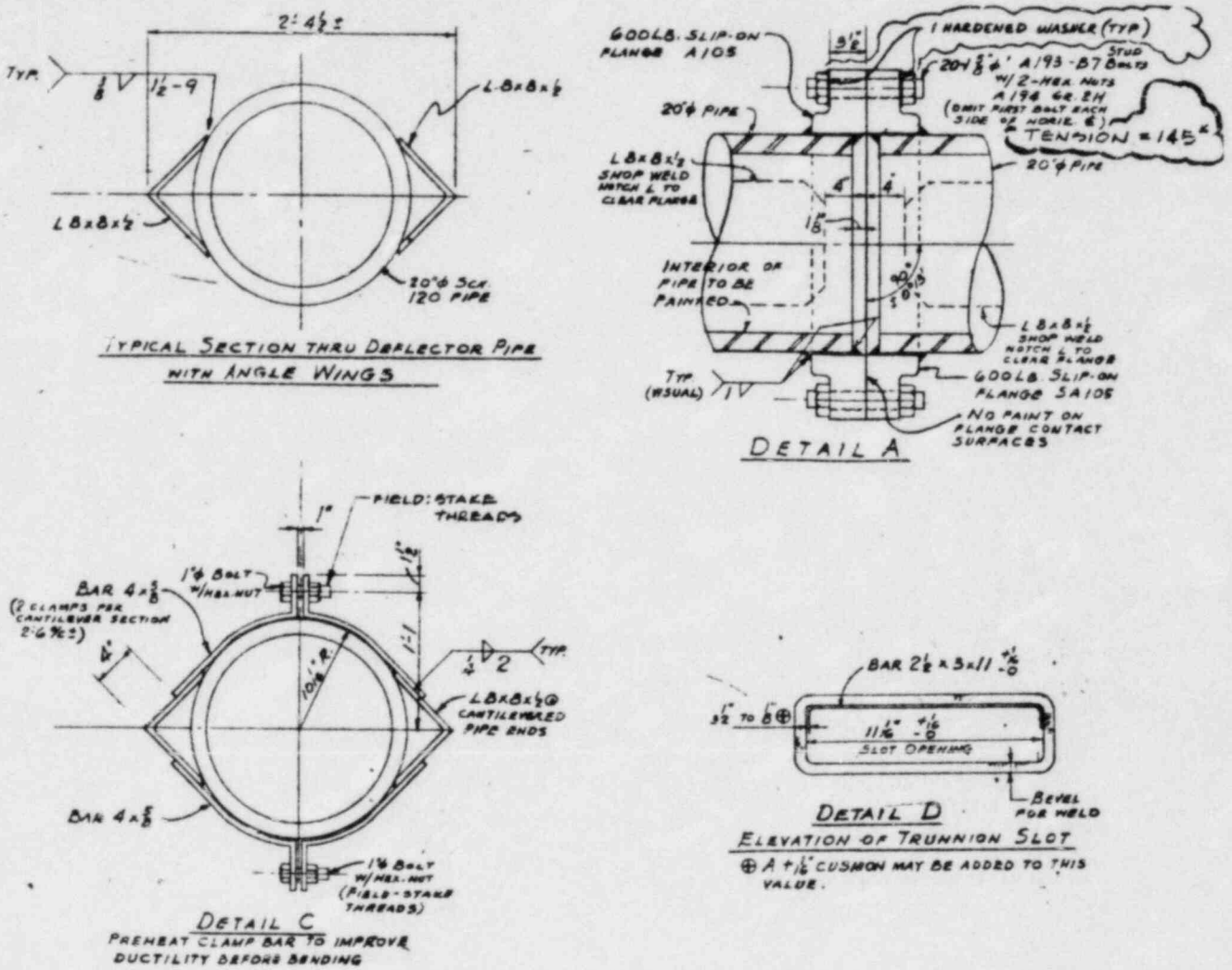

Figure 3.2-6 Sketches for Ring Header Deflector
(Page 3 of 4)

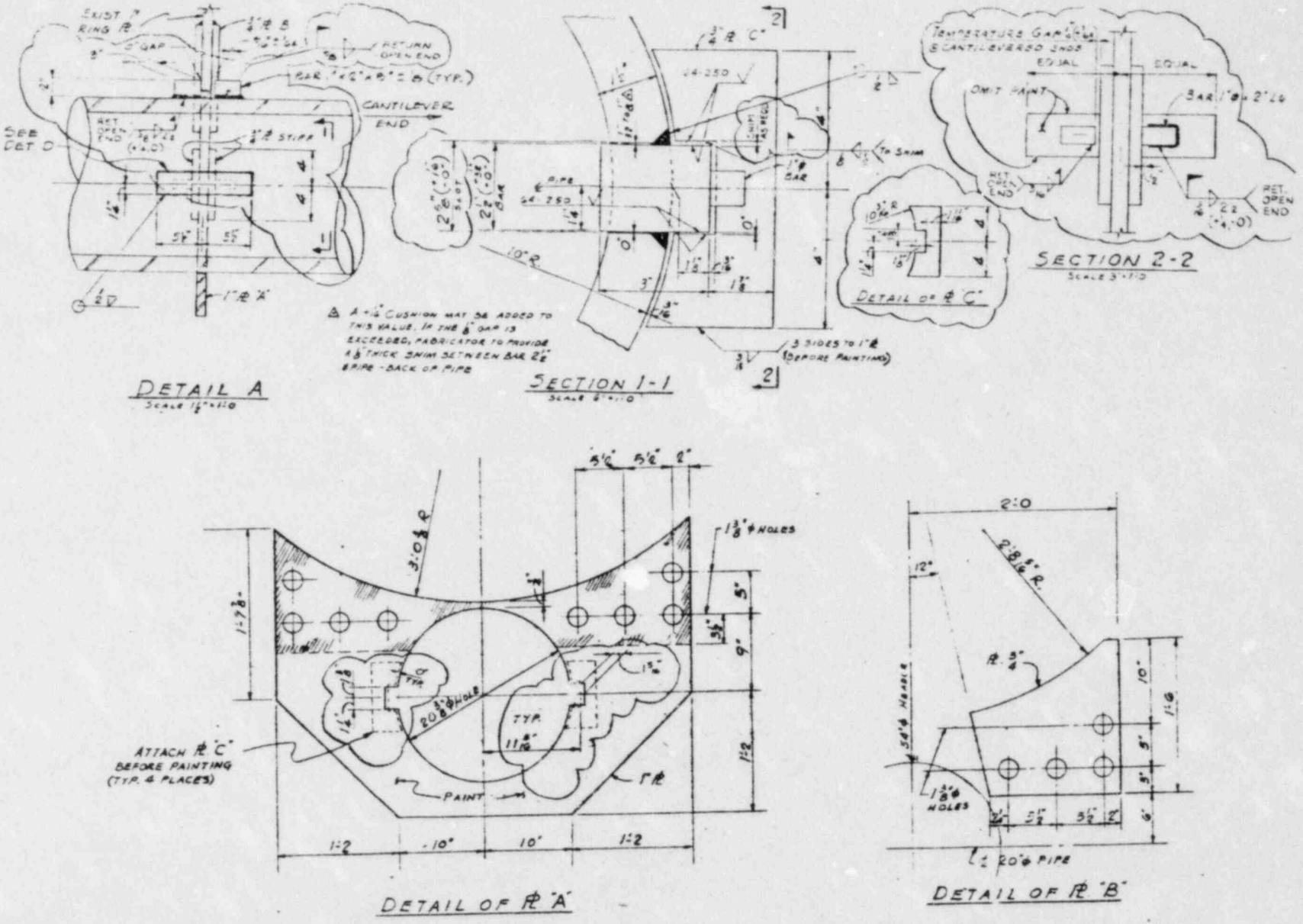

Figure 3.2-6 Sketches for Ring Header Deflector
(Page 4 of 4)

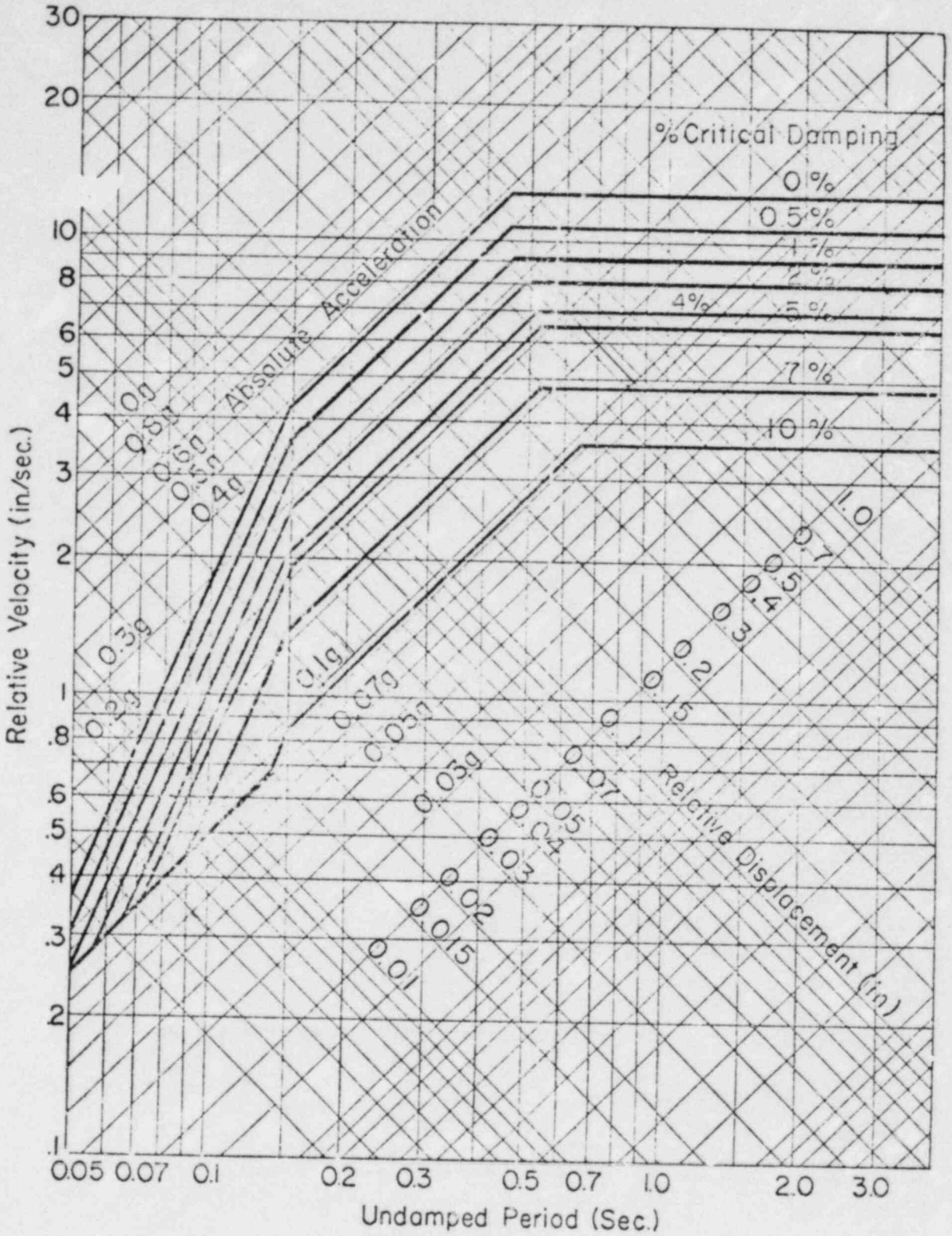

Figure 3.3.1.4-1 Design Response Spectra Curves

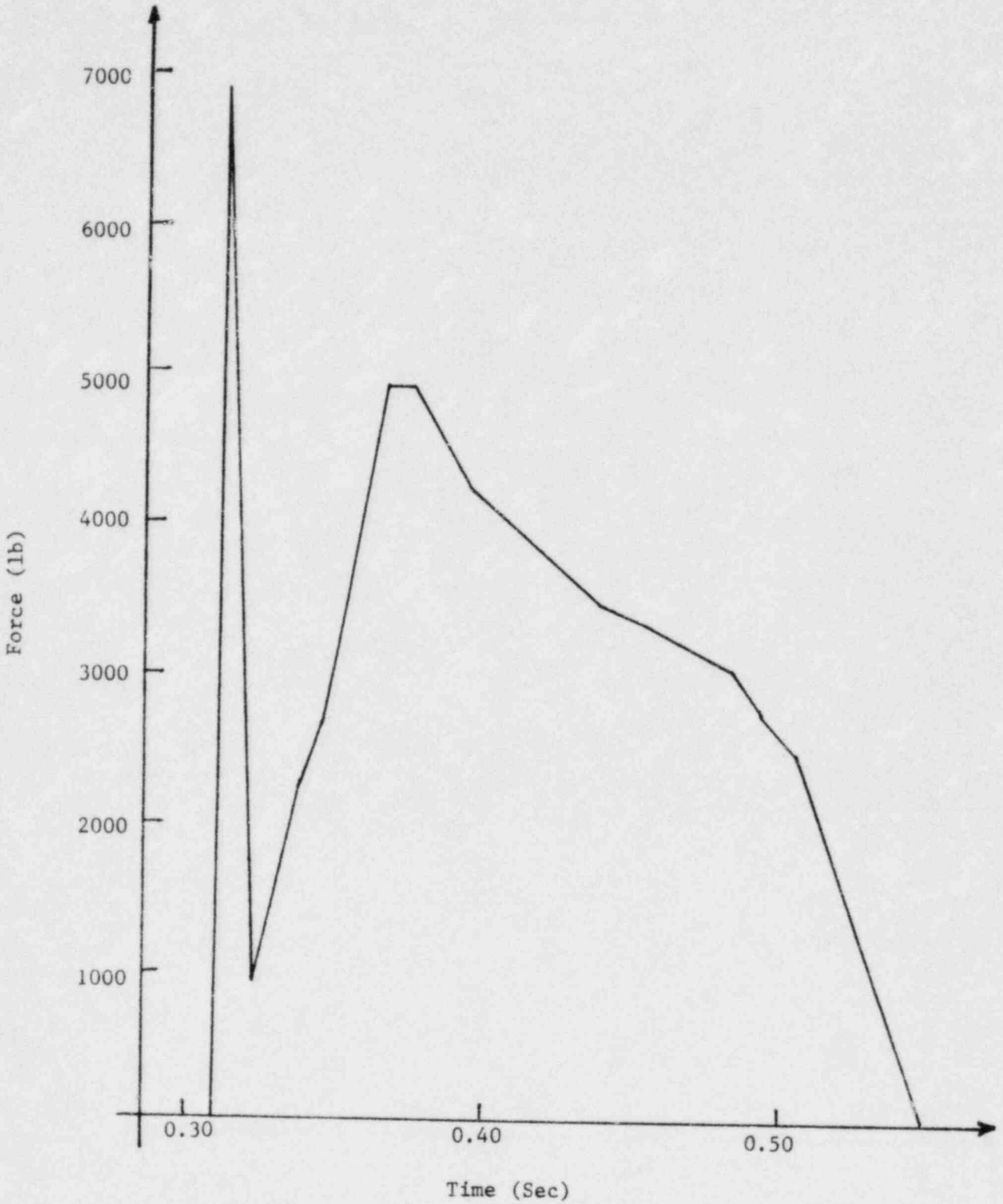

Figure 3.3.2.3-1 Typical Pool Swell Impact and Drag Load on Deflector

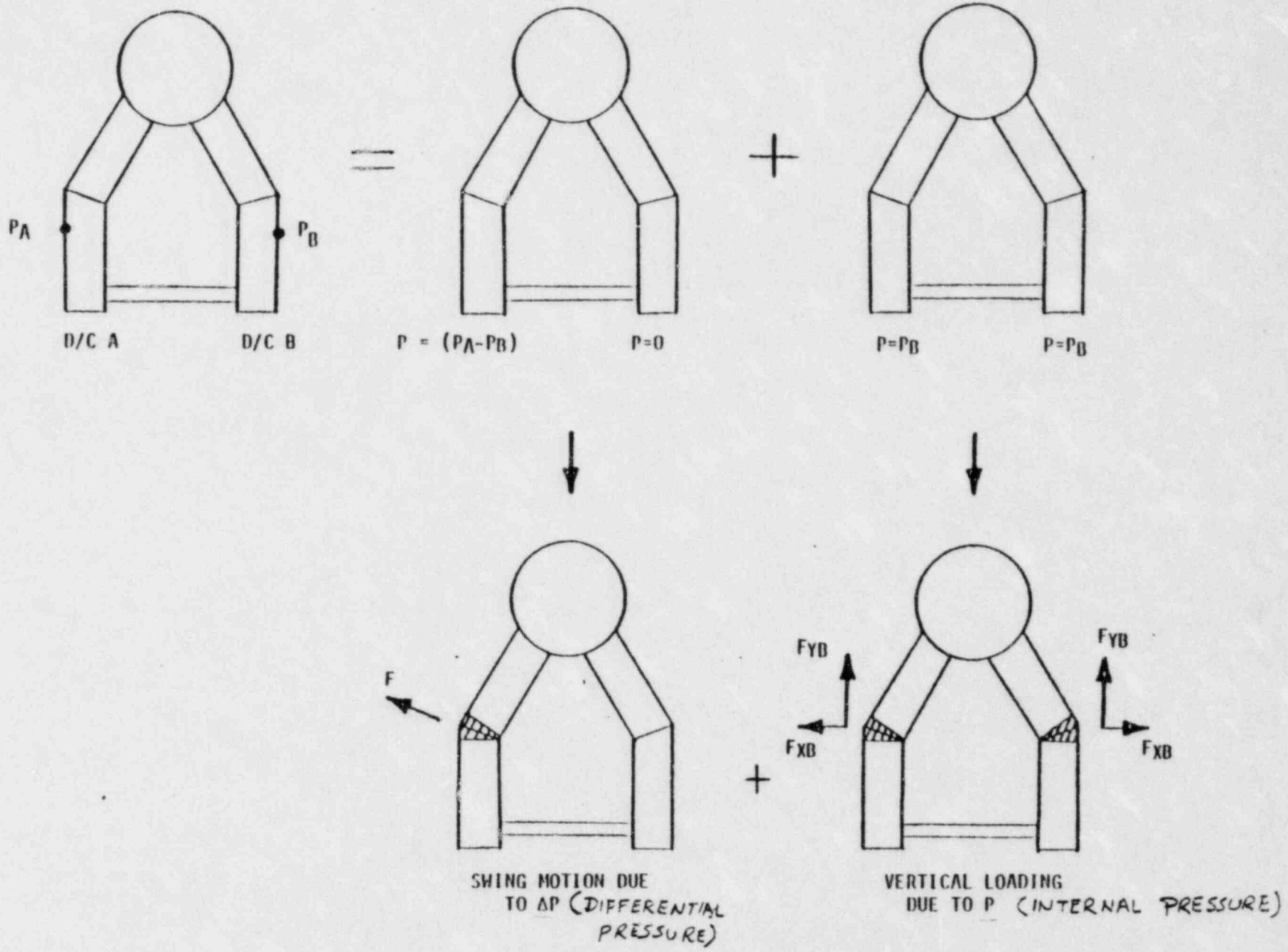

Figure 3.3.2.4-1 Downcomer Dynamic Load, Sum Of Differential And Internal Pressure

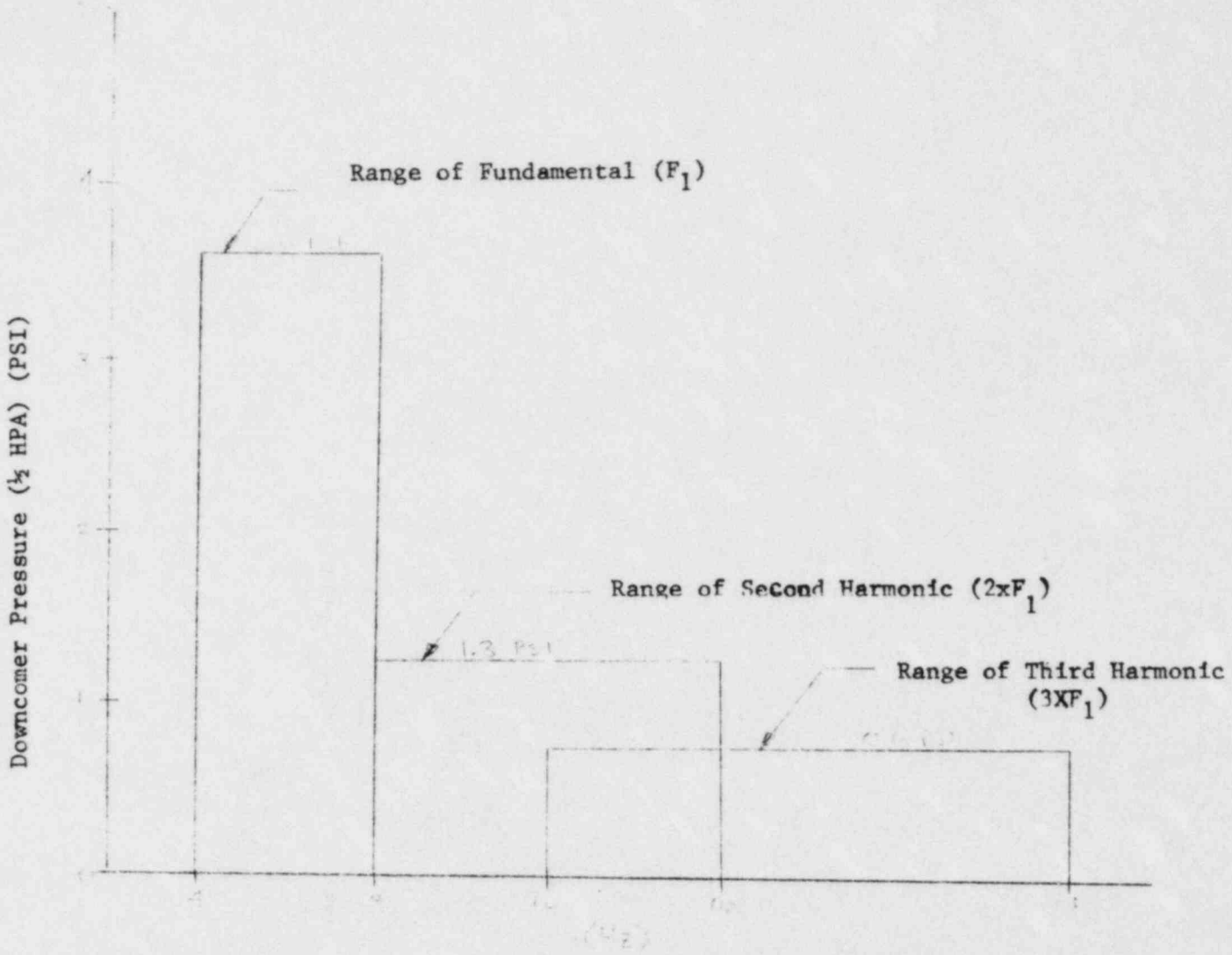

Figure 3.3.2.4-2 Downcomer Pair Internal Pressure Loading for DBA CO

NOTES:
1. THE AMPLITUDE SHOWN ARE HALF RANGE (ONE-HALF OF THE PEAK TC PEAK VALUE)
2. F_1 IS THE SINGLE FREQUENCY IN THE RANGE OF THE FUNDAMENTAL

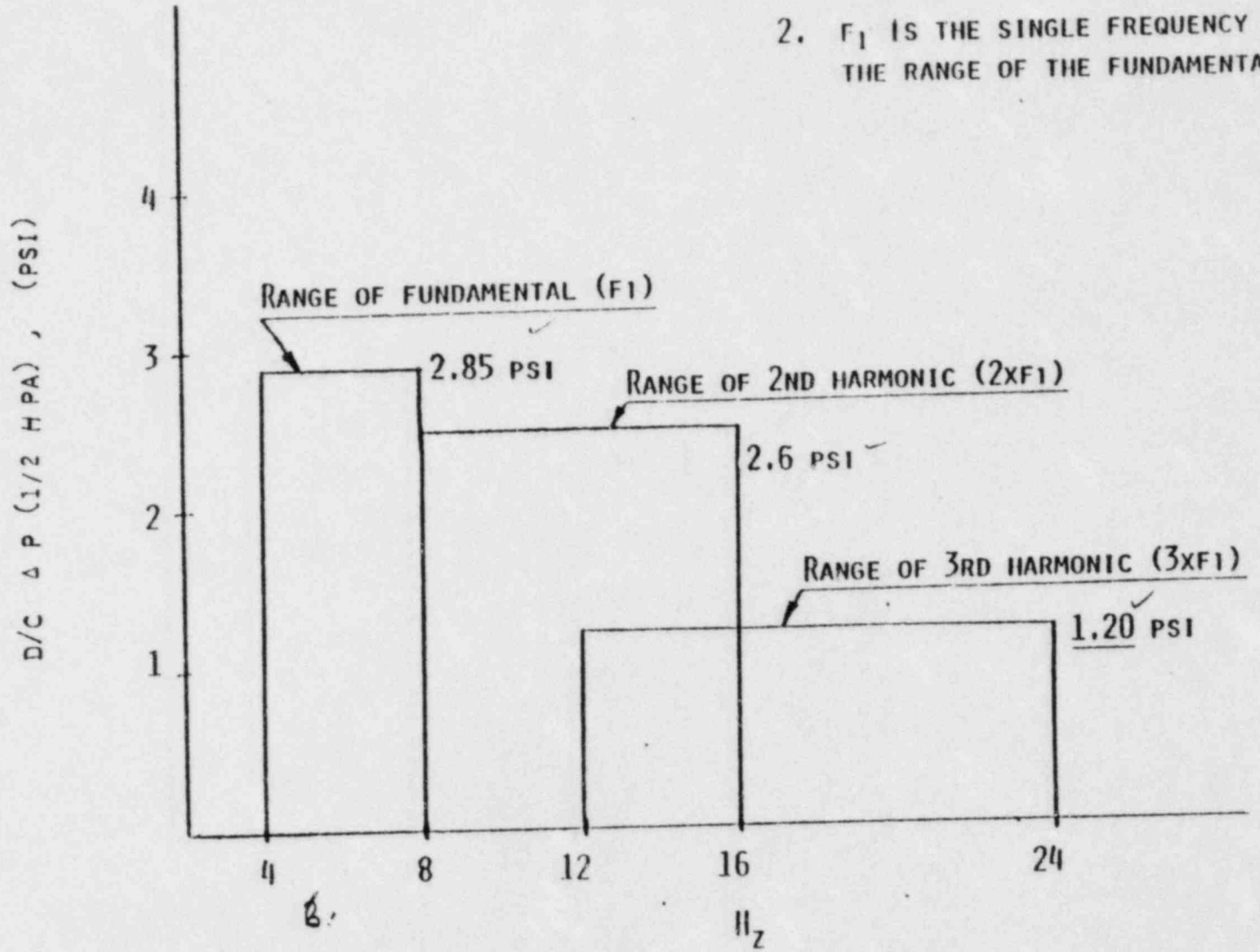

Figure 3.3.2.4-3 Downcomer Pair Differential Pressure Loading for DBA CO

NOTES: 1. The amplitudes shown are half range (one ... of the peak to peak value).

2. F_1 is the single frequency in the range of the fundamental.

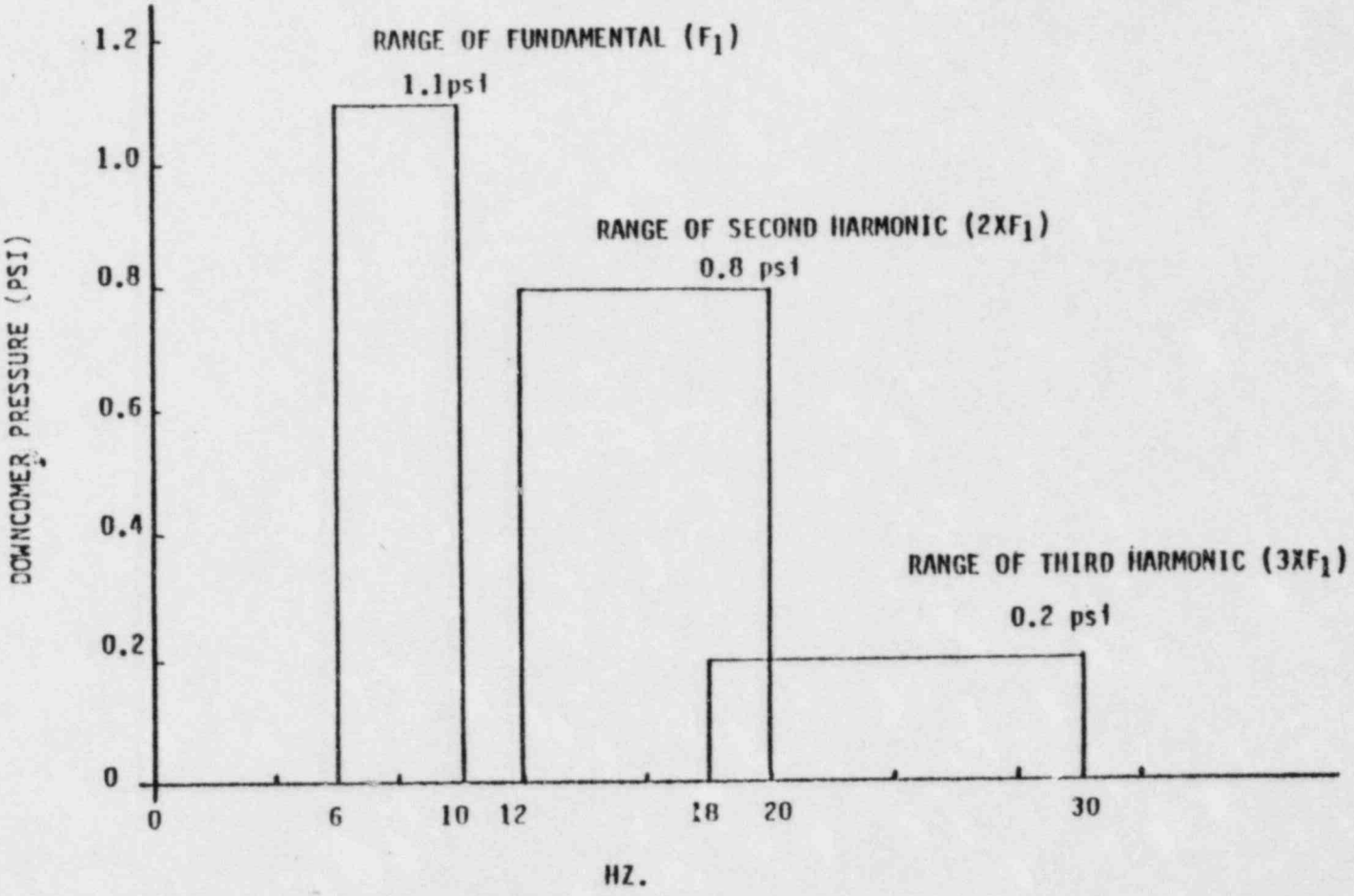

Figure 3.3.2.4-4 Downcomer Pair Internal Pressure Loading for IBA CO

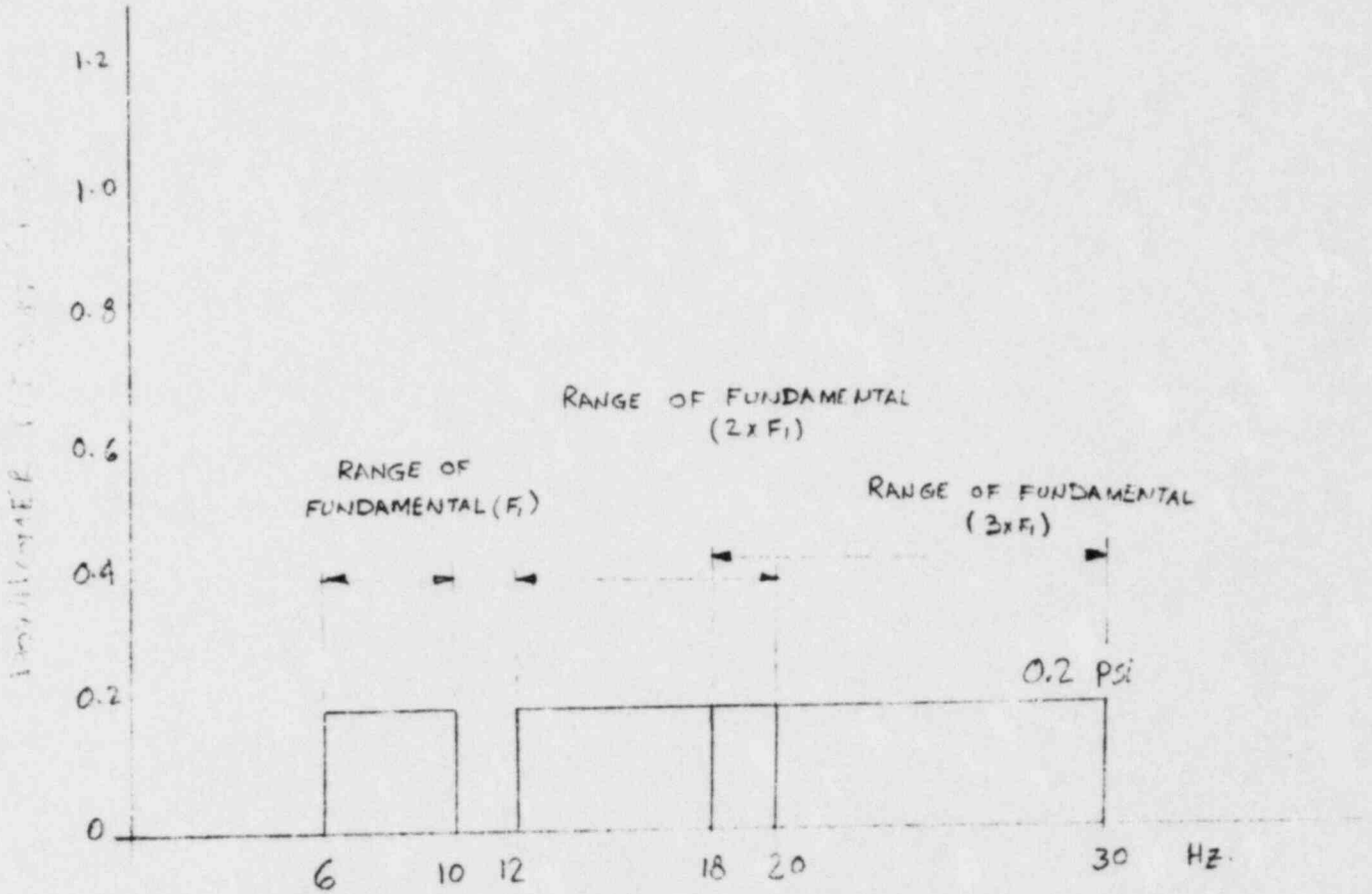

Figure 3.3.2.4-5 Downcomer Pair Differential Pressure Loading for IBA CO

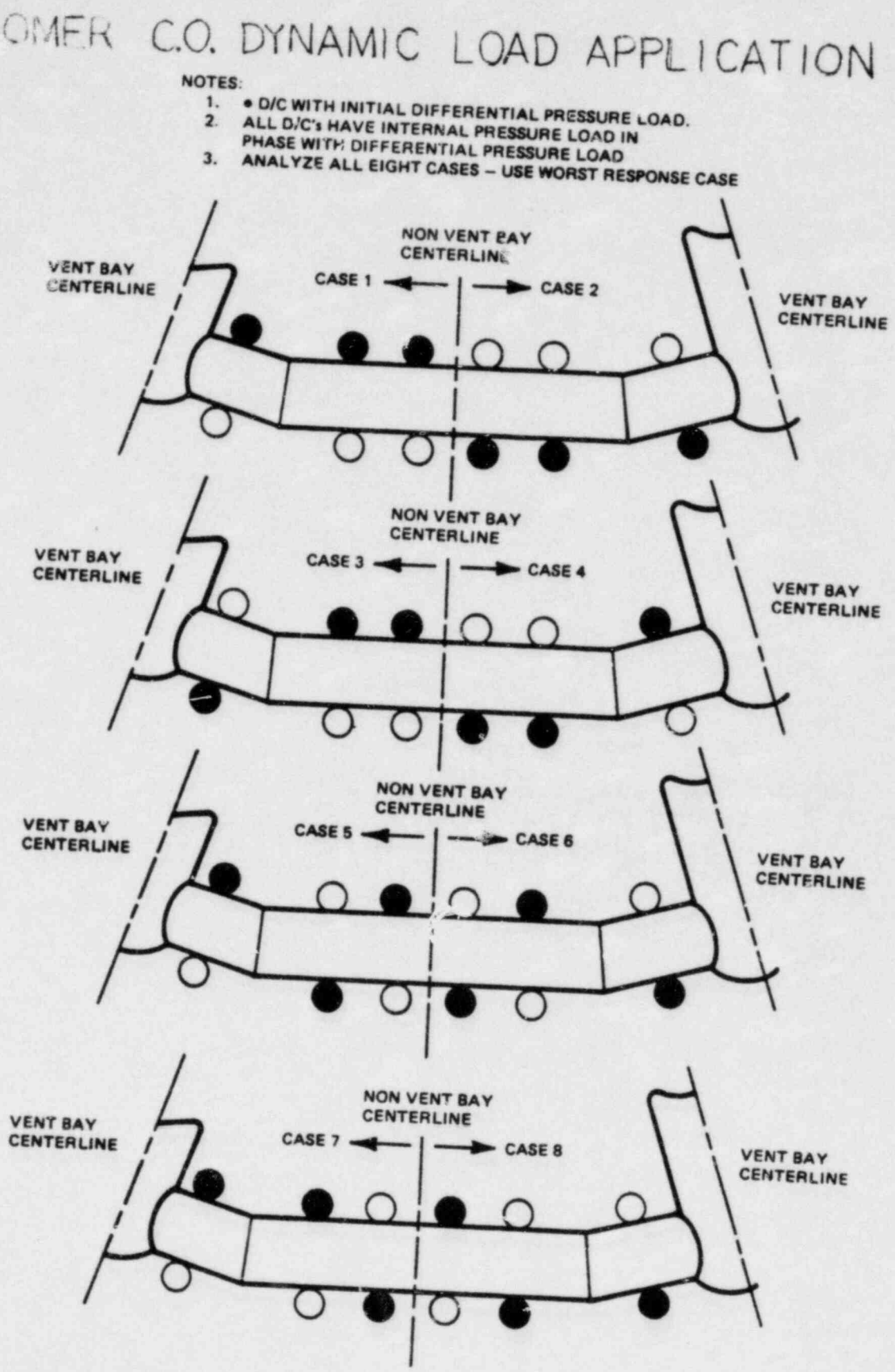

Figure 3.3.2.4-6 Dynamic Load Cases

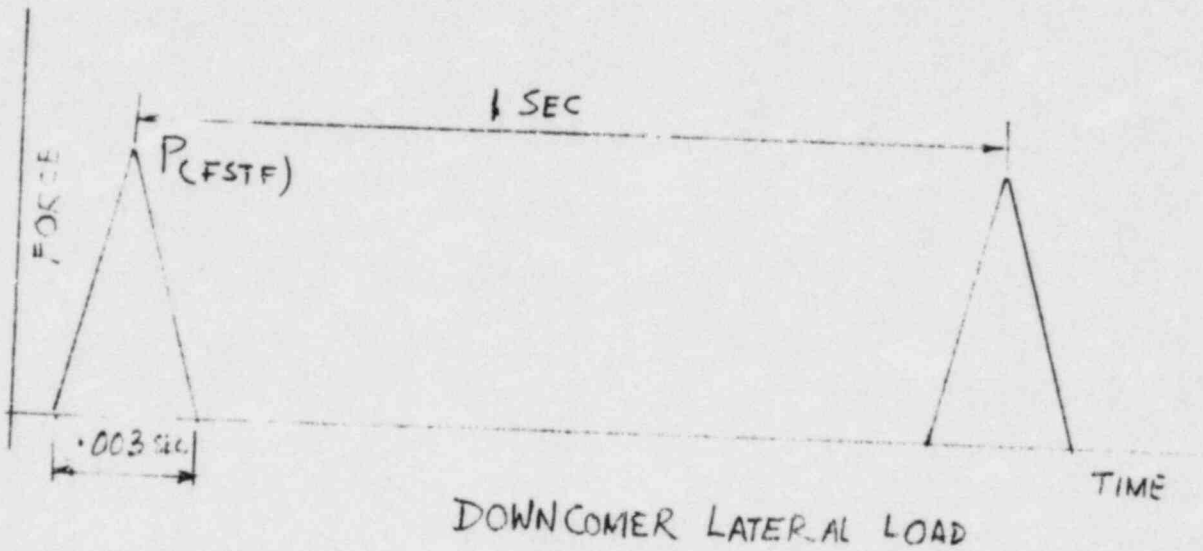

Figure 3.3.2.4-7 Chugging Load Transient

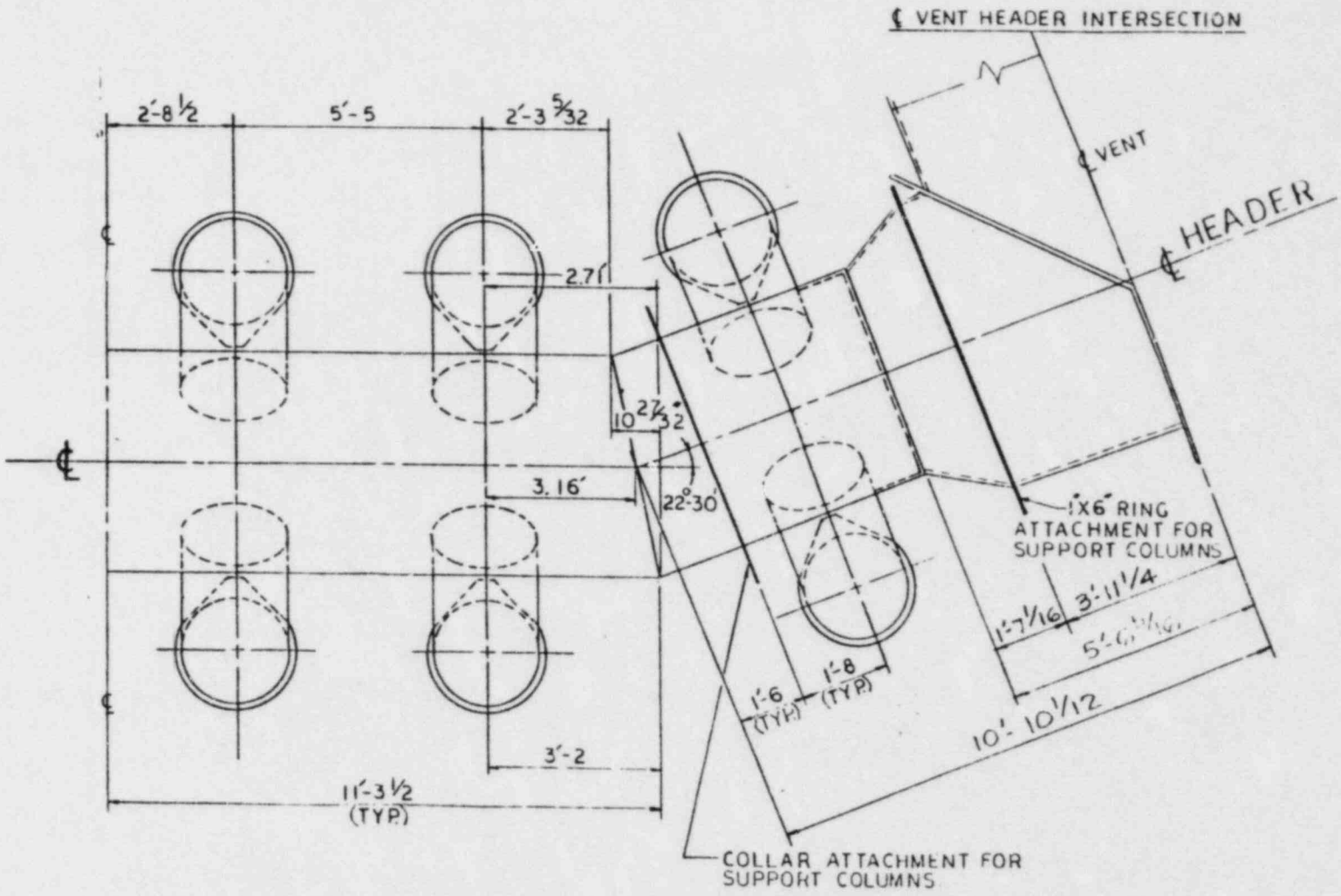

Figure 3.5.2-1 View of 22½° Segment of Vent Header System

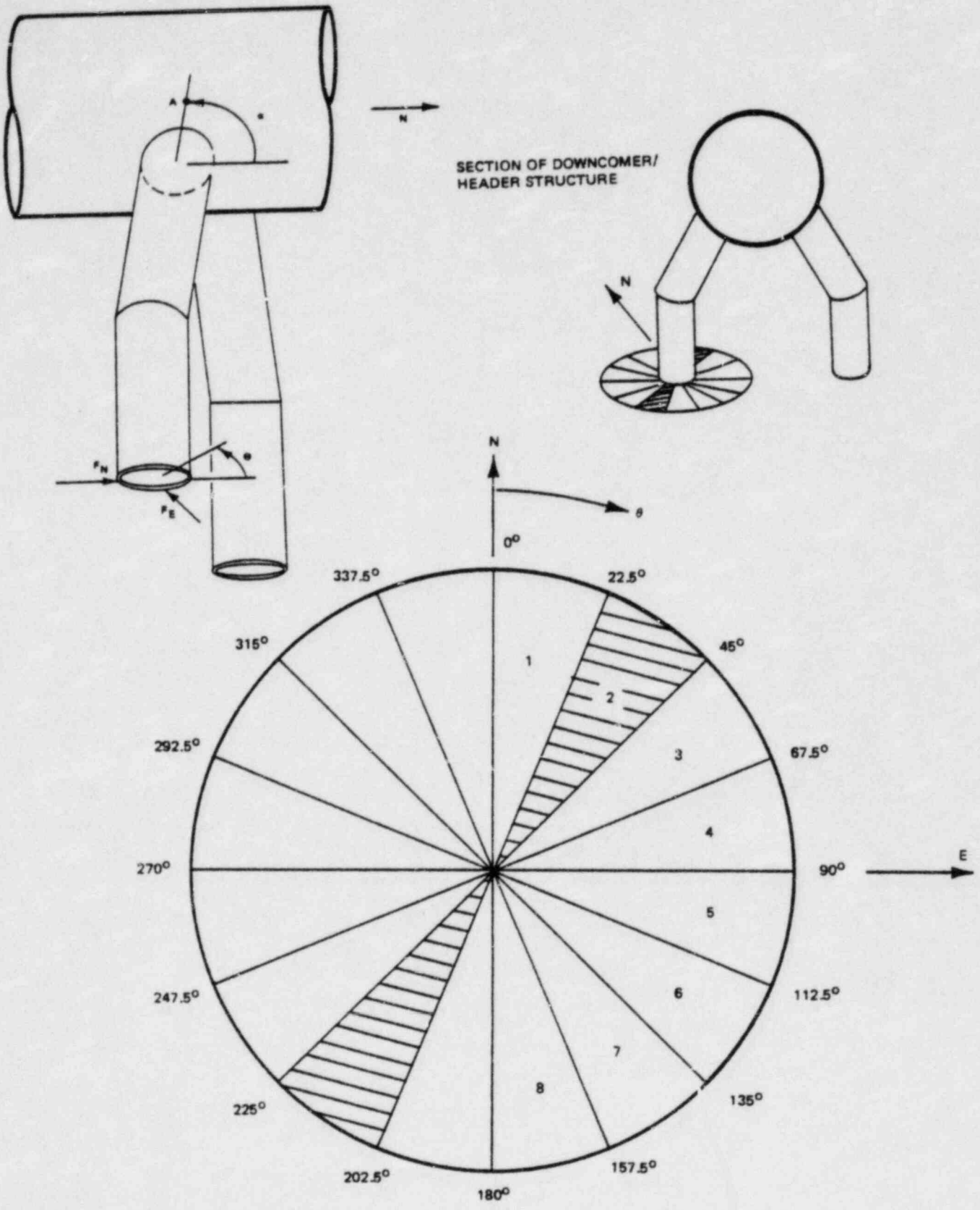

Figure 3.5.3-1 Sectors Used to Define Directions of Lateral Loads on Downcomer Ends

Analysis For Chugging Loads

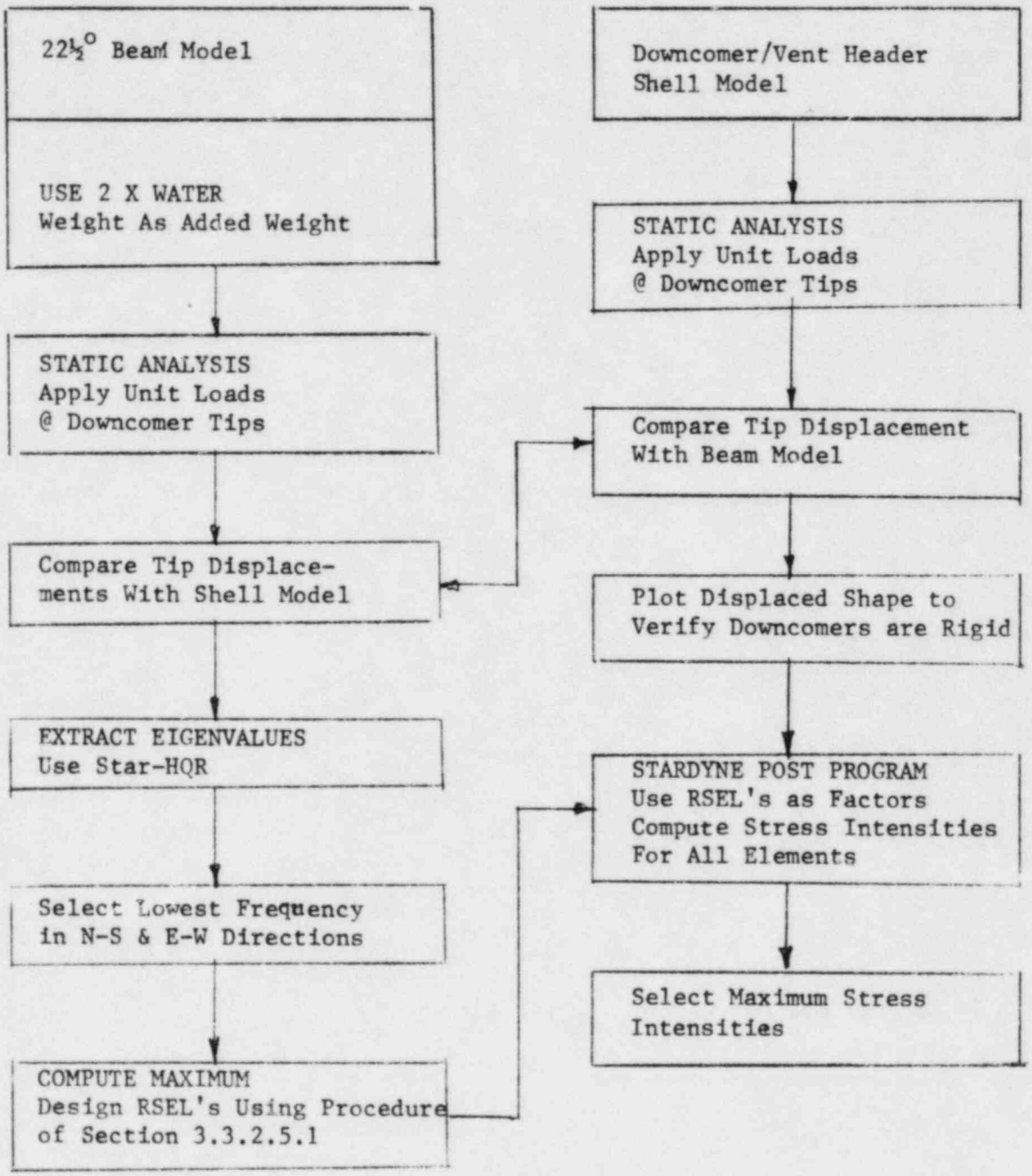

Figure 3.5.3-2 Methods for Analysis for Chugging Load Schematic

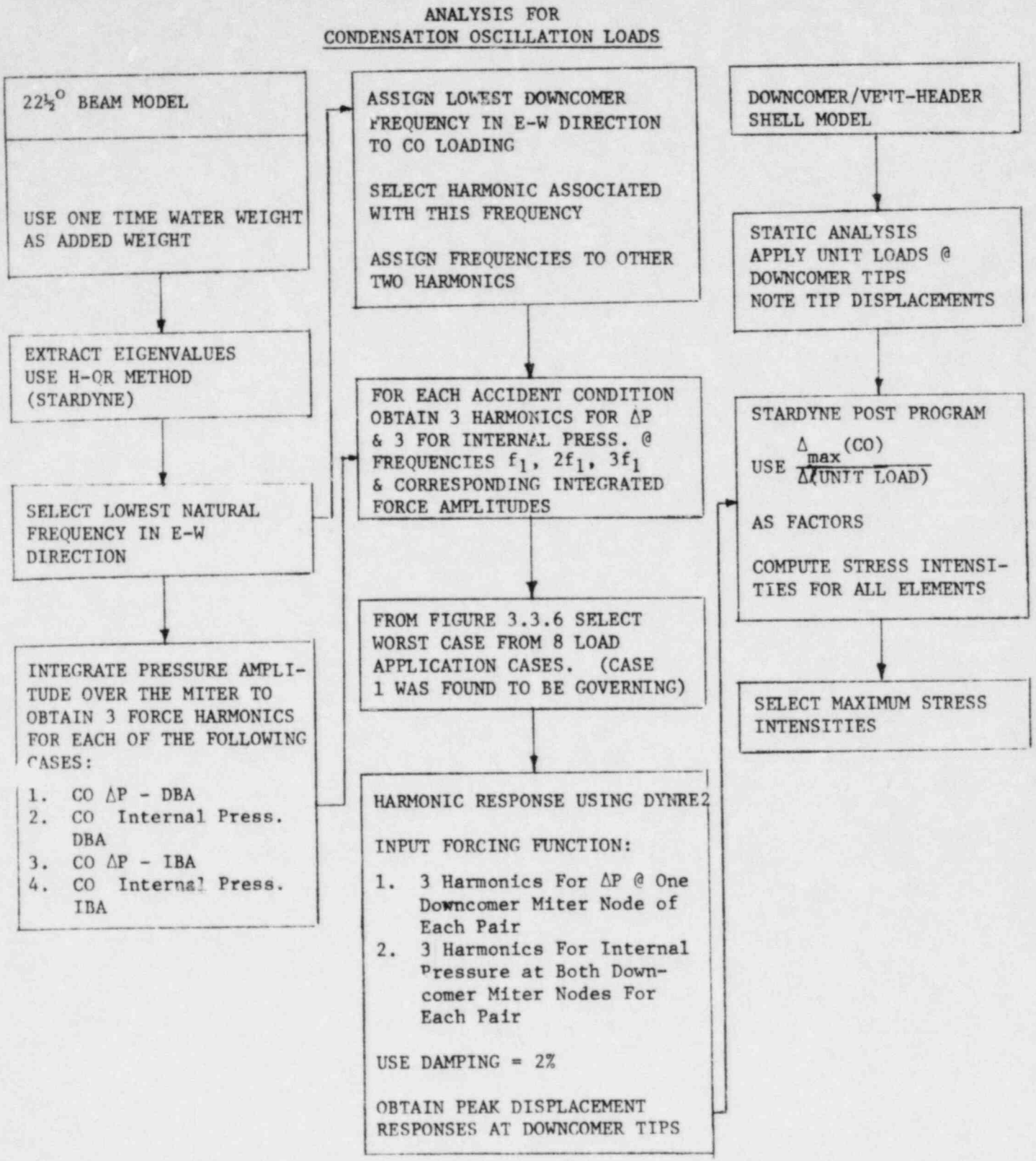

Figure 3.5.4-1 Methods of Analysis for Condensation Oscillation Load Schematic

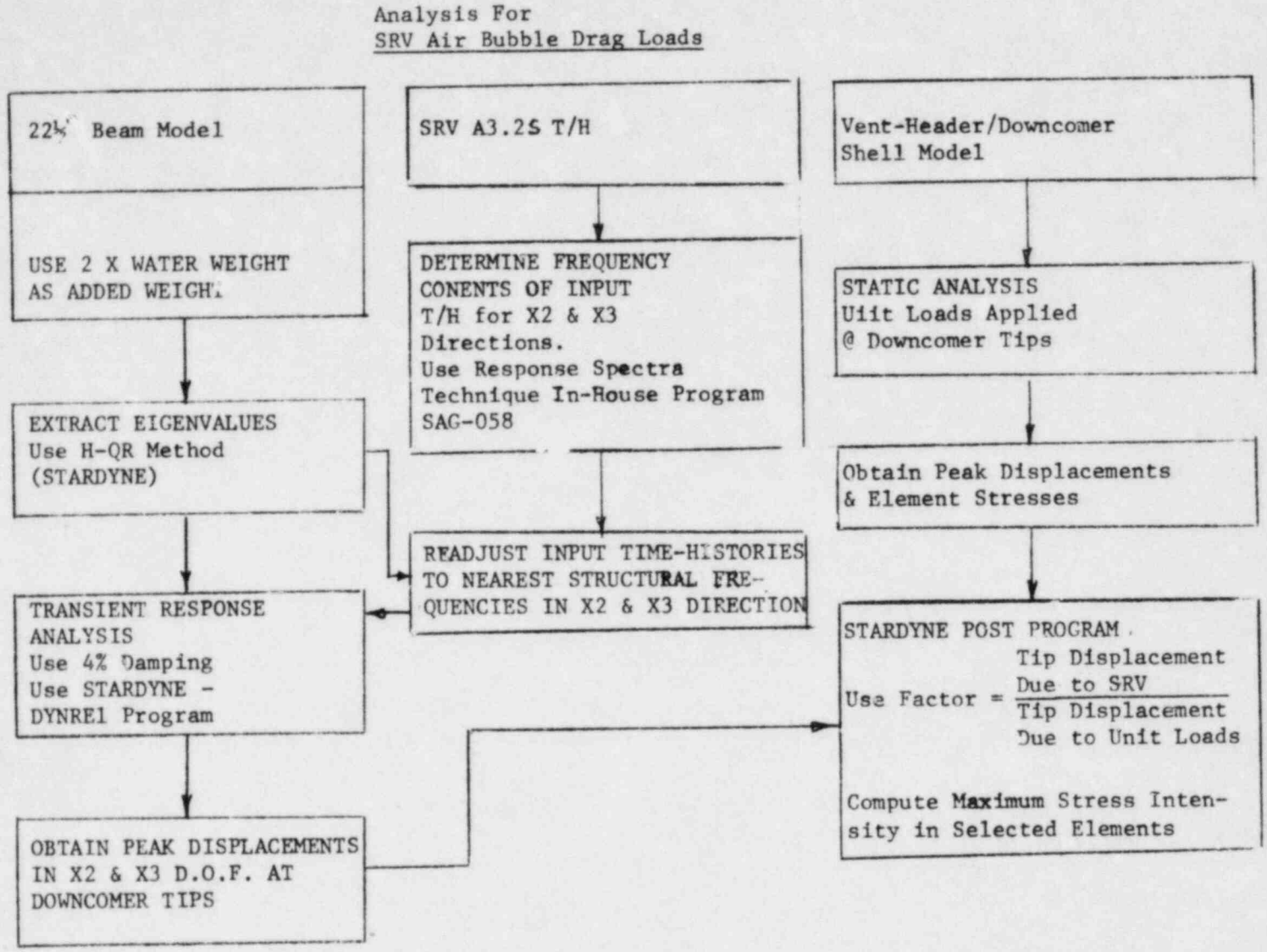

Figure 3.5.5-1 Methods of Analysis for SRV Air Bubble Drag Loads Schematic

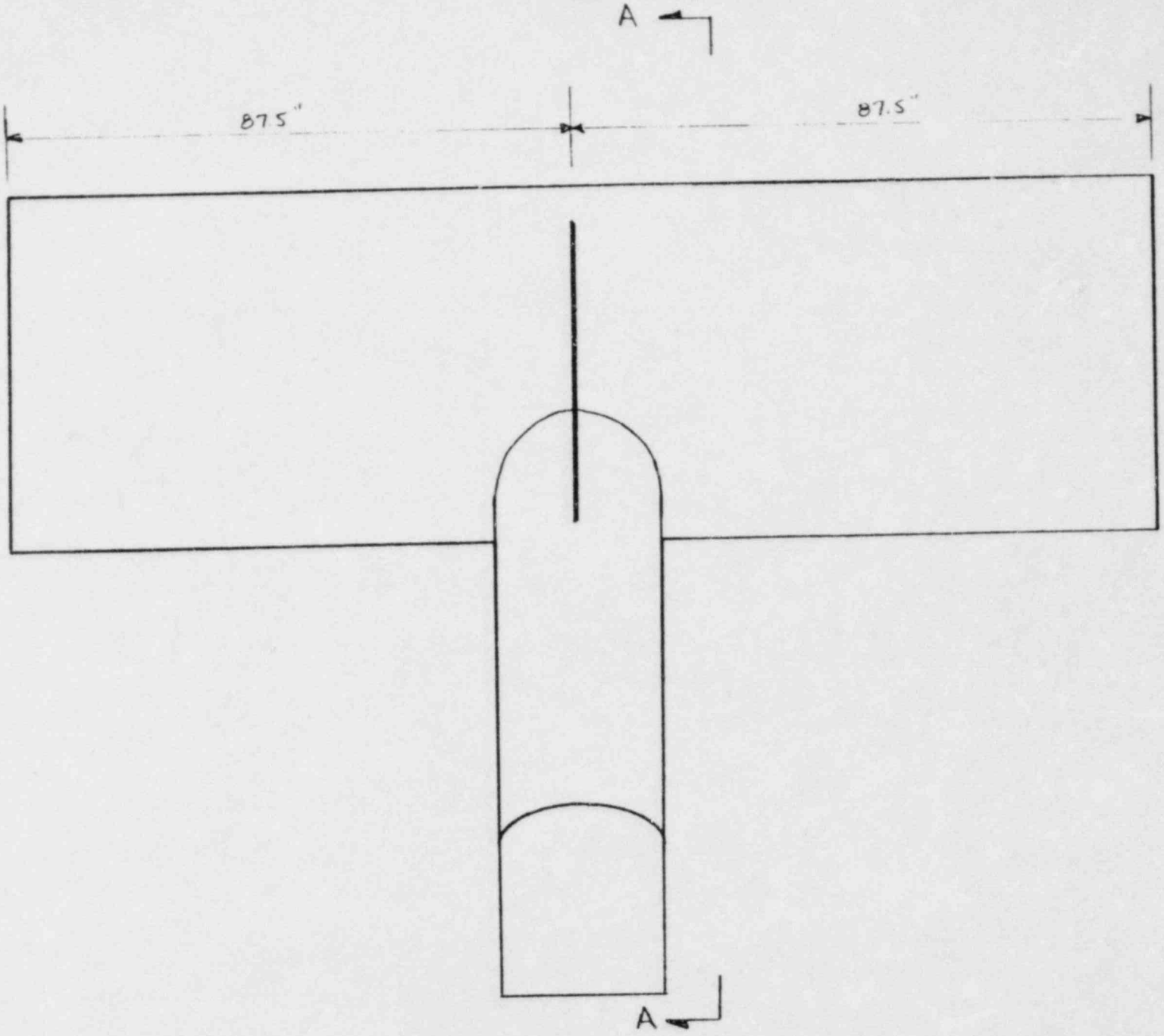

Figure 3.6.1.1-1 Downcomer/Vent Header Projected on X_1 - X_3 Plane

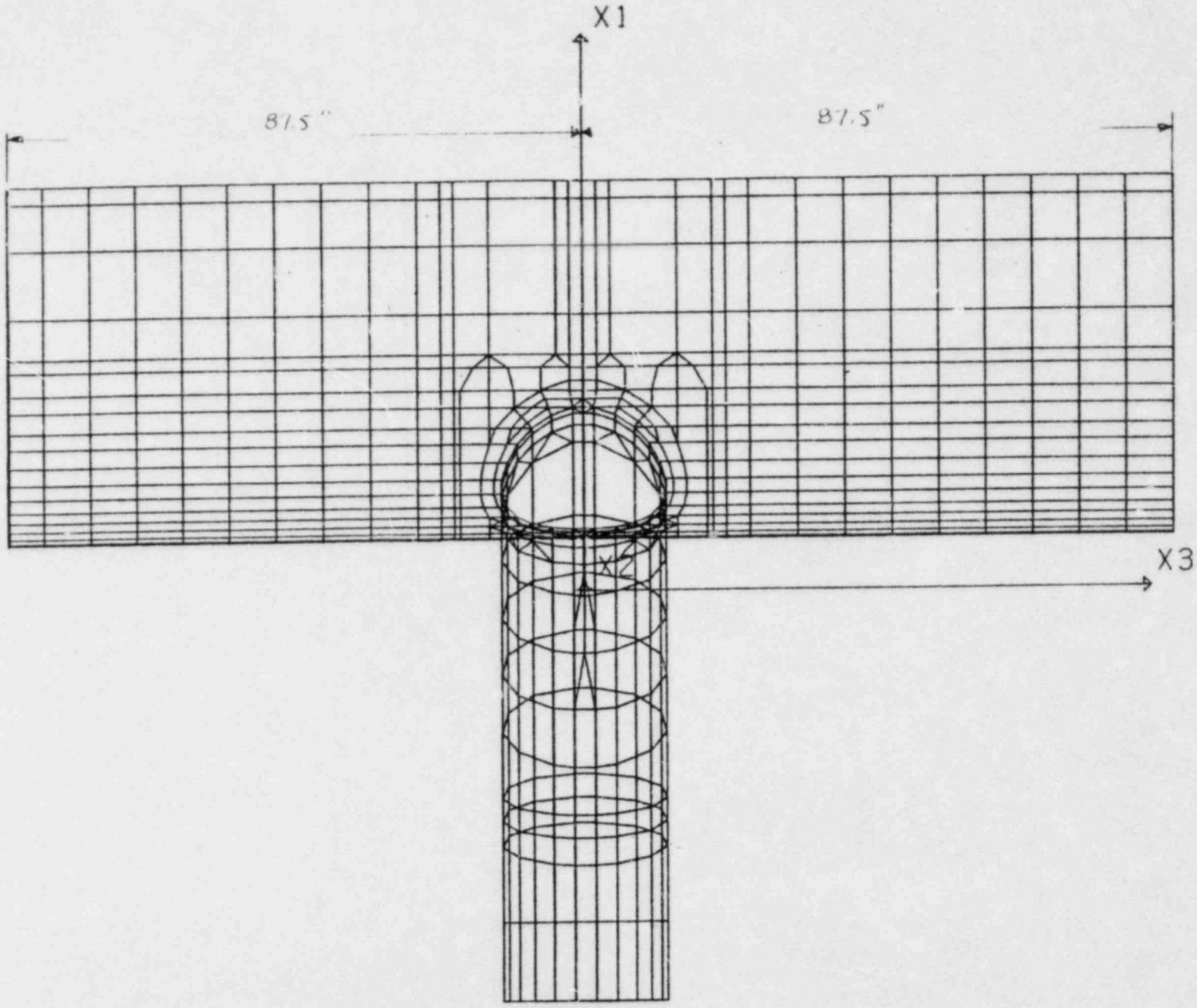

Figure 3.6.1.1-11 Downcomer/Vent Header Finite Element Projection on X_1 - X_3 Plane

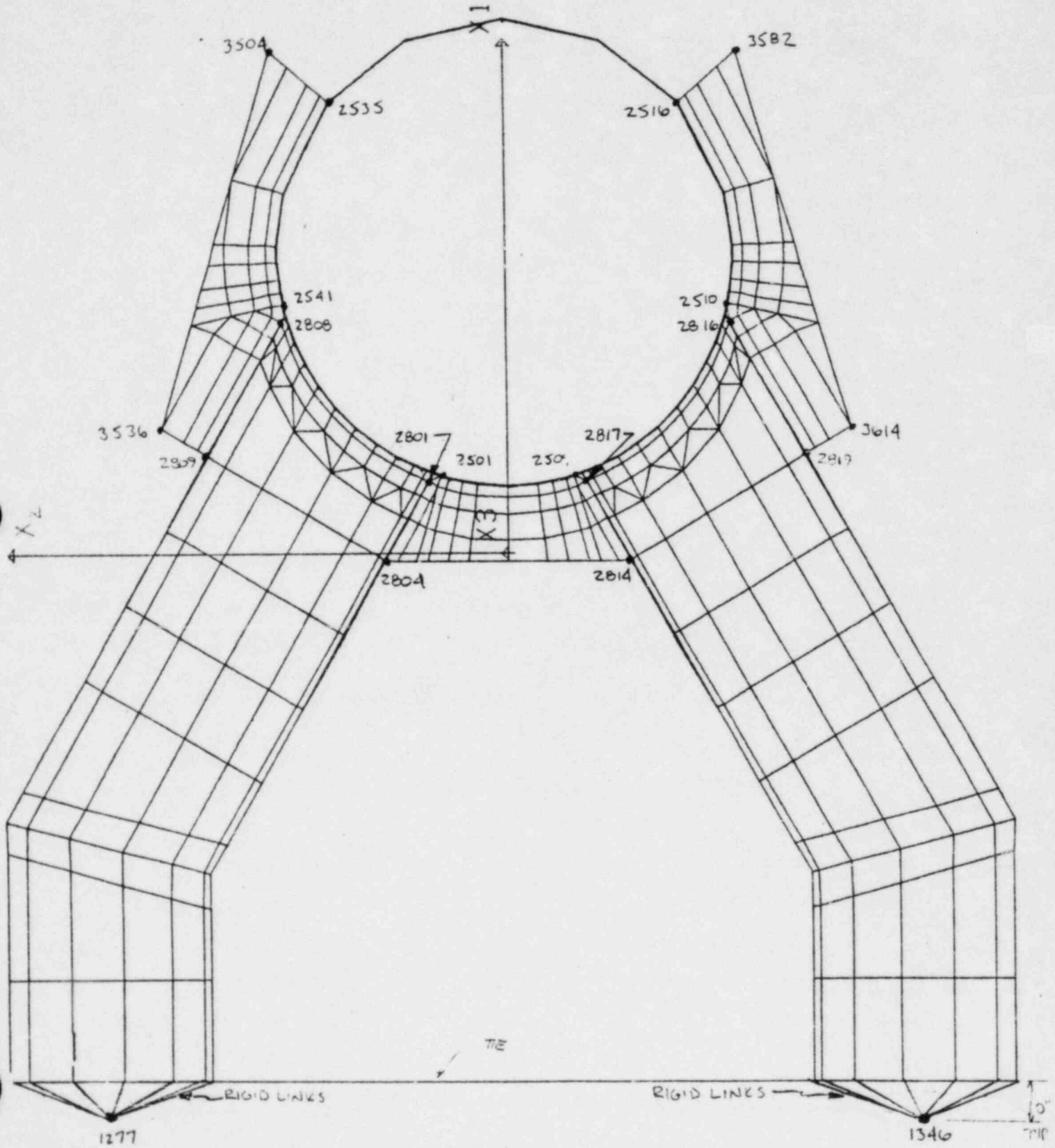

Figure 3.6.1.1-12 Downcomer/Vent Header Finite Element Projection on X_1 - X_2 Plane

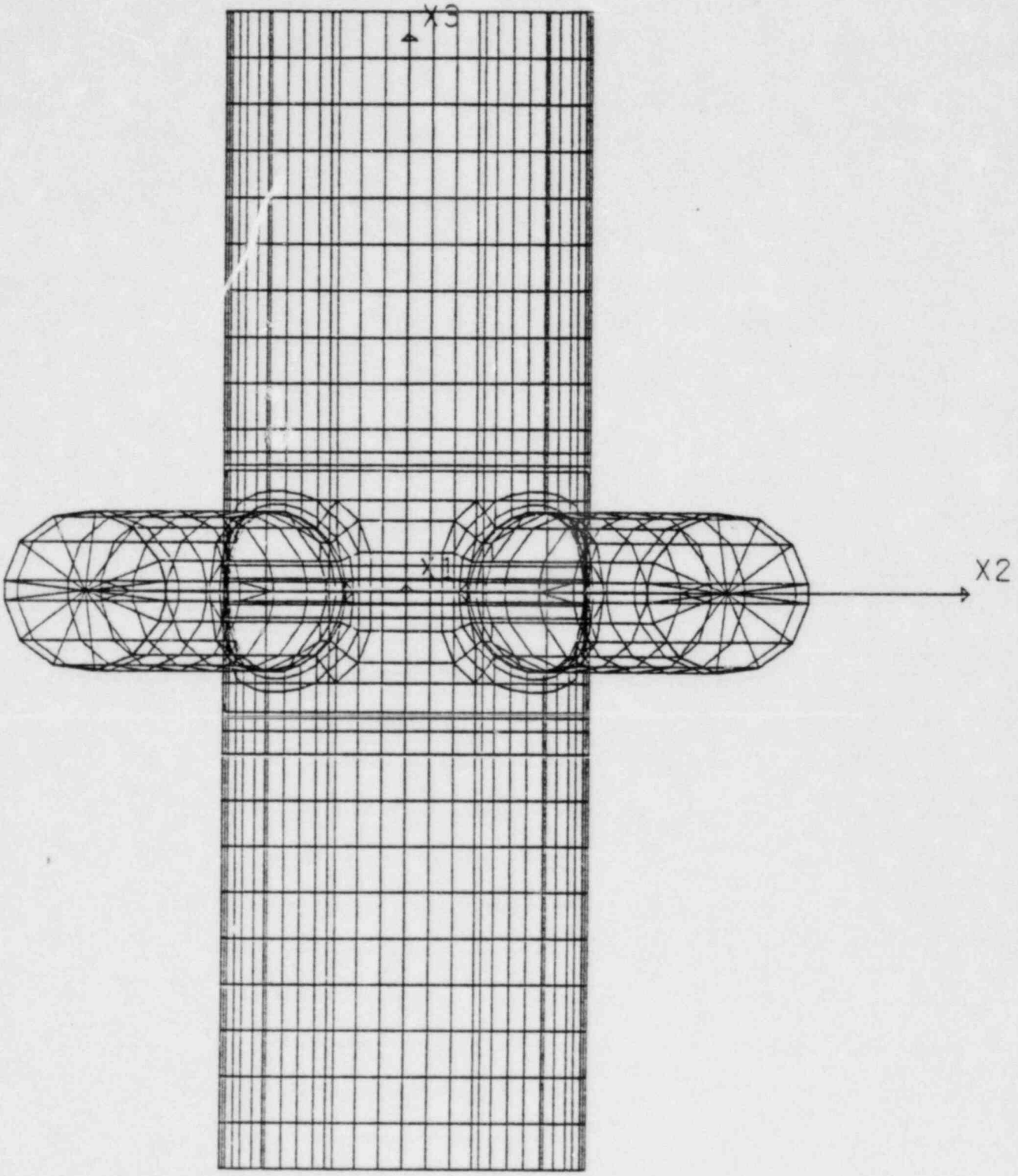

Figure 3.6.1.1-13 Downcomer/Vent Header Finite Element Projection on X_2 - X_3 Plane

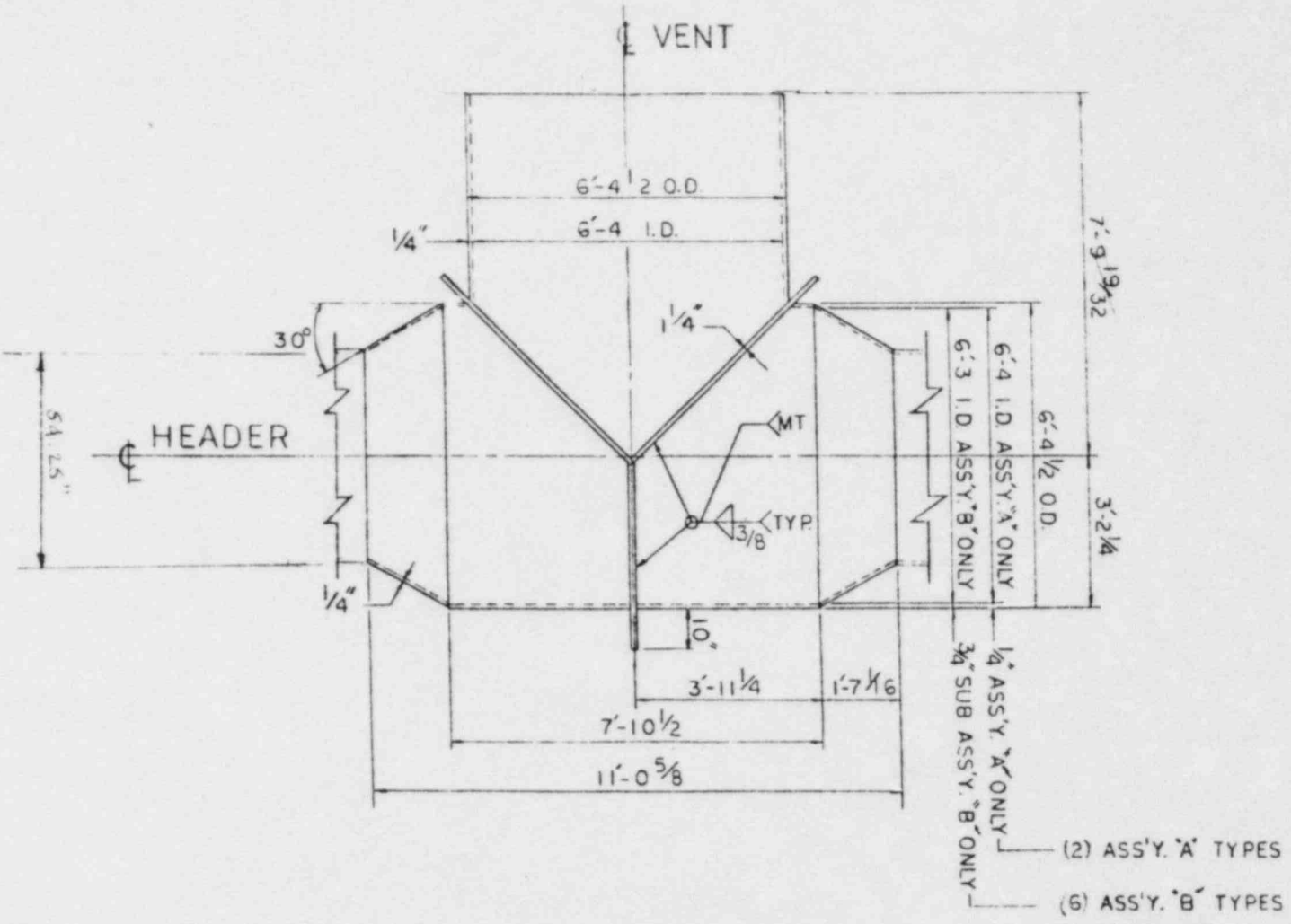

Figure 3.6.1.2-1 Vent & Vent Header Intersection

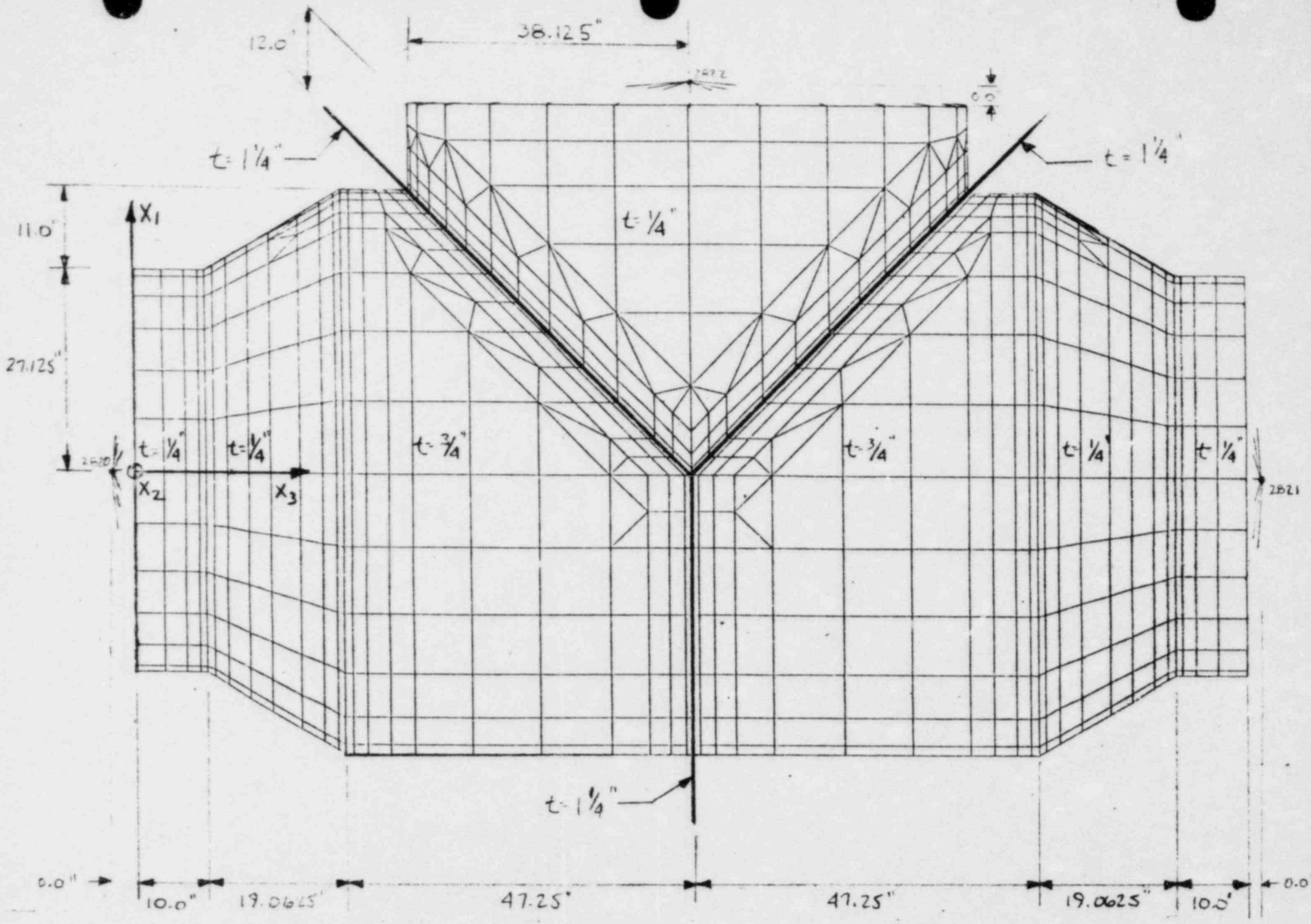

Figure 3.6.1.2-2 Geometry of Vent/Vent Header Intersection

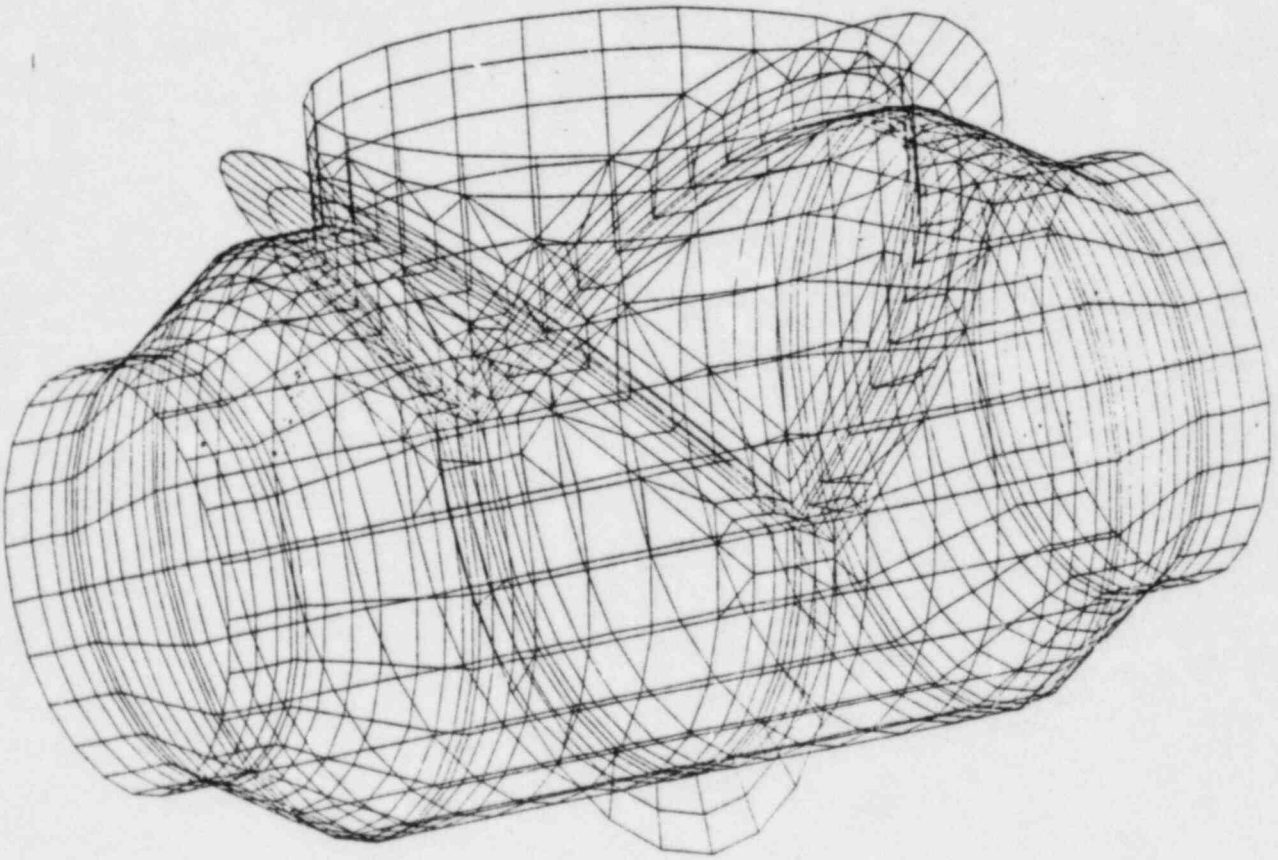

Figure 3.6.1.2-3 Vent Header System Shell Model 3

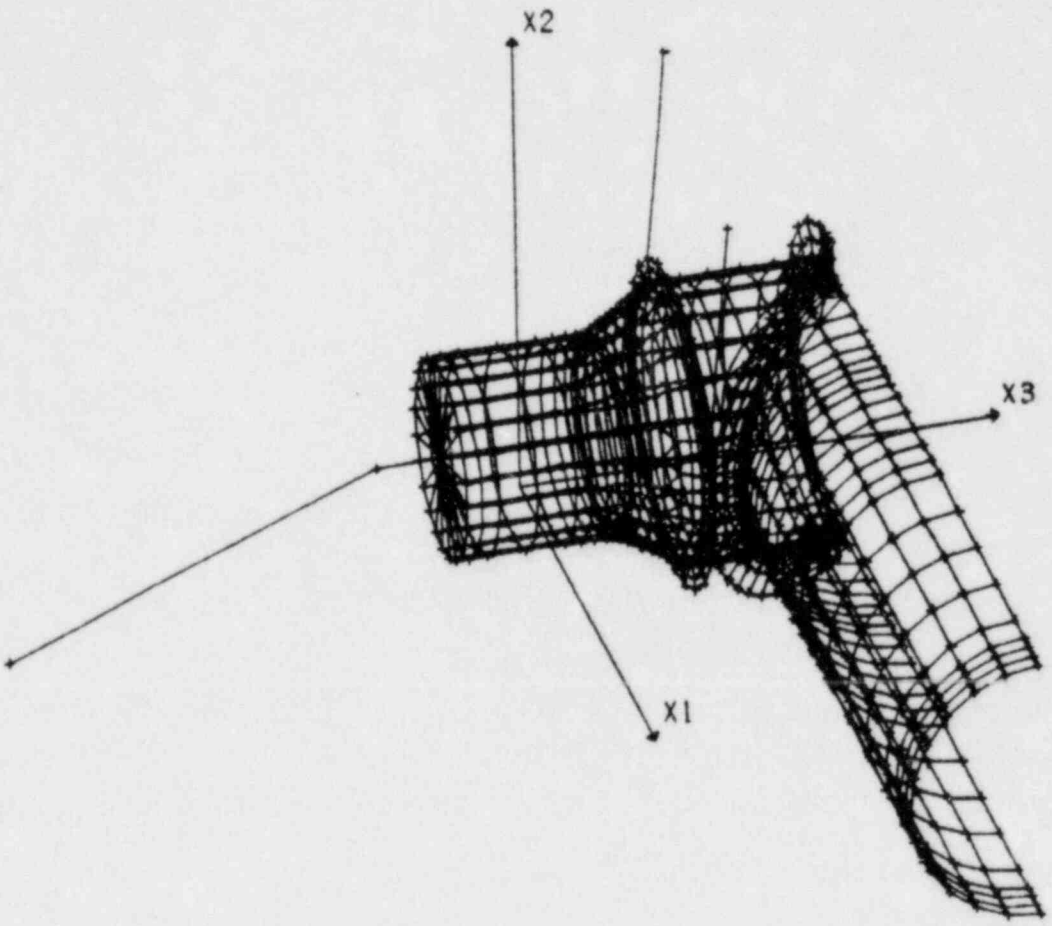

Figure 3.6.1.3-1 Half Shell Model 3

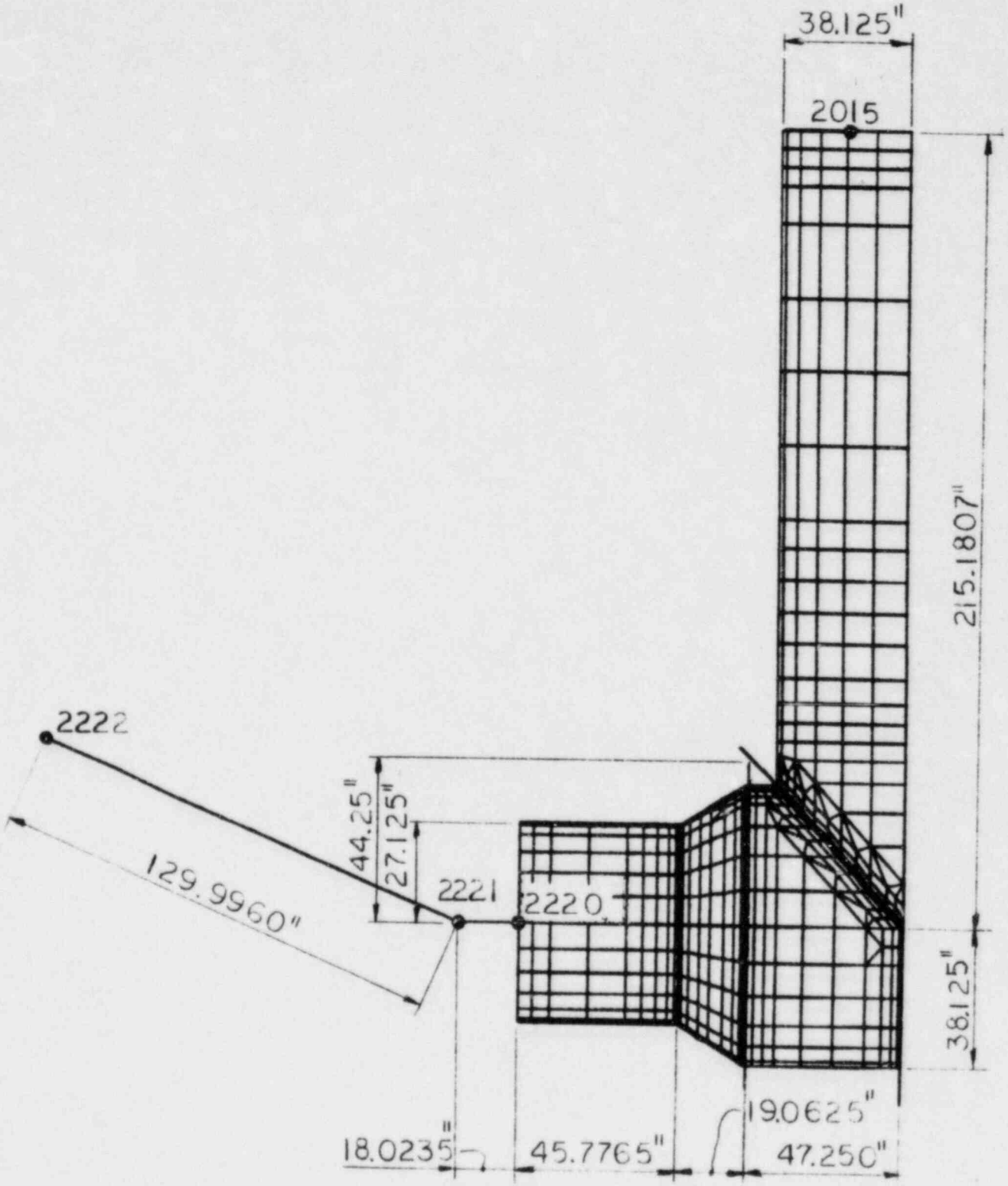

Figure 3.6.1.3-2 Half Shell Model 3 Plan View

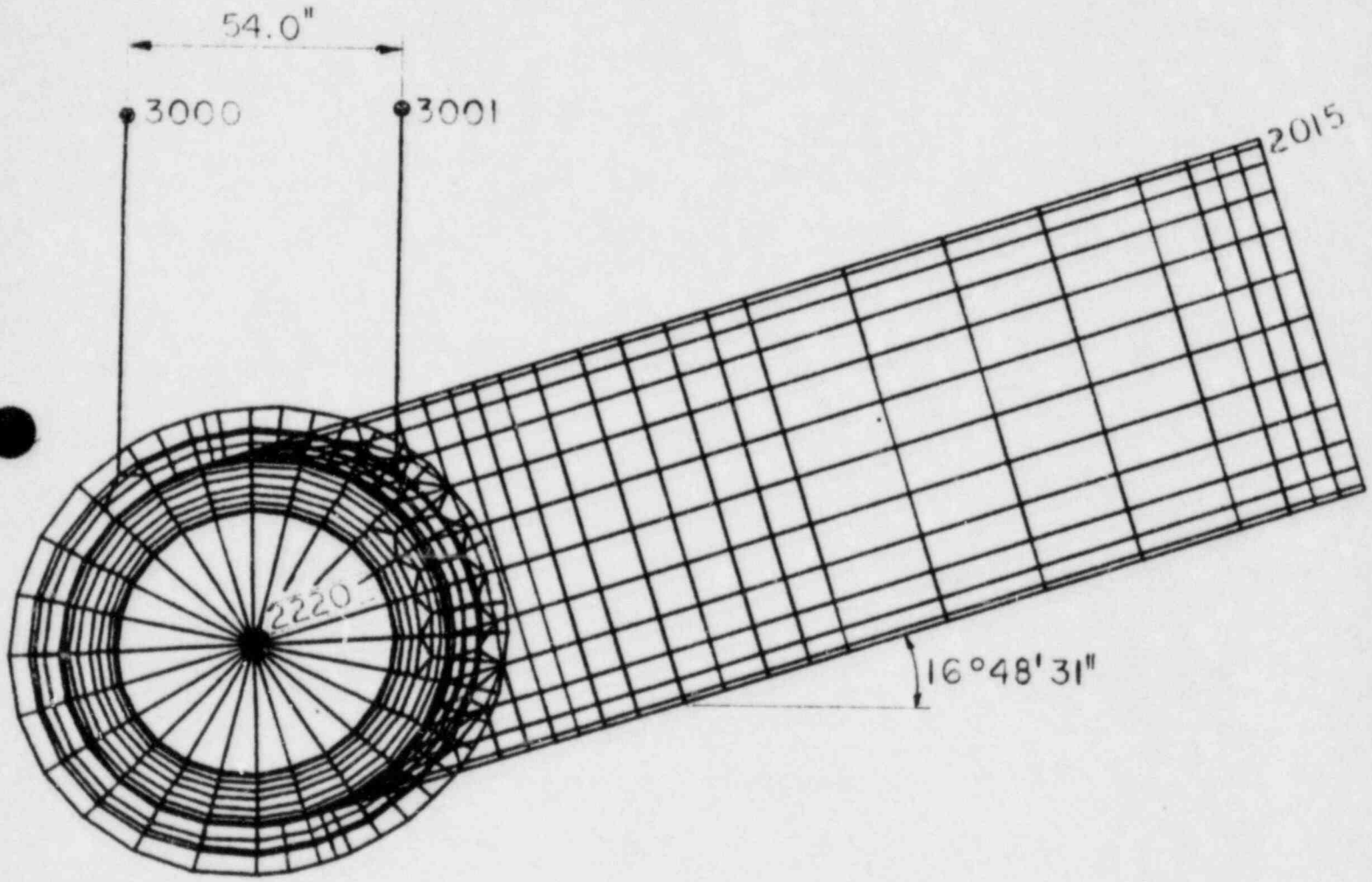

Figure 3.6.1.3-3 Half Shell Model 3 Looking Along the Vent-Header

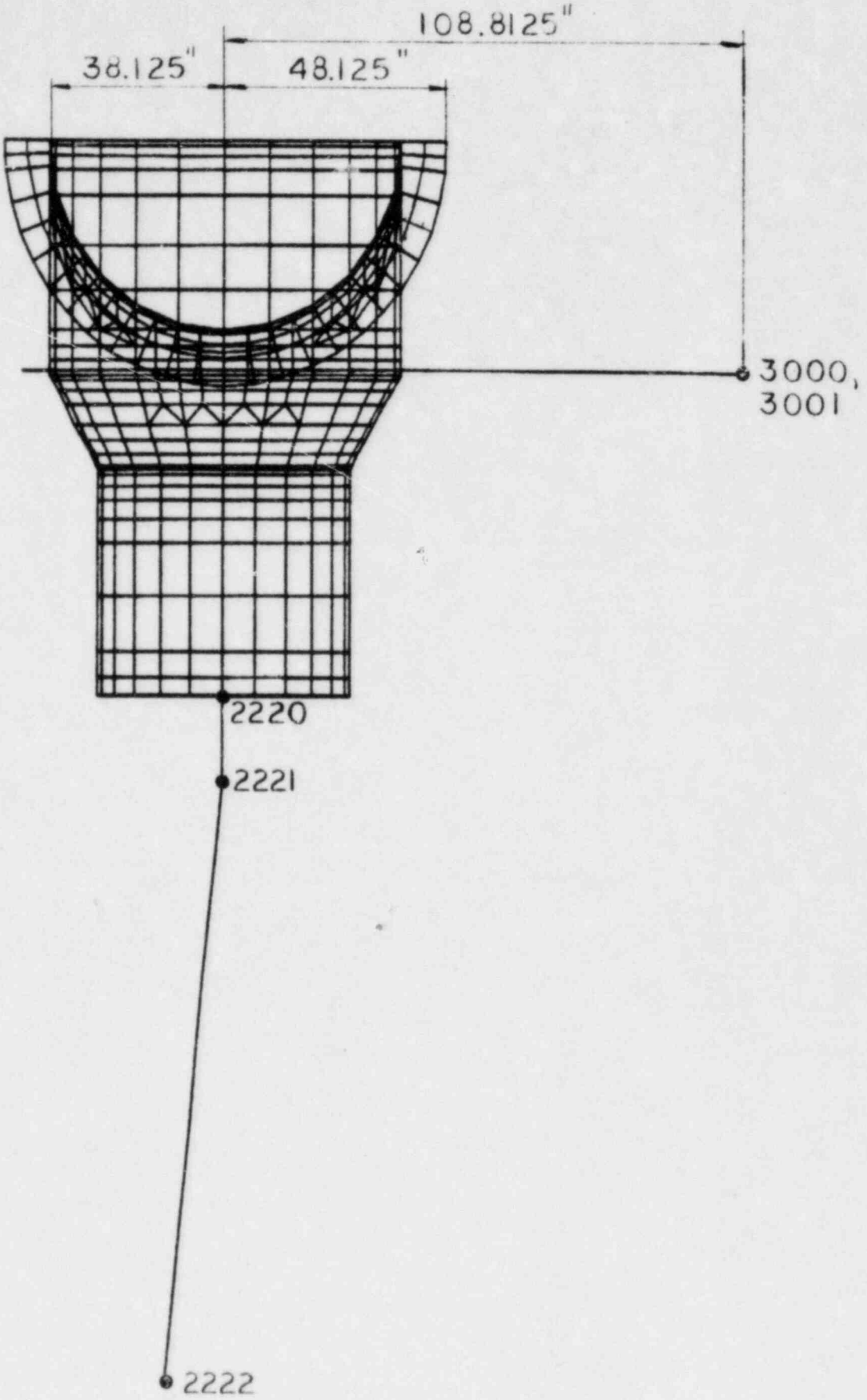

Figure 3.6.1.3-4 Half Shell Model 3 Looking Down the Vent

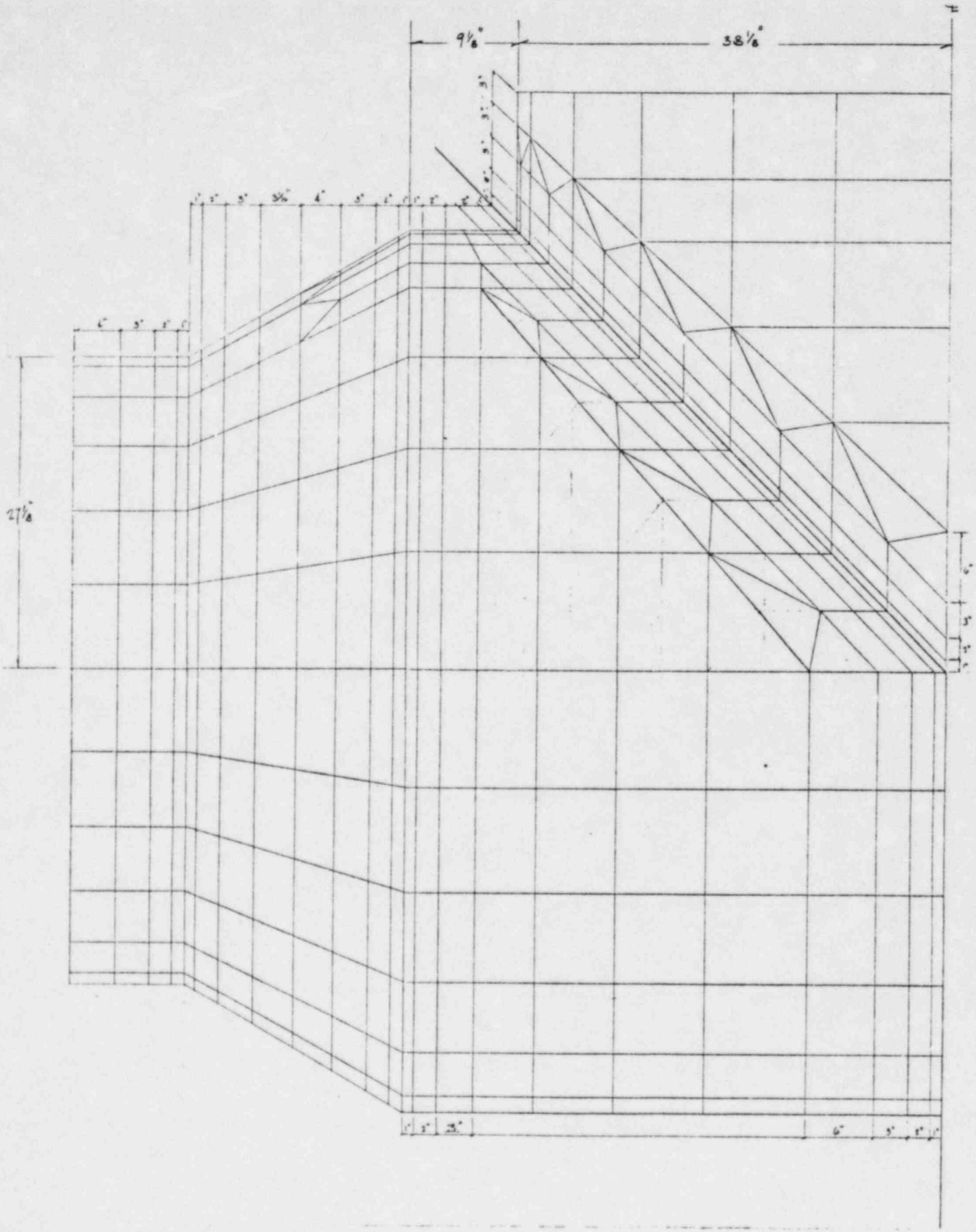

Figure 3.6.1.3-5 Vent Header Intersection Finite Element Mesh
Half Shell Model 3

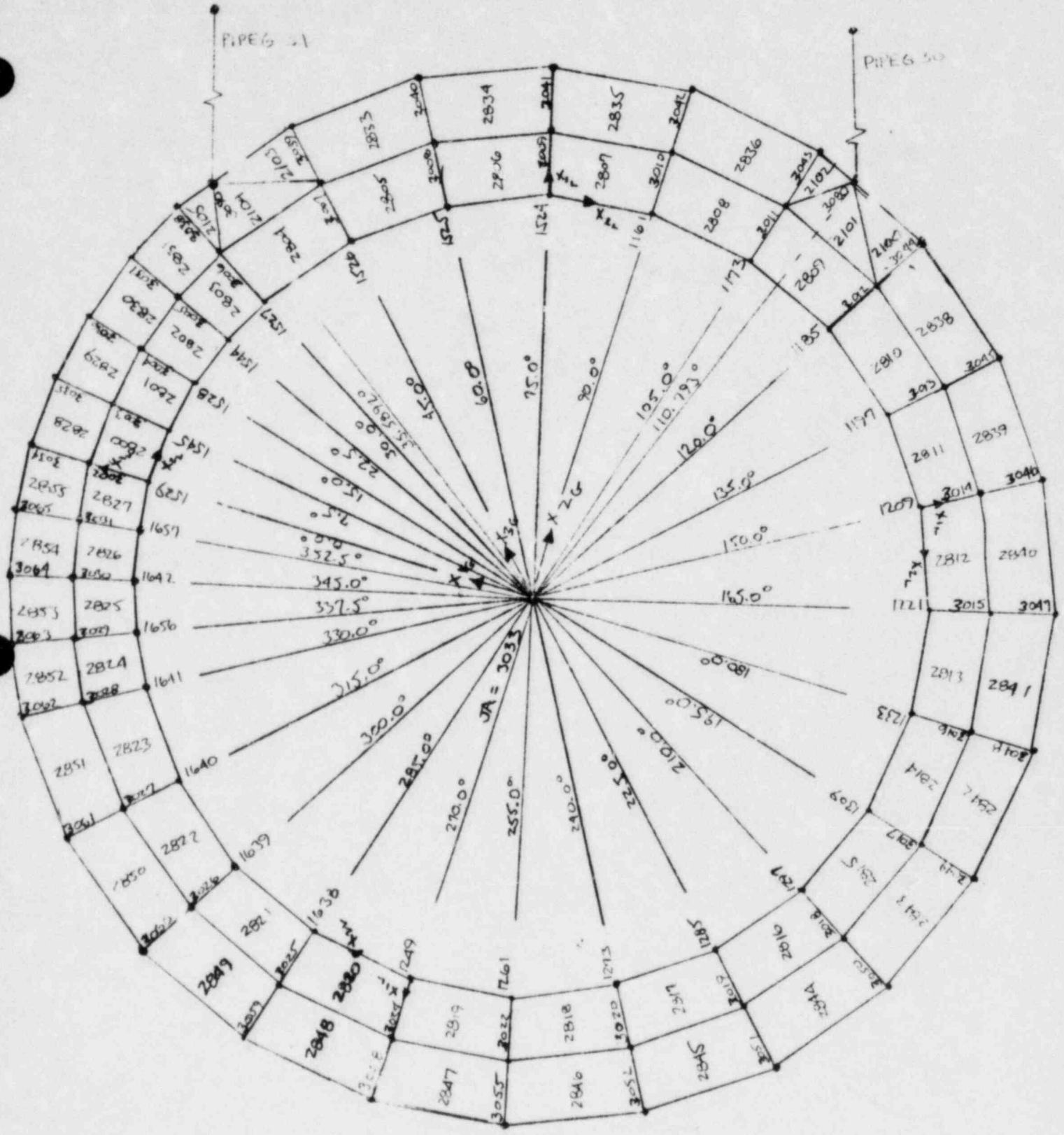

Figure 3.6.1.3-6 Stiffener Ring Finite Element Mesh
Half Shell Model 3

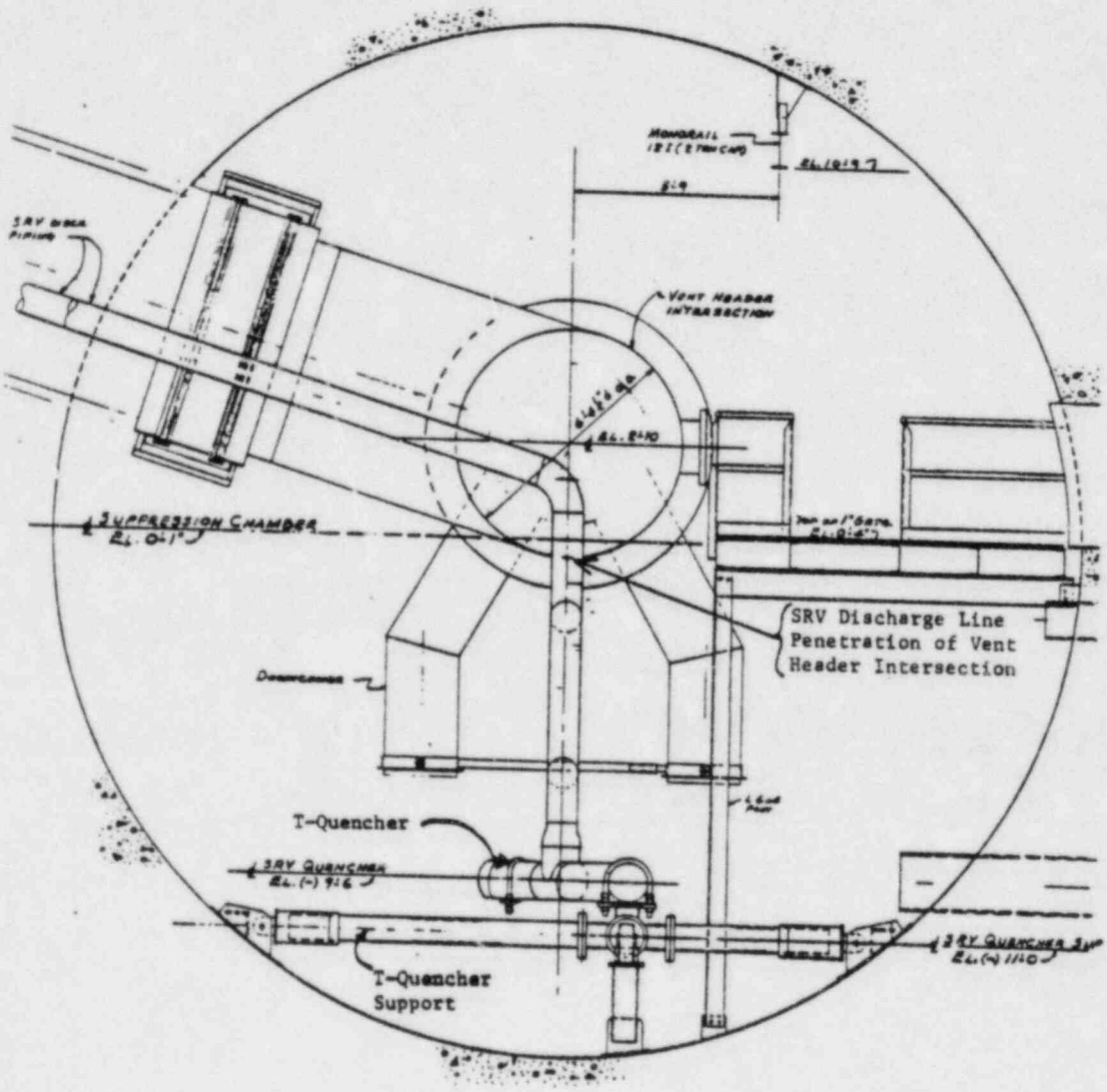

Figure 3.6.1.4-1 Location of SRV Discharge Line in Suppression Chamber

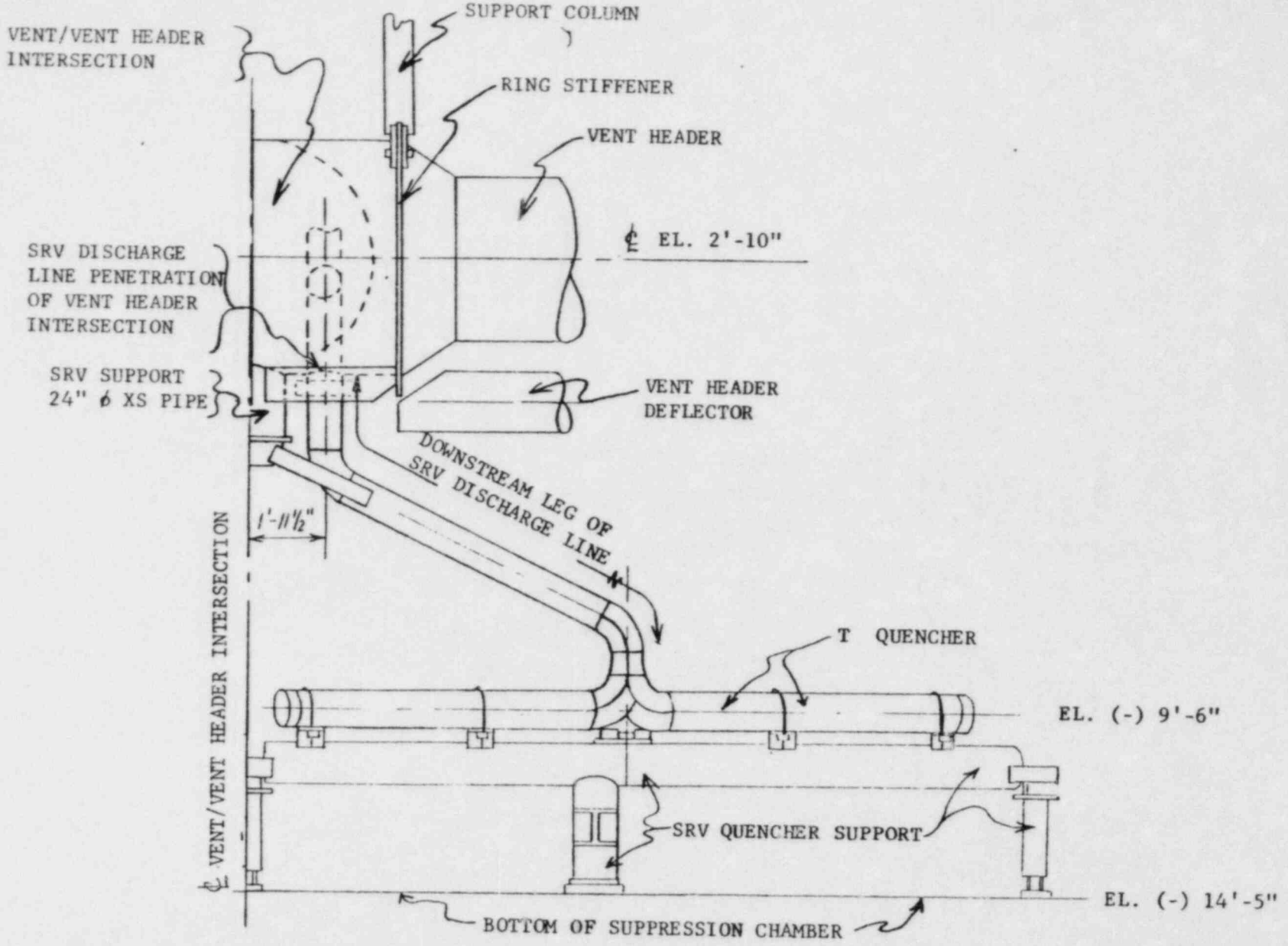

Figure 3.6.1.4-2 Location of SRV Discharge Line in Relation to the Vent Header Intersection

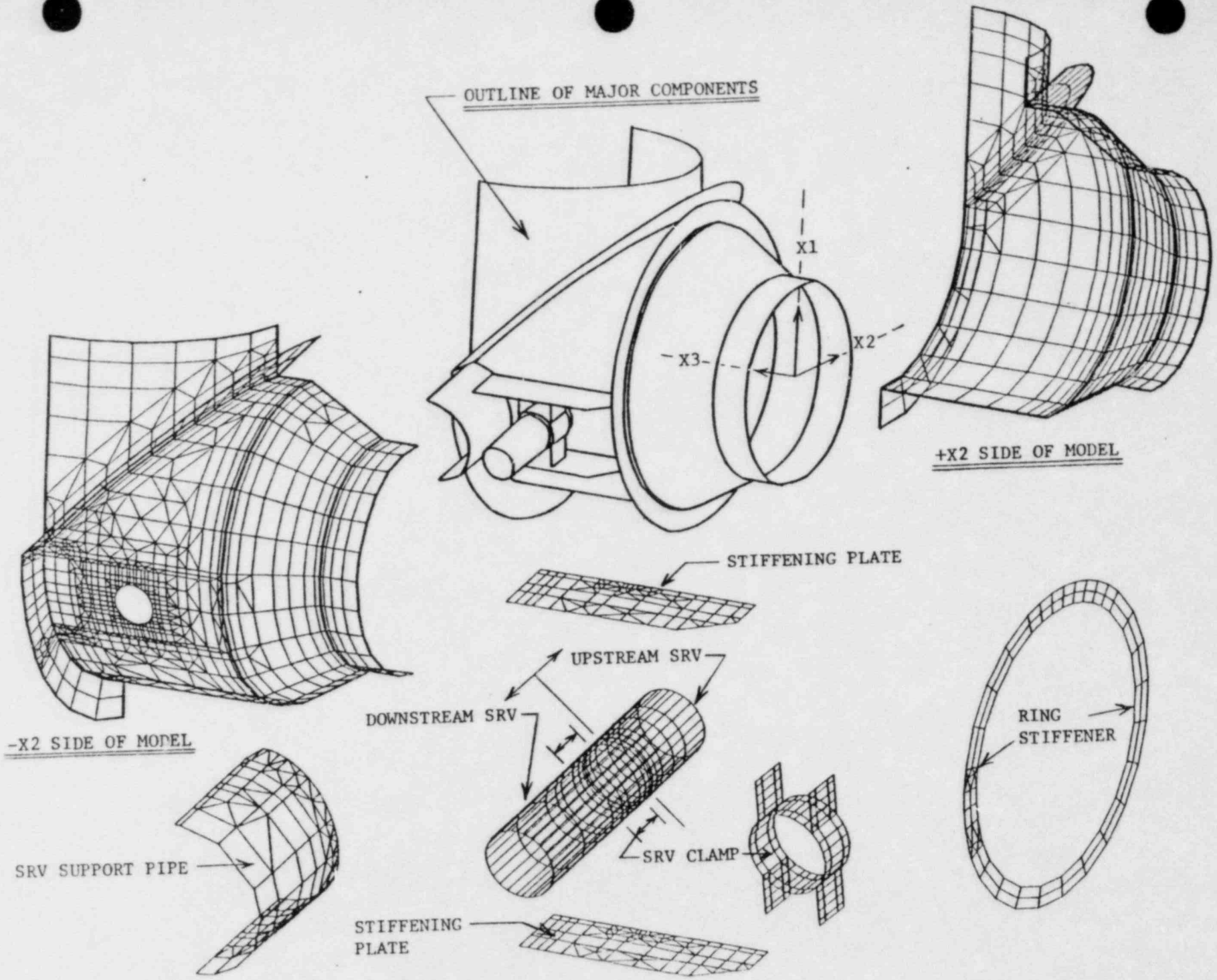

Figure 3.6.1.4-3 Components of SRV Penetration Finite Element Model

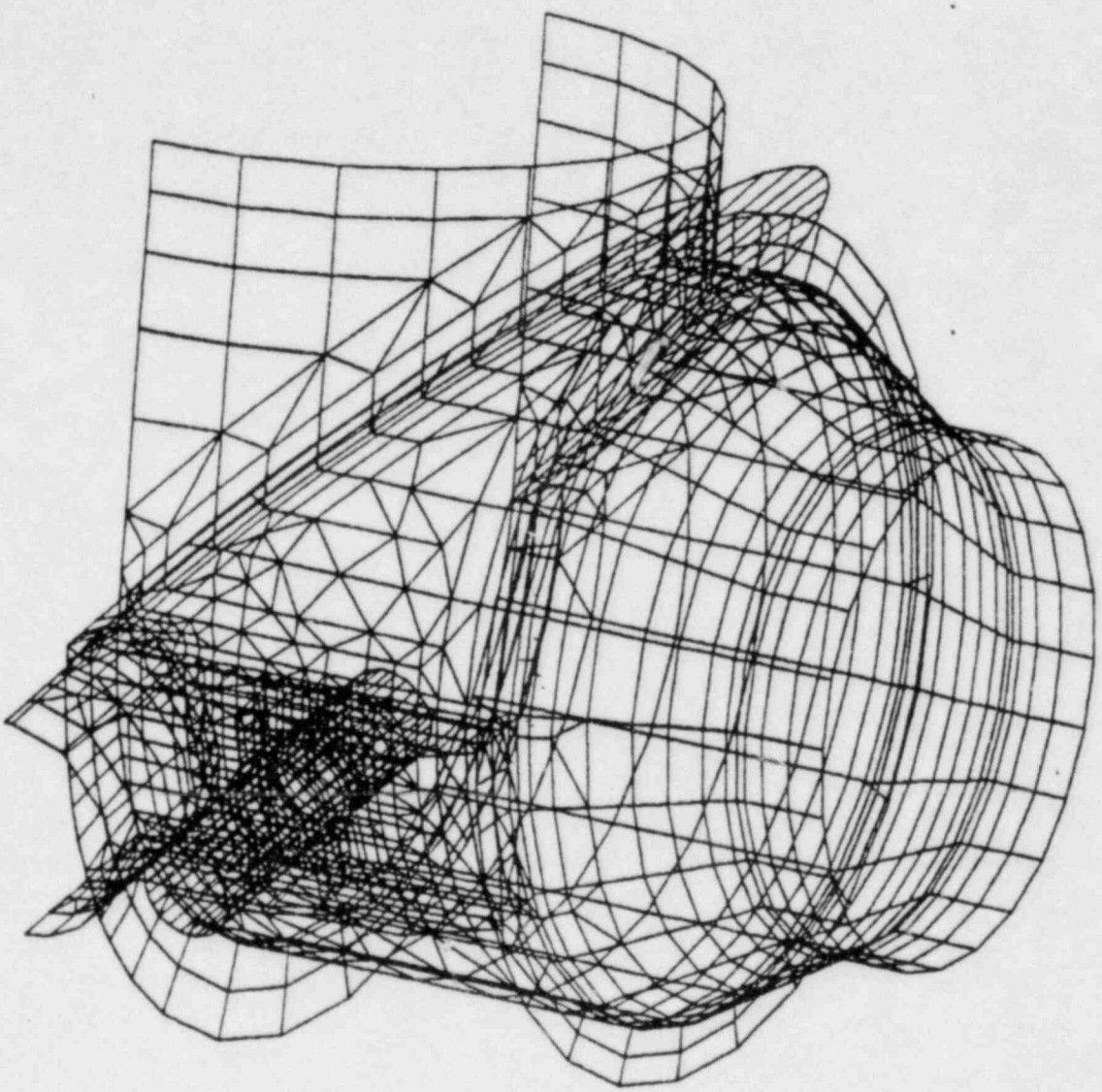

Figure 3.6.1.4-4 SRV Penetration Finite Element Model

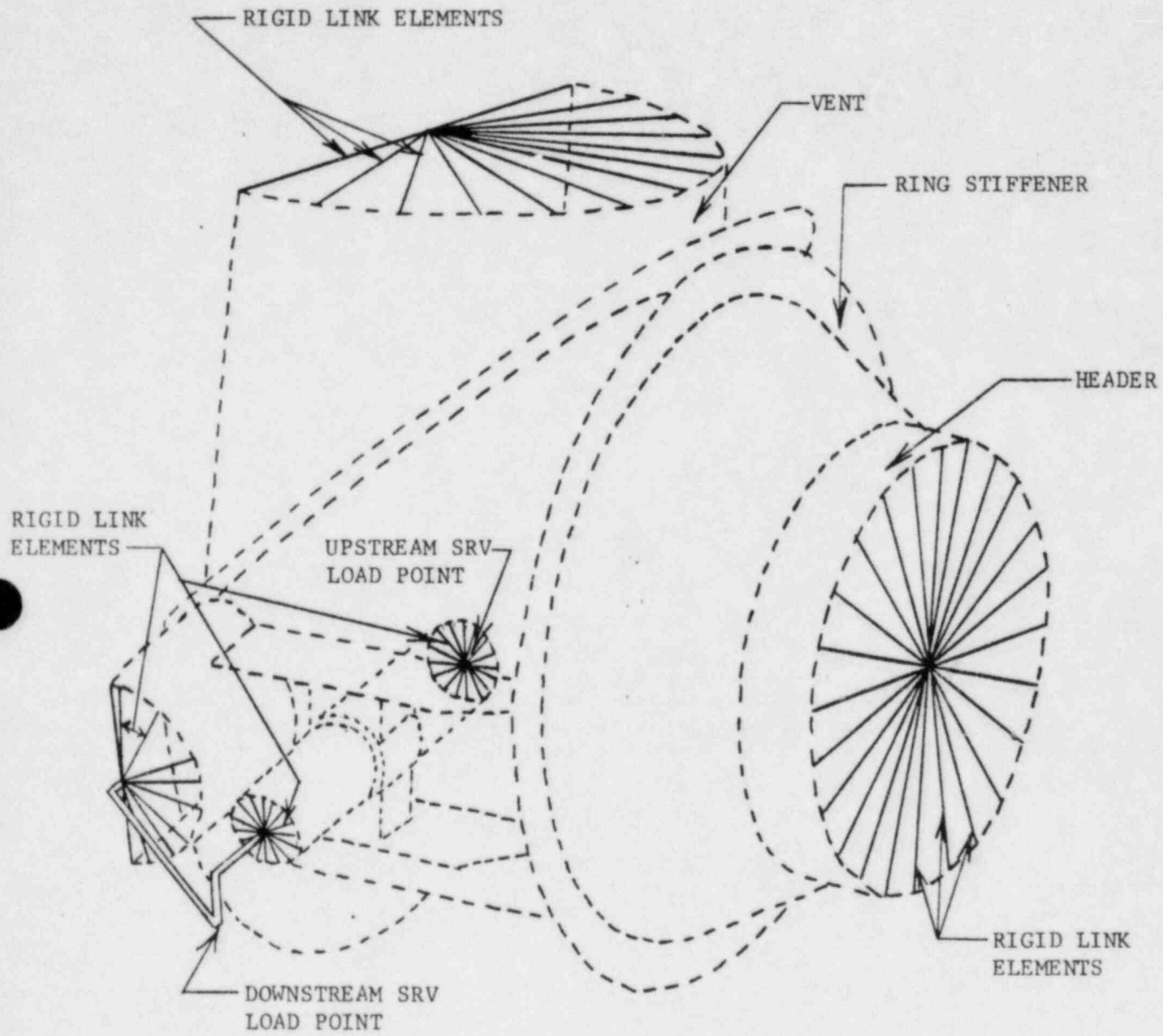

Figure 3.6.1.4-5 Load Points and Rigid Link Element Configuration

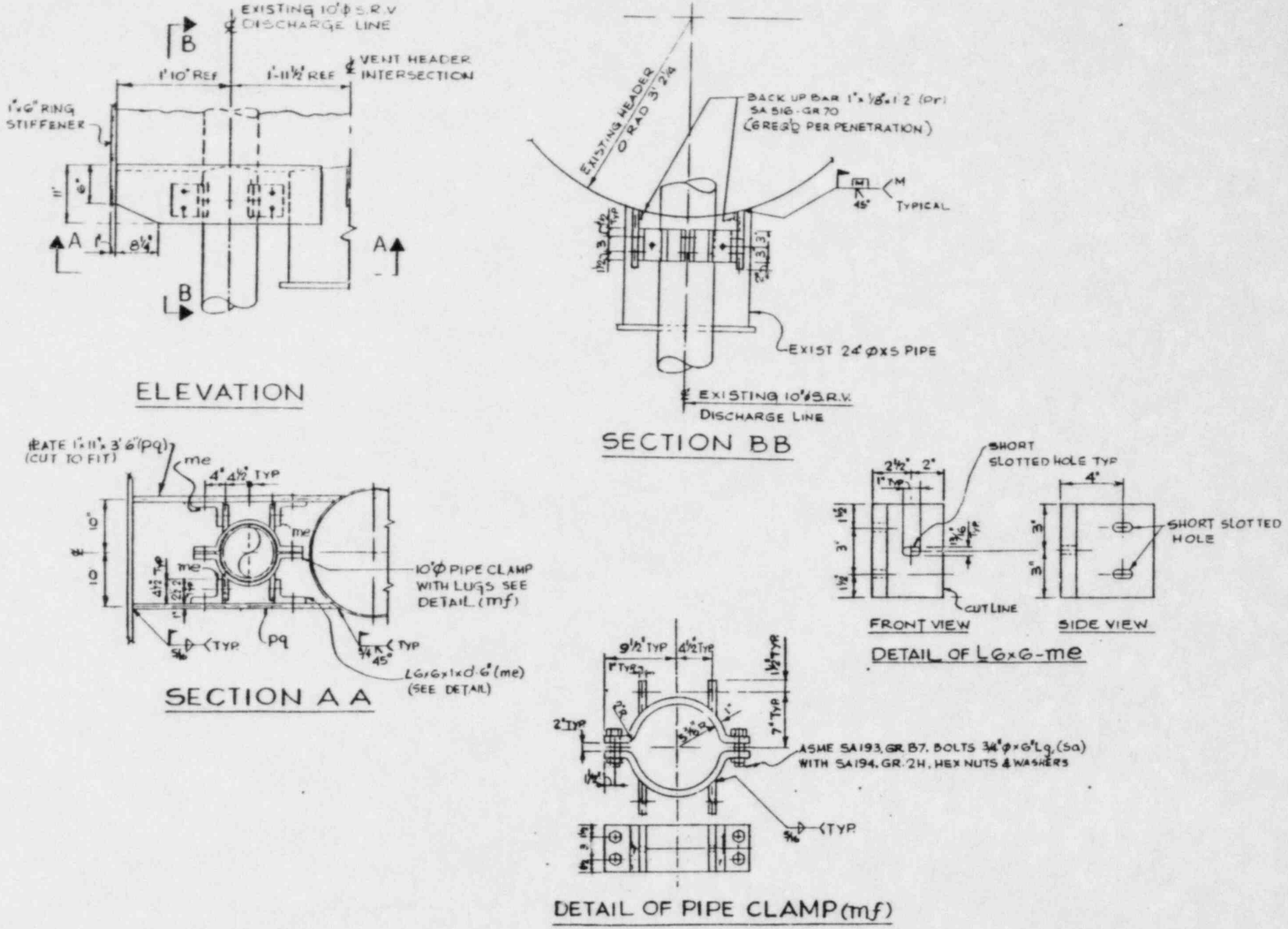

Figure 3.6.1.4-6 Detail of SRV Penetration Reinforcement

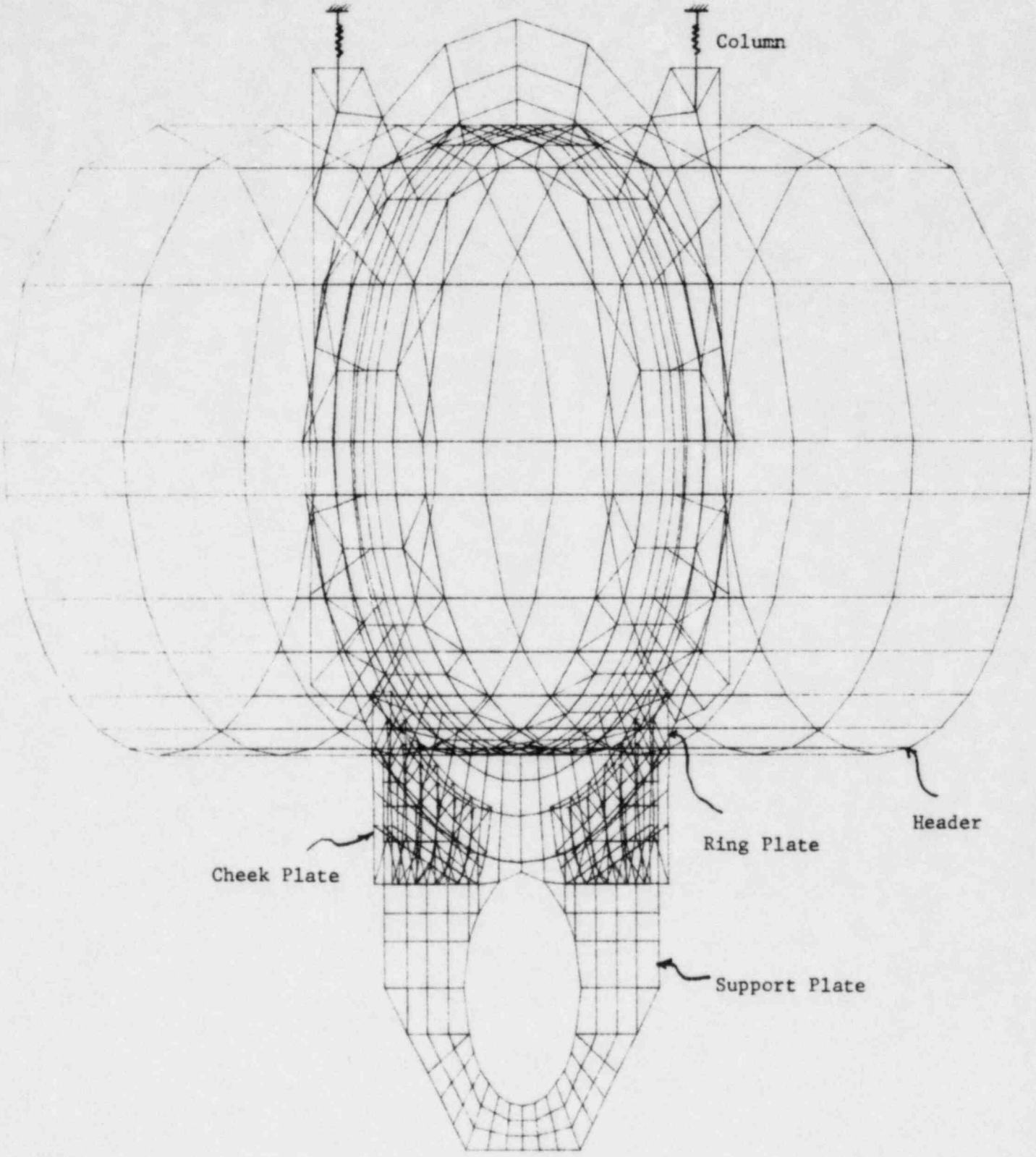

Figure 3.6.1.5-1 Finite Element Shell Model of Deflector Support (Page 1 of 3)

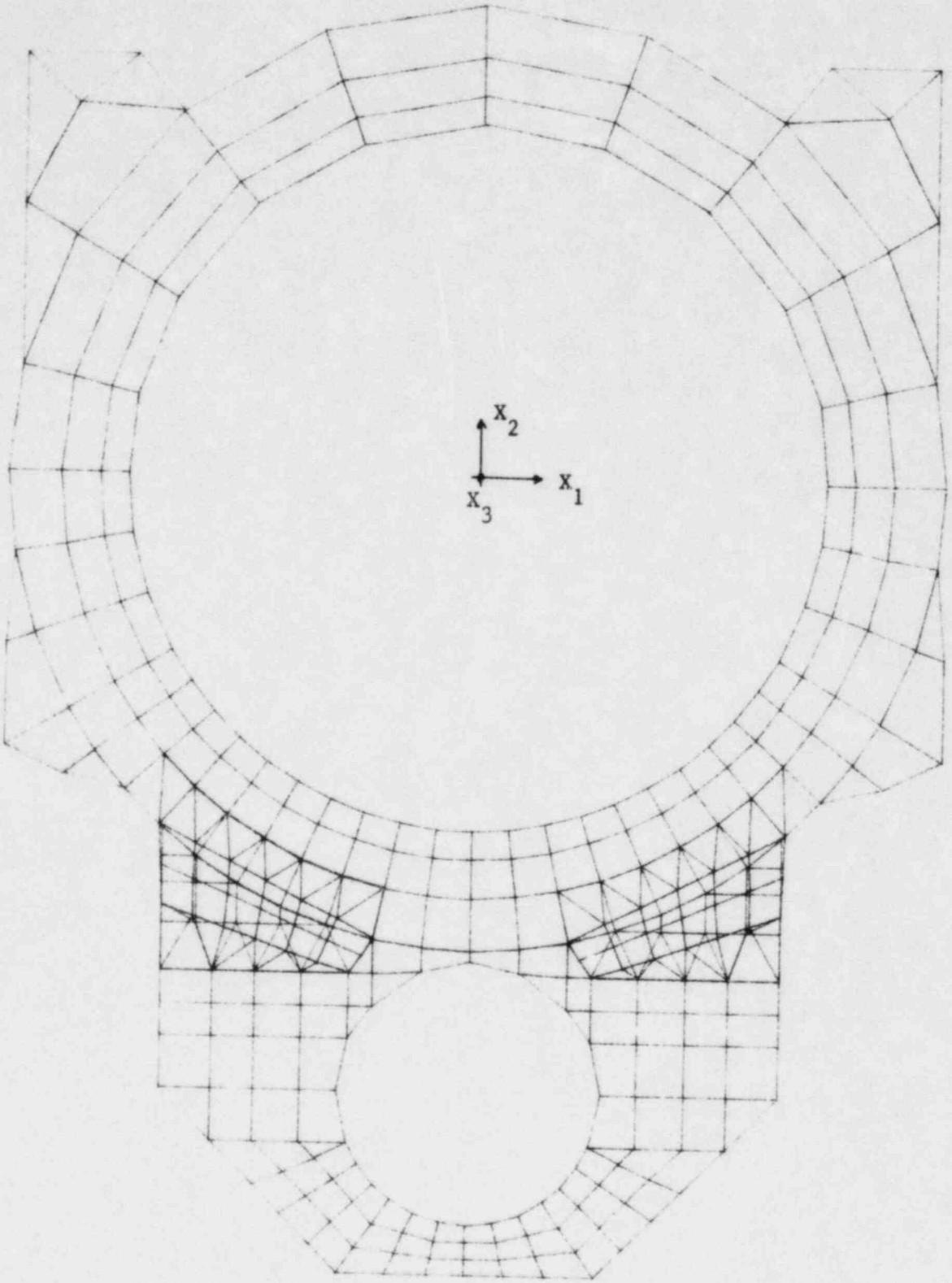

Figure 3.6.1.5-1 Finite Element Shell Model
of Deflector Support (Page 2 of 3)

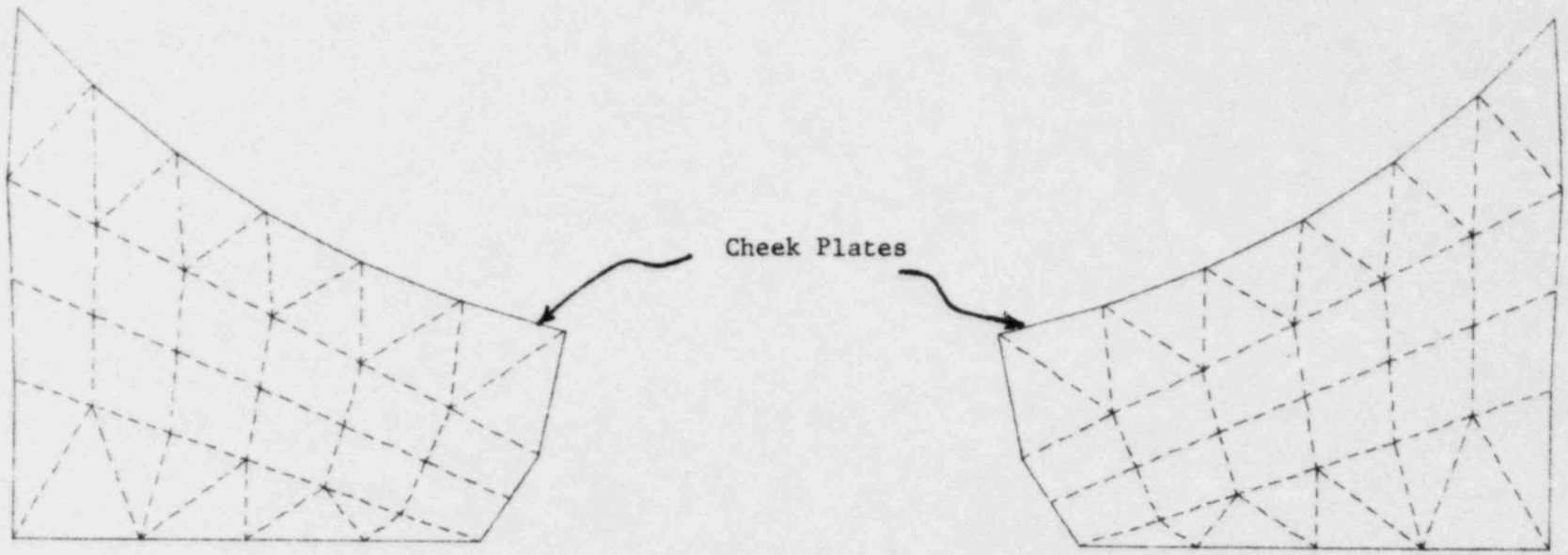

Figure 3.6.1.5-1 Finite Element Shell Model of
Deflector Support (Page 3 of 3)

CP&L Brunswick Steam Electric Plant Units 1&2

Reactor Building Idealized Structure

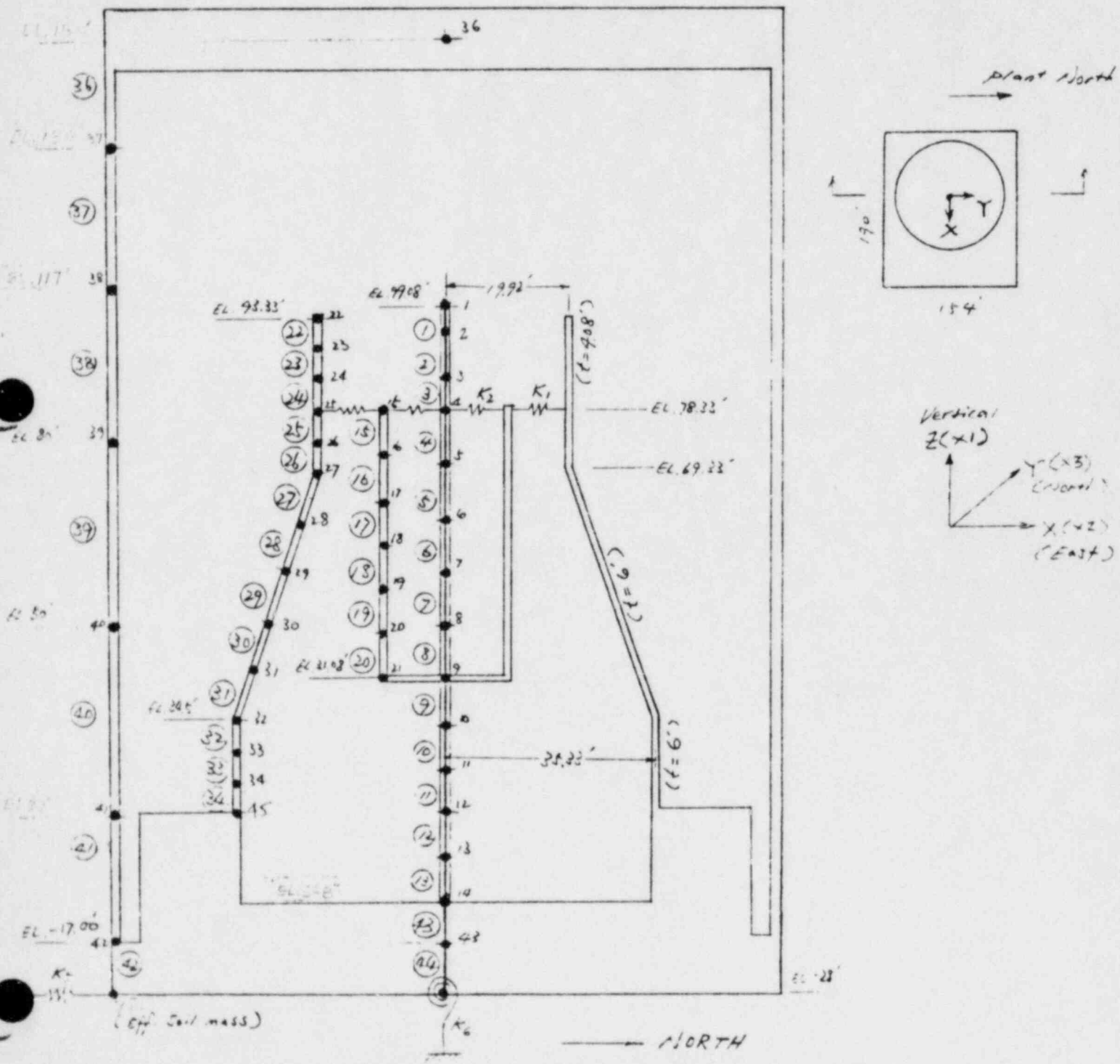

Figure 3.6.2.1-1 Brunswick Containment Beam Model

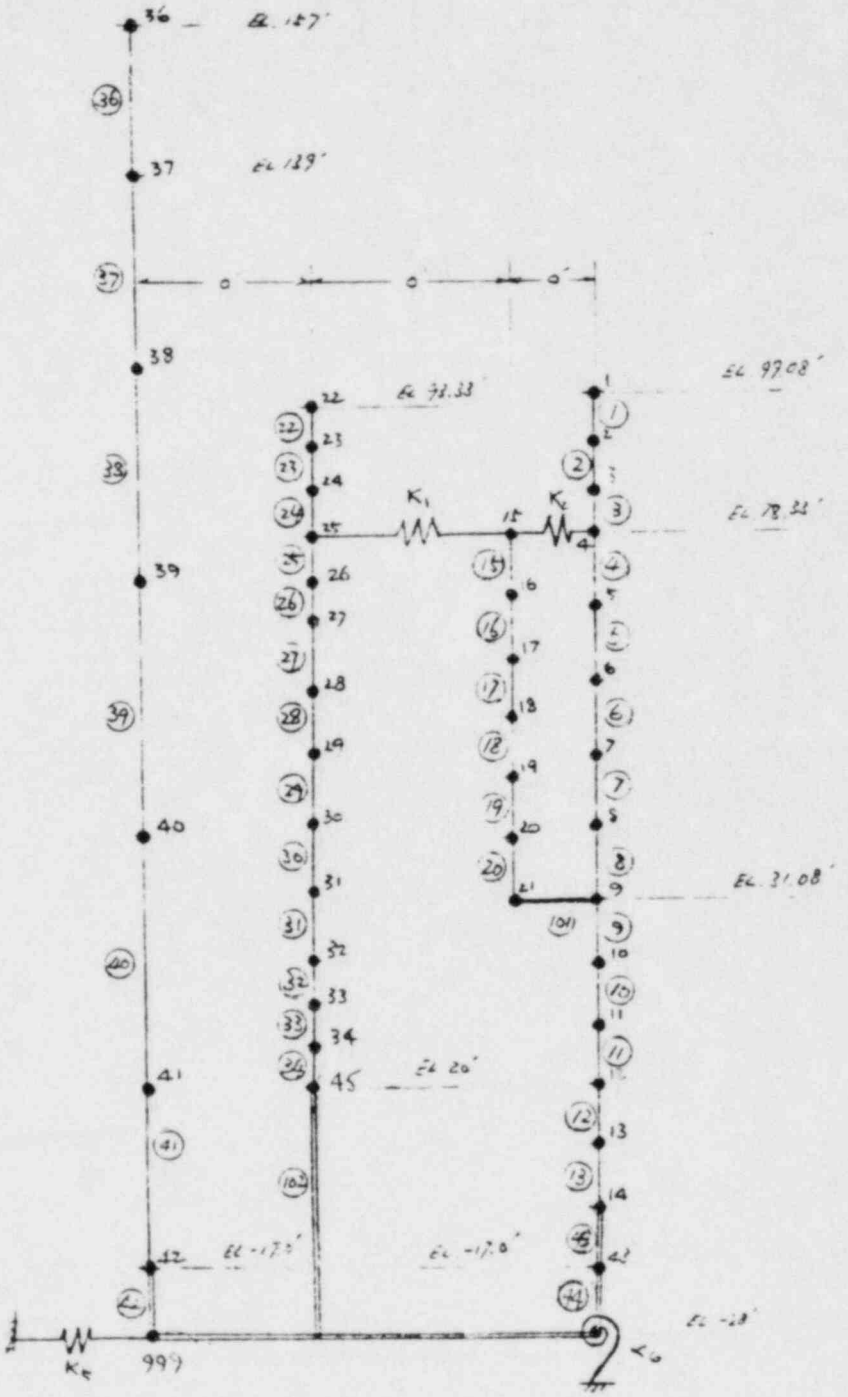

Figure 3.6.2.1-2 Brunswick Containment Lump Mass Stick Model

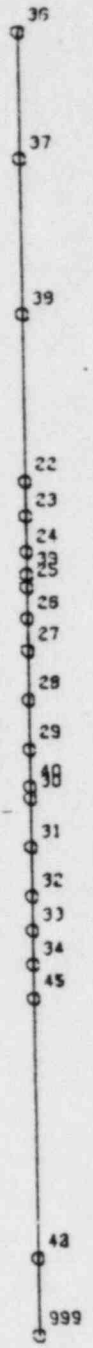

Figure 3.6.2.1-3 Brunswick Containment Model Projection on X3-X1 Plane

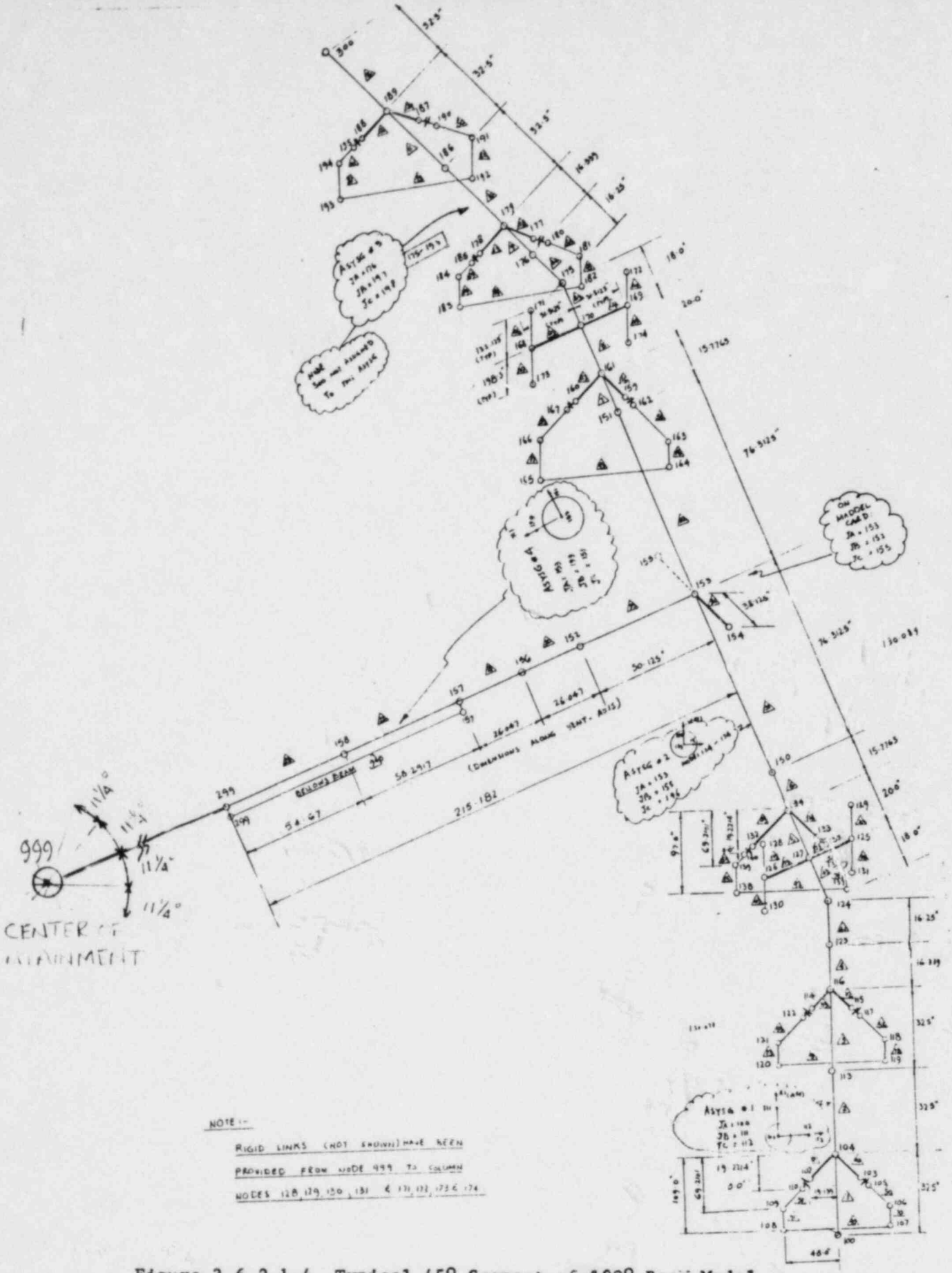

Figure 3.6.2.1-4 Typical 45° Segment of 180° Beam Model

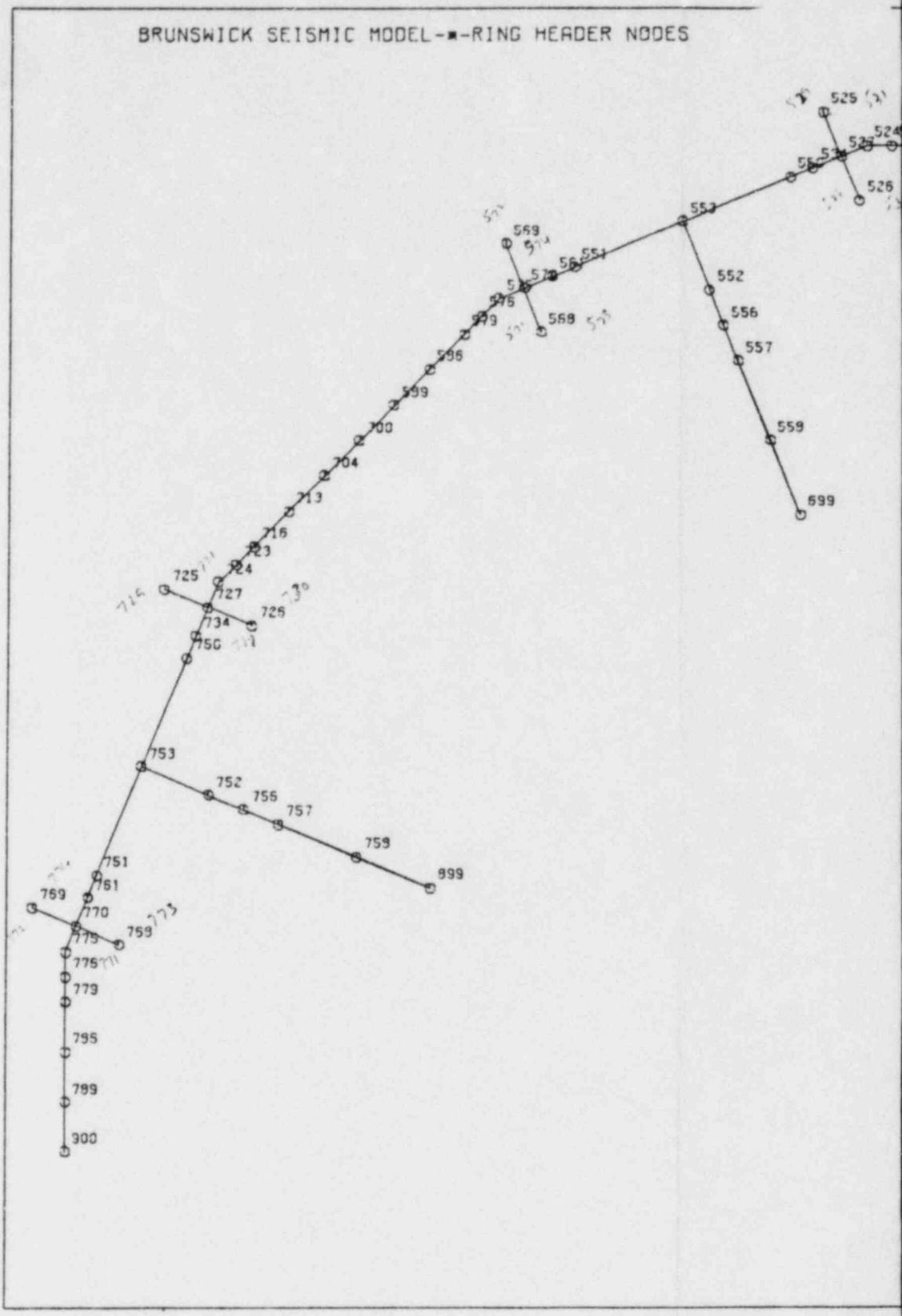

Figure 3.6.2.1-5 Vent/Vent Header/Dow

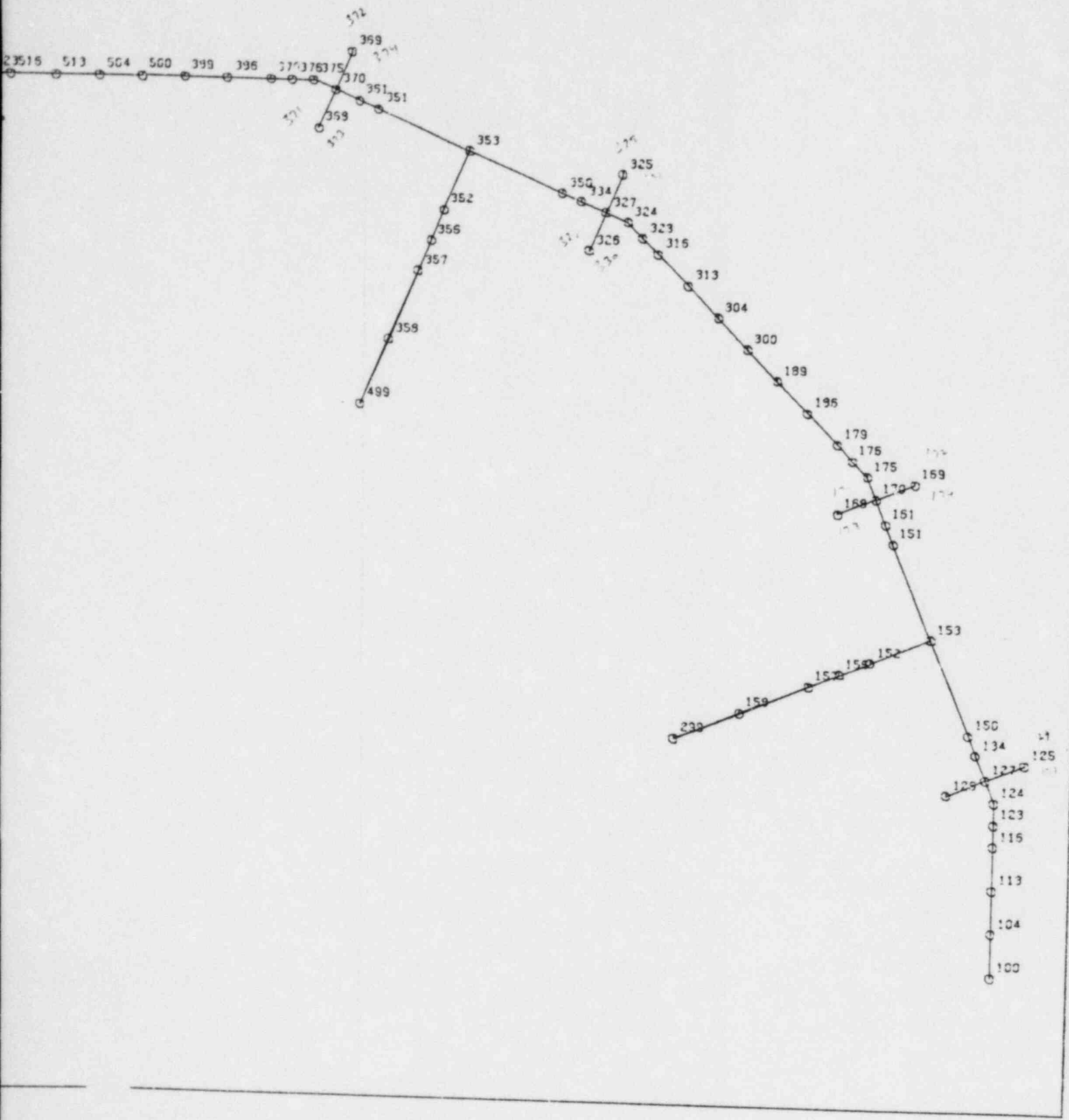

ncomer System 180° Beam Model Nodes

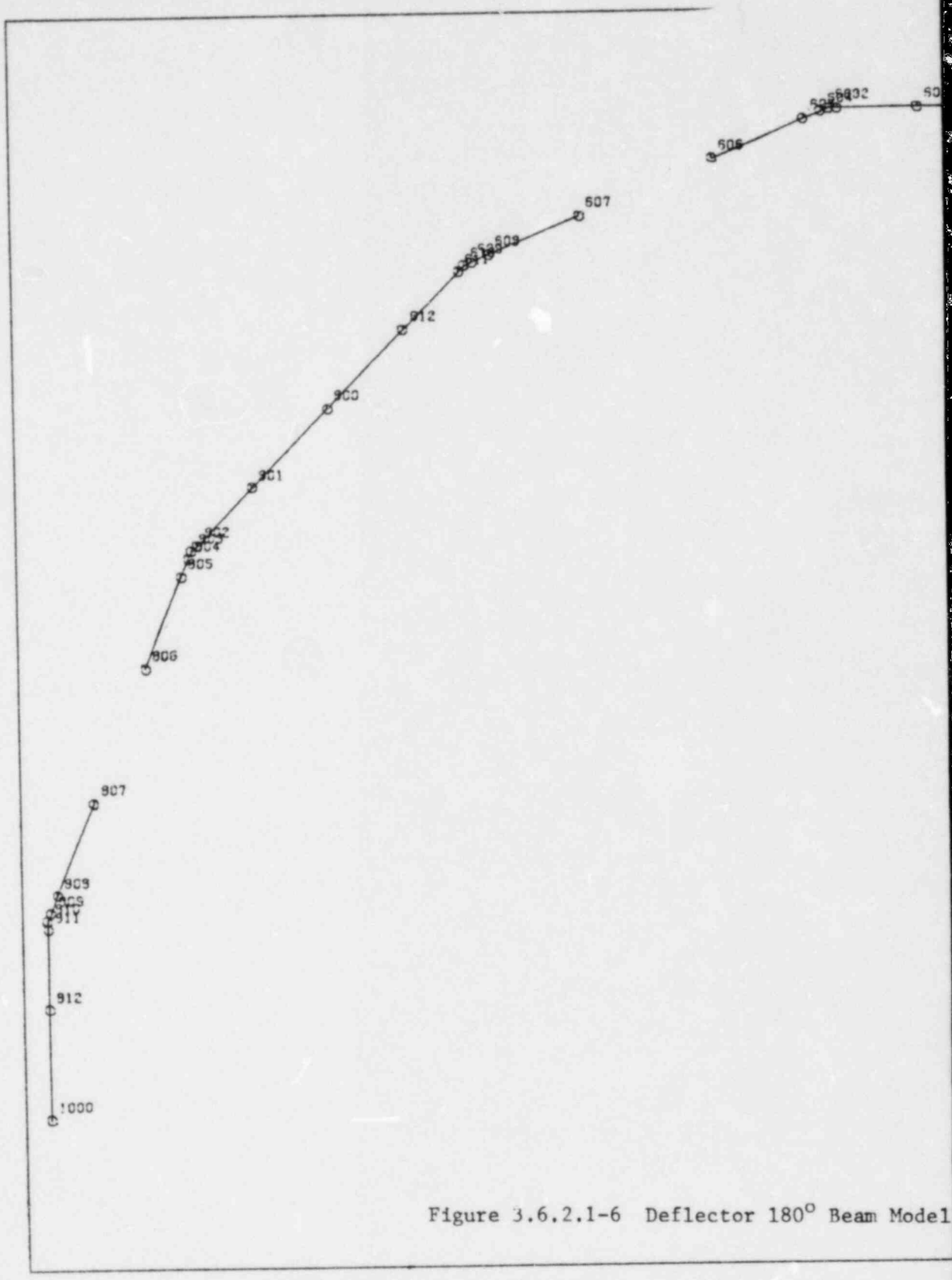

Figure 3.6.2.1-6 Deflector 180° Beam Model

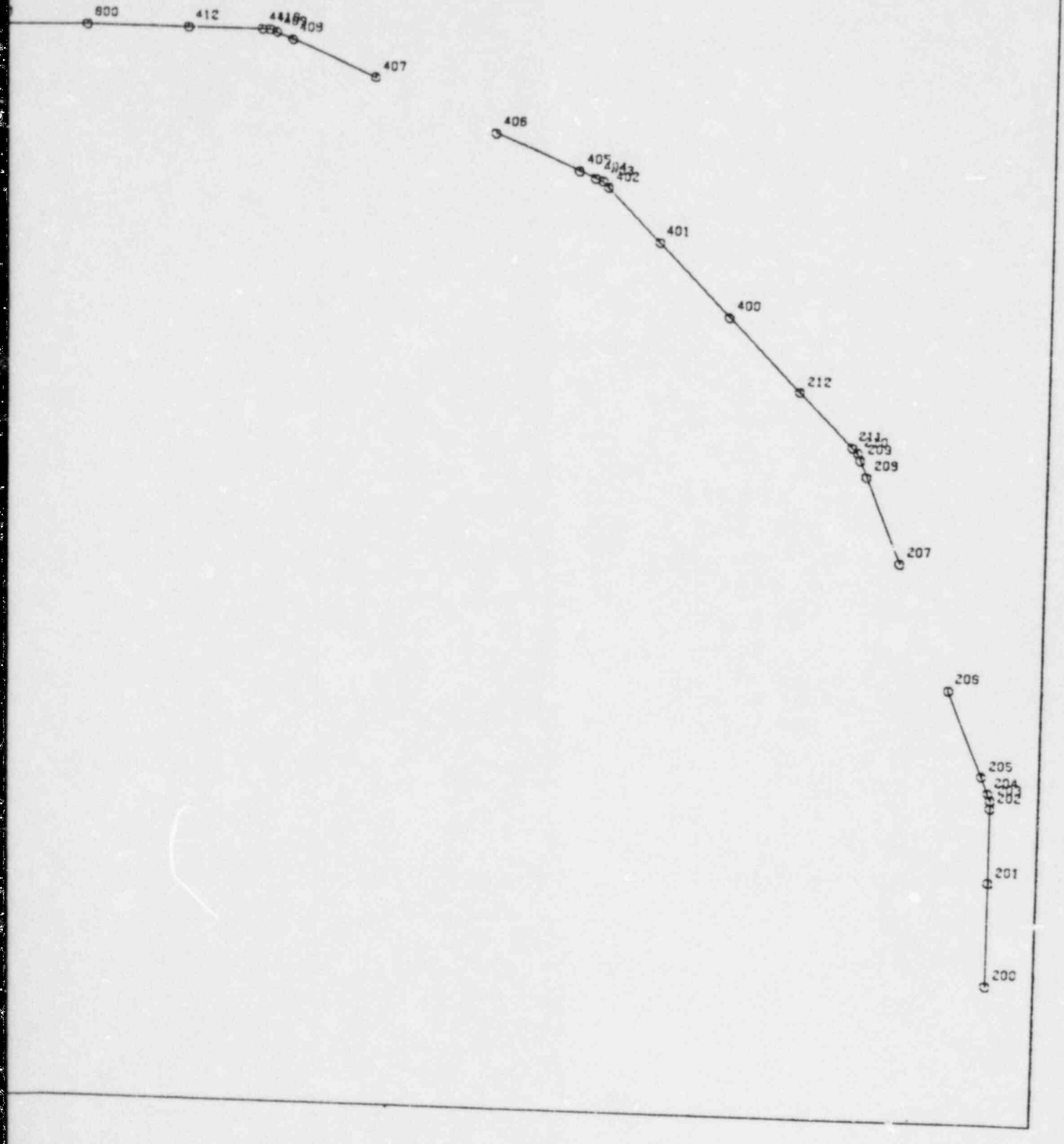
600
412
407
406
401
400
212
209
207
206
205
201
200

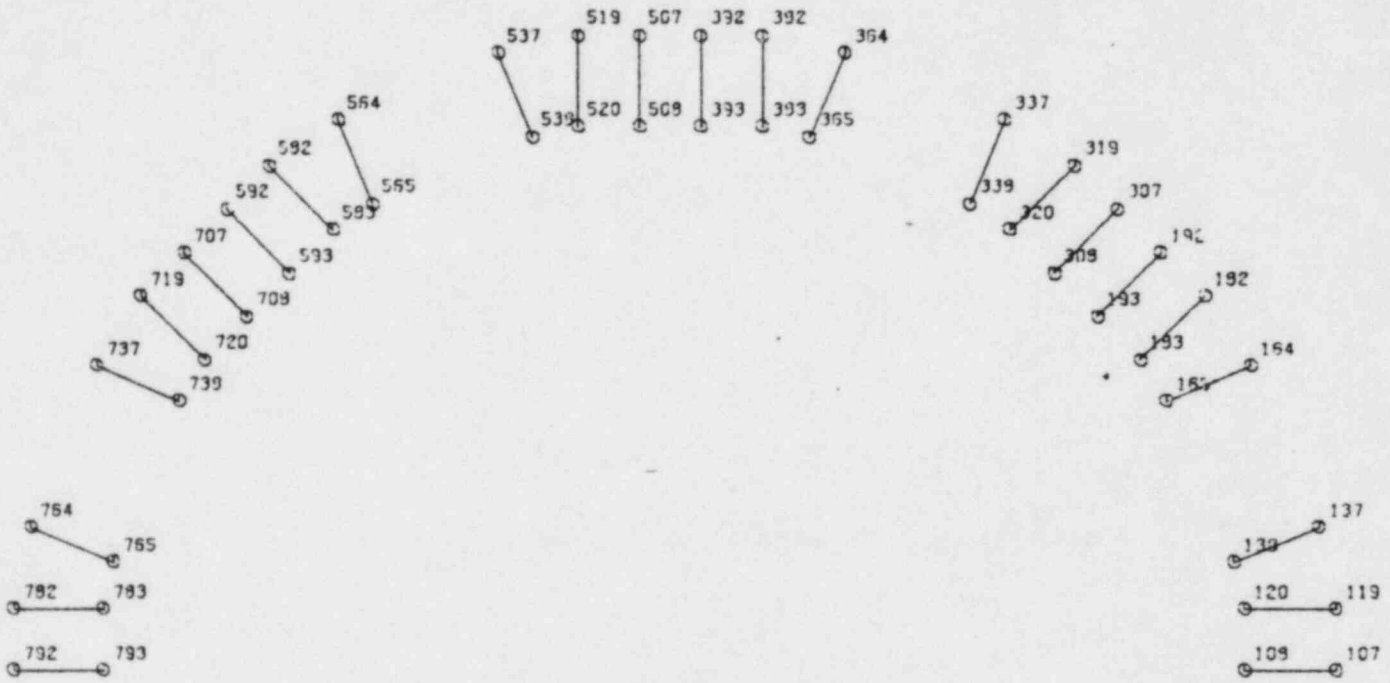

Figure 3.6.2.1-7 Downcomer Ties

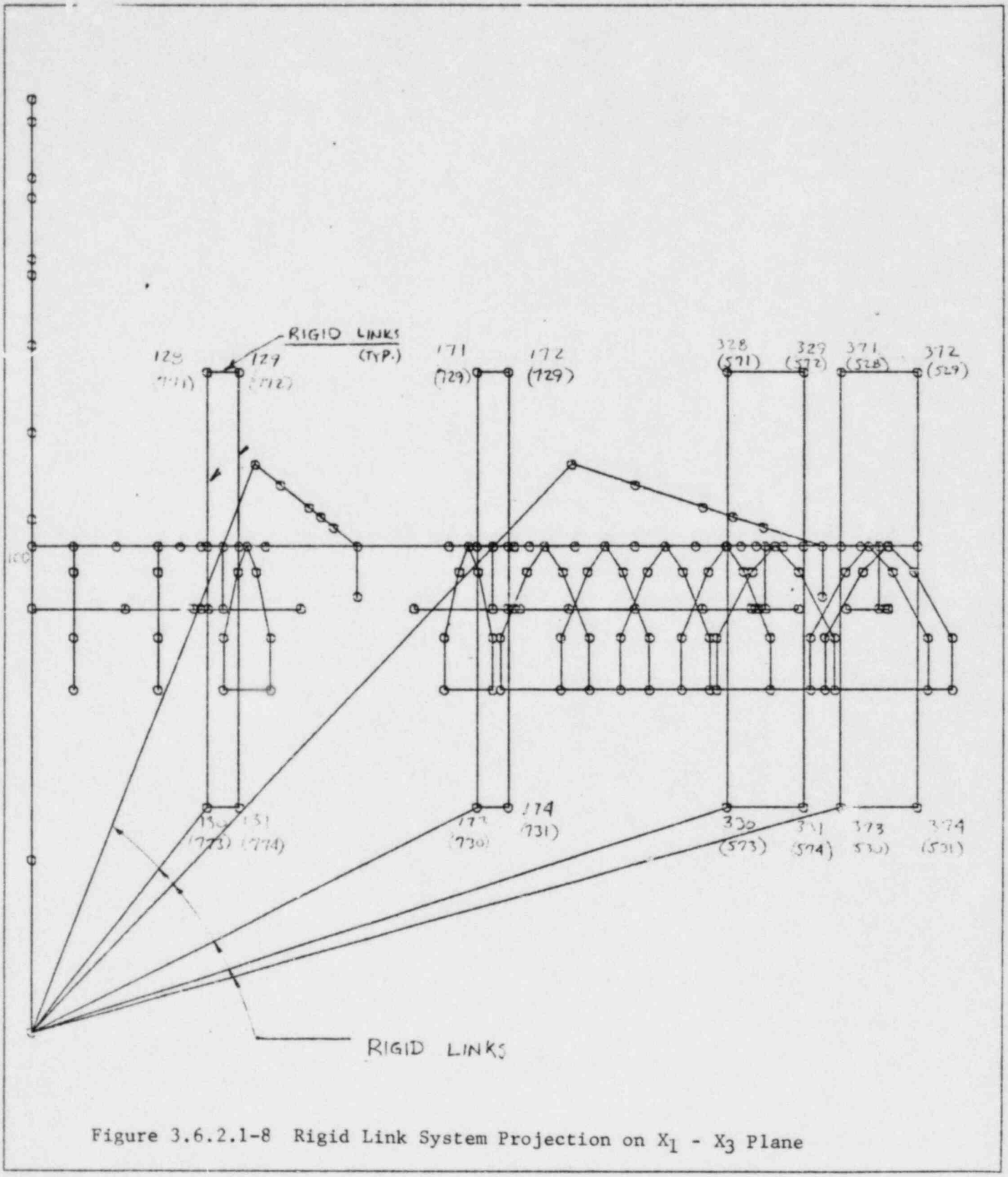

Figure 3.6.2.1-8 Rigid Link System Projection on X_1 - X_3 Plane

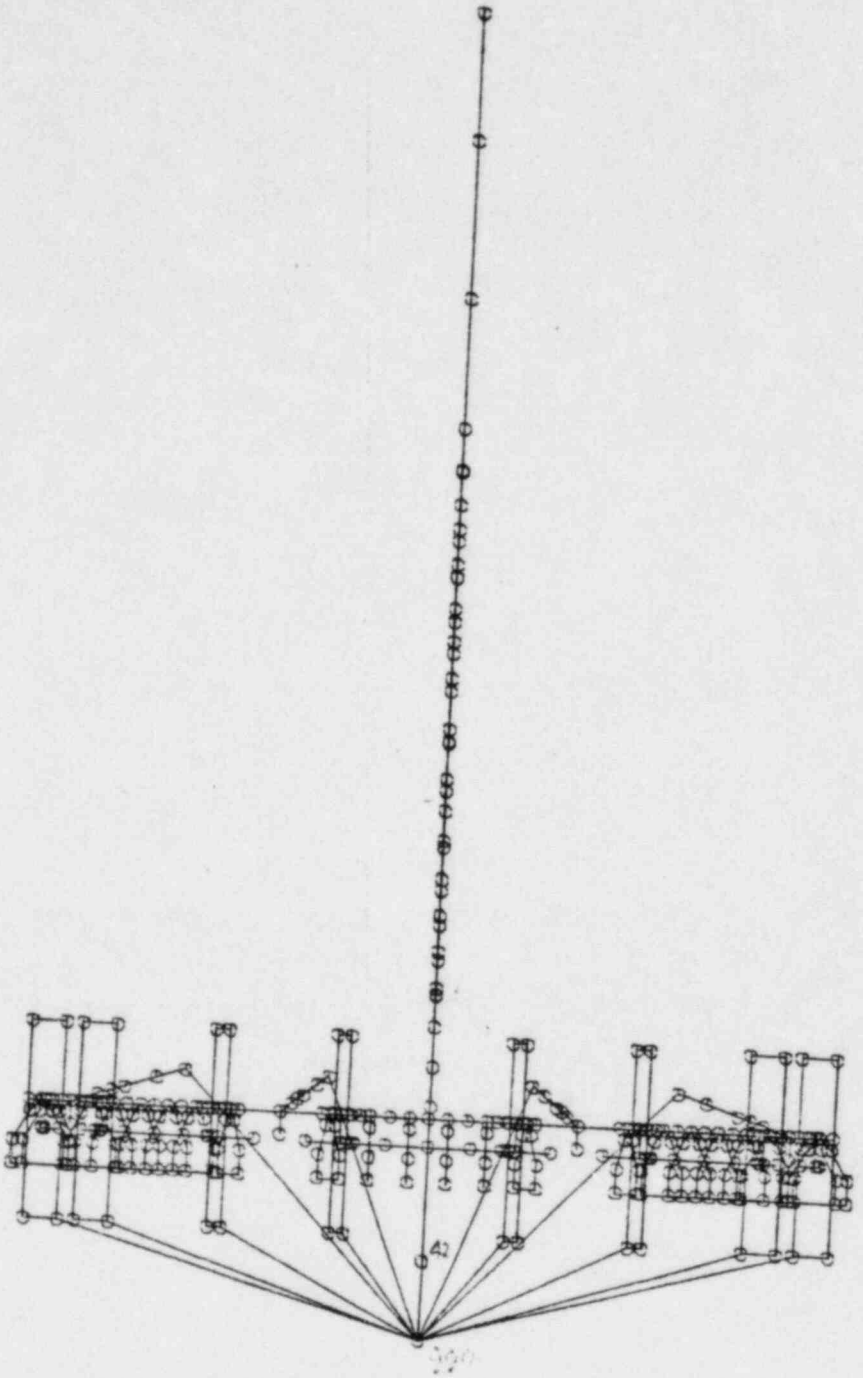

Figure 3.6.2.1-9 Rigid Link System Projection on X1-X2 Plane

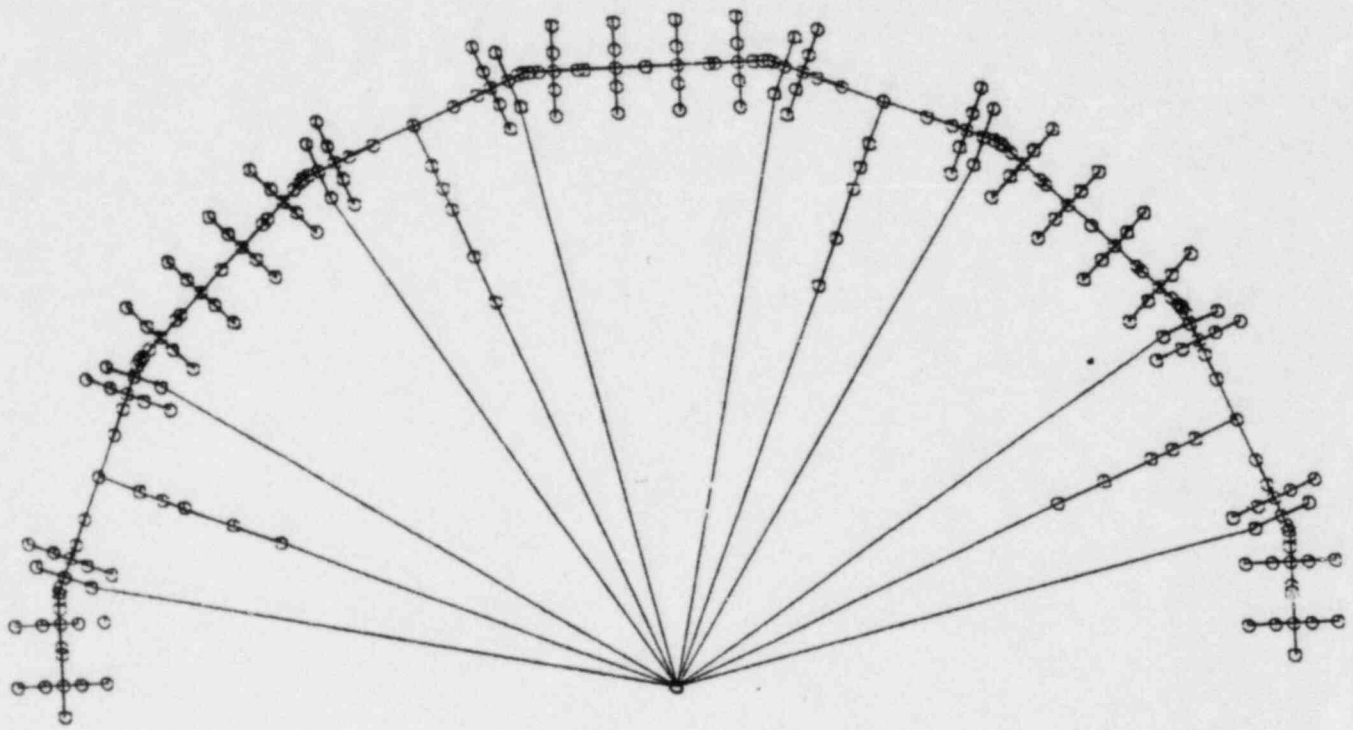

Figure 3.6.2.1-10 Rigid Link System Projection on X_2 - X_3 Plane

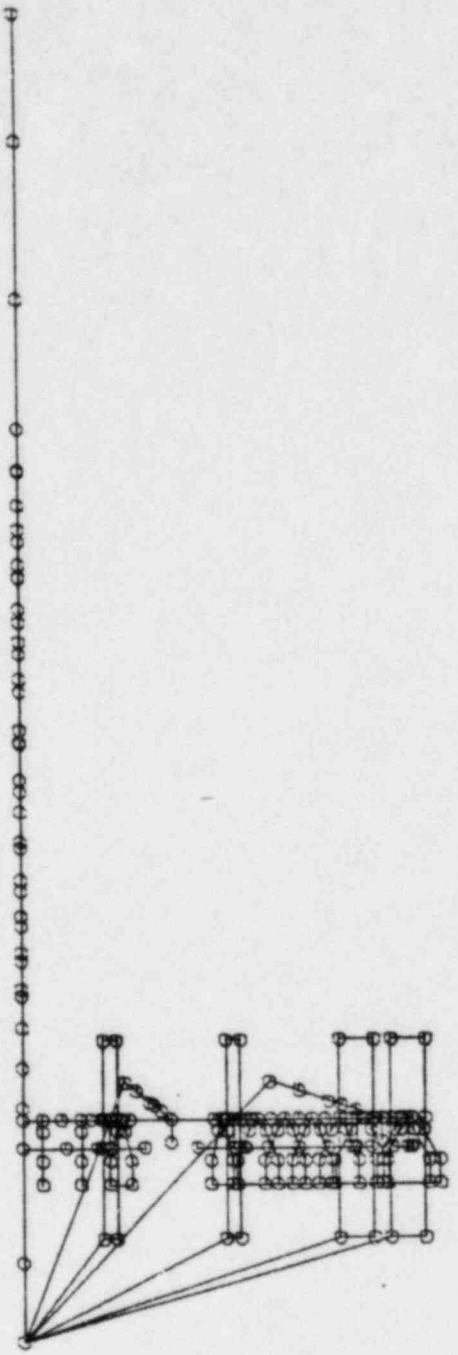

Figure 3.6.2.1-11 Rigid Link System Projection on X_1 - X_3 Plane

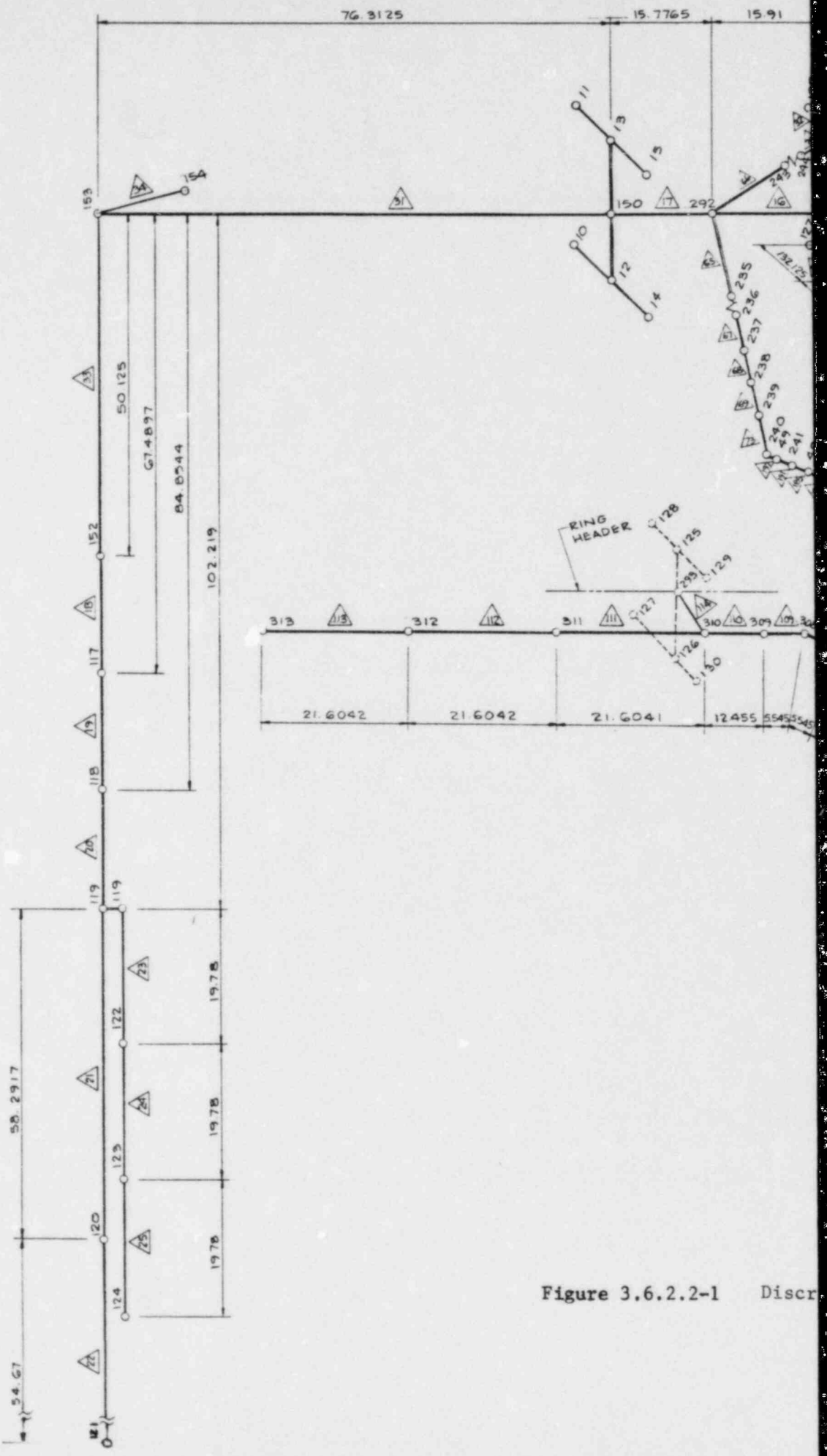

Figure 3.6.2.2-1 Discr

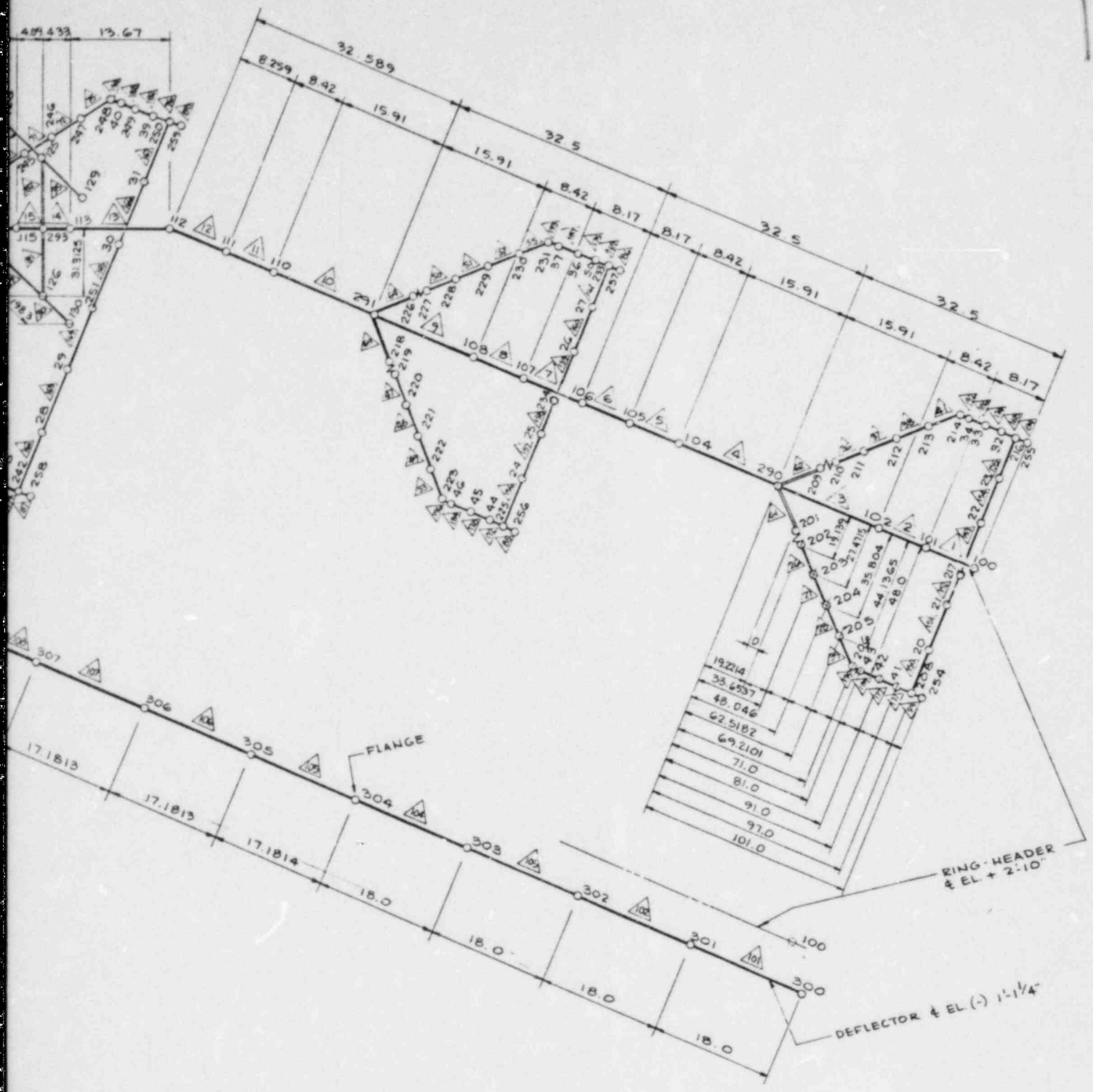

ete Model of $22\frac{1}{2}^{o}$ Beam Model

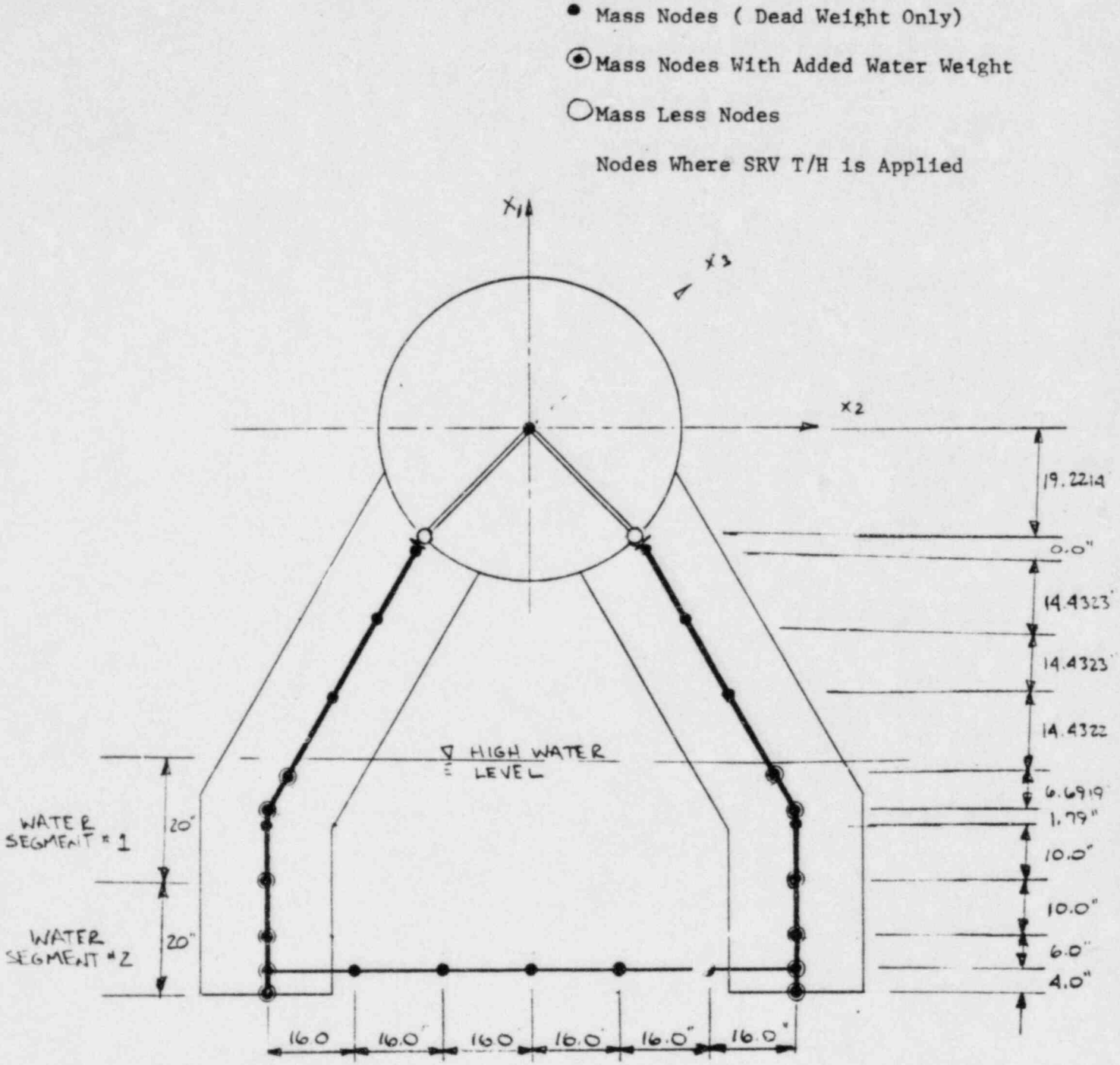

Figure 3.6.2.2-2 Typical Downcomer Pair

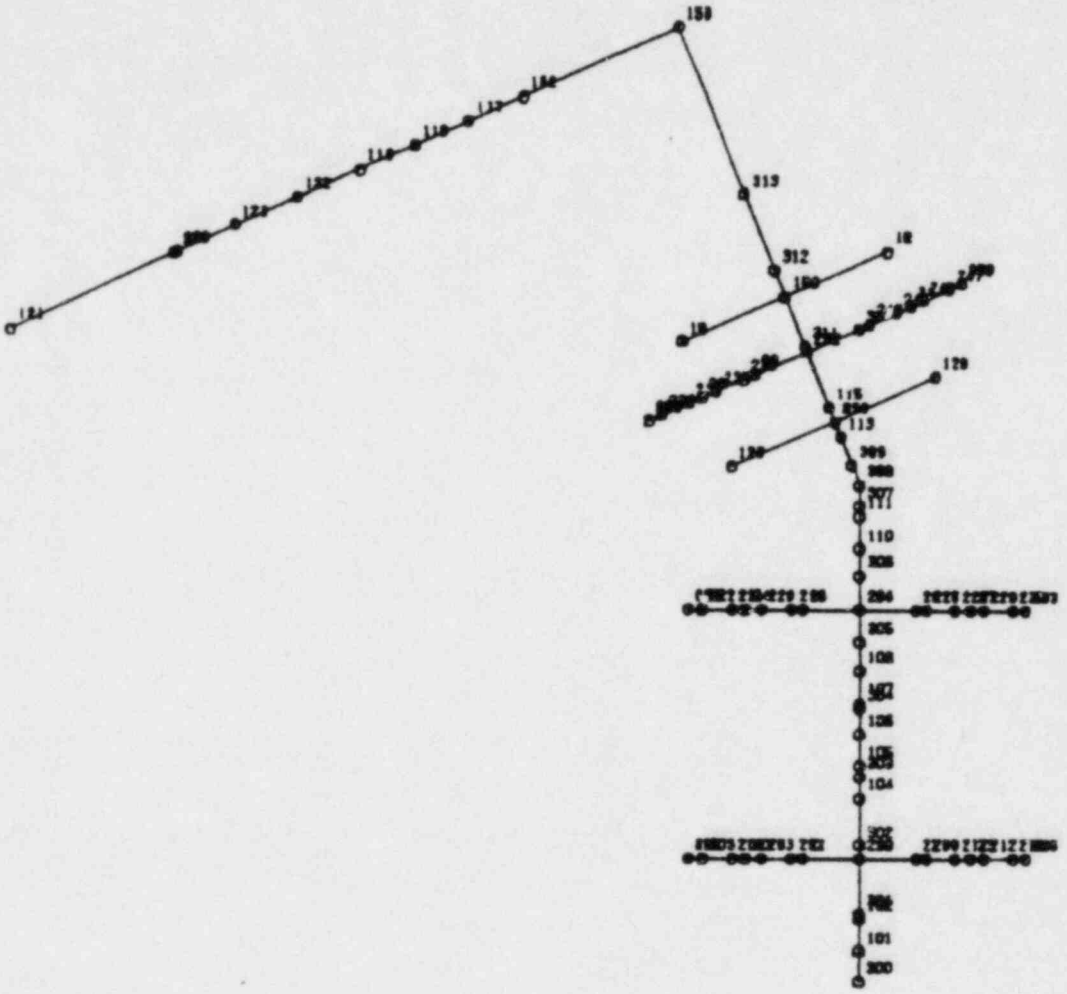

Figure 3.6.2.2-3 $22\frac{1}{2}^{o}$ Beam Model
Projection on X_2 - X_3 Plane

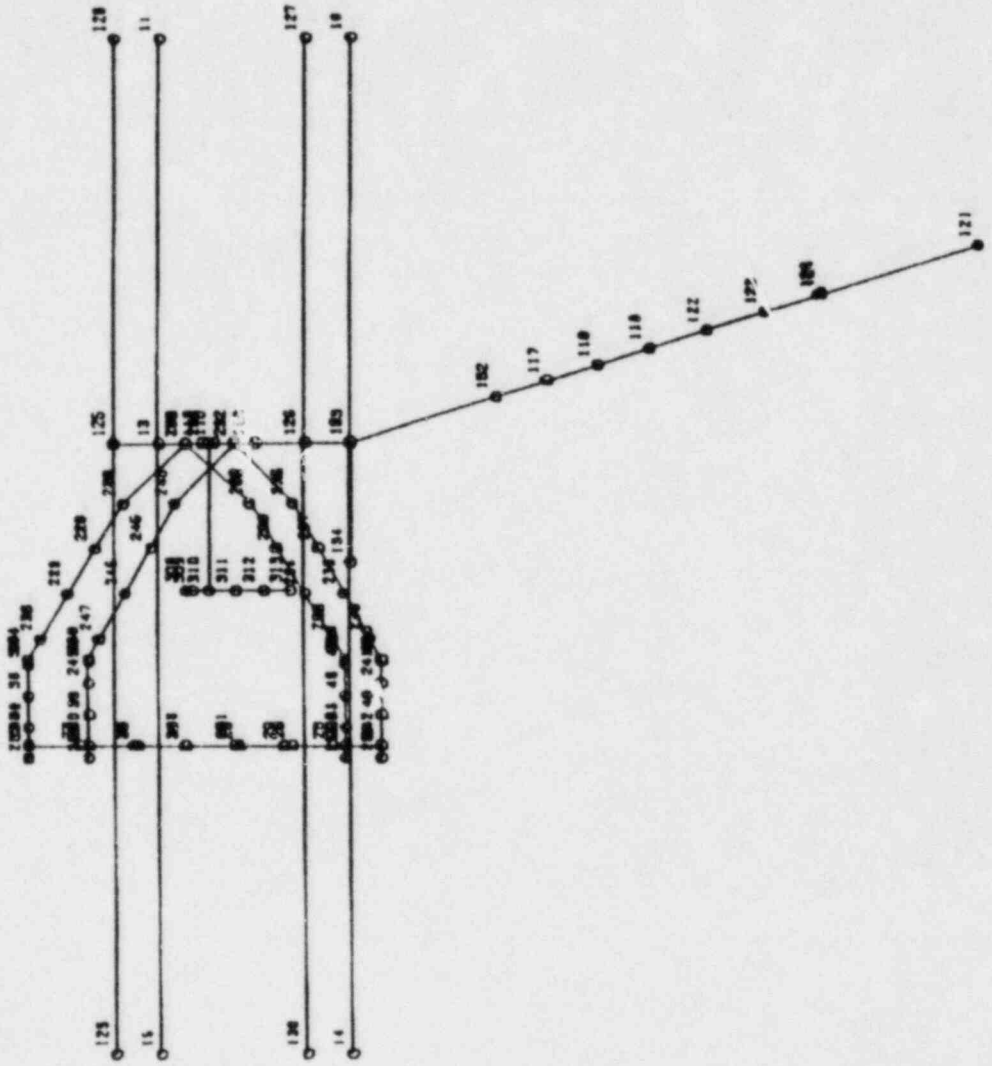

Figure 3.6.2.2-4 22½° Beam Model

Projection on X_1 - X_2 Plane

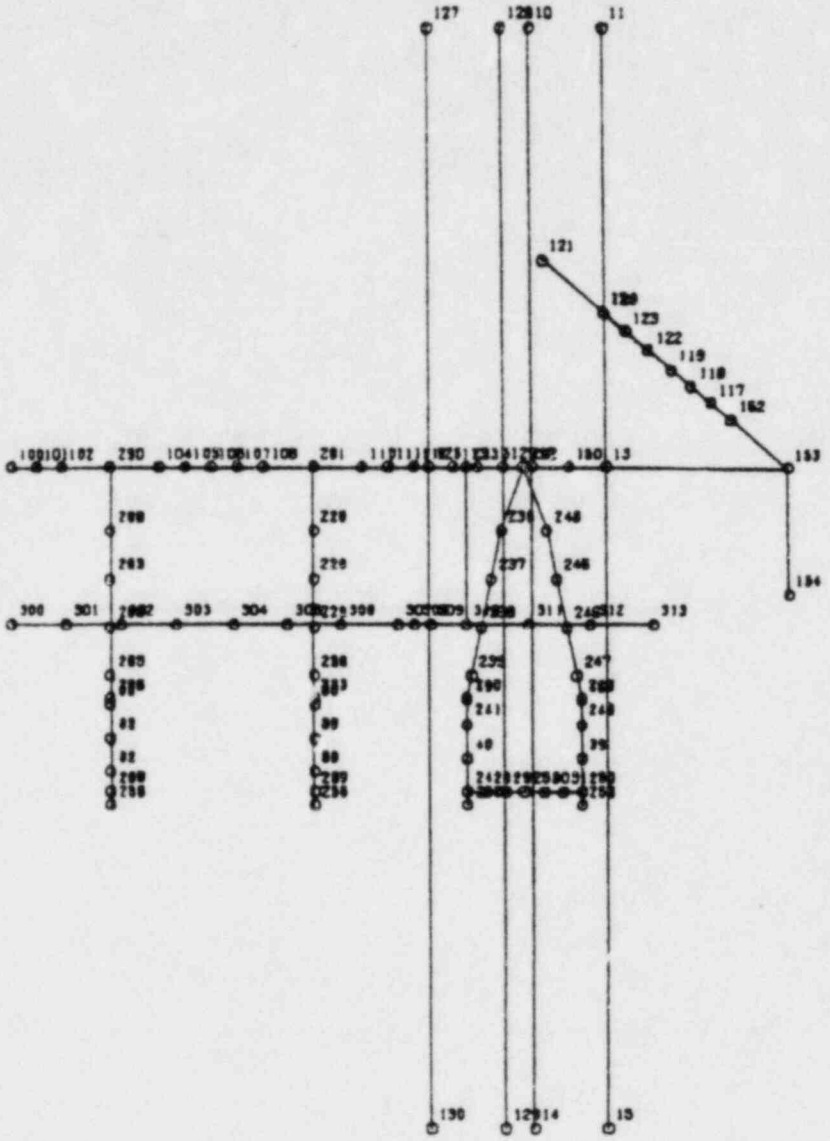

Figure 3.6.2.2-5 $22\frac{1}{2}^{o}$ Beam Model

Projection on $X_3 - X_1$ Plane

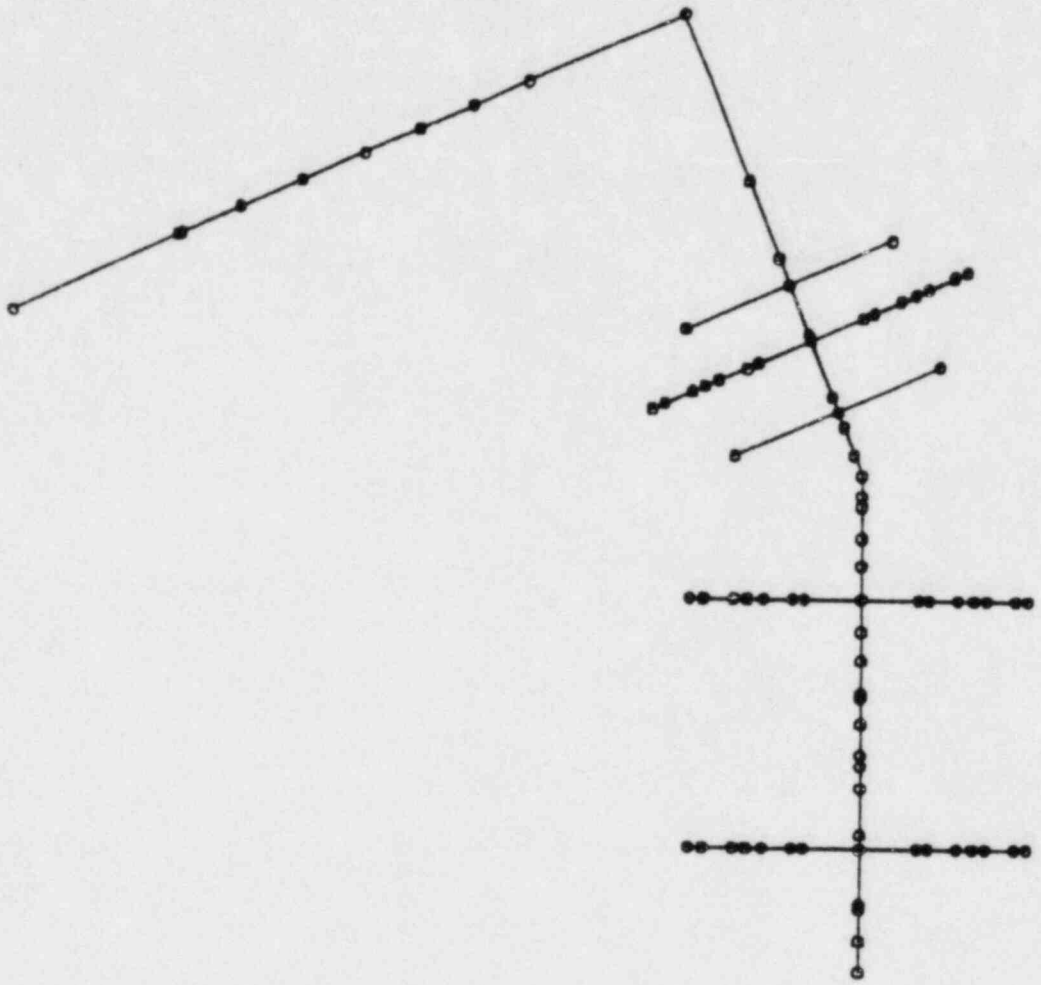

Figure 3.6.2.2-6 $22\frac{1}{2}^{\circ}$ Beam Model

Projection on X_2 - X_3 Plane

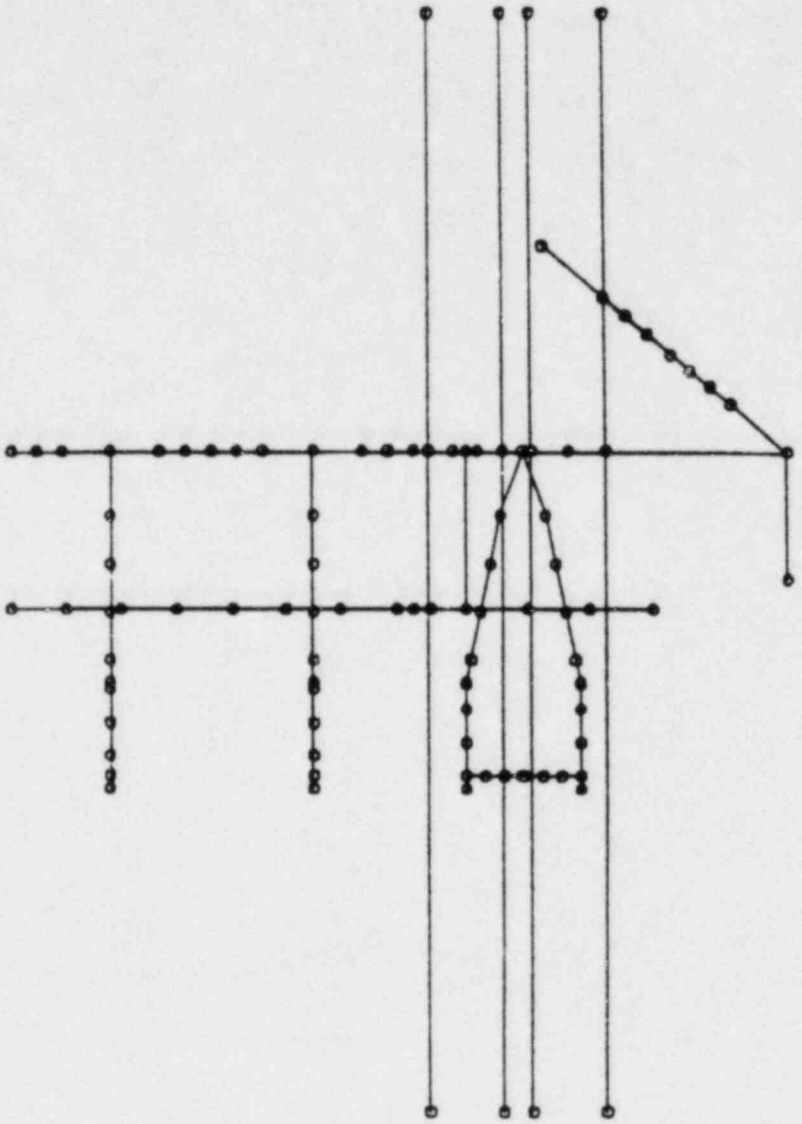

Figure 3.6.2.2-7 $22\frac{1}{2}^{o}$ Beam Model

Projection on $X_3 - X_1$ Plane

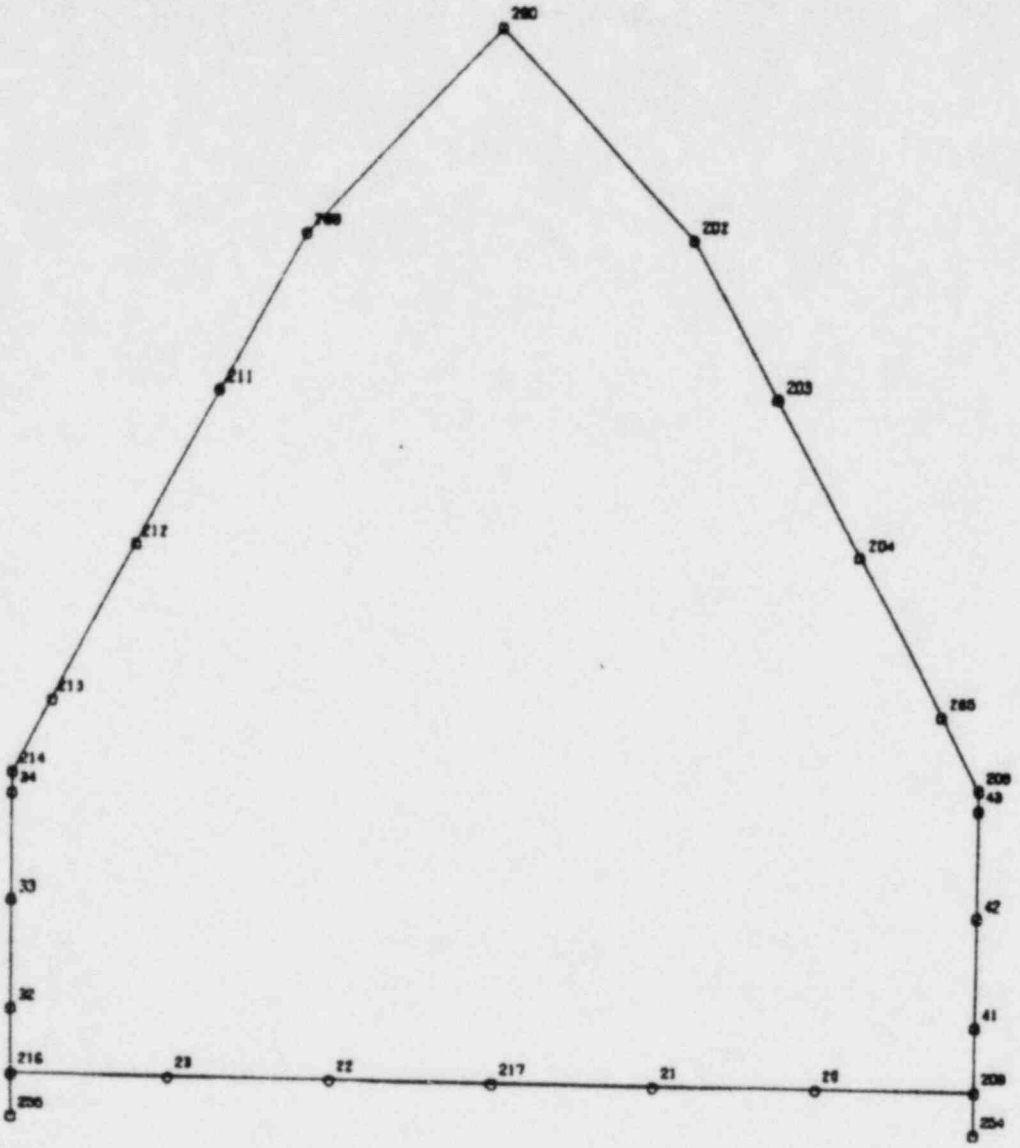

Figure 3.6.2.2-8 Downcomer Pair 1

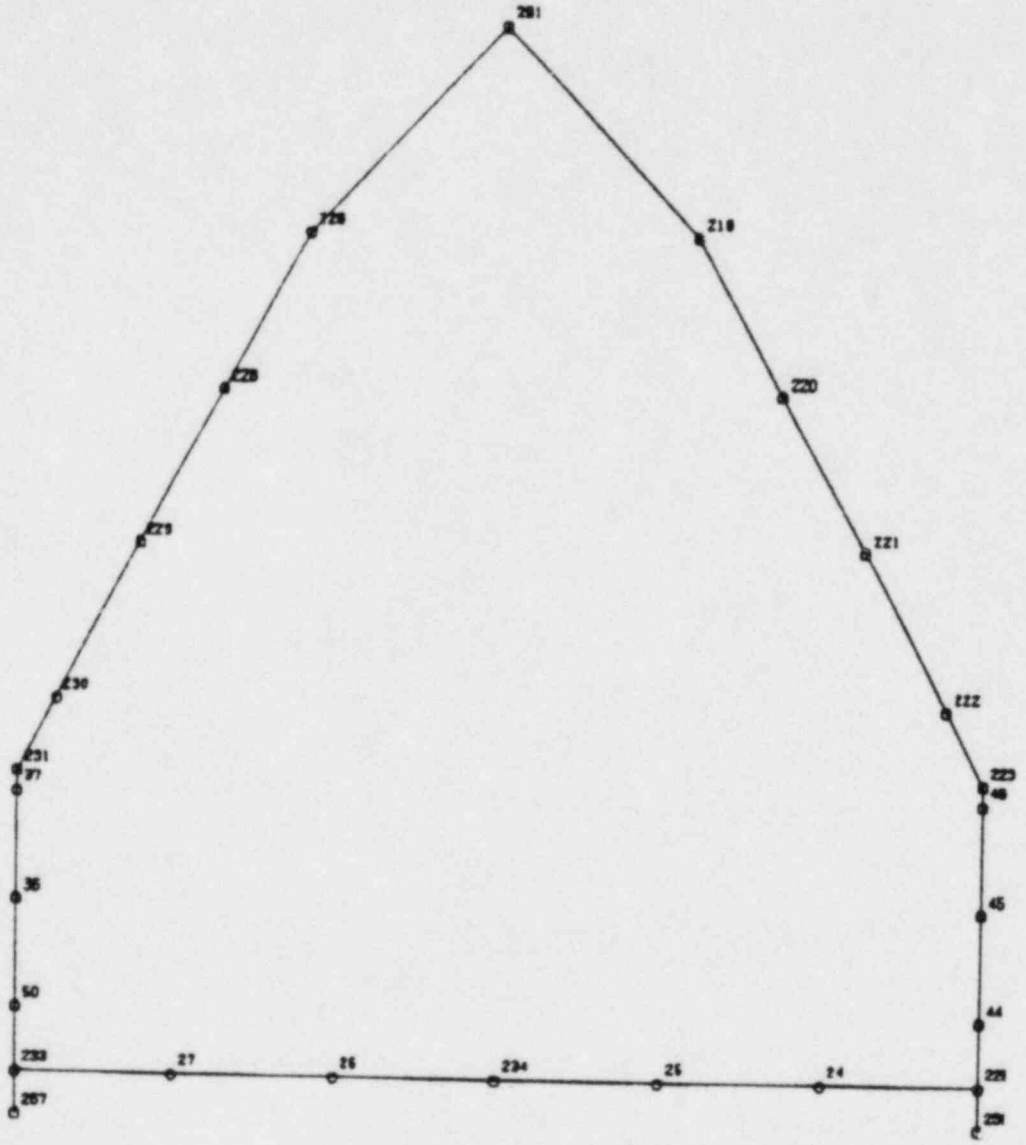

Figure 3.6.2.2-9 Downcomer Pair 2

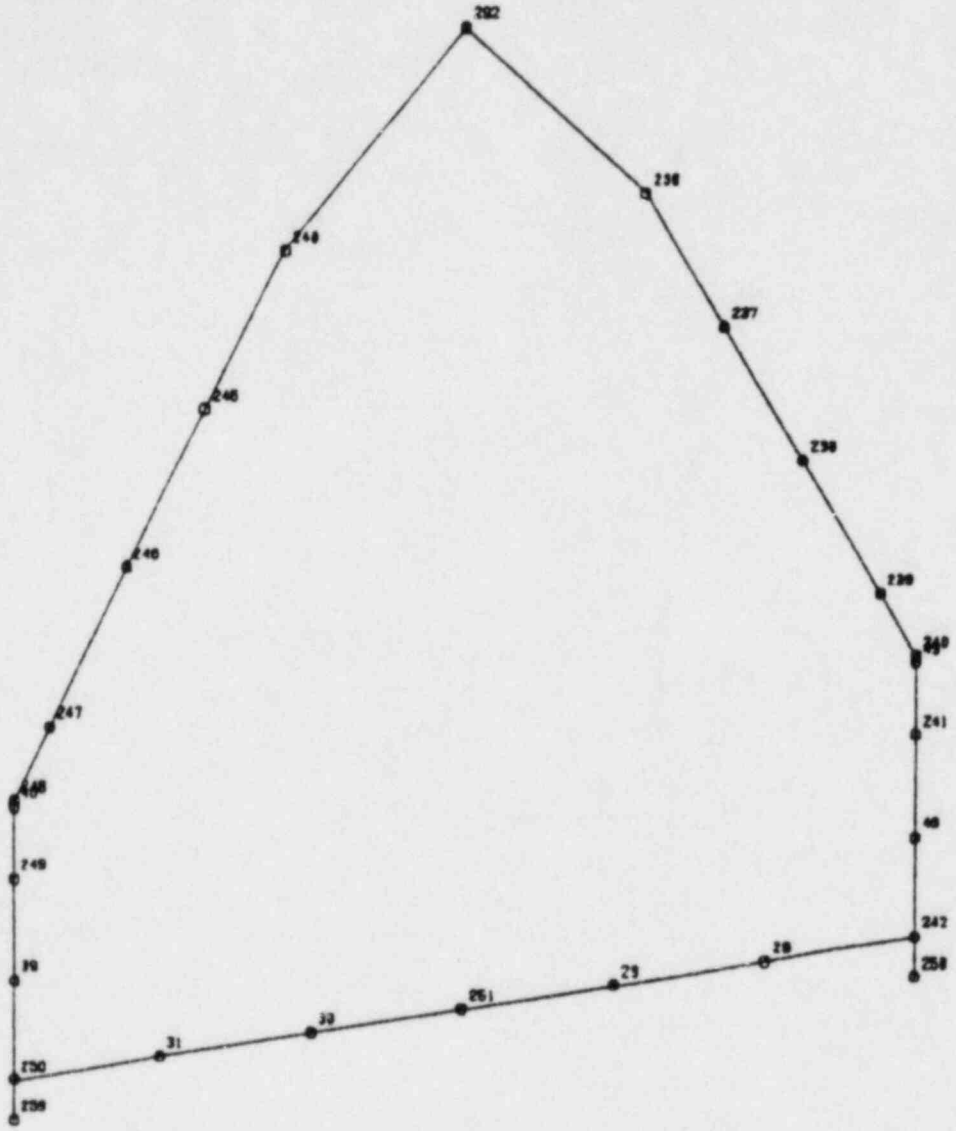

Figure 3.6.2.2-10 Downcomer Pair 3

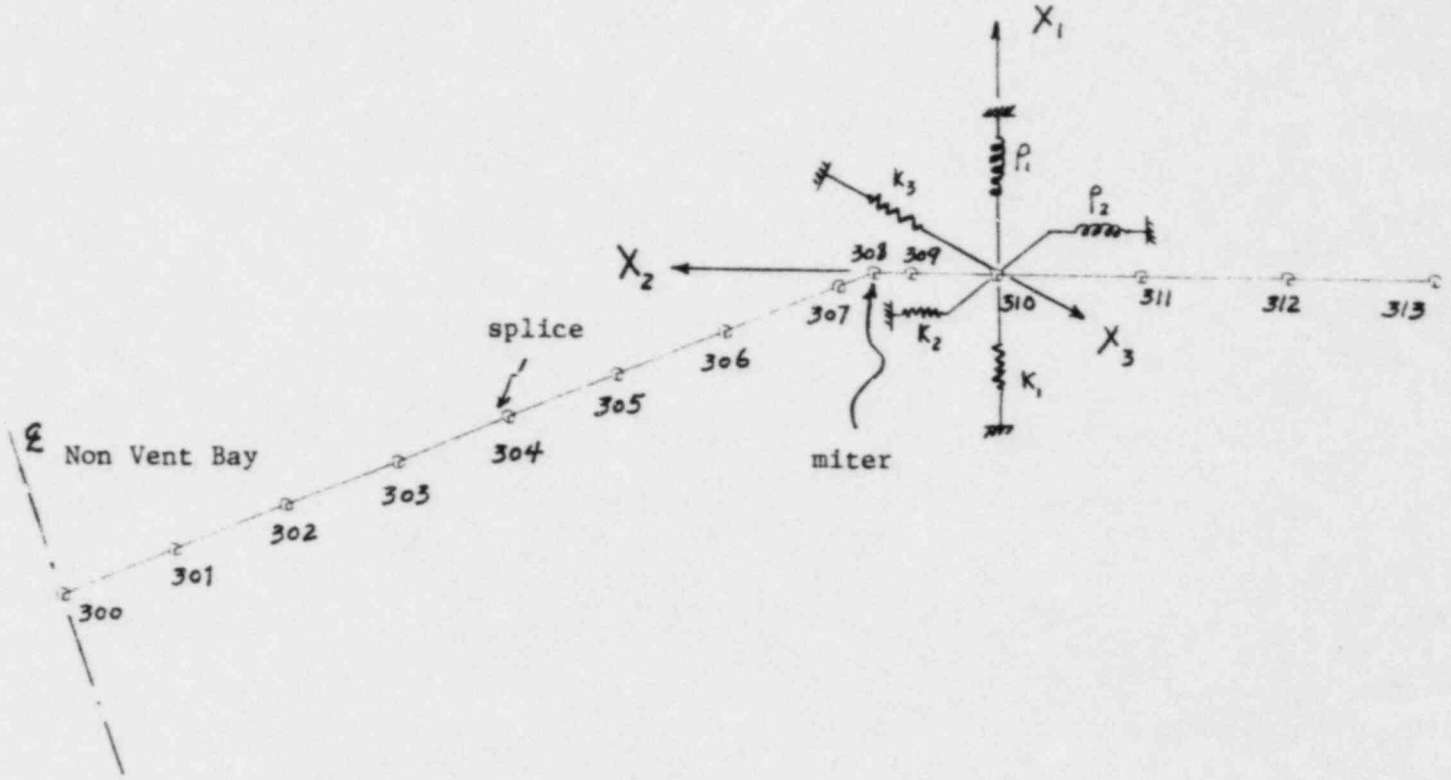

Figure 3.6.2.3-1 Finite Element Beam Model of Deflector

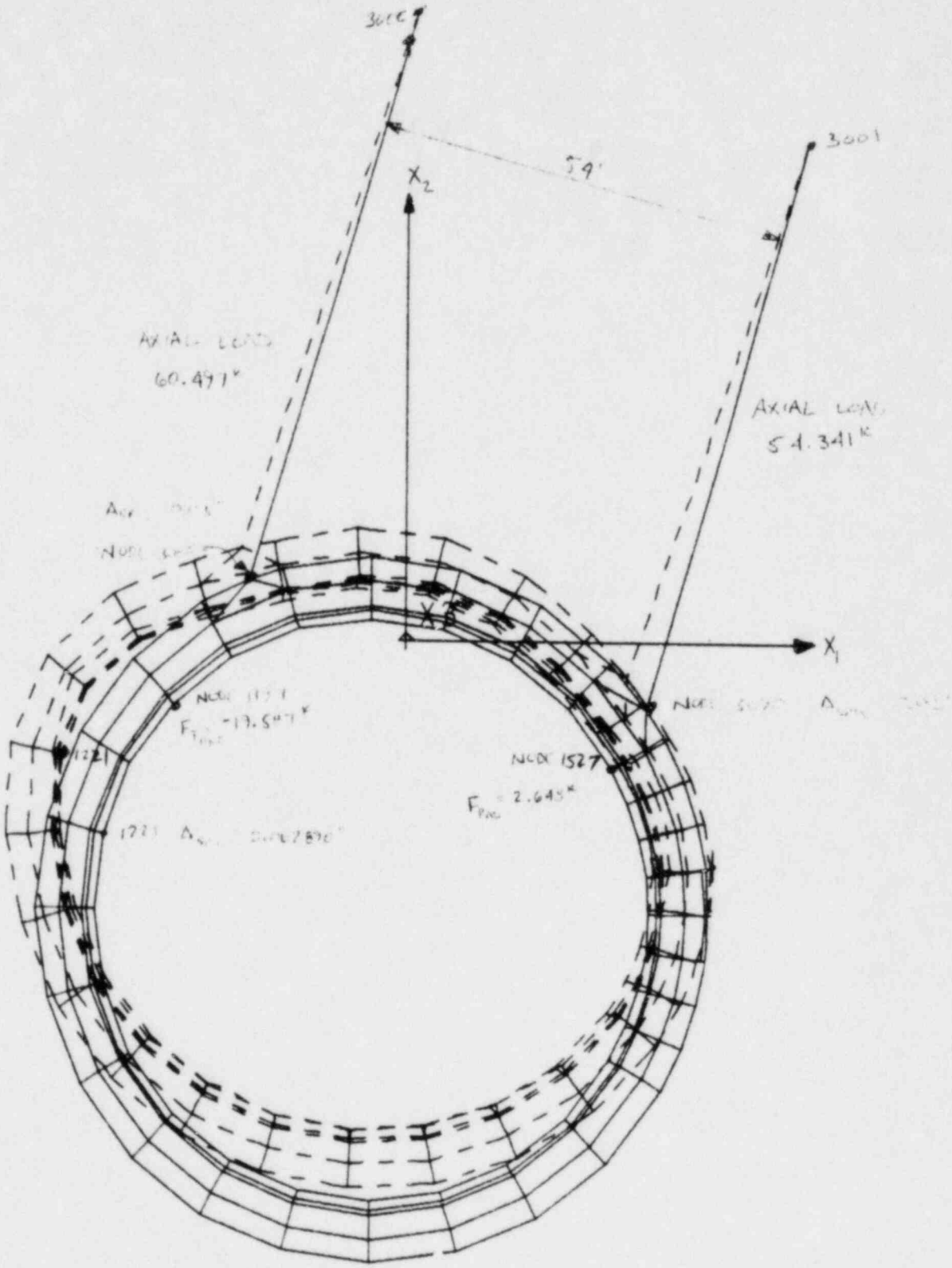

Figure 3.7.1-1 Vent & Vent Header Column Displacements and Reactions

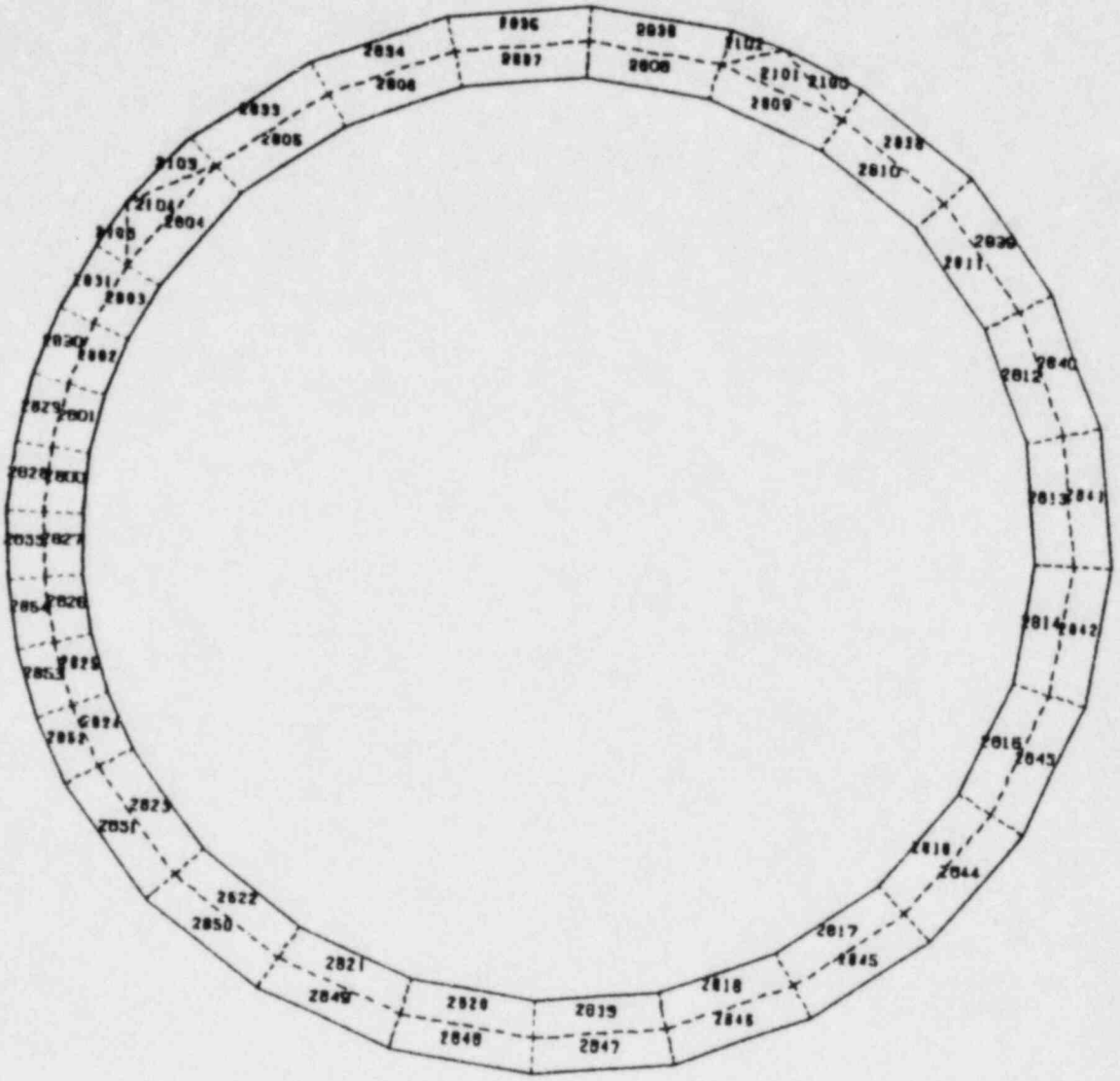

Figure 3.7.1-2 Stiffener Ring at Vent Header Column Supports Geometry Plot

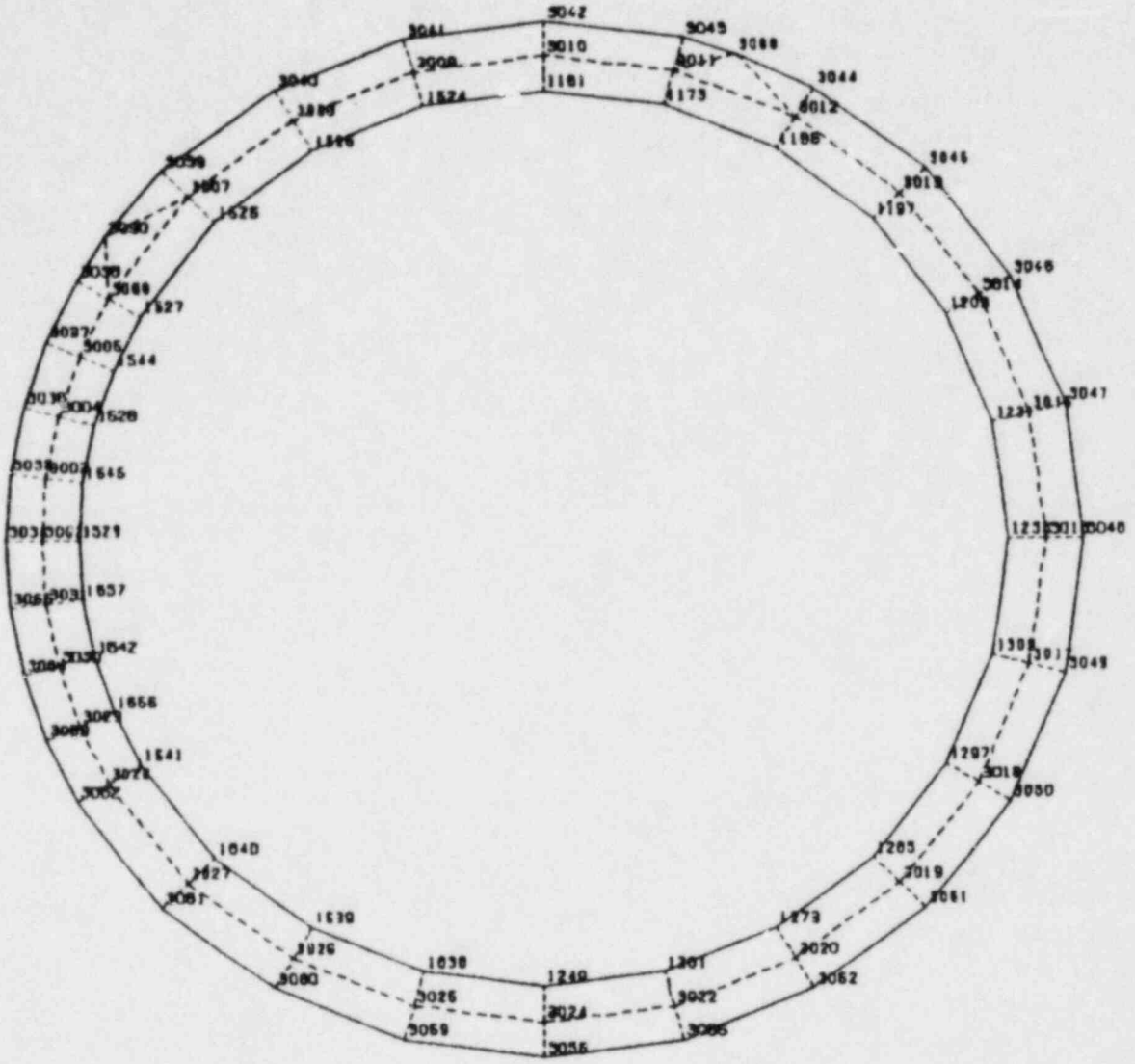

Figure 3.7.1-3 Stiffener Ring at Vent Header Column Supports
Geometry Plot

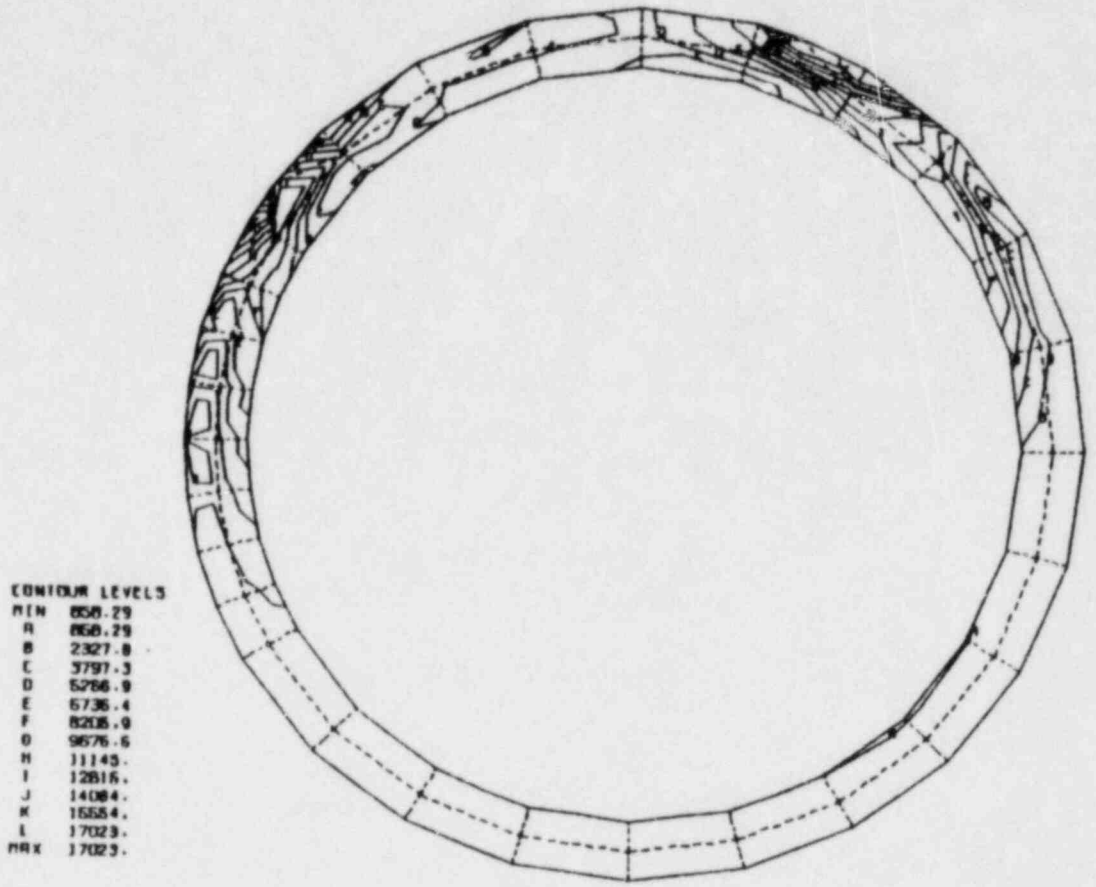

Figure 3.7.1-4 Stiffener Ring at Vent Header Column Supports Absolute Principal Stress Plot For Stress Intensity Qualification of Pool Swell Loads

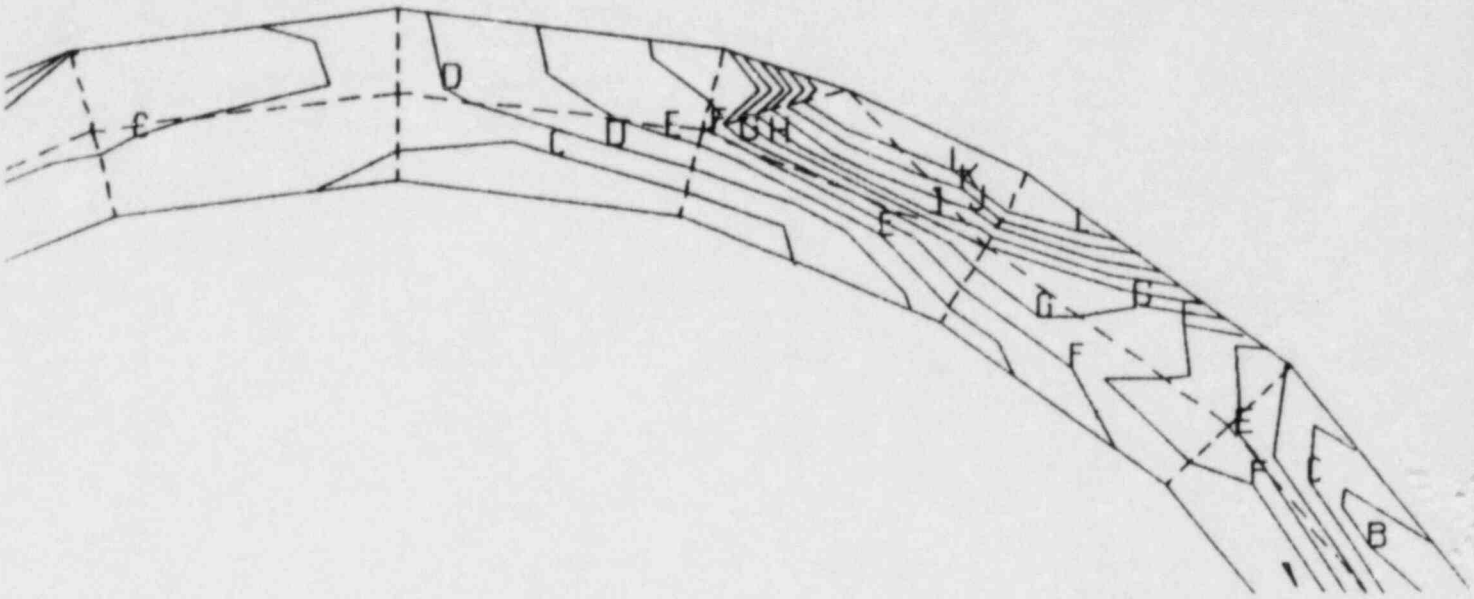

Figure 3.7.1-5 (Blow Up of 3.7.1-4)

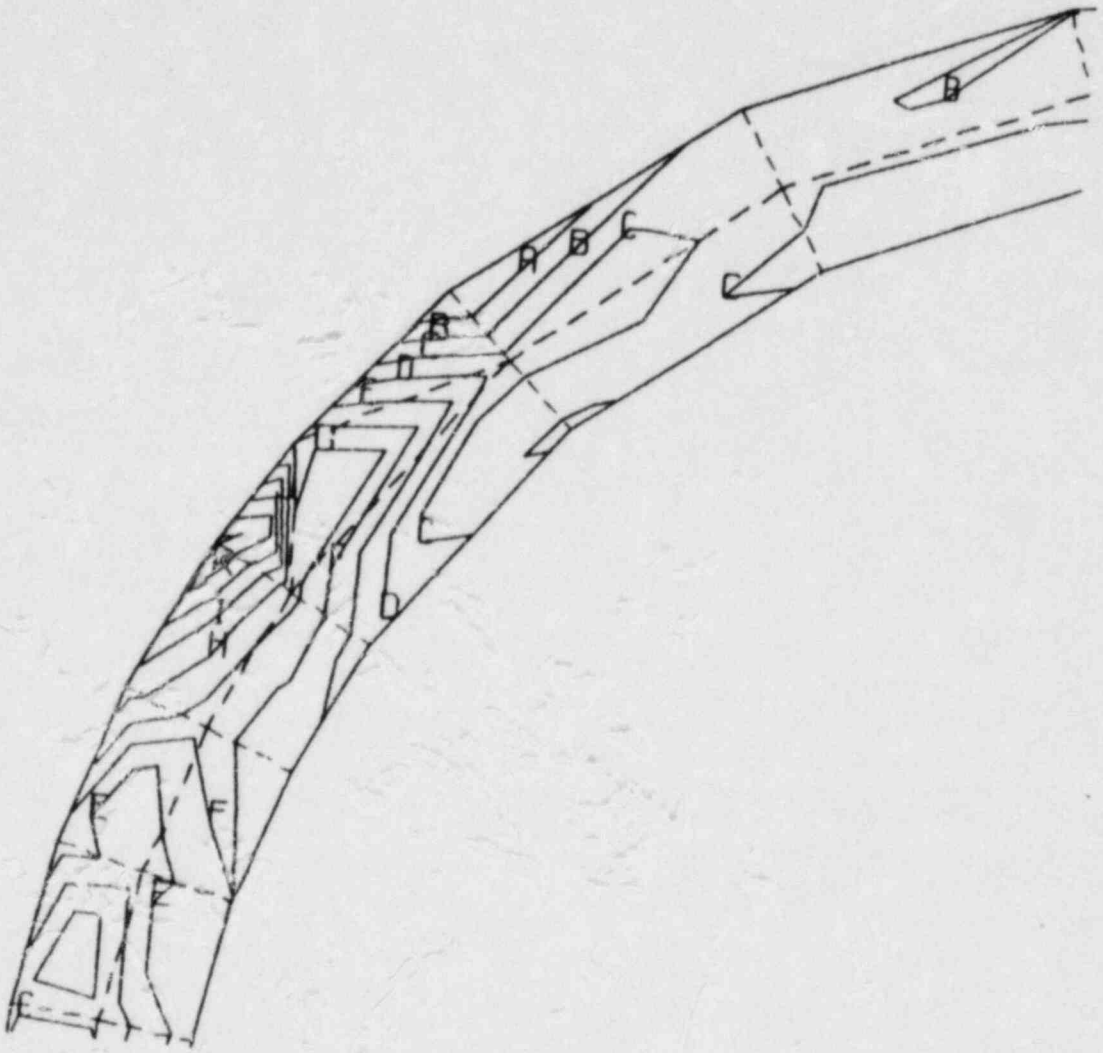

Figure 3.7.1-6 (Blow Up of 3.7.1-4)

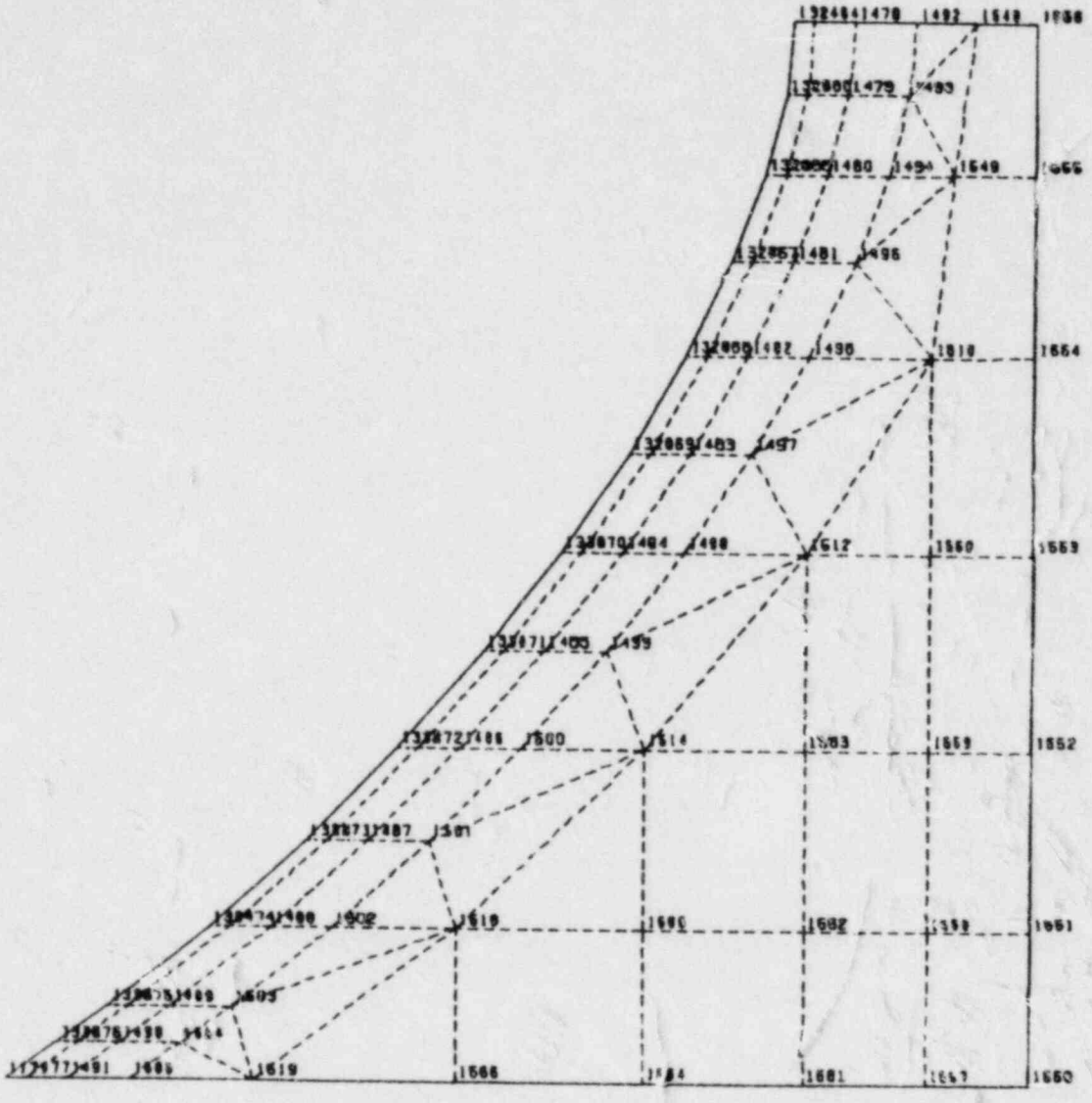

Figure 3.7.1-7 Main Vent Section E-1 Geometry Plot

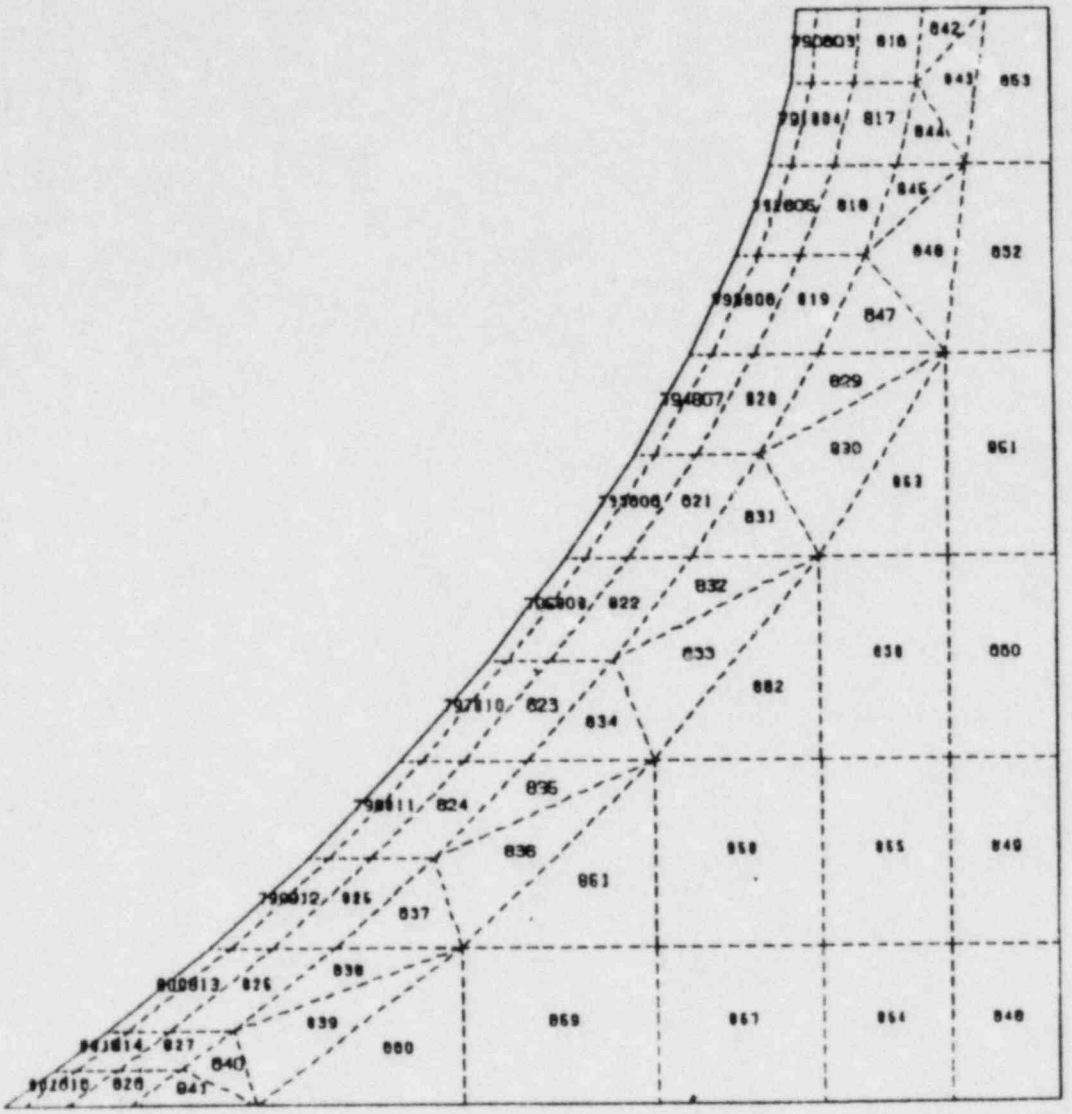

Figure 3.7.1-8 Main Vent Section E-1 Geometry Plot

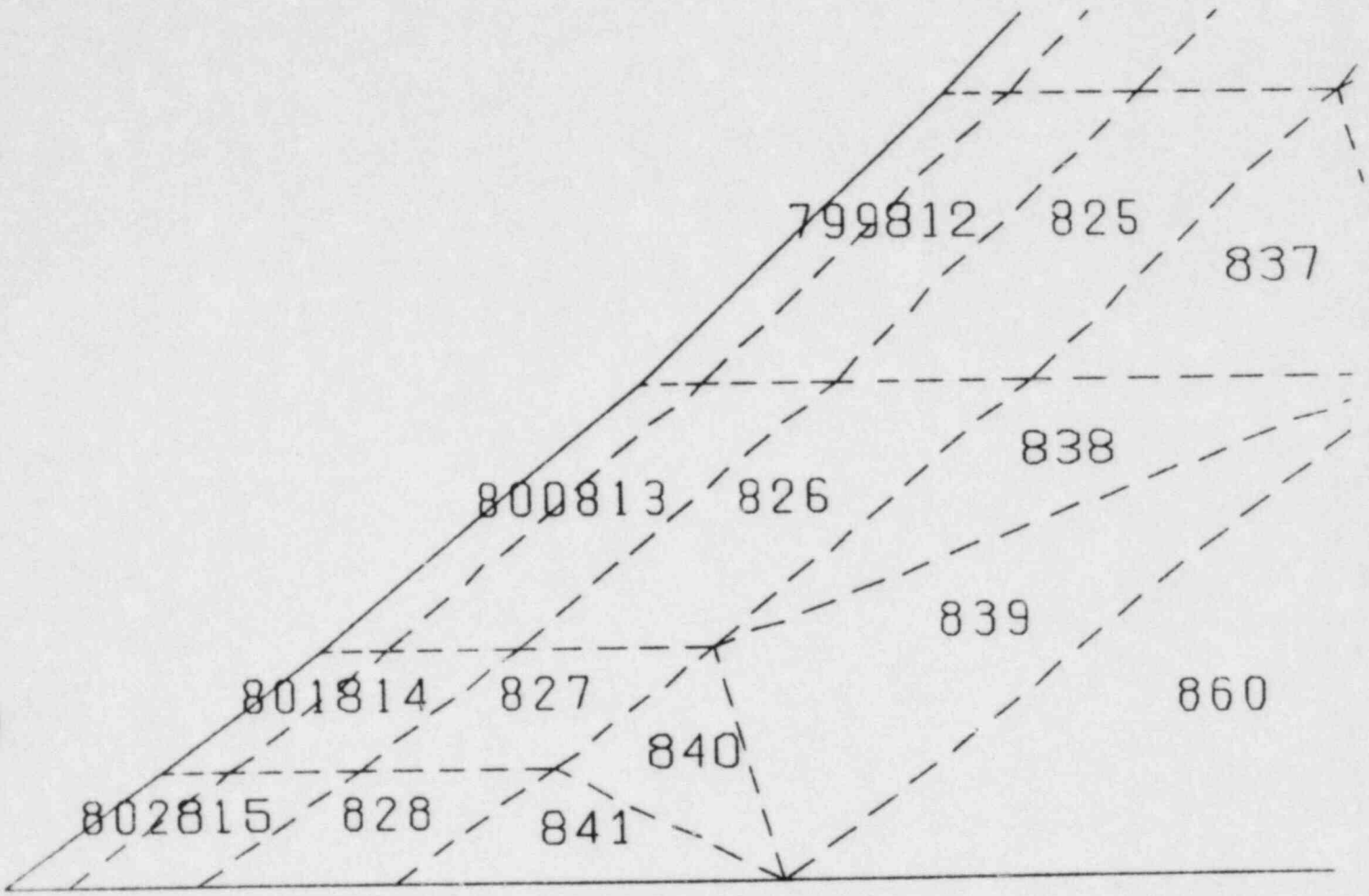

Figure 3.7.1-9 Main Vent Section E-1 Geometry Plot Blow Up

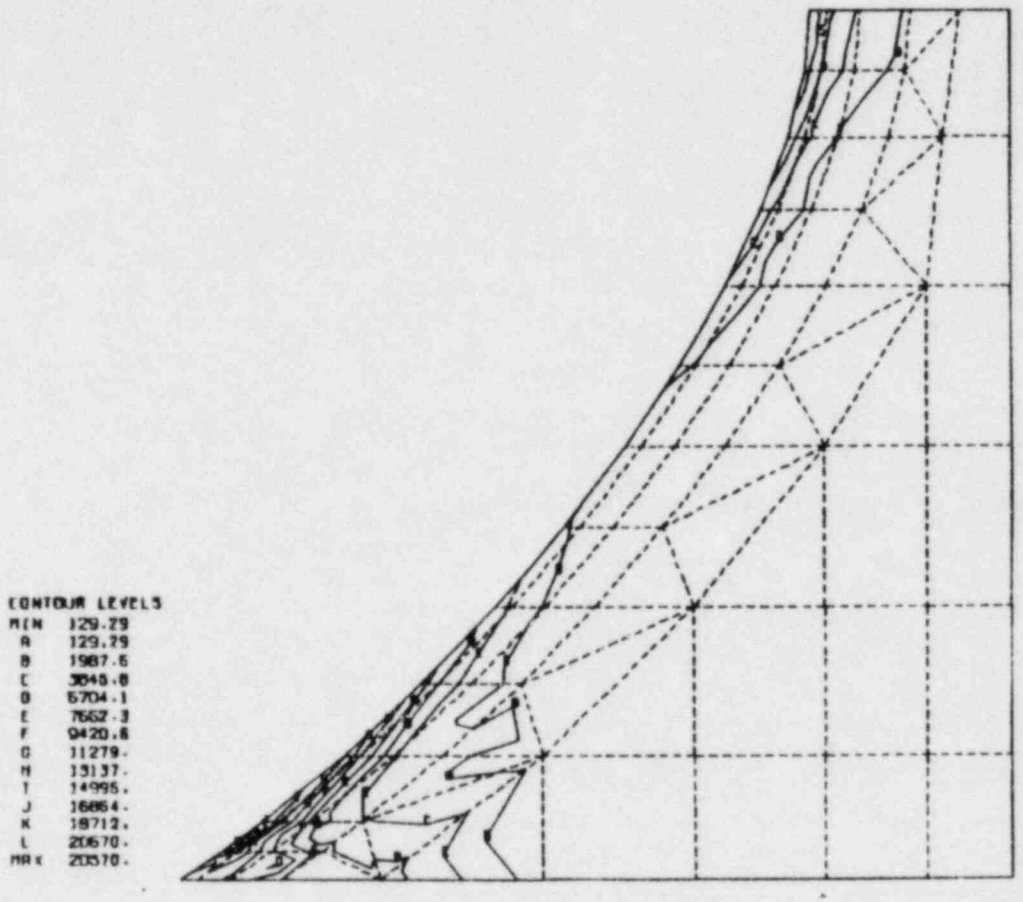

Figure 3.7.1-10 Main Vent Section E-1 Absolute Shear Stress Plot

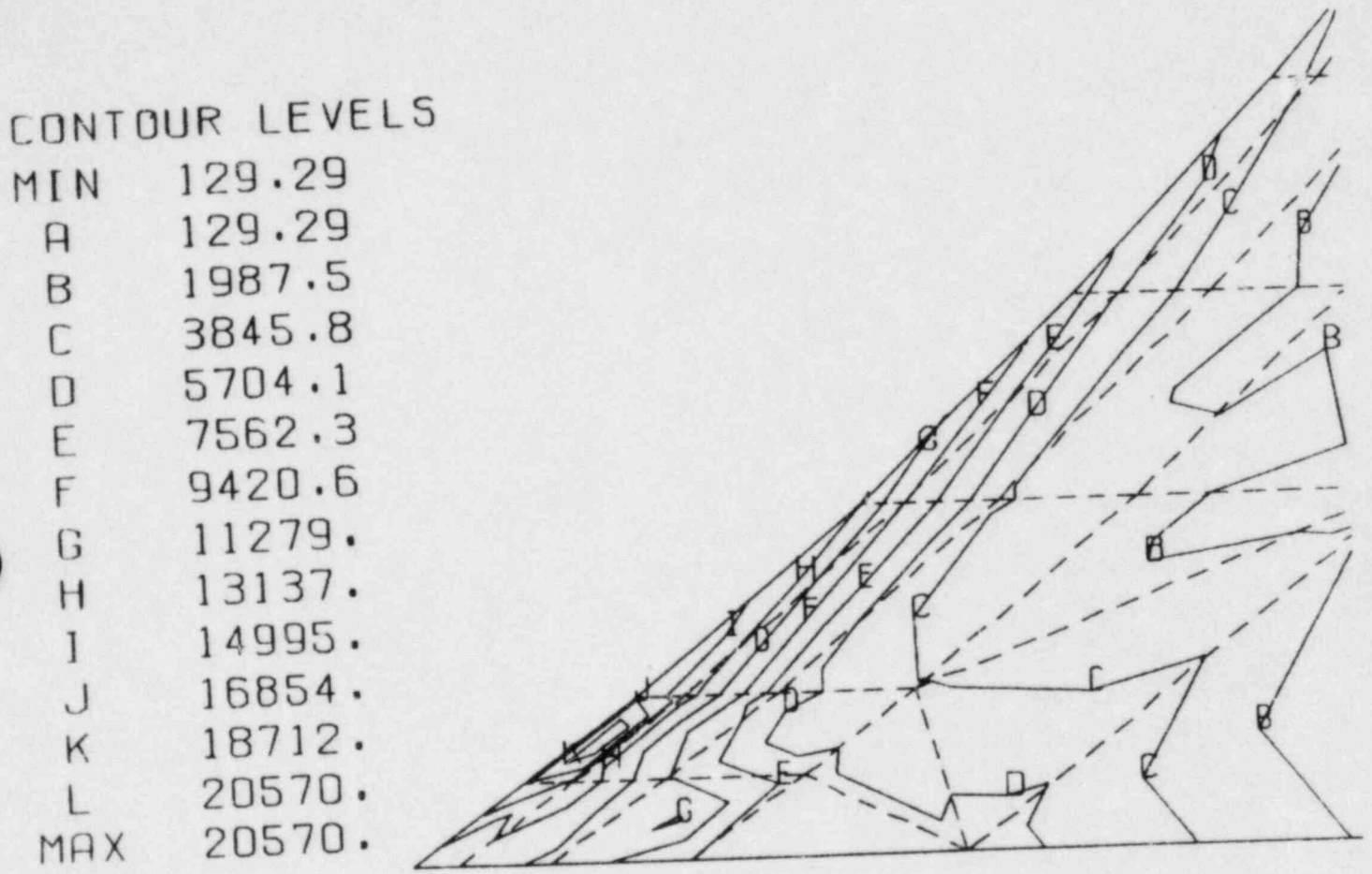

Figure 3.7.1-11 Main Vent Section E-1 Absolute Shear Stress Plot Blow Up

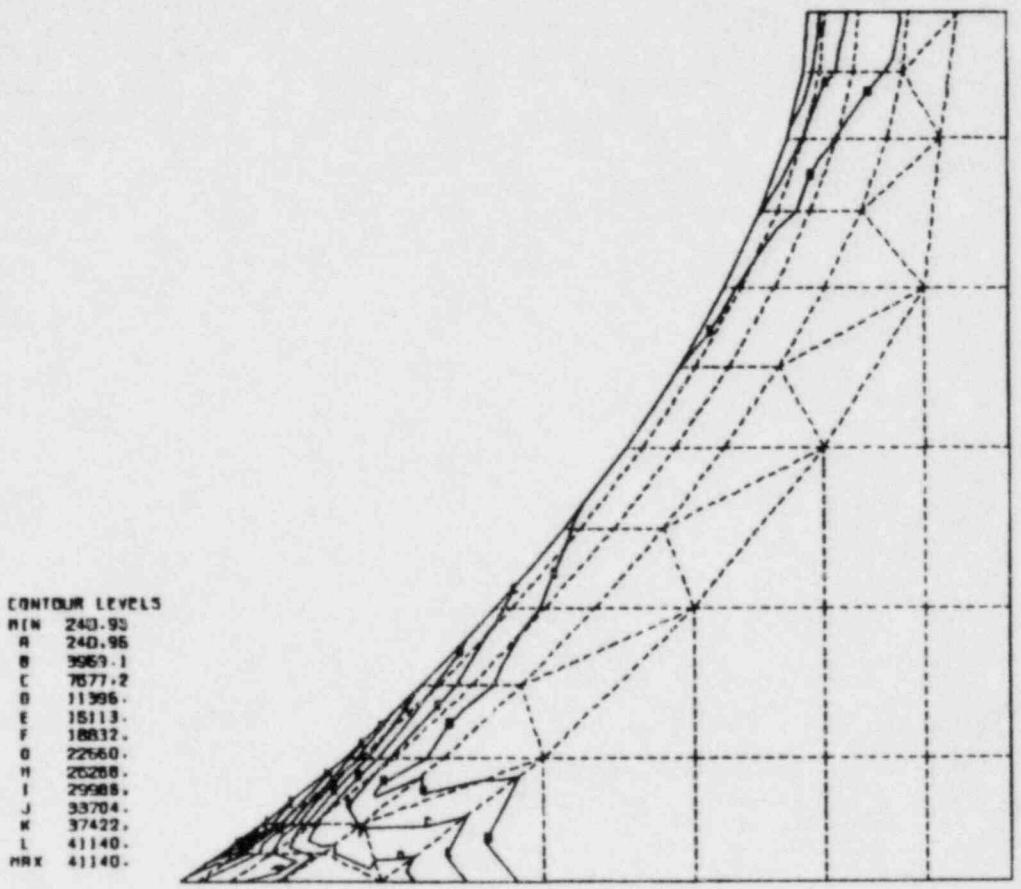

Figure 3.7.1-12 Main Vent Section E-1 Absolute Principal Stress Plot

CONTOUR LEVELS

MIN	240.95
A	240.95
B	3959.1
C	7677.2
D	11395.
E	15113.
F	18832.
G	22550.
H	26268.
I	29986.
J	33704.
K	37422.
L	41140.
MAX	41140.

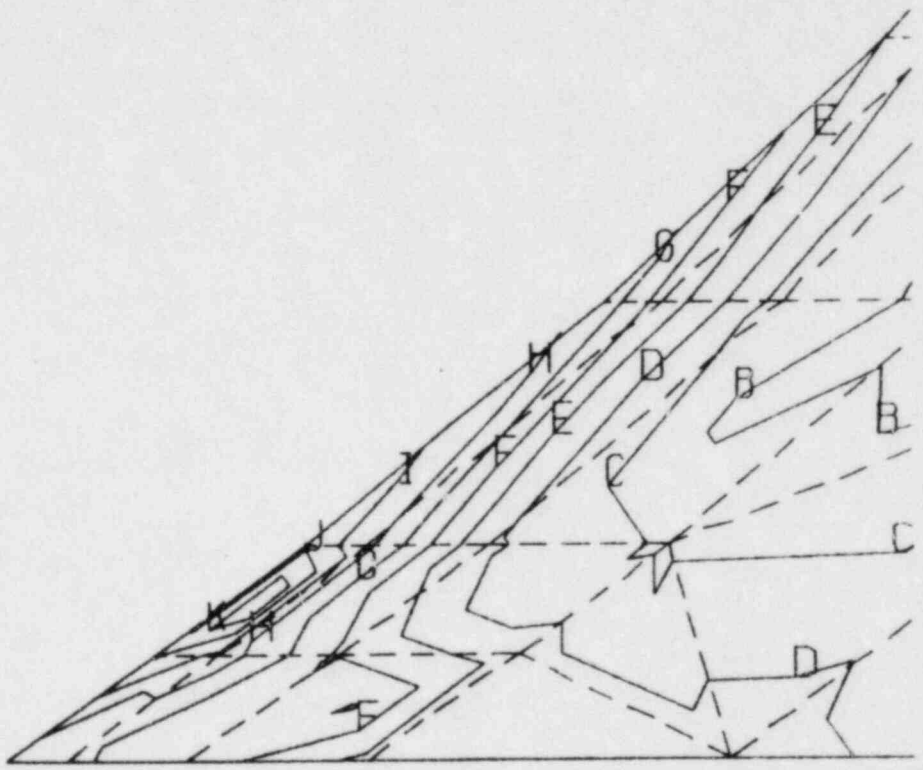

Figure 3.7.1-13 Main Vent Section E-1 Absolute Principal Stress Plot Blow Up

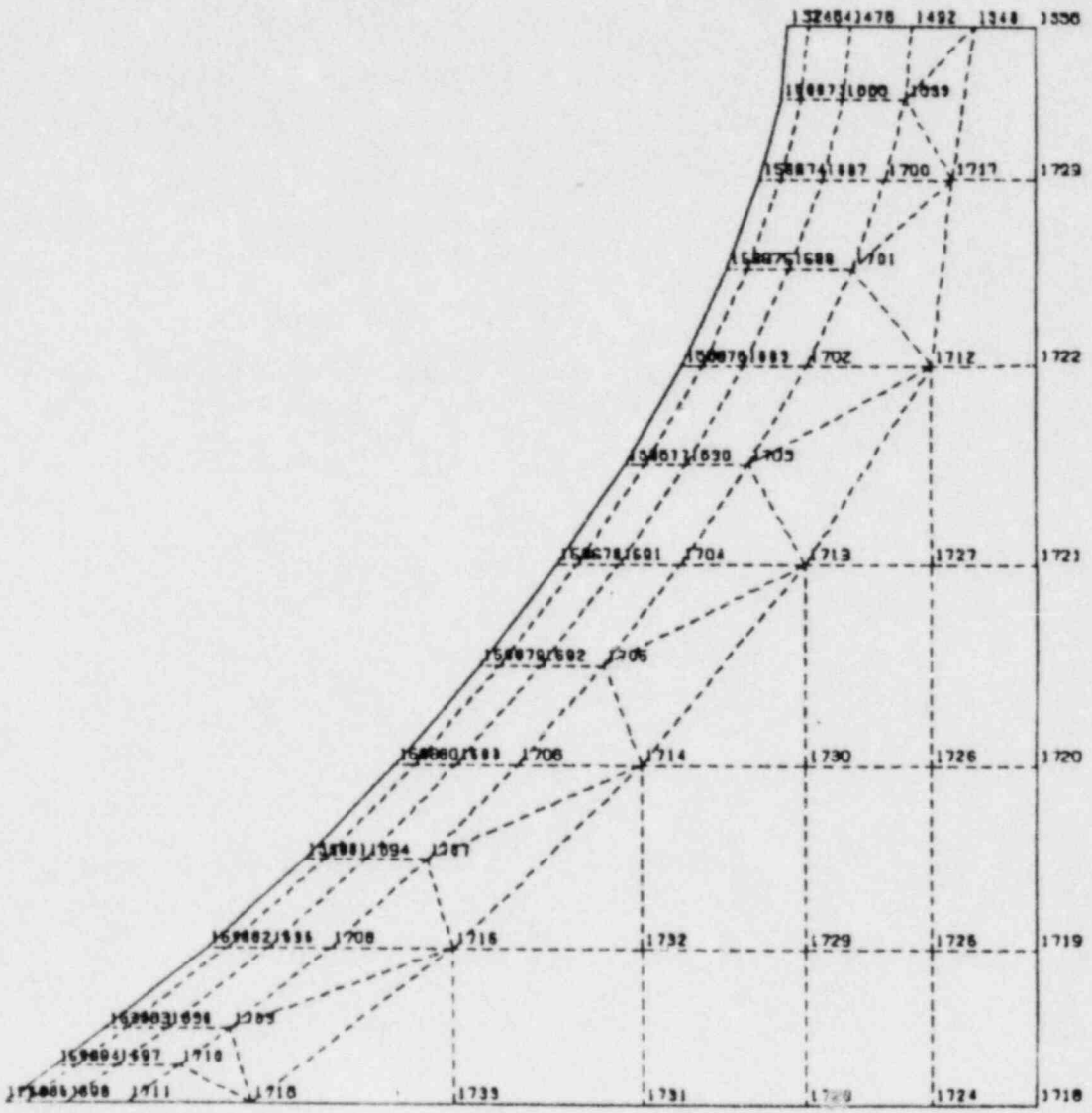

Figure 3.7.1-14 Main Vent Section E-2 Geometry Plot

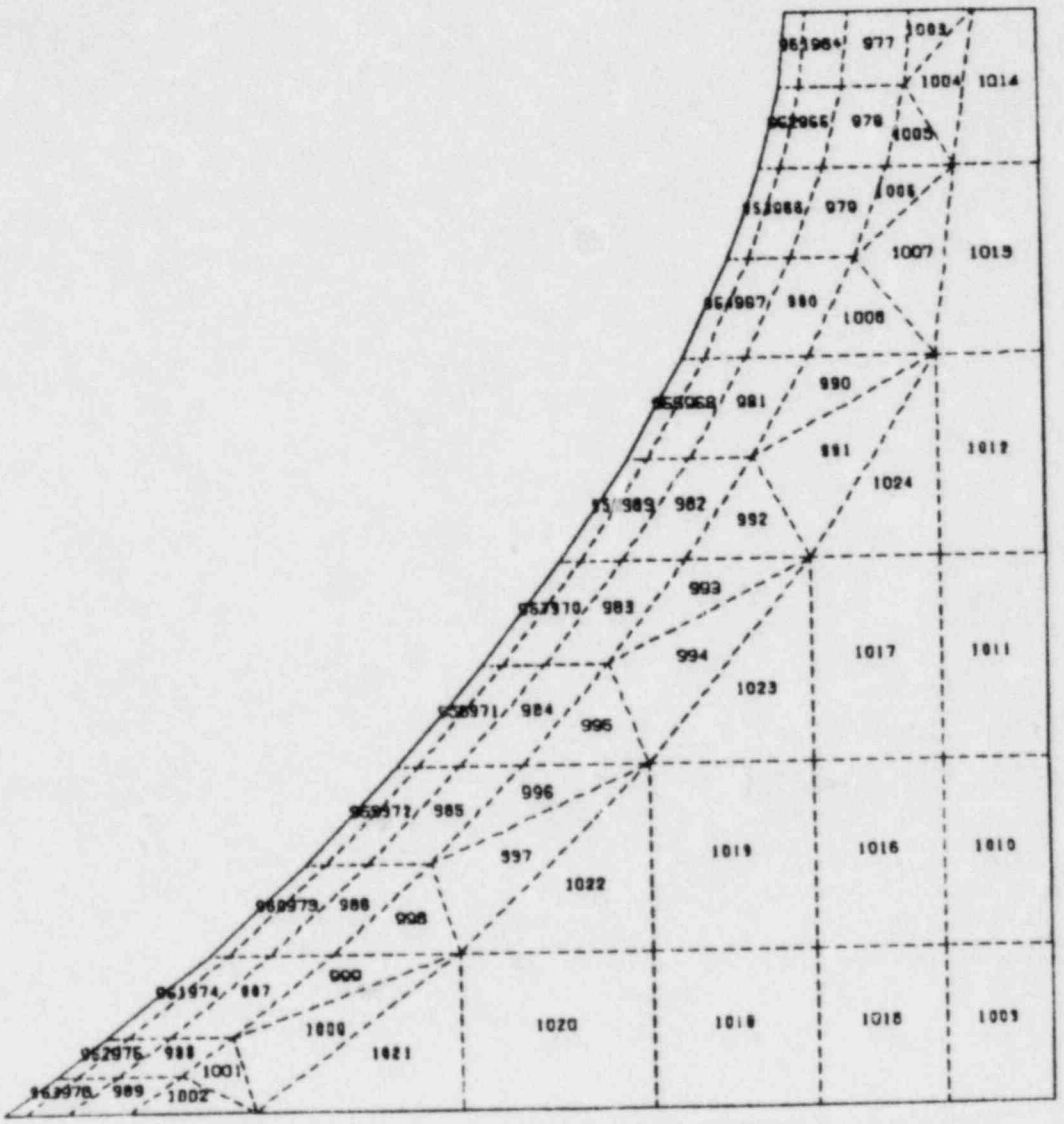

Figure 3.7.1-15 Main Vent Section E-2 Geometry Plot

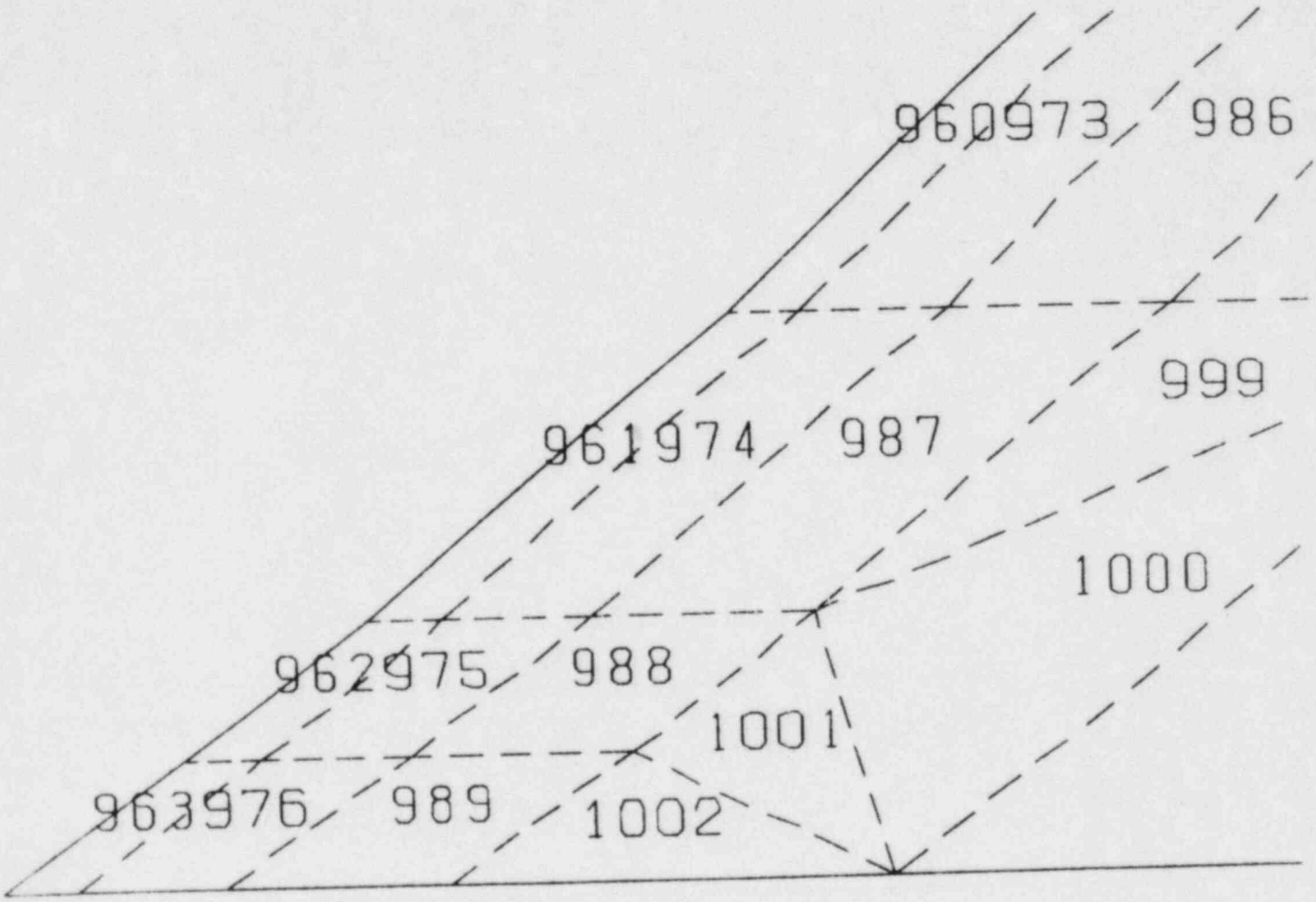

Figure 3.7.1-16 Main Vent Section E-2 Geometry Plot Blow Up

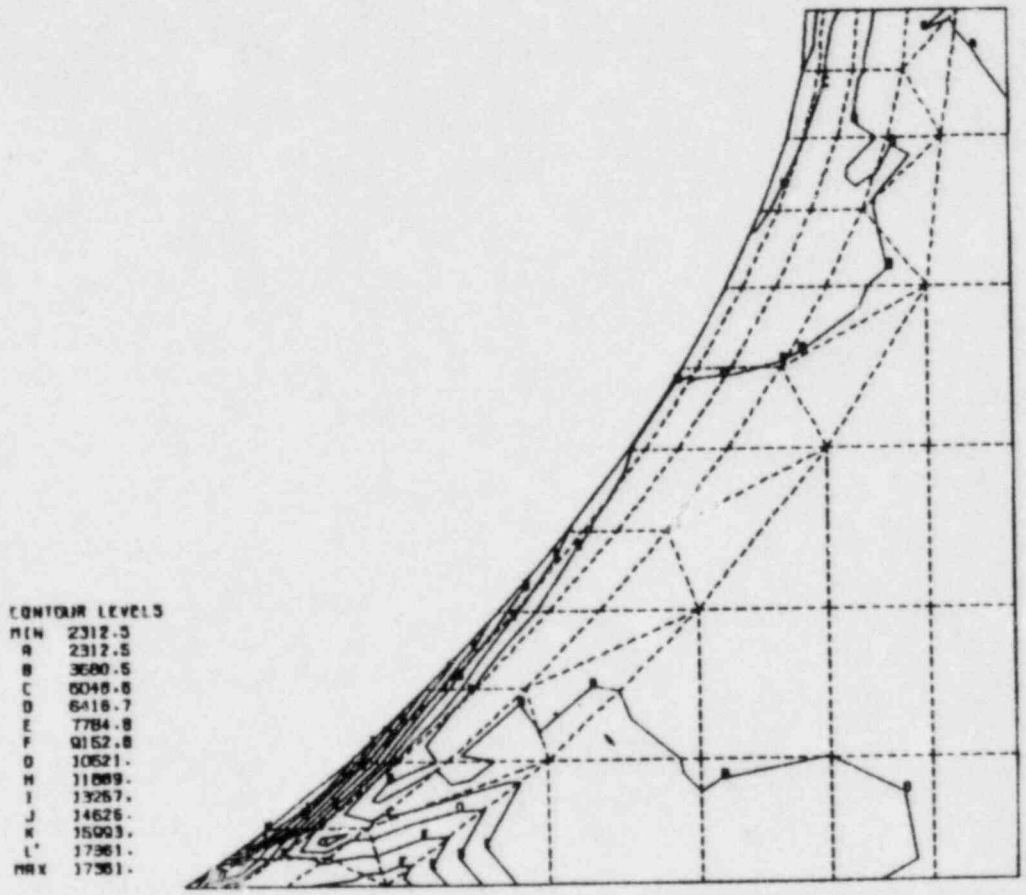

Figure 3.7.1-17 Main Vent Section E-2 Absolute Shear Stress Plot

CONTOUR LEVELS

MIN	2312.5
A	2312.5
B	3680.5
C	5048.6
D	6416.7
E	7784.8
F	9152.8
G	10521.
H	11889.
I	13257.
J	14625.
K	15993.
L	17361.
MAX	17361.

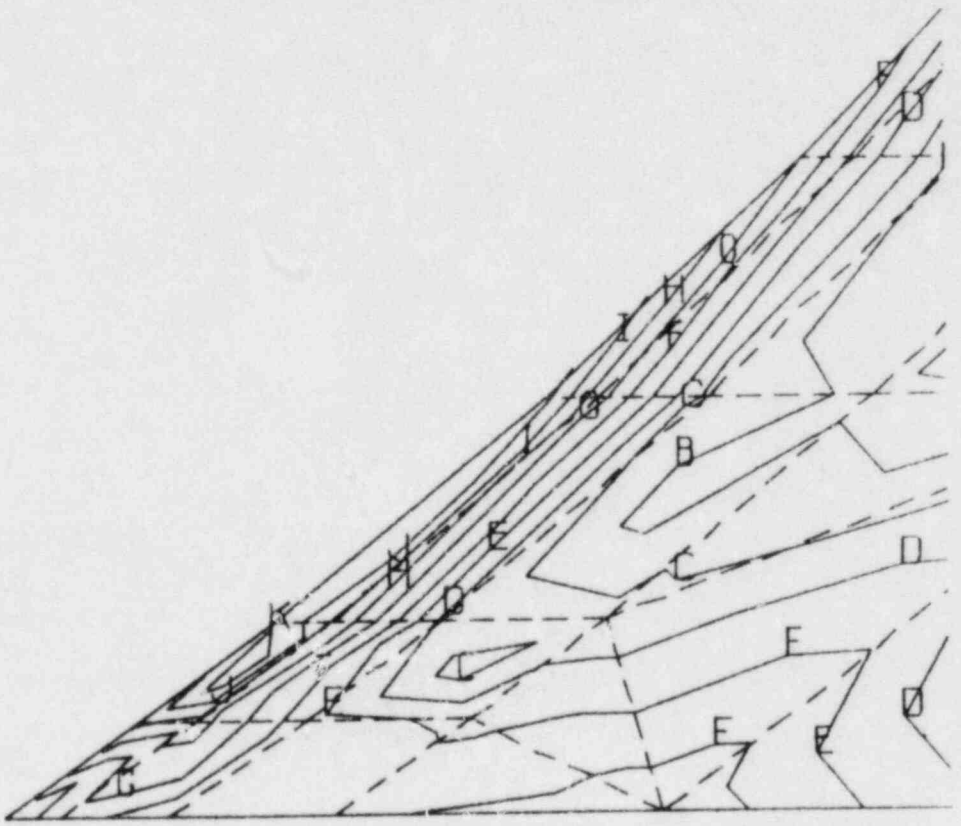

Figure 3.7.1-18 Main Vent Section E-2 Absolute Shear Stress Plot Blow Up

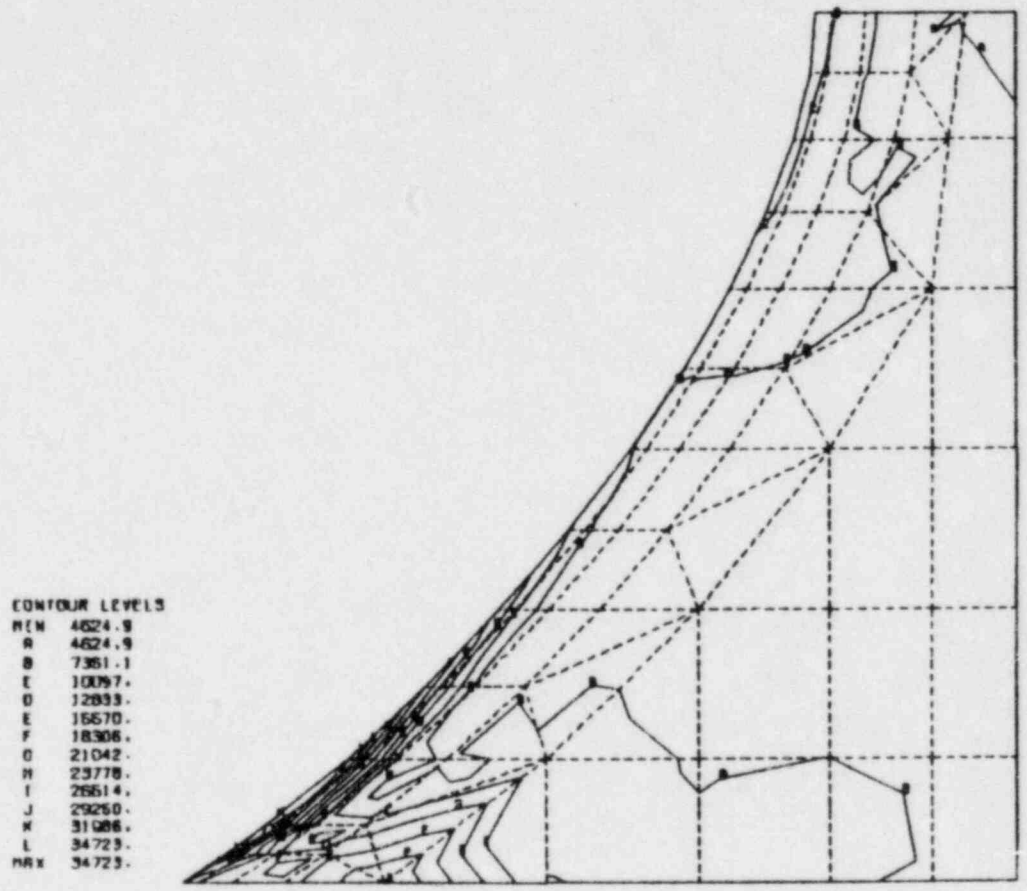

Figure 3.7.1-19 Main Vent Section E-2 Absolute Principal Stress Plot

CONTOUR LEVELS

MIN	4624.9
A	4624.9
B	7361.1
C	10097.
D	12833.
E	15570.
F	18306.
G	21042.
H	23778.
I	26514.
J	29250.
K	31986.
L	34723.
MAX	34723.

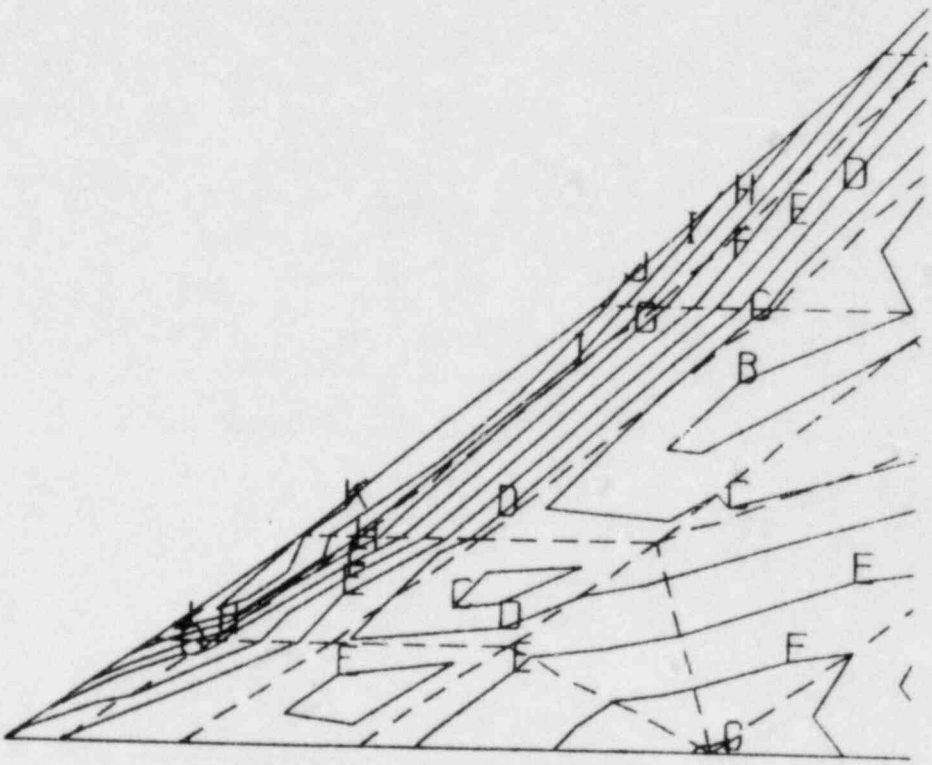

Figure 3.7.1-20 Main Vent Section E-2 Absolute Principal Stress Plot Blow Up

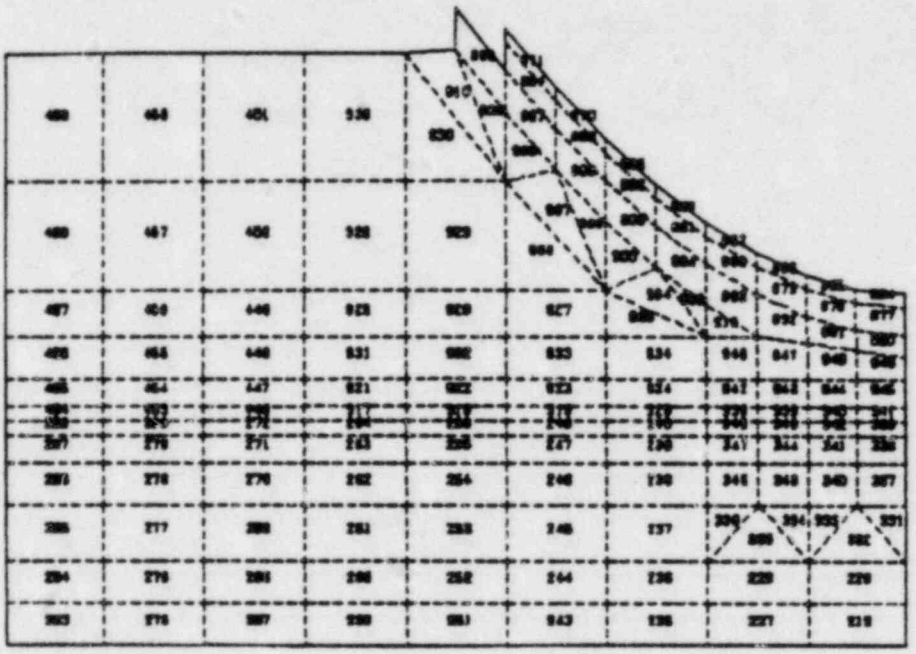

Figure 3.7.1-21 Vent Header X_1, - X_2 Quadrant Geometry Plot

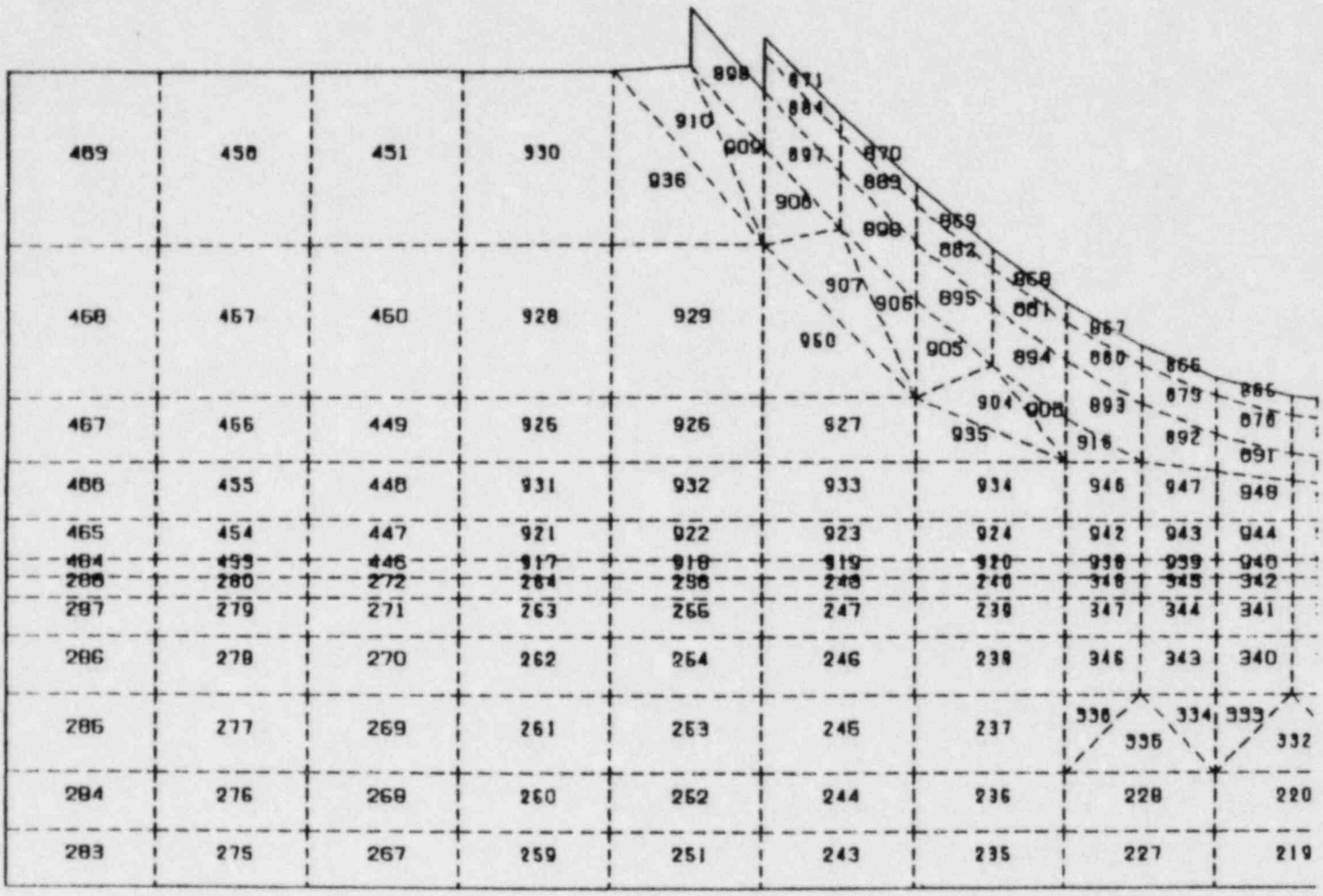

Figure 3.7.1-22 Vent Header X_1, $-X_2$ Quadrant Geometry Plot

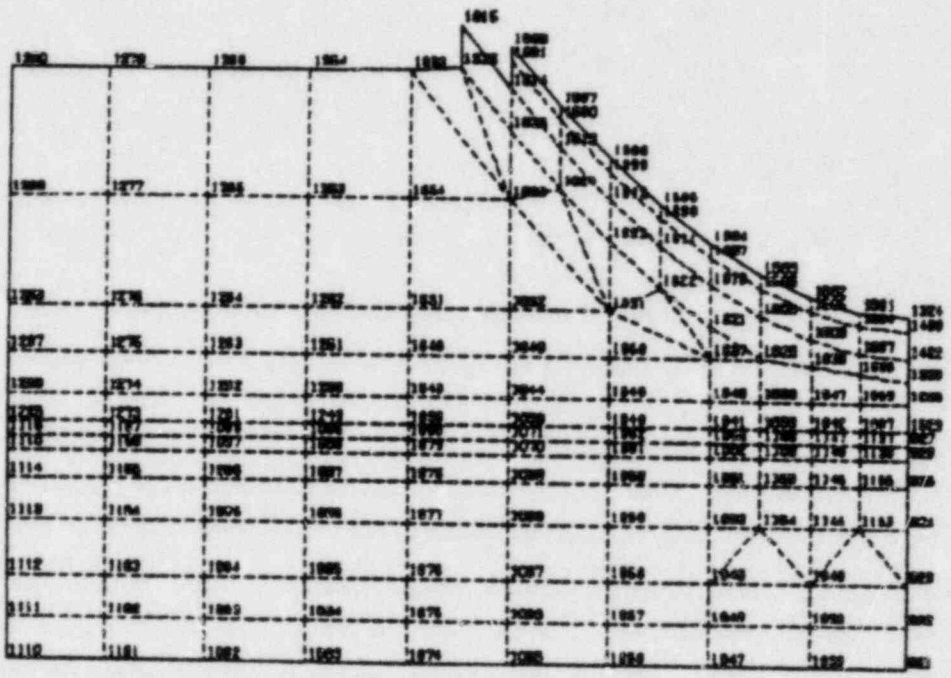

Figure 3.7.1-23 Vent Header X_1, - X_2 Quadrant Geometry Plot

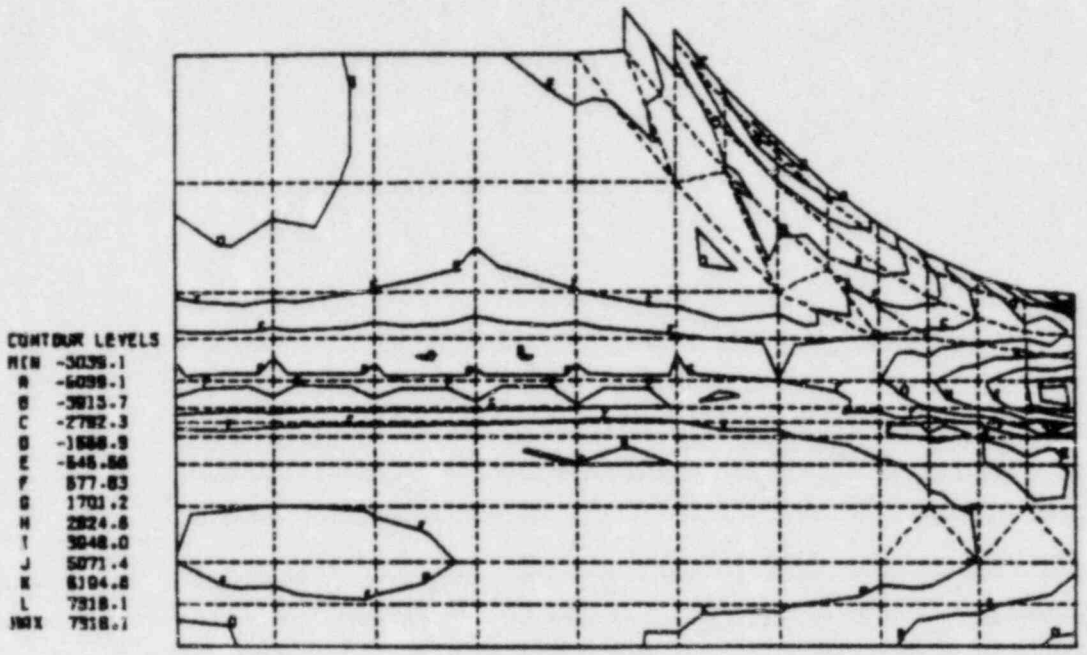

Figure 3.7.1-24 Vent Header X_1, - X_2 Quadrant Maximum Principal Stress -X_3 Plot

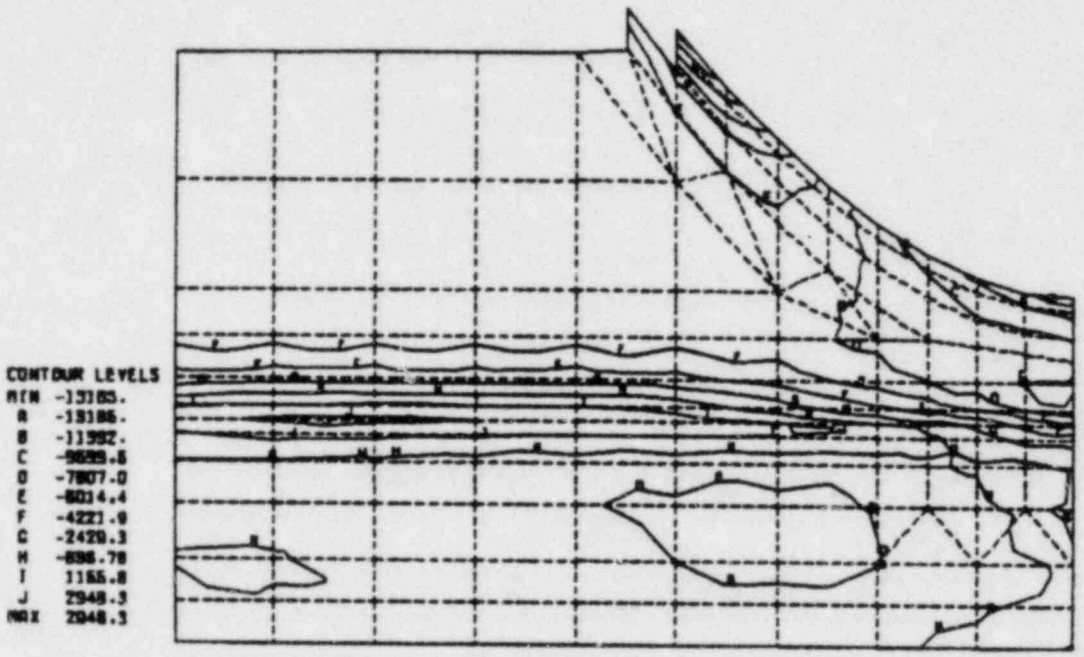

Figure 3.7.1-25 Vent Header X_1, - X_2 Quadrant Minimum Principal Stress $+X_3$ Plot

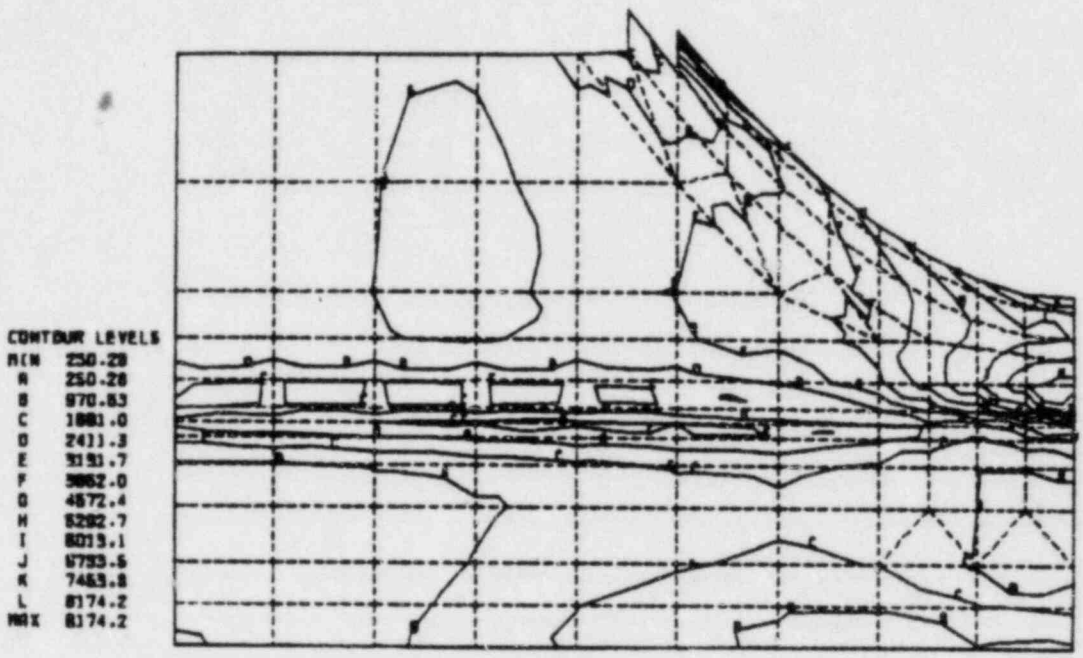

Figure 3.7.1-26 Vent Header X_1, - X_2 Quadrant Maximum Shear Stress -X_3 Plot

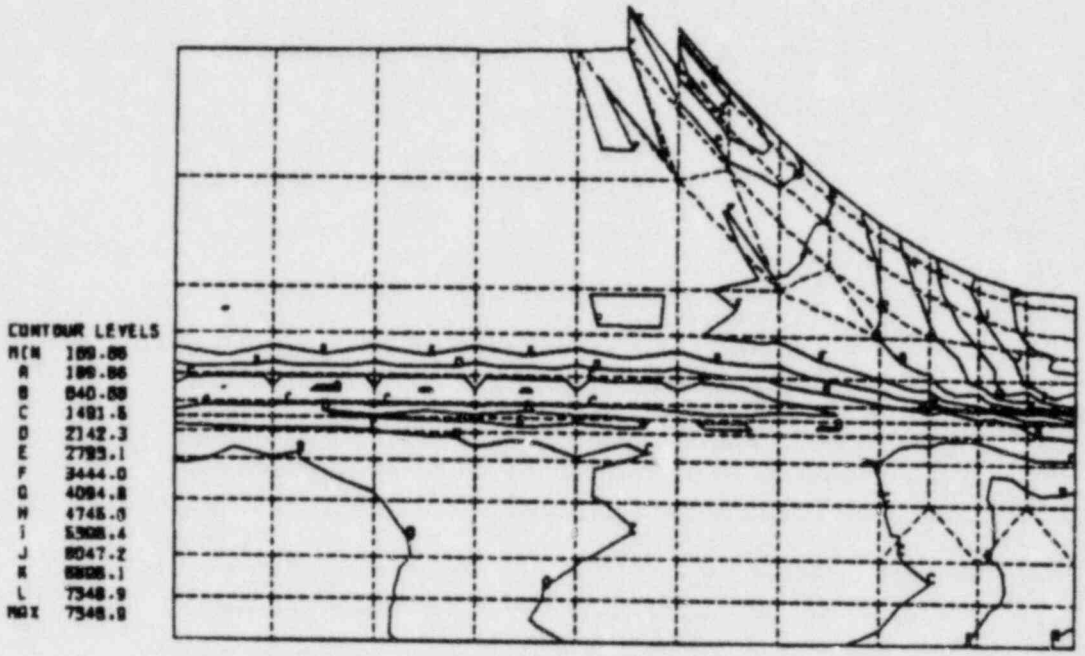

Figure 3.7.1-27 Vent Header X_1, - X_2 Quadrant Maximum Shear Stress $+X_3$ Plot

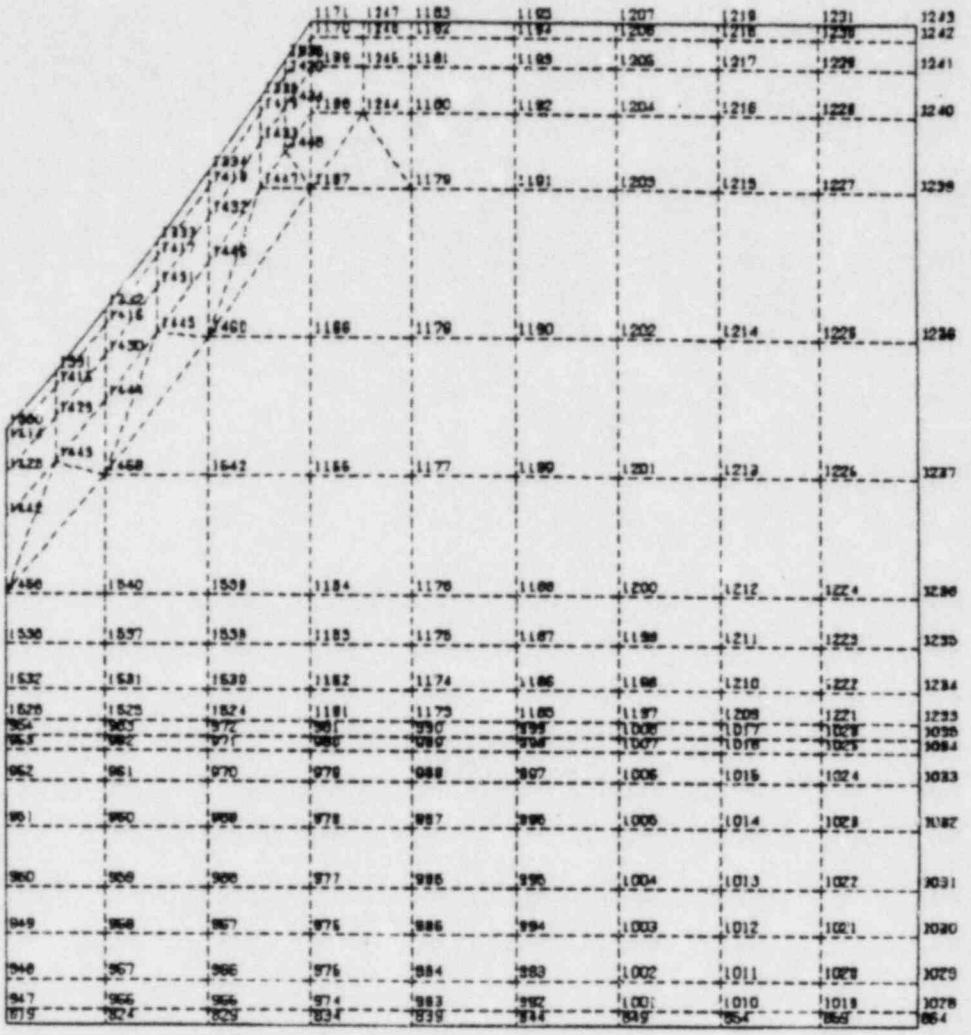

Figure 3.7.1-28 Vent Header -X_1, X_2 Quadrant Geometry Plot

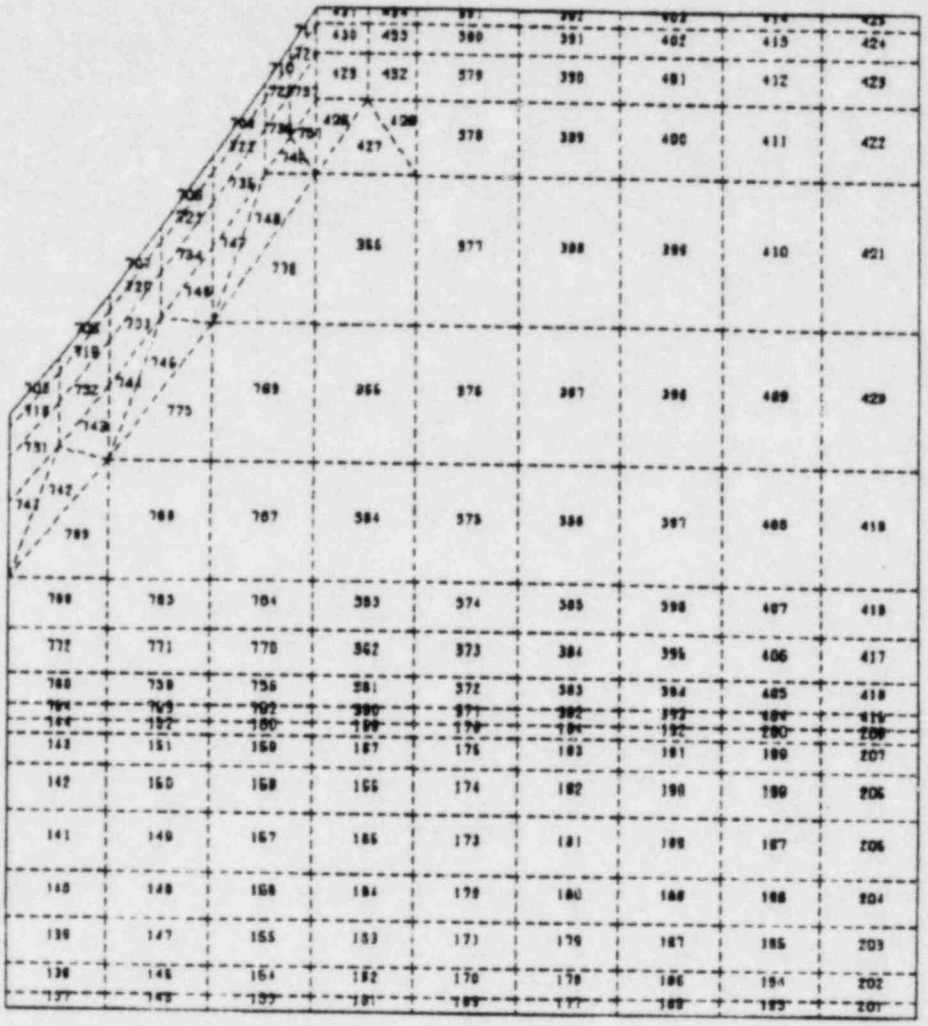

Figure 3.7.1-29 Vent Header -X_1, X_2 Quadrant Geometry Plot

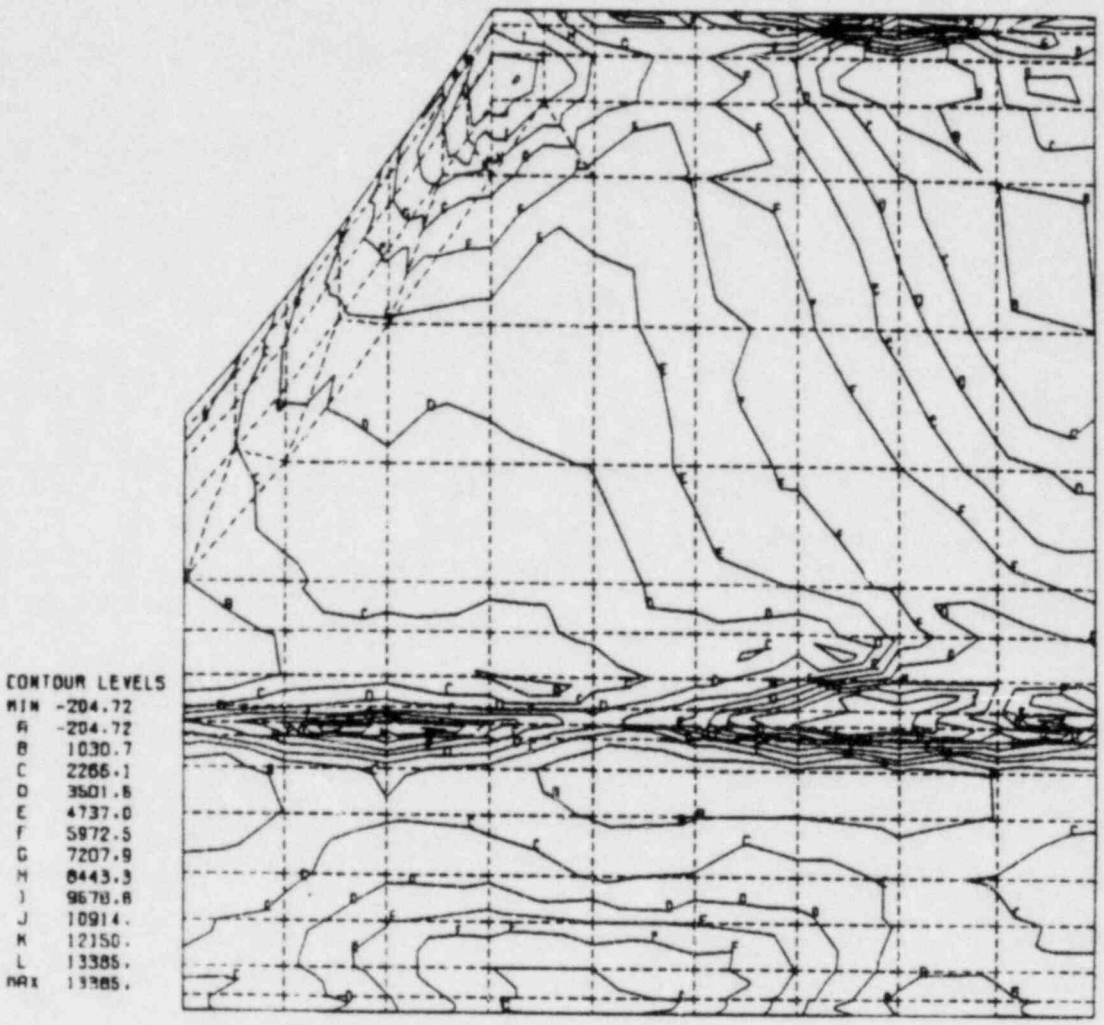

Figure 3.7.1-30 Vent Header $-X_1$, X_2 Quadrant Minimum Principal Stress $-X_3$ Plot

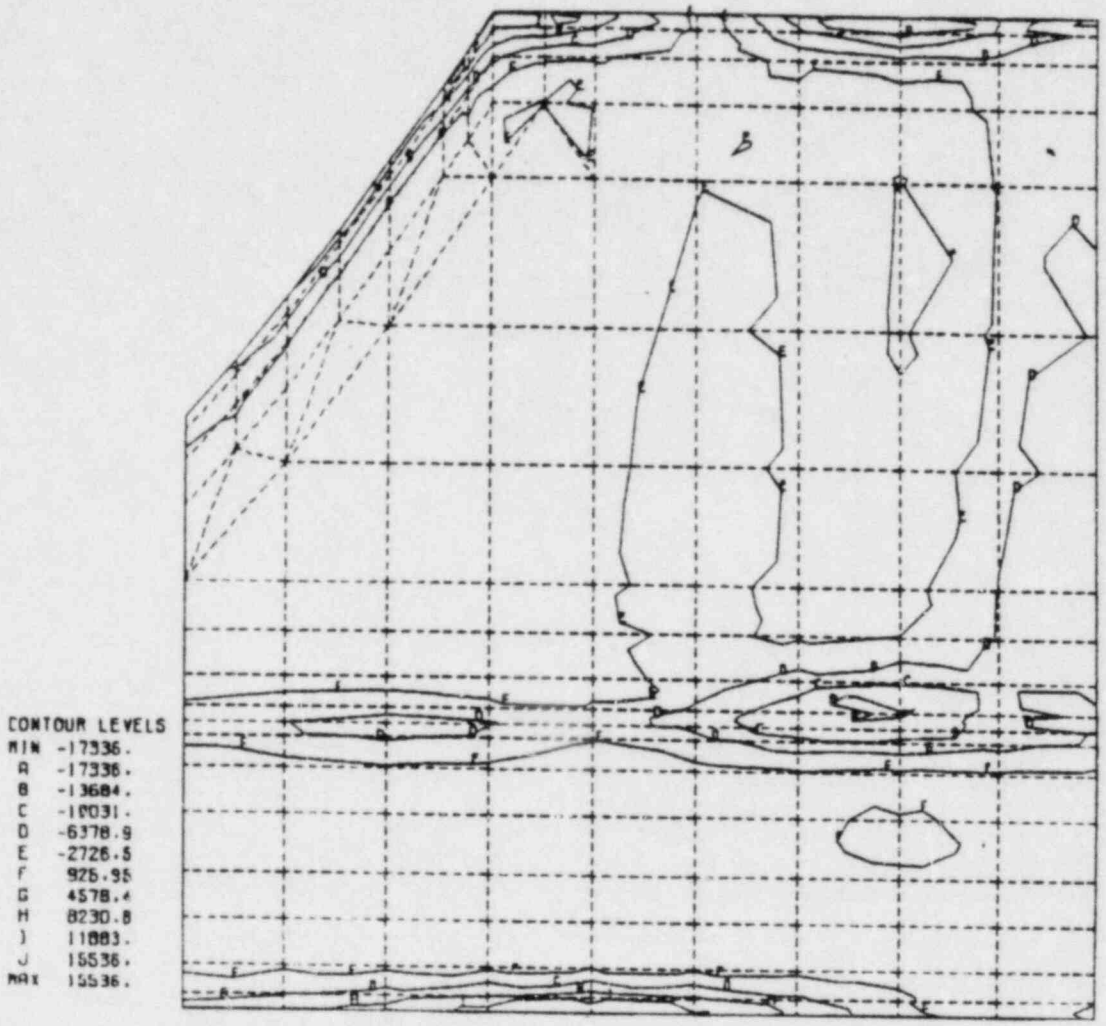

Figure 3.7.1-31 Vent Header $-X_1$, X_2 Quadrant Minimum Principal Stress $+X_3$ Plot

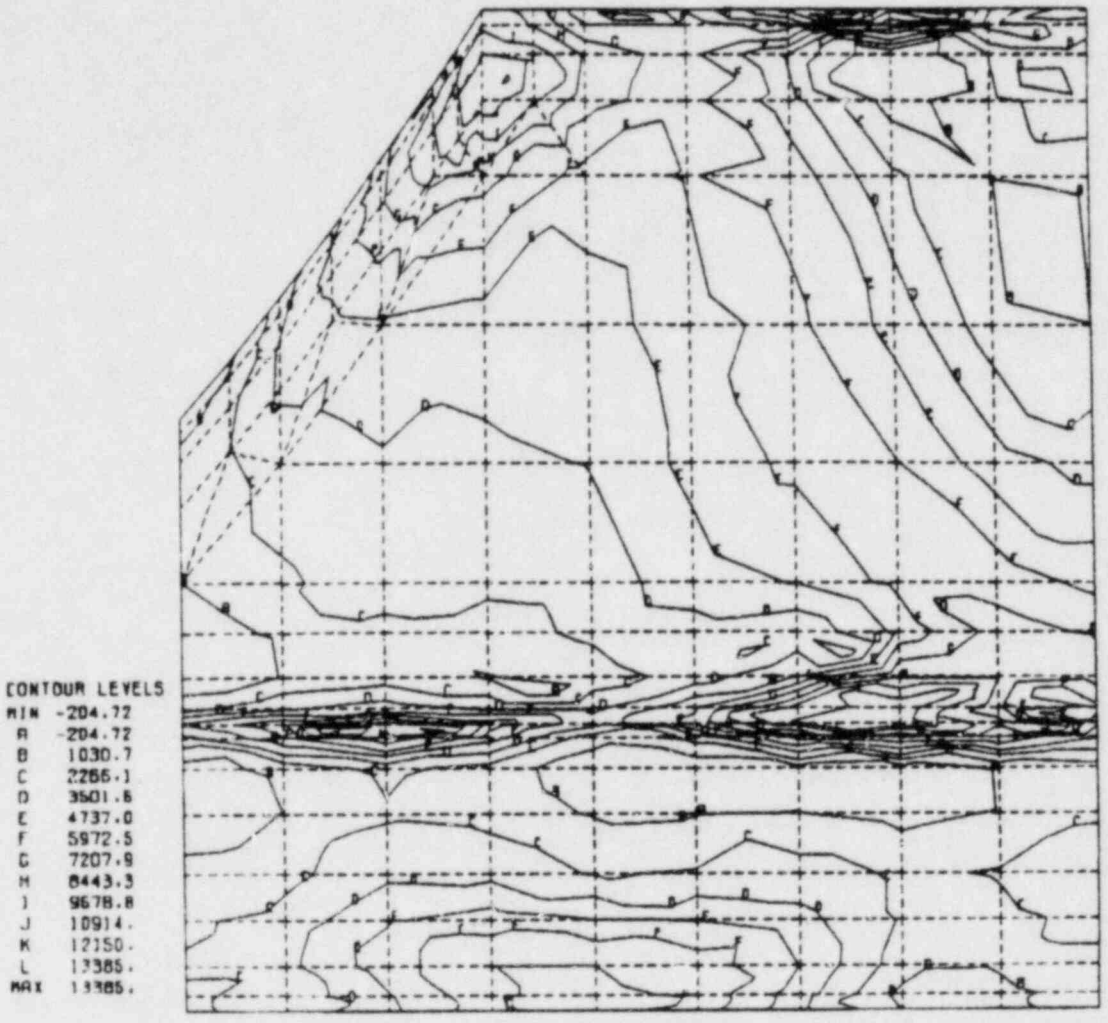

Figure 3.7.1-32 Vent Header -X_1, X_2 Quadrant Maximum Principal Stress -X_3 Plot

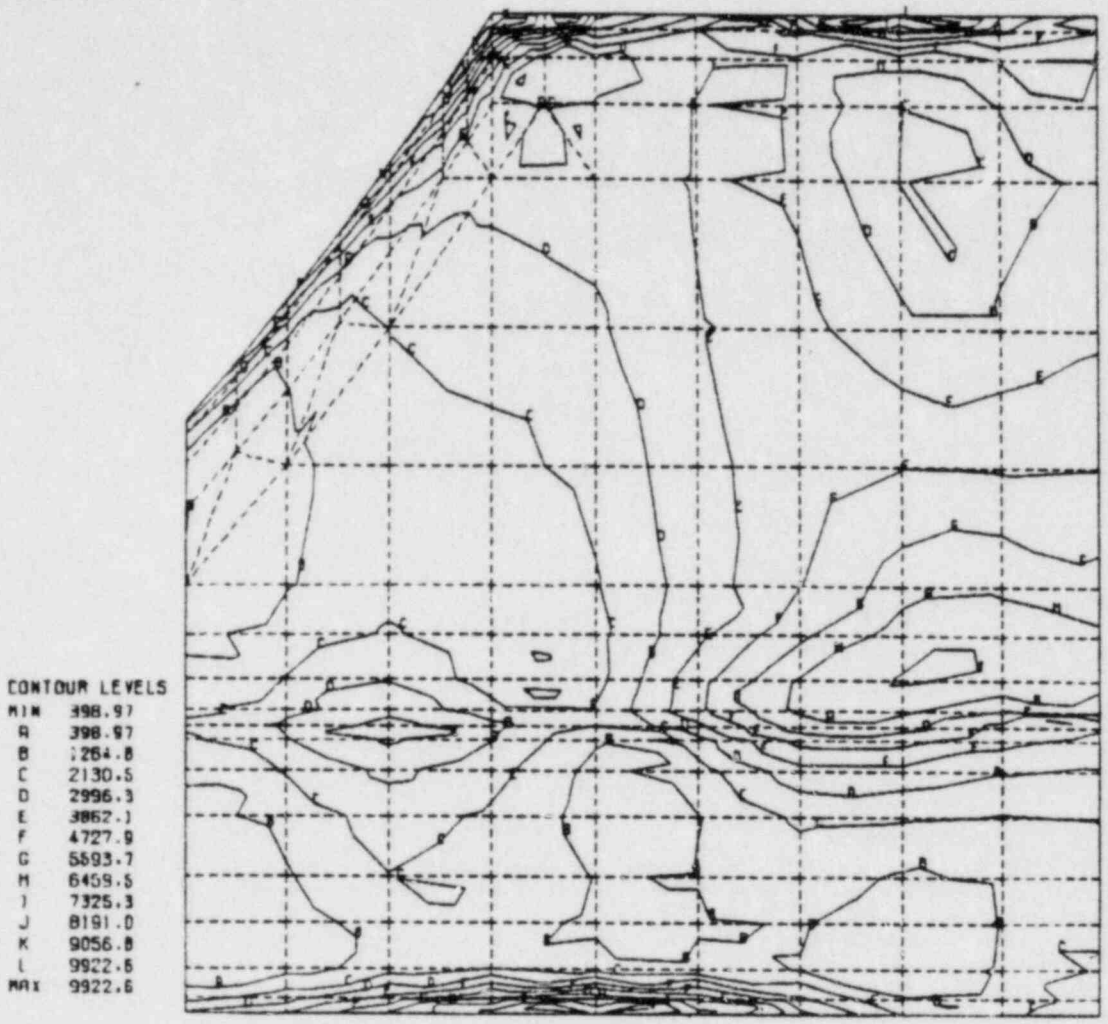

Figure 3.7.1-33 Vent Header -X_1, Y_2 Quadrant Maximum Shear Stress +X_3 Plot

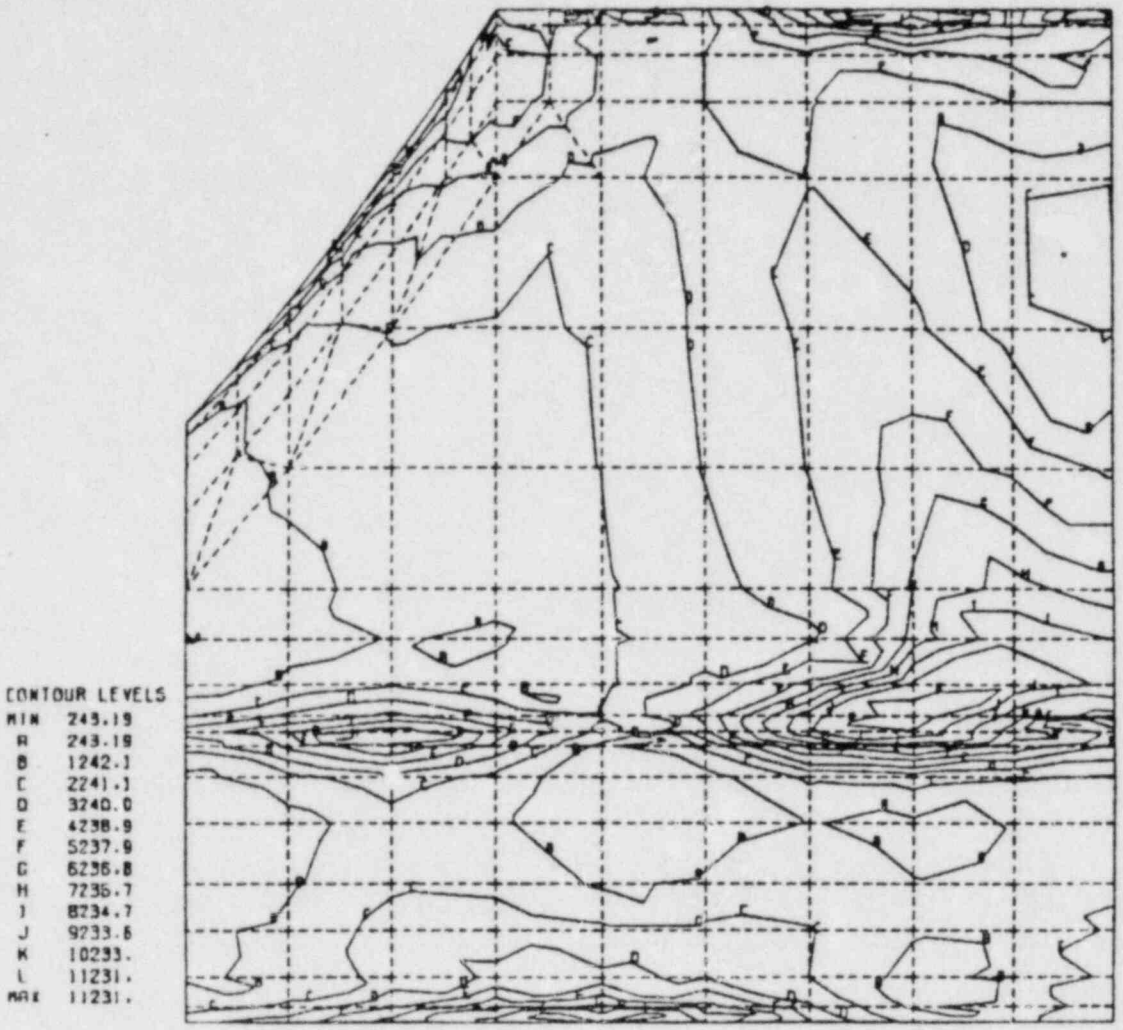

Figure 3.7.1-34 Vent Header -X_1, X_2 Quadrant Maximum Shear Stress -X_3 Plot

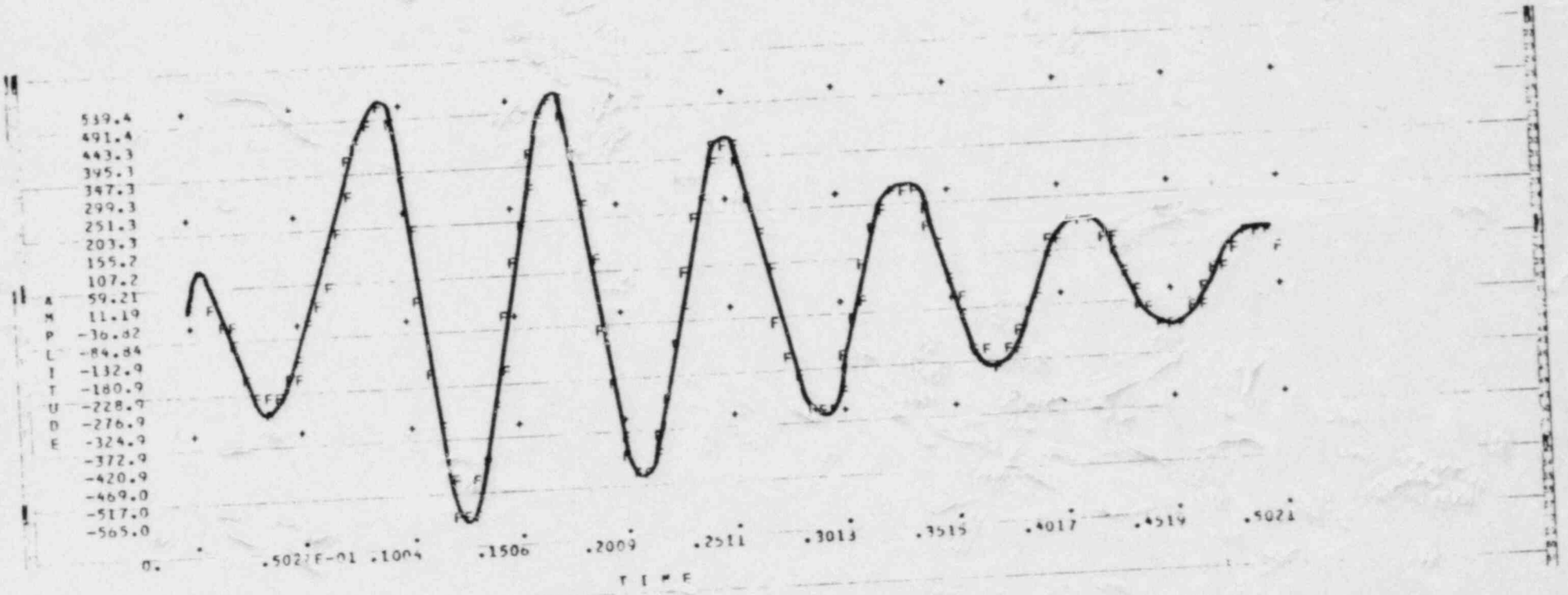

Figure 3.8.1-1 Plot of a Typical Input SRV T/H Adjusted for Resonance at f=11.274 Hz

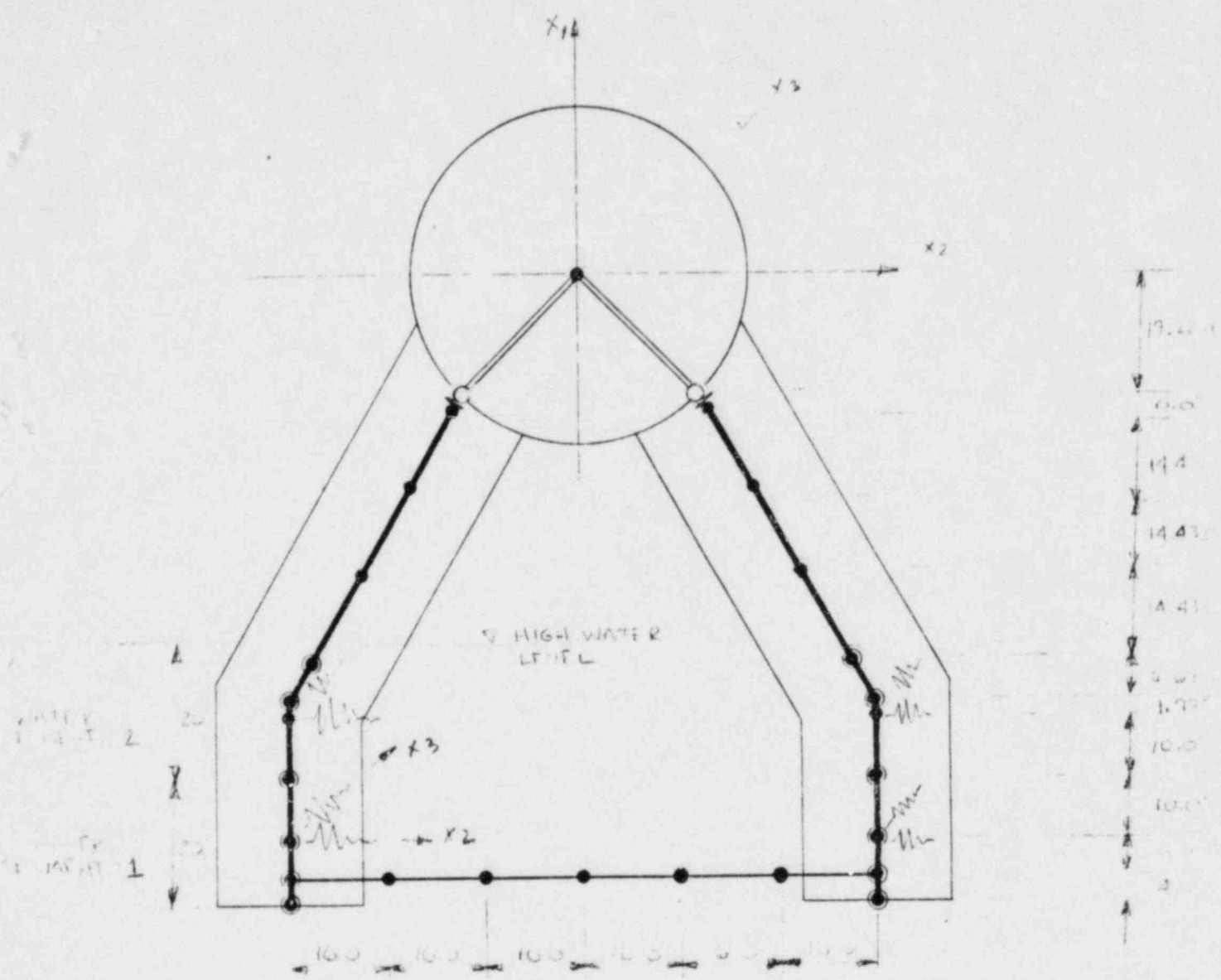

Figure 3.8.1-2 Typical Downcomer Showing Nodes Where SRV T/H is Applied

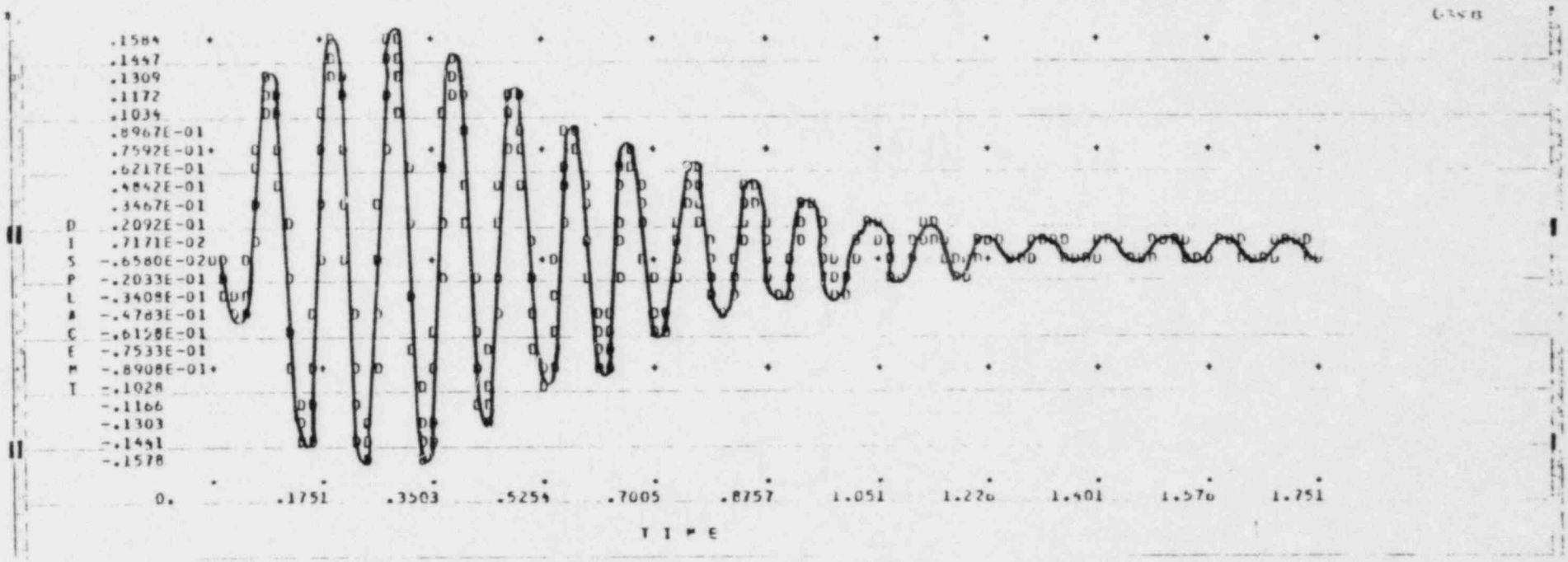

Node 216 DOF_2 Peak Displacement = 0.158428 @ T = 0.291890

Figure 3.8.1 - 3 Peak Displacement Response at Node 216 $-X_2$, D.O.F.

(For SRV T/H A3.2 S Adjusted to Resonate @ f = 11.274 Hz.

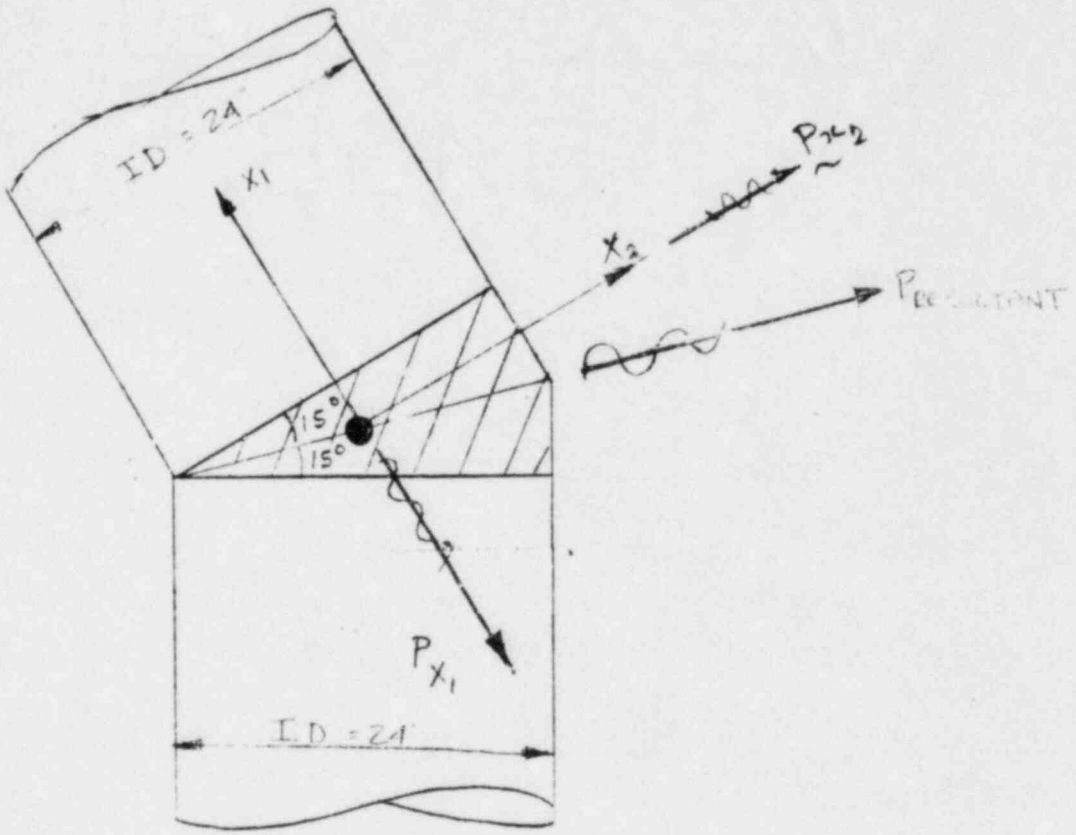

Figure 3.8.2-1 Unbalanced CO Harmonic Load at Downcomer Miter

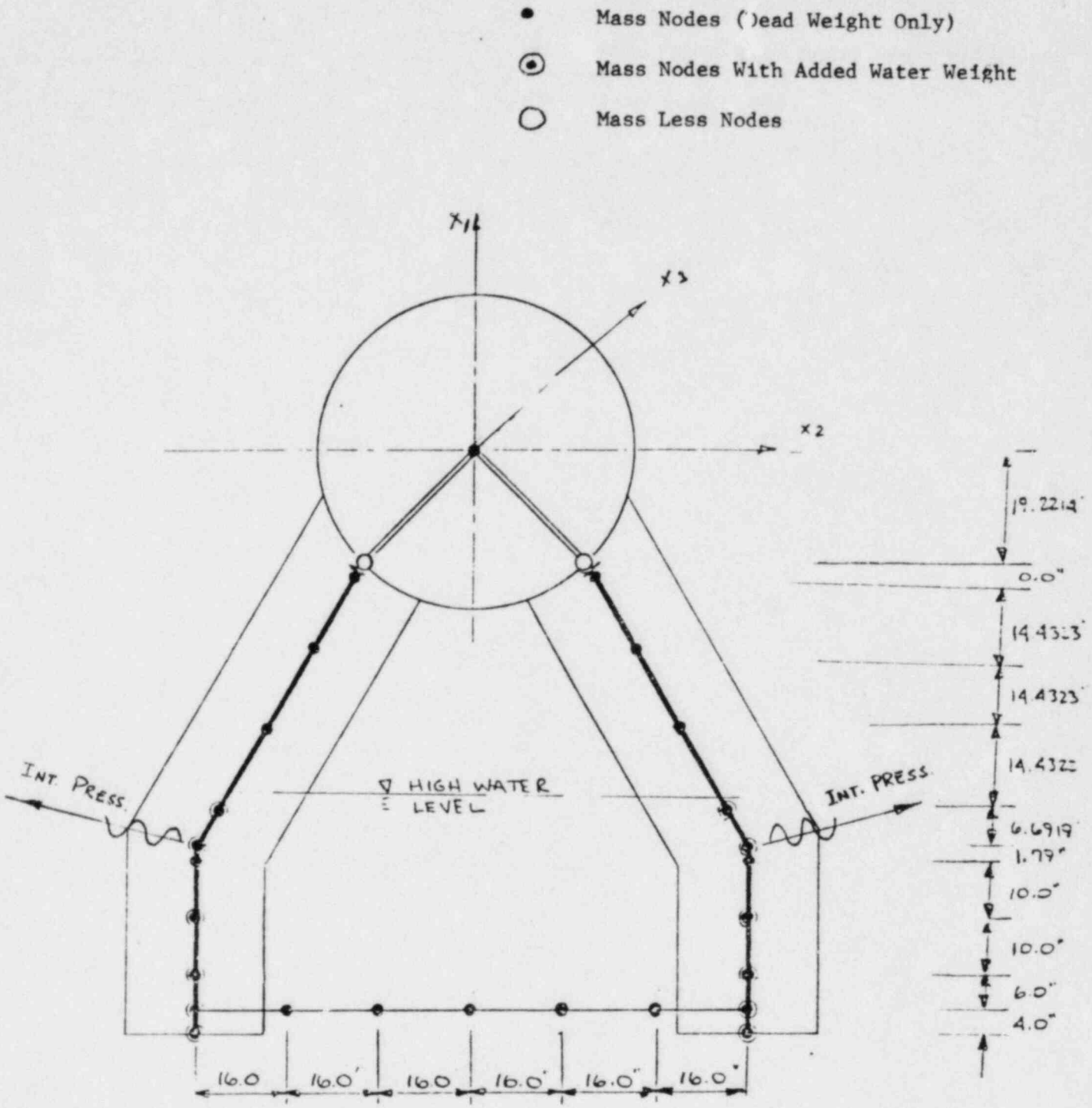

Figure 3.8.2-2 Nodes Where Internal Pressure Harmonics are Applied

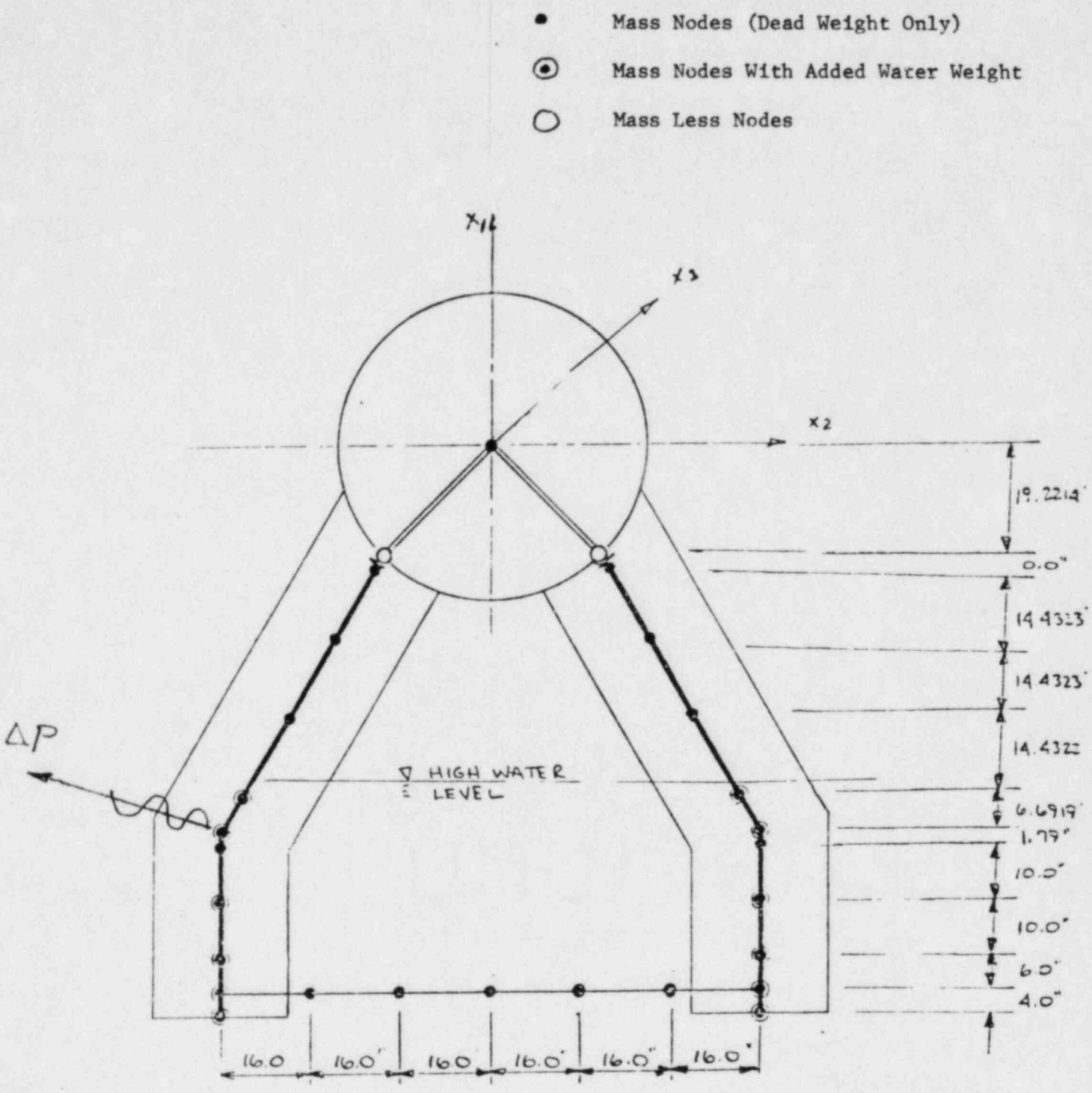

Figure 3.8.2-3 Nodes Where ΔP Harmonics are Applied

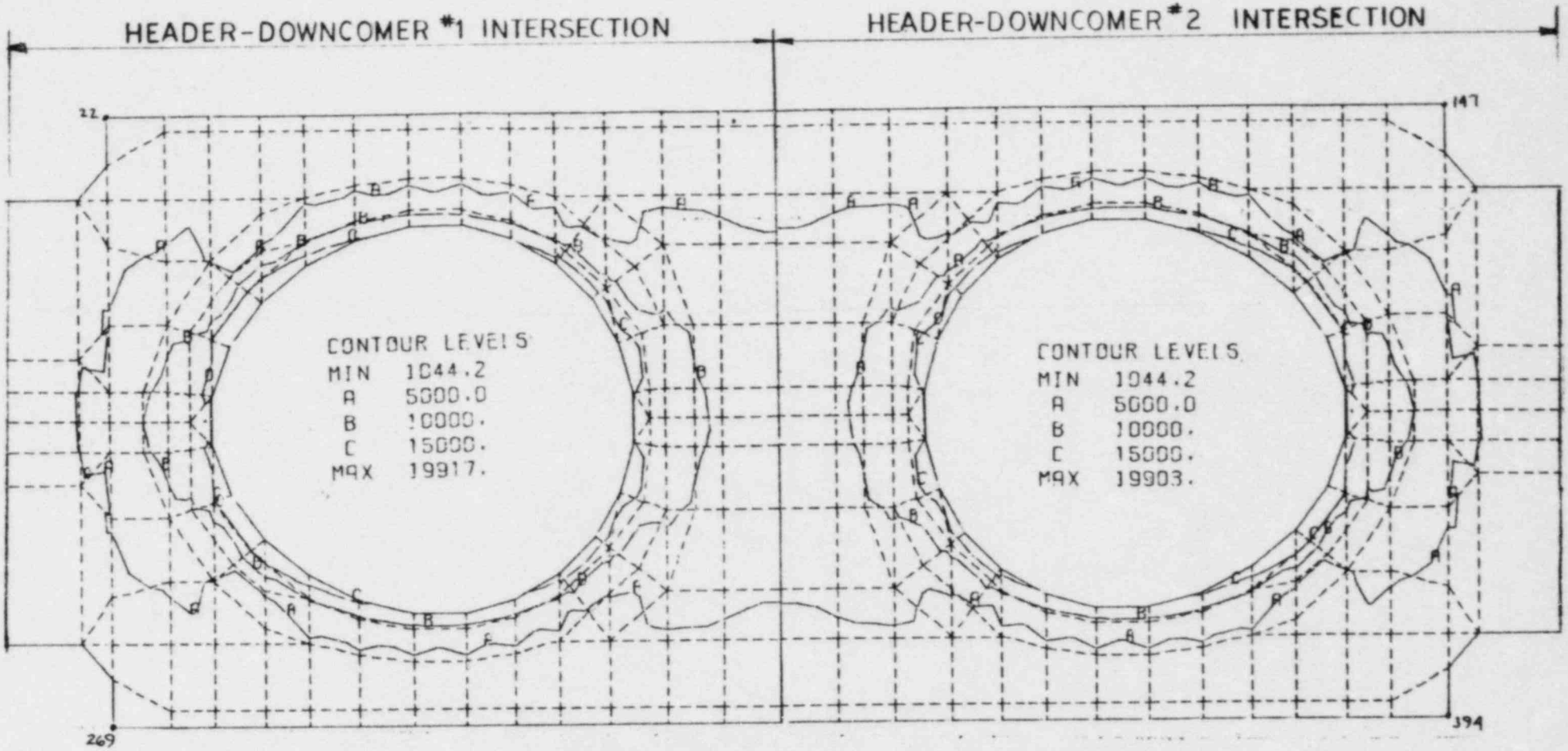

Figure 3.8.4.2-1 Shell Model 1 Plot of Maximum Absolute Shear Stress
(Load Combination #6 Chugging and SRV
$\left[(\text{Chugging } X_2)^2 + (\text{SRV})^2\right]^{\frac{1}{2}}$)

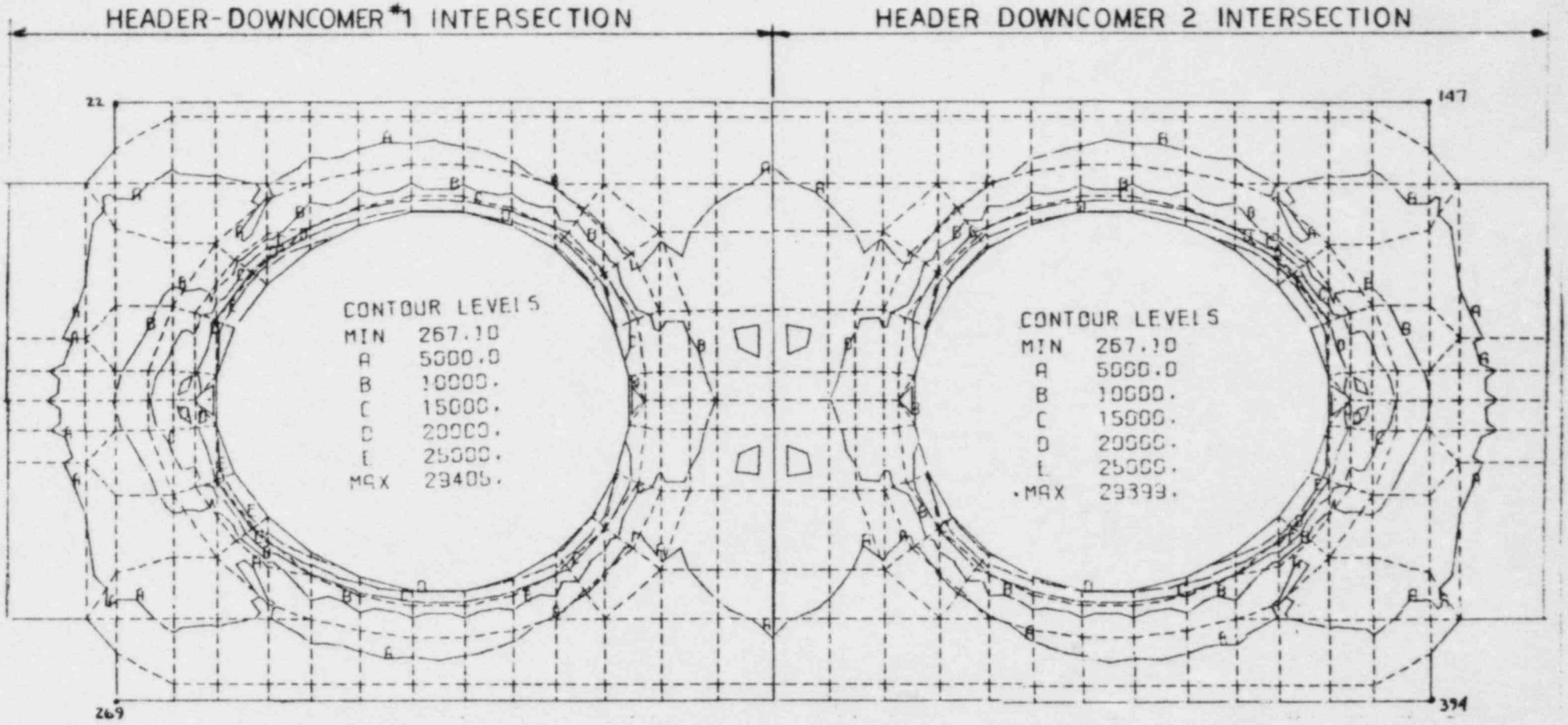

Figure 4.8.4.2-2 Shell Model 1 Plot of Maximum Absolute Shear Stress (Load Combination #7 Chugging and SRV $\pm$ (Chugging X_3)^2 + (SRV X_3)$^2 \pm \frac{1}{2}$)

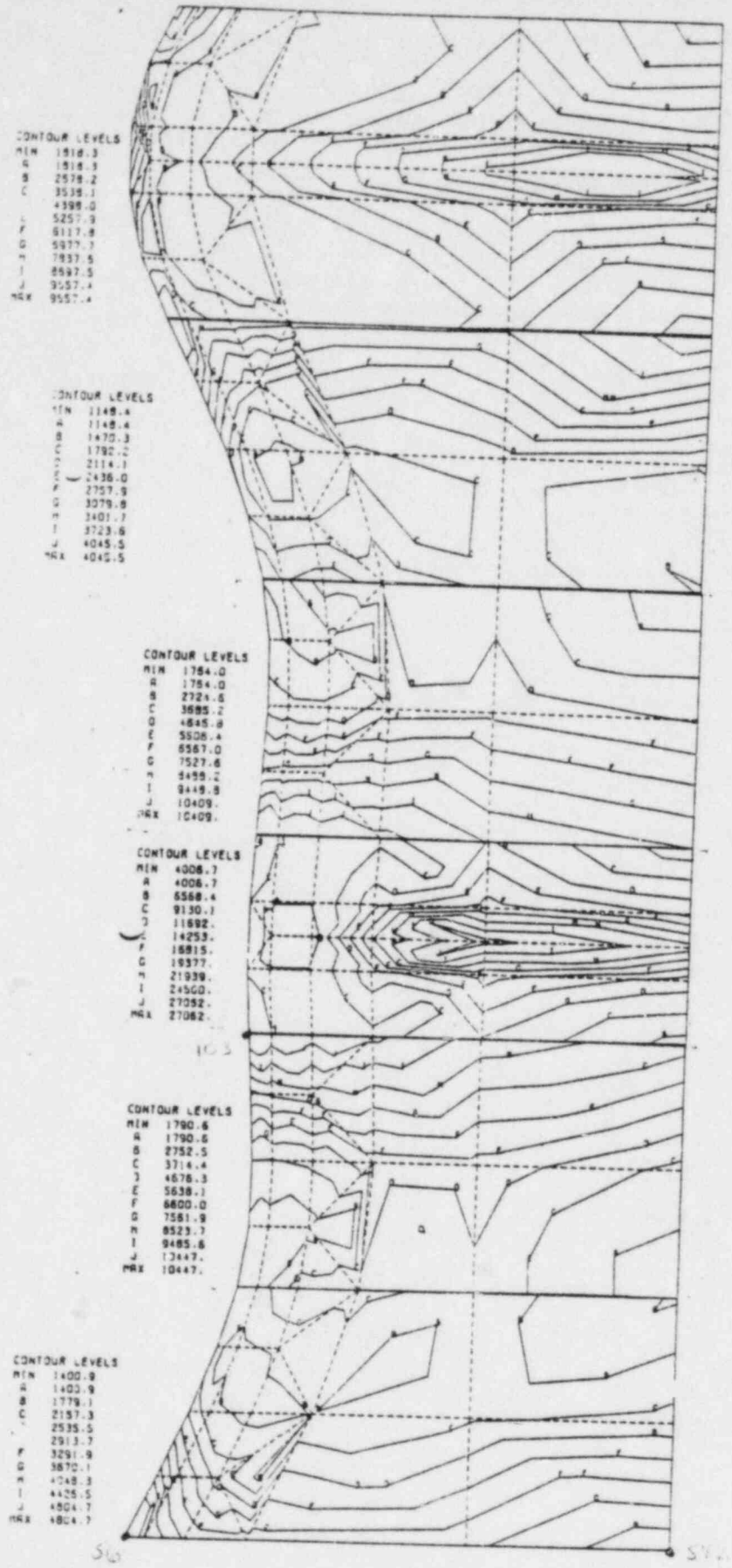

Figure 3.8.4.2-3 Downcomer 1 Plot of Maximum Absolute Shear Stress (Load Combination #2 Chugging and SRV $\left[(\text{Chugging } X_2)^2 + (\text{SRV } X_2)^2 \right]^{1/2}$)

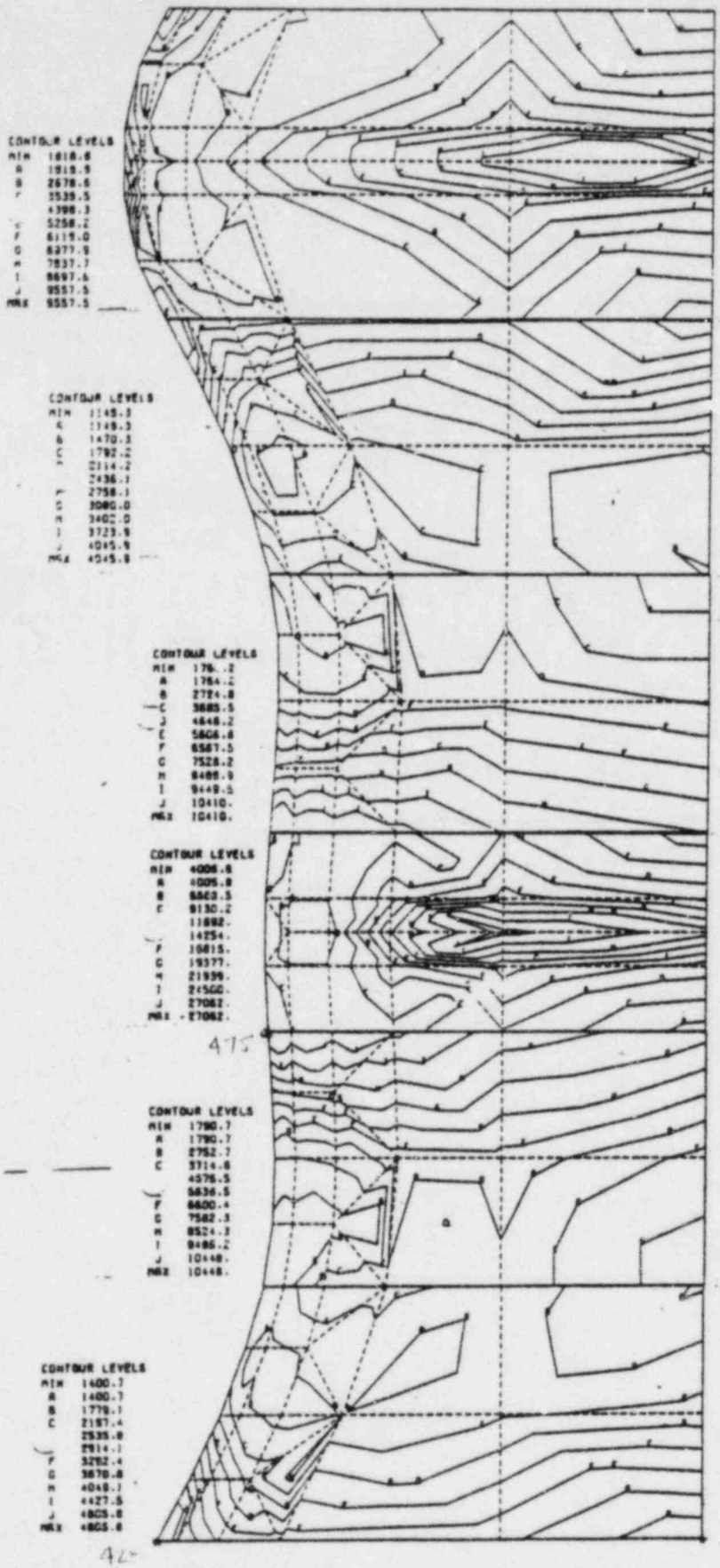

Figure 3.8.4.2-4 Downcomer 2 Plot of Maximum Absolute Shear Stress (Load Combination #2 Chugging and SRV $[\ (\text{Chugging } X_2)^{\ 2} + (\text{SRV } X_2)^{\ 2}\ ]^{\frac{1}{2}}$)

MAX DESIGN LOAD FOR FATIGUE EVALUATION

PMAX (E-W) = 15490.0 lbs.

PMAX (N-S) = 5918.0 lbs.

$$\text{WEIGHTING FACTOR} = \frac{\text{PMAX (N-S)}}{\text{PMAX (E-W)}} = \frac{5.918}{15.49} = 0.382$$

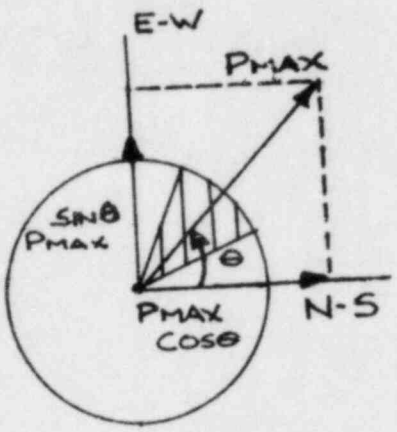

Figure 3.8.5.3-1 Chugging Load Evaluation for Fatigue

SECTION 4 PHOTOGRAPHS AND DRAWINGS OF MODIFICATIONS

4.1 The photographs and drawings listed below depict the modifications that CP&L has installed or is proposing to install as part of the Mark I Program.

4.1.1 Listing of Drawings

9527-F-1322	Ring Vent Header Deflector - South Half
9527-F-1323	Ring Vent Header Deflector - North Half
9527-F-1325	SRV Quencher Support, Plan, South Half
9527-F-1326	SRV Quencher Support, Plan, North Half
9527-F-1352	Ring Vent Header Supports
9527-D-2792	Main Steam Relief Valve Discharge Piping, Plan and Sections - Sheet No. 1 Unit 2
Z812041011	Pipe Support Details
Z820671008	Piping and Arrangement Unit 1 (RHR Test Line, HPCI Turbine Exhaust Line, RCIC Barometric Condenser, HPCI Drain Pot, RCIC Turbine Exhaust Line).
Z820671010	RHR Test Line Pipe Support Details
Z812041013	Pipe Support Details Sheet 2 (Torus Spray Header Supports)
Sketch	Support for HPCI Turbine Exhaust Sparger
Sketch	Torus Section at Azimuth 315° (Reinforcement of downcomers and downcomer cut off)
Sketch	Torus Section Near Vent Header Support and Center SRV Quencher Support (Existing Header Columns, New Header Columns, Deflector, SRV Sparger and Support)
Sketch	Torus Section at Azimuth 315° (New overhead columns at vent).

4.1.2 List of Photographs of CP&L, BSEP
Unit 2 Torus

1. HPCI Turbine Exhaust Anchor (1980)
2. HPCI Turbine Exhaust Anchor (1980)
3. Steam Relief Discharge Line Sparger and Support (1980)
4. Steam Relief Discharge Line Spargers and Supports (1980)
5. Steam Relief Discharge Line Sparger and Support (1980)
6. Steam Relief Discharge Line Sparger and Support (1980)
7. Steam Relief Discharge Line Support (1980)
8. Vent Header Columns (1980)
9. Core Spray Test Line Supports (1982)
10. HPCI Drainpot Line Support (1982)
11. RHR Test Line Support 1982

9527-F-1322

K
L
M
20'-0
25'-0
0'
EXIST. 54"ϕ HEADER
EL. 0'-6
EL. 10'-0
EL. 11'-0
EL. 2'-6
STAIR DOWN FROM EL. 20'-0
NOTE 'A'
SUGGESTED PROCEDURE FOR WELDING RG. 3 TO 1" RING A / B4.
A1. BOLT RG. 3 TO W.A - RAISE AND ALIGN ASSEMBLY.
A2. CLAMP RG. 3 TO 1" RING W. AND TORQUE BOLTS TO 3/4 ϕ HELD TO W.A.
A3. WELD ALONG EDGES ① START WELD AT OUTER EDGE OF 1" RING W.
A4. WELD ALONG EDGE ②.
A5. ALL WELDS SEQUENCED TO PREVENT DISTORTION.
A6. REMOVE CLAMPS AFTER WELDS ARE COOL.
NOTE 'B'
MAXIMUM GAP AT WELDS ① & ②
IS '0'. WELD SIZE SHALL BE DESIGN
SIZE + GAP, ROUNDED UP TO NEAREST 1/16"
EXIST. 54"ϕ TEST HEADER
EXIST. 1"ϕ RING
SEE DETAIL 'A' DWG. F-1324
24"ϕ O.D. TOWN COMBER
CANTILEVER END OF PIPE
L 8x8x1/2 TO PIPE DETAIL C
L 8x8x1/2 W.S.&F.S. SHOP WELD
SEE DETAIL 'A' (F-1324)
L8x8 CLAMP TO PIPE
EXIST. 6"ϕ SCH 80 PIPE
LOW WATER LEVEL EL. 0'-2"
10"ϕ SCH 120 PIPE
EXIST. 1"ϕ RING (54"ϕ I.D.)
FIELD REMOVE PAINT TO LEAVE WELD 3" ϕ MIN. BOTH SIDES
SEE DWG. F-1324 FOR SHIMS
NOTE FOR REINFORCEMENT TO HEADER AT SAW PENETRATIONS SEE DWG. 9527-F-1352
SECTION 1-1
SECTION 2-2
See Det. A (F-1324) for addl information
FIELD OPTION
LUGS MAY BE LEFT ON AFTER ERECTION PROVIDED THEY DO NOT INTERFERE WITH
MODIFICATION BUT MUST BE PAINTED, OR MAY BE BURNT OFF (BURNED AREA PAINTE

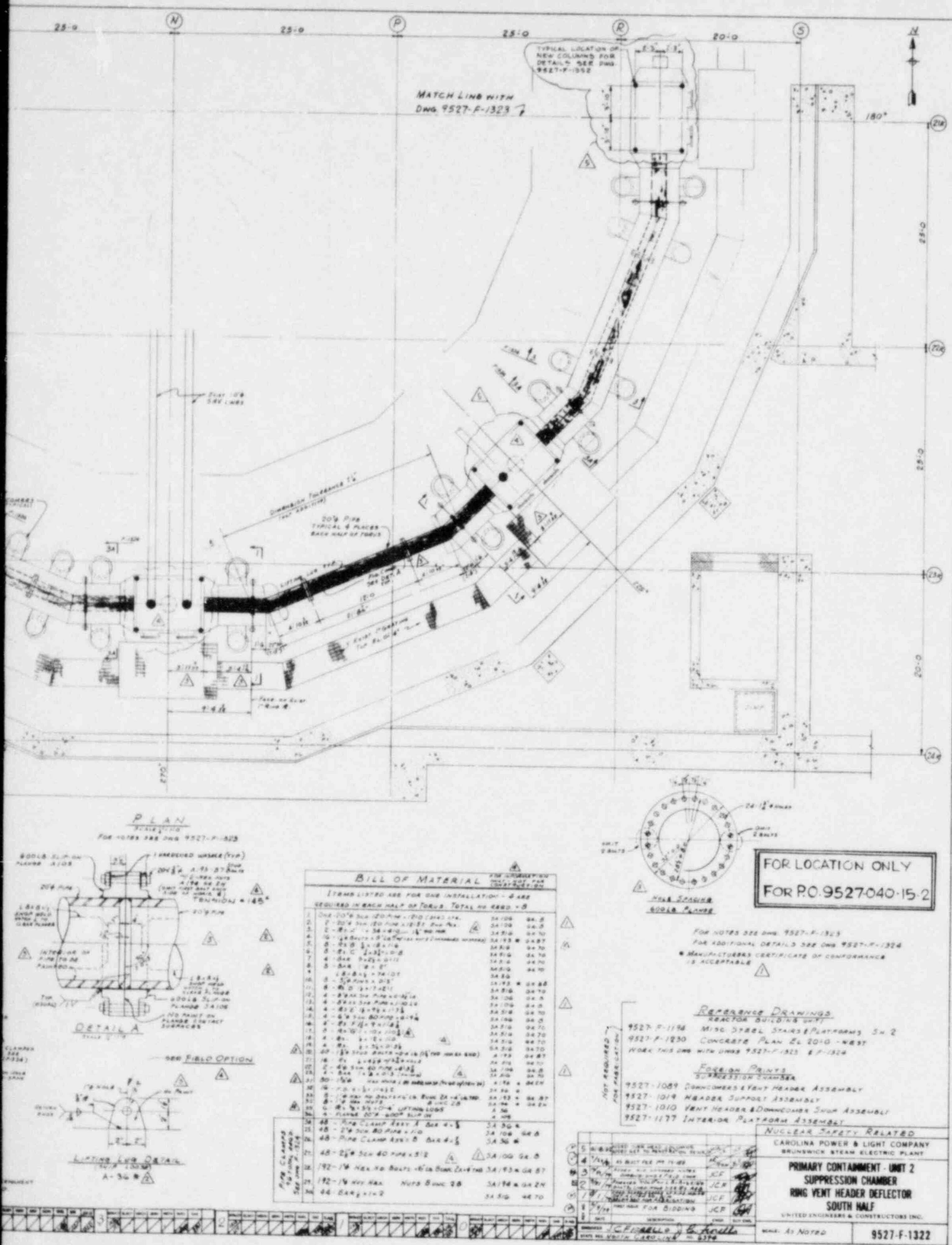

MATCH LINE WITH DWG 9527-F-1323
TYPICAL LOCATION OF NEW COLUMNS FOR DETAILS SEE DWG 9527-F-1352
180°
270°
20" PIPE TYPICAL 4 PLACES EACH HALF OF TORUS
P L A N
FOR NOTES SEE DWG 9527-F-1323
DETAIL A
LIFTING LUG DETAIL
A-34
SEE FIELD OPTION
TENSION = 145°
BILL OF MATERIAL
ITEMS LISTED ARE FOR ONE INSTALLATION - 4 ARE REQUIRED IN EACH HALF OF TORUS. TOTAL NO REQD = 8
48 - PIPE CLAMP ASSY A
48 - PIPE CLAMP ASSY B
192 - 1/4 HEX HD BOLTS
192 - 1/4 HVY HEX NUTS
HOLE SPACING 600LB FLANGE
FOR LOCATION ONLY
FOR P.O. 9527-040-15-2
FOR NOTES SEE DWG 9527-F-1323
FOR ADDITIONAL DETAILS SEE DWG 9527-F-1324
* MANUFACTURERS CERTIFICATE OF CONFORMANCE IS ACCEPTABLE
REFERENCE DRAWINGS
REACTOR BUILDING UNIT 1
9527-F-1194 MISC STEEL STAIRS & PLATFORMS SH 2
9527-F-1230 CONCRETE PLAN EL 20'-0 - WEST
WORK THIS DWG WITH DWGS 9527-F-1323 & F-1324
FOREIGN PRINTS
SUPPRESSION CHAMBER
9527-1089 DOWNCOMERS & VENT HEADER ASSEMBLY
9527-1019 HEADER SUPPORT ASSEMBLY
9527-1010 VENT HEADER & DOWNCOMER SHOP ASSEMBLY
9527-1177 INTERIOR PLATFORM ASSEMBLY
NOT REQUIRED FOR FABRICATION
NUCLEAR SAFETY RELATED
CAROLINA POWER & LIGHT COMPANY
BRUNSWICK STEAM ELECTRIC PLANT
PRIMARY CONTAINMENT - UNIT 2
SUPPRESSION CHAMBER
RING VENT HEADER DEFLECTOR
SOUTH HALF
UNITED ENGINEERS & CONSTRUCTORS INC.
FOR BIDDING
SCALE: AS NOTED
9527-F-1322

9527-F-1223

K
L
M
20'-0
25'-0
EL 19'-11"
ACCESS HATCH
OPNG AT EL 20'-0
NOTES & DIMENSIONS TYPICAL 4 PLACES
EXISTING 54"ϕ HEADER
℄ VENT HEADER INTERSECTION
SECTION C-C
SCALE 1"=1'-0"
ELEVATION OF SRVDL SUPPORT AT BOTTOM OF HEADER
SECTION A-A
SECTION B-B
NOTE: FOR REINFORCEMENT TO HEADER AT SRV PENETRATIONS SEE DWG 9527-F-1332

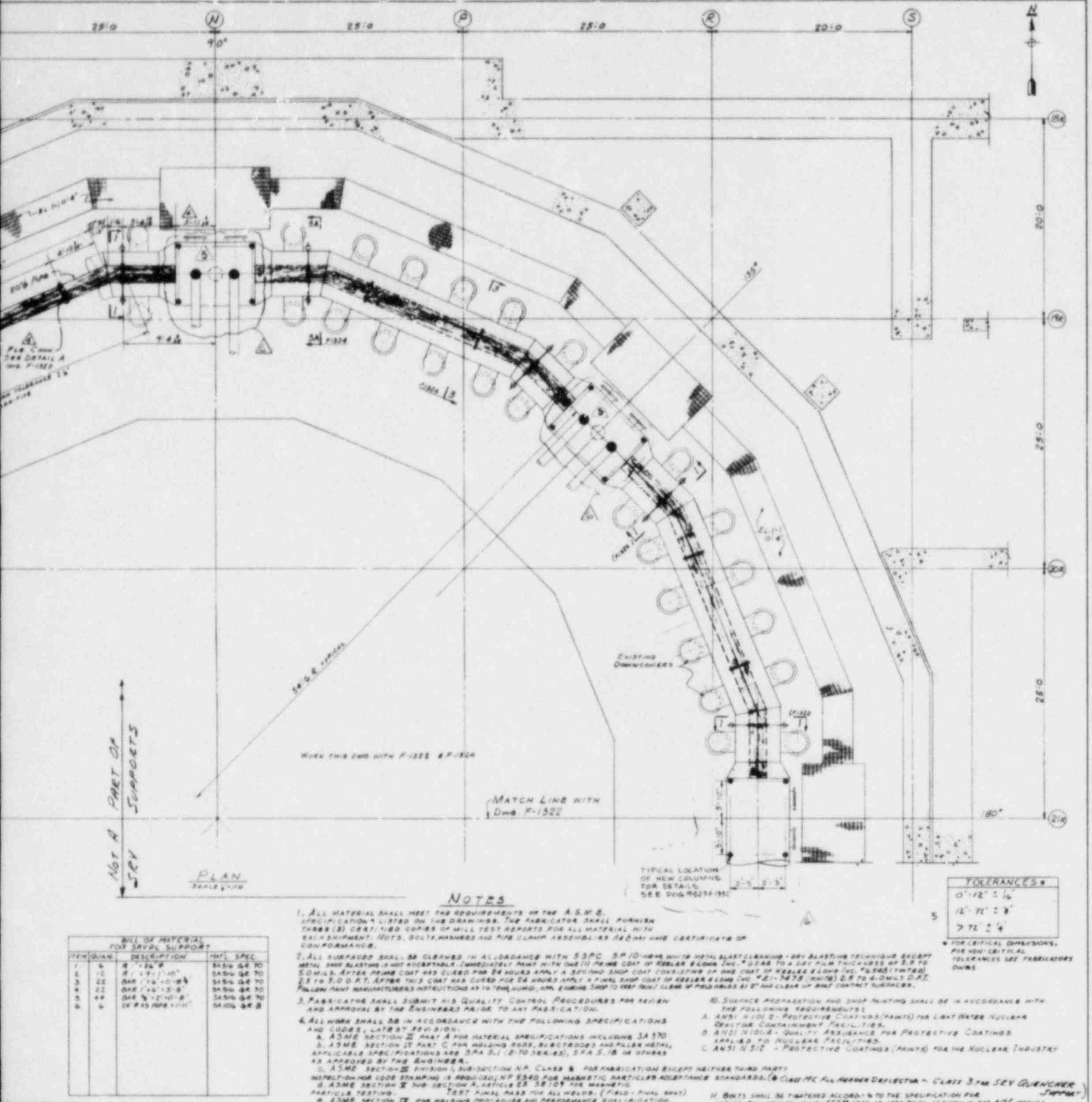

NOTES

1. ALL MATERIAL SHALL MEET THE REQUIREMENTS OF THE A.S.M.E. SPECIFICATIONS LISTED ON THE DRAWINGS. THE FABRICATOR SHALL FURNISH THREE (3) CERTIFIED COPIES OF MILL TEST REPORTS FOR ALL MATERIAL WITH EACH SHIPMENT. NUTS, BOLTS, WASHERS AND PIPE CLAMP ASSEMBLIES AS ONLY HAVE CERTIFICATE OF CONFORMANCE.

2. ALL SURFACES SHALL BE CLEANED IN ACCORDANCE WITH SSPC SP 10 - NEAR WHITE METAL BLAST CLEANING - DRY BLASTING TECHNIQUE EXCEPT METAL SHOT BLASTING IS NOT ACCEPTABLE. IMMEDIATELY PAINT WITH ONE (1) PRIME COAT OF KEELER & LONG INC. #6548 TO A DRY FILM THICKNESS OF 2.5 TO 5.0 MILS. AFTER PRIME COAT HAS CURED FOR 24 HOURS APPLY A SECOND SHOP COAT CONSISTING OF ONE COAT OF KEELER & LONG INC. #6548 (TINTED) 2.5 TO 5.0 D.F.T. AFTER THIS COAT HAS CURED FOR 24 HOURS APPLY A FINAL SHOP COAT OF KEELER & LONG INC. #E1-7475 (WHITE) 2.5 TO 4.0 MILS D.F.T. FOLLOW PAINT MANUFACTURER'S INSTRUCTIONS AS TO TIME, HUMIDITY, APPLICATION, ETC. KEEP PAINT CLEAR OF FIELD WELDS BY 2" AND CLEAR OF BOLT CONTACT SURFACES.

3. FABRICATOR SHALL SUBMIT HIS QUALITY CONTROL PROCEDURES FOR REVIEW AND APPROVAL BY THE ENGINEERS PRIOR TO ANY FABRICATION.

4. ALL WORK SHALL BE IN ACCORDANCE WITH THE FOLLOWING SPECIFICATIONS AND CODES, LATEST REVISION.
   a. ASME SECTION II PART A FOR MATERIAL SPECIFICATIONS INCLUDING SA 370
   b. ASME SECTION II PART C FOR WELDING RODS, ELECTRODES AND FILLER METAL, APPLICABLE SPECIFICATIONS ARE SFA 5.1 (E-70 SERIES), SFA 5.18 OR OTHERS AS APPROVED BY THE ENGINEER.
   c. ASME SECTION III DIVISION I, SUB-SECTION NF, CLASS 3 FOR FABRICATION EXCEPT NEITHER THIRD PARTY INSPECTION NOR CODE STAMPING IS REQUIRED; NF 5340 FOR MAGNETIC PARTICLES ACCEPTANCE STANDARDS. (3 CLASS MC FOR HEADER DEFLECTOR ~ CLASS 3 FOR SRV QUENCHER SUPPORT)
   d. ASME SECTION V SUB-SECTION A, ARTICLE 25 SE 109 FOR MAGNETIC PARTICLE TESTING. TEST FINAL PASS FOR ALL WELDS. (FIELD - FINAL SHOP)
   e. ASME SECTION IX FOR WELDING PROCEDURE AND PERFORMANCE QUALIFICATION.
   f. ASME SECTION V SUB-SECTION A, ARTICLE 1 FOR QUALIFICATION OF PERSONNEL FOR NON DESTRUCTIVE EXAMINATION.

5. ERECTOR TO GRIND AND WELD EXISTING STRUCTURE AND MAKE MINOR ADJUSTMENTS TO NEW MEMBERS IN FIELD AS NECESSARY.

6. AFTER ERECTION, ABRADED AREAS WHERE NOT PAINTED.

7. FABRICATOR AND ERECTOR TO SUBMIT TEST REPORTS AND LOGS SHOWING AREAS PAINTED OF BOTH PRIME AND FINISH COATS, BATCH NUMBER OF PAINT, TEMPERATURE OF SURFACE, SURFACE PREPARATION, HUMIDITY, AIR TEMPERATURE AND D.F.T.

8. ALL SA 106 GR. B. PIPE HAVING A WALL THICKNESS GREATER THAN 5/8" SHALL BE IMPACT TESTED AT A TEMPERATURE OF 40°F. TESTS SHALL MEET THE REQUIREMENTS OF A.S.M.E. SECTION III, DIVISION I, SUBSECTION NF-2331 AND SHALL BE REPORTED ON THE CERTIFIED MATERIAL TEST REPORT.

9. FIELD WELDS THAT ARE TO BE MAGNETIC PARTICLE TESTED SHALL HAVE THE LETTER M IN THE TAIL OF THE WELD SYMBOL THUS. MAGNETIC PARTICLE TESTING SHALL BE IN ACCORDANCE WITH NOTE 4d (ABOVE). FIELD, AS AN ALTERNATE TO MAGNETIC PARTICLE TESTING, MAY USE LIQUID PENETRANT TESTING ACCORDING TO ASME SECTION V, SUBSECTION B, ARTICLE 24 SE 165. ALL FIELD WELDS SHALL BE VISUALLY INSPECTED IN ACCORDANCE WITH ASME SECTION V, SUBSECTION A, ARTICLE 9. WELDS TO LINER INDICATED "M" HERE MAG. PARTICLE TESTED. SEE NOTE B ON APPLICABLE DRAWINGS.

10. SURFACE PREPARATION AND SHOP PAINTING SHALL BE IN ACCORDANCE WITH THE FOLLOWING REQUIREMENTS:
   A. ANSI N101.2 - PROTECTIVE COATINGS (PAINTS) FOR LIGHT WATER NUCLEAR REACTOR CONTAINMENT FACILITIES.
   B. ANSI N101.4 - QUALITY ASSURANCE FOR PROTECTIVE COATINGS APPLIED TO NUCLEAR FACILITIES.
   C. ANSI N 512 - PROTECTIVE COATINGS (PAINTS) FOR THE NUCLEAR INDUSTRY

11. BOLTS SHALL BE TIGHTENED ACCORDING TO THE SPECIFICATION FOR STRUCTURAL JOINTS USING ASTM A325 OR A490 BOLTS AS GIVEN IN THE AISC MANUAL OF STEEL CONSTRUCTION. EACH BOLT SHALL BE TIGHTENED TO PROVIDE, WHEN ALL BOLTS IN THE CONNECTION ARE TIGHT, AT LEAST THE MINIMUM TENSION SHOWN ON THE DWGS. USE SKIDMORE-WILHELM DIRECT TENSION INDICATOR TO CALIBRATE TORQUE WRENCH. TIGHTEN ALL BOLTS SNUG, THEN TIGHTEN TO MIN. TENSION IN THE FOLLOWING ORDER. HARDENED STEEL WASHERS TO BE ASTM F436. USE TWO PER BOLT: ONE UNDER HEAD AND ONE UNDER NUT.

NOTE: AT 225° THERE IS ONE SRV DISCHARGE LINE SEE DWG F-1330

BILL OF MATERIAL FOR SRVDL SUPPORT

ITEM	QUAN.	DESCRIPTION	MATL. SPEC
1	4	℞ 1"×26"℞	SA 516 GR. 70
2	16	℞ 1"×9½"×1'-10"	SA 516 GR. 70
3	22	BAR 1"×6"×1'-8"	SA 516 GR. 70
4	22	BAR 1"×6"×1'-3"	SA 516 GR. 70
5	44	BAR ¾"×2'-10"-8"	SA 516 GR. 70
6	4	24" ⌀ XS PIPE ×1'-0"	SA 106 GR. B

TOLERANCES *

0'-12" ± 1/16
12"-72" ± 1/8
> 72" ± 1/4

* FOR CRITICAL DIMENSIONS, FOR NON-CRITICAL TOLERANCES SEE FABRICATORS DWGS

FOR LOCATION ONLY
FOR P.O. 9527-040-15-2

NO.	DATE	DESCRIPTION	CHKD.	SUP. ENG.
6		ADDED DIEN. HEAT COLUMNS ...		
5	1/14/80	AS BUILT PER ... 79-188		
4		ADDED NOTE 9, CHG'D DIMENSIONS FOR CMA	JCF	
3		RELEASED FOR FABRICATION SRV SUPPORTS	JCF	
2	4/13/79	FOR BIDDING SRV SUPPORTS	JCF	
1		RELEASED FOR FABRICATION	JCF	
0	5/4/79	FOR BIDDING	JCE	

CAROLINA POWER & LIGHT COMPANY
BRUNSWICK STEAM ELECTRIC PLANT

PRIMARY CONTAINMENT - UNIT 2
SUPPRESSION CHAMBER
RING VENT HEADER DEFLECTOR
NORTH HALF

UNITED ENGINEERS & CONSTRUCTORS INC.

SCALE: AS NOTED

9527-F-1323

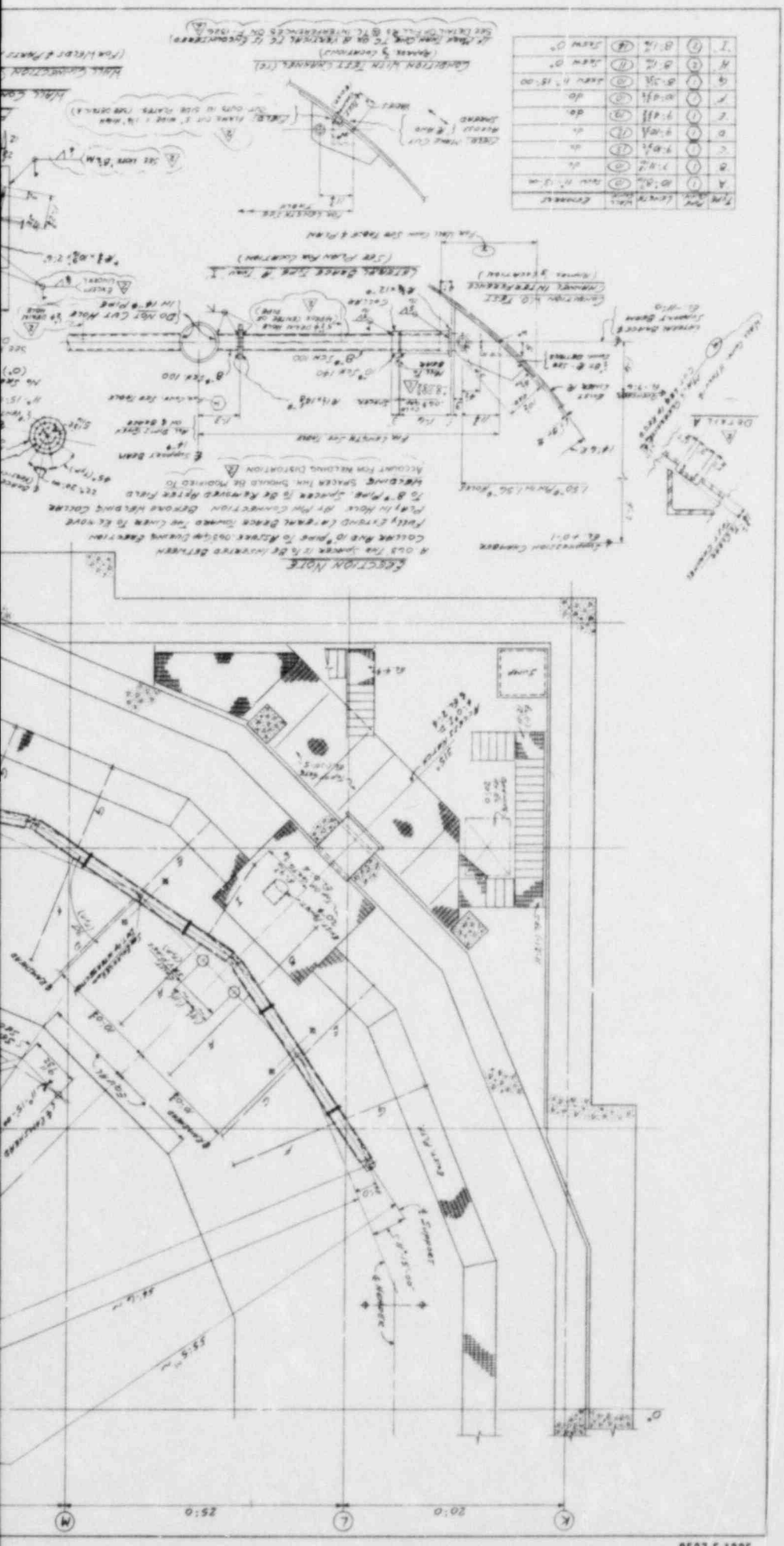

9527-F-1325

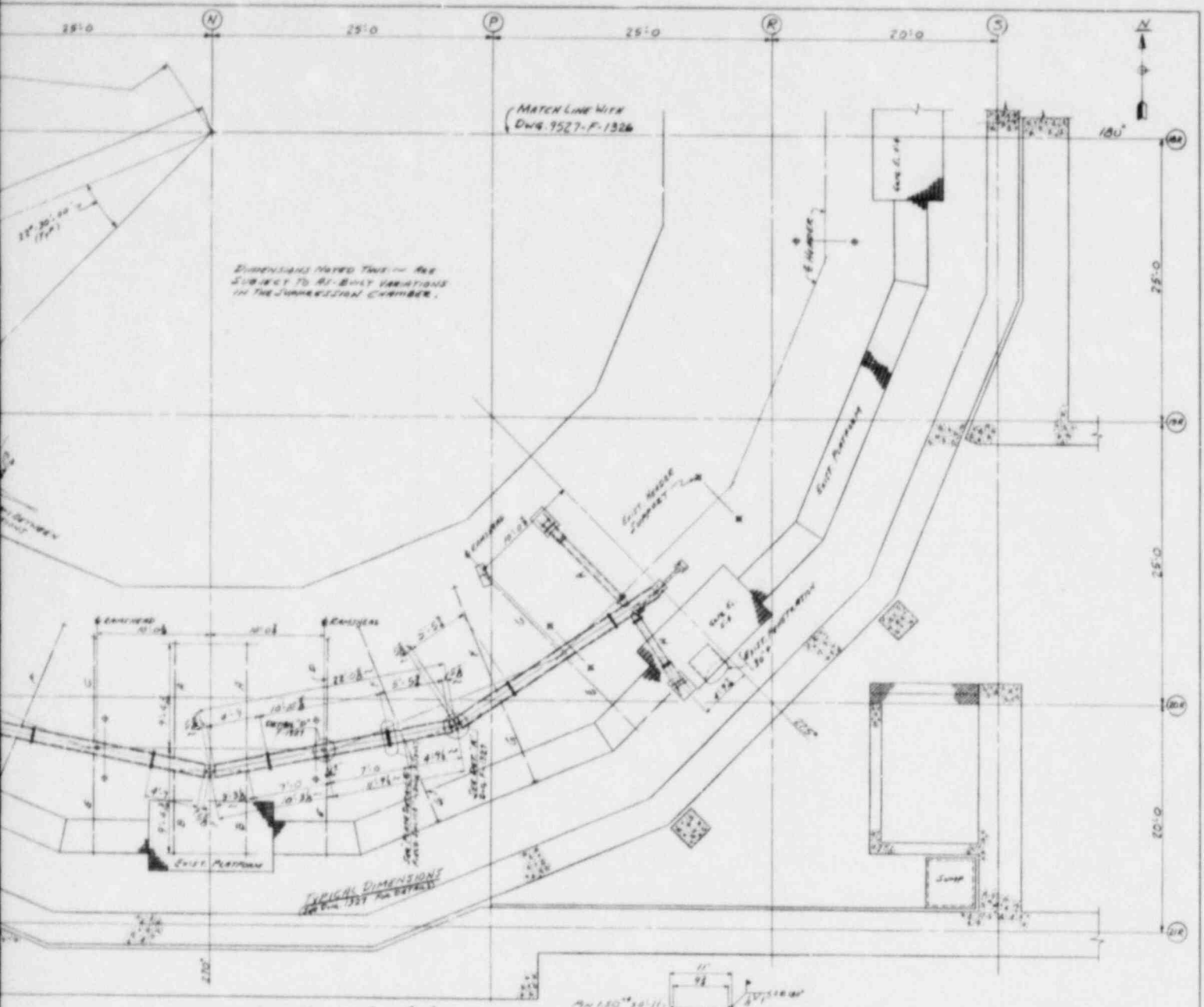

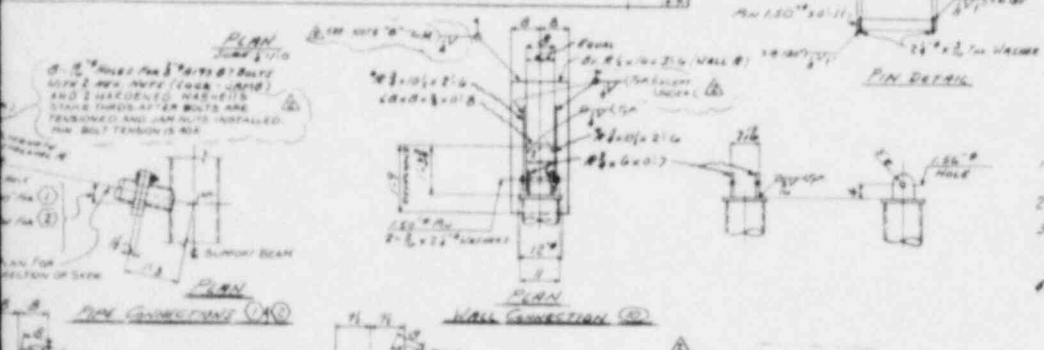

NOTES:

1. WORK THIS DRAWING WITH DRAWINGS F-1323, F-1326 & F-1327
2. FOR ADDITIONAL NOTES SEE DWG. F-1323
3. SHIM TO CUT PLATES MARKED THUS -B- TO FIT CURVATURE OF WALL (B), FIELD TO TRIM AS REQUIRED TO FIT AS BUILT CONDITION
4. DIMENSION TOLERANCES TO BE AS INDICATED BELOW FOR CRITICAL DIMENSIONS FOR NON CRITICAL TOLERANCES SEE FABRICATOR'S DETAIL.

DECIMALS - INCH	FRACTIONS
.X ± .100	0"-12" ± 1/16
.XX ± .050	12"-72" ± 1/8
.XXX ± .010	OVER 72" ± 1/4
RADIUS ± 1°	TAPER TOLERANCE 1/8" PER FOOT

5. SURFACE PREPARATION AND SHOP PAINTING SHALL BE IN ACCORDANCE WITH THE FOLLOWING REQUIREMENTS:
   A. ANSI N101.6 - PROTECTIVE COATINGS (PAINTS) FOR LIGHT WATER NUCLEAR REACTOR CONTAINMENT FACILITIES
   B. ANSI N101.4 - QUALITY ASSURANCE FOR PROTECTIVE COATINGS APPLIED TO NUCLEAR FACILITIES
   C. ANSI N512 - PROTECTIVE COATINGS (PAINTS) FOR THE NUCLEAR INDUSTRY

NUCLEAR SAFETY RELATED

CAROLINA POWER & LIGHT COMPANY
BRUNSWICK STEAM ELECTRIC PLANT

PRIMARY CONTAINMENT - UNIT 2
SUPPRESSION CHAMBER
S/RV QUENCHER SUPPORT
PLAN - SOUTH HALF

UNITED ENGINEERS & CONSTRUCTORS INC.

SCALE: AS NOTED

9527-F-1325

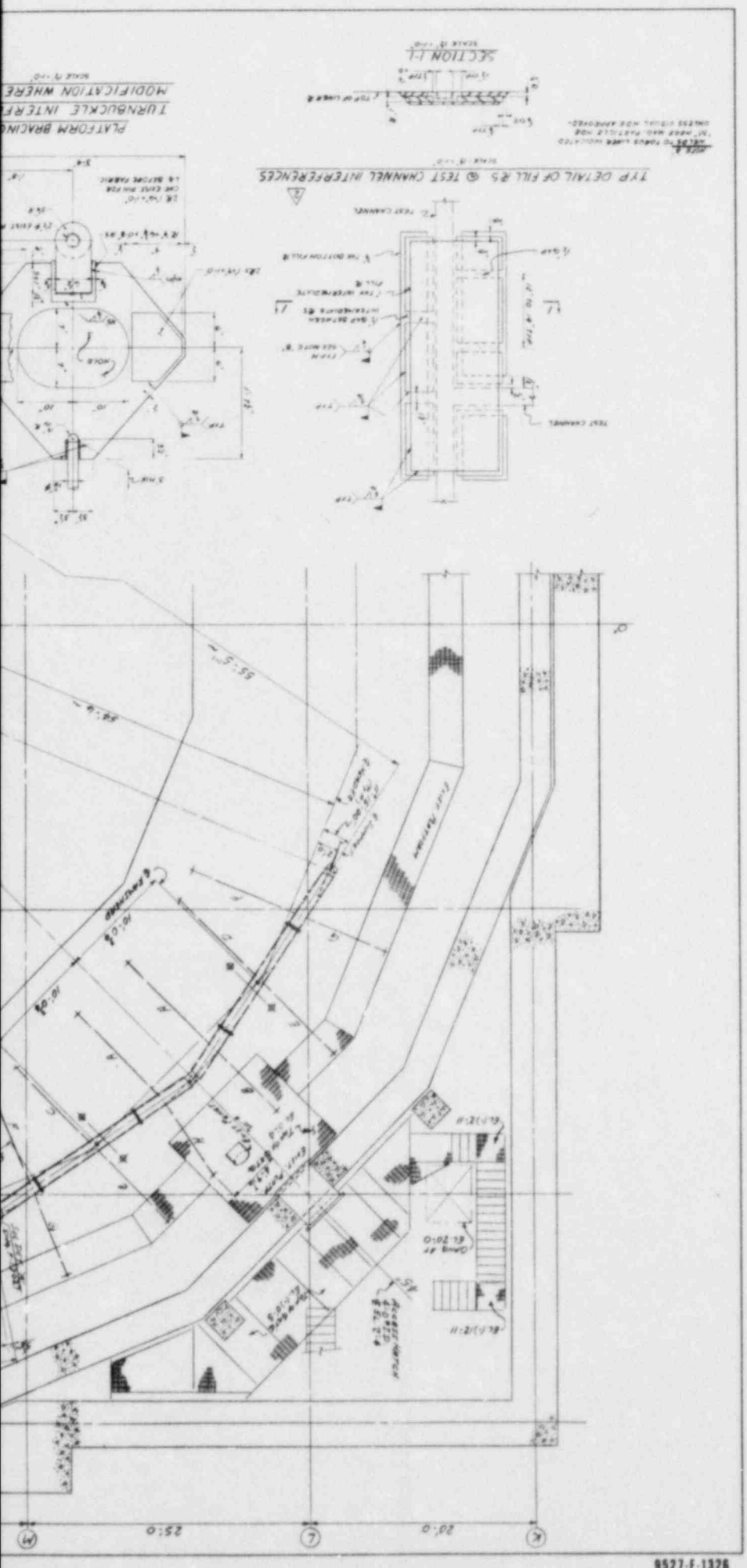

9527-F-1326

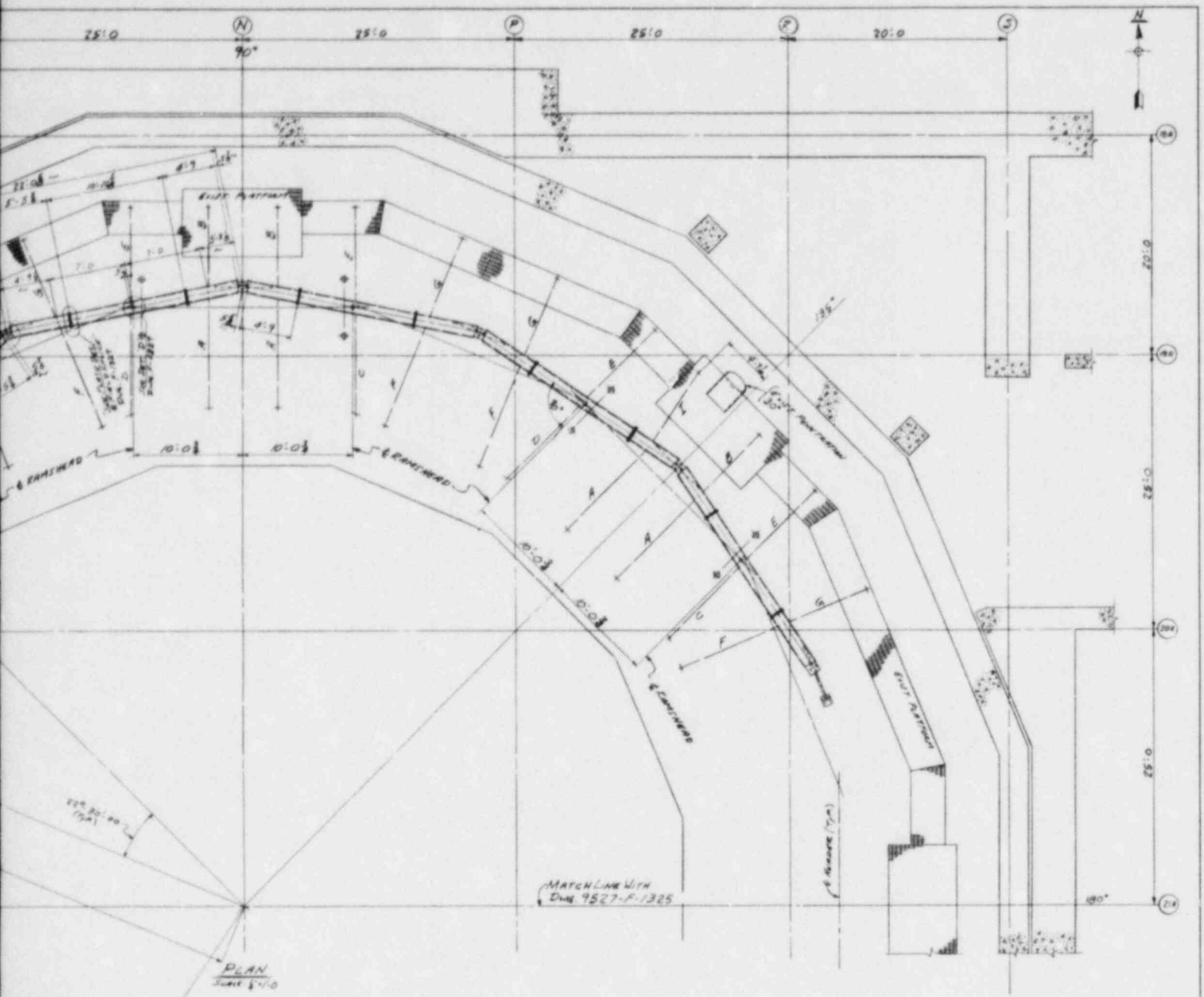

REFERENCE DRAWINGS (NOT REQUIRED FOR FABRICATION OR ERECTION)

	CBI	FP 9527
MONORAIL	- 221	- 1041
PLATFORM	- 215 THRU 219	- 1035 THRU 1039
TEST CHANNELS	- 208 & 209	- 1111 & 1112
VENT HEADER & DOWNCOMMERS	- 206	- 1010
HEADER INTERSECTION	- 210	- 1028
VENT HEADER ASSEMBLY	- 202	- 1024
HEADER SUPPORT	- 203	- 1019

NOT REQUIRED FOR FABRICATION

NOTES:
1. WORK THIS DRAWING WITH DRAWINGS F-1323 F-1325 & F-1327
2. FOR ADDITIONAL NOTES SEE DRAWING F-1323

NUCLEAR SAFETY RELATED

CAROLINA POWER & LIGHT COMPANY
BRUNSWICK STEAM ELECTRIC PLANT

PRIMARY CONTAINMENT - UNIT 2
SUPPRESSION CHAMBER
SRV QUENCHER SUPPORT
PLAN - NORTH HALF

UNITED ENGINEERS & CONSTRUCTORS INC.

SCALE: AS NOTED

9527-F-1326

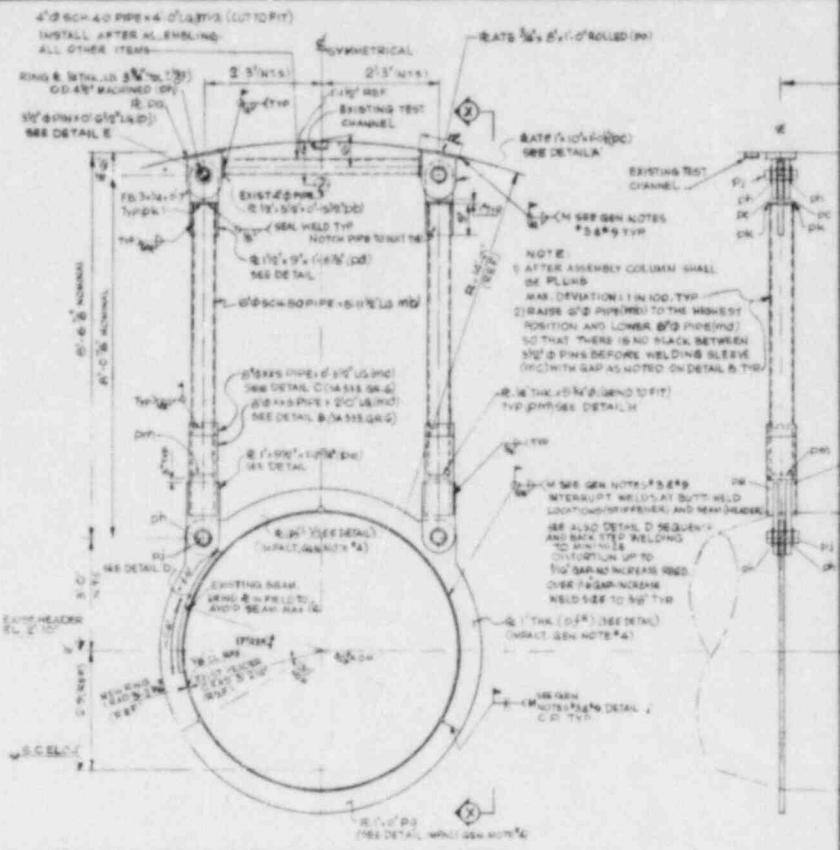

ELEVATION OF UPPER SUPPORT FOR VENT HEADER

(ALLOCATIONS SEE DWGS 9527-F-1322 & 9527-F-1523

REFERENCE DRAWINGS

1. 9527-F-1322 SUPPRESSION CHAMBER RING VENT HEADER DEFLECTOR & CUTH HALF
2. 9527-F-1523 SUPPRESSION CHAMBER RING VENT HEADER DEFLECTOR NORTH HALF
3. F.P. 9527-01-1019 SUPPRESSION CHAMBER HEADER SUPPORT A (LOCATION) (SEE DWG NO 205 REV.)
4. F.P. 9527-01-1190 SHOP ASSEMBLY VENT HEADER INTERSECTION (SEE DRGN. 2 DIA REV. 0)
5. F.P. 9527-01-1030 SHOP ASSEMBLY VENT HEADER INTERSECTION (SEE DRG NO 2 REV. 1)

VENT SY

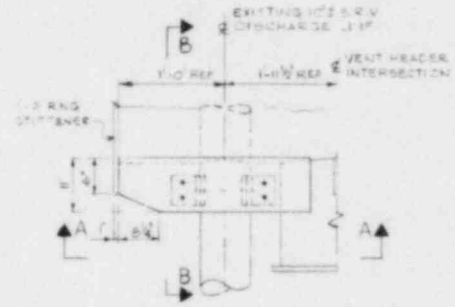

ELEVATION

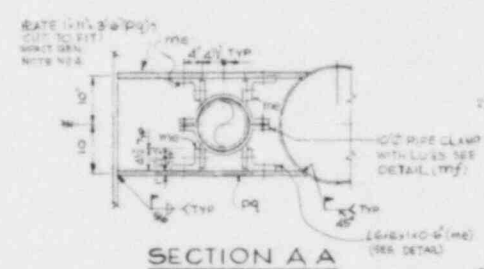

SECTION A A

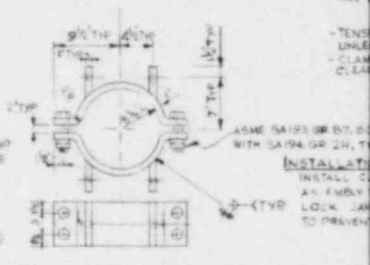

DETAIL OF PIPE CLAMP (mf)

SEC

S.R.V. LINE PENETRATION REINFORCEMENT FO

(S. R.V. LINE SUPPORTS IN THE WET WELL)

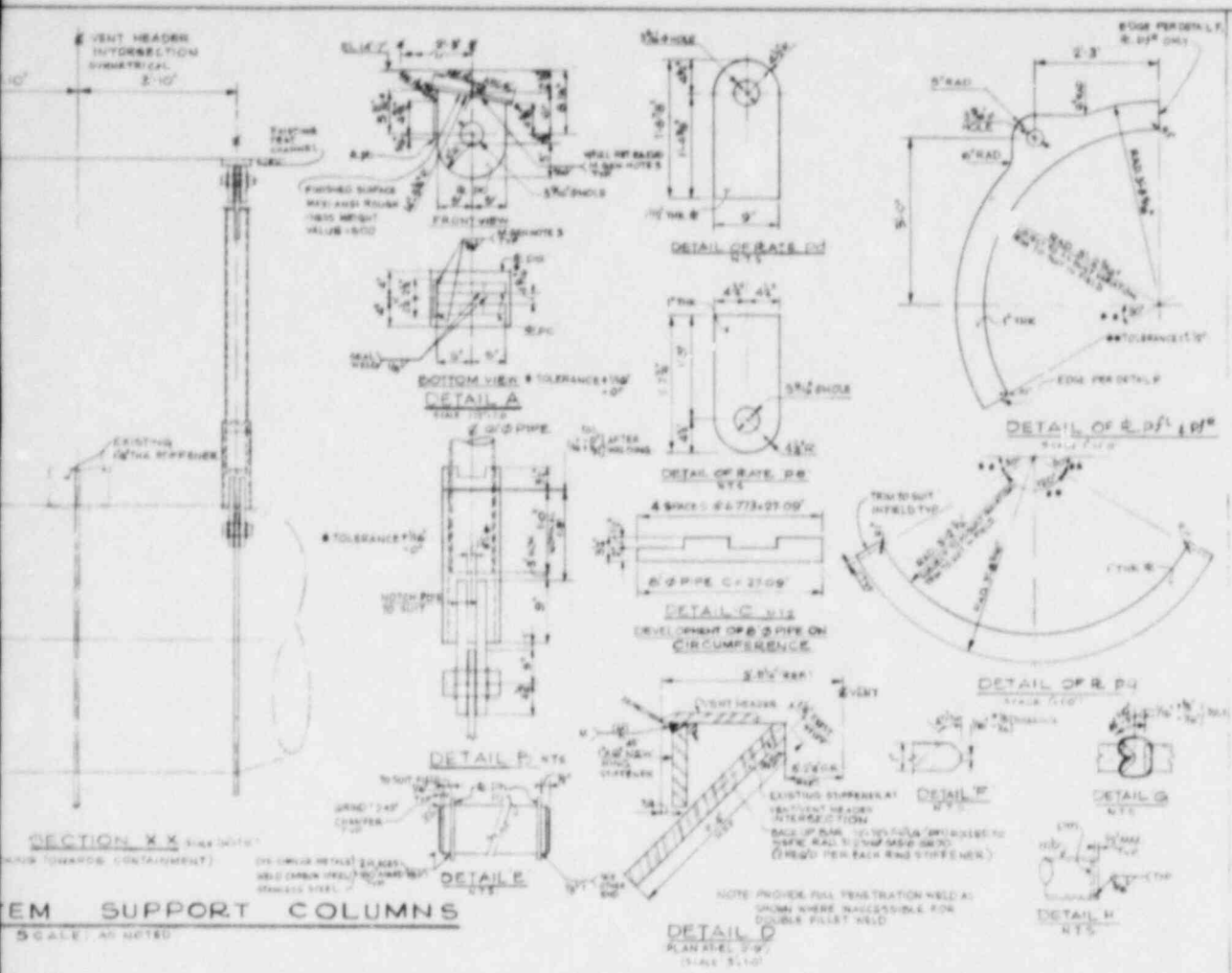

GENERAL NOTES

1) ALL FABRICATION SHALL BE IN ACCORDANCE WITH U.S.A.E.C. SPECIFICATION NO. 9527-040 (2-1961).

2) UNLESS NOTED OTHERWISE ALL MATERIALS SHALL BE AS FOLLOWS:
ALL PLATES ASME SA-516 GR70
ALL PIPE STRUCTURAL MEMBERS ASME SA-53 GR B
ALL PIPE ASME SA-106 GR B

3) WELDS DENOTED M SHALL BE MAGNETIC PARTICLE TESTED. WELDS DENOTED R SHALL BE RADIOGRAPHED. ALL OTHER WELDS SHALL BE VISUALLY INSPECTED PER SPECIFICATION FOR ACCEPTANCE STANDARDS BUT ALTERNATE METHODS OF INSPECTION.

4) ALL MATERIAL DENOTED IMPACT SHALL BE IMPACT TESTED AT A TEMPERATURE OF 10°F. TESTS SHALL MEET THE REQUIREMENTS OF ASME SECTION III, DIV.1, SUBSECTION NE, ARTICLE NE-2300 AND SHALL BE REPORTED ON THE CERTIFIED MATERIAL TEST REPORT.

5) LINER PADS SHALL BE ROLLED TO A RADIUS OF 4'-0".

6) DIMENSIONS AND LOCATIONS OF EXISTING STRUCTURE AND COMPONENTS ARE OBTAINED FROM LATEST DRAWINGS AND ARE SUBJECT TO AS-BUILT VARIATIONS. THESE ARE FURNISHED FOR REFERENCE ONLY.

7) LINEAR DIMENSIONAL TOLERANCE UNLESS NOTED:

0'-0"	± 1/16"
12'-0"	± 3/8"
>12'-0"	± 1/4"

8) CONNECTIONS TO THE TORUS LINER MAY HAVE TO BE ALTERED DUE TO UNKNOWN TEE CHANNEL OR OTHER INTERFERENCE. NOTIFY ENGINEER PRIOR TO FABRICATION.

9) ASME CODE CLASSIFICATIONS:
LINER AND WELDS TO LINER: ASME SECT III, DIV 2
ATTACHMENTS AND WELDS TO HEADER: ASME SECT III DIV 1 SUBSECT NE CLASS MC
REMAINDER ASME SECT III DIV 3 SUBSECTION NF CLASS 3 COMPONENT SUPPORT

10) TOLERANCES FOR FILLET WELDS:
A. INCREASE LEG SIZE BY AN AMOUNT EQUAL TO THE GAP BETWEEN ITEMS TOBE WELDED. THIS INCREASE IS NOT CONSIDERED AN INCREASE IN WELD SIZE. MAX GAP = 3/16"
B. WELDS TO TORUS LINER ONLY:
MIN SIZE = AS SHOWN
MAX SIZE = MIN SIZE + 1/8 IN
ALL OTHERS:
MIN SIZE = AS SHOWN
MAX SIZE = THICKNESS OF THICKER MATERIAL JOINED

11) TOLERANCE FOR ANGLES UNLESS NOTED ± 1/2°

12) TOLERANCE FOR DIMENSIONS ± 1/32"

13) WELD FILLER MATERIAL SHALL BE IMPACT TESTED PER SPECIFICATIONS.

14) 1977 EDITION, INCLUDING ADDENDA THROUGH SUMMER 1977.

EM SUPPORT COLUMNS

SCALE: AS NOTED

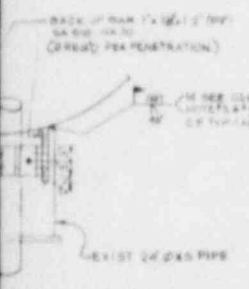

ON BB

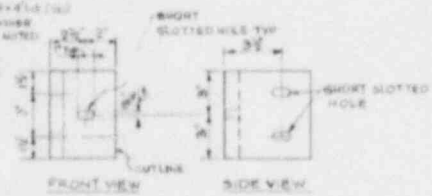

DETAIL OF L@x@-m@
SCALE: 3"=1'-0"

VENT HEADER (LOCATIONS 45° CW FROM 90°-1 TO 315° & 135°)

CAROLINA POWER & LIGHT COMPANY
BRUNSWICK STEAM ELECTRIC PLANT

PRIMARY CONTAINMENT - UNIT NO 1
SUPPRESSION CHAMBER
RING VENT HEADER SUPPORTS

United Engineers

DWG NO. 9527-F-1352 REV NO. 2

SCALE AS NOTED

9527-0-2792

PLAN VIEW
SCALE 1/8" = 1'-0"

GENERAL NOTES

1. PIPING PREFIXED BY SYSTEM NUMBER 2-82" UNLESS OTHERWISE NOTED.
2. ALL PIPING SHALL BE IN A-E ORDANCE WITH" DESIGN SPECIFICATION 2-82-1, DATED JAN. 1, 1973 OTHERWISE NOTED.
3. THIS DIVISION INCLUDES 3" FOR FIELD FIT.
4. REMOVE EXISTING WELDED COVER PLATE OVER 15" DIA. HOLE IN JET DEFLECTOR ASSY. AT 135° AZIMUTH. INSTALL 17 DIA. HOLE IN JET DEFLECTOR ASSY.

REFERENCE DWG'S.

1. GEN. ARRG'T. PLAN BELOW GR. EL. 117'-0"
2. CONTAINMENT LINER DETAILS SHT. 4
3. MAIN STEAM REL VAL DISCH PIPING, PLAN/SECT SHT. 2
4. MAIN STEAM REL VAL DISCH PIPING, PLAN/SECT SHT. 3
5. VALVE SCHEDULE INDEX
6. MAIN STEAM SAFETY REL VAL DISCH PIPING, PLAN/SECT.
7. SUPPRESSION CHAMBER-RING VENT HDR. DEFLECTOR-SOUTH HA
8. SUPPRESSION CHAMBER-RING VENT HDR DEFLECTOR-NORTH HA
9. SUPPRESSION CHAMBER-RING VENT HDR DEFLECTOR SECTION
10. SUPPRESSION CHAMBER SRV QUENCHER SUPPORT PLAN SOU
11. SUPPRESSION CHAMBER SRV QUENCHER SUPPORT PLAN NOR
12. SUPPRESSION CHAMBER SRV QUENCHER SUPPORT PLAN SEC
13. STRESS ANALYSIS DIAGRAMS
(SHEET 119, 120, 121, 122, 123, 124, 125, 126, 127, 187, 2

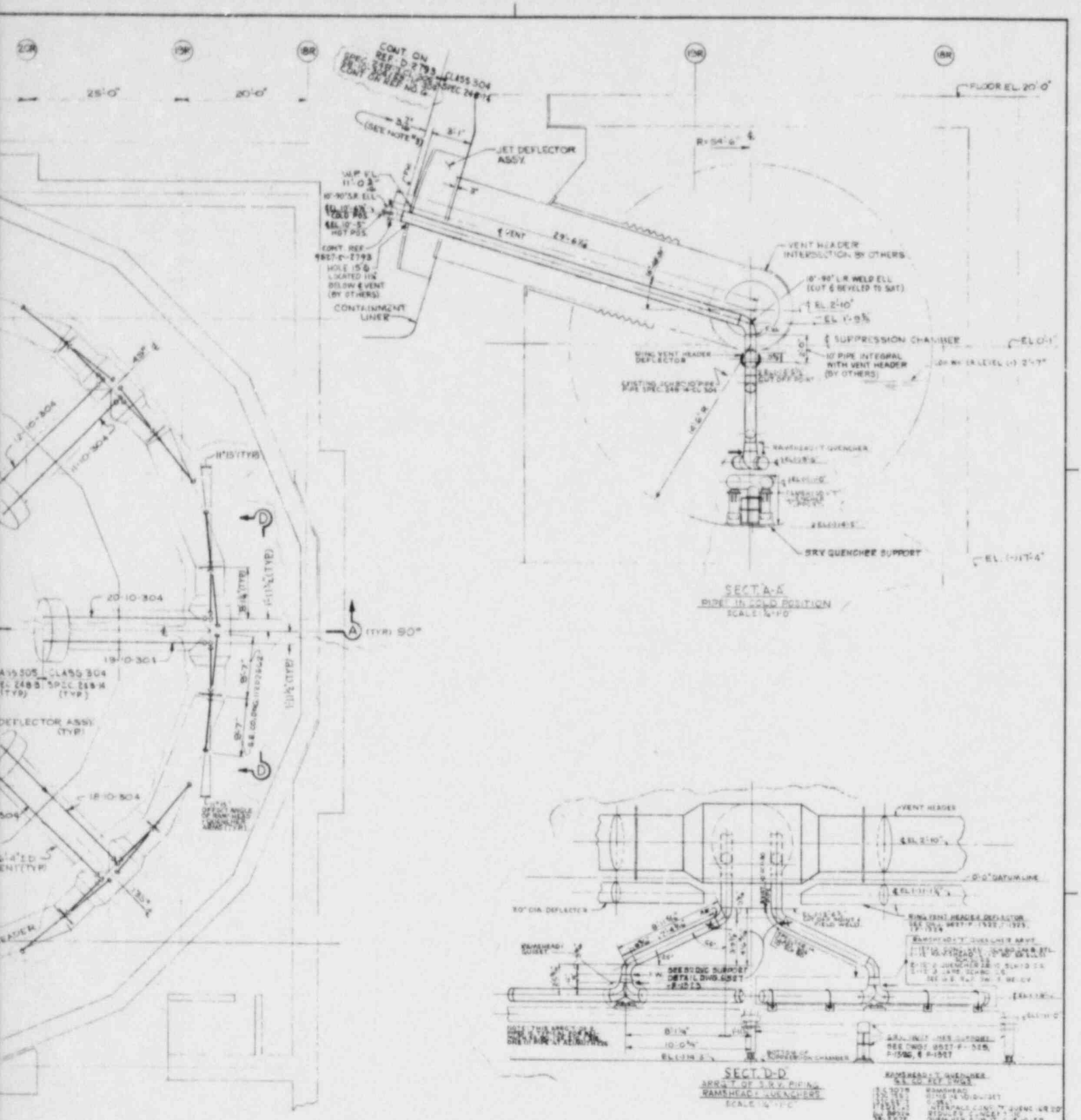

DATE	DESCRIPTION	ENGR.	SUP. ENGR.
6-17-71	FIRST ISSUE		

ENGINEER

STATE REG. NORTH CAROLINA NO. 4885

CAROLINA POWER & LIGHT COMPANY
BRUNSWICK STEAM ELECTRIC PLANT

REACTOR BUILDING
MAIN STM. RELIEF VALVE DISCH. PIPING
PLAN AND SECTIONS - SHEET NO. 1
UNIT NO. 2

UNITED ENGINEERS & CONSTRUCTORS INC.

SCALE: AS NOTED

9527-D-2792

D-2840

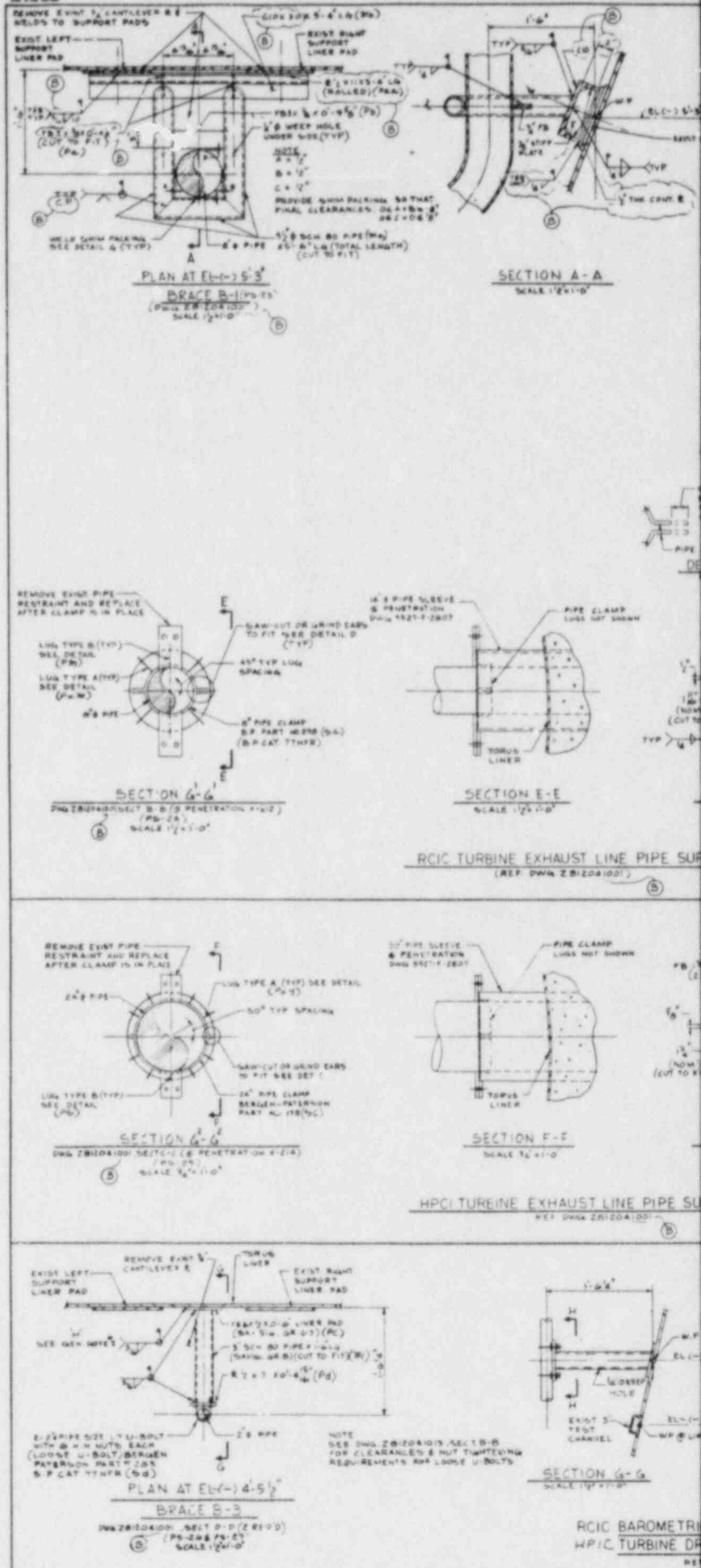
PLAN AT EL(-) 5'-3"
BRACE B-1
SECTION A-A
SECTION G¹-G¹
SECTION E-E
RCIC TURBINE EXHAUST LINE PIPE SU
SECTION G²-G²
SECTION F-F
HPCI TURBINE EXHAUST LINE PIPE SU
PLAN AT EL(-) 4'-5½"
BRACE B-3
SECTION G-G
RCIC BAROMETRI
HPIC TURBINE DR

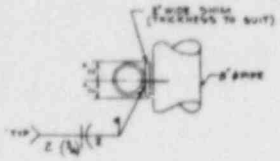

DETAIL G

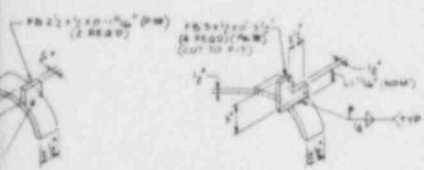

LUG DETAIL (TYPE B) NOT TO SCALE

LUG DETAIL (TYPE A) NOT TO SCALE

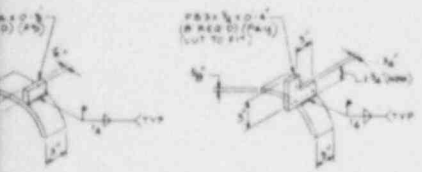

LUG DETAIL (TYPE B)

LUG DETAIL (TYPE A) NOT TO SCALE

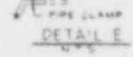

DETAIL E

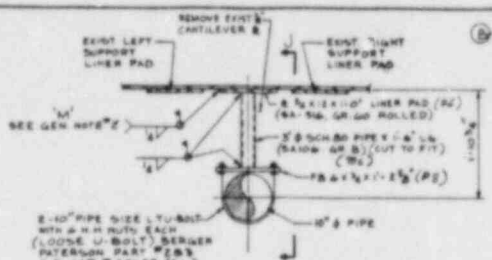

PLAN AT EL (-) 4'-5½"

BRACE B-4 (PS 18) (PS 35)

(Dwg Z81204100) SCALE 1"=1'-0"

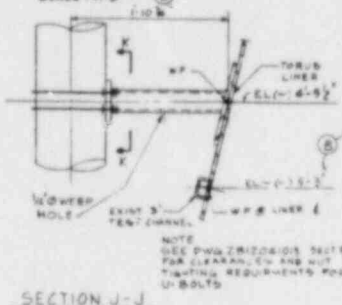

SECTION J-J

SCALE 1"=1'-0"

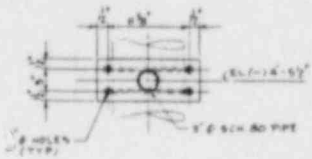

SECTION K-K

SCALE 1½"=1'-0"

CORE SPRAY TEST LINE PIPE SUPPORT

(REF. Dwg Z81204001)

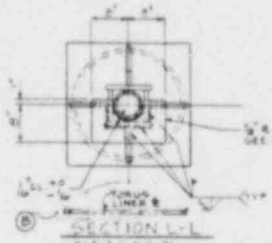

SECTION L-L

SCALE 1"=1'-0"

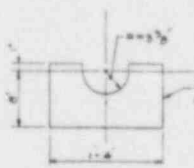

DETAIL F

SCALE 1"=1'-0"

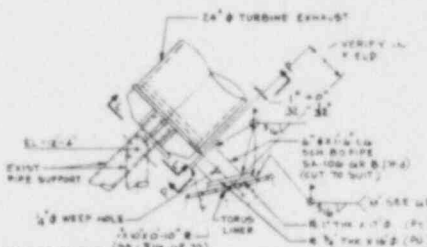

SECTION N-N

Dwg Z81204001 (PS-4075) NOT TO SCALE

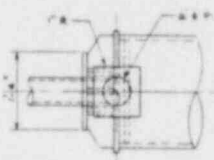

SECTION P-P

SCALE 1"=1'-0"

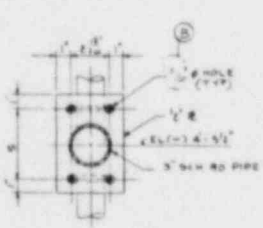

SECTION H-H

SCALE 3"=1'-0"

ONDENSER LINE PIPE SUPPORT (PS 26)

POT LINE PIPE SUPPORT (PS-27)

(Dwg Z81204100)

GENERAL NOTES

1. UNLESS NOTED OTHERWISE ALL MATERIALS SHALL BE AS FOLLOWS
   - a. STRUCTURAL STEEL SHAPES AND PLATES ASME SA-36
   - b. PIPE STRUCTURAL MEMBERS ASME SA-106 GR.B
   - c. STRUCTURAL STEEL TUBE ASTM A-500 GR.B
2. WELDS TO TORUS LINER ARE CLASSIFIED AS ASME SECT III DIVE. (USSAR M INDICATES MAGNETIC PARTICLE NON-DESTRUCTIVE EXAMINATION. WELDS NOT INDICATED W WILL BE VISUALLY INSPECTED PER SPECIFICATION
3. CENTER NEW LINER PADS UNDER CENTERS OF CONNECTING MEMBERS.
4. ALL WORK SHALL BE IN ACCORDANCE WITH UE&C SPECIFICATION NO. 9527-040-12-7
5. MEMBERS CONNECTED TO THE LINER PLATE OR LINER PADS SHALL BE ROLLED AND/OR CUT TO MIT TO A RADIUS OF 18'-0"
6. CONNECTION DETAILS TO TORUS LINER MAY HAVE TO BE ALTERED TO SUIT FIELD CONDITIONS. NOTIFY ENGINEER PRIOR TO FABRICATION.
7. ALL BOLTED CONNECTIONS ARE BEARING TYPE ⅞ Ø A325 - A325 UNLESS NOTED
8. ELEVATIONS AND LOCATIONS OF EXIST PIPING AND DIMENSIONS OF EXISTING PIPE SUPPORTS ARE OBTAINED FROM LATENT DRAWINGS AND ARE FURNISHED FOR REFERENCE ONLY.
9. BERGEN-PATTERSON PART NUMBERS ARE FROM CATALOG NO. 17HPR UNLESS NOTED
10. LINEAR DIMENSIONAL TOLERANCES UNLESS NOTED

0'-12"	± 1/16
12"-72"	± 1/8
> 72"	± 1/4

11. TOLERANCE FOR FILET WELDS
    - a. INCREASE LEG SIZE BY AN AMOUNT EQUAL TO THE GAP BETWEEN ITEMS TO BE WELDED. THIS INCREASE IS NOT CONSIDERED AN INCREASE IN WELD SIZE.
    - b. WELDS TO TORUS LINER ONLY: MIN SIZE = AS SHOWN MAX SIZE = MIN SIZE + ⅛ IN. ALL OTHERS: MIN SIZE = AS SHOWN MAX SIZE = THICKNESS OF THICKER MATERIAL JOINED.
12. GROOVE DIMENSIONS FOR GROOVE WELDS: ALL ROOT OPENINGS SHALL BE ¼ IN TOL. (± 1/16 IN.) AND ALL GROOVE ANGLES SHALL BE 45° TOL. (± 5°) UNLESS NOTED OTHERWISE.
13. ALL PIPE SUPPORTS ARE CLASSIFIED AS ASME SECTION III SUBSECTION NF CLASS 3 COMPONENT SUPPORTS, UNLESS NOTED.

REFERENCE DRAWINGS

1. Z81204001 — REACTOR BLDG. SUPPRESSION POOL PIPING & ARRANGEMENT
2. 9527-F-2407 — CONTAINMENT LINER SUPPRESSION CHAMBER PENETRATIONS
3. Z81204013 — PRIMARY CONTAINMENT UNIT NO.2 SUPPRESSION CHAMBER PIPE SUPPORT DETAILS SH.2

ALL WORK ON THIS DWG. UNDER

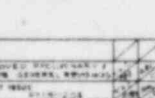

REV.	DATE	DESCRIPTION	BY	CHK	APP
B		REMOVED EXCLUSION ZONE / MAIN SEWERS, REVISED			
A		FIRST ISSUE			

DESIGNED | DRAWN | CHECKED | ENGINEER | STATE REG.

CAROLINA POWER & LIGHT COMPANY
BRUNSWICK STEAM ELECTRIC PLANT

PRIMARY CONTAINMENT UNIT NO. 2
SUPPRESSION CHAMBER
PIPE SUPPORT DETAILS SH. 1

united engineers

DWG. NO. Z81204101 1A 9527 A2A — REV. NO. B

SCALE AS NOTED

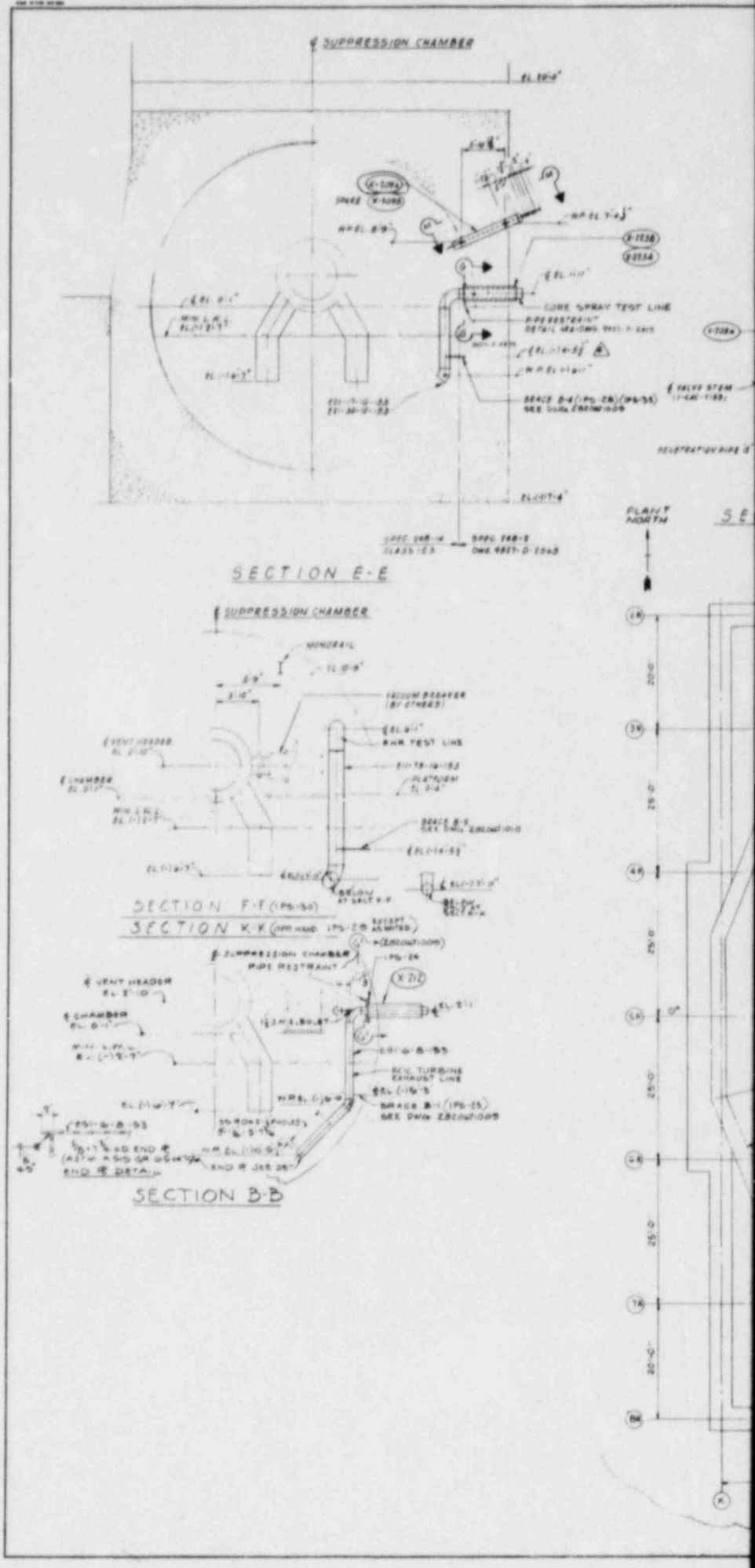
℄ SUPPRESSION CHAMBER
EL 20'-0"
SPARE
CORE SPRAY TEST LINE
PLANT NORTH
SECTION E-E
℄ SUPPRESSION CHAMBER
MONORAIL
VACUUM BREAKER
RHR TEST LINE
SECTION F-F
SECTION K-K
SECTION B-B
RCIC TURBINE EXHAUST LINE

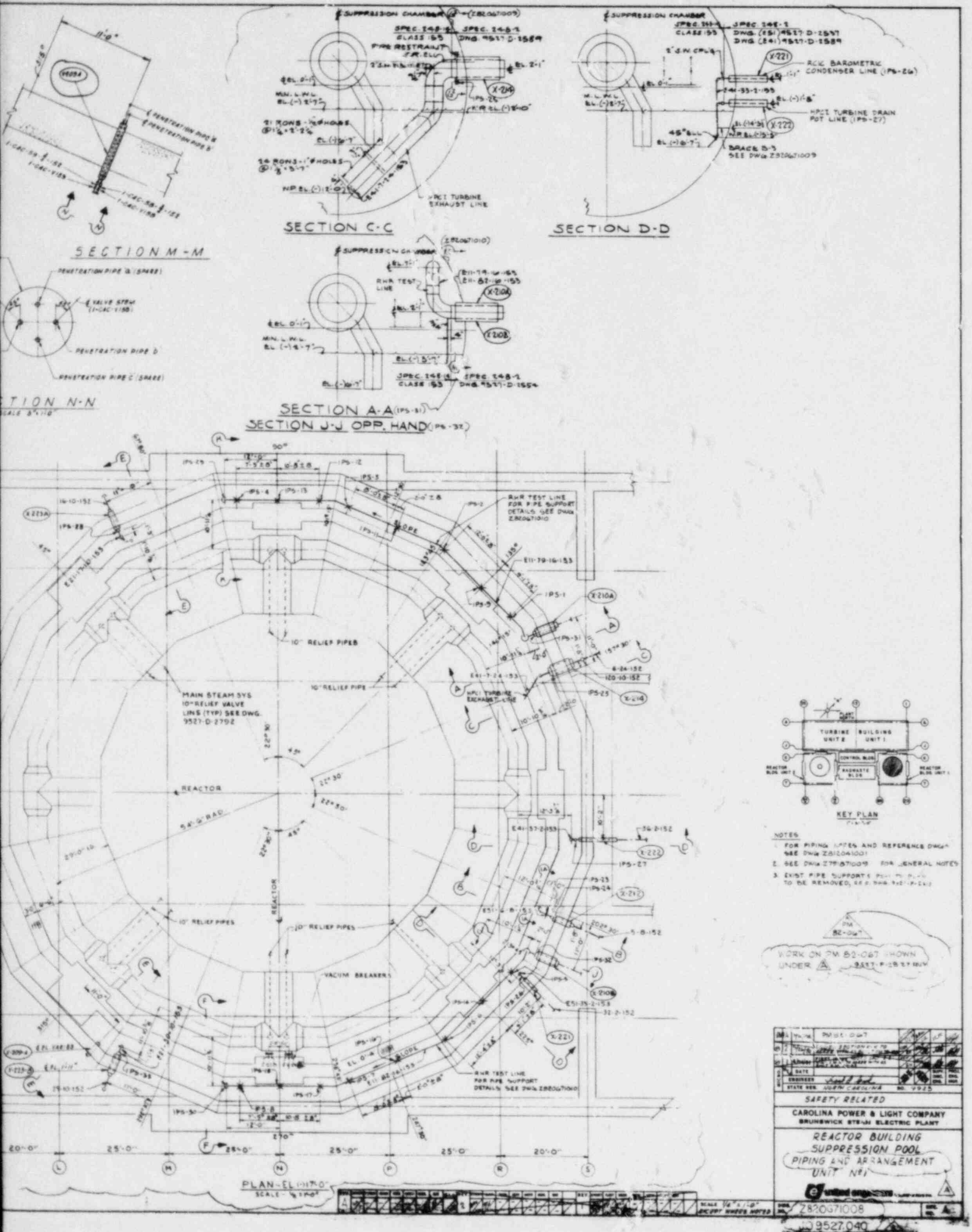
SECTION M-M
SECTION C-C
SECTION D-D
SECTION A-A (IPS-31)
SECTION J-J OPP. HAND (IPS-32)
PLAN-EL. 130'-0"
SCALE - 1/8"=1'-0"
KEY PLAN
NOTES
1. FOR PIPING NOTES AND REFERENCE DWGS SEE DWG Z81204100 1
2. SEE DWG Z7708710009 FOR GENERAL NOTES
3. EXIST PIPE SUPPORTS TO BE REMOVED, SEE DWG
WORK ON PM 82-067 SHOWN UNDER A
SAFETY RELATED
CAROLINA POWER & LIGHT COMPANY
BRUNSWICK STEAM ELECTRIC PLANT
REACTOR BUILDING
SUPPRESSION POOL
PIPING AND ARRANGEMENT
UNIT NO 1
Z820671008
9527.040

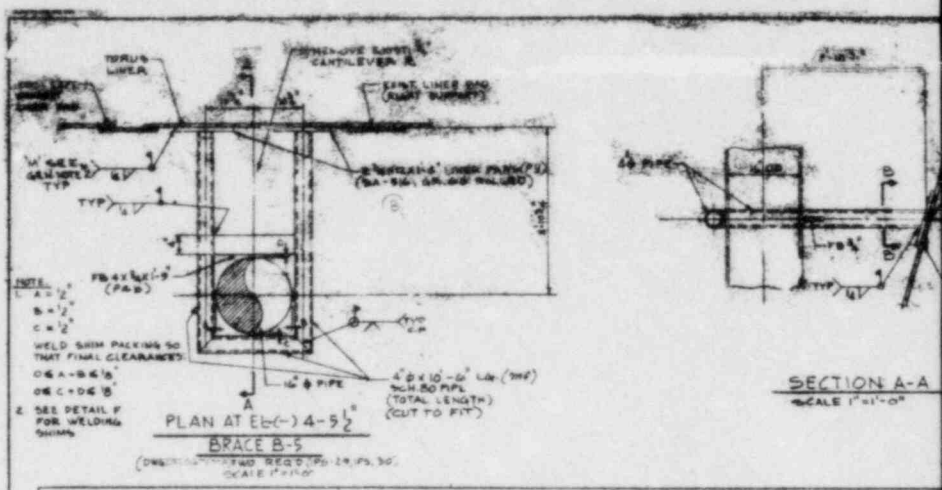
PLAN AT EL (-) 4-5½"
BRACE B-5
SECTION A-A

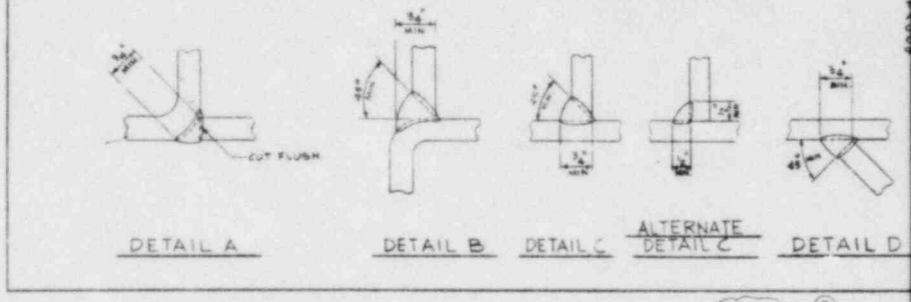
WELD DETAILS FOR
TUBE TO TUBE CONNECTIONS
DETAIL A
DETAIL B
DETAIL C
ALTERNATE
DETAIL C
DETAIL D

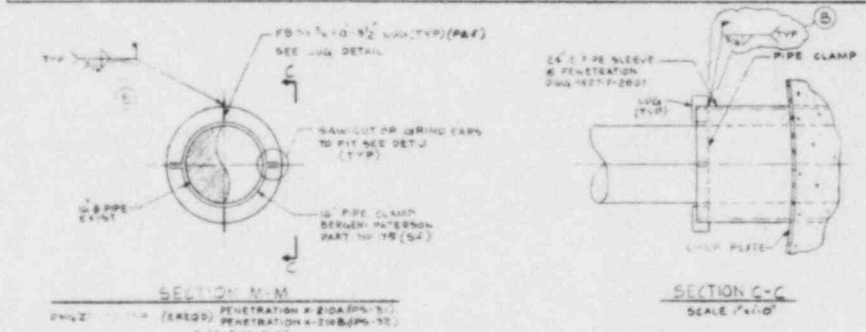
SECTION M-M
SECTION C-C
PIPE CLAMP

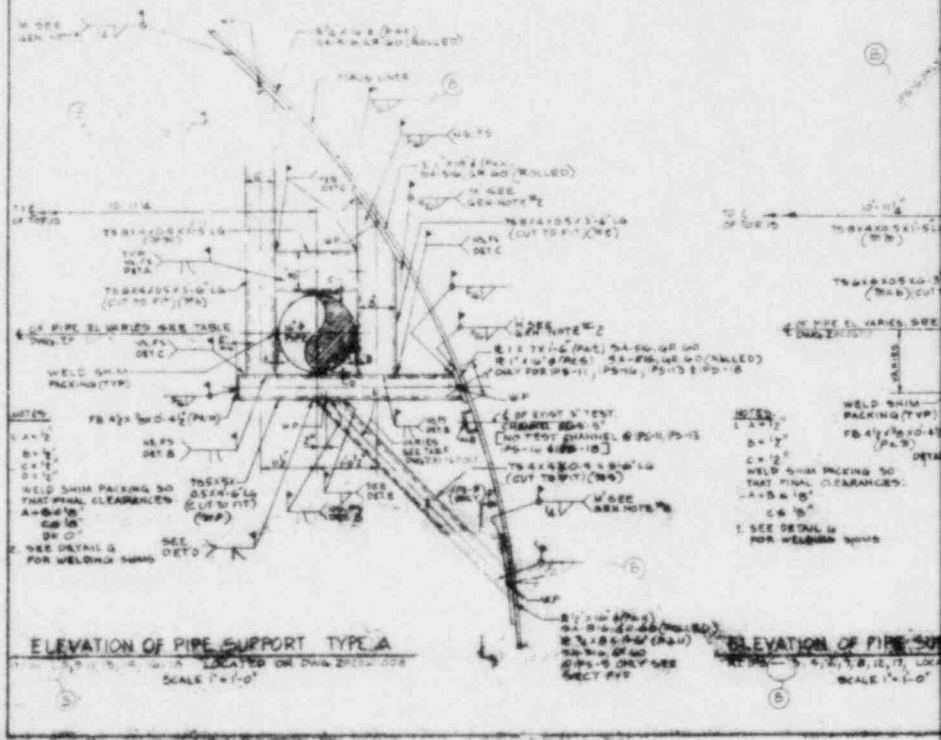
ELEVATION OF PIPE SUPPORT TYPE A

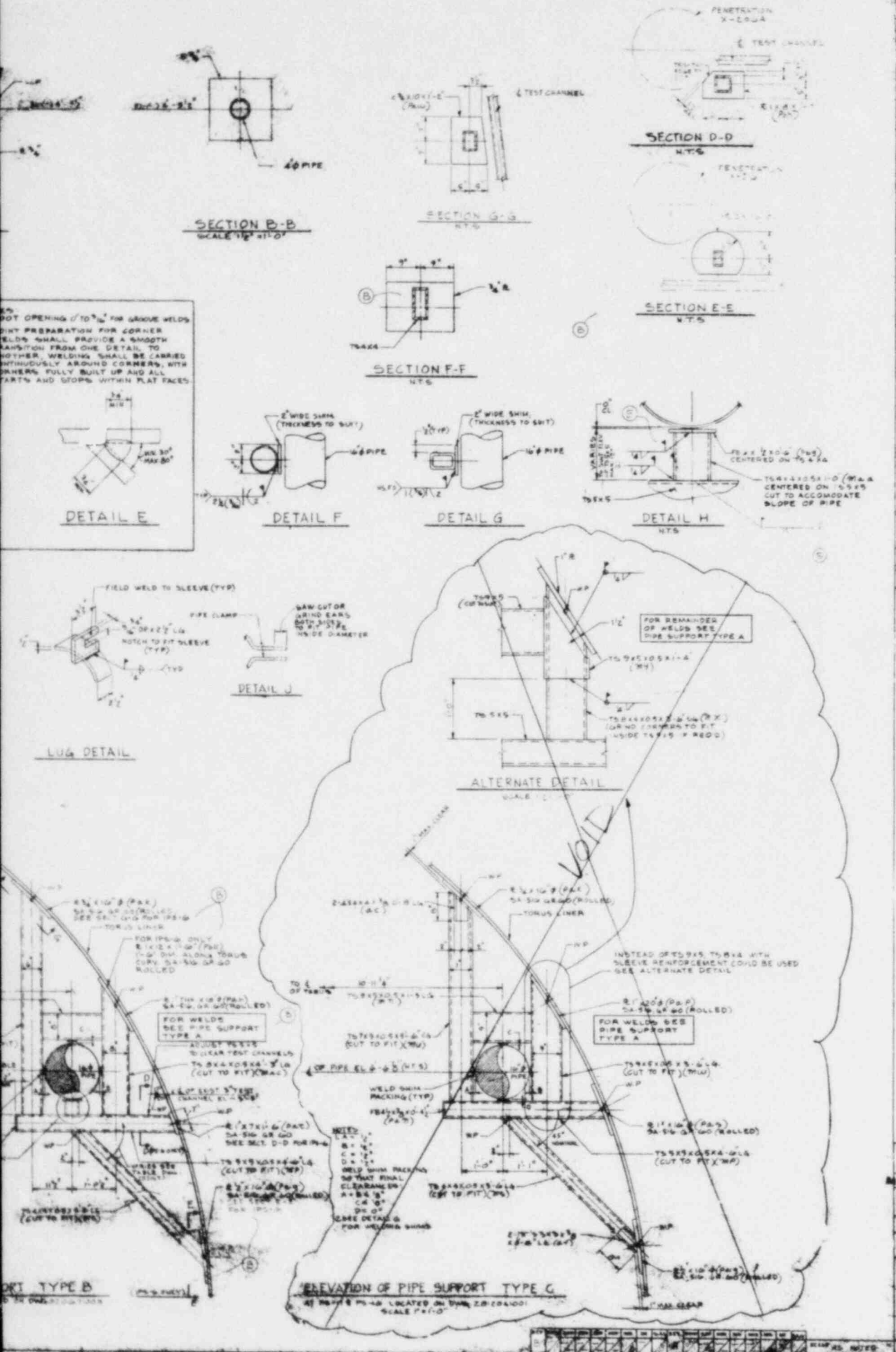
SECTION B-B
SCALE 1"=1'-0"
SECTION G-G
N.T.S.
SECTION D-D
N.T.S.
SECTION E-E
N.T.S.
SECTION F-F
N.T.S.
DETAIL E
DETAIL F
DETAIL G
DETAIL H
N.T.S.
DETAIL J
LUG DETAIL
ALTERNATE DETAIL
SCALE 1"=1'-0"
ELEVATION OF PIPE SUPPORT TYPE C
SCALE 1"=1'-0"
PIPE SUPPORT TYPE B
NOTE
REFERENCE DRAWINGS
CAROLINA POWER & LIGHT COMPANY
BRUNSWICK STEAM ELECTRIC PLANT
PRIMARY CONTAINMENT UNIT NO. 2
SUPPRESSION CHAMBER
RHR TEST LINE PIPE SUPPORT DET'S
VOID

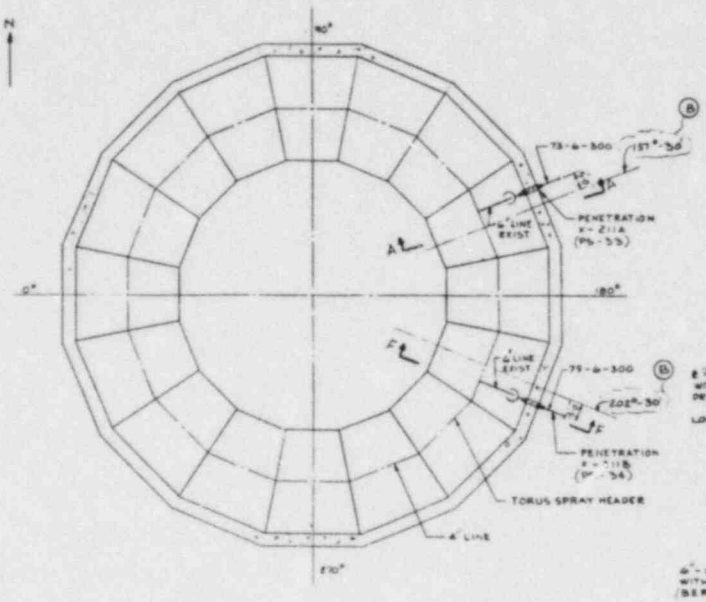

PLAN VIEW OF SUPPRESSION CHAMBER

SCALE 1/16"=1'-0"

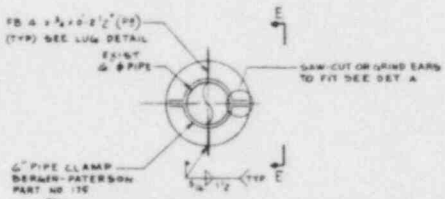

SECTION D-D

PENETRATION X-21A (PS-33)
PENETRATION X-21B (PS-34)
SCALE 1"=1'-0"

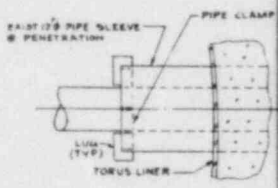

SECTION E-E

SCALE 1"=1'-0"

TO

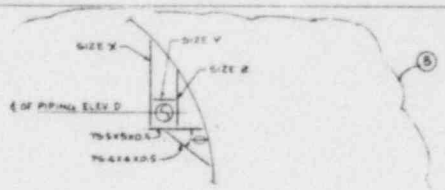

ELEVATION OF PIPE SUPPORT

(SEE DWG 2BD2040102 FOR DETAILS)

SUMMARY

PIPE SUPPORT MARK	NO OF PIPING SUPPORTED BY THIS MARK	SIZE X	SIZE Y	SIZE Z	NOMINAL ϕ ANGLE	FRAME TYPE *	NOMINAL ELEV D
PS-1	9	PL ⅜x10.5	PL ⅜x10.5	PL ⅜x10.5	37½°	A	6'-11½"
PS-2	13				45°	B	6'-8½"
PS-3	8				45°	B	6'-7½"
PS-4	22				45°	B	6'-0½"
PS-5	9				45°	A	6'-11½"
PS-6	15				41°	B	6'-8½"
PS-7	18				45°	B	6'-9½"
PS-8	22				45°	B	6'-0½"
PS-9	11				35°	A	6'-10½"
PS-11	16				45°	A	6'-8½"
PS-12	40				45°	B	6'-3½"
PS-13	21				45°	A	6'-11½"
PS-14	11				45°	A	6'-10½"
PS-16	16				45°	A	6'-6½"
PS-17	40				45°	B	6'-3½"
PS-18	21	↑	↑	↑	45°	A	6'-11½"

* NOMINAL ANGLE OF BRACE AND FRAME TYPE (A OR B WITH OR WITHOUT SHOE) HAVE BEEN DETERMINED FROM FIELD MEASUREMENTS MADE FOR UNIT 1 TO CLEAR PENETRATIONS, TEST CHANNELS AND OTHER INTERFERENCES. VERIFY IN FIELD GEOMETRY OF FRAME AND DETERMINE CUT LENGTHS PRIOR TO FABRICATION. ANGLE OF BRACE MAY BE VARIED MIN 30°, MAX 60°

RHR TEST LINE PIPE SUPPORTS

PS-1 THRU PS-18

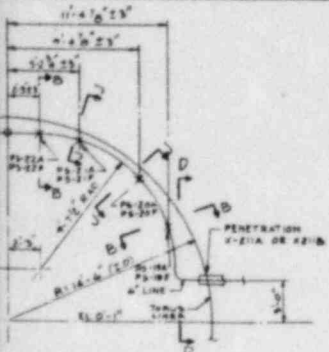

CTION A-A PS-19A THRU PS-22A

TION F-F PS-19F THRU PS-22F

SCALE 1/4"=1'-0"

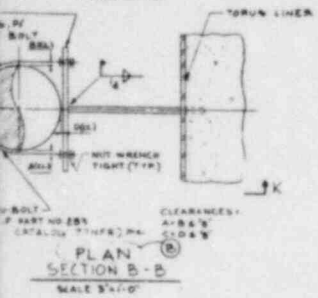

PLAN
SECTION B-B
SCALE 3"=1'-0"

PS MARK NO	A MIN	LENGTH OF E	ASSEMBLY MARK NO
PS-19A PS-19B	1'-3"	1'-1"	pa SEE SECT BB
PS-20A PS-20F	8"	5"	pb SEE SECT JJ
PS-21A PS-21F	1"	4"	pc SEE SECT JJ
PS-22A PS-22F	11"	8"	pd SEE SECT BB

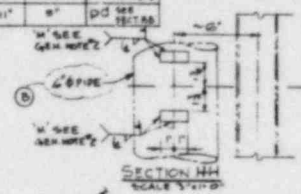

SECTION HH
SCALE 3"=1'-0"

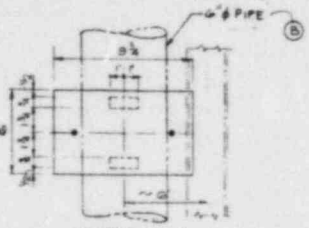

SECTION G-G
SCALE 3"=1'-0"

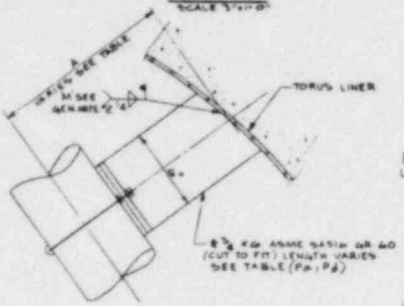

SECTION K-K
SCALE 3"=1'-0"

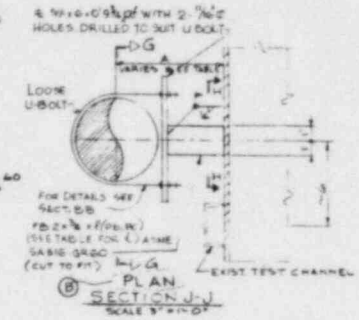

PLAN
SECTION J-J
SCALE 3"=1'-0"

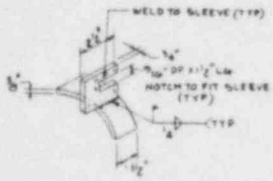

LUG DETAIL

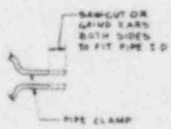

DETAIL A

US SPRAY HEADER PIPE SUPPORTS (RHR LOOP COOLING LINE PIPE SUPPORTS)

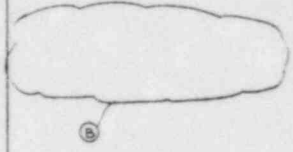

NOTES:

1. SEE 2NAS-0102A-0001 FOR GENERAL NOTES

REFERENCE DRAWINGS

1. FP-9557-01-104 SUPPRESSION CHAMBER INTERNAL SPRAY HEADER ASSEMBLY
2. 9557-F-1 PRIMARY CONTAINMENT LINER SUPPRESSION CHAMBER PENETRATIONS
3. FP-9557-01-112 SUPPRESSION CHAMBER PENETRATION SCHEDULE AND ORIENTATION

(B)

ALL WORK ON THIS DWG UNDER

B REV PW B-204

SCH-9557-040-63

REVISIONS					
NO.	BY	DESCRIPTION	DATE	APPROVED	
B		REVISED PER CHANGE IN PIP NOZ GENERAL REVISIONS			
A		FIRST ISSUE P.W. B-204			

CAROLINA POWER & LIGHT COMPANY
BRUNSWICK STEAM ELECTRIC PLANT

PRIMARY CONTAINMENT UNIT NO. 2

SUPPRESSION CHAMBER

PIPE SUPPORT DETAILS SH. 2

united engineers

DWG NO. 2812041013 REV NO. B

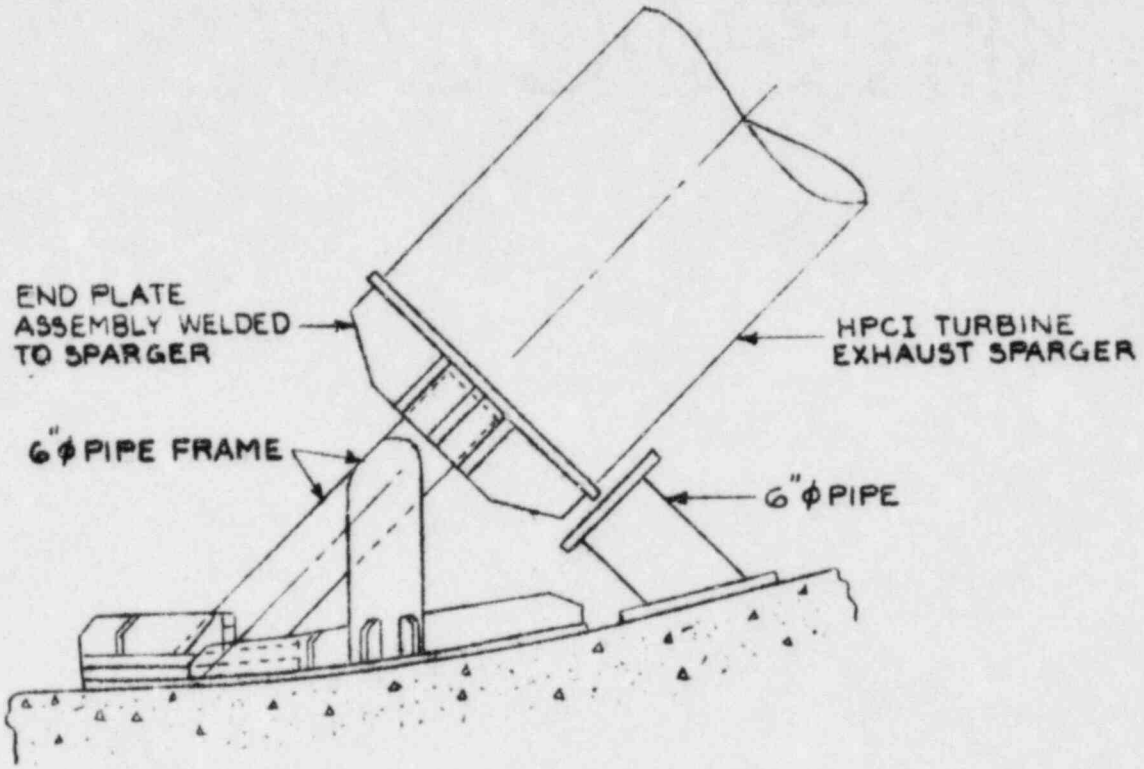

SUPPORT FOR HPCI TURBINE EXHAUST SPARGER

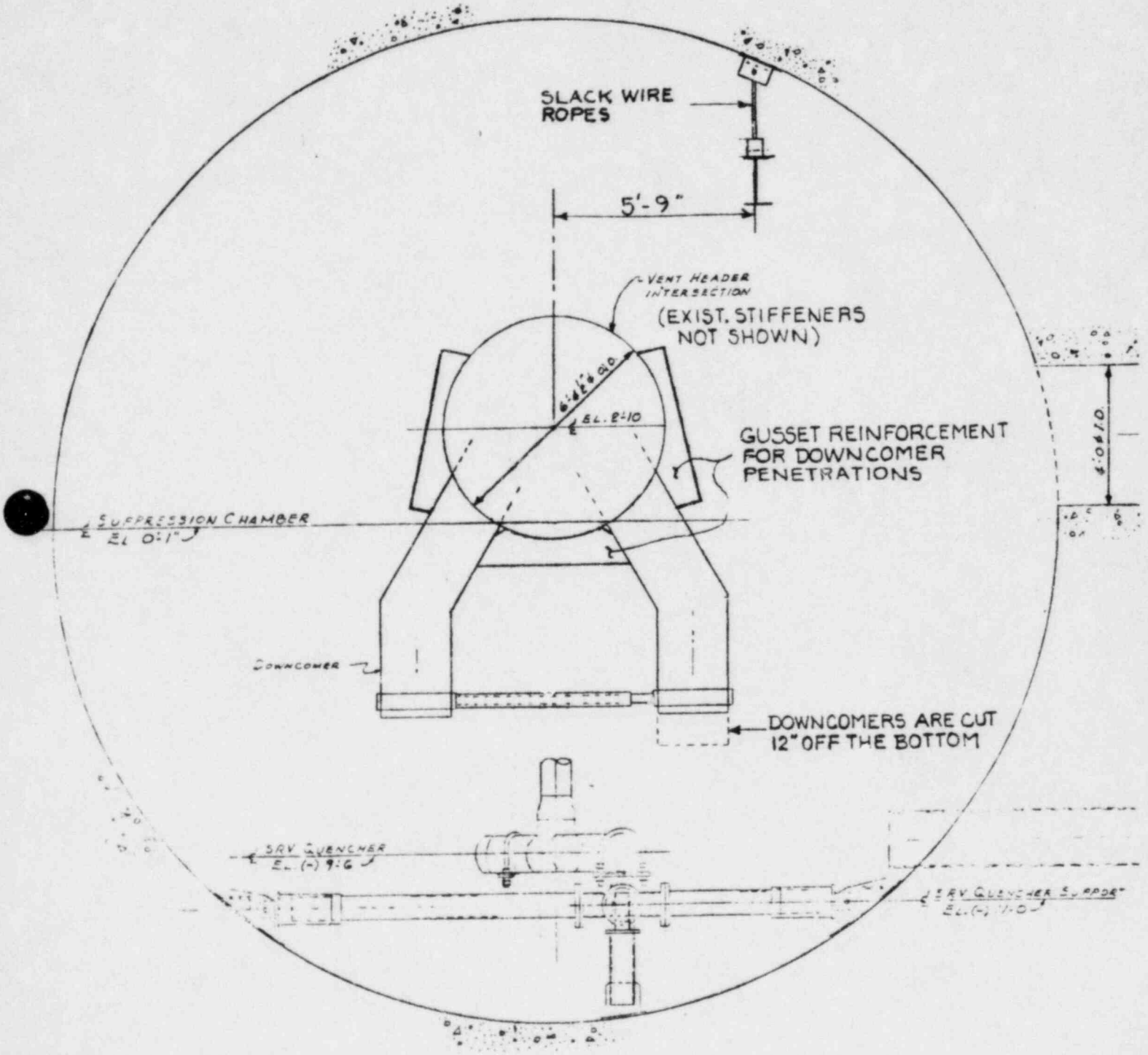

SECTION AT AZM 315°
LOOKING SOUTHEAST

EL. 20'-0"

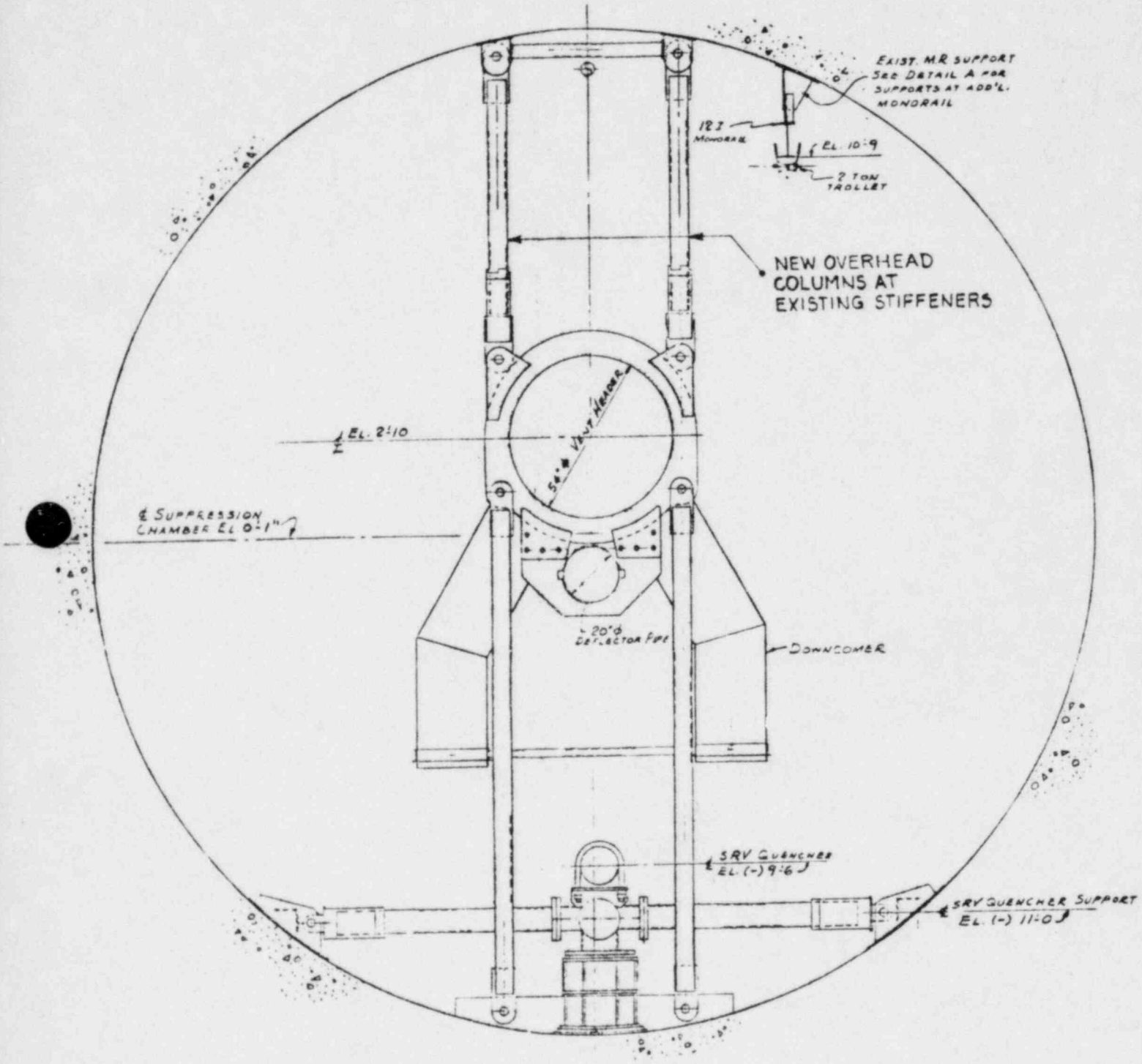

TYPICAL SECTION NEAR VENT HEADER SUPPORT
℄ CENTER SRV QUENCHER SUPPORT

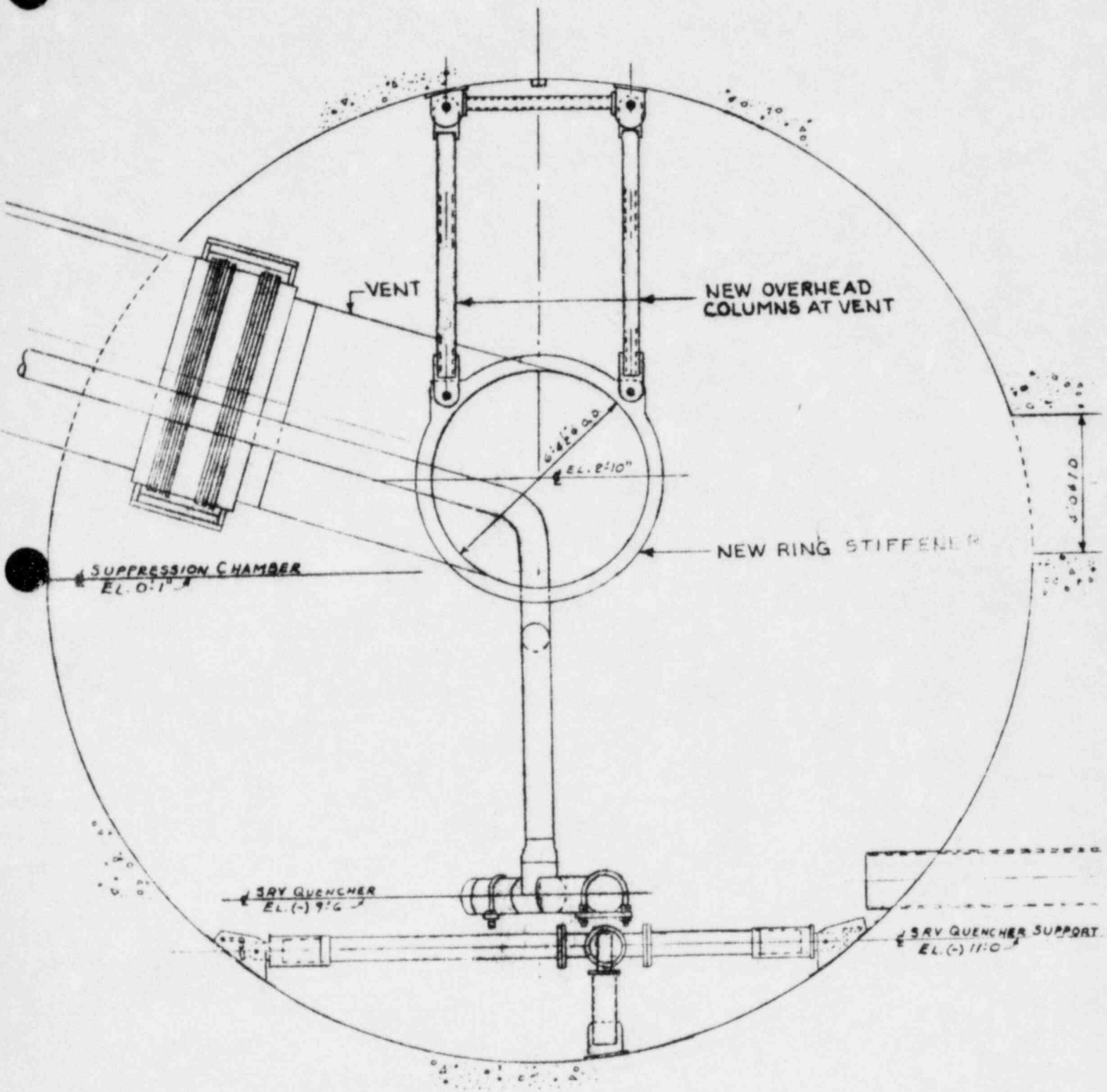

SECTION AT AZM. 315°
LOOKING SOUTHEAST

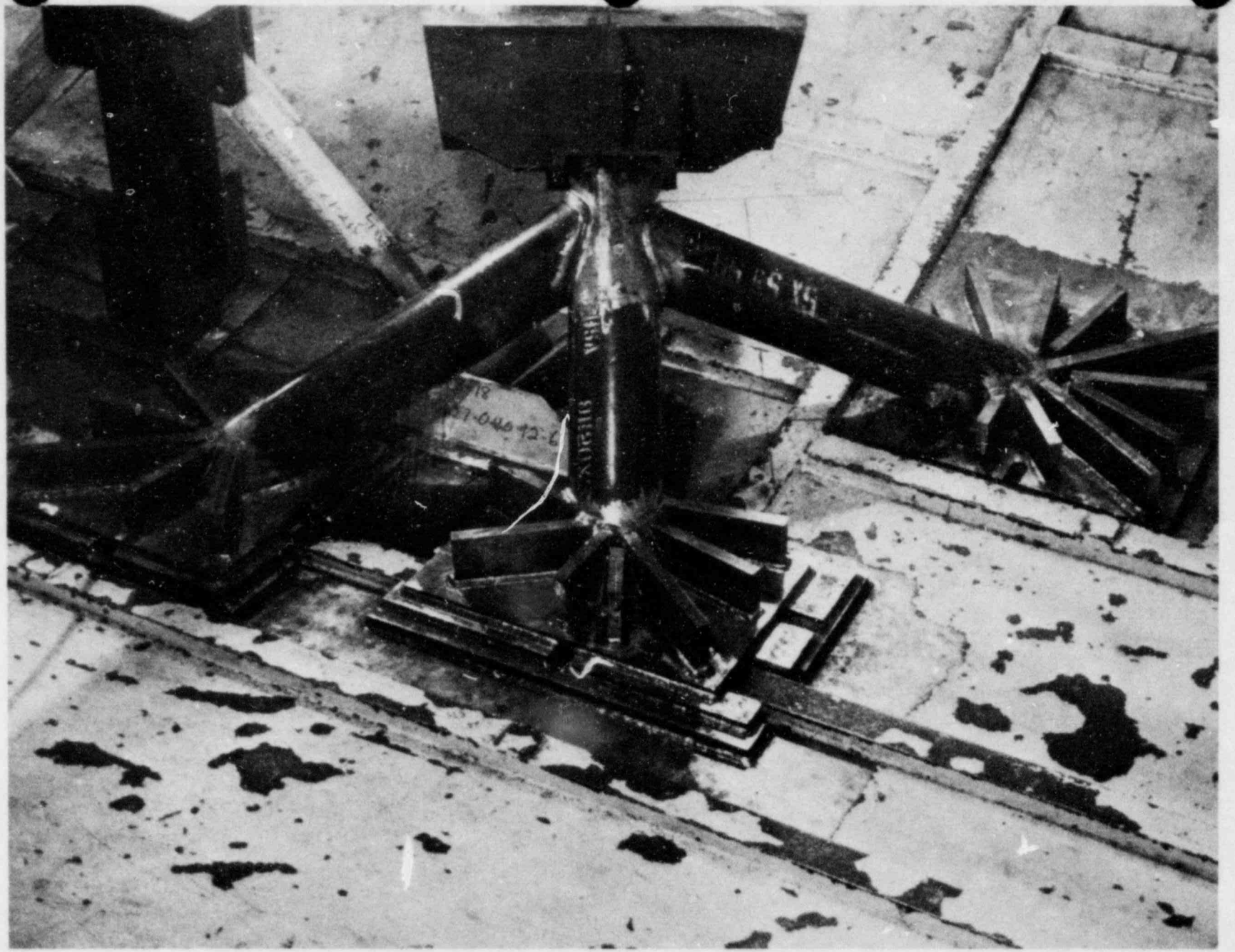

CAROLINA POWER AND LIGHT
BRUNSWICK STEAM ELECTRIC PLANT
UNIT 2
TORUS (1980)

HPCI TURBINE EXHAUST ANCHOR

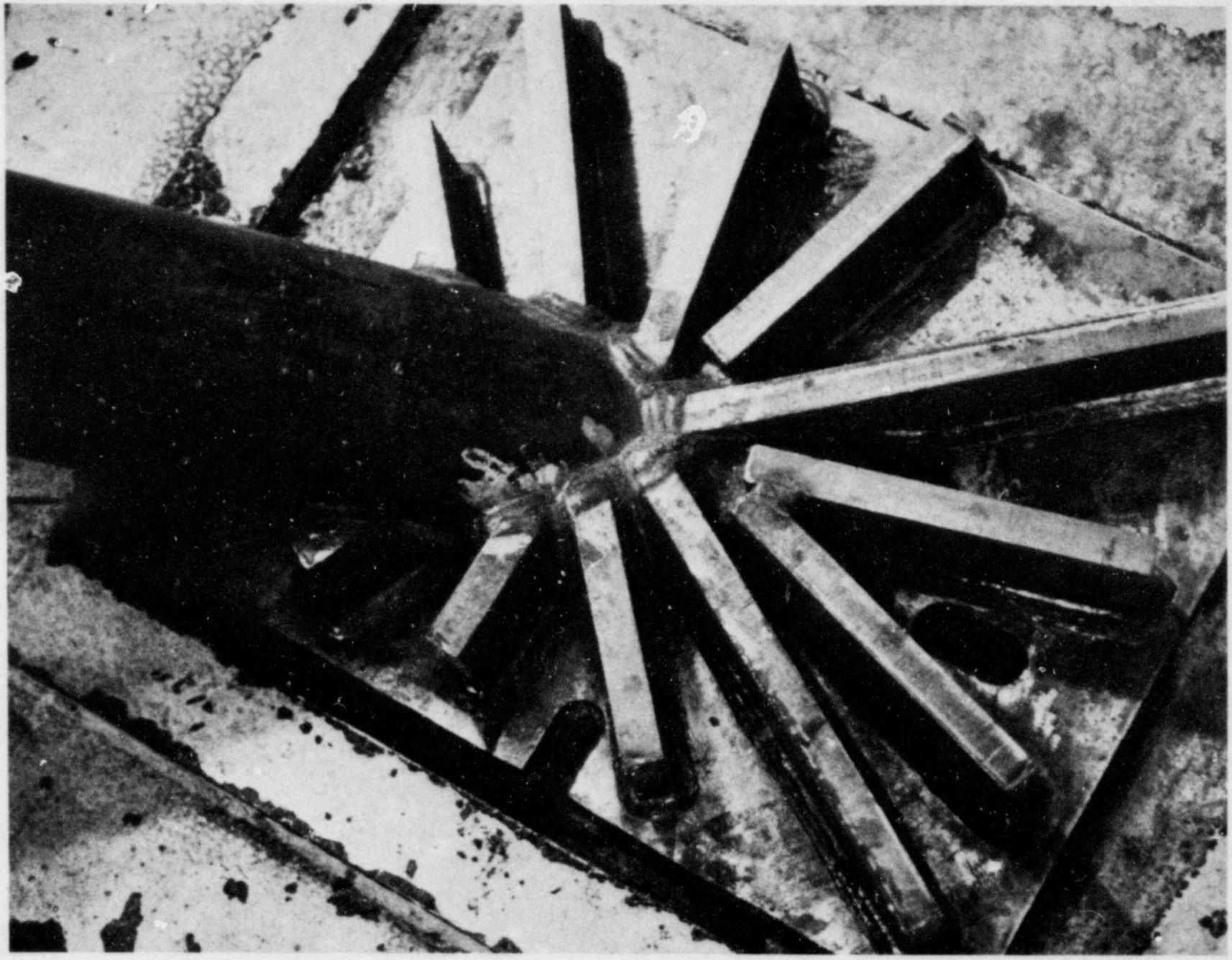

CAROLINA POWER AND LIGHT
BRUNSWICK STEAM ELECTRIC PLANT
UNIT 2
TORUS (1980)

HPCI TURBINE EXHAUST ANCHOR

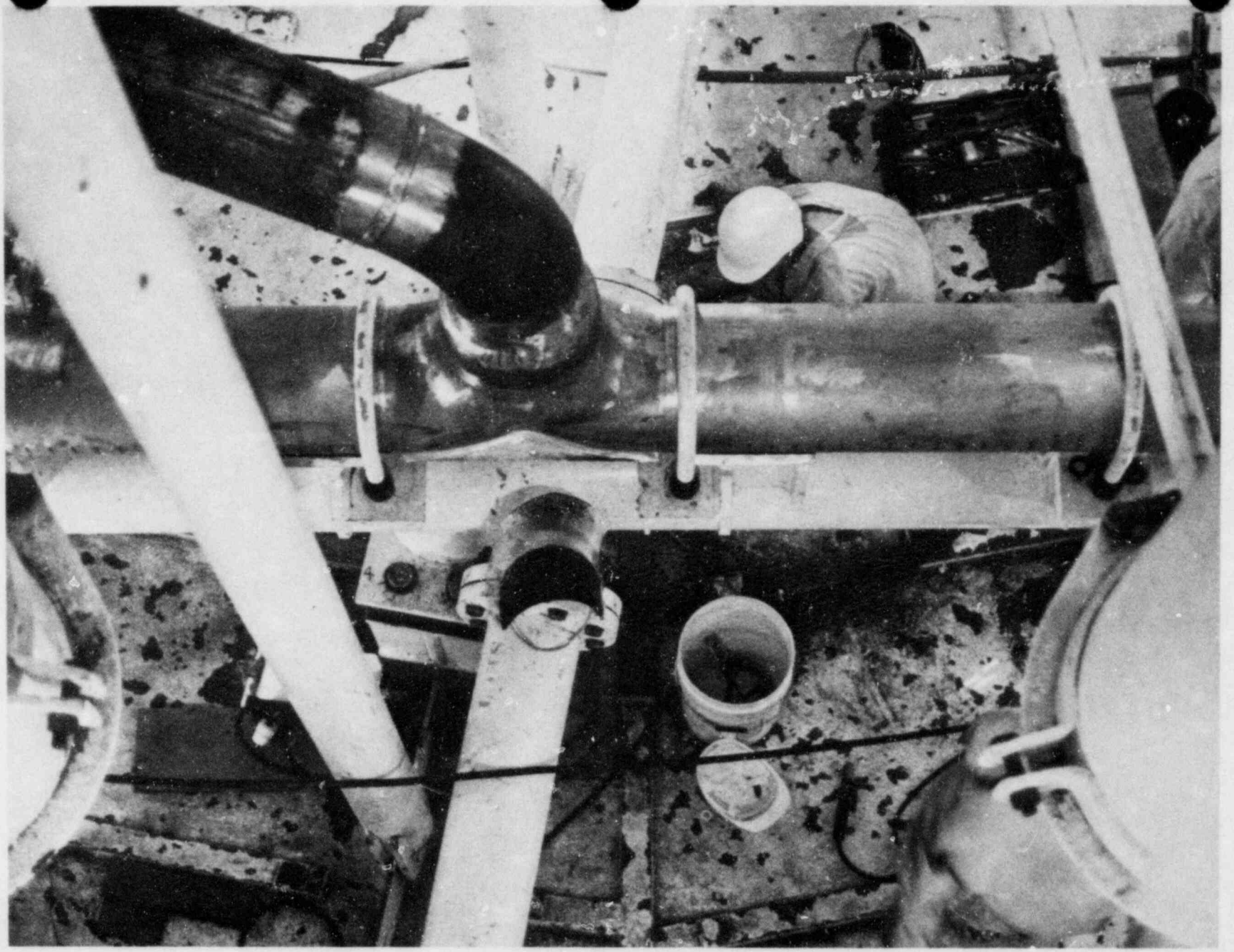

CAROLINA POWER AND LIGHT
BRUNSWICK STEAM ELECTRIC PLANT
UNIT 2
TORUS (1980)

STEAM RELIEF DISCHARGE LINE SPARGER & SUPPORT

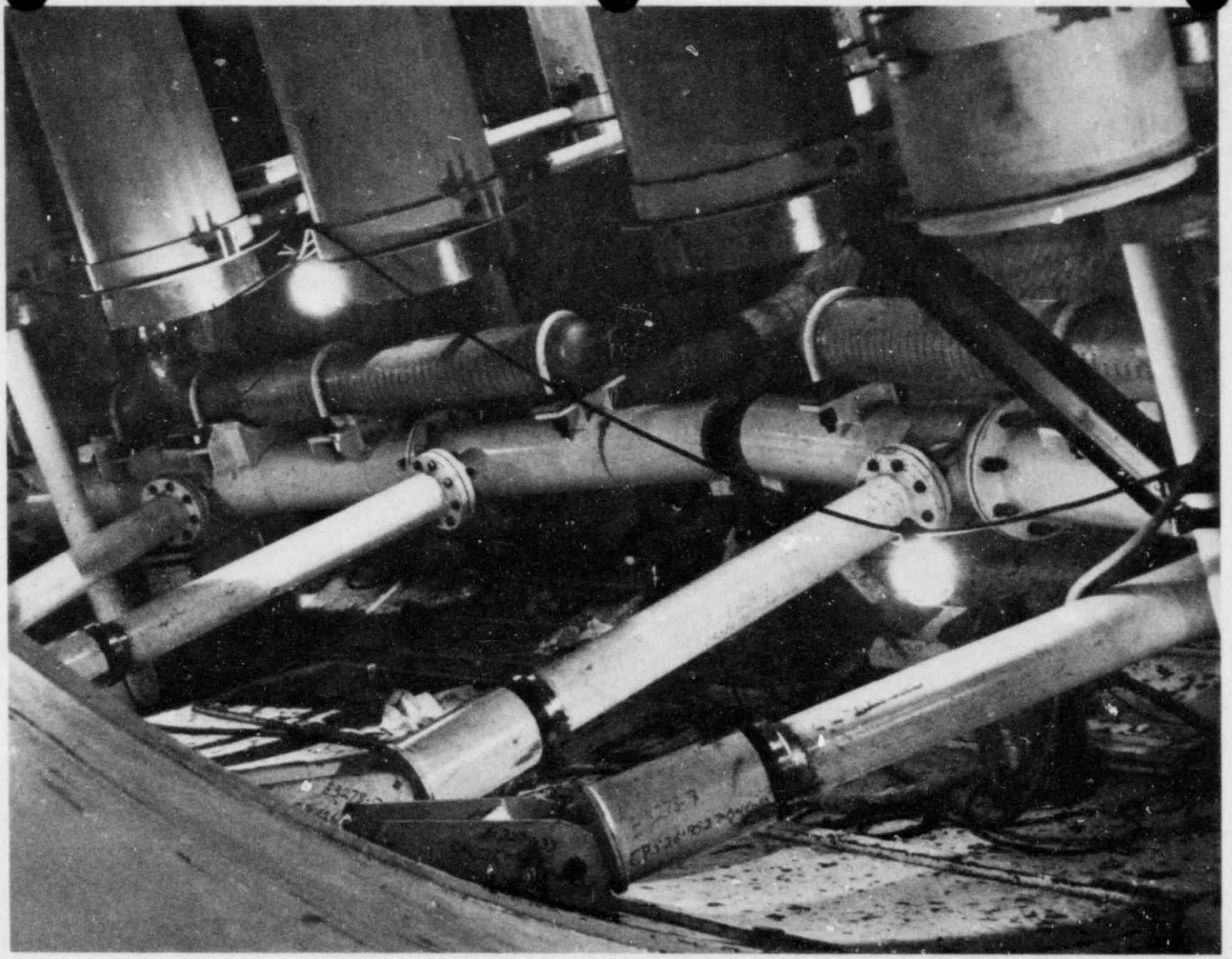

CAROLINA POWER AND LIGHT
BRUNSWICK STEAM ELECTRIC PLANT
UNIT 2
TORUS (1980)

STEAM RELIEF DISCHARGE LINE SPARGER & SUPPORTS

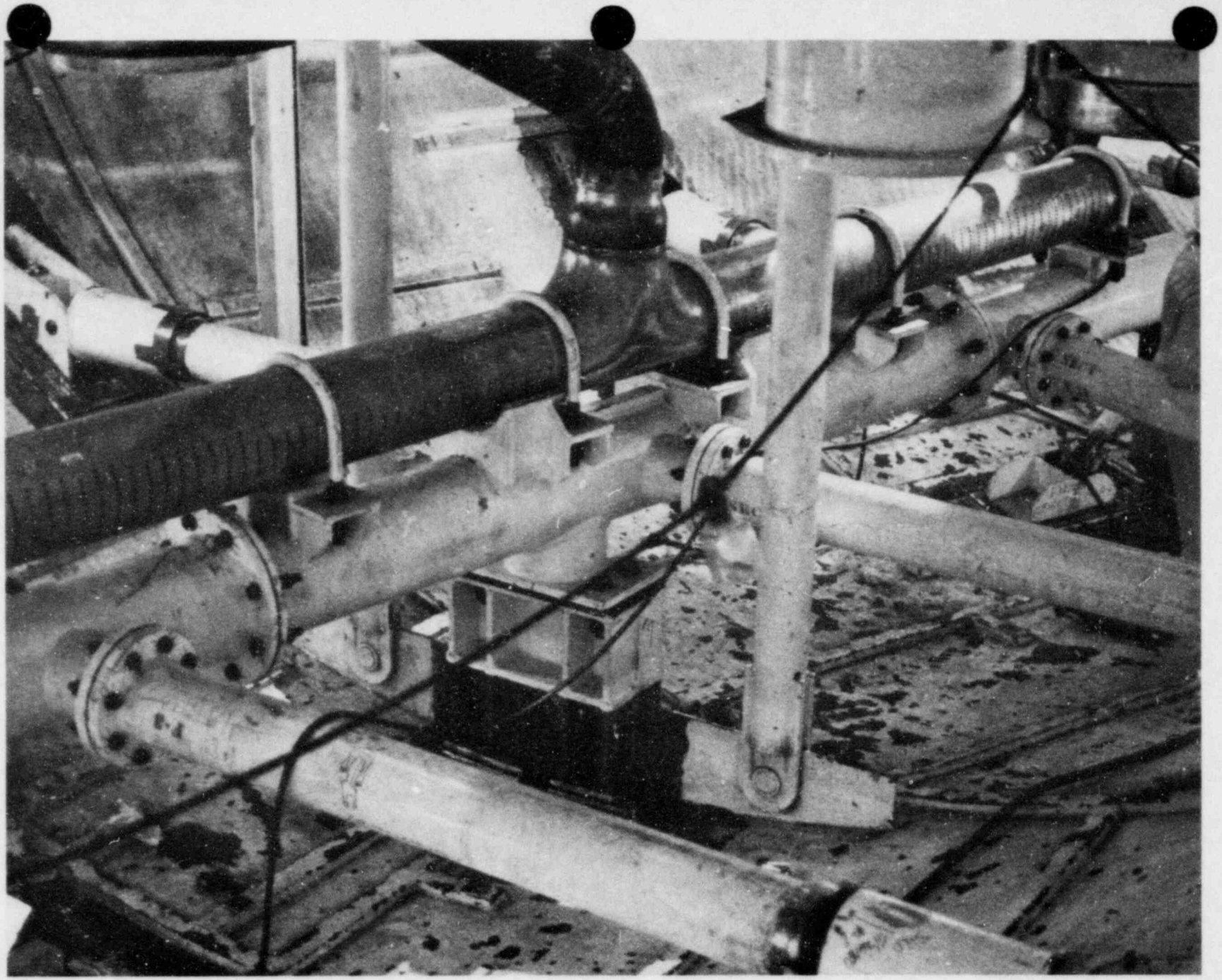

CAROLINA POWER AND LIGHT
BRUNSWICK STEAM ELECTRIC PLANT
UNIT 2
TORUS (1980)

STEAM RELIEF DISCHARGE LINE SPARGER & SUPPORT

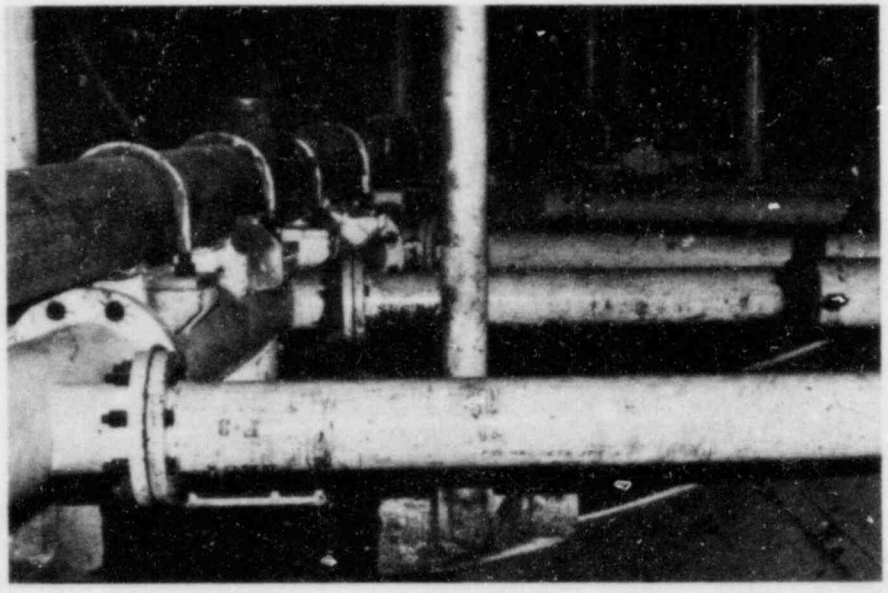

CAROLINA POWER AND LIGHT
BRUNSWICK STEAM ELECTRIC PLANT
UNIT 2
TORUS (1980)

STEAM RELIEF DISCHARGE LINE SPARGER & SUPPORT

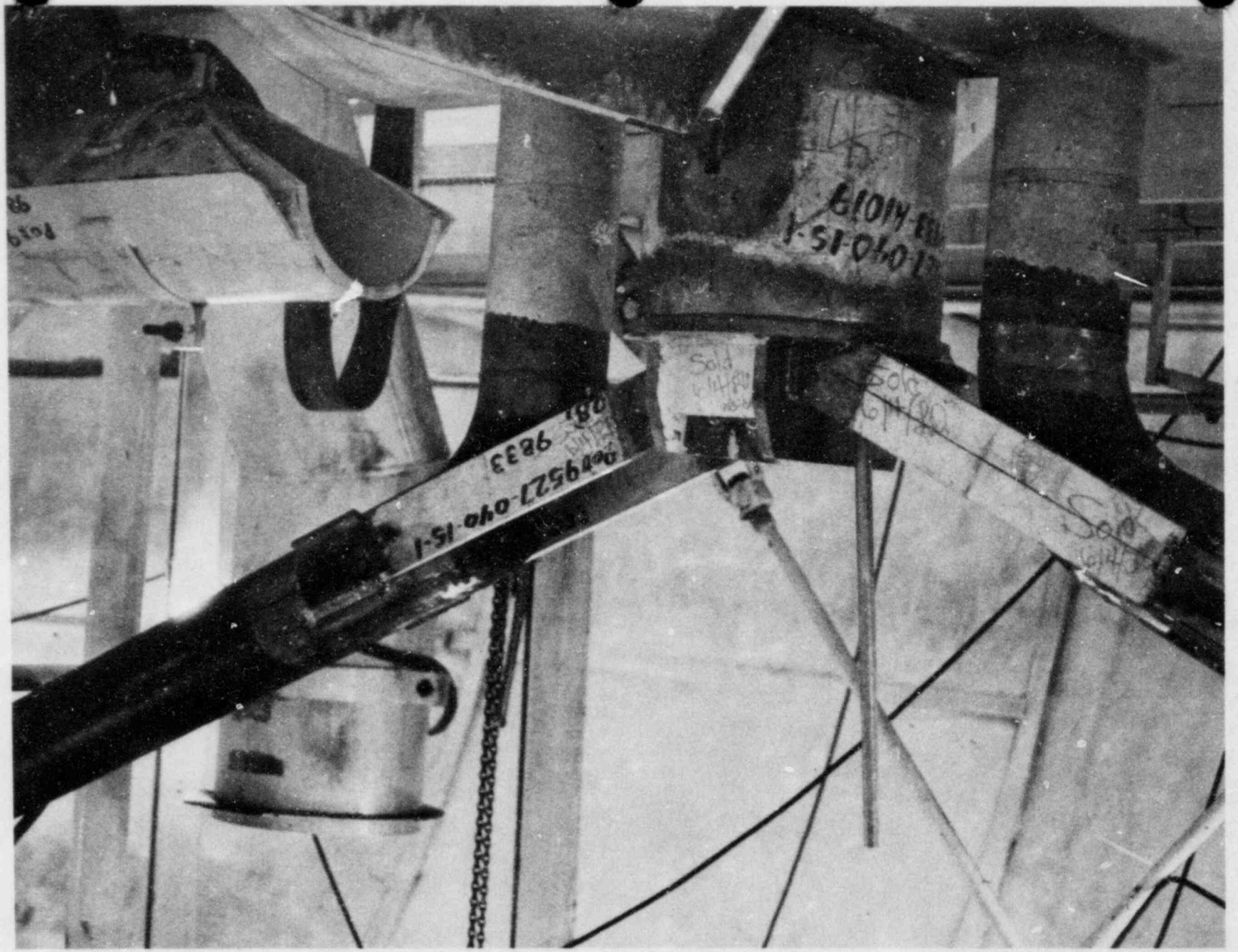

CAROLINA POWER AND LIGHT
BRUNSWICK STEAM ELECTRIC PLANT
UNIT 2
TORUS (1980)

STEAM RELIEF DISCHARGE LINE SUPPORT

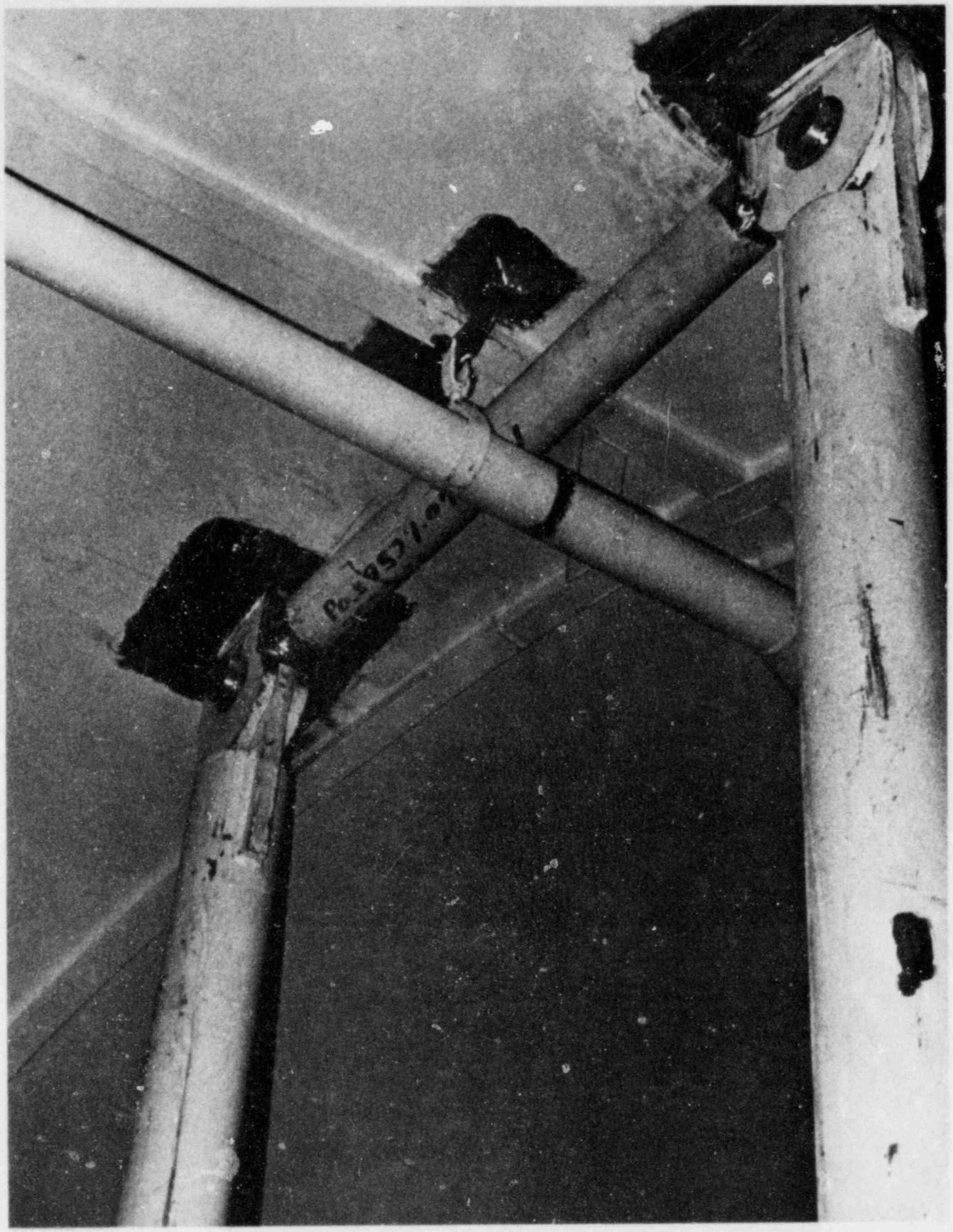

CAROLINA POWER AND LIGHT
BRUNSWICK STEAM ELECTRIC PLANT
UNIT 2
TORUS (1980)

VENT HEADER COLUMNS

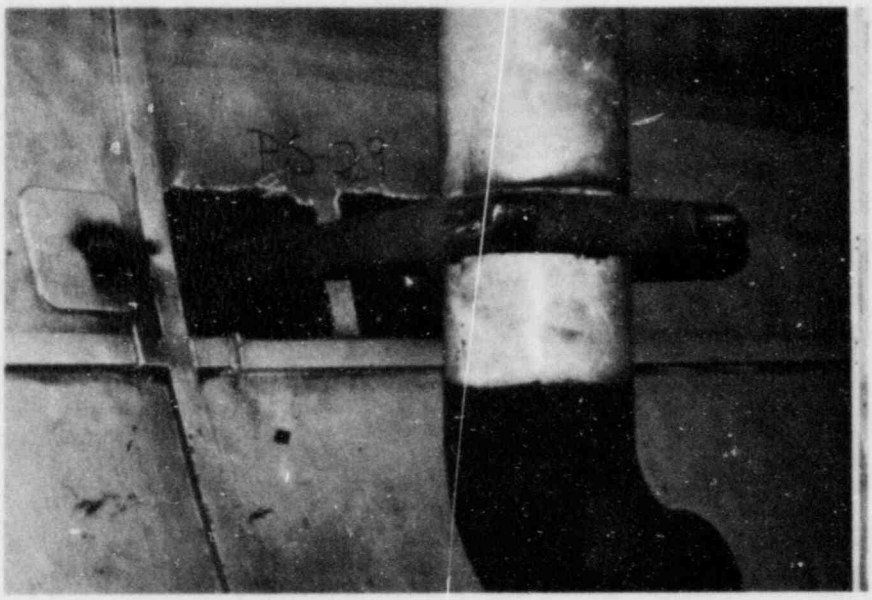

CAROLINA POWER AND LIGHT
BRUNSWICK STEAM ELECTRIC PLANT
UNIT 2
TORUS (1982)

RHR TEST LINE SUPPORT

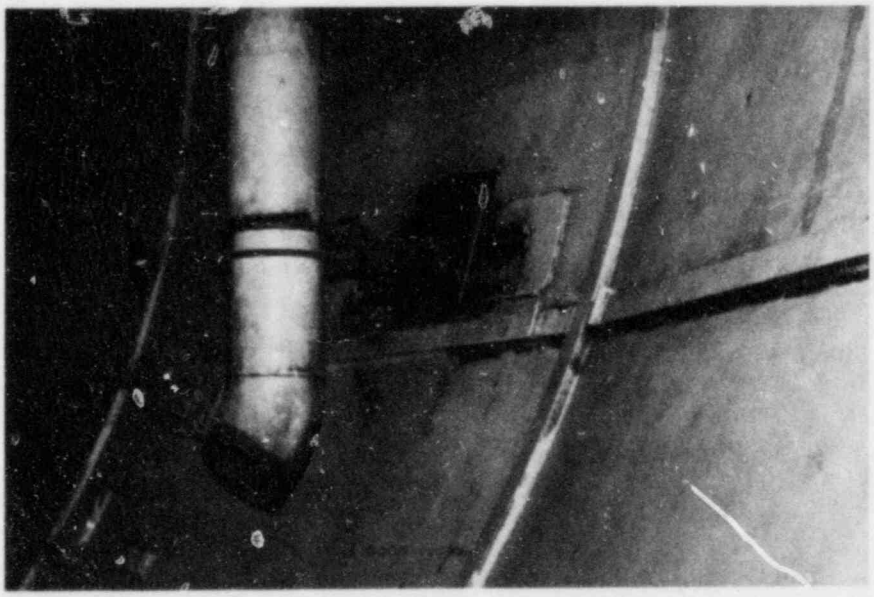

CAROLINA POWER AND LIGHT
BRUNSWICK STEAM ELECTRIC PLANT
UNIT 2
TORUS (1982)

CORE SPRAY TEST LINE SUPPORT

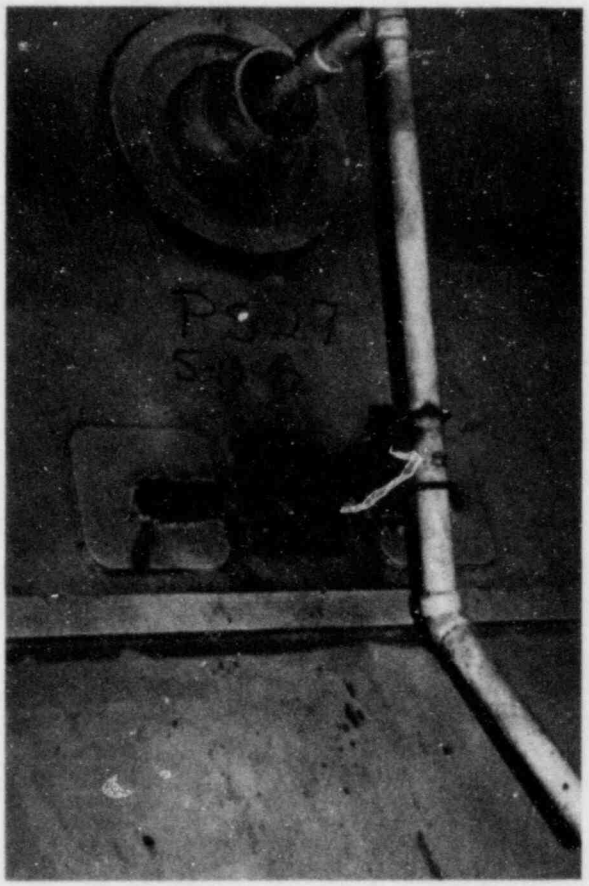

CAROLINA POWER AND LIGHT
BRUNSWICK STEAM ELECTRIC PLANT
UNIT 2
TORUS (1982)

HPCI DRAINPOT LINE SUPPORT